DISS. ETH No. 30063

Electrostatic and Magnetostatic Force Computation With Shape Calculus and BEM

A thesis submitted to attain the degree of

DOCTOR OF SCIENCES
(Dr. sc. ETH Zürich)

presented by

PIYUSH PANCHAL

MSc ETH in Computational Science and Engineering, ETH Zürich

born on 17.12.1995
citizen of India

accepted on the recommendation of
Prof. Dr. Ralf Hiptmair, ETH Zürich, examiner
Prof. Dr. Helmut Harbrecht, Universität Basel, co-examiner
Prof. Dr. Alberto Paganini, University of Leicester, co-examiner

2024

Abstract

Local and global forces are important quantities of interest in electrostatic and magnetostatic settings. They are important for the mechanical design or analysis of an electromechanical system and their computation via numerical simulations is thus a valuable tool. They are obtained through post-processing of the numerically computed fields and, generally speaking, can be obtained via either a volume-based or a boundary-based approach. For classical schemes based on the Maxwell Stress Tensor, the boundary-based computation yields lower convergence rates and total errors compared to the volume-based computations, especially for the case of non-smooth domains with sharp corners. When working with the boundary element method (BEM), the boundary data is obtained directly from the solvers, making it convenient to do a boundary-based computation of forces. Alas, it suffers from low convergence rates. Yet, it is not efficient to reconstruct the field solution inside the domain and use a volume-based computation in this case.

This work is aimed at obtaining better boundary-based computation algorithms for electromagnetic forces. The central idea comes from the Virtual Work Principle which relates the change of field energy for a deformation of the geometric configuration to the work done by the force fields. These energy changes are tracked using the shape derivative of the field energy which yields the forces in the sense of a distribution over the space of velocity fields. The computation of the shape derivative can be done with a variational constraint using the adjoint method which provides another point of attack. By choosing a variational constraint in the volume, we recover the Maxwell Stress Tensor based formulas, but by choosing a boundary integral equation constraint we obtain novel expressions which resemble boundary integral operators and thus have certain smoothing properties, making them superior to the classical boundary based approaches. In this work we compute these boundary integral equation constrained shape derivatives for various electrostatic and magnetostatic settings and compare their performance to the classical boundary based algorithms via numerical computation of forces and torques. In the process of computing the energy shape derivatives, we also attempt to provide more clarity to the idea of "holding the fluxes constant" while using the Virtual Work Principle, which emerges as a natural by-product of the adjoint calculus in our computations. Finally, for the case of permanent magnets, we show how the equivalent charge and equivalent current models are related to each other.

1

Abstrakt

Lokale und globale Kräfte sind wichtige Größen von Interesse in elektrostatischen und magnetostatischen Umgebungen. Sie spielen eine entscheidende Rolle beim mechanischen Design oder der Analyse eines elektromechanischen Systems, und ihre Berechnung mittels numerischer Simulationen ist somit ein wertvolles Werkzeug. Diese Größen werden durch die Nachverarbeitung der numerisch berechneten Felder erhalten und können im Allgemeinen entweder durch einen volumenbasierten oder einen grenzbasierten Ansatz ermittelt werden. Bei klassischen Methoden, die auf dem Maxwell-Spannungstensor basieren, ergibt die grenzbasierte Berechnung niedrigere Konvergenzraten und Gesamtfehler im Vergleich zu volumenbasierten Berechnungen, insbesondere für den Fall von nicht glatten Domänen mit scharfen Ecken. Bei der Arbeit mit der Randelementmethode (BEM) werden die Randdaten direkt von den Lösungsalgorithmen erhalten, was die Durchführung einer grenzbasierten Berechnung von Kräften erleichtert. Leider leidet sie unter niedrigen Konvergenzraten. Es ist jedoch nicht effizient, die Feldlösung im Inneren der Domäne zu rekonstruieren und in diesem Fall eine volumenbasierte Berechnung durchzuführen.

Diese Arbeit zielt darauf ab, bessere grenzbasierte Berechnungsalgorithmen für elektromagnetische Kräfte zu entwickeln. Die zentrale Idee stammt vom Prinzip der virtuellen Arbeit, das die Änderung der Feldenergie für eine Verformung der geometrischen Konfiguration mit der durch die Kraftfelder verrichteten Arbeit in Beziehung setzt. Diese Energieänderungen werden mithilfe der Formableitung der Feldenergie verfolgt, die die Kräfte im Sinne einer Verteilung über den Raum der Geschwindigkeitsfelder liefert. Die Berechnung der Formableitung kann mithilfe einer Variationsbedingung unter Verwendung der adjungierten Methode erfolgen, die einen weiteren Ansatzpunkt bietet. Durch die Wahl einer Variationsbedingung im Volumen erhalten wir Formeln, die auf dem Maxwell-Spannungstensor basieren. Durch die Wahl einer Randintegralgleichungsbedingung erhalten wir jedoch neuartige Ausdrücke, die Randintegraloperatoren ähneln und somit bestimmte Glättungseigenschaften aufweisen, die sie den klassischen grenzbasierten Ansätzen überlegen machen. In dieser Arbeit berechnen wir diese durch Randintegralgleichungen eingeschränkten Formableitungen für verschiedene elektrostatische und magnetostatische Umgebungen und vergleichen ihre Leistung mit den klassischen grenzbasierten Algorithmen durch numerische Berechnung von Kräften und Drehmomenten. Im Prozess der Berechnung der Formableitungen der Energie versuchen wir auch, mehr Klarheit in die Idee des "Konstantenhaltens der Flüsse" zu bringen, während wir das Prinzip der virtuellen Arbeit verwenden, das in unseren Berechnungen als natürlicher Nebenprodukt des adjungierten Kalküls entsteht. Schließlich zeigen wir für den Fall permanenter Magneten, wie die Modelle des äquivalenten Ladungs- und äquivalenten Stroms miteinander verbunden sind.

2

Acknowledgments

I am very grateful to Prof. Ralf Hiptmair for giving me this opportunity to pursue my Ph.D. studies. I have learned a lot from him about mathematics, numerics and life. I highly appreciate all the contribution and support he has provided to me at every step during this journey. I really enjoyed the hikes, the bike rides to Disentis, the car rides to Sollerhaus and the chess games with him. I am also very thankful to the staff at SAM, the secretaries and the ISG who have been very helpful in making my time at SAM go smoothly.

I am grateful to all the SAMmies, especially my office mates Erick and Ignacio who were always there for me in discussions concerning mathematics, programming or other things in life. I am very thankful to Martin who introduced our group to Gypsilab, a tool which I used for a lot of numerical experiments in this thesis, and all the interesting chess games he played with me. I had a good time with the next-door office mates Joost, Konstantin, Marcello and Oliver who was a great help in relocating in Zurich twice. I had a great time organizing NumCSE for several years with Tandri, Jinghao, Tianwei and Liu Ping. I am also very thankful to Vignesh whose help was invaluable for me while living in Zurich. I am very thankful to Ning Ren who did a tremendous job on force computation for 2D dielectric setting during her semester project and produced excellent results that are included in this thesis. Finally, I am very thankful to my family which has been very supportive of my endeavors all these years.

Contents

Chapter 1

Introduction

> "The electromagnetic field is something fundamental in the universe, whether it's in galaxies, atoms, or you and me."
>
> - Michael Faraday

Electromagnetic phenomena have long piqued our curiosity, manifesting in seemingly simple ways—such as the creation of static electric charge through friction leading to forces of attraction and tiny sparks, or the alignment of a magnetic material with the Earth's magnetic north. The laws governing electromagnetic phenomena were discovered incrementally by Coulomb, Faraday, Biot-Savart, and Ampère, and were later unified into a set of mathematical equations by Maxwell. This natural phenomenon not only stimulates contemplation but also forms the basis of many modern-day developments, becoming an indispensable part of our lives.

In the realm of mechanical devices operating in conjunction with electromagnetism, the forces of attraction and repulsion become crucial considerations. Mathematical models for forces between static charges and steady currents and magnetic fields were established over a century ago through Coulomb's law and Lorentz force law. These laws describe scenarios where the charges, currents, and fields are known. However, modeling becomes more intricate when dealing with physical scenarios where all the fields and charge/current distributions are not directly known. In such situations, an additional step is required to estimate the fields, typically utilizing numerical solvers like the finite element method or boundary element method. Forces can then be obtained as a post-processing step based on the computed field solution. Popular methods involve using Coulomb's law or Lorentz's law directly or employing computations based on the Maxwell Stress Tensor [23, 38].

Electrostatics and magnetostatics can also be viewed from an energetic perspective, a concept known for a considerable period. In the spirit of the Virtual Work Principle, an alternative approach emerged for force computation—one that considers virtual deformations of the geometrical configuration, linking changes in energy to force fields. This idea has been extensively explored and applied in mechanics. Several authors, such as Bossavit [4–7], Henrotte and Hameyer [20, 27–29], Medeiros et al. [39, 40], and Sanchez-Grandia [51], have contributed significantly in this direction. While their work has clarified the use of the Virtual Work Principle in the context of electrostatics and magnetostatics, it has also generated some confusion, particularly in the interpretation of the principle. A mathematically satisfying

answer to the question is given in the work by Henrotte and Hameyer which proposes to look at the deformations through the lens of differential forms and moving the relevant quantities as appropriate differential forms which implicitly preserves their "flux". Work by Bossavit, for example, takes a slightly different approach where he tracks the total energy change and algebraically extracts the mechanical power from it, which contains only the partial derivative of the field energy with respect to the configuration. Although an interesting approach, it often fails to give a detailed picture of what is being done. It also adds to the confusion when sometimes a quasi-static model is used to model a static setting as done in [7]. Some works further add to the confusion when their application of the Virtual Work Principle holds the fields constant.

This work aims to bring clarity to these issues by deriving force expressions through tracking energy changes in explicitly defined deformed configurations. Our approach is similar to Bossavit's, although the tools we employ differ. We define deformed configurations in terms of explicit boundary/transmission conditions and deformed sources (if any, as appropriate differential forms). Every deformed configuration has an associated field solution encoded through a variational formulation, which is linked to the energy for that configuration. The change in field energy is then tracked by computing the energy shape derivative, and the variational constraint is taken into account via the adjoint method. To facilitate this computation, we utilize tools from differential geometry and shape calculus. The novelty of this work lies not only in this methodology but also in using boundary integral equation (BIE) based variational formulations. While volume-based variational formulations yield classical force expressions, also obtained through the Maxwell Stress Tensor, BIE-based variational formulations produce entirely new force expressions. At the final step of our methodology we also see the connection with holding the fluxes constant and how it emerges naturally from the adjoint calculus.

As BIE constrained shape derivatives are the focal point of this work, we commence by introducing the BIEs for the Laplace and curl-curl equations in Chapter 2. In Chapter 3, we outline the tools from shape calculus and differential geometry that we will employ to compute the shape derivatives. Subsequently, in Chapter 4 and Chapter 5, we present the energy shape derivatives for various electrostatic and magnetostatic models, respectively, along with numerical experiments comparing the performance of the methods.

Chapter 2

Boundary Integral Equations

2.1 Laplace Equation

2.1.1 Representation Formula

For a bounded Lipschitz domain $\Omega \subset \mathbb{R}^d$, $d = 2, 3$, and $u \in C^2(\overline{\Omega})$[1] we have the representation formula [58, Equation. 6.1], [54, Theorem 3.1.6], [43, Theorem 6.10]

$$u(\boldsymbol{x}) = \int_\Gamma G(\boldsymbol{x}, \boldsymbol{y}) \, \nabla u(\boldsymbol{y}) \cdot \boldsymbol{n}(\boldsymbol{y}) \, dS_{\boldsymbol{y}} - \int_\Gamma \nabla_{\boldsymbol{y}} G(\boldsymbol{x}, \boldsymbol{y}) \cdot \boldsymbol{n}(\boldsymbol{y}) \, u(\boldsymbol{y}) \, dS_{\boldsymbol{y}}$$

$$- \int_\Omega G(\boldsymbol{x}, \boldsymbol{y}) \, \Delta u(\boldsymbol{y}) \, d\boldsymbol{y}, \quad \boldsymbol{x} \in \Omega, \qquad (2.1.1)$$

where $\boldsymbol{n}$ is the exterior unit normal vector field on the boundary $\Gamma := \partial\Omega$. $G : \{(\boldsymbol{x}, \boldsymbol{y}) \in \mathbb{R}^d \times \mathbb{R}^d, \, \boldsymbol{x} \neq \boldsymbol{y}\} \to \mathbb{R}$ is the fundamental solution for the Laplace operator, and is given as

$$G(\boldsymbol{x}, \boldsymbol{y}) := \begin{cases} -\frac{1}{2\pi} \log \|\boldsymbol{x} - \boldsymbol{y}\| & \text{for } d = 2 \,, \\ \dfrac{1}{4\pi \, \|\boldsymbol{x} - \boldsymbol{y}\|} & \text{for } d = 3 \,. \end{cases} \qquad (2.1.2)$$

For an exterior Lipschitz domain $\Omega_c := \mathbb{R}^d \setminus \overline{\Omega}$, that is the open complement of the bounded Lipschitz domain Ω, the representation formula still holds in 3D if Δu is compactly supported, and u satisfies the decay conditions [58, Section 7.5]

$$|u(\boldsymbol{x})| = O(\|\boldsymbol{x}\|^{-1}), \quad \|\nabla u(\boldsymbol{x})\| = O(\|\boldsymbol{x}\|^{-2}) \quad \text{for } \|\boldsymbol{x}\| \to \infty \text{ uniformly.}$$

2.1.2 Traces

The appearance of the boundary data of u in the integrals over Γ in Equation (2.1.1) leads us to the definition of traces. For $u \in C^1(\overline{\Omega})$ we define its Dirichlet trace $\gamma_D u$ and the Neumann

---

[1]We use standard notations for function spaces and, in particular, Sobolev spaces: $C^\infty(\Omega)$, $L^2(\Omega)$, $H^s(\Omega)$, $W^{m,\infty}(\Omega)$, etc., where Ω denotes a "generic domain". We adopt the conventions of [54, Sect 2.3 & 2.4].

trace (also called the co-normal derivative in literature) $\gamma_N u$ at $\boldsymbol{x} \in \Gamma$ as

$$\gamma_D u(\boldsymbol{x}) := \lim_{\Omega \ni \boldsymbol{y} \to \boldsymbol{x} \in \Gamma} u(\boldsymbol{y}), \quad \gamma_N u(\boldsymbol{x}) := \lim_{\Omega \ni \boldsymbol{y} \to \boldsymbol{x} \in \Gamma} \nabla u(\boldsymbol{y}) \cdot \boldsymbol{n}(\boldsymbol{x}),$$

where $\boldsymbol{n}$ is the exterior unit normal on the boundary Γ. The trace operators can be extended to bounded linear operators between the following spaces [54, Section 2.6,2.7]

$$\gamma_N : H^1_\Delta(\Omega) \to H^{-\frac{1}{2}}(\Gamma), \quad \gamma_D : H^1(\Omega) \to H^{\frac{1}{2}}(\Gamma),$$

where $H^1_\Delta(\Omega) := \{u \in H^1_{loc}(\Omega) : \Delta u \in L^2_{comp}(\Omega)\}$ (see [54, Equation 2.108]). The traces can also be defined from the unbounded complement domain Ω_c. In the subsequent chapters we will denote the interior traces with a superscript " $-$ " and the exterior traces with a superscript " $+$ " following the notation in [54, Remark 2.7.10].

2.1.3   Layer Potentials

The boundary integrals in Equation (2.1.1) motivate the definition of the single layer potential Ψ_{SL} and double layer potential Ψ_{DL}. For $f \in L^1(\Gamma)$ and $\boldsymbol{x} \in \mathbb{R}^d \setminus \Gamma$ [54, Section 3.1]

$$\Psi_{SL}(f)(x) := \int_\Gamma G(\boldsymbol{x}, \boldsymbol{y})\, f(\boldsymbol{y})\, d\mathrm{S}_{\boldsymbol{y}},$$

$$\Psi_{DL}(f)(x) := \int_\Gamma \nabla_y G(\boldsymbol{x}, \boldsymbol{y}) \cdot \boldsymbol{n}(\boldsymbol{y})\, f(\boldsymbol{y})\, d\mathrm{S}_{\boldsymbol{y}}. \tag{2.1.3}$$

The layer potentials also have a more general, abstract definiton in terms of the Newton potential and adjoint trace operators, which can be found in [54, Definition 3.1.5], and which leads to bounded linear operators

$$\Psi_{SL} : H^{-\frac{1}{2}+s}(\Gamma) \to H^{1+s}_{loc}(\mathbb{R}^3), \quad \Psi_{DL} : H^{\frac{1}{2}+s}(\Gamma) \to H^{1+s}_\Delta(\mathbb{R}^3 \setminus \Gamma),$$

where $|s| < \frac{1}{2}$ for Lipschitz domains. The abstract definition coincides with the integral representations (2.1.3) for L^1 densities which holds true in the numerical implementations. The representation formula itself can be defined in a more abstract fashion for $u \in H^1_\Delta(\mathbb{R}^d \setminus \Gamma)$ using the abstract definitions of the layer potentials [54, Section 3.1.1], [43, Chapter 6].

2.1.4   Boundary Integral Operators

Since the layer potentials map into H^1_Δ in both Ω and its complement $\Omega_c := \mathbb{R}^3 \setminus \overline{\Omega}$, we can apply the trace operators from both sides. Averaging these traces on Γ gives us boundary integral operators. We write the average traces on the boundary $\frac{1}{2}(\gamma^-_* u + \gamma^+_* u)$, $* \in \{N, D\}$, using the shorthand notation $\{\gamma_* u\}_\Gamma$. Using this convention, we can write down the definition of the boundary integral operators

$$\mathrm{V}\,\psi := \{\gamma_D \Psi_{SL}(\psi)\}_\Gamma, \quad \mathrm{K}\,g := \{\gamma_D \Psi_{DL}(g)\}_\Gamma, \tag{2.1.4}$$

$$\mathrm{K}'\,\psi := \{\gamma_N \Psi_{SL}(\psi)\}_\Gamma, \quad \mathrm{W}\,g := -\{\gamma_N \Psi_{DL}(g)\}_\Gamma, \tag{2.1.5}$$

where V, K, K', W are called the single layer, double layer, adjoint double layer and hypersingular boundary integral operators, respectively. These boundary integral operators are bounded linear maps between trace spaces

$$V : H^{-\frac{1}{2}}(\Gamma) \to H^{\frac{1}{2}}(\Gamma), \qquad K : H^{\frac{1}{2}}(\Gamma) \to H^{\frac{1}{2}}(\Gamma), \tag{2.1.6}$$

$$K' : H^{-\frac{1}{2}}(\Gamma) \to H^{-\frac{1}{2}}(\Gamma), \quad W : H^{\frac{1}{2}}(\Gamma) \to H^{-\frac{1}{2}}(\Gamma). \tag{2.1.7}$$

It is also well known that the single layer BIO is elliptic on $H^{-\frac{1}{2}}(\Gamma)$ for $d = 3$ [58, Theorem 6.22] and for $d = 2$ it is elliptic under the assumption $\text{diam}(\Omega) < 1$ [58, Theorem 6.23]. The hypersingular BIO is elliptic on $H_*^{\frac{1}{2}}(\Gamma) := \{u \in H^{\frac{1}{2}}(\Gamma) : \int_\Gamma u \, dS = 0\}$ [58, Section 6.6].

For Γ belonging to the class C_{pw}^2 and argument functions in $L^\infty(\Gamma)$ the boundary integral operators have integral representations in terms of weakly singular integrals which will be heavily used in subsequent chapters:

$$V(\psi)(\boldsymbol{x}) = \int_\Gamma G(\boldsymbol{x}, \boldsymbol{y}) \, \psi(\boldsymbol{y}) \, dS_{\boldsymbol{y}}, \tag{2.1.8}$$

$$K(g)(\boldsymbol{x}) = \int_\Gamma \nabla_y G(\boldsymbol{x}, \boldsymbol{y}) \cdot \boldsymbol{n}(\boldsymbol{y}) \, g(\boldsymbol{y}) \, dS_{\boldsymbol{y}}, \tag{2.1.9}$$

$$K'(\psi)(\boldsymbol{x}) = \int_\Gamma \nabla_x G(\boldsymbol{x}, \boldsymbol{y}) \cdot \boldsymbol{n}(\boldsymbol{x}) \, \psi(\boldsymbol{y}) \, dS_{\boldsymbol{y}}. \tag{2.1.10}$$

The hypersingular BIO W has an explicit integral representation as a finite part integral. We have a more convenient representation for the bilinear form it induces [58, Section 6.5], which we will use. We call the bilinear form induced by the hypersingular BIO b_W. It is given as

$$\mathsf{b}_W(g, v) = \int_\Gamma \int_\Gamma G(\boldsymbol{x}, \boldsymbol{y}) \frac{dg}{dt}(\boldsymbol{y}) \frac{dv}{dt}(\boldsymbol{x}) \, dS_{\boldsymbol{y}} \, dS_{\boldsymbol{x}} \qquad \text{(2D)}, \tag{2.1.11}$$

$$\mathsf{b}_W(g, v) = \int_\Gamma \int_\Gamma G(\boldsymbol{x}, \boldsymbol{y}) \, \mathbf{curl}_\Gamma \, g(\boldsymbol{y}) \cdot \mathbf{curl}_\Gamma \, v(\boldsymbol{x}) \, dS_{\boldsymbol{y}} \, dS_{\boldsymbol{x}} \quad \text{(3D)}, \tag{2.1.12}$$

where in the 2D case $\frac{d}{dt}$ represents the arclength derivative.

Remark 1. Note that the assumptions required for the integral representations to be valid hold true for boundary element approximations where the basis functions are piecewise smooth and so are the boundaries.

The traces of layer potentials also satisfy certain jump relations which we mention next [58, Chapter 6], [54, Theorem 3.3.1]. We denote a jump using $[\![\cdot]\!]_\Gamma$, which is given as the exterior trace minus the interior trace. For example, $[\![\gamma_D \, \Psi_{SL}(\psi)]\!]_\Gamma = \gamma_D^+ \, \Psi_{SL}(\psi) - \gamma_D^- \, \Psi_{SL}(\psi)$. Using this notation, the jump relations are expressed as

$$[\![\gamma_D \Psi_{SL}(\psi)]\!]_\Gamma = 0, \qquad [\![\gamma_D \Psi_{DL}(g)]\!]_\Gamma = g, \tag{2.1.13}$$

$$[\![\gamma_N \Psi_{SL}(\psi)]\!]_\Gamma = -\psi, \quad [\![\gamma_N \Psi_{DL}(g)]\!]_\Gamma = 0. \tag{2.1.14}$$

Combining the definition of the BIOs and the jump relations gives us

$$\gamma_D^- \Psi_{SL}(\psi) = \mathrm{V}(\psi), \qquad \gamma_D^+ \Psi_{SL}(\psi) = \mathrm{V}(\psi), \tag{2.1.15}$$

$$\gamma_N^- \Psi_{SL}(\psi) = \frac{\psi}{2} + \mathrm{K}'(\psi), \quad \gamma_N^+ \Psi_{SL}(\psi) = -\frac{\psi}{2} + \mathrm{K}'(\psi), \tag{2.1.16}$$

$$\gamma_D^- \Psi_{DL}(g) = -\frac{g}{2} + \mathrm{K}(g), \quad \gamma_D^+ \Psi_{DL}(g) = \frac{g}{2} + \mathrm{K}(g), \tag{2.1.17}$$

$$\gamma_N^- \Psi_{DL}(g) = -\mathrm{W}(g), \qquad \gamma_N^+ \Psi_{DL}(g) = -\mathrm{W}(g). \tag{2.1.18}$$

2.1.5   Boundary Integral Equations

Let $\Omega \subset \mathbb{R}^d$ be a bounded Lipschitz domain. Let $\Omega_c := \mathbb{R}^d \setminus \overline{\Omega}$ denote its complement and let $u \in C^2(\Omega \cup \Omega_c)$. We have the representation formulas for u in both domains:
For $\boldsymbol{x} \in \Omega$

$$u(\boldsymbol{x}) = \Psi_{SL}(\gamma_N^- u)(\boldsymbol{x}) - \Psi_{DL}(\gamma_D^- u)(\boldsymbol{x}) - \int_\Omega G(\boldsymbol{x}, \boldsymbol{y}) \, \Delta u(\boldsymbol{y}) \, d\boldsymbol{y}. \tag{2.1.19}$$

For $\boldsymbol{x} \in \Omega_c$

$$u(\boldsymbol{x}) = -\Psi_{SL}(\gamma_N^+ u)(\boldsymbol{x}) + \Psi_{DL}(\gamma_D^+ u)(\boldsymbol{x}) - \int_{\Omega_c} G(\boldsymbol{x}, \boldsymbol{y}) \, \Delta u(\boldsymbol{y}) \, d\boldsymbol{y}. \tag{2.1.20}$$

Notice the sign flip for the layer potentials in the representation formula for the exterior domain. This is because when considering the representation formula 2.1.1 on Ω_c the exterior unit normal vector field points into Ω. Writing the integral expressions and traces in terms of the exterior unit normal gives us the sign flip. Applying the traces to these representation formulas yields the two sets of boundary integral equations.

$$\begin{bmatrix} \mathrm{V} & -\frac{\mathsf{Id}}{2} - \mathrm{K} \\ -\frac{\mathsf{Id}}{2} + \mathrm{K}' & \mathrm{W} \end{bmatrix} \begin{bmatrix} \gamma_N^- u \\ \gamma_D^- u \end{bmatrix} = \begin{bmatrix} \gamma_D^- \int_\Omega G(\boldsymbol{x}, \boldsymbol{y}) \, \Delta u(\boldsymbol{y}) \, d\boldsymbol{y} \\ \gamma_N^- \int_\Omega G(\boldsymbol{x}, \boldsymbol{y}) \, \Delta u(\boldsymbol{y}) \, d\boldsymbol{y} \end{bmatrix}, \tag{2.1.21}$$

$$\begin{bmatrix} -\mathrm{V} & -\frac{\mathsf{Id}}{2} + \mathrm{K} \\ -\frac{\mathsf{Id}}{2} - \mathrm{K}' & -\mathrm{W} \end{bmatrix} \begin{bmatrix} \gamma_N^+ u \\ \gamma_D^+ u \end{bmatrix} = \begin{bmatrix} \gamma_D^+ \int_\Omega G(\boldsymbol{x}, \boldsymbol{y}) \, \Delta u(\boldsymbol{y}) \, d\boldsymbol{y} \\ \gamma_N^+ \int_\Omega G(\boldsymbol{x}, \boldsymbol{y}) \, \Delta u(\boldsymbol{y}) \, d\boldsymbol{y} \end{bmatrix}. \tag{2.1.22}$$

2.2   Curl Curl Equation

2.2.1   Representation Formula

For any Lipschitz domain $\Omega \in \mathbb{R}^3$ and a vector field $\mathbf{A} \in C^2(\overline{\Omega})^3$ which has $\mathrm{div}\,\mathbf{A}$ and **curlcurlA** compactly supported and decaying like $\mathbf{A}(\boldsymbol{x}) = O(\|\boldsymbol{x}\|^{-1}), \mathbf{curlA}(\boldsymbol{x}) = O(\|\boldsymbol{x}\|^{-1})$

for $\|\boldsymbol{x}\| \to \infty$, we have the representation formula [33, Equation 5.1]

$$
\mathbf{A}(\boldsymbol{x}) = -\,\mathbf{curl}_{\boldsymbol{x}} \int_{\Gamma} (\mathbf{n} \times \mathbf{A})(\boldsymbol{y})\, G(\boldsymbol{x},\boldsymbol{y})\, d\mathrm{S}_{\boldsymbol{y}} - \int_{\Gamma} (\mathbf{n} \times \mathbf{curl}\mathbf{A})(\boldsymbol{y})\, G(\boldsymbol{x},\boldsymbol{y})\, d\mathrm{S}_{\boldsymbol{y}}
$$

$$
+ \operatorname{grad}_{\boldsymbol{x}} \int_{\Gamma} (\mathbf{n} \cdot \mathbf{A})(\boldsymbol{y})\, G(\boldsymbol{x},\boldsymbol{y})\, d\mathrm{S}_{\boldsymbol{y}} + \int_{\Omega} \mathbf{curlcurl}\mathbf{A}(\boldsymbol{y})G(\boldsymbol{x},\boldsymbol{y})\, \mathrm{d}\boldsymbol{y}
$$

$$
- \int_{\Omega} \operatorname{div} \mathbf{A}(\boldsymbol{y})\ \operatorname{grad}_{\boldsymbol{x}} G(\boldsymbol{x},\boldsymbol{y})\, \mathrm{d}\boldsymbol{y}, \quad \boldsymbol{x} \in \Omega, \tag{2.2.1}
$$

where $G(\boldsymbol{x},\boldsymbol{y})$ is the fundamental solution for the Laplacian in 3D (2.1.2).

2.2.2 Layer Potentials

The three boundary integrals that appear in the representation formula (2.2.1) lead us to three layer potentials. To express their properties, we require the relevant tangential trace spaces for vector fields in $\boldsymbol{H}(\mathbf{curl}, \Omega) := \{\mathbf{u} \in \boldsymbol{L}^2(\Omega) : \mathbf{curl}\mathbf{u} \in \boldsymbol{L}^2(\Omega)\}$, where $\boldsymbol{L}^2(\Omega)$ is the space of square integrable vector fields on a bounded domain Ω. We will simply mention the relevant tangential trace spaces as $\boldsymbol{H}^{-\frac{1}{2}}(\mathbf{curl}_\Gamma, \Gamma)$ and $\boldsymbol{H}^{-\frac{1}{2}}(\operatorname{div}_\Gamma, \Gamma)$ which are dual to each other with respect to the pivot space $\boldsymbol{L}_t^2(\Gamma)$ of square integrable tangential vector fields on Γ, and refer the reader to [8, 10, 33] for technical details.

The vectorial single layer potential is defined as

$$
\boldsymbol{\Psi}_{\mathbf{A}}(\boldsymbol{\lambda})(\boldsymbol{x}) := \int_{\Gamma} G(\boldsymbol{x},\boldsymbol{y})\, \boldsymbol{\lambda}(\boldsymbol{y})d\mathrm{S}_{\boldsymbol{y}}, \quad \boldsymbol{x} \notin \Gamma, \tag{2.2.2}
$$

and its continuity properties are made explicit in [33, Theorem 5.1]. The vectorial double layer potential is defined as

$$
\boldsymbol{\Psi}_{\mathbf{M}}(\mathbf{u})(\boldsymbol{x}) := \mathbf{curl}_{\boldsymbol{x}} \int_{\Gamma} G(\boldsymbol{x},\boldsymbol{y}) \big(\mathbf{n}(\boldsymbol{y}) \times \mathbf{u}(\boldsymbol{y})\big)d\mathrm{S}_{\boldsymbol{y}} \quad \boldsymbol{x} \notin \Gamma \tag{2.2.3}
$$

$$
= \mathbf{curl}\boldsymbol{\Psi}_{\mathbf{A}}(\mathbf{n} \times \mathbf{u}), \tag{2.2.4}
$$

and its continuity properties are made explicit in [33, Theorem 5.3]. Next we define the scalar single layer potential, which we already saw in the case of the Laplace operator:

$$
\Psi_{SL}(\phi)(\boldsymbol{x}) := \int_{\Gamma} G(\boldsymbol{x},\boldsymbol{y})\, \phi(\boldsymbol{y})d\mathrm{S}_{\boldsymbol{y}}, \quad \boldsymbol{x} \notin \Gamma. \tag{2.2.5}
$$

The mapping property for the single layer potential is mentioned in Section 2.1.3.

2.2.3 Traces

For a bounded Lipschitz domain $\Omega \subset \mathbb{R}^3$ with a unit normal $\mathbf{n}$ on its boundary $\Gamma = \partial\Omega$, we can define three traces for a vector field $\mathbf{A} \in (C^1(\overline{\Omega}))^3$. The tangential trace is defined as

$$
\gamma_{\mathbf{t}}\mathbf{A}(\boldsymbol{x}) := \mathbf{n}(\boldsymbol{x}) \times (\mathbf{A}(\boldsymbol{x}) \times \mathbf{n}(\boldsymbol{x})), \tag{2.2.6}
$$

14

for almost all $\boldsymbol{x} \in \Gamma$. It represents the tangential component of the vector field on Γ and can be extended to a continuous and surjective mapping $\gamma_{\mathbf{t}} : \boldsymbol{H}(\mathbf{curl}, \Omega) \to \boldsymbol{H}^{-\frac{1}{2}}(\mathbf{curl}_\Gamma, \Gamma)$ with a continuous right inverse [33, Theorem 3.2]. The magnetic trace is defined as

$$\gamma_{\mathbf{M}}\mathbf{A}(\boldsymbol{x}) = \mathbf{curl}\mathbf{A}(\boldsymbol{x}) \times \mathbf{n}(\boldsymbol{x}), \tag{2.2.7}$$

which can be extended to a continuous and surjective mapping $\gamma_{\mathbf{M}} : \boldsymbol{H}(\mathbf{curl}^2; \Omega) \to \boldsymbol{H}^{-\frac{1}{2}}(\text{div}_\Gamma, \Gamma)$, where $\boldsymbol{H}(\mathbf{curl}^2; \Omega) := \{\mathbf{u} \in \boldsymbol{H}(\mathbf{curl}; \Omega) : \mathbf{curl}\mathbf{curl}\mathbf{u} \in \boldsymbol{L}^2(\Omega)\}$ [33, Section 3]. The normal trace γ_n is defined as

$$\gamma_n\mathbf{A}(\boldsymbol{x}) := \mathbf{A}(\boldsymbol{x}) \cdot \mathbf{n}(\boldsymbol{x}), \tag{2.2.8}$$

and can be extended to a mapping $\gamma_n : \boldsymbol{H}(\text{div}; \Omega) \to H^{-\frac{1}{2}}(\Gamma)$ [33, Section 3]. The traces can also be defined from the unbounded complement $\Omega_c = \mathbb{R}^3 \setminus \overline{\Omega}$. To distinguish the traces from the inside and outside we will use the superscript "$-$" and "$+$" respectively as in the Laplace case. The notation for the jump remains the same and we use the same convention of "exterior trace minus interior trace".

2.2.4   Boundary Integral Operators

To get the boundary integral operators, we take the traces of the layer potentials. Here we assume boundaries of class C_{pw}^2 and use the results from [14, Chapter 2, Section 2.6] for the traces. We mention the BIOs in their integral representations which will be used subsequently, but similar to the Laplace case, they have an abstract definition as well for which we refer to [33, Section 5,6].

The interior and exterior tangential trace of the vectorial single layer potential gives us

$$\gamma_{\mathbf{t}}^+\boldsymbol{\Psi}_{\mathbf{A}}(\boldsymbol{\lambda})(\boldsymbol{x}) = \gamma_{\mathbf{t}}^-\boldsymbol{\Psi}_{\mathbf{A}}(\boldsymbol{\lambda})(\boldsymbol{x}) = \mathbf{n}(\boldsymbol{x}) \times \left(\int_\Gamma G(\boldsymbol{x}, \boldsymbol{y}) \, \boldsymbol{\lambda}(\boldsymbol{y}) dS_{\boldsymbol{y}} \times \mathbf{n}(\boldsymbol{x}) \right), \quad \boldsymbol{x} \in \Gamma,$$

where the integral is defined as an improper integral. This leads to the definition of the boundary integral operator

$$\mathcal{A}(\boldsymbol{\lambda})(\boldsymbol{x}) := \mathbf{n}(\boldsymbol{x}) \times \left(\int_\Gamma G(\boldsymbol{x}, \boldsymbol{y}) \, \boldsymbol{\lambda}(\boldsymbol{y}) dS_{\boldsymbol{y}} \times \mathbf{n}(\boldsymbol{x}) \right), \quad \boldsymbol{x} \in \Gamma. \tag{2.2.9}$$

It has the mapping property $\mathcal{A} : \boldsymbol{H}^{-\frac{1}{2}}(\text{div}_\Gamma, \Gamma) \to \boldsymbol{H}^{-\frac{1}{2}}(\mathbf{curl}_\Gamma, \Gamma)$ and induces an elliptic bilinear form on $\boldsymbol{H}^{-\frac{1}{2}}(\text{div}_\Gamma 0, \Gamma)$ [33, Theorem 6.2]. Thus we have the relations

$$\gamma_{\mathbf{t}}^+\boldsymbol{\Psi}_{\mathbf{A}}(\boldsymbol{\lambda})(\boldsymbol{x}) = \gamma_{\mathbf{t}}^-\boldsymbol{\Psi}_{\mathbf{A}}(\boldsymbol{\lambda})(\boldsymbol{x}) = \mathcal{A}(\boldsymbol{\lambda})(\boldsymbol{x}). \tag{2.2.10}$$

Assuming $\boldsymbol{\lambda}$ is a continuous tangential density, the magnetic trace of the vectorial single layer potential gives

$$\gamma_{\mathbf{M}}^+\boldsymbol{\Psi}_{\mathbf{A}}(\boldsymbol{\lambda})(\boldsymbol{x}) = \int_\Gamma \mathbf{curl}_{\boldsymbol{x}}\big(G(\boldsymbol{x}, \boldsymbol{y}) \, \boldsymbol{\lambda}(\boldsymbol{y})\big) \times \mathbf{n}(\boldsymbol{x}) \, dS_{\boldsymbol{y}} - \frac{1}{2}\boldsymbol{\lambda}(\boldsymbol{x}), \quad \boldsymbol{x} \in \Gamma, \tag{2.2.11}$$

$$\gamma_{\mathbf{M}}^-\boldsymbol{\Psi}_{\mathbf{A}}(\boldsymbol{\lambda})(\boldsymbol{x}) = \int_\Gamma \mathbf{curl}_{\boldsymbol{x}}\big(G(\boldsymbol{x}, \boldsymbol{y}) \, \boldsymbol{\lambda}(\boldsymbol{y})\big) \times \mathbf{n}(\boldsymbol{x}) \, dS_{\boldsymbol{y}} + \frac{1}{2}\boldsymbol{\lambda}(\boldsymbol{x}), \quad \boldsymbol{x} \in \Gamma, \tag{2.2.12}$$

where the integrals exist as Cauchy Principal Value integrals. This leads to definition of the boundary integral operator

$$\mathcal{B}(\boldsymbol{\lambda})(\boldsymbol{x}) := \int_{\Gamma} \mathbf{curl}_{\boldsymbol{x}}\big(G(\boldsymbol{x}, \boldsymbol{y})\, \boldsymbol{\lambda}(\boldsymbol{y})\big) \times \mathbf{n}(\boldsymbol{x})\, dS_{\boldsymbol{y}}, \quad \boldsymbol{x} \in \Gamma, \tag{2.2.13}$$

which has the mapping property $\mathcal{B} : \boldsymbol{H}^{-\frac{1}{2}}(\mathrm{div}_{\Gamma}, \Gamma) \to \boldsymbol{H}^{-\frac{1}{2}}(\mathrm{div}_{\Gamma}, \Gamma)$ [33, Theorem 6.1]. The existence of the integral as an improper integral can be seen from the integrand

$$\mathbf{curl}_{\boldsymbol{x}}\big(G(\boldsymbol{x}, \boldsymbol{y})\, \boldsymbol{\lambda}(\boldsymbol{y})\big) \times \mathbf{n}(\boldsymbol{x}) = \mathbf{n}(\boldsymbol{x}) \cdot \nabla_{\boldsymbol{x}} G(\boldsymbol{x}, \boldsymbol{y})\, \boldsymbol{\lambda}(\boldsymbol{y}) - \mathbf{n}(\boldsymbol{x}) \cdot \boldsymbol{\lambda}(\boldsymbol{y}) \nabla_{\boldsymbol{x}} G(\boldsymbol{x}, \boldsymbol{y})$$
$$= \mathbf{n}(\boldsymbol{x}) \cdot \nabla_{\boldsymbol{x}} G(\boldsymbol{x}, \boldsymbol{y})\, \boldsymbol{\lambda}(\boldsymbol{y}) - \mathbf{n}(\boldsymbol{x}) \cdot (\boldsymbol{\lambda}(\boldsymbol{y}) - \boldsymbol{\lambda}(\boldsymbol{x}))\, \nabla_{\boldsymbol{x}} G(\boldsymbol{x}, \boldsymbol{y}).$$

By jump relations, the trace relations can be rewritten as

$$\gamma_{\mathbf{M}}^{+} \boldsymbol{\Psi}_{\mathbf{A}}(\boldsymbol{\lambda})(\boldsymbol{x}) = \mathcal{B}(\boldsymbol{\lambda})(\boldsymbol{x}) - \frac{1}{2}\boldsymbol{\lambda}(\boldsymbol{x}), \quad \gamma_{\mathbf{M}}^{-} \boldsymbol{\Psi}_{\mathbf{A}}(\boldsymbol{\lambda})(\boldsymbol{x}) = \mathcal{B}(\boldsymbol{\lambda})(\boldsymbol{x}) + \frac{1}{2}\boldsymbol{\lambda}(\boldsymbol{x}), \quad \boldsymbol{x} \in \Gamma. \tag{2.2.14}$$

Now applying the tangential trace to the vectorial double layer potential gives us

$$\gamma_{\mathbf{t}}^{+} \boldsymbol{\Psi}_{\mathbf{M}}(\mathbf{u})(\boldsymbol{x}) = \mathbf{n}(\boldsymbol{x}) \times \int_{\Gamma} \Big(\nabla_{\boldsymbol{x}} G(\boldsymbol{x}, \boldsymbol{y}) \times (\mathbf{n} \times \mathbf{u})(\boldsymbol{y})\Big) \times \mathbf{n}(\boldsymbol{x})\, dS_{\boldsymbol{y}} + \frac{1}{2}\mathbf{u}(\boldsymbol{x}), \quad \boldsymbol{x} \in \Gamma$$

$$\gamma_{\mathbf{t}}^{-} \boldsymbol{\Psi}_{\mathbf{M}}(\mathbf{u})(\boldsymbol{x}) = \mathbf{n}(\boldsymbol{x}) \times \int_{\Gamma} \Big(\nabla_{\boldsymbol{x}} G(\boldsymbol{x}, \boldsymbol{y}) \times (\mathbf{n} \times \mathbf{u})(\boldsymbol{y})\Big) \times \mathbf{n}(\boldsymbol{x})\, dS_{\boldsymbol{y}} - \frac{1}{2}\mathbf{u}(\boldsymbol{x}) \quad \boldsymbol{x} \in \Gamma.$$
$$\tag{2.2.15}$$

The integrals are defined as Cauchy Principal Value integrals, which can be shown using the argument above. This leads us to the boundary integral operator

$$\mathcal{C}(\mathbf{u})(\boldsymbol{x}) := \mathbf{n}(\boldsymbol{x}) \times \int_{\Gamma} \Big(\nabla_{\boldsymbol{x}} G(\boldsymbol{x}, \boldsymbol{y}) \times (\mathbf{n} \times \mathbf{u})(\boldsymbol{y})\Big) \times \mathbf{n}(\boldsymbol{x})\, dS_{\boldsymbol{y}}, \tag{2.2.16}$$

which has the mapping property $\mathcal{C} : \boldsymbol{H}^{-\frac{1}{2}}(\mathbf{curl}_{\Gamma}, \Gamma) \to \boldsymbol{H}^{-\frac{1}{2}}(\mathbf{curl}_{\Gamma}, \Gamma)$ [33, Theorem 6.1]. The jump relations are compactly written as

$$\gamma_{\mathbf{t}}^{+} \boldsymbol{\Psi}_{\mathbf{M}}(\mathbf{u})(\boldsymbol{x}) = \mathcal{C}(\mathbf{u})(\boldsymbol{x}) + \frac{1}{2}\mathbf{u}(\boldsymbol{x}), \quad \gamma_{\mathbf{t}}^{-} \boldsymbol{\Psi}_{\mathbf{M}}(\mathbf{u})(\boldsymbol{x}) = \mathcal{C}(\mathbf{u})(\boldsymbol{x}) - \frac{1}{2}\mathbf{u}(\boldsymbol{x}), \quad \boldsymbol{x} \in \Gamma. \tag{2.2.17}$$

Applying the Neumann trace to the vectorial double layer potential gives us

$$\gamma_{\mathbf{M}}^{+} \boldsymbol{\Psi}_{\mathbf{M}}(\mathbf{u})(\boldsymbol{x}) = \gamma_{\mathbf{M}}^{-} \boldsymbol{\Psi}_{\mathbf{M}}(\mathbf{u})(\boldsymbol{x}) = \int_{\Gamma} \nabla_{\boldsymbol{x}} G(\boldsymbol{x}, \boldsymbol{y})\, \mathrm{div}_{\Gamma}(\mathbf{n} \times \mathbf{u})(\boldsymbol{y})\, dS(\boldsymbol{y}) \times \mathbf{n}(\boldsymbol{x}), \tag{2.2.18}$$

which leads us to the boundary integral operator

$$\mathbf{N}(\mathbf{u})(\boldsymbol{x}) := \int_{\Gamma} \nabla_{\boldsymbol{x}} G(\boldsymbol{x}, \boldsymbol{y})\, \mathrm{div}_{\Gamma}(\mathbf{n} \times \mathbf{u})(\boldsymbol{y})\, dS(\boldsymbol{y}) \times \mathbf{n}(\boldsymbol{x}), \quad \boldsymbol{x} \in \Gamma. \tag{2.2.19}$$

It has the mapping property $\mathcal{N} : \boldsymbol{H}^{-\frac{1}{2}}(\mathbf{curl}_{\Gamma}, \Gamma) \to \boldsymbol{H}^{-\frac{1}{2}}(\mathrm{div}_{\Gamma}, \Gamma)$ [33, Theorem 6.1]. The integral exists as a Cauchy-Principal Value [14] but the operator has an associated bilinear form with improper integrals [33, Lemma 6.3].

16

Remark 2. The bilinear form associated with $\mathcal{N}$ can be made elliptic if we consider it on a subspace of $\boldsymbol{H}^{-\frac{1}{2}}(\mathbf{curl}_\Gamma, \Gamma)$ with the kernel of the operator removed, that is the space $\{\mathbf{u} \in \boldsymbol{H}^{-\frac{1}{2}}(\mathbf{curl}_\Gamma, \Gamma) : (\mathbf{u}, \mathbf{grad}_\Gamma v)_{-\frac{1}{2}} = 0 \quad v \in H_*^{\frac{1}{2}}(\Gamma)\}$, where $H_*^{\frac{1}{2}}(\Gamma) := \{v \in H^{\frac{1}{2}}(\Gamma) : \int_\Gamma v\, d\mathrm{S} = 0\}$ and $(\cdot, \cdot)_{-\frac{1}{2}}$ denotes the inner product for the Hilbert space $\boldsymbol{H}^{-\frac{1}{2}}(\mathbf{curl}_\Gamma, \Gamma)$. This characterization is valid only for trivial topologies, for a more general treatment, we refer to [13].

Writing the trace relation compactly we have

$$\gamma_{\mathbf{M}}^+ \boldsymbol{\Psi}_{\mathbf{M}}(\mathbf{u})(\boldsymbol{x}) = \gamma_{\mathbf{M}}^- \boldsymbol{\Psi}_{\mathbf{M}}(\mathbf{u})(\boldsymbol{x}) = \mathcal{N}(\mathbf{u})(\boldsymbol{x}). \tag{2.2.20}$$

2.2.5 Boundary Integral Equations

Using the notation for traces and layer potentials, we have the following representation in the interior of a bounded Lipschitz domain Ω

$$
\begin{aligned}
\mathbf{A}(\boldsymbol{x}) = {}& - \boldsymbol{\Psi}_{\mathbf{M}}(\gamma_{\mathbf{t}}^- \mathbf{A})(\boldsymbol{x}) + \boldsymbol{\Psi}_{\mathbf{A}}(\gamma_{\mathbf{M}}^- \mathbf{A})(x) + \mathrm{grad}_{\boldsymbol{x}}\, \Psi_V(\gamma_n^- \mathbf{A})(\boldsymbol{x}) \\
& + \int_\Omega \mathbf{curlcurl} \mathbf{A}(\boldsymbol{y}) G(\boldsymbol{x}, \boldsymbol{y})\, \mathrm{d}\boldsymbol{y} - \int_\Omega \mathrm{div}\, \mathbf{A}(\boldsymbol{y})\, \mathrm{grad}_{\boldsymbol{x}}\, G(\boldsymbol{x}, \boldsymbol{y})\, \mathrm{d}\boldsymbol{y}, \quad \boldsymbol{x} \in \Omega. \tag{2.2.21}
\end{aligned}
$$

For the exterior domain $\Omega_c = \mathbb{R}^3 \setminus \overline{\Omega}$, we get a sign flip for the unit normal which leads to the representation

$$
\begin{aligned}
\mathbf{A}(\boldsymbol{x}) = {}& \boldsymbol{\Psi}_{\mathbf{M}}(\gamma_{\mathbf{t}}^+ \mathbf{A})(\boldsymbol{x}) - \boldsymbol{\Psi}_{\mathbf{A}}(\gamma_{\mathbf{M}}^+ \mathbf{A})(x) - \mathrm{grad}_{\boldsymbol{x}}\, \Psi_V(\gamma_n^+ \mathbf{A})(\boldsymbol{x}) \\
& + \int_{\Omega_c} \mathbf{curlcurl} \mathbf{A}(\boldsymbol{y}) G(\boldsymbol{x}, \boldsymbol{y})\, \mathrm{d}\boldsymbol{y} - \int_{\Omega_c} \mathrm{div}\, \mathbf{A}(\boldsymbol{y})\, \mathrm{grad}_{\boldsymbol{x}}\, G(\boldsymbol{x}, \boldsymbol{y})\, \mathrm{d}\boldsymbol{y}, \quad \boldsymbol{x} \in \Omega_c. \tag{2.2.22}
\end{aligned}
$$

In the subsequent chapters, we will be dealing with vector potentials with zero divergence. Applying the Dirichlet and Neumann traces to the two representation formulas yields two sets of boundary integral equations given as

$$
\begin{aligned}
&\begin{bmatrix} -\mathcal{A} & \mathcal{C} + \frac{\mathrm{Id}}{2} \\ -\mathcal{B} + \frac{\mathrm{Id}}{2} & \mathcal{N} \end{bmatrix} \begin{bmatrix} \gamma_{\mathbf{M}}^- \mathbf{A} \\ \gamma_{\mathbf{t}}^- \mathbf{A} \end{bmatrix} - \begin{bmatrix} \mathbf{grad}_\Gamma\, \Psi_V(\gamma_n^- \mathbf{A}) \\ 0 \end{bmatrix} = \begin{bmatrix} \gamma_{\mathbf{t}}^- \int_\Omega \mathbf{curlcurl} \mathbf{A}(\boldsymbol{y})\, G(\boldsymbol{x}, \boldsymbol{y})\, d\boldsymbol{y} \\ \gamma_{\mathbf{M}}^- \int_\Omega \mathbf{curlcurl} \mathbf{A}(\boldsymbol{y})\, G(\boldsymbol{x}, \boldsymbol{y})\, d\boldsymbol{y} \end{bmatrix}, \\[2ex]
&\begin{bmatrix} \mathcal{A} & -\mathcal{C} + \frac{\mathrm{Id}}{2} \\ \mathcal{B} + \frac{\mathrm{Id}}{2} & -\mathcal{N} \end{bmatrix} \begin{bmatrix} \gamma_{\mathbf{M}}^+ \mathbf{A} \\ \gamma_{\mathbf{t}}^+ \mathbf{A} \end{bmatrix} + \begin{bmatrix} \mathbf{grad}_\Gamma\, \Psi_V(\gamma_n^+ \mathbf{A}) \\ 0 \end{bmatrix} = \begin{bmatrix} \gamma_{\mathbf{t}}^+ \int_{\Omega_c} \mathbf{curlcurl} \mathbf{A}(\boldsymbol{y})\, G(\boldsymbol{x}, \boldsymbol{y})\, d\boldsymbol{y} \\ \gamma_{\mathbf{M}}^+ \int_{\Omega_c} \mathbf{curlcurl} \mathbf{A}(\boldsymbol{y})\, G(\boldsymbol{x}, \boldsymbol{y})\, d\boldsymbol{y} \end{bmatrix}.
\end{aligned}
$$
$$\tag{2.2.23}$$

Chapter 3

Virtual Work Principle and Shape Calculus

In solid mechanics, the Virtual Work Principle states that for a system in equilibrium, the virtual work done by the external forces adds up to zero. Virtual work is defined as the work done by the forces along virtual displacements. This idea has also been applied to electrostatic and magnetostatic settings, where general deformations of a domain assume the role of virtual displacements [4, 11, 15, 28, 29]. One can imagine an external entity applying an equal and opposite force to the one generated by the electric or magnetic field to slowly cause the deformation. Obviously the total virtual work done is zero, but the virtual work done by the electric or magnetic field corresponds to a change in the energy contained in the fields. We can calculate this change in the field energy and obtain the force field from it. We use tools from shape calculus to track this change in energy, specifically via the shape derivative of the field energy.

3.0.1 Shape Differentiation via Perturbation of Identity

In the subsequent chapters, we will think of the field energy as a shape functional $\mathcal{E}_F = \mathcal{E}_F(\Omega)$, a mapping from a set of admissible domains to $\mathbb{R}$. To shape differentiate $\mathcal{E}_F$ at a reference Lipschitz domain Ω^0, we will use the perturbation of identity approach [57, Sect. 2.8]. Starting with a fixed velocity field $\boldsymbol{\mathcal{V}} \in (C_0^\infty(\mathbb{R}^d))^d$, we define the perturbation map

$$\mathbf{T}_s^{\boldsymbol{\nu}} : \mathbb{R}^d \to \mathbb{R}^d, \quad \mathbf{T}_s^{\boldsymbol{\nu}}(\boldsymbol{x}) := \boldsymbol{x} + s\boldsymbol{\mathcal{V}}(\boldsymbol{x}), \quad s \in \mathbb{R}. \tag{3.0.1}$$

There exists a $\delta(\boldsymbol{\mathcal{V}}) > 0$ such that $\mathbf{T}_s^{\boldsymbol{\nu}}$ is bijective for $|s| < \delta(\boldsymbol{\mathcal{V}})$, as seen in [19, Chapter 4, Section 4.3]. Thus, the family of one-parameter domains

$$\Omega^s := \mathbf{T}_s^{\boldsymbol{\nu}}(\Omega^0), \quad |s| < \delta(\boldsymbol{\mathcal{V}}), \tag{3.0.2}$$

will still have connected Lipschitz boundaries $\Gamma^s := \partial\Omega^s = \mathbf{T}_s^{\boldsymbol{\nu}}(\Gamma^0)$. This family gives us the admissible set on which we can consider our shape functional $\mathcal{E}_F$. We call the limit

$$\frac{d\mathcal{E}_F}{d\Omega}(\Omega^0; \boldsymbol{\mathcal{V}}) := \lim_{s \to 0} \frac{\mathcal{E}_F(\Omega^s) - \mathcal{E}_F(\Omega^0)}{s} = \frac{d}{ds}\{s \mapsto \mathcal{E}_F(\Omega^s)\}\Big|_{s=0}, \tag{3.0.3}$$

if it exists, the shape (Gateaux) derivative in the direction of $\boldsymbol{\mathcal{V}}$. If, in addition, $\boldsymbol{\mathcal{V}} \mapsto \frac{d\mathcal{E}_F}{d\Omega}(\Omega^0; \boldsymbol{\mathcal{V}}) \in \mathbb{R}$ is a distribution on $\left(C_0^\infty(\mathbb{R}^d)\right)^d$, a 1-current in words of de Rham [17, Ch. 3, § 8], then $\Omega \mapsto \mathcal{E}_F(\Omega)$ is called *shape-differentiable* and that distribution is the *shape derivative* $\frac{d\mathcal{E}_F}{d\Omega}(\Omega)$ of $\mathcal{E}_F$ in Ω^0.

Remark 3. Note that we are talking about the unconstrained case when $\boldsymbol{\mathcal{V}} \in (C_0^\infty(\mathbb{R}^d))^d$ [19, Chapter 4, Section 4]. For the computation of shape derivatives we will place additional constraints on the velocity field $\boldsymbol{\mathcal{V}}$ depending on the model problem we are working with. These constraints will mainly be fixing the velocity field to zero at some part of the geometric configuration which would not be of interest when calculating forces. This part of the space would usually be associated with charge or current sources or some boundary conditions. The mathematical developments for this case are presented in [19, Chapter 4, Section 5], where the bijective property of the map $\mathbf{T}_s^\nu$ is shown to still hold.

Remark 4. The Hadamard structure theorem [18, Ch. 9, Thm 3.6] states that if Γ is C^∞-smooth, the shape derivative $\boldsymbol{\mathcal{V}} \mapsto \frac{d\mathcal{E}_F}{d\Omega}(\Omega^0; \boldsymbol{\mathcal{V}})$ admits a representative h in the space of distributions on Γ^0 such that

$$\frac{d\mathcal{E}_F}{d\Omega}(\Omega^0; \boldsymbol{\mathcal{V}}) = \langle h, \, \boldsymbol{\mathcal{V}} \cdot \boldsymbol{n}|_{\Gamma^0}\rangle \, , \quad \boldsymbol{\mathcal{V}} \in \left(C_0^\infty(\mathbb{R}^d)\right)^d . \tag{3.0.4}$$

This distribution h can be regarded as representing a *normal surface force density*.

3.0.2 Forces and Torques From Energy Shape Derivative

The Cartesian components of the *total force* $\mathbf{F} = (F_1, \ldots, F_d) \in \mathbb{R}^d$ acting on an object of interest $D \subset \mathbb{R}^d$ are the shape derivatives of the energy with respect to deformation fields that agree with Cartesian coordinate vectors in a neighborhood of D:

$$F_k = \frac{d\mathcal{E}_F}{d\Omega}(\Omega^0; \{\boldsymbol{x} \mapsto \mathbf{e}_k \chi(\boldsymbol{x})\}) \, , \tag{3.0.5}$$

where $\chi \in C_0^\infty(\mathbb{R}^d)$ is a cut-off function such that $\chi \equiv 1$ close to the object of interest D. It would also carry the additional constraints that are imposed on the velocity field $\boldsymbol{\mathcal{V}}$ for the concrete computation of the shape derivative in subsequent chapters.

The *total torque* T experienced by D with respect to the pivot point $\boldsymbol{c} \in \mathbb{R}^d$ (and axis $\boldsymbol{a} \in \mathbb{R}^3$, $\|\boldsymbol{a}\| = 1$, for $d = 3$) is given by

$$T = \begin{cases} \dfrac{d\mathcal{E}_F}{d\Omega}(\Omega^0, \{\boldsymbol{x} \mapsto (\boldsymbol{x} - \boldsymbol{c})^\perp\}) & \text{for} \quad d = 2 \, , \\[3mm] \dfrac{d\mathcal{E}_F}{d\Omega}(\Omega^0, \{\boldsymbol{x} \mapsto \boldsymbol{a} \times (\boldsymbol{x} - \boldsymbol{c})\}) & \text{for} \quad d = 3 \, , \end{cases} \tag{3.0.6}$$

with $\perp$ indicating an anti-clockwise plane rotation by $\pi/2$ and $\times$ denoting the vector product.

The energy functionals we will work with will have a dependence on the domain Ω which manifests itself in two ways: through integrals defined on the domain Ω or its boundary Γ, and through the solution of a variational problem which also depends on the domain or its boundary. The field energy functional will be $\mathcal{E}_F = \mathcal{E}_F(\Omega; u(\Omega))$ which expresses this dependence. For computing the shape derivative of such a functional, we will resort to the adjoint method, the details of which will be elaborated in the subsequent chapters.

3.0.3 Shape Transformations and Derivatives

To compute shape derivatives with a variational constraint, we will always try to formulate the problem for a deformed configuration, obtained using the perturbation map, using an equivalent formulation on the reference configuration. The procedure to accomplish this consists of two steps: transformation of the integrals in the variational formulation to the reference configuration using the perturbation map (3.0.1) and in the second step, pulling back functions to the reference configuration. In this sub-section we will mention the important transformation rules that we will need and the associated derivatives that will occur in the computations.

For transforming the integrals in the variational formulations, we will mainly use the following two formulas for transformation of volume and boundary based integrals. Let $\Omega^0 \subset \mathbb{R}^d$ be a bounded Lipschitz domain and $\Gamma^0 := \partial \Omega^0$ be its boundary. Let $\Omega^s := \mathbf{T}_s^{\boldsymbol{\nu}}(\Omega^0)$ and $\Gamma^s := \mathbf{T}_s^{\boldsymbol{\nu}}(\Gamma^0)$, then for $f \in L^1(\Gamma^s)$ and $F \in L^1(\Omega^s)$ we have the identities [18, Ch. 9, Sec. 4.2, eq. 4.9], [57, Sect. 2.17]

$$\int_{\Gamma^s} f(\boldsymbol{x}) \, d\mathrm{S}_{\boldsymbol{x}} = \int_{\Gamma^0} f(\mathbf{T}_s^{\boldsymbol{\nu}}(\hat{\boldsymbol{x}})) \, \omega_s(\hat{\boldsymbol{x}}) \, d\mathrm{S}_{\hat{\boldsymbol{x}}}, \tag{3.0.7}$$

$$\int_{\Omega^s} F(\boldsymbol{x}) \, d\boldsymbol{x} = \int_{\Omega^0} F(\mathbf{T}_s^{\boldsymbol{\nu}}(\hat{\boldsymbol{x}})) \, |\det \mathsf{D}\mathbf{T}_s^{\boldsymbol{\nu}}(\hat{\boldsymbol{x}})| \, d\hat{\boldsymbol{x}}, \tag{3.0.8}$$

where $\mathsf{D}\mathbf{T}_s^{\boldsymbol{\nu}}$ is the Jacobian matrix of the transformation and

$$\omega_s(\hat{\boldsymbol{x}}) := \|\mathbf{C}(\mathsf{D}\mathbf{T}_s^{\boldsymbol{\nu}}(\hat{\boldsymbol{x}})) \, \hat{\mathbf{n}}(\hat{\boldsymbol{x}})\|, \tag{3.0.9}$$

where $\mathbf{C}(\mathsf{D}\mathbf{T}_s^{\boldsymbol{\nu}})$ is the cofactor matrix of $\mathsf{D}\mathbf{T}_s^{\boldsymbol{\nu}}$ and $\hat{\mathbf{n}}$ is the unit normal vector field on the reference boundary Γ^0. In our computations, we will also require the transformation rule for the unit normal vector field. Denoting the normal on Γ^s by $\mathbf{n}$, we have the identity [18, Ch. 9, Thm. 4.4]

$$\mathbf{n}(\boldsymbol{x}) = \frac{\mathbf{C}(\mathsf{D}\mathbf{T}_s^{\boldsymbol{\nu}}(\hat{\boldsymbol{x}})) \, \hat{\mathbf{n}}(\hat{\boldsymbol{x}})}{\omega_s(\hat{\boldsymbol{x}})} = \frac{\mathbf{C}(\mathsf{D}\mathbf{T}_s^{\boldsymbol{\nu}}(\hat{\boldsymbol{x}})) \, \hat{\mathbf{n}}(\hat{\boldsymbol{x}})}{\|\mathbf{C}(\mathsf{D}\mathbf{T}_s^{\boldsymbol{\nu}}(\hat{\boldsymbol{x}})) \, \hat{\mathbf{n}}(\hat{\boldsymbol{x}})\|}. \tag{3.0.10}$$

In the computation of shape derivatives, we will encounter derivatives of certain quantities which we will mention next. These partial derivatives can be obtained using the definition of $\mathbf{T}_s^{\boldsymbol{\nu}}$ and the formulas in [57, Sect. 2.13]

$$\frac{d(\mathsf{D}\mathbf{T}_s^{\boldsymbol{\nu}})}{ds}\bigg|_{s=0} = \mathsf{D}\boldsymbol{\mathcal{V}}, \quad \frac{d\det(\mathsf{D}\mathbf{T}_s^{\boldsymbol{\nu}})}{ds}\bigg|_{s=0} = \boldsymbol{\nabla} \cdot \boldsymbol{\mathcal{V}}, \quad \frac{d(f \circ \mathbf{T}_s^{\boldsymbol{\nu}})}{ds}\bigg|_{s=0} = \nabla f \cdot \boldsymbol{\mathcal{V}}, \quad (3.0.11)$$

$$\frac{d(\mathsf{D}\mathbf{T}_s^{\boldsymbol{\nu}})^{-1}}{ds}\bigg|_{s=0} = -(\mathsf{D}\mathbf{T}_s^{\boldsymbol{\nu}})^{-1} \frac{d\,\mathsf{D}\mathbf{T}_s^{\boldsymbol{\nu}}}{ds} (\mathsf{D}\mathbf{T}_s^{\boldsymbol{\nu}})^{-1}\bigg|_{s=0} = -\mathbf{I}_d \, \mathsf{D}\boldsymbol{\mathcal{V}} \, \mathbf{I}_d = -\mathsf{D}\boldsymbol{\mathcal{V}}, \quad (3.0.12)$$

$$\frac{d\mathbf{C}(\mathsf{D}\mathbf{T}_s^{\boldsymbol{\nu}})}{ds}\bigg|_{s=0} = \frac{d\left(\det \mathsf{D}\mathbf{T}_s^{\boldsymbol{\nu}} (\mathsf{D}\mathbf{T}_s^{\boldsymbol{\nu}})^{-\top}\right)}{ds}\bigg|_{s=0} = (\boldsymbol{\nabla} \cdot \boldsymbol{\mathcal{V}}) \, \mathbf{I}_d - (\mathsf{D}\boldsymbol{\mathcal{V}})^{\top}, \quad (3.0.13)$$

$$\frac{d\omega_s}{ds}\bigg|_{s=0} = \frac{d\|\mathbf{C}(\mathsf{D}\mathbf{T}_s^{\boldsymbol{\nu}})\hat{\mathbf{n}}\|}{ds}\bigg|_{s=0} = \hat{\mathbf{n}} \cdot (\boldsymbol{\nabla} \cdot \boldsymbol{\mathcal{V}} \hat{\mathbf{n}} - (\mathsf{D}\boldsymbol{\mathcal{V}})^{\top}\hat{\mathbf{n}}) = \boldsymbol{\nabla} \cdot \boldsymbol{\mathcal{V}} - \hat{\mathbf{n}}^{\top} \mathsf{D}\boldsymbol{\mathcal{V}}^{\top} \hat{\mathbf{n}}. \tag{3.0.14}$$

3.0.4 Pullbacks

After transforming the integrals to the reference configuration, the integrands still contain functions on the deformed configuration. We need appropriate pullbacks to equivalently express the integrals in terms of functions on the reference configuration and get an equivalent formulation. The tools for accomplishing this can be borrowed from Differential Geometry. Here we simply mention the pullbacks we will require and refer the reader to [5, 32, 35] for more details.

3.0.4.1 0-Form

Let $u : \Omega^s \to \mathbb{R}$ be the vector proxy of a 0-form and its pullback (vector proxy) be denoted by $\hat{u} : \Omega^0 \to \mathbb{R}$ which satisfies the relation [35, Table 2]

$$u(\mathbf{T}^{\boldsymbol{\nu}}_s(\hat{\boldsymbol{x}})) = \hat{u}(\hat{\boldsymbol{x}}). \tag{3.0.15}$$

Its gradient (exterior derivative) is a 1-form for which we have the pullback relation [35, Table 2]

$$\nabla u(\mathbf{T}^{\boldsymbol{\nu}}_s(\hat{\boldsymbol{x}})) = \mathsf{D}\mathbf{T}^{\boldsymbol{\nu}}_s(\hat{\boldsymbol{x}})^{-T}\,\nabla \hat{u}(\hat{\boldsymbol{x}}). \tag{3.0.16}$$

The restriction of u to the boundary is still a 0-form [35, Section 2.2.3]. Let $g := \gamma_D u$, $\psi := \gamma_N u$ be the Dirichlet and Neumann boundary data associated with it respectively. Denoting their pullbacks by $\hat{g} : \Gamma^0 \to \mathbb{R}$, $\hat{\psi} : \Gamma^0 \to \mathbb{R}$ we have the relations

$$g(\mathbf{T}^{\boldsymbol{\nu}}_s(\hat{\boldsymbol{x}})) = \hat{g}(\hat{\boldsymbol{x}}), \quad \psi(\mathbf{T}^{\boldsymbol{\nu}}_s(\hat{\boldsymbol{x}})) = \frac{\hat{\psi}(\hat{\boldsymbol{x}})}{\omega_s(\hat{\boldsymbol{x}})}. \tag{3.0.17}$$

The above relations are obtained by using the fact that pullback and trace commute with each other [32, Section 2.2]. So the pullback for the trace of a 0 form is the trace of the pullback, that is $\hat{g} = \gamma_D \hat{u}$. The Neumann trace is a 2-form which becomes clear when we look at its more general definition $(\boldsymbol{\epsilon}\nabla u) \cdot \mathbf{n}$, where $\boldsymbol{\epsilon}$ is a symmetric positive definite tensor. In the formalism of differential geometry, it is called a Hodge operator [35, Section 2.4.3]. We will see an explaination for the pullback shown above when discussing 2 forms.

We will also encounter $\mathbf{curl}_\Gamma\, u$ when working with the hypersingular operator associated with the Laplace BIE. Writing $\mathbf{curl}_\Gamma\, u = \nabla u \times \mathbf{n}$ and using the individual transformation rules, we get

$$\nabla u(\mathbf{T}^{\boldsymbol{\nu}}_s(\hat{\boldsymbol{x}})) \times \mathbf{n}(\mathbf{T}^{\boldsymbol{\nu}}_s(\hat{\boldsymbol{x}})) = \left(\mathsf{D}\mathbf{T}^{\boldsymbol{\nu}}_s(\hat{\boldsymbol{x}})^{-T}\nabla \hat{u}(\hat{\boldsymbol{x}})\right) \times \left(\frac{\det \mathsf{D}\mathbf{T}^{\boldsymbol{\nu}}_s(\hat{\boldsymbol{x}})\, \mathsf{D}\mathbf{T}^{\boldsymbol{\nu}}_s(\hat{\boldsymbol{x}})^{-T}\, \hat{\mathbf{n}}(\hat{\boldsymbol{x}})}{\omega_s(\hat{\boldsymbol{x}})}\right) \tag{3.0.18}$$

$$= \frac{\mathsf{D}\mathbf{T}^{\boldsymbol{\nu}}_s(\hat{\boldsymbol{x}})\left(\nabla \hat{u}(\hat{\boldsymbol{x}}) \times \hat{\mathbf{n}}(\hat{\boldsymbol{x}})\right)}{\omega_s(\hat{\boldsymbol{x}})}, \tag{3.0.19}$$

where we used the identity $(\mathbf{M}\mathbf{a})\times(\mathbf{M}\mathbf{b}) = \det(\mathbf{M})\mathbf{M}^{-T}(\mathbf{a}\times\mathbf{b})$ for a regular matrix $\mathbf{M} \in \mathbb{R}^{3,3}$ and $\mathbf{a}, \mathbf{b} \in \mathbb{R}^3$. In the manipulations above, $\mathbf{n}$ and $\hat{\mathbf{n}}$ denote the normals on Γ^s and Γ^0 respectively. Thus we have the relation

$$\mathbf{curl}_\Gamma\, u(\mathbf{T}^{\boldsymbol{\nu}}_s(\hat{\boldsymbol{x}})) = \frac{\mathsf{D}\mathbf{T}^{\boldsymbol{\nu}}_s(\hat{\boldsymbol{x}})}{\omega_s(\hat{\boldsymbol{x}})}\, \mathbf{curl}_\Gamma\, \hat{u}(\hat{\boldsymbol{x}}). \tag{3.0.20}$$

3.0.4.2   1-Form

Fixing $d = 3$, let $\mathbf{A} : \Omega^s \to \mathbb{R}^3$ be the vector proxy of a 1-form. Its pullback (vector proxy) is denoted as $\hat{\mathbf{A}} : \Omega^0 \to \mathbb{R}$ and satisfies the relation [35, Table 2]

$$\mathbf{A}(\mathbf{T}_s^{\boldsymbol{\nu}}(\hat{\boldsymbol{x}})) = D\mathbf{T}_s^{\boldsymbol{\nu}}(\hat{\boldsymbol{x}})^{-T}\, \hat{\mathbf{A}}(\hat{\boldsymbol{x}}). \tag{3.0.21}$$

We know that $\mathbf{curlA}$ (exterior derivative) is a 2-form. Using the fact that exterior derivative and pullback commute [32, Equation 2.13], we can use the pullback of 2 forms [35, Table 2] to get the relation

$$\mathbf{curlA}(\mathbf{T}_s^{\boldsymbol{\nu}}(\hat{\boldsymbol{x}})) = \frac{1}{\det D\mathbf{T}_s^{\boldsymbol{\nu}}(\hat{\boldsymbol{x}})} D\mathbf{T}_s^{\boldsymbol{\nu}}(\hat{\boldsymbol{x}})\, \mathbf{curl\hat{A}}(\hat{\boldsymbol{x}}). \tag{3.0.22}$$

The vector potential (1-form) will be encountered in curl curl type problems. Let the associated tangential trace $\mathbf{n} \times (\mathbf{A} \times \mathbf{n})$ and magnetic trace $\mathbf{curlA} \times \mathbf{n}$ be denoted as $\mathbf{g} : \Gamma^s \to \mathbb{R}^3$, $\boldsymbol{\psi} : \Gamma^s \to \mathbb{R}^3$ respectively. Let their pullbacks be denoted as $\hat{\mathbf{g}} : \Gamma^0 \to \mathbb{R}^3$, $\hat{\boldsymbol{\psi}} : \Gamma^0 \to \mathbb{R}^3$. They satisfy the relations

$$\boldsymbol{\psi}(\mathbf{T}_s^{\boldsymbol{\nu}}(\hat{\boldsymbol{x}})) = \frac{D\mathbf{T}_s^{\boldsymbol{\nu}}(\hat{\boldsymbol{x}})}{\omega_s(\hat{\boldsymbol{x}})}\, \hat{\boldsymbol{\psi}}(\hat{\boldsymbol{x}}), \tag{3.0.23}$$

$$\mathbf{g}(\mathbf{T}_s^{\boldsymbol{\nu}}(\hat{\boldsymbol{x}})) = D\mathbf{T}_s^{\boldsymbol{\nu}}(\hat{\boldsymbol{x}})^{-T}\, \hat{\mathbf{g}}(\hat{\boldsymbol{x}}). \tag{3.0.24}$$

For the pullback of the tangential trace, we again used the commutative property of the trace and pullback [32, Section 2.2]. We can find the pullback of the magnetic trace by preserving the inner product of the two traces

$$\int_{\Gamma^s} \boldsymbol{\psi}(\boldsymbol{x}) \cdot \mathbf{g}(\boldsymbol{x})\, d\mathrm{S}_{\boldsymbol{x}} = \int_{\Gamma^0} \hat{\boldsymbol{\psi}}(\hat{\boldsymbol{x}}) \cdot \hat{\mathbf{g}}(\hat{\boldsymbol{x}})\, d\mathrm{S}_{\hat{\boldsymbol{x}}}. \tag{3.0.25}$$

In the BIE formulation we will encounter $\mathrm{curl}_\Gamma\, \mathbf{g}$, which is the scalar surface curl. It can be written as $\mathbf{curl}_\Gamma\, \mathbf{g} = \mathbf{curlA} \cdot \mathbf{n}$, which allows us to obtain the pullback after plugging in the pullbacks for individual terms.

$$\mathbf{curlA}(\mathbf{T}_s^{\boldsymbol{\nu}}(\hat{\boldsymbol{x}})) \cdot \mathbf{n}(\mathbf{T}_s^{\boldsymbol{\nu}}(\hat{\boldsymbol{x}})) = \left(\frac{1}{\det D\mathbf{T}_s^{\boldsymbol{\nu}}(\hat{\boldsymbol{x}})} D\mathbf{T}_s^{\boldsymbol{\nu}}(\hat{\boldsymbol{x}})\, \mathbf{curl\hat{A}}(\hat{\boldsymbol{x}}) \right) \cdot \left(\frac{\det D\mathbf{T}_s^{\boldsymbol{\nu}}(\boldsymbol{x})\, D\mathbf{T}_s^{\boldsymbol{\nu}}(\hat{\boldsymbol{x}})^{-T}\, \hat{\mathbf{n}}(\hat{\boldsymbol{x}})}{\omega_s(\hat{\boldsymbol{x}})} \right)$$

$$= \frac{\mathbf{curl\hat{A}}(\hat{\boldsymbol{x}}) \cdot \hat{\mathbf{n}}(\hat{\boldsymbol{x}})}{\omega_s(\hat{\boldsymbol{x}})}.$$

Thus we get the pullback relation

$$\mathrm{curl}_\Gamma\, \mathbf{g}(\mathbf{T}_s^{\boldsymbol{\nu}}(\hat{\boldsymbol{x}})) = \frac{\mathrm{curl}_\Gamma\, \hat{\mathbf{g}}(\hat{\boldsymbol{x}})}{\omega_s(\hat{\boldsymbol{x}})}.$$

3.0.4.3   2-Form

For $d = 3$, let $\mathbf{B} : \Omega^s \to \mathbb{R}^3$ be the vector proxy of a 2-form. Its vector proxy pullback, denoted by $\hat{\mathbf{B}} : \Omega^0 \to \mathbb{R}^3$ satisfies the relation [35, Table 2]

$$\mathbf{B}(\mathbf{T}_s^{\boldsymbol{\nu}}(\hat{\boldsymbol{x}})) = \frac{D\mathbf{T}_s^{\boldsymbol{\nu}}(\hat{\boldsymbol{x}})}{\det D\mathbf{T}_s^{\boldsymbol{\nu}}(\hat{\boldsymbol{x}})}\, \hat{\mathbf{B}}(\hat{\boldsymbol{x}}). \tag{3.0.26}$$

22

Let us denote $\operatorname{div}\mathbf{B}$ by $\rho : \Omega^s \to \mathbb{R}$ which is the exterior derivative of a 2-form. Let its pullback be denoted as $\hat{\rho} : \Omega^0 \to \mathbb{R}$. It satisfies the relation [35, Table 2]

$$\rho(\mathbf{T}_s^{\boldsymbol{\nu}}(\hat{\boldsymbol{x}})) = \frac{\hat{\rho}(\hat{\boldsymbol{x}})}{\det \mathsf{D}\mathbf{T}_s^{\nu}(\hat{\boldsymbol{x}})}. \tag{3.0.27}$$

Let the associated normal trace $\mathbf{B} \cdot \mathbf{n}$ be denoted as $\lambda : \Gamma^s \to \mathbb{R}$. Its pullback $\hat{\lambda} : \Gamma^0 \to \mathbb{R}$ can be obtained by plugging in the individual pullbacks

$$\begin{aligned}
\mathbf{B}(\mathbf{T}_s^{\boldsymbol{\nu}}(\hat{\boldsymbol{x}})) \cdot \mathbf{n}(\mathbf{T}_s^{\boldsymbol{\nu}}(\hat{\boldsymbol{x}})) &= \left(\frac{\mathsf{D}\mathbf{T}_s^{\boldsymbol{\nu}}(\hat{\boldsymbol{x}})}{\det \mathsf{D}\mathbf{T}_s^{\nu}(\hat{\boldsymbol{x}})} \, \hat{\mathbf{B}}(\hat{\boldsymbol{x}}) \right) \cdot \left(\frac{\det \mathsf{D}\mathbf{T}_s^{\boldsymbol{\nu}}(\hat{\boldsymbol{x}}) \, \mathsf{D}\mathbf{T}_s^{\boldsymbol{\nu}}(\hat{\boldsymbol{x}})^{-T} \, \hat{\mathbf{n}}(\hat{\boldsymbol{x}})}{\omega_s(\hat{\boldsymbol{x}})} \right) \\
&= \frac{\hat{\mathbf{B}}(\hat{\boldsymbol{x}}) \cdot \hat{\mathbf{n}}(\hat{\boldsymbol{x}})}{\omega_s(\hat{\boldsymbol{x}})}.
\end{aligned}$$

Thus we get

$$\lambda(\mathbf{T}_s^{\boldsymbol{\nu}}(\hat{\boldsymbol{x}})) = \frac{\hat{\lambda}(\hat{\boldsymbol{x}})}{\omega_s(\hat{\boldsymbol{x}})}. \tag{3.0.28}$$

The expression above is precisely the pullback we used for the Neumann trace in (3.0.17)

Chapter 4

Energy Shape Derivatives for Electrostatic Models

In this chapter we look at the field energy shape derivatives for different electrostatic models. All the shape derivative expressions are derived using a common framework: we start from either a BIE based or a volume based variational formulation, construct a perturbed formulation using the perturbation map 3.0.1 and then compute the energy shape derivative using pullbacks and the adjoint method. We will see that the final expressions obtained from the volume based variational formulation yield the known classical formulas that are related to the Maxwell Stress Tensor (MST). However, the BIE based formulations would yield novel expressions that are better behaved when evaluated numerically.

4.1 Dirichlet Boundary Value Problem

The contents of this section are reproduced from [48]. A solid conducting object filling the bounded open connected domain $D \subset \mathbb{R}^d$, $d = 2, 3$, with C_{pw}^2 boundary, is embedded in a non-conducting homogeneous isotropic dielectric medium. Both together occupy a larger bounded open domain $B \subset \mathbb{R}^d$ with C_{pw}^2 boundary, $\overline{D} \subset B$, which represents the geometry of a container with metal walls.

A potential difference U is imposed between the object and the metal box by a voltage source, see Figure 4.1. For $d = 3$ this arrangement represents a realistic laboratory setup, for $d = 2$ it is to be read as a cross-section description of a situation with translational symmetry. We use the short notations $\Omega := B \setminus \overline{D}$ for the "field domain", $\Gamma := \partial D$ for the boundary of the object, and assume that Γ is connected.
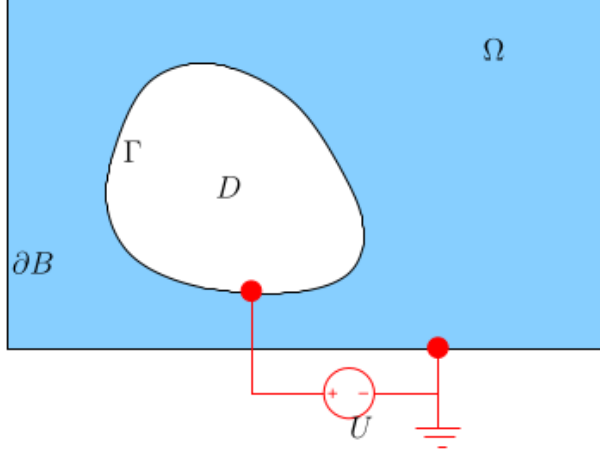
Figure 4.1: Geometric setting for model problem

The (non-dimensional, rescaled) electrostatic scalar potential $u : \Omega \to \mathbb{R}$ can be obtained as the unique weak solution in $H^1(\Omega)$ of the linear elliptic boundary value problem

$$\Delta u = 0 \quad \text{in} \quad \Omega, \quad u = g \quad \text{on} \quad \partial\Omega . \tag{4.1.1}$$

The physical setting of Figure 4.1 corresponds to constant Dirichlet data on the boundaries Γ and ∂B, that is $g|_\Gamma \equiv U$ and $g|_{\partial B} \equiv 0$, but we prefer to admit general $g \in H^{\frac{1}{2}}(\partial\Omega)$ at this point.

The field energy we consider for shape differentiation is

$$\mathcal{E}_F := \frac{1}{2} \int_\Omega \|\nabla u(\boldsymbol{x})\|^2 \ d\boldsymbol{x} = \frac{1}{2} \int_{\partial\Omega} g \, \nabla u \cdot \mathbf{n} \ d\mathrm{S}. \tag{4.1.2}$$

Integration limit of Ω in the above expression instead of the usual $\mathbb{R}^d$ can be justified if we consider deformations that do not affect the boundary ∂B of metal box. This is because due to Dirichlet shielding, the field energy outisde will not change and consequently not affect the shape derivative.

4.1.1 Variational Boundary Integral Equations

From [54, Section 2.9.2.1], [43, Thm. 7.5] we learn that the unknown co-normal/Neumann trace $\psi := \nabla u \cdot \boldsymbol{n}|_{\partial\Omega}$ of the solution of Equation (4.1.1) can be recovered as the solution of the following first-kind boundary integral equation

$$\psi \in H^{-\frac{1}{2}}(\partial\Omega) : \quad \mathsf{a}_V(\psi, \varphi) = \tfrac{1}{2}\ell_g(\varphi) + \mathsf{b}_K(g, \varphi) \quad \forall \varphi \in H^{-\frac{1}{2}}(\partial\Omega) , \tag{4.1.3}$$

with

$$\mathsf{a}_V(\psi, \varphi) := \int_{\partial\Omega} \int_{\partial\Omega} G(\boldsymbol{x}, \boldsymbol{y}) \, \psi(\boldsymbol{y}) \, \varphi(\boldsymbol{x}) \, d\mathrm{S}(\boldsymbol{y}) d\mathrm{S}(\boldsymbol{x}) ,$$

$$\mathsf{b}_K(g, \varphi) := \int_{\partial\Omega} \int_{\partial\Omega} \nabla_{\boldsymbol{y}} G(\boldsymbol{x}, \boldsymbol{y}) \cdot \boldsymbol{n}(\boldsymbol{y}) \, g(\boldsymbol{y}) \, \varphi(\boldsymbol{x}) \, d\mathrm{S}(\boldsymbol{y}) d\mathrm{S}(\boldsymbol{x}) , \tag{4.1.4}$$

$$\ell_g(\varphi) := \int_{\partial\Omega} g(\boldsymbol{x}) \, \varphi(\boldsymbol{x}) \, d\mathrm{S}(\boldsymbol{x}) ,$$

and the fundamental solutions $G : \{(\boldsymbol{x}, \boldsymbol{y}) \in \mathbb{R}^d \times \mathbb{R}^d, \; \boldsymbol{x} \neq \boldsymbol{y}\} \to \mathbb{R}$

$$G(\boldsymbol{x}, \boldsymbol{y}) := -\frac{1}{2\pi} \log(||\boldsymbol{x} - \boldsymbol{y}||) \quad \text{for } d = 2 \quad , \quad G(\boldsymbol{x}, \boldsymbol{y}) := \frac{1}{4\pi ||\boldsymbol{x} - \boldsymbol{y}||} \quad \text{for } d = 3 \; .$$

Existence and uniqueness of the solution of (4.1.3) follows from the $H^{-\frac{1}{2}}(\partial\Omega)$-ellipticity of a_V [54, Theorem 3.5.3], ensured after a suitable rescaling for $d = 2$.

4.1.2 Variational Formulation on Deformed Domain

We consider the Dirichlet boundary value problem Equation (4.1.1) for the 1-parameter family of domains $(\Omega^s := \mathbf{T}_s^{\boldsymbol{\nu}}(\Omega^0))$ induced by the perturbation map (3.0.1). To make the notation simpler, we will skip the sub/super-script for quantities in the reference configuration, that is $s = 0$. The velocity field inducing deformations is compactly supported in the metallic box, that is $\boldsymbol{\mathcal{V}} \in (C_0^\infty(B))^d$. In the deformed configuration, we impose Dirichlet boundary conditions via the restriction of $\widetilde{g} \in H_0^1(B)$ to the boundary $\partial\Omega^s$, that is $g = \tilde{g}|_{\partial\Omega^s} \in H^{\frac{1}{2}}(\partial\Omega^s)$. The variational formulation for this deformed s-configuration carries the exact same structure as Equation (4.1.4), and to account for the dependence on the scalar parameter s, we augment the notation.

$$\psi_s \in H^{-\frac{1}{2}}(\partial\Omega^s) : \quad \mathsf{a}_V(s)(\psi_s, \varphi) = \tfrac{1}{2}\ell_g(s)(\varphi) + \mathsf{b}_K(s)(g, \varphi) \quad \forall \varphi \in H^{-\frac{1}{2}}(\partial\Omega^s), \qquad (4.1.5)$$

where the (bi)linear forms $\mathsf{a}_V(s), \mathsf{b}_K(s), l_g(s)$ denote that the integration is over $\partial\Omega^s$. Field energy for the deformed s-configuration is given as:

$$\mathcal{E}_F(s) := \tfrac{1}{2} \int_{\partial\Omega^s} g \, \psi_s \, d\mathrm{S}. \qquad (4.1.6)$$

4.1.3 Equivalent Formulation on Reference Domain

To achieve an equivalent formulation to (4.1.5) on the reference boundary, we start by transforming the surface integrals using identities from Section 3.0.3. The building blocks of (4.1.5) can be written by means of integrals over $\partial\Omega$:

$$\mathsf{a}_V(s)(\psi, \varphi) = \int_{\partial\Omega} \int_{\partial\Omega} G(\mathbf{T}_s^{\boldsymbol{\nu}}(\hat{\boldsymbol{x}}), \mathbf{T}_s^{\boldsymbol{\nu}}(\hat{\boldsymbol{y}})) \, \psi(\mathbf{T}_s^{\boldsymbol{\nu}}(\hat{\boldsymbol{y}})) \, \varphi(\mathbf{T}_s^{\boldsymbol{\nu}}(\hat{\boldsymbol{x}})) \, \omega_s(\hat{\boldsymbol{y}}) \, \omega_s(\hat{\boldsymbol{x}}) \, d\mathrm{S}(\hat{\boldsymbol{y}}) d\mathrm{S}(\hat{\boldsymbol{x}}) \; ,$$

$$\mathsf{b}_K(s)(g, \varphi) = \int_{\partial\Omega} \int_{\partial\Omega} \{\nabla_{\boldsymbol{y}} G(\mathbf{T}_s^{\boldsymbol{\nu}}(\hat{\boldsymbol{x}}), \mathbf{T}_s^{\boldsymbol{\nu}}(\hat{\boldsymbol{y}})) \cdot \mathbf{C}(\mathrm{D}\mathbf{T}_s^{\boldsymbol{\nu}}(\hat{\boldsymbol{y}})) \boldsymbol{n}(\hat{\boldsymbol{y}})\} \cdot$$
$$g(\mathbf{T}_s^{\boldsymbol{\nu}}(\hat{\boldsymbol{y}})) \, \varphi(\mathbf{T}_s^{\boldsymbol{\nu}}(\hat{\boldsymbol{x}})) \, \omega_s(\hat{\boldsymbol{x}}) \, d\mathrm{S}(\hat{\boldsymbol{y}}) d\mathrm{S}(\hat{\boldsymbol{x}}) \; ,$$

$$\ell_g(s)(\varphi) = \int_{\partial\Omega} g(\mathbf{T}_s^{\boldsymbol{\nu}}(\hat{\boldsymbol{x}})) \, \varphi(\mathbf{T}_s^{\boldsymbol{\nu}}(\hat{\boldsymbol{x}})) \, \omega_s(\hat{\boldsymbol{x}}) \, d\mathrm{S}(\hat{\boldsymbol{x}}) \; ,$$

and the expression for the energy becomes

$$\mathcal{E}_F(s) = \tfrac{1}{2} \int_\Gamma \psi_s(\mathbf{T}_s^{\boldsymbol{\nu}}(\hat{\boldsymbol{x}})) \, g(\mathbf{T}_s^{\boldsymbol{\nu}}(\hat{\boldsymbol{x}})) \, \omega_s(\hat{\boldsymbol{x}}) \, d\mathrm{S}(\hat{\boldsymbol{x}}) \; .$$

Since the nature of ψ_s is that of a surface charge density, we pull back ψ_s to the space $H^{-\frac{1}{2}}(\partial\Omega)$ using the pullback of surface densities (3.0.17)

$$\hat{\varphi}(\hat{\boldsymbol{x}}) := \varphi(\mathbf{T}^{\boldsymbol{\nu}}_s(\hat{\boldsymbol{x}}))\,\omega_s(\hat{\boldsymbol{x}})\,, \quad \hat{\boldsymbol{x}} \in \partial\Omega\,, \quad \varphi \in H^{-\frac{1}{2}}(\partial\Omega^s)\,. \tag{4.1.7}$$

Thus, we find that $\hat{\psi}_s$ satisfies the transformed variational boundary integral equation

$$\hat{\psi}_s \in H^{-\frac{1}{2}}(\partial\Omega): \quad \hat{\mathsf{a}}_V(s; \hat{\psi}_s, \hat{\varphi}) = \tfrac{1}{2}\hat{\ell}_{\widetilde{g}}(s; \hat{\varphi}) + \hat{\mathsf{b}}_K(s; \widetilde{g}, \varphi) \quad \forall \hat{\varphi} \in H^{-\frac{1}{2}}(\partial\Omega)\,, \tag{4.1.8}$$

with the abbreviations $(\hat{\sigma}, \hat{\varphi} \in H^{-\frac{1}{2}}(\partial\Omega))$

$$\hat{\mathsf{a}}_V(s; \hat{\sigma}, \hat{\varphi}) := \int_{\partial\Omega}\int_{\partial\Omega} G(\mathbf{T}^{\boldsymbol{\nu}}_s(\hat{\boldsymbol{x}}), \mathbf{T}^{\boldsymbol{\nu}}_s(\hat{\boldsymbol{y}}))\,\hat{\sigma}(\hat{\boldsymbol{y}})\,\hat{\varphi}(\hat{\boldsymbol{x}})\,dS(\hat{\boldsymbol{y}})dS(\hat{\boldsymbol{x}})\,, \tag{4.1.9a}$$

$$\hat{\mathsf{b}}_K(s; \widetilde{g}, \hat{\varphi}) := \int_{\partial\Omega}\int_{\partial\Omega} \{\nabla_{\boldsymbol{y}}G(\mathbf{T}^{\boldsymbol{\nu}}_s(\hat{\boldsymbol{x}}), \mathbf{T}^{\boldsymbol{\nu}}_s(\hat{\boldsymbol{y}})) \cdot \mathbf{C}(D\mathbf{T}^{\boldsymbol{\nu}}_s(\hat{\boldsymbol{y}}))\boldsymbol{n}(\hat{\boldsymbol{y}})\} \cdot \tag{4.1.9b}$$
$$\widetilde{g}(\mathbf{T}^{\boldsymbol{\nu}}_s(\hat{\boldsymbol{y}}))\,\hat{\varphi}(\hat{\boldsymbol{x}})\,dS(\hat{\boldsymbol{y}})dS(\hat{\boldsymbol{x}})\,,$$

$$\hat{\ell}_{\widetilde{g}}(s; \hat{\varphi}) := \int_{\partial\Omega} \widetilde{g}(\mathbf{T}^{\boldsymbol{\nu}}_s(\hat{\boldsymbol{x}}))\,\hat{\varphi}(\hat{\boldsymbol{x}})\,dS(\hat{\boldsymbol{x}})\,. \tag{4.1.9c}$$

The field energy can be written in terms of the pulled back Neumann trace solution $\hat{\psi}_s$

$$\hat{\mathcal{E}}_F(\boldsymbol{\mathcal{V}}; s) = \tfrac{1}{2}\int_{\Gamma} \hat{\psi}_s(\hat{\boldsymbol{x}})\,\widetilde{g}(\mathbf{T}^{\boldsymbol{\nu}}_s(\hat{\boldsymbol{x}}))\,dS(\hat{\boldsymbol{x}})\,. \tag{4.1.10}$$

4.1.4 BIE-Constrained Shape Derivative

In order to compute the shape derivative $\frac{d\mathcal{E}_F}{d\Omega}(\Omega; \boldsymbol{\mathcal{V}}) = \frac{d\hat{\mathcal{E}}_F}{ds}(\boldsymbol{\mathcal{V}}; 0)$ for $s \mapsto \hat{\mathcal{E}}_F(\boldsymbol{\mathcal{V}}; s)$ from (4.1.10) with $s \mapsto \hat{\psi}_s$ defined through the linear variational equation (4.1.8) we resort to the well-established adjoint approach [31, Sect. 1.6.4]. The relevant Lagrangian is given by

$$L(s; \hat{\sigma}, \hat{\varphi}) := \tfrac{1}{2}\hat{\ell}_{\widetilde{g}}(s; \hat{\sigma}) + \hat{\mathsf{a}}_V(s; \hat{\sigma}, \hat{\varphi}) - \tfrac{1}{2}\hat{\ell}_{\widetilde{g}}(s; \hat{\varphi}) - \hat{\mathsf{b}}_K(s; \widetilde{g}, \hat{\varphi})\,, \quad \hat{\sigma}, \hat{\varphi} \in H^{-\frac{1}{2}}(\partial\Omega)\,, \tag{4.1.11}$$

and, writing $\hat{\psi}_s$ for the solution of (4.1.8), it permits us to express $\hat{\mathcal{E}}_F(\boldsymbol{\mathcal{V}}; s)$ as

$$\hat{\mathcal{E}}_F(\boldsymbol{\mathcal{V}}; s) = L(s; \hat{\psi}_s, \hat{\varphi}) \quad \forall \hat{\varphi} \in H^{-\frac{1}{2}}(\partial\Omega)\,. \tag{4.1.12}$$

We exploit the freedom of being able to insert any $\hat{\varphi} \in H^{-\frac{1}{2}}(\partial\Omega)$ into (4.1.12) and choose it as the solution ρ of the *adjoint variational problem*: seek $\rho \in H^{-\frac{1}{2}}(\partial\Omega)$ such that

$$\hat{\mathsf{a}}_V(0; \hat{\varphi}, \rho) = -\tfrac{1}{2}\left\langle \frac{\partial\hat{\ell}_{\widetilde{g}}}{\partial\hat{\sigma}}(0; \hat{\psi}_0), \hat{\varphi} \right\rangle \quad \forall \hat{\varphi} \in H^{-\frac{1}{2}}(\partial\Omega)$$

$$\Leftrightarrow \qquad \hat{\mathsf{a}}_V(0; \varphi, \rho) = -\frac{1}{2}\int_{\Gamma} \varphi(\hat{\boldsymbol{x}})\,g(\hat{\boldsymbol{x}})\,dS(\hat{\boldsymbol{x}}) \quad \forall \varphi \in H^{-\frac{1}{2}}(\partial\Omega)\,. \tag{4.1.13}$$

Noting that $\hat{\psi}_0 = \psi$, ψ the solution of the BIE (4.1.3), this yields the formula

$$\frac{d\hat{\mathcal{E}}_F}{ds}(\boldsymbol{\mathcal{V}}; 0) = \frac{\partial L}{\partial s}(0; \hat{\psi}_0, \rho) = \tfrac{1}{2}\frac{\partial\hat{\ell}_{\widetilde{g}}}{\partial s}(0; \psi) + \frac{\partial\hat{\mathsf{a}}_V}{\partial s}(0; \psi, \rho) - \tfrac{1}{2}\frac{\partial\hat{\ell}_{\widetilde{g}}}{\partial s}(0; \rho) - \frac{\partial\hat{\mathsf{b}}_K}{\partial s}(0; \widetilde{g}, \rho)\,. \tag{4.1.14}$$

27

It expresses the directional shape derivative of $\hat{\mathcal{E}}_F$ by means of partial derivatives with respect to s of the terms in (4.1.8). Those partial derivatives can be computed using the formulas mentioned in Section 3.0.3. Thus, swapping differentiation and integration in (4.1.9) we get

$$\frac{\partial \hat{\mathsf{a}}_V}{\partial s}(0; \psi, \rho) = \int_{\partial\Omega} \int_{\partial\Omega} \left. \frac{d\, G(\mathbf{T}_s^{\boldsymbol{\nu}}(\hat{\boldsymbol{x}}), \mathbf{T}_s^{\boldsymbol{\nu}}(\hat{\boldsymbol{y}}))}{ds} \right|_{s=0} \psi(\hat{\boldsymbol{y}})\, \rho(\hat{\boldsymbol{x}})\, dS(\hat{\boldsymbol{y}})dS(\hat{\boldsymbol{x}})\ ,$$

$$= \int_{\partial\Omega} \int_{\partial\Omega} \left(\nabla_{\boldsymbol{x}} G(\hat{\boldsymbol{x}},\hat{\boldsymbol{y}}) \cdot \boldsymbol{\mathcal{V}}(\hat{\boldsymbol{x}}) + \nabla_{\boldsymbol{y}} G(\hat{\boldsymbol{x}},\hat{\boldsymbol{y}}) \cdot \boldsymbol{\mathcal{V}}(\hat{\boldsymbol{y}}) \right)\, \psi(\hat{\boldsymbol{y}})\, \rho(\hat{\boldsymbol{x}})\, dS(\hat{\boldsymbol{y}})dS(\hat{\boldsymbol{x}})\ .$$

$$\frac{\partial \hat{\mathsf{b}}_K}{\partial s}(0; \widetilde{g}, \rho) = \int_{\partial\Omega} \int_{\partial\Omega} \rho(\hat{\boldsymbol{x}}) \left. \frac{d\left(\left(\nabla_{\boldsymbol{y}} G(\mathbf{T}_s^{\boldsymbol{\nu}}(\hat{\boldsymbol{x}}), \mathbf{T}_s^{\boldsymbol{\nu}}(\hat{\boldsymbol{y}})) \cdot \mathbf{C}(\mathrm{D}\mathbf{T}_s^{\boldsymbol{\nu}}(\hat{\boldsymbol{y}}))\, \mathbf{n}(\hat{\boldsymbol{y}}) \right) \widetilde{g}(\mathbf{T}_s^{\boldsymbol{\nu}}(\hat{\boldsymbol{y}})) \right)}{ds} \right|_{s=0} dS(\hat{\boldsymbol{y}})dS(\hat{\boldsymbol{x}})$$

$$= \int_{\partial\Omega} \int_{\partial\Omega} p(\hat{\boldsymbol{x}})\, \widetilde{g}(\hat{\boldsymbol{y}})\ \left. \frac{d\nabla_{\boldsymbol{y}} G(\mathbf{T}_s^{\boldsymbol{\nu}}(\hat{\boldsymbol{x}}), \mathbf{T}_s^{\boldsymbol{\nu}}(\hat{\boldsymbol{y}}))}{ds} \right|_{s=0} \cdot \mathbf{n}(\hat{\boldsymbol{y}})\, dS(\hat{\boldsymbol{y}})dS(\hat{\boldsymbol{x}})$$

$$+ \int_{\partial\Omega} \int_{\partial\Omega} \rho(\hat{\boldsymbol{x}})\, \widetilde{g}(\hat{\boldsymbol{y}})\, \nabla_{\boldsymbol{y}} G(\hat{\boldsymbol{x}},\hat{\boldsymbol{y}}) \cdot \left(\boldsymbol{\nabla} \cdot \boldsymbol{\mathcal{V}}(\hat{\boldsymbol{y}})\, \mathbf{n}(\hat{\boldsymbol{y}}) - \mathrm{D}\boldsymbol{\mathcal{V}}^{\top}(\hat{\boldsymbol{y}})\mathbf{n}(\hat{\boldsymbol{y}}) \right) dS(\hat{\boldsymbol{y}})dS(\hat{\boldsymbol{x}})$$

$$+ \int_{\partial\Omega} \int_{\partial\Omega} \rho(\hat{\boldsymbol{x}}) \left(\nabla_{\boldsymbol{y}} G(\hat{\boldsymbol{x}},\hat{\boldsymbol{y}}) \cdot \mathbf{n}(\hat{\boldsymbol{y}}) \right) \left(\nabla \widetilde{g}(\hat{\boldsymbol{y}}) \cdot \boldsymbol{\mathcal{V}}(\hat{\boldsymbol{y}}) \right) dS(\hat{\boldsymbol{y}})dS(\hat{\boldsymbol{x}})\ ,$$

$$\frac{\partial \hat{\ell}_{\widetilde{g}}}{\partial s}(0; \rho) = \int_{\partial\Omega} \rho(\hat{\boldsymbol{x}}) \left. \frac{d\, \widetilde{g}(\mathbf{T}_s^{\boldsymbol{\nu}}(\hat{\boldsymbol{x}}))}{ds} \right|_{s=0} dS(\boldsymbol{x}) = \int_{\partial\Omega} \rho(\hat{\boldsymbol{x}}) \nabla \widetilde{g}(\hat{\boldsymbol{x}}) \cdot \boldsymbol{\mathcal{V}}(\hat{\boldsymbol{x}})\, dS(\hat{\boldsymbol{x}})\ . \qquad (4.1.15)$$

Adding up individual contributions gives us the directional shape derivative

$$\frac{d\hat{\mathcal{E}}_F}{ds}(\boldsymbol{\mathcal{V}}; 0)\, [\psi, \rho] =$$

$$\frac{1}{2} \int_{\Gamma} \psi(\hat{\boldsymbol{x}})\, (\nabla \widetilde{g}(\hat{\boldsymbol{x}}) \cdot \boldsymbol{\mathcal{V}}(\hat{\boldsymbol{x}}))\, dS(\hat{\boldsymbol{x}}) \qquad\qquad =: \mathbf{T_1}(\psi)$$

$$+ \int_{\partial\Omega} \int_{\partial\Omega} \psi(\hat{\boldsymbol{y}}) \left\{ \nabla_{\boldsymbol{x}} G(\hat{\boldsymbol{x}},\hat{\boldsymbol{y}}) \cdot \boldsymbol{\mathcal{V}}(\hat{\boldsymbol{x}}) + \nabla_{\boldsymbol{y}} G(\hat{\boldsymbol{x}},\hat{\boldsymbol{y}}) \cdot \boldsymbol{\mathcal{V}}(\hat{\boldsymbol{y}}) \right\} \rho(\hat{\boldsymbol{x}})\, dS(\hat{\boldsymbol{y}})dS(\hat{\boldsymbol{x}}) \quad =: \mathbf{T_2}(\psi, \rho)$$

$$- \int_{\partial\Omega} \int_{\partial\Omega} \rho(\hat{\boldsymbol{x}})\widetilde{g}(\hat{\boldsymbol{y}})\ \left. \frac{d\nabla_{\boldsymbol{y}} G(\mathbf{T}_s^{\boldsymbol{\nu}}(\hat{\boldsymbol{x}}), \mathbf{T}_s^{\boldsymbol{\nu}}(\hat{\boldsymbol{y}}))}{ds} \right|_{s=0} \cdot \mathbf{n}(\hat{\boldsymbol{y}})\, dS(\hat{\boldsymbol{y}})dS(\hat{\boldsymbol{x}}) \qquad =: \mathbf{T_3}(\rho)$$

$$+ \int_{\partial\Omega} \int_{\partial\Omega} \rho(\hat{\boldsymbol{x}})\widetilde{g}(\hat{\boldsymbol{y}})\, \nabla_{\boldsymbol{y}} G(\hat{\boldsymbol{x}},\hat{\boldsymbol{y}}) \cdot \left((\mathrm{D}\boldsymbol{\mathcal{V}})^{\top}(\hat{\boldsymbol{y}})\mathbf{n}(\hat{\boldsymbol{y}}) \right) dS(\hat{\boldsymbol{y}})dS(\hat{\boldsymbol{x}}) \qquad\quad =: \mathbf{T_4}(\rho)$$

$$- \int_{\partial\Omega} \int_{\partial\Omega} \rho(\hat{\boldsymbol{x}}) \left(\nabla_{\boldsymbol{y}} G(\hat{\boldsymbol{x}},\hat{\boldsymbol{y}}) \cdot \hat{\mathbf{n}}(\hat{\boldsymbol{y}}) \right) \boldsymbol{\nabla} \cdot \left(\widetilde{g}(\hat{\boldsymbol{y}})\boldsymbol{\mathcal{V}}(\hat{\boldsymbol{y}}) \right) dS(\hat{\boldsymbol{y}})dS(\hat{\boldsymbol{x}}) \qquad\quad =: \mathbf{T_5}(\rho)$$

$$- \frac{1}{2} \int_{\partial\Omega} \rho(\hat{\boldsymbol{x}})\, (\nabla \widetilde{g}(\hat{\boldsymbol{x}}) \cdot \boldsymbol{\mathcal{V}}(\hat{\boldsymbol{x}}))\, dS(\hat{\boldsymbol{x}})\ . \qquad\qquad =: \mathbf{T_6}(\rho)$$

$$(4.1.16)$$

The notation $\frac{d\hat{\mathcal{E}}_F}{ds}(\boldsymbol{\mathcal{V}}; 0)\, [\psi, \rho]$ hints that this expression can be viewed as a function of the two arguments $\psi \in H^{-\frac{1}{2}}(\partial\Omega)$ and $\rho \in H^{-\frac{1}{2}}(\partial\Omega)$, for which we have to plug in the solutions of the "state problem" (4.1.3) and of the adjoint problem (4.1.13), respectively, in order to

recover the force in direction $\boldsymbol{\mathcal{V}}$. Note that

$$\frac{d\nabla_y G(\mathbf{T}_s^{\boldsymbol{\nu}}(\hat{\boldsymbol{x}}), \mathbf{T}_s^{\boldsymbol{\nu}}(\hat{\boldsymbol{y}}))}{ds}\bigg|_{s=0} = \mathsf{D}_x \nabla_y G(\hat{\boldsymbol{x}}, \hat{\boldsymbol{y}}) \, \boldsymbol{\mathcal{V}}(\hat{\boldsymbol{x}}) + \mathsf{D}_y \nabla_y G(\hat{\boldsymbol{x}}, \hat{\boldsymbol{y}}) \, \boldsymbol{\mathcal{V}}(\hat{\boldsymbol{y}}) \tag{4.1.17}$$

$$= \nabla_y \nabla_y G(\hat{\boldsymbol{x}}, \hat{\boldsymbol{y}}) \Big(\boldsymbol{\mathcal{V}}(\hat{\boldsymbol{y}}) - \boldsymbol{\mathcal{V}}(\hat{\boldsymbol{x}}) \Big), \tag{4.1.18}$$

where

$$\nabla_y \nabla_y G(\boldsymbol{x}, \boldsymbol{y}) = \nabla_x \nabla_x G(\boldsymbol{x}, \boldsymbol{y}) = \frac{3}{4\pi} \frac{(\boldsymbol{x} - \boldsymbol{y})(\boldsymbol{x} - \boldsymbol{y})^T}{\|\boldsymbol{x} - \boldsymbol{y}\|^5} - \frac{1}{4\pi} \frac{\mathsf{Id}}{\|\boldsymbol{x} - \boldsymbol{y}\|^3}. \tag{4.1.19}$$

4.1.5 Boundary-Element Galerkin Discretization

We introduce a mesh partition $\partial\Omega_h$ of $\partial\Omega$ whose cells are curve segments ($d = 2$) or curved triangular panels ($d = 3$). We perform a Galerkin discretization of (4.1.3) employing so-called boundary element spaces $\mathcal{S}_q^{-1}(\partial\Omega_h)$ of $\partial\Omega_h$-piecewise (mapped) polynomial functions of degree $q \in \mathbb{N}_0$. The simplest option $q = 0$ uses the boundary element space spanned by the characteristic functions of the cells of the mesh. For the details of the construction of $\mathcal{S}_q^{-1}(\partial\Omega_h)$ refer to [58, Chapter 10] or [54, Chapter 4]. The choice of basis functions and the computation of the Galerkin matrices is presented in [54, Chapter 5].

We restrict ourselves to the boundary element space $\mathcal{S}_0^{-1}(\partial\Omega_h)$ and write $\psi_h \in \mathcal{S}_0^{-1}(\partial\Omega_h)$ for the Galerkin boundary element solution of (4.1.3). The results of [54, Section 4.3] predict asymptotic convergence $\|\psi - \psi_h\|_{H^{-\frac{1}{2}}(\partial\Omega)} = O(h^{3/2})$ when the meshwidth h of $\partial\Omega_h$ is sent to zero through uniform regular refinement, and the exact solution ψ of (4.1.3) is sufficiently smooth.

4.1.6 BEM-Based Approximation of Forces

To evaluate the shape derivative (4.1.16) for a displacement vector field $\boldsymbol{\mathcal{V}}$, beside the data $\widetilde{g}$ we need the solutions $\psi \in H^{-\frac{1}{2}}(\partial\Omega)$ (state solution) and $\rho \in H^{-\frac{1}{2}}(\partial\Omega)$ (adjoint solution) of the weakly singular variational boundary integral equations (4.1.3) and (4.1.13), respectively.

In general, those will only be available through boundary element Galerkin approximations as introduced in Section 4.1.5. In other words, we evaluate (4.1.16) after replacing ψ and ρ with Galerkin approximations ψ_h and ρ_h. This gives an approximation for the action of the surface force density on the displacement $\boldsymbol{\mathcal{V}}$, the "force in direction $\boldsymbol{\mathcal{V}}$",

$$\int_\Gamma \mathbf{f}^\Gamma(\boldsymbol{x}) \cdot \boldsymbol{\mathcal{V}}(\boldsymbol{x}) \, d\mathsf{S}(\boldsymbol{x}) \approx -\frac{d\hat{\mathcal{E}}_F}{dt}(\boldsymbol{\mathcal{V}}; 0)\, [\psi_h, \rho_h] \ . \tag{4.1.20}$$

Neglecting potential variational crimes this perfectly fits the abstract framework laid out in the following proposition

Proposition 1. Let $V_{0,h} \subset V_0 \subset V$ be closed subspaces of a Banach space V, and let $\mathsf{a} : V \times V \to \mathbb{R}$ be a bounded V_0-elliptic bilinear form, $\ell \in V'$, $\widetilde{g} \in V$, and consider the variational problems

$$u \in V_0 + \widetilde{g}: \qquad \mathsf{a}(u, v) = \ell(v) \quad \forall v \in V_0 \ , \tag{4.1.21}$$

$$u_h \in V_{0,h} + \widetilde{g}: \qquad \mathsf{a}(u_h, v_h) = \ell(v_h) \quad \forall v_h \in V_{0,h} \ . \tag{4.1.22}$$

If $F \in C^2(V, \mathbb{R})$, then the output error estimate[1]

$$|F(u) - F(u_h)| \leq \|\mathsf{a}\| \, \|u - u_h\|_V \inf_{v_h \in V_{0,h}} \|z - v_h\|_V + \tag{4.1.23}$$

$$\tfrac{1}{2} \max_{0 \leq \tau \leq 1} \left\| \mathsf{D}^2 F(\tau u_h + (1 - \tau) u) \right\| \, \|u - u_h\|_V^2$$

holds true, where u, u_h designate the solutions of (4.1.21) and (4.1.22), respectively, and $z \in V_0$ is the solution of the *adjoint variational problem*

$$z \in V_0 : \quad \mathsf{a}(v, z) = \mathsf{D}F(u)(v) \quad \forall v \in V_0 . \tag{4.1.24}$$

Proof. By the Lax-Milgram lemma [12, Sect. 6.2] existence and uniqueness of both u and u_h is guaranteed. We write $e := u_h - u \in V_0$ for the Galerkin discretization error and recall its property known as Galerkin orthogonality: $\mathsf{a}(e, v_h) = 0$ for all $v_h \in V_{0,h}$. By second-order Taylor expansion [12, Theorem 7.9-1] we find

$$F(u + e) - F(u) = \mathsf{D}F(u)(e) + \int_0^1 (1 - t) \mathsf{D}^2 F(u + te)(e, e) \, \mathrm{d}t . \tag{4.1.25}$$

Thanks to the defining equation (4.1.24) for $z \in V_0$ and Galerkin orthogonality, we can rewrite

$$\mathsf{D}F(u)(e) = \mathsf{a}(e, z) = \mathsf{a}(e, z - v_h) \quad \forall v_h \in V_{0,h} . \tag{4.1.26}$$

The continuity estimate $|\mathsf{a}(v, v')| \leq \|\mathsf{a}\| \, \|v\|_V \, \|v'\|_V$ for all $v, v' \in V_0$ together with the definition of the norm of $\mathsf{D}^2 F$ finishes the proof. $\square$

For the h-version of the finite-element method (FEM) the message of Proposition 1 is that the output error $F(u) - F(u_h)$ can converge to zero faster than the energy norm $\|u - u_h\|_V$ of the Galerkin discretization error provided that the best-approximation error $\inf_{v_h \in V_{0,h}} \|z - v_h\|_V$ for the solution z of the adjoint variational problem tends to zero with some rate. In this case we observe *superconvergence* of $F(u_h) \to F(u)$ for $h \to 0$.

Proposition 1 can be applied to the evaluation of (4.1.20) with $V := H^{-\frac{1}{2}}(\partial \Omega) \times H^{-\frac{1}{2}}(\partial \Omega)$, $\mathsf{a} := \mathsf{a}_V \times \mathsf{a}_V$, and $F((\varphi, \sigma)) := \dfrac{d\hat{\mathcal{E}}_F}{dt}(\boldsymbol{\mathcal{V}}; 0)\,[\varphi, \sigma]$. The linear form is a combination of the linear form appearing in (4.1.8) and (4.1.13).

Obviously the mapping $(\varphi, \sigma) \in H^{-\frac{1}{2}}(\partial \Omega) \times H^{-\frac{1}{2}}(\partial \Omega) \mapsto F((\varphi, \sigma))$ is a *quadratic functional*:

$$F((\varphi, \sigma)) := \frac{d\hat{\mathcal{E}}_F}{dt}(\boldsymbol{\mathcal{V}}; 0)\,[\varphi, \sigma] = \mathsf{q}_{\boldsymbol{\mathcal{V}}}((\varphi, \sigma), (\varphi, \sigma)) + p_{\boldsymbol{\mathcal{V}}}(\varphi) + r_{\boldsymbol{\mathcal{V}}}(\sigma) , \tag{4.1.27}$$

with a bilinear form $\mathsf{q}_{\boldsymbol{\mathcal{V}}}$ on $H^{-\frac{1}{2}}(\partial \Omega) \times H^{-\frac{1}{2}}(\partial \Omega)$ and linear forms $p_{\boldsymbol{\mathcal{V}}}$ and $r_{\boldsymbol{\mathcal{V}}}$, given as

$$\mathsf{q}_{\boldsymbol{\mathcal{V}}}((\varphi, \sigma), (\varphi, \sigma)) := \mathbf{T_2}(\varphi, \sigma) \quad , \quad p_{\boldsymbol{\mathcal{V}}}(\varphi) := \mathbf{T_1}(\varphi) \quad , \tag{4.1.28}$$

$$r_{\boldsymbol{\mathcal{V}}}(\sigma) := \mathbf{T_3}(\sigma) + \mathbf{T_4}(\sigma) + \mathbf{T_5}(\sigma) + \mathbf{T_6}(\sigma) , \tag{4.1.29}$$

---

[1] $\|\mathsf{a}\|$ and $\|\mathsf{D}^2 F\|$ designate the operator norms of bounded bilinear mappings $V \times V \to \mathbb{R}$

in terms of the abbreviations from (4.1.16). Thus, F will be C^∞-smooth with first derivative

$$\mathsf{D}F((\varphi,\sigma))((\varphi',\sigma')) = \mathsf{q}_{\boldsymbol{\mathcal{V}}}((\varphi,\sigma),(\varphi',\sigma')) + \mathsf{q}_{\boldsymbol{\mathcal{V}}}((\varphi',\sigma'),(\varphi,\sigma)) + p_{\boldsymbol{\mathcal{V}}}(\varphi') + r_{\boldsymbol{\mathcal{V}}}(\sigma') , \quad (4.1.30)$$

and constant second derivative, if and only if $\mathsf{q}_{\boldsymbol{\mathcal{V}}}$ and $p_{\boldsymbol{\mathcal{V}}}$, $r_{\boldsymbol{\mathcal{V}}}$ are bounded on $H^{-\frac{1}{2}}(\partial\Omega) \times H^{-\frac{1}{2}}(\partial\Omega)$ and $H^{-\frac{1}{2}}(\partial\Omega)$, respectively.

From (4.1.30) we also learn that the adjoint variational problem (4.1.24) becomes: seek $(\nu,\kappa) \in H^{-\frac{1}{2}}(\partial\Omega) \times H^{-\frac{1}{2}}(\partial\Omega)$ such that

$$\mathsf{a}_V(\varphi,\nu) + \mathsf{a}_V(\sigma,\kappa) = \mathsf{q}_{\boldsymbol{\mathcal{V}}}((\psi,\rho),(\varphi,\sigma)) + \mathsf{q}_{\boldsymbol{\mathcal{V}}}((\varphi,\sigma),(\psi,\rho)) + p_{\boldsymbol{\mathcal{V}}}(\varphi) + r_{\boldsymbol{\mathcal{V}}}(\sigma) \qquad (4.1.31)$$

for all $(\varphi,\sigma) \in H^{-\frac{1}{2}}(\partial\Omega) \times H^{-\frac{1}{2}}(\partial\Omega)$. A decoupling is possible: From the special structure of $\mathbf{T_2}$ we infer

$$\mathsf{q}_{\boldsymbol{\mathcal{V}}}((0,\sigma),(\varphi',\sigma')) = \mathsf{q}_{\boldsymbol{\mathcal{V}}}((\varphi,\sigma),(\varphi',0)) = 0 \quad \forall \varphi, \varphi', \sigma, \sigma' \in H^{-\frac{1}{2}}(\partial\Omega) .$$

This reveals that (4.1.31) is equivalent to the two decoupled variational equations

$$\mathsf{a}_V(\varphi,\nu) = \mathsf{q}_{\boldsymbol{\mathcal{V}}}((\varphi,0),(\psi,\rho)) + p_{\boldsymbol{\mathcal{V}}}(\varphi) \quad \forall \varphi \in H^{-\frac{1}{2}}(\partial\Omega) , \qquad (4.1.32\text{a})$$

$$\mathsf{a}_V(\sigma,\kappa) = \mathsf{q}_{\boldsymbol{\mathcal{V}}}((\psi,\rho),(0,\sigma)) + r_{\boldsymbol{\mathcal{V}}}(\sigma) \quad \forall \sigma \in H^{-\frac{1}{2}}(\partial\Omega) . \qquad (4.1.32\text{b})$$

Proposition 1 sends the message that for predicting superconvergence of forces it will be important to establish enhanced smoothness of the solutions ν and κ of (4.1.32). Therefore we have to understand the regularity of the right-hand sides of these variational equations.

4.1.7 Mapping properties of Shape Derivative

In this section we study the continuity of the quadratic functional $(\varphi,\sigma) \in H^{-\frac{1}{2}}(\partial\Omega) \times H^{-\frac{1}{2}}(\partial\Omega) \mapsto F((\varphi,\sigma)) := \frac{d\hat{\mathcal{E}}_F}{ds}(\boldsymbol{\mathcal{V}};0)[\varphi,\sigma]$ from (4.1.27), (4.1.28). This boils down to establishing the continuity of its bilinear and linear terms $\mathsf{q}_{\boldsymbol{\mathcal{V}}}$, $p_{\boldsymbol{\mathcal{V}}}$, $r_{\boldsymbol{\mathcal{V}}}$ on the trace space $H^{-\frac{1}{2}}(\partial\Omega)$. We do this by a close inspection of the integral kernels occurring in (4.1.16). To avoid technical complications we impose smoothness requirements on $\boldsymbol{\mathcal{V}}$ and $\widetilde{g}$, which can certainly be relaxed.

Assumption 1. We assume that both $\boldsymbol{\mathcal{V}} \in \left(C_0^\infty(B)\right)^d$ and $\widetilde{g} \in C_0^\infty(B)$.

4.1.7.1 Analysis of $\mathsf{q}_{\boldsymbol{\mathcal{V}}}$

Using elementary properties of the fundamental solutions

$$G(\boldsymbol{x},\boldsymbol{y}) = \begin{cases} -\frac{1}{2\pi} \log \|\boldsymbol{x}-\boldsymbol{y}\| & \text{for } d = 2 , \\ \dfrac{1}{4\pi\|\boldsymbol{x}-\boldsymbol{y}\|} & \text{for } d = 3 , \end{cases} \quad \nabla_{\boldsymbol{y}} G(\boldsymbol{x},\boldsymbol{y}) = \frac{1}{2^{d-1}\pi} \frac{\boldsymbol{x}-\boldsymbol{y}}{\|\boldsymbol{x}-\boldsymbol{y}\|^d} , \qquad (4.1.33)$$

and the fact $\nabla_{\boldsymbol{x}} G(\boldsymbol{x},\boldsymbol{y}) = -\nabla_{\boldsymbol{y}} G(\boldsymbol{x},\boldsymbol{y})$ the term $\mathbf{T_2}$ from (4.1.16) can be recast as

$$\mathsf{q}_{\boldsymbol{\mathcal{V}}}((\varphi,\sigma),(\varphi',\sigma')) = \int_{\partial\Omega} \int_{\partial\Omega} \varphi(\boldsymbol{y}) \left\{ \nabla_{\boldsymbol{x}} G(\boldsymbol{x},\boldsymbol{y}) \cdot \boldsymbol{\mathcal{V}}(\boldsymbol{x}) + \nabla_{\boldsymbol{y}} G(\boldsymbol{x},\boldsymbol{y}) \cdot \boldsymbol{\mathcal{V}}(\boldsymbol{y}) \right\} \sigma'(\boldsymbol{x}) \, d\mathrm{S}(\boldsymbol{y}) d\mathrm{S}(\boldsymbol{x})$$

$$= -\frac{1}{2^{d-1}\pi} \int_{\partial\Omega} \int_{\partial\Omega} \varphi(\boldsymbol{y}) \, \sigma'(\boldsymbol{x}) \, \frac{\boldsymbol{x}-\boldsymbol{y}}{\|\boldsymbol{x}-\boldsymbol{y}\|^d} \cdot (\boldsymbol{\mathcal{V}}(\boldsymbol{x}) - \boldsymbol{\mathcal{V}}(\boldsymbol{y})) \, d\mathrm{S}(\boldsymbol{x}) d\mathrm{S}(\boldsymbol{y}) .$$

Thus, $q_{\mathcal{V}}$ can be expressed as

$$q_{\mathcal{V}}((\varphi, \sigma), (\varphi', \sigma')) = -\int_{\partial\Omega} \mathsf{V}(\varphi)(\boldsymbol{x})\, \sigma'(\boldsymbol{x})\, d\mathrm{S}(\boldsymbol{x})\,, \tag{4.1.34}$$

with an integral operator

$$\mathsf{V}(\psi)(\boldsymbol{x}) := \int_{\partial\Omega} K_V(\boldsymbol{x}, \boldsymbol{x} - \boldsymbol{y})\, \psi(\boldsymbol{y}) d\mathrm{S}(\boldsymbol{y})\,, \quad \boldsymbol{x} \in \partial\Omega\,, \tag{4.1.35a}$$

whose kernel is given by ($\boldsymbol{z} := \boldsymbol{x} - \boldsymbol{y}$)

$$K_V(\boldsymbol{x}, \boldsymbol{z}) := \frac{1}{2^{d-1}\pi} \frac{\boldsymbol{z}}{\|\boldsymbol{z}\|^d} \cdot (\boldsymbol{\mathcal{V}}(\boldsymbol{x}) - \boldsymbol{\mathcal{V}}(\boldsymbol{x} - \boldsymbol{z}))\,, \quad \boldsymbol{x}, \boldsymbol{z} \in \mathbb{R}^d,\, \boldsymbol{z} \neq \boldsymbol{0}\,. \tag{4.1.35b}$$

Thanks to Assumption 1 we can insert a local Taylor expansion of $\boldsymbol{\mathcal{V}}$

$$\boldsymbol{\mathcal{V}}(\boldsymbol{x}) - \boldsymbol{\mathcal{V}}(\boldsymbol{x} - \boldsymbol{z}) = \mathsf{D}\boldsymbol{\mathcal{V}}(\boldsymbol{x})\boldsymbol{z} - \tfrac{1}{2}\mathsf{D}^2\boldsymbol{\mathcal{V}}(\boldsymbol{x})(\boldsymbol{z}, \boldsymbol{z}) + O(\|\boldsymbol{z}\|^3) \quad \text{for} \quad \boldsymbol{z} \to \boldsymbol{0}\,, \tag{4.1.36}$$

and the apparently strong singularity of the kernel can be canceled. For $d = 2$ we find

$$K_V(\boldsymbol{x}, \boldsymbol{z}) = K_0(\boldsymbol{x}, \boldsymbol{z}) + \widetilde{K}_V(\boldsymbol{x}, \boldsymbol{z})\,, \quad K_0(\boldsymbol{x}, \boldsymbol{z}) := \frac{\boldsymbol{z}^\top \mathsf{D}\boldsymbol{\mathcal{V}}(\boldsymbol{x})\boldsymbol{z}}{2\pi \|\boldsymbol{z}\|^2}\,, \quad \boldsymbol{x}, \boldsymbol{z} \in \mathbb{R}^2,\, \boldsymbol{z} \neq \boldsymbol{0}\,, \tag{4.1.37}$$

where

- $K_0(\boldsymbol{x}, \boldsymbol{z})$ is smooth on $B \times \mathbb{R}^2 \setminus \{\boldsymbol{0}\}$,

- $\boldsymbol{z} \in \mathbb{R}^2 \setminus \{\boldsymbol{0}\} \mapsto \nabla_{\boldsymbol{z}} K_0(\boldsymbol{x}, \boldsymbol{z})$ is *homogeneous of degree* $-1 = 1 - d$ and *odd*,

- $\boldsymbol{z} \mapsto \widetilde{K}_V(\boldsymbol{x}, \boldsymbol{z})$ belongs to $W^{1,\infty}(\mathbb{R}^2)$ for all $\boldsymbol{x} \in B$.

According to [44, Sect. 4.3.3] this qualifies K_V as a *pseudo-homogeneous* kernel of class -1.
For $d = 3$ we get (redefining notations)

$$K_V(\boldsymbol{x}, \boldsymbol{z}) = \underbrace{\frac{\boldsymbol{z}^\top \mathsf{D}\boldsymbol{\mathcal{V}}(\boldsymbol{x})\boldsymbol{z}}{\|\boldsymbol{z}\|^3}}_{=:K_0(\boldsymbol{x}, \boldsymbol{z})} - \frac{1}{2} \underbrace{\frac{\boldsymbol{z}^\top \mathsf{D}^2\boldsymbol{\mathcal{V}}(\boldsymbol{x})(\boldsymbol{z}, \boldsymbol{z})}{\|\boldsymbol{z}\|^3}}_{=:K_1(\boldsymbol{x}, \boldsymbol{z})} + \widetilde{K}_V(\boldsymbol{x}, \boldsymbol{z})\,. \tag{4.1.38}$$

The terms satisfy that

- both K_0 and K_1 belong to $C^\infty(B \times \mathbb{R}^2 \setminus \{\boldsymbol{0}\})$,

- $\boldsymbol{z} \in \mathbb{R}^2 \setminus \{\boldsymbol{0}\} \mapsto \nabla_{\boldsymbol{z}} K_0(\boldsymbol{z}, \boldsymbol{z})$ is homogeneous of degree $-2 = 1 - d$ and odd, and so is $\boldsymbol{z} \in \mathbb{R}^2 \setminus \{\boldsymbol{0}\} \mapsto \mathsf{D}_{\boldsymbol{z}}^2 K_1(\boldsymbol{x}, \boldsymbol{z})$, and,

- again, $\boldsymbol{z} \mapsto \widetilde{K}_V(\boldsymbol{x}, \boldsymbol{z})$ belongs to $W^{1,\infty}(\mathbb{R}^3)$ for all $\boldsymbol{x} \in B$.

As a consequence, also for $d = 3$, the kernel K_V meets the requirements of [44, Sect. 4.3.3] for being *pseudo-homogeneous* of class -1.

Now we can invoke [44, Thm. 4.3.2] together with results from [24, Sect. 1.3] on scales of Sobolev spaces $H^s(\partial\Omega)$ supported on boundaries of class $C^{r,1}$, $r \in \mathbb{N}_0$ [24, Def. 1.2.1.1].

Lemma 1. *Under Assumption 1 and for $\partial\Omega$ of class $C^{r,1}$, $r \in \mathbb{N}_0$, the boundary integral operator* V *as defined in* (4.1.35) *provides a bounded operator* $H^{s-\frac{1}{2}}(\partial\Omega) \to H^{s+\frac{1}{2}}(\partial\Omega)$ *for all* $r - \frac{1}{2} \le s \le r + \frac{1}{2}$.

This means that for $\partial\Omega$ of class $C^{r,1}$ the bilinear form $\mathsf{q}_{\boldsymbol{\mathcal{V}}}$ is continuous as a mapping

$$\mathsf{q}_{\boldsymbol{\mathcal{V}}} : \left(H^{-\frac{1}{2}+s}(\partial\Omega) \times H^{-\frac{1}{2}+s}(\partial\Omega) \right) \times \left(H^{-\frac{1}{2}-s}(\partial\Omega) \times H^{-\frac{1}{2}-s}(\partial\Omega) \right) \to \mathbb{R} , \qquad (4.1.39)$$

for any $s \in [r - \frac{1}{2}, r + \frac{1}{2}]$.

4.1.7.2 Analysis of $r_{\boldsymbol{\mathcal{V}}}$

Inspecting (4.1.16) we see that the linear form $r_{\boldsymbol{\mathcal{V}}}$ as introduced in (4.1.28) can be expressed in terms of integral operators:

$$r_{\boldsymbol{\mathcal{V}}}(\sigma) = \int_{\partial\Omega} \mathsf{R}(\widetilde{g}|_{\partial\Omega})(\boldsymbol{x})\, \sigma(\boldsymbol{x})\, d\mathrm{S}(\boldsymbol{x}) + \int_{\partial\Omega} \mathsf{K}(\boldsymbol{\nabla} \cdot (\widetilde{g}\boldsymbol{\mathcal{V}})|_{\partial\Omega})(\boldsymbol{x})\, \sigma(\boldsymbol{x})\, d\mathrm{S}(\boldsymbol{x}) \qquad (4.1.40)$$
$$- \frac{1}{2} \int_{\partial\Omega} \sigma(\boldsymbol{x})(\nabla\widetilde{g} \cdot \boldsymbol{\mathcal{V}}(\boldsymbol{x}))\, d\mathrm{S}(\boldsymbol{x})$$

with integral operators

$$\mathsf{R}(f)(\boldsymbol{x}) := \int_{\partial\Omega} K_R(\boldsymbol{y}, \boldsymbol{x} - \boldsymbol{y}) f(\boldsymbol{y})\, d\mathrm{S}(\boldsymbol{y}) , \qquad (4.1.41)$$

$$K_R(\boldsymbol{y}, \boldsymbol{z}) := \left. - \frac{d\, \nabla_{\boldsymbol{y}} G(\mathbf{T}^{\boldsymbol{\nu}}_s(\boldsymbol{y} + \boldsymbol{z}), \mathbf{T}^{\boldsymbol{\nu}}_s(\boldsymbol{y}))}{ds} \right|_{s=0} \cdot \boldsymbol{n}(\boldsymbol{y})$$
$$+ \nabla_{\boldsymbol{y}} G(\boldsymbol{y} + \boldsymbol{z}, \boldsymbol{y}) \cdot \left((\mathsf{D}\boldsymbol{\mathcal{V}}(\boldsymbol{y}))^{\top} \boldsymbol{n}(\boldsymbol{y}) \right) , \quad \boldsymbol{z} \ne \boldsymbol{0} ,$$

$$\mathsf{K}(f)(\boldsymbol{x}) := \int_{\partial\Omega} K_K(\boldsymbol{y}, \boldsymbol{x} - \boldsymbol{y}) f(\boldsymbol{y})\, d\mathrm{S}(\boldsymbol{y}) , \qquad (4.1.42)$$

$$K_K(\boldsymbol{y}, \boldsymbol{z}) := \nabla_{\boldsymbol{y}} G(\boldsymbol{y} + \boldsymbol{z}, \boldsymbol{y}) \cdot \boldsymbol{n}(\boldsymbol{y}) , \quad \boldsymbol{z} \ne \boldsymbol{0} .$$

To begin with, the boundary integral operator K is the standard double-layer boundary integral operator for $-\Delta$ and, as such, $\mathsf{K} : H^s(\partial\Omega) \to H^s(\partial\Omega)$ is continuous for $-r - 1 \le s \le r + 1$, if $\partial\Omega$ is of class $C^{r,1}$ [43, Thms. 7.1 & 7.2].

We continue with an inspection of the kernels of the integral operator R using (4.1.33):

$$- \left. \frac{d\, \nabla_{\boldsymbol{y}} G(\mathbf{T}^{\boldsymbol{\nu}}_s(\boldsymbol{y} + \boldsymbol{z}), \mathbf{T}^{\boldsymbol{\nu}}_s(\boldsymbol{y}))}{ds} \right|_{s=0} \cdot \boldsymbol{n}(\boldsymbol{y}) + \nabla_{\boldsymbol{y}} G(\boldsymbol{y} + \boldsymbol{z}, \boldsymbol{y}) \cdot \left((\mathsf{D}\boldsymbol{\mathcal{V}}(\boldsymbol{y}))^{\top} \boldsymbol{n}(\boldsymbol{y}) \right)$$

$$= \frac{1}{2^{d-1}\pi} \left\{ - \frac{\boldsymbol{n}(\boldsymbol{y}) \cdot (\boldsymbol{\mathcal{V}}(\boldsymbol{y} + \boldsymbol{z}) - \boldsymbol{\mathcal{V}}(\boldsymbol{y}))}{\|\boldsymbol{z}\|^d} + d\, \frac{\boldsymbol{z} \cdot \boldsymbol{n}(\boldsymbol{y}) \left(\boldsymbol{z} \cdot (\boldsymbol{\mathcal{V}}(\boldsymbol{y} + \boldsymbol{z}) - \boldsymbol{\mathcal{V}}(\boldsymbol{y})) \right)}{\|\boldsymbol{z}\|^{d+2}} + \right. \qquad (4.1.43)$$
$$\left. \frac{\boldsymbol{z}}{\|\boldsymbol{z}\|^d} \cdot \mathsf{D}\boldsymbol{\mathcal{V}}(\boldsymbol{y})^{\top} \boldsymbol{n}(\boldsymbol{y}) \right\} .$$

Inserting the Taylor expansion

$$\boldsymbol{V}(\boldsymbol{y}+\boldsymbol{z}) - \boldsymbol{V}(\boldsymbol{y}) = \mathsf{D}\boldsymbol{V}(\boldsymbol{y})\boldsymbol{z} + \tfrac{1}{2}\mathsf{D}^2\boldsymbol{V}(\boldsymbol{y})(\boldsymbol{z},\boldsymbol{z}) + O(\|\boldsymbol{z}\|^3) \quad \text{for} \quad \boldsymbol{z} \to \boldsymbol{0}\,, \qquad (4.1.44)$$

we are rewarded with a serendipitous cancellation of the third term and get (redefining notation from Section 4.1.7.1)

$$K_R(\boldsymbol{y},\boldsymbol{z}) = \frac{d}{2^{d-1}\pi} \underbrace{\frac{\boldsymbol{z}\cdot\boldsymbol{n}(\boldsymbol{y})}{\|\boldsymbol{z}\|^d}\frac{\boldsymbol{z}^\top\mathsf{D}\boldsymbol{V}(\boldsymbol{y})\boldsymbol{z}}{\|\boldsymbol{z}\|^2}}_{=:K_0(\boldsymbol{y},\boldsymbol{z})} +$$

$$\frac{1}{2^{d-1}\pi} \underbrace{\left\{-\frac{1}{2}\frac{\boldsymbol{n}(\boldsymbol{y})\cdot\mathsf{D}^2\boldsymbol{V}(\boldsymbol{y})(\boldsymbol{z},\boldsymbol{z})}{\|\boldsymbol{z}\|^d} + \frac{d}{2}\frac{\boldsymbol{z}\cdot\boldsymbol{n}(\boldsymbol{y})}{\|\boldsymbol{z}\|^d}\frac{\boldsymbol{z}\cdot\mathsf{D}^2\boldsymbol{V}(\boldsymbol{y})(\boldsymbol{z},\boldsymbol{z})}{\|\boldsymbol{z}\|^2}\right\}}_{=:K_1(\boldsymbol{y},\boldsymbol{z})} + \widetilde{K}_R(\boldsymbol{y},\boldsymbol{z})\,, \quad (4.1.45)$$

for which we find that

- as functions of $(\boldsymbol{y},\boldsymbol{z})$ both K_0 and K_1 feature the same smoothness as the kernel K_K of the double-layer boundary integral operator,

- $\boldsymbol{z} \in \mathbb{R}^2 \setminus \{\boldsymbol{0}\} \mapsto K_0(\boldsymbol{y},\boldsymbol{z})$ is odd and homogeneous of degree $1-d$,

- $\boldsymbol{z} \in \mathbb{R}^2 \setminus \{\boldsymbol{0}\} \mapsto \nabla_{\boldsymbol{z}}K_1(\boldsymbol{y},\boldsymbol{z})$ is odd and homogeneous of degree $1-d$,

- and $\widetilde{K}_R \in W^{1,\infty}(\partial\Omega \times \mathbb{R}^2)$.

We conclude that K_R is a *pseudo-homogeneous* integral kernel of class 0 in the sense of [44, Sect. 4.3.3], which means that the integral operator R enjoys the same continuity properties as K: It maps continuously $H^s(\partial\Omega) \to H^s(\partial\Omega)$ for $-r-1 \le s \le r+1$, if $\partial\Omega$ is of class $C^{r,1}$ [44, Thm. 4.3.2].

Summing up, under Assumption 1 for $\partial\Omega$ of class $C^{r,1}$ this ensures

$$\mathsf{R}(\widetilde{g}|_{\partial\Omega}) \in H^{r+1}(\partial\Omega) \quad,\quad \mathsf{K}(\boldsymbol{\nabla}\cdot(\widetilde{g}\boldsymbol{V})|_{\partial\Omega}) \in H^{r+1}(\partial\Omega)\,,$$

which means that $r_{\boldsymbol{V}}$ is a continuous linear functional on $H^{-r-1}(\partial\Omega)$, which, by duality, can be identified with a function in $H^{r+1}(\partial\Omega)$.

4.1.7.3 Analysis of $p_{\boldsymbol{V}}$

The simple formula

$$p_{\boldsymbol{V}}(\varphi) = \frac{1}{2}\int_{\partial\Omega} \varphi(\boldsymbol{x})(\nabla\widetilde{g}(\boldsymbol{x})\cdot\boldsymbol{V}(\boldsymbol{x}))\,d\mathrm{S}(\boldsymbol{x}) \qquad (4.1.46)$$

combined with the smoothness assumption Assumption 1 for $\widetilde{g}$ and $\boldsymbol{V}$ means that $p_{\boldsymbol{V}}$ is a continuous linear functional on $H^{-s}(\partial\Omega)$ for $s = r+1$, if $\partial\Omega$ is of class $C^{r,1}$. Thus, by duality, $p_{\boldsymbol{V}}$ can be regarded as an element of $H^{r+1}(\partial\Omega)$.

4.1.8 Section 4.1.6 continued: BEM-Based Approximation of Forces

As announced in Section 4.1.5, we consider only the lowest-order boundary element space $\mathcal{S}_0^{-1}(\partial\Omega_h)$ of $\partial\Omega_h$-piecewise constant functions. Then, Proposition 1 gives us the following concrete estimate for the error of the computed force in the direction $\boldsymbol{\mathcal{V}}$: With a constant $C > 0$ independent of the boundary element space

$$\left| \frac{d\hat{\mathcal{E}}_F}{ds}(\boldsymbol{\mathcal{V}}; 0)\,[\psi, \rho] - \frac{d\hat{\mathcal{E}}_F}{ds}(\boldsymbol{\mathcal{V}}; 0)\,[\psi_h, \rho_h] \right| \leq C E_1 (E_2 + E_1) , \qquad (4.1.47)$$

with the best approximation error norms, which are equal to the Galerkin discretization error by Cea's lemma [58, Sect. 8.1, Theorem 8.1]

$$E_1 := \inf_{\psi_h \in \mathcal{S}_0^{-1}(\partial\Omega_h)} \|\psi - \psi_h\|_{H^{-\frac{1}{2}}(\partial\Omega)} + \inf_{\rho_h \in \mathcal{S}_0^{-1}(\partial\Omega_h)} \|\rho - \rho_h\|_{H^{-\frac{1}{2}}(\partial\Omega)} ,$$

$$E_2 := \inf_{\kappa_h \in \mathcal{S}_0^{-1}(\partial\Omega_h)} \|\kappa - \kappa_h\|_{H^{-\frac{1}{2}}(\partial\Omega)} + \inf_{\nu_h \in \mathcal{S}_0^{-1}(\partial\Omega_h)} \|\nu - \nu_h\|_{H^{-\frac{1}{2}}(\partial\Omega)} ,$$

where $\psi, \rho, \nu, \kappa \in H^{-\frac{1}{2}}(\partial\Omega)$ are the solutions of (4.1.3), (4.1.13), (4.1.32a), and (4.1.32b), respectively.

For the following discussion we maintain Assumption 1 and also assume that $\partial\Omega$ is of class $C^{r,1}$, $r \in \mathbb{N}_0$, which entails that

- the right-hand side of the BIE (4.1.3) can be regarded as a function in $H^{r+1}(\partial\Omega)$,

- the right-hand side of the adjoint variational problem (4.1.13) belongs to $H^{r+1}(\partial\Omega)$, too,

- by the results from Section 4.1.7.3 the right-hand side of (4.1.32a) is in $H^{r+1}(\partial\Omega)$, and,

- as we have seen in Section 4.1.7.1 and Section 4.1.7.2, the right-hand side of (4.1.32b) corresponds to a an element of $H^{\min\{s+1,r+1\}}(\partial\Omega)$, if $\psi \in H^s(\partial\Omega)$.

By the following elliptic lifting theorem for the single-layer boundary integral equation, regularity of the right-hand sides can be transferred to solutions.

Theorem 1 ([43, Theorem 7.16]). Given $f \in H^{\frac{1}{2}}(\partial\Omega)$ let $\eta \in H^{-\frac{1}{2}}(\partial\Omega)$ be the solution of

$$\mathsf{a}_V(\eta, \varphi) = \int_{\partial\Omega} f(\boldsymbol{x})\varphi(\boldsymbol{x})\,d\mathrm{S}(\boldsymbol{x}) \quad \forall \varphi \in H^{-\frac{1}{2}}(\partial\Omega) ,$$

the integral to be read as duality pairing. Then extra smoothness of f induces more regularity of η:

(i) If $\partial\Omega$ is Lipschitz, $f \in H^1(\partial\Omega)$, then $\eta \in L^2(\partial\Omega)$.

(ii) If $\partial\Omega$ is of class $C^{r,1}$, $r \in \mathbb{N}$, and $f \in H^{r+\frac{1}{2}}(\partial\Omega)$, then $\eta \in H^{r-\frac{1}{2}}(\partial\Omega)$.

In addition, in [54, Sect. 4.3.4] we find the following approximation estimate for piecewise smooth $\partial\Omega$ and shape-regular sequences of meshes

$$\inf_{\varphi_h \in \mathcal{S}_0^{-1}(\partial\Omega_h)} \|\varphi - \varphi_h\|_{H^{-\frac{1}{2}}(\partial\Omega)} \le C h^{\min\{1,s\}+\frac{1}{2}} \|\varphi\|_{H^s(\partial\Omega)} \quad \forall \varphi \in H^s(\partial\Omega) , \qquad (4.1.48)$$

where h stands for the mesh width of $\partial\Omega_h$. We discuss two cases.

(I) If $\partial\Omega$ is of class $C^{r,1}$ with $r \in \mathbb{N}$, then Theorem 1 together with the right-hand side regularities listed above yields

$$\psi, \rho, \nu, \kappa \in H^{r-\frac{1}{2}}(\partial\Omega) .$$

The $\mathcal{S}_0^{-1}(\partial\Omega_h)$ best-approximation errors in the $H^{-\frac{1}{2}}(\partial\Omega)$-norm for all of these functions will converge like $O(h^{\min\{\frac{3}{2},r\}})$ for $h \to 0$, for instance on sequences of uniformly refined meshes. Plugging this into (4.1.47), we end up with

$$\left| \frac{d\hat{\mathcal{E}}_F}{ds}(\boldsymbol{\mathcal{V}}; 0)\,[\psi, \rho] - \frac{d\hat{\mathcal{E}}_F}{ds}(\boldsymbol{\mathcal{V}}; 0)\,[\psi_h, \rho_h] \right| = O(h^{\min\{3, 2r\}}) \quad \text{for} \quad h \to 0 . \qquad (4.1.49)$$

(II) If we merely know that $\partial\Omega$ is Lipschitz, we can still conclude

$$\psi, \rho, \nu, \kappa \in L^2(\partial\Omega) ,$$

and the $H^{-\frac{1}{2}}(\partial\Omega)$-norms of the best approximation errors decay asymptotically like $O(h^{\frac{1}{2}})$ for $h \to 0$. By (4.1.47) this involves a minimal $O(h)$-convergence of the error in the force.

Remark 5. The above crude convergence estimates can be refined for piecewise smooth domains taking into account the special corner and edge singular functions present in the solutions of the variational problems [16]. This a-priori knowledge about the structure of the solution can be exploited through the use of algebraically graded meshes, see [25, Chapter 7], [21], [53], in a BEM framework with fixed polynomial degree, or by employing geometrically graded meshes combined with hp-BEM, see [30, 41, 59] and [25, Chapter 8]. A flexible alternative is adaptive mesh refinement controlled by an a-posteriori error estimator, refer to [3] and the references therein.

Remark 6. Throughout this section we took for granted a given fixed smooth displacement field $\boldsymbol{\mathcal{V}}$. As an extension of the investigations in this section one could also aim for $\boldsymbol{\mathcal{V}}$-uniform estimates of the approximation error for shape derivatives as has been done in [34].

4.1.9 Forces from Volume Variational Formulations

The derivation of formulas for the directional shape derivative $\frac{d\mathcal{E}_F}{d\Omega}(\Omega; \boldsymbol{\mathcal{V}})$ is well established for the standard variational formulation of (4.3.1) [18, 36, 57] given as

$$u \in V_g := H_0^1(\Omega) + \widetilde{g} : \quad \mathsf{a}(u, v) := \int_\Omega \nabla u \cdot \nabla v \, \mathrm{d}\boldsymbol{x} = 0 \quad \forall v \in V_0 := H_0^1(\Omega) , \qquad (4.1.50)$$

where $\widetilde{g} \in H^1(\Omega)$ extends the Dirichlet data g, $\widetilde{g}|_\Gamma = g$, and vanishes on ∂B. With details postponed to Section 4.1.11.1, we remark that "implicit shape differentiation" of (4.1.50) yields the boundary-based formula

$$\frac{d\mathcal{E}_F}{d\Omega}(\Omega; \boldsymbol{\mathcal{V}}) = \frac{1}{2} \int_\Gamma \left(\left((\nabla\widetilde{g} - \nabla u) \cdot \boldsymbol{n} \right) \left(\nabla u \cdot \boldsymbol{n} \right) + \nabla\widetilde{g} \cdot \nabla u \right) (\boldsymbol{\mathcal{V}} \cdot \boldsymbol{n}) \, dS \, , \tag{4.1.51}$$

where u is the solution of (4.3.1), and $\boldsymbol{\mathcal{V}} \in \left(C_0^\infty(B) \right)^d$. Obviously, extra smoothness of u and $\widetilde{g}$ beyond merely $u \in H^1(\Omega)$ and $\widetilde{g} \in H_0^1(B)$ is required to render (4.1.51) meaningful. For $\widetilde{g} \equiv U$ and $\boldsymbol{\mathcal{V}}$ constant in a neighborhood of Γ we recover the classical formula (4.1.56).

In fact, also the volume-based force formula (4.1.57) can be obtained as a shape derivative. Again, we start from the standard variational formulation on Ω^s:

$$u = u(\Omega^s) \in H_0^1(\Omega^s) + \widetilde{g} : \quad \int_{\Omega^s} \nabla u(\boldsymbol{x}) \cdot \nabla v(\boldsymbol{x}) \, d\boldsymbol{x} = 0 \quad \forall v \in H_0^1(\Omega^s) \, , \tag{4.1.52}$$

and then pull it back to $\Omega = \Omega^0$. We arrive at a variational characterization of the pullback $\hat{u}_s := u(\Omega^s) \circ \mathbf{T}_s^{\boldsymbol{\nu}}$: Seek $\hat{u} = \hat{u}_s \in H_0^1(\Omega) + \widetilde{g} \circ \mathbf{T}_s^{\boldsymbol{\nu}}$ such that

$$\int_\Omega \left((\mathbf{DT}_s^{\boldsymbol{\nu}}(\hat{\boldsymbol{x}}))^{-1} (\mathbf{DT}_s^{\boldsymbol{\nu}}(\hat{\boldsymbol{x}}))^{-\top} \nabla\hat{u}(\hat{\boldsymbol{x}}) \right) \cdot \nabla v(\hat{\boldsymbol{x}}) \, |\det \mathbf{DT}_s^{\boldsymbol{\nu}}(\hat{\boldsymbol{x}})| \, d\hat{\boldsymbol{x}} = 0 \tag{4.1.53}$$

for all $v \in H_0^1(\Omega)$. This confines the s-dependence to the integrand. The same trick works for the field energy

$$\mathcal{E}_F(s) := \int_\Omega ||(\mathbf{DT}_s^{\boldsymbol{\nu}}(\hat{\boldsymbol{x}}))^{-\top} \nabla\hat{u}_s(\hat{\boldsymbol{x}})||^2 |\det \mathbf{DT}_s^{\boldsymbol{\nu}}(\hat{\boldsymbol{x}})| \, d\hat{\boldsymbol{x}} \, . \tag{4.1.54}$$

Then computing the shape derivative $\frac{d\mathcal{E}_F}{d\Omega}(\Omega; \boldsymbol{\mathcal{V}}) = \frac{d\mathcal{E}_F}{ds}(0)$ using the adjoint approach from PDE-constraint optimization, see Section 4.1.11.2, yields a volume-based formula, which boils down to (4.1.57) for $\widetilde{g} \equiv U$ in a neighborhood of Γ and suitably chosen $\boldsymbol{\mathcal{V}}$.

4.1.10 Numerical Experiments

Now we study the convergence of the new pullback approach formula from (4.1.16) empirically and compare it to the classical boundary based evaluation resulting from the Maxwell Stress Tensor, and the volume based evaluation also known as the "egg-shell method" [27, 28, 42]. The convergence studies are done in 2D entirely and are divided into two parts. In the first part we restrict ourselves to physically meaningful quantities: net forces and torques. In the second part, aligned with our view of force as a shape derivative, a linear functional on displacements, we examine the convergence of a dual norm of the approximation error.

We remind that standard methods employ the Maxwell stress tensor[2] [38, Section 6.9]

$$\mathbf{T}(u) := \nabla u \nabla u^\top - \tfrac{1}{2} ||\nabla u||^2 \, \mathbf{I}_d : \Omega \to \mathbb{R}^{d,d} \, , \tag{4.1.55}$$

---

[2]$\mathbf{I}_d$ stands for the $d \times d$ identity matrix.

involving the electrostatic potential u, which solves (4.3.1). Then, writing $\boldsymbol{n}$ for the exterior unit normal vector field on $\partial\Omega$, the vector field $\mathbf{f}^\Gamma(\boldsymbol{x}) := \mathbf{T}(u(\boldsymbol{x}))\boldsymbol{n}(\boldsymbol{x})$, $\boldsymbol{x} \in \Gamma$ gives the electrostatic surface force density, and, consequently,

$$\mathbf{F} := \int_\Gamma \mathbf{f}^\Gamma \, \mathrm{d}S = \int_\Gamma \mathbf{T}(u)\boldsymbol{n} \, \mathrm{d}S = \frac{1}{2}\int_\Gamma |\nabla u \cdot \boldsymbol{n}|^2 \boldsymbol{n} \, \mathrm{d}S \tag{4.1.56}$$

is the total force on the object, where the last equality holds for constant Dirichlet data $g \equiv U$. Since $\boldsymbol{\nabla} \cdot \mathbf{T}(u) = \mathbf{0}$, by elementary computations using $\Delta u = 0$, integration by parts yields the *equivalent* formula [3]

$$\mathbf{F} = \int_\Omega \mathbf{T}(u)\nabla w \, \mathrm{d}\boldsymbol{x} = \int_\Omega \nabla u(\nabla u \cdot \nabla w) - \tfrac{1}{2}||\nabla u||^2 \nabla w \, \mathrm{d}\boldsymbol{x} \; . \tag{4.1.57}$$

for *any* $w \in W^{1,\infty}(\Omega)$ with $w|_\Gamma \equiv 1$ and $w|_{\partial B} \equiv 0$.

4.1.10.1   Implementation

Both the pullback approach formula (4.1.16) and the stress tensor formula (4.1.51) were implemented using exact parametrizations for the boundaries[4]. Quasi-uniform sequences of mesh partitions of $\partial\Omega$ were employed with increasing resolution. As explained in Section 4.1.5 and Section 4.1.6, boundary-element Galerkin discretization with trial and test space $\mathcal{S}_0^{-1}(\partial\Omega_h)$ is employed to solve the variational equations (4.1.3) and (4.1.13) approximately. The obtained solutions ψ_h and ρ_h are used to compute approximations of the forces according to (4.1.20). For the evaluation of integrals with singular kernels we use log weighted gauss quadrature and regularization by transformation to polar coordinates [26, Section 9.4.5]. All integrals with smooth integrands are evaluated using Gauss quadrature of order 16. The required derivatives of $\widetilde{g}$ and $\boldsymbol{\mathcal{V}}$ are assumed to be explicitly available in the implementation.

4.1.10.2   Total Force and Torque

Experiment 1. We solved (4.3.1) for $g \equiv 1$ by means of piecewise linear C^0 finite elements on quasi-uniform shape-regular sequences of triangular meshes for $d = 2$, and

(i) a smooth "kite-shaped" D, given by the parameterization $\gamma : [0, 2\pi] \to \mathbb{R}^2$, $t \mapsto [0.3 + 0.35\cos(t) + 0.1625\cos(2t), 0.5 + 0.35\sin(t)]$ and a square-shaped $B =]{-2}, 2[\times]{-2}, 2[$, and

(ii) a unit square $D :=]0, 1[^2$ inside $B :=]{-3}, 3[\times]{-3}, 3[$.

The coarsest meshes used for each geometry are displayed in Figure 4.2.

---

[3]We write $\cdot$ for the inner product in Euclidean space $\mathbb{R}^d$ and $|| \cdot ||$ for the associated norm.

[4]Code available at https://gitlab.ethz.ch/ppanchal/fcsc.git. Instructions on how to repeat some of the numerical experiments of this section are given in a README file.
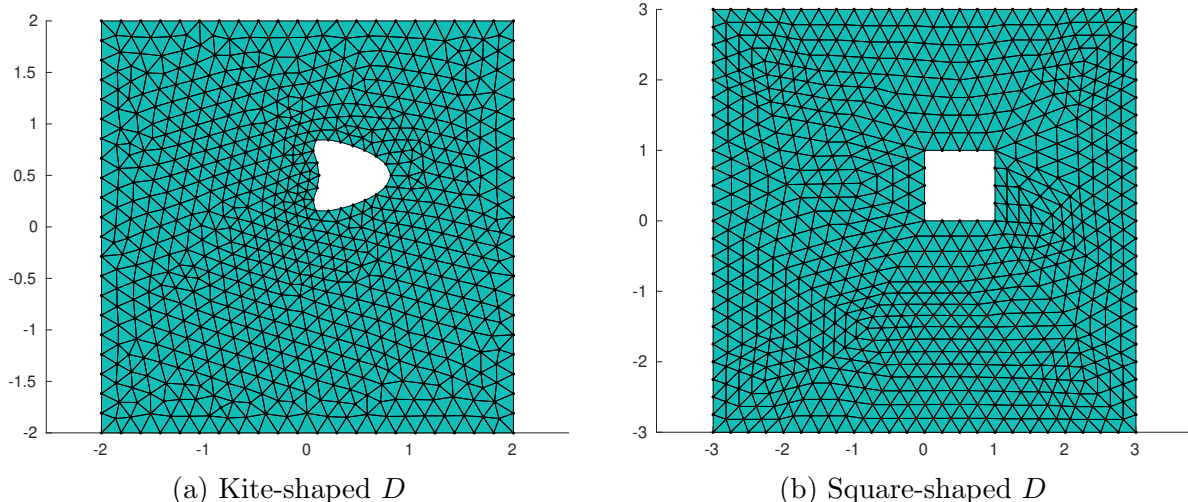
(a) Kite-shaped D (b) Square-shaped D

Figure 4.2: Geometries and coarsest finite element meshes for the numerical tests covered in Experiment 1

We directly evaluate both formulas (4.1.56) and (4.1.57) for the finite element solution and use the following C^1 cut-off function in the volume-based formula (4.1.57):

$$
w(\boldsymbol{x}) := \begin{cases} 1 & \text{for } ||\boldsymbol{x}|| < 1.2 \text{ ,} \\ \cos^2\big(\frac{||\boldsymbol{x}||-1.2}{0.7}\big) & \text{for } 1.2 \leq ||\boldsymbol{x}|| \leq 1.9 \text{ ,} \\ 0 & \text{for } ||\boldsymbol{x}|| > 1.9 \text{ ,} \end{cases} \tag{4.1.58}
$$

The Euclidean norm of the error in the computed forces is shown in Figure 4.3 as a function of the mesh width h of the underlying triangulations. [5]
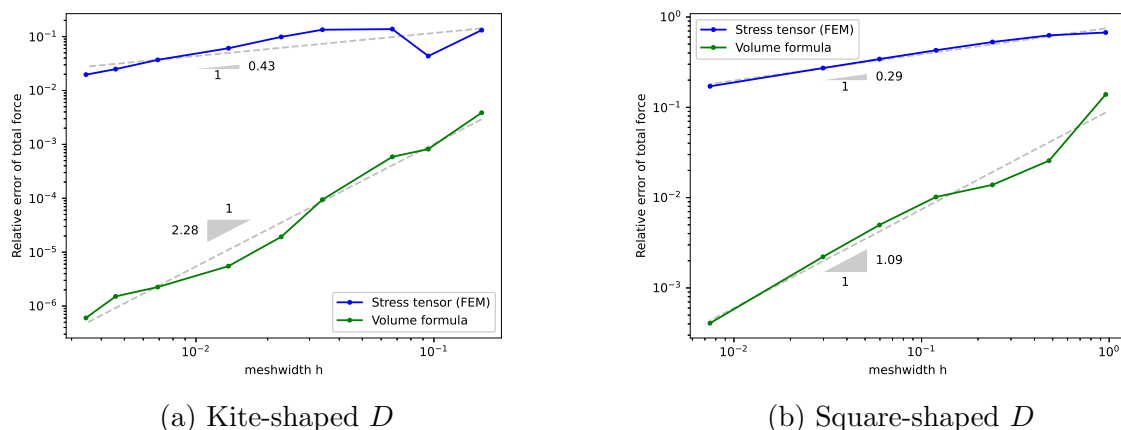

(a) Kite-shaped D (b) Square-shaped D

Figure 4.3: Euclidean norm of errors in approximate total force for finite-element solution inserted into (4.1.56) (blue, "Stress tensor (FEM)") and (4.1.57) (green, "Volume formula"), respectively. The dashed lines represent the linear regression fit.

---

[5]As reference solution we used the total force computed by the pullback approach (4.1.16) on a uniform mesh with 9000 (kite-shaped D)/7200 (square-shaped D) cells

We make the striking observation that, when used with a finite-element solution, the volume-based formula (4.1.57) enjoys a vast superiority over the boundary-based formula (4.1.56), both in terms of absolute accuracy and in terms of rate of asymptotic (algebraic) convergence.

Proposition 1 is key to understanding Experiment 1: The boundary-based output functional (4.1.56) is not even continuous on $H^1(\Omega)$, let alone differentiable. We conclude this from the failure of the co-normal trace $u \mapsto \nabla u \cdot \boldsymbol{n}|_\Gamma$ to map from $H^1(\Omega)$ into $L^2(\Gamma)$. Conversely, if $w \in W^{1,\infty}(\Omega)$, then the volume-based functional (4.1.57) is a smooth quadratic functional on $H^1(\Omega)$. If $w \in W^{2,\infty}(\Omega)$ as in Experiment 1 and $u \in H^2(\Omega)$, then the first derivative of the volume-based force functional will even be continuous on $L^2(\Omega)$, which entails extra smoothness of the dual solution z by virtue of elliptic lifting results. This explains the "superconvergence" of the forces computed by means of (4.1.57) in Experiment 1.

Experiment 2. We compute the total force for the geometric setting introduced in Experiment 1 by evaluating (4.1.56) for $\mathcal{S}_0^{-1}(\partial\Omega_h)$ boundary-element Galerkin solutions on quasi-uniform sequences of mesh partitions $\partial\Omega_h$ of $\partial\Omega$ with increasing resolution. An exact parametric representation of curved boundary parts was employed along with polar-coordinate transformation techniques for singular integrals [26, Section 9.4.5]. We add the resulting error curves to the plots of Experiment 1, see Figure 4.4.
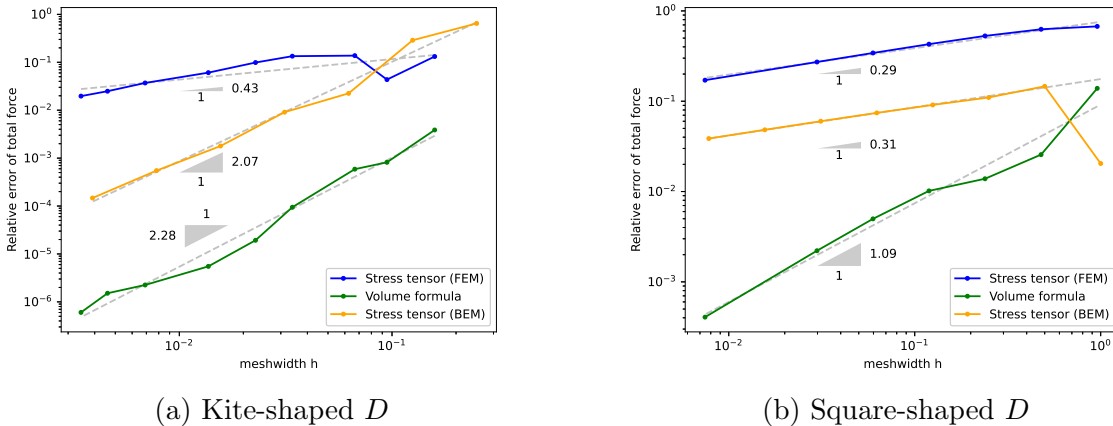

(a) Kite-shaped D (b) Square-shaped D

Figure 4.4: Error of $\mathcal{S}_0^{-1}(\partial\Omega_h)$-BEM based forces by (4.1.56) ("Stress tensor (BEM)") as a function of the meshwidth h of $\partial\Omega_h$. Dashed lines represent the linear regression fits.

For the non-smooth square-shaped object we observe that both accuracy and convergence of the forces obtained from (4.1.56) using a BEM solution are as poor as those for the ones obtained using a FEM solution. Yet, for the kite-shaped smooth object, (4.1.56) with the BEM solution delivers remarkable accuracy almost on par with that of volume-based formula used with the FEM.

Experiment 3. We use the same geometric settings as introduced already in Experiment 1. In particular we use $\widetilde{g} \equiv 1$ close to ∂D and $\widetilde{g} \equiv 0$ close to ∂B. For constant Dirichlet data we compute the total force according to (3.0.5) based on the deformation fields discussed in Section 3.0.2. We employ both (4.1.16) ("Pullback approach (BEM)") and (4.1.51) ("Stress

tensor (BEM)") on a quasi-uniform sequence of meshes of $\partial\Omega_h$. As before we monitor the Euclidean norm of the error in the total force as a function of the mesh width. As reference bona-fide close-to-exact solution we used the total force computed by the pullback approach on a uniform mesh with 9000 (kite-shaped D)/7200 (square-shaped D) cells. The resulting error curves are added to the plots of Experiment 2 and are shown in Figure 4.5 for comparison.
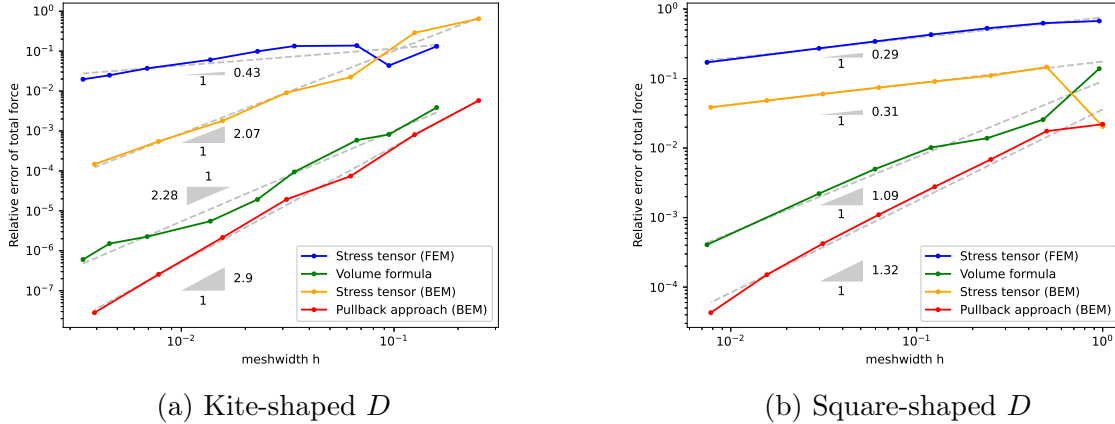

(a) Kite-shaped D (b) Square-shaped D

Figure 4.5: Error of $S_0^{-1}(\partial\Omega_h)$ - BEM based forces as a function of the meshwidth h of $\partial\Omega_h$. Dashed lines represent the linear regression fit.

We see that the pullback approach outperforms every other method not only in terms of the absolute accuracy but also in terms of the asymptotic rate of (algebraic) convergence. For the smooth kite-shaped D (Figure 4.5 (A)) it achieves the optimal convergence $O(h^3)$ for $h \to 0$ predicted in Section 4.1.8. For the square-shaped D (Figure 4.5 (A)) strong singularities of the electrostatic potential u at the re-entrant corners make the rates of convergence deteriorate substantially for all methods, with the pullback approach maintaining its clear lead.

Remark 7. The surprisingly good performance of the BEM-based evaluation of the stress tensor formula (4.1.51) for smooth Γ remains a mystery. It reminds us of a similarly unexpected fast convergence of a boundary-based shape-derivative formula reported in [34, Sect. 4] and, later, theoretically explained in [22, Sect. 3.2].

Experiment 4. In the setting of Experiment 3 we also compute the total torque on D according to (3.0.6), with $\boldsymbol{c} = (0.5, 0)^\top$ for square-shaped D and $\boldsymbol{c} = (0.38, 0.5)^\top$ for kite-shaped D, using the pullback approach (4.1.16) and stress tensor formula (BEM) (4.1.51). The errors of the approximate torques are plotted against the meshwidth h in Figure 4.6.
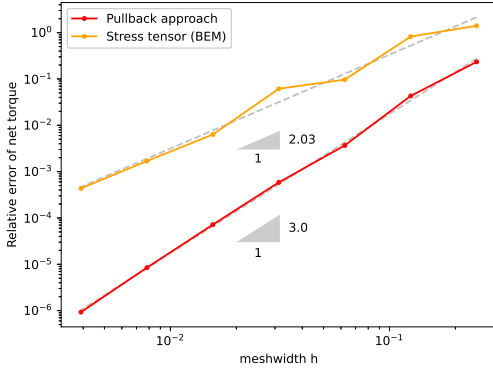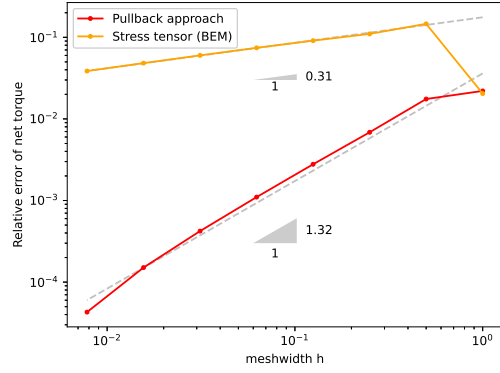
41

(a) Kite-shaped D (b) Square-shaped D

Figure 4.6: Errors of $S_0^{-1}(\partial\Omega_h)$ - BEM based torques by (4.1.16) ("Pullback approach") and (4.1.51) ("Stress tensor (BEM)") as a function of the meshwidth h of $\partial\Omega_h$

The observations closely match those made in Experiment 3. The pullback approach gives the best results both in terms of absolute accuracy and in terms of asymptotic rate of convergence. Its advantage is more pronounced for non-smooth D.

4.1.10.3   Approximation of Force Functionals

Experiment 5. Inspired by [34, Sect. 4] we consider the dual norm of the force as a linear mapping from displacements $\boldsymbol{V}$ to the real numbers over a finite dimensional subspace W_N of $(H^1(B))^2$ and measure the error

$$\text{err} := \max_{\boldsymbol{V} \in W_N} \frac{1}{\|\boldsymbol{V}\|_{H^1(B)}} \left| \frac{d\hat{\mathcal{E}}_F}{dt}(\boldsymbol{V}; 0)\,[\psi, \rho] - \frac{d\hat{\mathcal{E}}_F}{dt}(\boldsymbol{V}; 0)\,[\psi_h, \rho_h] \right|, \tag{4.1.59}$$

both for the pullback approach (4.1.16) and stress tensor (BEM) (4.1.51). We adopt the setting of Experiment 3 and we use the same BEM to compute $\psi_h, \rho_h \in \mathcal{S}_0^{-1}(\partial\Omega_h)$. Two choices for $W_N := U \times U$ are used in this numerical experiment,

$$(I) \qquad U := \text{span}\{\boldsymbol{x} = (x, y)^\top \mapsto x^m y^n,\ 1 \le m, n \le 5\}, \tag{4.1.60}$$

$$(II) \qquad U := \text{span}\{\boldsymbol{x} = (x, y)^\top \mapsto \sin(mx)\sin(ny),\ 1 \le m, n \le 5\}. \tag{4.1.61}$$

Since we are dealing with purely boundary-based expressions, we don't need to introduce cut-off functions for the velocity fields. As reference solutions we use the directional forces obtained by the pullback approach on meshes created by one more step of refinement. The dual norms (4.1.59) are plotted in Figure 4.7.

42
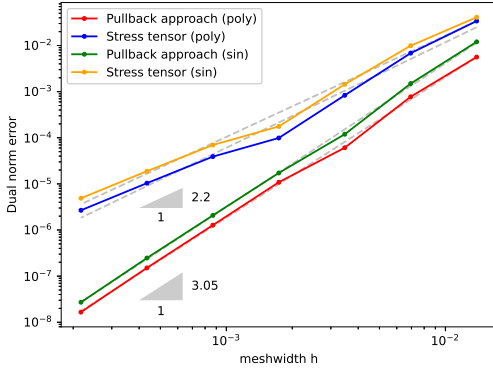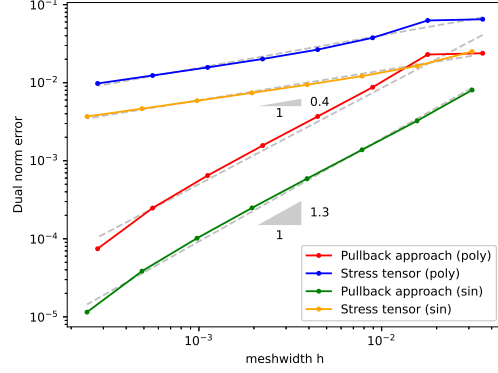
(a) Kite-shaped D (b) Square-shaped D

Figure 4.7: Dual norm errors (4.1.59) for polynomial (poly) and sinusoidal (sin) basis, as a function of the meshwidth h of $\partial\Omega_h$. Dashed lines represent the linear regression fit.

Obviously, the BEM-based pullback approach (4.1.16) offers better accuracy also in the approximate dual norm, but for the kite-shaped D the stress tensor formula (4.1.51) achieves similar empiric rates of convergence for $h \to 0$. We cannot offer an explanation for this surprising observation. Conversely, for the square-shaped D the pullback approach is much better also in terms of the rate of asymptotic (algebraic) convergence. It seems to be less affected by the presence of strong corner singularities in ψ and ρ.

Experiment 6. For the computation of the shape derivative we had always taken for granted that the Dirichlet data g possess a sufficiently regular extension $\widetilde{g}$ to the hold-all domain B. In this experiment we demonstrate the importance of the smoothness of $\tilde{g}$ as regards the approximations of shape derivatives. The experiment shown next uses two different functions $\tilde{g}_1$ and $\tilde{g}_2$ such that $\tilde{g}_1|_\Gamma = \tilde{g}_2|_\Gamma = g$. We work with the model geometry of the square-shaped D from Experiment 1 and with $g = 1$.

For imposing $g = 1$ on Γ we use $\tilde{g}_1 \equiv 1$ in a neighborhood of Γ and for $\tilde{g}_2$ we use four corner singular functions located at the four corners of the square shaped D. These corner singular functions are rotations and reflections of the simple function

$$(r,\theta) \mapsto r^{\frac{2}{3}} \sin(\frac{2}{3}\theta) \quad \text{(polar coordinates)} \,,$$

which is harmonic but its gradient blows up for $r \to 0$.

By comparing the green and red curves in Figure 4.8 we see that a smoother g drastically improves the performance of the pullback approach (4.1.16) as regards both absolute accuracy and the asymptotic (algebraic) convergence rates. For the case of stress tensor formula (4.1.51), a smoother g makes little difference.
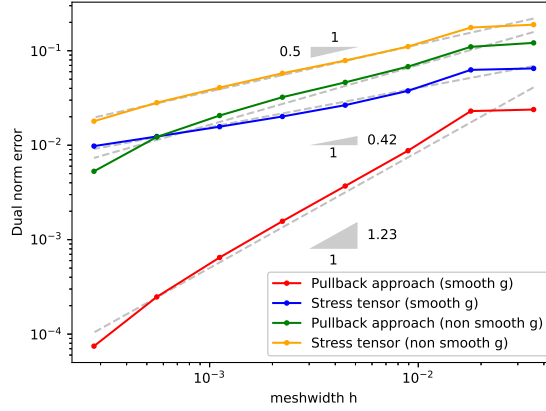
43

Figure 4.8: Dual norm errors (4.1.59) with polynomial basis, using a smooth and non-smooth $\widetilde{g}$, as a function of the meshwidth h of $\partial\Omega_h$

4.1.11 Shape Derivatives From Volume Based Variational Formulation

4.1.11.1 Derivation of Boundary-Based Shape Derivative Formula (4.1.51)

We start from a mixed variational formulation of (4.3.1) in $H^1(B) \times \boldsymbol{H}(\mathrm{div}0, B)$ [58, Sec. 4.1.2]. We seek $(u, \boldsymbol{\mu}) \in H^1(B) \times \boldsymbol{H}(\mathrm{div}0, B)$ such that

$$\int_\Omega \nabla u \cdot \nabla v \, \mathrm{d}\boldsymbol{x} + \int_{\partial\Omega} v \, \boldsymbol{\mu} \cdot \boldsymbol{n} \, d\mathrm{S} = 0 \qquad \forall v \in H^1(B) \,, \tag{4.1.62}$$

$$\int_{\partial\Omega} u \, \boldsymbol{\lambda} \cdot \boldsymbol{n} \, d\mathrm{S} = \int_\Gamma g \, \boldsymbol{\lambda} \cdot \boldsymbol{n} \, d\mathrm{S} \qquad \forall \boldsymbol{\lambda} \in \boldsymbol{H}(\mathrm{div}0, B) \,, \tag{4.1.63}$$

where $g = \widetilde{g}|_\Gamma$ for a $\widetilde{g} \in H^1(B)$ that vanishes on ∂B. There is a unique solution only for u but not for the Lagrange multiplier $\boldsymbol{\mu}$. We define the associated symmetric bilinear form a and linear form $l_{\widetilde{g}}$ for $(w, \boldsymbol{\kappa}), (v, \boldsymbol{\lambda}) \in H^1(B) \times \boldsymbol{H}(\mathrm{div}0, B)$:

$$\mathsf{a}((w, \boldsymbol{\kappa}), (v, \boldsymbol{\lambda})) := \int_\Omega \nabla w \cdot \nabla v \, \mathrm{d}\boldsymbol{x} + \int_{\partial\Omega} v \, \boldsymbol{\kappa} \cdot \boldsymbol{n} \, d\mathrm{S} + \int_{\partial\Omega} u \, \boldsymbol{\lambda} \cdot \boldsymbol{n} \, d\mathrm{S} \,, \tag{4.1.64}$$

$$l_{\widetilde{g}}((v, \boldsymbol{\lambda})) := \int_\Gamma g \, \boldsymbol{\lambda} \cdot \boldsymbol{n} \, d\mathrm{S} \,. \tag{4.1.65}$$

The system in (4.1.62) can be compactly written as: Seek $(u, \boldsymbol{\mu}) \in H^1(B) \times \boldsymbol{H}(\mathrm{div}0, B)$:

$$\mathsf{a}((u, \boldsymbol{\mu}), (v, \boldsymbol{\lambda})) = l_{\widetilde{g}}((v, \boldsymbol{\lambda})) \quad \forall (v, \boldsymbol{\lambda}) \in H^1(B) \times \boldsymbol{H}(\mathrm{div}0, B) \,. \tag{4.1.66}$$

We use the field energy in the volume integral form:

$$\mathcal{E}_F(\Omega) := \frac{1}{2} \int_\Omega \|\nabla u(\boldsymbol{x})\|^2 \, \mathrm{d}\boldsymbol{x} = \frac{1}{2} \mathsf{a}((u, \boldsymbol{0}), (u, \boldsymbol{0})) \,, \tag{4.1.67}$$

44

where $u = u(\Omega)$ solves (4.1.62). Following the developments in section 4.1.2, we write $(\Omega^s := \mathbf{T}^{\boldsymbol{\nu}}_s(\Omega))_{|s|<\delta}$ for the 1-parameter family of slightly deformed domains induced by a given deformation vector field $\boldsymbol{\mathcal{V}} \in \left(C_0^\infty(B)\right)^d$. Replacing $\Omega \to \Omega^s$, $\partial\Omega \to \partial\Omega^s$ and $\Gamma \to \Gamma^s$ in (4.1.64) yields a s-dependent version of its constituent parts. For $(w, \boldsymbol{\kappa}), (v, \boldsymbol{\lambda}) \in H^1(B) \times \boldsymbol{H}(\mathrm{div}0, B)$:

$$\mathsf{a}(s; (w, \boldsymbol{\kappa}), (v, \boldsymbol{\lambda})) := \int_{\Omega^s} \nabla w \cdot \nabla v \, d\boldsymbol{x} + \int_{\partial\Omega^s} v \, \boldsymbol{\kappa} \cdot \boldsymbol{n} \, dS + \int_{\partial\Omega^s} u \, \boldsymbol{\lambda} \cdot \boldsymbol{n} \, dS , \qquad (4.1.68)$$

$$l_{\widetilde{g}}(s; (v, \boldsymbol{\lambda})) := \int_{\Gamma^s} \widetilde{g} \, \boldsymbol{\lambda} \cdot \boldsymbol{n} \, dS . \qquad (4.1.69)$$

The s dependent energy functional is given as

$$\mathcal{E}_F(s) := J(s; (u_s, \boldsymbol{\mu}_s)) , \quad J(s; (w, \boldsymbol{\kappa})) := \frac{1}{2}\mathsf{a}(s; (w, \mathbf{0}), (w, \mathbf{0})) , \qquad (4.1.70)$$

where $(u_s, \boldsymbol{\mu}_s) \in H^1(B) \times \boldsymbol{H}(\mathrm{div}0, B)$ solves the state problem on Ω^s:

$$\mathsf{a}(s; (u_s, \boldsymbol{\mu}_s), (v, \boldsymbol{\lambda})) = l_{\widetilde{g}}(s; (v, \boldsymbol{\lambda})) \quad \forall (v, \boldsymbol{\lambda}) \in H^1(B) \times \boldsymbol{H}(\mathrm{div}0, B) . \qquad (4.1.71)$$

Notice that in this derivation, the function space framework is already independent of s. Following the adjoint approach [31, Sect. 1.6.4] from section 4.1.4, we can define the relevant Lagrangian. For $(w, \boldsymbol{\kappa}), (v, \boldsymbol{\lambda}) \in H^1(B) \times \boldsymbol{H}(\mathrm{div}0, B)$:

$$L(s; (w, \boldsymbol{\kappa}), (v, \boldsymbol{\lambda})) := J(s; (w, \boldsymbol{\kappa})) + \mathsf{a}(s; (w, \boldsymbol{\kappa}), (v, \boldsymbol{\lambda})) - l_{\widetilde{g}}(s; (v, \boldsymbol{\lambda})) . \qquad (4.1.72)$$

Plugging in $(w, \boldsymbol{\kappa}) = (u_s, \boldsymbol{\mu}_s)$, the solution for (4.1.71), we recover an expression for the field energy

$$\mathcal{E}_F(s) = L(s; (u_s, \boldsymbol{\mu}_s), (v, \boldsymbol{\lambda})) \quad \forall (v, \boldsymbol{\lambda}) \in H^1(B) \times \boldsymbol{H}(\mathrm{div}0, B) . \qquad (4.1.73)$$

Exploiting the freedom to choose $(v, \boldsymbol{\lambda})$, we choose it as the adjoint solution $(\rho, \boldsymbol{\pi}) \in H^1(B) \times \boldsymbol{H}(\mathrm{div}0, B)$ such that

$$\mathsf{a}(0; (v, \boldsymbol{\lambda}), (\rho, \boldsymbol{\pi})) = -\left\langle \frac{\partial J}{\partial(w, \boldsymbol{\kappa})}(0; (u(0), \boldsymbol{\mu}(0))), (v, \boldsymbol{\lambda}) \right\rangle \quad \forall (v, \boldsymbol{\lambda}) \in H^1(B) \times \boldsymbol{H}(\mathrm{div}0, B)$$
$$(4.1.74)$$

$$\Leftrightarrow \qquad \mathsf{a}((v, \boldsymbol{\lambda}), (\rho, \boldsymbol{\pi})) = -\mathsf{a}((v, \mathbf{0}), (u, \mathbf{0})) \quad \forall (v, \boldsymbol{\lambda}) \in H^1(B) \times \boldsymbol{H}(\mathrm{div}0, B) , \qquad (4.1.75)$$

where we used $u(0) = u$ and $\boldsymbol{\mu}(0) = \boldsymbol{\mu}$. The equations can easily be decoupled by putting $v = 0$ or $\boldsymbol{\lambda} = \mathbf{0}$. Thus we see that adjoint solution is $(\rho, \boldsymbol{\pi}) = (0, -\nabla u)$. Now the shape derivative can be computed using only the partial derivatives with respect to s:

$$\frac{d\mathcal{E}_F}{ds}(0) = \frac{\partial L}{\partial s}(0; (u, \boldsymbol{\mu}), (0, -\nabla u)) = \frac{\partial J}{\partial s}(0; (u, \boldsymbol{\mu})) + \frac{\partial \mathsf{a}}{\partial s}(0; (u, \boldsymbol{\mu}), (0, -\nabla u)) - \frac{\partial l_{\widetilde{g}}}{\partial s}(0; (0, -\nabla u)) .$$
$$(4.1.76)$$

Using the identities in section 4.1.4 and [18, Ch. 9, Thm. 4.1], the *partial derivatives* with respect to s can be easily computed, because the integrands are independent of s:

$$\frac{\partial J}{\partial s}(0; (u, \boldsymbol{\mu})) = \frac{1}{2} \int_\Gamma \|\nabla u\|^2 (\boldsymbol{\mathcal{V}} \cdot \boldsymbol{n}) \, dS \,, \tag{4.1.77}$$

$$\frac{\partial \mathsf{a}}{\partial s}(0; (u, \boldsymbol{\mu}), (0, -\nabla u)) = - \int_\Gamma \|\nabla u\|^2 (\boldsymbol{\mathcal{V}} \cdot \boldsymbol{n}) \, dS \,, \tag{4.1.78}$$

$$\frac{\partial l_{\widetilde{g}}}{\partial s}(0; (0, -\nabla u)) = - \int_\Gamma \nabla u \cdot \nabla \widetilde{g} \, (\boldsymbol{\mathcal{V}} \cdot \boldsymbol{n}) \, dS \,. \tag{4.1.79}$$

Summing up and using the fact that $\nabla \widetilde{g} - \nabla u$ is in the normal direction at the surface, we get the shape derivative:

$$\frac{d\mathcal{E}_F}{d\Omega}(\Omega; \boldsymbol{\mathcal{V}}) = \frac{1}{2} \int_\Gamma \left(\left((\nabla \widetilde{g} - \nabla u) \cdot \boldsymbol{n} \right) \left(\nabla u \cdot \boldsymbol{n} \right) + \nabla \widetilde{g} \cdot \nabla u \right) (\boldsymbol{\mathcal{V}} \cdot \boldsymbol{n}) \, dS \,. \tag{4.1.80}$$

4.1.11.2   Derivation of Volume-based Shape Derivative Formula

We start from the variational formulation of (4.1.1) in the Sobolev space $H_0^1(\Omega)$ using $w := u - \widetilde{g} \in H_0^1(\Omega)$:

$$w \in H_0^1(\Omega): \quad \mathsf{a}(w, v) := \int_\Omega \nabla w \cdot \nabla v \, d\boldsymbol{x} = l_{\widetilde{g}}(v) := - \int_\Omega \boldsymbol{G} \cdot \nabla v \, d\boldsymbol{x} \quad \forall v \in H_0^1(\Omega) \,, \tag{4.1.81}$$

where $g = \widetilde{g}|_\Gamma$ for a $\widetilde{g} \in H^1(\Omega)$ that vanishes on ∂B and $\boldsymbol{G} := \nabla \widetilde{g}$. By the Lax-Milgram lemma [12, Sect. 6.2] existence and uniqueness of w is guaranteed. We use the energy functional in the volume integral form

$$\mathcal{E}_F(\Omega) := \frac{1}{2} \int_\Omega \|\nabla u(\boldsymbol{x})\|^2 \, d\boldsymbol{x} = \frac{1}{2} \int_\Omega \|\nabla w(\boldsymbol{x}) + \boldsymbol{G}(\boldsymbol{x})\|^2 \, d\boldsymbol{x} \,, \tag{4.1.82}$$

where $w = w(\Omega)$ solves (4.1.81). Following the definitions in section 4.1.2, we write $(\Omega^s := \mathbf{T}_s^{\boldsymbol{\nu}}(\Omega))_{|s| < \delta}$ for the 1-parameter family of slightly deformed domains induced by a given deformation vector field $\boldsymbol{\mathcal{V}} \in \left(C_0^\infty(B) \right)^d$. Considering $\widetilde{g} \in H_0^1(B)$ and replacing $\Omega \to \Omega^s$ in (4.1.81) yields a s-dependent version:

$$w_s \in H_0^1(\Omega^s): \quad \mathsf{a}(s; w_s, v) = l_{\widetilde{g}}(s; v) \quad \forall v \in H_0^1(\Omega^s) \,, \tag{4.1.83}$$

where, for $w, v \in H_0^1(\Omega^s)$,

$$\mathsf{a}(s; w, v) := \int_{\Omega^s} \nabla w \cdot \nabla v \, d\boldsymbol{x}, \quad l_{\widetilde{g}}(s; v) := - \int_{\Omega^s} \boldsymbol{G} \cdot \nabla v \, d\boldsymbol{x} \,. \tag{4.1.84}$$

Transforming integrals back to the reference domain Ω we arrive at a variational characterization of the pullback $\hat{w}_s := w(\Omega^s) \circ \mathbf{T}_s^{\boldsymbol{\nu}}$: Seek $\hat{w}_s \in H_0^1(\Omega)$ such that

$$\hat{\mathsf{a}}(s; \hat{w}_s, \hat{v}) = \hat{l}_{\widetilde{g}}(s; \hat{v}) \quad \forall \hat{v} \in H_0^1(\Omega) \,, \tag{4.1.85}$$

where, for $\hat{w}, \hat{v} \in H_0^1(\Omega)$,

$$\hat{\mathsf{a}}(s; \hat{w}, \hat{v}) := \int_\Omega (\mathsf{D}\mathbf{T}_s^\nu(\hat{\boldsymbol{x}})^{-\top} \nabla \hat{w}) \cdot (\mathsf{D}\mathbf{T}_s^\nu(\hat{\boldsymbol{x}})^{-\top} \nabla \hat{v}) |\det \mathsf{D}\mathbf{T}_s^\nu(\hat{\boldsymbol{x}})| \, \mathrm{d}\hat{\boldsymbol{x}} \,, \tag{4.1.86}$$

$$\hat{l}_{\widetilde{g}}(s; \hat{v}) := -\int_\Omega \boldsymbol{G}(\mathbf{T}_s^\nu(\hat{\boldsymbol{x}})) \cdot (\mathsf{D}\mathbf{T}_s^\nu(\hat{\boldsymbol{x}})^{-\top} \nabla \hat{v}) \, |\det \mathsf{D}\mathbf{T}_s^\nu(\hat{\boldsymbol{x}})| \, \mathrm{d}\hat{\boldsymbol{x}} \,. \tag{4.1.87}$$

The field energy is also dependent on the parameter s and is given as:

$$\mathcal{E}_F(s) = \hat{J}(s; \hat{w}_s) \,, \quad \hat{J}(s; \hat{w}) := \frac{1}{2} \int_\Omega \left\| \mathsf{D}\mathbf{T}_s^\nu(\hat{\boldsymbol{x}})^{-\top} \nabla \hat{w}(\hat{\boldsymbol{x}}) + \boldsymbol{G}(\mathbf{T}_s^\nu(\hat{\boldsymbol{x}})) \right\|^2 \, |\det \mathsf{D}\mathbf{T}_s^\nu(\hat{\boldsymbol{x}})| \, \mathrm{d}\hat{\boldsymbol{x}} \,.$$
$$\tag{4.1.88}$$

Following the steps in section. 4.1.4, we use the adjoint approach [31, Sect. 1.6.4] and define the relevant Lagrangian for $\hat{w}, \hat{v} \in H_0^1(\Omega)$:

$$L(s; \hat{w}, \hat{v}) := \hat{J}(s; \hat{w}) + \hat{\mathsf{a}}(s; \hat{w}, \hat{v}) - \hat{l}_{\widetilde{g}}(s; \hat{v}) \,. \tag{4.1.89}$$

Plugging in $\hat{w} = \hat{w}_s$, we recover the expression for field energy

$$\mathcal{E}_F(s) = L(s; \hat{w}_s, \hat{v}) \quad \forall \hat{v} \in H_0^1(\Omega) \,. \tag{4.1.90}$$

Since we are free to choose $\hat{v}$, we choose it as the adjoint solution ρ which solves

$$\rho \in H_0^1(\Omega) : \quad \hat{\mathsf{a}}(0; \hat{v}, \rho) = -\left\langle \frac{\partial \hat{J}}{\partial \hat{w}}(0; \hat{w}(0)), \hat{v} \right\rangle \quad \forall \hat{v} \in H_0^1(\Omega) \tag{4.1.91}$$

$$\Leftrightarrow \qquad \mathsf{a}(v, \rho) = -\int_\Omega (\nabla w + \boldsymbol{G}) \cdot \nabla v \, \mathrm{d}\boldsymbol{x} = 0 \quad \forall v \in H_0^1(\Omega) \,, \tag{4.1.92}$$

where in the last equality we used (4.1.81) and the fact that $\hat{w}_0 = w$. This gives us the adjoint solution $\rho \equiv 0$ and allows us to calculate the shape derivative in terms of partial derivatives of s:

$$\frac{d\mathcal{E}_F}{ds}(0) = \frac{\partial L}{\partial s}(0; \hat{w}(0), \rho) = \frac{\partial \hat{J}}{\partial s}(0; w) + \frac{\partial \hat{\mathsf{a}}}{\partial s}(0; w, \rho) - \frac{\partial \hat{\ell}_{\widetilde{g}}}{\partial s}(0; \rho) \,. \tag{4.1.93}$$

The last two terms go to zero and we are left with the partial derivative of $\hat{J}(0; w)$ defined in (4.1.88). We can swap integration with the partial derivative and using the required expressions from section 4.1.4 we get

$$\frac{d\mathcal{E}_F}{ds}(0) = \frac{1}{2} \int_\Omega ||\nabla u||^2 \nabla \cdot \boldsymbol{\mathcal{V}} + 2\nabla u \cdot (-\nabla \boldsymbol{\mathcal{V}} \nabla u + \nabla \boldsymbol{\mathcal{V}} \nabla \widetilde{g} + \nabla \nabla \widetilde{g} \boldsymbol{\mathcal{V}}) \, \mathrm{d}\boldsymbol{x} \,, \tag{4.1.94}$$

where we used $w = u - \widetilde{g}$.

4.1.11.3 Equivalence of volume based and boundary based shape derivatives

We start with the Volume formula from (4.1.94):

$$\frac{1}{2}\int_{\Omega}\Big(\|\nabla u\|^{2}\,\nabla\cdot\boldsymbol{\mathcal{V}}+2\,\nabla u\cdot\Big(-\nabla\boldsymbol{\mathcal{V}}\nabla u+\nabla\boldsymbol{\mathcal{V}}\nabla\widetilde{g}+\nabla\nabla\widetilde{g}^{T}\boldsymbol{\mathcal{V}}\Big)\Big)dx\ .$$

This can be written as :

$$\frac{1}{2}\int_{\Omega}\Big(\nabla\cdot\Big(\|\nabla u\|^{2}\,\boldsymbol{\mathcal{V}}\Big)+2\ \nabla u\cdot\Big(-\nabla\boldsymbol{\mathcal{V}}\nabla u\ +\ \nabla\boldsymbol{\mathcal{V}}\nabla\widetilde{g}+\nabla\nabla\widetilde{g}^{T}\boldsymbol{\mathcal{V}}\ -\ \nabla\nabla u^{T}\boldsymbol{\mathcal{V}}\Big)\Big)dx\ .$$

Since $\nabla\nabla u$ and $\nabla\nabla\widetilde{g}$ are symmetric, the highlighted terms can be combined together to give:

$$\frac{1}{2}\int_{\Omega}\nabla\cdot\Big(\|\nabla u\|^{2}\,\boldsymbol{\mathcal{V}}\Big)+2\,\nabla u\cdot\Big(-\nabla(\boldsymbol{\mathcal{V}}\cdot\nabla u)\ +\ \nabla(\boldsymbol{\mathcal{V}}\cdot\nabla\widetilde{g})\Big)dx\ .$$

This can be further simplified by combining the two highlighted terms:

$$\frac{1}{2}\int_{\Omega}\nabla\cdot\Big(\|\nabla u\|^{2}\,\boldsymbol{\mathcal{V}}\Big)+2\nabla u\cdot\nabla\Big(\boldsymbol{\mathcal{V}}\cdot(\nabla\widetilde{g}-\nabla u)\Big)dx\ .$$

Using the Divergence theorem for the first term and Green's first formula for the second term with $\Delta u=0$, we get:

$$\frac{1}{2}\int_{\partial\Omega}\|\nabla u\|^{2}\,\boldsymbol{\mathcal{V}}\cdot\mathbf{n}\,d\mathrm{S}+\int_{\partial\Omega}\nabla u\cdot\mathbf{n}\,\Big(\boldsymbol{\mathcal{V}}\cdot(\nabla\widetilde{g}-\nabla u)\Big)d\mathrm{S}\ .$$

On the boundary, we know that $\nabla\widetilde{g}-\nabla u$ is in the normal direction. Using that we get:

$$\frac{1}{2}\int_{\partial\Omega}\|\nabla u\|^{2}\,\boldsymbol{\mathcal{V}}\cdot\mathbf{n}\,d\mathrm{S}+\int_{\partial\Omega}\nabla u\cdot\mathbf{n}\,(\nabla\widetilde{g}-\nabla u)\cdot\mathbf{n}\,\boldsymbol{\mathcal{V}}\cdot\mathbf{n}\,d\mathrm{S}\ ,$$

Whis can be rewritten as:

$$\frac{1}{2}\int_{\partial\Omega}\|\nabla u\|^{2}\,\boldsymbol{\mathcal{V}}\cdot\mathbf{n}\,d\mathrm{S}+\int_{\partial\Omega}\nabla u\cdot(\nabla\widetilde{g}-\nabla u)\,\boldsymbol{\mathcal{V}}\cdot\mathbf{n}\,d\mathrm{S}\ .$$

Thus we recover the boundary based shape derivative seen in (4.1.51).

4.2 Floating Potential Problem in 3D

The contents concerning the floating potential problem have been reproduced with permission from Springer Nature [49]. We have two solid conducting objects occupying bounded, open and simply connected domains $D, B \subset \mathbb{R}^{3}$ with C^{2}_{pw} boundaries. The complement $M := \mathbb{R}^{3}\setminus(\overline{B}\cup\overline{D})$ is occupied by a homogeneous, linear and isotropic dielectric medium with its dielectric tensor given by the Kronecker delta, $\varepsilon_{ij} := \delta_{ij}, \ i,j \in \{1,2,3\}$. The solid object B is grounded (at electrostatic potential 0), whereas the solid object D has a

known net electric charge Q which resides entirely on its surface, a phenomenon well known for conductors in electrostatic equilibrium [23]. Writing ∂B and ∂D for the boundaries of these conducting objects, the electrostatic potential u can be obtained as the weak solution in $H^1(M)$ of the linear, constant coefficient homogeneous Poisson boundary value problem (BVP) on the unbounded domain M:

$$
\begin{aligned}
\Delta u &= 0 && \text{in} \quad M, \\
u &= 0 && \text{on} \quad \partial B, \\
u &= c && \text{on} \quad \partial D, \\
\int_{\partial D} \nabla u \cdot \boldsymbol{n}\, d\mathrm{S} &= -Q && \text{on} \quad \partial D, \\
u(\boldsymbol{x}) &= \mathcal{O}(\|\boldsymbol{x}\|^{-1}) && \text{as} \quad \|\boldsymbol{x}\| \to \infty,
\end{aligned}
\tag{4.2.1}
$$

where c is the unknown constant potential of the conducting body D and $\boldsymbol{n}$ is the exterior unit normal vector field on the conducting objects D and B. The model electrostatic boundary value problem (4.2.1) is known as the floating potential problem in literature [1].

Remark 8. The unbounded electrostatic setting chosen in our considerations becomes non-physical in $\mathbb{R}^2$ as the electric field energy in the unbounded domain goes to infinity due to a mere $O(\|\boldsymbol{x}\|^{-1})$ decay of the field for $\|\boldsymbol{x}\| \to \infty$. This problem can be circumvented with the additional constraint that the combined net charge on D and B is zero, leading to a faster $O(\|\boldsymbol{x}\|^{-2})$ decay for $\|\boldsymbol{x}\| \to \infty$.

For solving the model problem (4.2.1), we use the first BIE for the exterior traces in (2.1.22) also known as the direct first kind formulation [54, Sec. 3.4.2]. The corresponding boundary integral equation is

$$
\mathrm{V}(\gamma_N^+ u) = \left(-\tfrac{Id}{2} + \mathrm{K}\right)(\gamma_D^+ u),
\tag{4.2.2}
$$

where $\gamma_N^+ u$ and $\gamma_D^+ u$ are the exterior Neumann and Dirichlet traces respectively of the solution u. They are defined for smooth functions as

$$
\begin{aligned}
\gamma_N^+ u(\boldsymbol{x}^*) &:= \lim_{\boldsymbol{x} \in M \to \boldsymbol{x}^* \in \partial M} \nabla u(\boldsymbol{x}) \cdot \boldsymbol{n}(\boldsymbol{x}^*), \\
\gamma_D^+ u(\boldsymbol{x}^*) &:= \lim_{\boldsymbol{x} \in M \to \boldsymbol{x}^* \in \partial M} u(\boldsymbol{x}),
\end{aligned}
$$

where $\boldsymbol{n}$ is the unit exterior normal vector field on the boundary $\Gamma := \partial D \cup \partial B$. In Equation (4.2.2), V is the Single-layer BIO and K is the Double-layer BIO, introduced in Section 2.1. The BIOs V and K are continuous, linear operators between the following spaces:

$$
\mathrm{V} : H^{-\frac{1}{2}}(\Gamma) \to H^{\frac{1}{2}}(\Gamma), \quad \mathrm{K} : H^{\frac{1}{2}}(\Gamma) \to H^{\frac{1}{2}}(\Gamma).
$$

Writing the Dirichlet trace as $\gamma_D u = c\, \mathbb{1}_{\partial D}$ and the Neumann trace as $\gamma_N u = \psi$, Equation (4.2.2) becomes

$$
\mathrm{V}\,\psi(\boldsymbol{x}) = -\frac{c}{2}\mathbb{1}_{\partial D}(\boldsymbol{x}) + c\,\mathrm{K}\,\mathbb{1}_{\partial D}(\boldsymbol{x}) \quad \boldsymbol{x} \in \Gamma,
\tag{4.2.3}
$$

where K $\mathbb{1}_{\partial D}(\boldsymbol{x})$ can be simplified further as

$$
\begin{aligned}
\text{K } \mathbb{1}_{\partial D}(\boldsymbol{x}) &= \int_{\Gamma} \nabla G(\boldsymbol{x}, \boldsymbol{y}) \cdot \boldsymbol{n}(\boldsymbol{y}) \; \mathbb{1}_{\partial D}(\boldsymbol{y}) \; dS(\boldsymbol{y}) \\
&= \int_{\partial D} \nabla G(\boldsymbol{x}, \boldsymbol{y}) \cdot \boldsymbol{n}(\boldsymbol{y}) \; dS(\boldsymbol{y}) \qquad = \begin{cases} 0 & \text{if } \boldsymbol{x} \in \partial B, \\ -\frac{1}{2} & \text{almost everywhere on } \partial D, \end{cases}
\end{aligned}
\tag{4.2.4}
$$

which yields

$$
\text{V } \psi(\boldsymbol{x}) + c \; \mathbb{1}_{\partial D}(\boldsymbol{x}) = 0 \quad \boldsymbol{x} \in \Gamma.
\tag{4.2.5}
$$

4.2.1 Variational Boundary Integral Equations

To get the variational formulation we test Equation (4.2.2) with $\phi \in H^{-\frac{1}{2}}(\Gamma)$. Another equation is provided by the fixed charge constraint which we test with some non-zero constant $d \in \mathbb{R}$. We obtain the mixed formulation: seek $\psi, c \in H^{-\frac{1}{2}}(\Gamma) \times \mathbb{R}$ such that

$$
\int_{\Gamma} \text{V } \psi(\boldsymbol{x}) \; \phi(\boldsymbol{x}) \; dS(\boldsymbol{x}) + c \int_{\Gamma} \mathbb{1}_{\partial D}(\boldsymbol{x}) \; \phi(\boldsymbol{x}) \; dS(\boldsymbol{x}) = 0 \qquad \forall \phi \in H^{-\frac{1}{2}}(\Gamma),
$$

$$
p \int_{\Gamma} \mathbb{1}_{\partial D}(\boldsymbol{x}) \psi(\boldsymbol{x}) \; dS(\boldsymbol{x}) = -p \; Q \qquad \forall p \in \mathbb{R}
\tag{4.2.6}
$$

This system of equations can be written in a compact way by introducing notation for the bilinear forms that we encounter:

$$
\text{a}_\text{V} : \begin{cases} H^{-\frac{1}{2}}(\Gamma) \times H^{-\frac{1}{2}}(\Gamma) \to \mathbb{R} \\ (\psi, \phi) \mapsto \int_{\Gamma} \text{V } \psi(\boldsymbol{x}) \; \phi(\boldsymbol{x}) dS(\boldsymbol{x}) := \int_{\Gamma} \int_{\Gamma} G(\boldsymbol{x}, \boldsymbol{y}) \psi(\boldsymbol{x}) \phi(\boldsymbol{y}) \; dS(\boldsymbol{y}) dS(\boldsymbol{x}), \end{cases}
$$

$$
\text{b} : \begin{cases} H^{-\frac{1}{2}}(\Gamma) \times \mathbb{R} \to \mathbb{R} \\ (\phi, p) \mapsto p \int_{\Gamma} \mathbb{1}_{\partial D}(\boldsymbol{x}) \phi(\boldsymbol{x}) \; dS(\boldsymbol{x}). \end{cases}
$$

where $G(\boldsymbol{x}, \boldsymbol{y})$ is the fundamental solution for the Laplace operator. This notation allows us to write (4.2.6) compactly

$$
\begin{aligned}
\text{a}_\text{V}(\psi, \phi) + \text{b}(\phi, c) &= 0 \qquad \forall \phi \in H^{-\frac{1}{2}}(\Gamma), \\
\text{b}(\psi, p) &= -p \; Q \quad \forall p \in \mathbb{R}.
\end{aligned}
\tag{4.2.7}
$$

We note that the equations above have a saddle-point structure. The bilinear form a_V is bounded and elliptic on $H^{-\frac{1}{2}}(\Gamma)$ and we refer to [54, Thm. 3.5.3], [58] for the proof. The bilinear form b is bounded on $H^{-\frac{1}{2}}(\Gamma) \times \mathbb{R}$ which is trivial considering the $L^2(\Gamma)$ duality

pairing that appears in the expression. The stability condition [58, Thm. 3.11] for the bilinear form b can be shown easily:

$$\sup_{0 \neq \phi \in H^{-\frac{1}{2}}(\Gamma)} \frac{\mathrm{b}(\phi, p)}{\|\phi\|_{H^{-\frac{1}{2}}(\Gamma)}} \geq \frac{\mathrm{b}(-p\psi, p)}{\|-p\psi\|_{H^{-\frac{1}{2}}(\Gamma)}} = C \, |p|.$$

The conditions listed in [58, Thm. 3.11] are satisfied, thus we have the unique solvability of (4.2.7).

Remark 9. Due to the special structure of the bilinear form b we have $\mathrm{b}(\phi, c) = c \, \mathrm{b}(\phi, 1)$. Assuming $c \neq 0$ we can divide by c and get

$$\mathrm{a_V}(\frac{\psi}{c}, \phi) = -\mathrm{b}(\phi, 1) \quad \forall \phi \in H^{-\frac{1}{2}}(\Gamma).$$

The above equation has a unique solution $\psi_1 \in H^{-\frac{1}{2}}(\Gamma)$ due to the ellipticity of $\mathrm{a_V}$ in $H^{-\frac{1}{2}}(\Gamma)$. The solution $\psi = c \, \psi_1$ can be obtained by scaling and the solution c is obtained via Q given in fixed charge constraint.

$$c = -\frac{Q}{\mathrm{b}(\psi_1, 1)}.$$

To bring the system of equations to a standard variational form, we add the two equations in (4.2.7) and write: seek $\begin{bmatrix} \psi \\ c \end{bmatrix} \in V := H^{-\frac{1}{2}}(\Gamma) \times \mathbb{R}$ such that

$$\mathrm{A}(\begin{bmatrix} \psi \\ c \end{bmatrix}, \begin{bmatrix} \phi \\ p \end{bmatrix}) = \mathrm{L}(\begin{bmatrix} \phi \\ p \end{bmatrix}) \quad \forall \begin{bmatrix} \phi \\ p \end{bmatrix} \in V, \tag{4.2.8}$$

where the bilinear form A and the linear form L are defined as

$$\mathrm{A} : \begin{cases} V \times V \to \mathbb{R}, \\ \mathrm{A}(\begin{bmatrix} \psi \\ c \end{bmatrix}, \begin{bmatrix} \phi \\ p \end{bmatrix}) := \mathrm{a_V}(\psi, \phi) + \mathrm{b}(\phi, c) + \mathrm{b}(\psi, p), \end{cases}$$

$$\mathrm{L} : \begin{cases} V \to \mathbb{R}, \\ \mathrm{L}(\begin{bmatrix} \phi \\ p \end{bmatrix}) := -p \, Q. \end{cases}$$

This form is amenable to a Galerkin discretization for numerical solution.

4.2.2 Variational Formulation on Deformed Domain

Let $\Omega^0 := D^0 \cup B^0$ denote the reference configuration for which we want to compute forces, where D^0 and B^0 are the reference states for the conducting objects. To apply the Virtual Work Principle via shape calculus, we consider the floating potential problem from Section 4.2 for a set of admissible domains $\mathcal{A}_{\boldsymbol{\mathcal{V}}} := \{\Omega^s := \mathbf{T}_s^{\boldsymbol{\nu}}(\Omega^0), \; s \in (-\delta(\boldsymbol{\mathcal{V}}), \delta(\boldsymbol{\mathcal{V}}))\}$. For all configurations $s \in (-\delta(\boldsymbol{\mathcal{V}}), \delta(\boldsymbol{\mathcal{V}}))\}$, the conducting object $B^s := \mathbf{T}_s^{\boldsymbol{\nu}}(B^0)$ is grounded and $D^s := \mathbf{T}_s^{\boldsymbol{\nu}}(D^0)$ carries the net charge Q. The solution $\psi_s, c_s \in H^{-\frac{1}{2}}(\Gamma^s) \times \mathbb{R}$ now becomes

dependent on the configuration. Since the only connected conducting body is grounded, the total energy $\mathcal{E}(s)$ comprises of only the field energy $\mathcal{E}_F(s)$

$$\mathcal{E}_F(s) := \frac{1}{2} \int\limits_{\mathbb{R}^3 \setminus \overline{\Omega^s}} \|\nabla u_s(\boldsymbol{x})\|^2 \ \mathrm{d}\boldsymbol{x}, \tag{4.2.9}$$

where u_s is the solution corresponding to $\Omega^s \in \mathcal{A}_{\mathcal{V}}$. Using Green's identity and the decay condition for the solution u_s we can get a boundary integral expression for the energy functional.

$$\frac{1}{2} \int\limits_{\mathbb{R}^3 \setminus \overline{\Omega^s}} \|\nabla u_s(\boldsymbol{x})\|^2 \ \mathrm{d}\boldsymbol{x} = \lim_{R \to \infty} \frac{1}{2} \int\limits_{B_R(0) \cap (\mathbb{R}^3 \setminus \overline{\Omega^s})} \|\nabla u_s(\boldsymbol{x})\|^2 \ \mathrm{d}\boldsymbol{x}$$

$$= \lim_{R \to \infty} -\frac{1}{2} \int\limits_{\partial D^s} c_s \ \psi_s(\boldsymbol{x}) \ d\mathrm{S}(\boldsymbol{x}) + \lim_{R \to \infty} \frac{1}{2} \int\limits_{\partial B_R(0)} u_s(\boldsymbol{x}) \ \nabla u_s(\boldsymbol{x}) \cdot \boldsymbol{n}(\boldsymbol{x}) \ d\mathrm{S}(\boldsymbol{x})$$

$$= -\frac{1}{2} \int\limits_{\partial D^s} c_s \ \psi_s(\boldsymbol{x}) \ d\mathrm{S}(\boldsymbol{x}) = \frac{c_s \ Q}{2} =: J(s; (\psi_s, c_s)).$$

We recognize the final expression for energy being the familiar formula for energy stored in a capacitor [23, Eq. 2.5].

For the s configuration we seek $\begin{bmatrix} \psi_s \\ c_s \end{bmatrix} \in V_s := H^{-\frac{1}{2}}(\Gamma^s) \times \mathbb{R}$ such that

$$\mathrm{A}(s)(\begin{bmatrix} \psi_s \\ c_s \end{bmatrix}, \begin{bmatrix} \phi \\ d \end{bmatrix}) = \mathrm{L}(s)(\begin{bmatrix} \phi \\ d \end{bmatrix}) \quad \forall \begin{bmatrix} \phi \\ d \end{bmatrix} \in V_s, \tag{4.2.10}$$

where the augmented s dependent bilinear and linear forms are defined as:

$$\mathrm{A}(s) : \begin{cases} V_s \times V_s \to \mathbb{R}, \\ \mathrm{A}(s)(\begin{bmatrix} \psi \\ c \end{bmatrix}, \begin{bmatrix} \phi \\ d \end{bmatrix}) := \mathrm{a_V}(s)(\psi, \phi) + \mathrm{b}(s)(\phi, c) + \mathrm{b}(s)(\psi, d), \end{cases}$$

$$\mathrm{L}(s) : \begin{cases} V_s \to \mathbb{R}, \\ \mathrm{L}(s)(\begin{bmatrix} \phi \\ d \end{bmatrix}) := -d \ Q, \end{cases}$$

and

$$\mathrm{a_V}(s) : \begin{cases} H^{-\frac{1}{2}}(\Gamma^s) \times H^{-\frac{1}{2}}(\Gamma^s) \to \mathbb{R} \\ \mathrm{a_V}(s)(\psi, \phi) := \int\limits_{\Gamma^s} \int\limits_{\Gamma^s} G(\boldsymbol{x}, \boldsymbol{y}) \psi(\boldsymbol{x}) \phi(\boldsymbol{y}) \ d\mathrm{S}(\boldsymbol{y}) d\mathrm{S}(\boldsymbol{x}), \end{cases}$$

$$\mathrm{b}(s) : \begin{cases} H^{-\frac{1}{2}}(\Gamma^s) \times \mathbb{R} \to \mathbb{R} \\ \mathrm{b}(s)(\phi, d) := d \int\limits_{\Gamma^s} \mathbb{1}_{\partial D}(\boldsymbol{x}) \phi(\boldsymbol{x}) \ d\mathrm{S}(\boldsymbol{x}). \end{cases}$$

4.2.3 Equivalent Formulation on Reference Domain

The expressions appearing in eq. (4.2.10) contain integrals on Γ^s which can be transformed to integrals on the reference boundary Γ^0 using the formula

$$\int_{\Gamma^s} f(\boldsymbol{y})\, dS(\boldsymbol{y}) = \int_{\Gamma^0} f(\mathbf{T}_s^{\boldsymbol{\nu}}(\boldsymbol{x}))\, \omega_s(\boldsymbol{x})\, dS(\boldsymbol{x}), \quad \boldsymbol{y} = \mathbf{T}_s^{\boldsymbol{\nu}}(\boldsymbol{x}), \tag{4.2.11}$$

where $\omega_s(\boldsymbol{x}) := \|\mathbf{C}(D\mathbf{T}_s^{\boldsymbol{\nu}}(\boldsymbol{x}))\, \boldsymbol{n}_0(\boldsymbol{x})\|$ is the Jacobian of transformation, $\boldsymbol{n}_0$ is the exterior unit normal vector field on Γ^0 and $\mathbf{C}(\mathbf{A})$ denotes the cofactor matrix of $\mathbf{A}$. We get integral expressions on the reference boundary:

$$\begin{aligned}
&A(s)(\begin{bmatrix} \psi \\ c \end{bmatrix}, \begin{bmatrix} \phi \\ d \end{bmatrix}) \\
&= \int_{\Gamma^0}\int_{\Gamma^0} G(\mathbf{T}_s^{\boldsymbol{\nu}}(\boldsymbol{x}), \mathbf{T}_s^{\boldsymbol{\nu}}(\boldsymbol{y}))\, \psi(\mathbf{T}_s^{\boldsymbol{\nu}}(\boldsymbol{x}))\, \omega_s(\boldsymbol{x})\, \phi(\mathbf{T}_s^{\boldsymbol{\nu}}(\boldsymbol{y}))\, \omega_s(\boldsymbol{y})\, dS(\boldsymbol{x})\, dS(\boldsymbol{y}) \\
&\quad + c \int_{\partial D^0} \psi(\mathbf{T}_s^{\boldsymbol{\nu}}(\boldsymbol{x}))\, \omega_s(\boldsymbol{x})\, dS(\boldsymbol{x}) + d \int_{\partial D^0} \phi(\mathbf{T}_s^{\boldsymbol{\nu}}(\boldsymbol{x}))\, \omega_s(\boldsymbol{x})\, dS(\boldsymbol{x}).
\end{aligned}$$

This transformation is not necessary for the linear form $L(s)(\begin{bmatrix} \phi \\ d \end{bmatrix})$ or the energy functional $J(s; \begin{bmatrix} \phi \\ d \end{bmatrix})$ as they involve simple expressions without integrals. The next step is to get rid of function spaces on Γ^s which we accomplish using the pullback for surface charge densities (3.0.17):

$$\hat{\psi} \in H^{-\frac{1}{2}}(\Gamma^0): \quad \hat{\psi} := (\psi \circ \mathbf{T}_s^{\boldsymbol{\nu}})\, \omega_s, \quad \psi \in H^{-\frac{1}{2}}(\Gamma^s). \tag{4.2.12}$$

Since $\mathbf{T}_s^{\boldsymbol{\nu}}$ is a Lipschitz continuous mapping and $\omega_s \in L^\infty(\Gamma^0)$, the trace spaces are preserved under pullback. This allows us to write an equivalent formulation to (4.2.10): we seek $\hat{\psi}_s, c_s \in V_0 = H^{-\frac{1}{2}}(\Gamma^0) \times \mathbb{R}$ such that

$$\hat{A}(s; \begin{bmatrix} \hat{\psi}_s \\ c_s \end{bmatrix}, \begin{bmatrix} \hat{\phi} \\ d \end{bmatrix}) = \hat{L}(s; \begin{bmatrix} \hat{\phi} \\ d \end{bmatrix}) \quad \forall \begin{bmatrix} \hat{\phi} \\ d \end{bmatrix} \in V_0. \tag{4.2.13}$$

where the bilinear form $\hat{A} : \mathbb{R} \times V_0 \times V_0 \to \mathbb{R}$ and the linear form $\hat{L} : \mathbb{R} \times V_0 \to \mathbb{R}$ are defined as:

$$\hat{A}(s): \begin{cases} V_0 \times V_0 \to \mathbb{R} \\[4pt] \hat{A}(s; \begin{bmatrix} \psi \\ c \end{bmatrix}, \begin{bmatrix} \phi \\ d \end{bmatrix}) := \displaystyle\int_{\Gamma^0}\int_{\Gamma^0} G(\mathbf{T}_s^{\boldsymbol{\nu}}(\boldsymbol{x}), \mathbf{T}_s^{\boldsymbol{\nu}}(\boldsymbol{y}))\, \psi(\boldsymbol{x})\, \phi(\boldsymbol{y})\, dS(\boldsymbol{x})\, dS(\boldsymbol{y}) \\[10pt] \quad + c \displaystyle\int_{\partial D^0} \psi(\boldsymbol{x})\, dS(\boldsymbol{x}) + d \displaystyle\int_{\partial D^0} \phi(\boldsymbol{x})\, dS(\boldsymbol{x}) \end{cases}$$

$$\hat{L}(s): \begin{cases} V_0 \to \mathbb{R} \\[4pt] \hat{L}(s; \begin{bmatrix} \phi \\ d \end{bmatrix}) := -d\, Q, \end{cases}$$

In a similar fashion we need a pulled back version of the energy functional $\hat{J} : \mathbb{R} \times V_0 \to \mathbb{R}$,
$\hat{J}(s; \begin{bmatrix} \phi \\ d \end{bmatrix}) := \frac{dQ}{2}$.

4.2.4   BIE-Constrained Shape Derivative

The energy shape derivative has to be calculated taking the BIE constraint (4.2.13) into account. For computing such a constrained shape derivative we use the well known adjoint approach from literature [31, Sect. 1.6.4]. To perform the computation, we start with defining the lagrangian $\mathcal{L} : \mathbb{R} \times V_0 \times V_0 \to \mathbb{R}$

$$\mathcal{L}(s; \begin{bmatrix} \hat{\psi} \\ c \end{bmatrix}, \begin{bmatrix} \hat{\phi} \\ d \end{bmatrix}) := \hat{A}(s; \begin{bmatrix} \hat{\psi} \\ c \end{bmatrix}, \begin{bmatrix} \hat{\phi} \\ d \end{bmatrix}) - \hat{L}(s; \begin{bmatrix} \hat{\phi} \\ d \end{bmatrix}) + \hat{J}(s; \begin{bmatrix} \hat{\psi} \\ c \end{bmatrix}). \tag{4.2.14}$$

We observe that by plugging in the state solution $\begin{bmatrix} \hat{\psi} \\ c \end{bmatrix} = \begin{bmatrix} \hat{\psi}_s \\ c_s \end{bmatrix}$ we get

$$\mathcal{L}(s; \begin{bmatrix} \hat{\psi}_s \\ c_s \end{bmatrix}, \begin{bmatrix} \hat{\phi} \\ d \end{bmatrix}) = \hat{J}(s; \begin{bmatrix} \hat{\psi}_s \\ c_s \end{bmatrix}) = \mathcal{E}_F(s) \quad \forall \begin{bmatrix} \hat{\phi} \\ d \end{bmatrix} \in H^{-\frac{1}{2}}(\Gamma_0) \times \mathbb{R}. \tag{4.2.15}$$

From the above expression, the energy shape derivative can be calculated as

$$\frac{d}{ds}\mathcal{E}_F(s)|_{s=0} = \frac{\partial}{\partial s}\mathcal{L}(s; \begin{bmatrix} \hat{\psi}_s \\ c_s \end{bmatrix}, \begin{bmatrix} \hat{\zeta} \\ e \end{bmatrix})|_{s=0}, \tag{4.2.16}$$

where $\begin{bmatrix} \hat{\zeta} \\ e \end{bmatrix} \in H^{-\frac{1}{2}}(\Gamma_0) \times \mathbb{R}$ solves the adjoint equation

$$\left\langle \frac{\partial \mathcal{L}}{\partial \begin{bmatrix} \hat{\psi} \\ c \end{bmatrix}}(s; \begin{bmatrix} \hat{\psi}_s \\ c_s \end{bmatrix}, \begin{bmatrix} \hat{\zeta} \\ e \end{bmatrix}), \begin{bmatrix} \hat{\eta} \\ k \end{bmatrix} \right\rangle |_{s=0} = 0 \quad \forall \begin{bmatrix} \hat{\eta} \\ k \end{bmatrix} \in H^{-\frac{1}{2}}(\Gamma_0) \times \mathbb{R}. \tag{4.2.17}$$

Using the definition of Lagrangian the adjoint equation becomes

$$\hat{A}(0; \begin{bmatrix} \hat{\eta} \\ k \end{bmatrix}, \begin{bmatrix} \hat{\zeta} \\ e \end{bmatrix}) + \frac{kQ}{2} = 0 \quad \forall \begin{bmatrix} \hat{\eta} \\ k \end{bmatrix} \in H^{-\frac{1}{2}}(\Gamma_0) \times \mathbb{R}. \tag{4.2.18}$$

Using symmetry of the bilinear form and comparing with (4.2.13), we immediately get the adjoint solution $\begin{bmatrix} \hat{\zeta} \\ e \end{bmatrix} = \frac{1}{2} \begin{bmatrix} \psi_0 \\ c_0 \end{bmatrix}$ and the shape derivative can be obtained via the partial derivative with respect to s:

$$\begin{aligned} \frac{d}{ds}\mathcal{E}(s)|_{s=0} &= \frac{\partial}{\partial s}\mathcal{L}(0; \begin{bmatrix} \psi_0 \\ c_0 \end{bmatrix}, \frac{1}{2}\begin{bmatrix} \psi_0 \\ c_0 \end{bmatrix}) \\ &= \frac{\partial}{\partial s}\hat{A}(s; \begin{bmatrix} \psi_0 \\ c_0 \end{bmatrix}, \frac{1}{2}\begin{bmatrix} \psi_0 \\ c_0 \end{bmatrix}) + \frac{\partial}{\partial s}\hat{J}(0; \begin{bmatrix} \psi_0 \\ c_0 \end{bmatrix}). \end{aligned} \tag{4.2.19}$$

The partial derivatives wrt s are easy to calculate:

$$\frac{\partial}{\partial s}\hat{A}(s; \begin{bmatrix} \psi \\ c \end{bmatrix}, \begin{bmatrix} \hat{\zeta} \\ e \end{bmatrix}) = \int_{\Gamma^0}\int_{\Gamma^0} (\nabla_x G(\boldsymbol{x},\boldsymbol{y})\cdot\boldsymbol{\nu}(\boldsymbol{x}) + \nabla_y G(\boldsymbol{x},\boldsymbol{y})\cdot\boldsymbol{\nu}(\boldsymbol{y}))\,\psi(\boldsymbol{x})\,\zeta(\boldsymbol{y})\,dS(\boldsymbol{x})dS(\boldsymbol{y}),$$

$$\frac{\partial}{\partial s}\hat{J}(s; \begin{bmatrix} \psi \\ c \end{bmatrix}) = \frac{\partial}{\partial s}\hat{L}(s; \begin{bmatrix} \phi \\ d \end{bmatrix}) = 0.$$

Using these results we get the required energy shape derivative as

$$\frac{d}{ds}\mathcal{E}_F(s)|_{s=0}(\psi_0,\zeta) = \int_{\Gamma^0}\int_{\Gamma^0} (\nabla_x G(\boldsymbol{x},\boldsymbol{y})\cdot\boldsymbol{\nu}(\boldsymbol{x}) + \nabla_y G(\boldsymbol{x},\boldsymbol{y})\cdot\boldsymbol{\nu}(\boldsymbol{y}))\,\psi_0(\boldsymbol{x})\,\zeta(\boldsymbol{y})\,dS(\boldsymbol{x})dS(\boldsymbol{y}),$$

which after plugging in the adjoint solution becomes

$$= \frac{1}{2}\int_{\Gamma^0}\int_{\Gamma^0} (\nabla_x G(\boldsymbol{x},\boldsymbol{y})\cdot\boldsymbol{\nu}(\boldsymbol{x}) + \nabla_y G(\boldsymbol{x},\boldsymbol{y})\cdot\boldsymbol{\nu}(\boldsymbol{y}))\,\psi_0(\boldsymbol{x})\,\psi_0(\boldsymbol{y})\,dS(\boldsymbol{x})dS(\boldsymbol{y}). \qquad (4.2.20)$$

The notation $\frac{d\mathcal{E}_F}{ds}(0;\boldsymbol{\nu})(\psi,\zeta)$ hints that this expression can be viewed as a function of the two arguments $\psi,\zeta \in H^{-\frac{1}{2}}(\Gamma^0)$ where if we plug in the appropriate state and adjoint solutions, we get the shape derivative in direction $\boldsymbol{\nu}$. For a detailed analysis of the mapping properties of (4.2.20) we refer to [48, Sec. 4.4] and Section 4.1.7. Here we simply mention that it is a continuous, bilinear mapping $H^{-\frac{1}{2}}(\Gamma^0) \times H^{-\frac{1}{2}}(\Gamma^0) \to \mathbb{R}$ which makes its Galerkin approximation superconvergent, see Proposition 1.

An advantage of (4.2.20) over the shape derivative formula in (4.1.16) is its simplicity. It contains a single double integral expression which can be evaluated without computing the adjoint solution.

Remark 10. It can be shown that the expression (4.2.20) is equivalent to (4.1.16) under the condition that g is constant in a neighborhood of Γ. We start by seeing that the terms $\mathbf{T_1}$ and $\mathbf{T_6}$ in (4.1.16) vanish because $\nabla\tilde{g} \equiv 0$ at Γ. Terms $\mathbf{T_3}, \mathbf{T_4}$ and $\mathbf{T_5}$ come from $\frac{\partial\hat{b}_K}{\partial s}(0;\tilde{g},\rho)$ as seen in (4.1.15). Putting $\tilde{g}|_\Gamma \equiv 1, \tilde{g}|_{\partial B} \equiv 0$ in the expression for $\hat{b}_K(0;\tilde{g},\rho)$ in (4.1.9), we get

$$\hat{b}_K(0;\tilde{g},\rho) = \int_{\partial\Omega}\int_\Gamma \nabla_y G(\mathbf{T}_s^{\boldsymbol{\nu}}(\hat{\boldsymbol{x}}), \mathbf{T}_s^{\boldsymbol{\nu}}(\hat{\boldsymbol{y}}))\cdot(\mathbf{C}(D\mathbf{T}_s^{\boldsymbol{\nu}}(\hat{\boldsymbol{y}}))\,\hat{\mathbf{n}}(\hat{\boldsymbol{y}}))\,\rho(\hat{\boldsymbol{x}})\,dS_{\hat{\boldsymbol{y}}}\,dS_{\hat{\boldsymbol{x}}}. \qquad (4.2.21)$$

Transforming the inner integral back to Γ^s we get

$$\hat{b}_K(0;\tilde{g},\rho) = \int_{\partial\Omega}\int_{\Gamma^s} \nabla_y G(\mathbf{T}_s^{\boldsymbol{\nu}}(\hat{\boldsymbol{x}}),\boldsymbol{y})\cdot\mathbf{n}(\boldsymbol{y})\,\rho(\hat{\boldsymbol{x}})\,dS_{\boldsymbol{y}}\,dS_{\hat{\boldsymbol{x}}}. \qquad (4.2.22)$$

We see that the integral over $\boldsymbol{y}$ evaluates to a constant. It is zero when $\mathbf{T}_s^{\boldsymbol{\nu}}(\hat{\boldsymbol{x}}) \in \partial B$ and -0.5 almost everywhere for $\mathbf{T}_s^{\boldsymbol{\nu}}(\hat{\boldsymbol{x}}) \in \Gamma^s$. Thus we see that $\hat{b}_K(0;\tilde{g},\rho)$ is a constant, hence its partial derivative wrt s is zero. Thus we conclude that terms $\mathbf{T_3}, \mathbf{T_4}$ and $\mathbf{T_5}$ in (4.1.16) are zero. Thus we are left with

$$\mathbf{T_2}(\psi,\rho) = \int_{\partial\Omega}\int_{\partial\Omega} \{\nabla_x G(\hat{\boldsymbol{x}},\hat{\boldsymbol{y}})\cdot\boldsymbol{\mathcal{V}}(\hat{\boldsymbol{x}}) + \nabla_y G(\hat{\boldsymbol{x}},\hat{\boldsymbol{y}})\cdot\boldsymbol{\mathcal{V}}(\hat{\boldsymbol{y}})\}\,\psi(\hat{\boldsymbol{y}})\,\rho(\hat{\boldsymbol{x}})\,dS(\hat{\boldsymbol{y}})dS(\hat{\boldsymbol{x}}). \qquad (4.2.23)$$

Now we find the relation between the adjoint solution $\rho \in H^{-\frac{1}{2}}(\partial\Omega)$ that solves (4.1.13) and the state solution $\hat{\psi}_0 \in H^{-\frac{1}{2}}(\partial\Omega)$ that solves (4.1.8) for $s = 0$. Writing the representation formula for u, we see

$$u(\boldsymbol{x}) = \Psi_{SL}(\psi)(\boldsymbol{x}) - \Psi_{DL}(\tilde{g})(\boldsymbol{x}), \quad \boldsymbol{x} \in \Omega. \tag{4.2.24}$$

Since $\tilde{g}|_\Gamma \equiv 1$ and $\tilde{g}|_{\partial B} \equiv 0$, $\Psi_{DL}(\tilde{g})(\boldsymbol{x}) = 0$ for $\boldsymbol{x} \in \Omega$. Taking the Dirichlet trace, we obtain the relation

$$\mathrm{V}(\psi) = \tilde{g}|_{\partial\Omega}. \tag{4.2.25}$$

On comparing with the variational adjoint equation (4.1.13) we immediately see the relation $\psi = -\frac{1}{2}\rho$ and the shape derivative reduces to

$$\mathbf{T_2}(\psi, \rho) = -\frac{1}{2}\int_{\partial\Omega}\int_{\partial\Omega} \left\{\nabla_{\boldsymbol{x}}G(\hat{\boldsymbol{x}}, \hat{\boldsymbol{y}}) \cdot \boldsymbol{\mathcal{V}}(\hat{\boldsymbol{x}}) + \nabla_{\boldsymbol{y}}G(\hat{\boldsymbol{x}}, \hat{\boldsymbol{y}}) \cdot \boldsymbol{\mathcal{V}}(\hat{\boldsymbol{y}})\right\} \psi(\hat{\boldsymbol{y}})\, \psi(\hat{\boldsymbol{x}})\, d\mathrm{S}(\hat{\boldsymbol{y}})d\mathrm{S}(\hat{\boldsymbol{x}}), \tag{4.2.26}$$

which is exactly the expression obtained in (4.2.20), with an opposite sign.

4.2.5 Implementation

The numerical implementation is done in 3D and relies on the MATLAB based Gypsilab framework (Matthieu Aussal, 2019) [6]. For solving the state and adjoint problems, BIOs are assembled using the available implementation in Gypsilab, with a quadrature order of 3. For evaluating the BEM based force formula in eq. (4.2.20), we use Sauter and Schwab quadrature technique [54] to evaluate the weakly singular integral with a tensor product quadrature rule of 3^4 points. The implementation can be found in the repository[7].

For convergence study a quasi-uniform sequence of mesh partitions $\mathcal{M}_h$ of Γ with increasing resolution was employed, consisting of triangular panels. Net forces and torques were computed using available methods and the numerical error recorded against the meshwidth h.

4.2.6 Force and Torque Computation

For computing the cartesian components of the net force $\mathbf{F} = (F_1, F_2, F_3) \in \mathbb{R}^3$, and the total torque $\mathbf{T}$ about the axis $\boldsymbol{a} \in \mathbb{R}^3$ and point $\boldsymbol{c} \in \mathbb{R}^3$, we use the strategy mentioned in (3.0.5). Since we are interested in forces on the object D, the chosen cut off function ξ is such that $\xi \equiv 1$ in a neighborhood of ∂D and $\xi \equiv 0$ in a neighborhood of ∂B.

Comparison is done with the forces and torques computed using the Maxwell stress tensor based formulas

$$\mathbf{F} = \frac{1}{2}\int_{\partial D} (\nabla u(\mathbf{x}) \cdot \mathbf{n}(\mathbf{x}))^2\, \mathbf{n}(\mathbf{x})\, d\mathrm{S}_{\mathbf{x}},$$

$$\mathbf{T} = \frac{1}{2}\int_{\partial D} (\nabla u(\mathbf{x}) \cdot \mathbf{n}(\mathbf{x}))^2\, (\boldsymbol{x} - \boldsymbol{c}) \times \mathbf{n}(\mathbf{x})\, d\mathrm{S}_{\mathbf{x}}.$$

---

[6]https://github.com/matthieuaussal/gypsilab
[7]Code available at https://github.com/piyushplcr7/gypsilab_forces

Numerical experiments are done on two geometries shown in the figure:
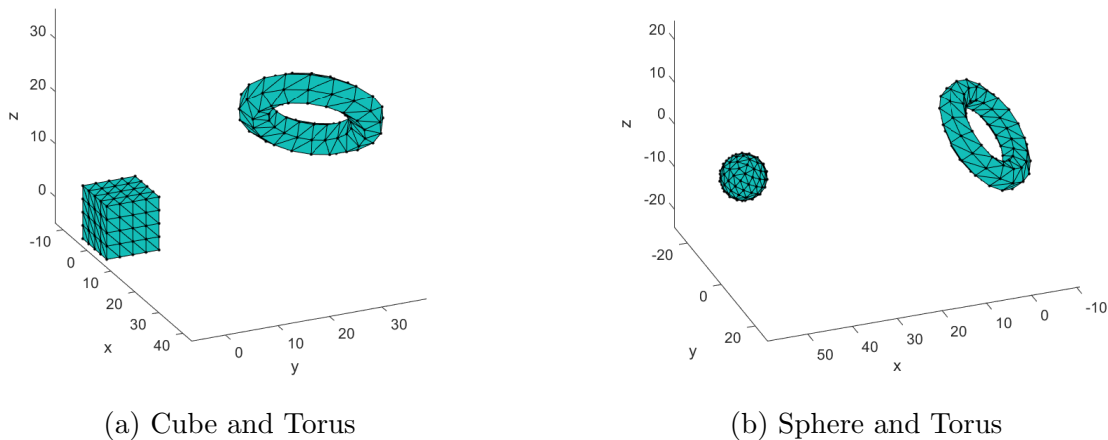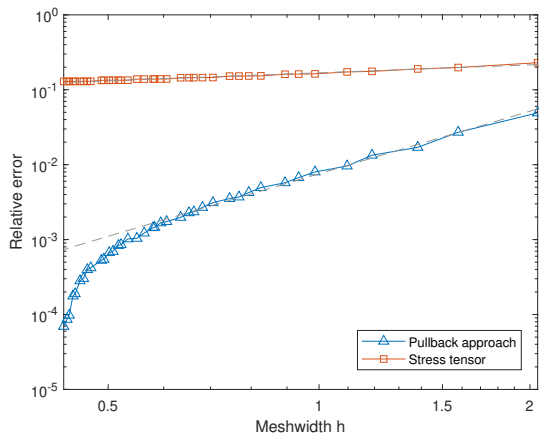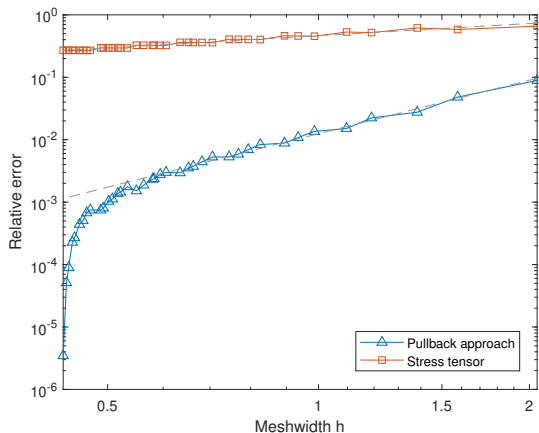

(a) Cube and Torus

(b) Sphere and Torus

Figure 4.9: Geometries for numerical experiments

4.2.7 Cube and Torus

In this experiment forces and torques are computed on the cube shaped domain $D := (-5, 5)^3$ while the torus shaped domain B is connected to ground. The torus with $R = 10$ and $r = 3$ is obtained via a rotation and translation, where r is the radius of the tube and R is the distance between center of tube and center of torus. Reference values are computed using (4.2.20) at a refinement level of $h = 0.42$. The results are computed using $Q = 10^2$ and plotted in Figure 4.10. We see the shape derivative formula is superior to the Maxwell Stress Tensor formula in absolute accuracy and asymptotic rate of convergence for both force and torque computation which are also tabulated in Table 4.1 and 4.2. The results are in agreement with the observations in Section 4.1.10 where we observed a clearly superior performance of the shape derivative formula, especially for geometries with corners.
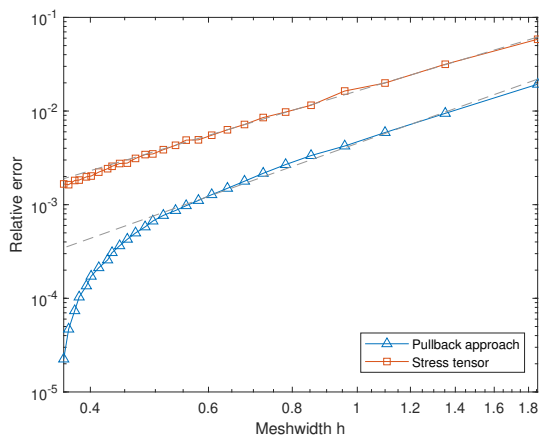
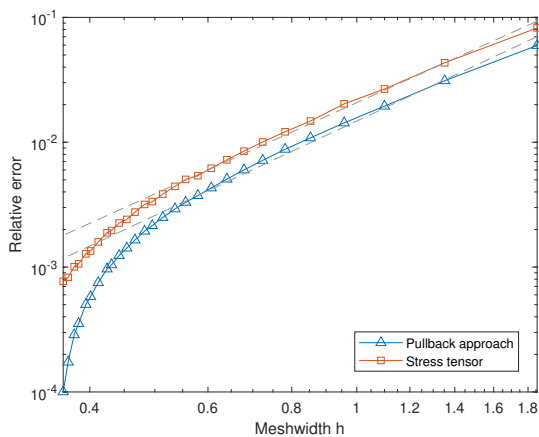(a) Force computation   (b) Torque computation

Figure 4.10: Error plots for Cube Torus geometry. Dashed lines represent the linear regression fit.

4.2.8 Sphere and Torus

In this experiment forces and torques are computed on a torus shaped domain D with $R = 10$ and $r = 3$, at the origin, while a grounded spherical body B of radius 5 is present at a distance. Reference values are computed using (4.2.20) at a refinement level of $h = 0.36$ and using $Q = 10^2$. The results are plotted in Figure 4.11. We see that the shape derivative formula is slightly superior to the Maxwell Stress Tensor formula in absolute accuracy and asymptotic rate of convergence for both force and torque computation for this smooth case.

(a) Force computation   (b) Torque computation

Figure 4.11: Error plots for Sphere Torus geometry. Dashed lines represent the linear regression fit.

Table 4.1: Asymptotic rate of algebraic convergence for forces

Method	Torus D, sphere B	Cubic D, Torus B
Pullback approach (BEM)	2.55	2.77
Stress tensor (BEM)	2.14	0.35

Table 4.2: Asymptotic rate of algebraic convergence for torques

Method	Torus D, sphere B	Cubic D, Torus B
Pullback approach (BEM)	2.51	2.85
Stress tensor (BEM)	2.43	0.65

4.3 Linear Dielectric and Mixed Boundary Conditions

The contents of this sub-section have been reproduced from [50]. To keep the presentation focused we confine ourselves to the following setting: We consider a parallel-plate capacitor where the gap between the plates is denoted by the simply connected, open domain $\Omega_c \subset \mathbb{R}^d$, $d = 2, 3$ which has C^2_{pw} boundary. The gap is filled with two homogeneous, isotropic, and linear dielectric materials, where one material is entirely embedded in another, as shown in Figure 4.12. The inner material occupies the domain $\Omega_i \subset \Omega_c$ and has dielectric constant $\varepsilon_i \in \mathbb{R}^+$, and the outer material occupies the domain $\Omega_e \subset \Omega_c$ and has dielectric constant $\varepsilon_e \in \mathbb{R}^+$. By Ω_i being embedded inside Ω_e, we mean $\overline{\Omega}_i \cup \Omega_e = \Omega_c$ and $\overline{\Omega}_i \cap \overline{\Omega}_e = \partial\Omega_i$. Both Ω_i and Ω_e have C^2_{pw} boundaries. Under operation of the capacitor, there is an imposed potential difference between the plates, giving rise to an electric field inside Ω_c which stores energy.

We define $\Gamma_I := \partial\Omega_i$ as the interface between two dielectrics, and $\Gamma_C := \partial\Omega_C$ as the outer boundary of the capacitor. We also introduce the notation $\Gamma_D \subset \Gamma_C$ for the part of the outer boundary touching the capacitor plates where the external voltage is applied (Dirichlet boundary conditions), and $\Gamma_N := \Gamma_C \setminus \Gamma_D$ for the free boundary of capacitor (Neumann boundary conditions). In the sequel, we admit a general Dirichlet boundary condition $\mathfrak{g} \in H^{\frac{1}{2}}(\Gamma_D)$. On the boundary Γ_N, a zero Neumann boundary condition is a sensible choice to model the ideal case where the electric field lines stay inside the dielectric and there is no fringing around the edges [23, Section 4.4]. Also here we may impose a more general Neumann boundary condition through an element $\eta \in H^{-\frac{1}{2}}(\Gamma_N)$.

Writing $\mathbf{n}_c$ for the exterior unit normal vector field on Γ_C, the electrostatic scalar potential $u : \Omega_c \to \mathbb{R}$ can be obtained as the weak solution in $H^1(\Omega_c)^8$ of the linear elliptic mixed boundary value problem

$$\nabla \cdot (\varepsilon \nabla u) = 0 \quad \text{in} \quad \Omega_c, \quad u = \mathfrak{g} \quad \text{on} \quad \Gamma_D, \quad \nabla u \cdot \mathbf{n}_c = \eta \quad \text{on} \quad \Gamma_N, \qquad (4.3.1)$$

where $\varepsilon(\mathbf{x}) = \varepsilon_i$ for $\mathbf{x} \in \Omega_i$ and $\varepsilon(\mathbf{x}) = \varepsilon_e$ for $\mathbf{x} \in \Omega_e$. BVP (4.3.1) can be reformulated as a transmission problem for the Laplacian. Using the notation u_i, u_e for the potentials inside subdomains Ω_i, Ω_e respectively, and $\mathbf{n}_i, \mathbf{n}_e$ for the exterior unit normal vector fields

---

[8]We adopt the convention of [54, Sec. 2.3 & Sec. 2.4] for function spaces and Sobolev spaces: $W^{k,p}(\Omega), H^1(\Omega), H^{\frac{1}{2}}(\Omega), L^2(\Omega), C^k(\Omega)$ etc., where Ω denotes a generic domain.

over $\partial\Omega_i, \partial\Omega_e$ respectively, we can write the equivalent problem

$$\Delta u_i = 0 \quad \text{in} \quad \Omega_i, \quad \Delta u_e = 0 \quad \text{in} \quad \Omega_e, \tag{4.3.2}$$

$$u_e = \mathfrak{g} \quad \text{on} \quad \Gamma_D, \quad \nabla u_e \cdot \mathbf{n}_e = \eta \quad \text{on} \quad \Gamma_N, \tag{4.3.3}$$

with the transmission conditions [54, Sec. 1.1] at the interface Γ_I which are given as

$$u_i|_{\Gamma_I} = u_e|_{\Gamma_I}, \quad \varepsilon_i \nabla u_i \cdot \mathbf{n}_i|_{\Gamma_I} = -\varepsilon_e \nabla u_e \cdot \mathbf{n}_e|_{\Gamma_I}. \tag{4.3.4}$$
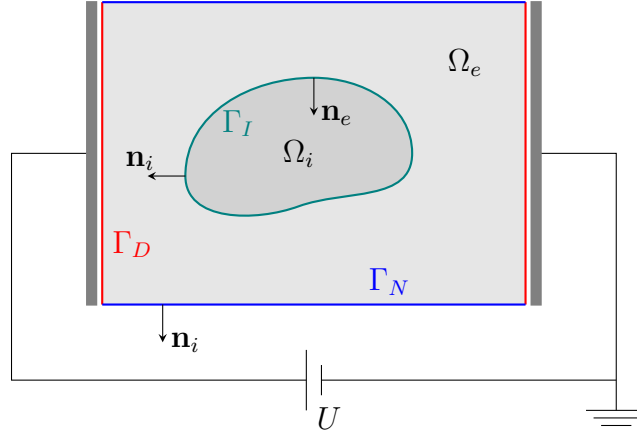

Figure 4.12: Geometric setting for the model problem. Ω_c comprises all shaded regions.

Since we deal with two domains with similar BIEs, we will write them compactly using the sub-script $*$ throughout this section, where $* \in \{i, e\}$ denotes the interior domain Ω_i and exterior domain Ω_e, respectively. For the bounded open Lipschitz domain Ω_*, the electrostatic potential $u_* \in H^1(\Omega_*)$ weakly satisfying the Laplace equation $\Delta u_* = 0$ in Ω_* also satisfies the following boundary integral equations:

$$\begin{bmatrix} -V_* & \frac{Id}{2} + K_* \\ \frac{Id}{2} - K'_* & -W_* \end{bmatrix} \begin{bmatrix} \gamma_*^N u_* \\ \gamma_*^D u_* \end{bmatrix} = \begin{bmatrix} 0 \\ 0 \end{bmatrix}. \tag{4.3.5}$$

In the equations above γ_*^N is the interior Neumann trace operator $\gamma_*^N : H^1(\Delta; \Omega_*) \to H^{-\frac{1}{2}}(\partial\Omega_*)$, and γ_*^D is the interior Dirichlet trace operator $\gamma_*^D : H^1(\Omega_*) \to H^{\frac{1}{2}}(\partial\Omega_*)$, defined for a function $f \in C^1(\overline{\Omega_*})$ as:

$$\gamma_*^N f(\mathbf{x}) := \lim_{\mathbf{x}_* \in \Omega_* \to \mathbf{x} \in \partial\Omega_*} \nabla f(\mathbf{x}_*) \cdot \mathbf{n}_*(\mathbf{x}), \quad \gamma_*^D f(\mathbf{x}) := \lim_{\mathbf{x}_* \in \Omega_* \to \mathbf{x} \in \partial\Omega_*} f(\mathbf{x}_*), \tag{4.3.6}$$

where $\mathbf{n}_*$ is the unit exterior normal vector field on $\partial\Omega_*$. The operators V_*, K_*, K'_* and W_* are the well known single-layer, double-layer, adjoint double-layer and hypersingular boundary integral operators (BIOs) for the Laplacian which are bounded linear operators acting between the following spaces:

$$V_* : H^{-\frac{1}{2}}(\partial\Omega_*) \to H^{\frac{1}{2}}(\partial\Omega_*), \qquad\qquad K_* : H^{\frac{1}{2}}(\partial\Omega_*) \to H^{\frac{1}{2}}(\partial\Omega_*),$$

$$K'_* : H^{-\frac{1}{2}}(\partial\Omega_*) \to H^{-\frac{1}{2}}(\partial\Omega_*), \qquad W_* : H^{\frac{1}{2}}(\partial\Omega_*) \to H^{-\frac{1}{2}}(\partial\Omega_*).$$

For input data lying in $L^\infty(\partial\Omega_*)$, the boundary integral operators also have explicit representations as improper integrals which we will use in the next sub-section. This regularity assumption will obviously be true for the boundary element spaces used for discretization.

4.3.1 Traces

To obtain a variational formulation of the BIEs, we first rely on the offset function technique used for the mixed boundary value problem [58, Ch. 7] [54, Ch. 4]. Let $\mathfrak{g}_{ex} \in H^{\frac{1}{2}}(\Gamma_C)$ and $\eta_{ex} \in H^{-\frac{1}{2}}(\Gamma_C)$ be suitable extensions of the given boundary data $\mathfrak{g}$ and η respectively, such that $\mathfrak{g}_{ex}|_{\Gamma_D} = \mathfrak{g}$ and $\eta_{ex}|_{\Gamma_N} = \eta$. Using these extensions, we decompose the traces[9] on Γ_C and define

$$
\begin{aligned}
\mathfrak{u} &:= \gamma_e^D u_e\big|_{\Gamma_C} - \mathfrak{g}_{ex}, \quad \mathfrak{u} \in \tilde{H}^{\frac{1}{2}}(\Gamma_N) := \{\mathfrak{v} \in H^{\frac{1}{2}}(\Gamma_C) : \mathrm{supp}(\mathfrak{v}) \subset \Gamma_N\}, \\
\psi &:= \gamma_e^N u_e\big|_{\Gamma_C} - \eta_{ex}, \quad \psi \in \tilde{H}^{-\frac{1}{2}}(\Gamma_D) := \{\phi \in H^{-\frac{1}{2}}(\Gamma_C) : \mathrm{supp}(\mathfrak{v}) \subset \Gamma_D\}.
\end{aligned}
\tag{4.3.7}
$$

The unknown traces on Γ_I are denoted as $\mathfrak{u}_I := \gamma_e^D u_e\big|_{\Gamma_I}$ and $\psi_I := \gamma_e^N u_e\big|_{\Gamma_I}$, where $\mathfrak{u}_I \in H^{\frac{1}{2}}(\Gamma_I)$ and $\psi_I \in H^{-\frac{1}{2}}(\Gamma_I)$. The task of solving the transmission problem (4.3.3) then reduces to finding the unknown traces $\mathfrak{u} \in \tilde{H}^{\frac{1}{2}}(\Gamma_N)$, $\psi \in \tilde{H}^{-\frac{1}{2}}(\Gamma_D)$, $\mathfrak{u}_I \in H^{\frac{1}{2}}(\Gamma_I)$ and $\psi_I \in H^{-\frac{1}{2}}(\Gamma_I)$. More information on the "tilde spaces" can be found in [54, Sec. 2.4.2], [58, Sec. 2.5].

4.3.2 Variational Boundary Integral Equations

To get the variational equations we rely on the duality of the Sobolev spaces $H^{-\frac{1}{2}}(\partial\Omega_*)$ and $H^{\frac{1}{2}}(\partial\Omega_*)$, and the corresponding duality pairing $\langle \cdot, \cdot \rangle_*$. Testing the first equation in (4.3.5) for $* = e$ with $\phi \in H^{-\frac{1}{2}}(\partial\Omega_e)$, we get

$$
\mathrm{a}_{V,e}(\gamma_e^N u_e, \phi) = \frac{1}{2}\left\langle \gamma_e^D u_e, \phi \right\rangle_e + \mathrm{a}_{K,e}(\gamma_e^D u_e, \phi) \quad \forall \phi \in H^{-\frac{1}{2}}(\partial\Omega_e),
\tag{4.3.8}
$$

where the bilinear forms are defined as:

$$
\begin{aligned}
\mathrm{a}_{V,*} &: H^{-\frac{1}{2}}(\partial\Omega_*) \times H^{-\frac{1}{2}}(\partial\Omega_*) \to \mathbb{R}, \quad \mathrm{a}_{a_{V_*}}(\psi, \phi) := \langle \mathrm{V}_* \psi, \phi \rangle_*, \\
\mathrm{a}_{K,*} &: H^{\frac{1}{2}}(\partial\Omega_*) \times H^{-\frac{1}{2}}(\partial\Omega_*) \to \mathbb{R}, \quad \mathrm{a}_{a_{K_*}}(g, \phi) := \langle \mathrm{K}_* g, \phi \rangle_*.
\end{aligned}
$$

We work with the integral representations of these bilinear forms which hold for functions in $L^\infty(\partial\Omega_*)$. In that case, the duality pairing $\langle \cdot, \cdot \rangle_*$ also reduces to the $L^2(\partial\Omega_*)$ pairing. The integral representations are

$$
\mathrm{a}_{a_{V,*}}(\psi, \phi) = \int_{\partial\Omega_*} \int_{\partial\Omega_*} G(\mathbf{x}, \mathbf{y}) \, \psi(\mathbf{y}) \, \phi(\mathbf{x}) \, dS(\mathbf{y}) dS(\mathbf{x}),
$$

$$
\mathrm{a}_{a_{K,*}}(g, \phi) = \int_{\partial\Omega_*} \int_{\partial\Omega_*} \nabla_y G(\mathbf{x}, \mathbf{y}) \cdot \mathbf{n}_*(\mathbf{y}) \, g(\mathbf{y}) \, \phi(\mathbf{x}) dS(\mathbf{y}) dS(\mathbf{x}),
$$

where $G(\mathbf{x}, \mathbf{y}) : \{(\mathbf{x}, \mathbf{y}) \in \mathbb{R}^d \times \mathbb{R}^d : \mathbf{x} \neq \mathbf{y}\} \to \mathbb{R}$ is the fundamental solution for the Laplace operator,

$$
G(\mathbf{x}, \mathbf{y}) := -\frac{1}{2\pi} \log(\|\mathbf{x} - \mathbf{y}\|) \quad \text{for } d = 2, \quad G(\mathbf{x}, \mathbf{y}) := \frac{1}{4\pi \|\mathbf{x} - \mathbf{y}\|} \quad \text{for } d = 3.
$$

---

[9]For functions in $H^{\frac{1}{2}}$ we use Roman letters and for those in $H^{-\frac{1}{2}}$ we use Greek letters

Let the chosen test function ϕ in (4.3.8) be such that $\phi|_{\Gamma_I} \equiv 0$, and $\phi|_{\Gamma_C} = \tilde{\phi} \in \tilde{H}^{-\frac{1}{2}}(\Gamma_D)$. The integrals over $\partial\Omega_e$ can be decomposed into integrals over the disjoint boundaries Γ_I and Γ_C, and we get

$$
\int_{\Gamma_C}\int_{\Gamma_I} G(\mathbf{x},\mathbf{y})\,\psi_I(\mathbf{y})\,\tilde{\phi}(\mathbf{x})\,dS(\mathbf{y})dS(\mathbf{x}) + \int_{\Gamma_C}\int_{\Gamma_C} G(\mathbf{x},\mathbf{y})\,(\eta_{ex}(\mathbf{y}) + \psi(\mathbf{y}))\,\tilde{\phi}(\mathbf{x})\,dS(\mathbf{y})dS(\mathbf{x})
$$

$$
= \frac{1}{2}\int_{\Gamma_C} \mathfrak{g}_{ex}(\mathbf{x})\,\tilde{\phi}(\mathbf{x})\,dS(\mathbf{x}) + \int_{\Gamma_C}\int_{\Gamma_I} \nabla_y G(\mathbf{x},\mathbf{y})\cdot\mathbf{n}_e(\mathbf{y})\,\mathfrak{u}_I(\mathbf{y})\,\tilde{\phi}(\mathbf{x})\,dS(\mathbf{y})dS(\mathbf{x})
$$

$$
+ \int_{\Gamma_C}\int_{\Gamma_C} \nabla_y G(\mathbf{x},\mathbf{y})\cdot\mathbf{n}_e(\mathbf{y})\,(\mathfrak{u}(\mathbf{y}) + \mathfrak{g}_{ex}(\mathbf{y}))\,\tilde{\phi}(\mathbf{x})\,dS(\mathbf{y})dS(\mathbf{x}) \quad \forall\tilde{\phi}\in\tilde{H}^{-\frac{1}{2}}(\Gamma_D), \qquad (4.3.9)
$$

where $\psi_I = \gamma_e^N u_e|_{\Gamma_I}$, $\mathfrak{u}_I = \gamma_e^D u_e$, and $\psi, \mathfrak{u}$ are the unknown traces on Γ_C defined in (4.3.7). We introduce some notation to write the variational equations in a compact way. For $\bullet, \blacktriangle \in \{I, C\}$, we define

$$
a_V^{\bullet,\blacktriangle} : \begin{cases} H^{-\frac{1}{2}}(\Gamma_\bullet) \times H^{-\frac{1}{2}}(\Gamma_\blacktriangle) \to \mathbb{R} \\ \qquad (\psi, \phi) \mapsto \displaystyle\int_{\Gamma_\blacktriangle}\int_{\Gamma_\bullet} G(\mathbf{x},\mathbf{y})\,\psi(\mathbf{y})\,\phi(\mathbf{x})\,dS(\mathbf{y})dS(\mathbf{x}). \end{cases}
$$

$$
l^\bullet : \begin{cases} H^{\frac{1}{2}}(\Gamma_\bullet) \times H^{-\frac{1}{2}}(\Gamma_\bullet) \to \mathbb{R} \\ \qquad (g, \phi) \mapsto \displaystyle\int_{\Gamma_\bullet} g(\mathbf{x})\,\phi(\mathbf{x})\,dS(\mathbf{x}) \end{cases}
$$

$$
a_K^{\bullet,\blacktriangle} : \begin{cases} H^{\frac{1}{2}}(\Gamma_\bullet) \times H^{-\frac{1}{2}}(\Gamma_\blacktriangle) \to \mathbb{R} \\ \qquad (g, \phi) \mapsto \displaystyle\int_{\Gamma_\blacktriangle}\int_{\Gamma_\bullet} \nabla_y G(\mathbf{x},\mathbf{y})\cdot\mathbf{n}_e(\mathbf{y})\,g(\mathbf{y})\,\phi(\mathbf{x})\,dS(\mathbf{y})dS(\mathbf{x}) \end{cases}
$$

$$
a_W^{\bullet,\blacktriangle} : \begin{cases} H^{\frac{1}{2}}(\Gamma_\bullet) \times H^{\frac{1}{2}}(\Gamma_\blacktriangle) \to \mathbb{R} \\ \qquad (g, v) \mapsto \displaystyle\int_{\Gamma_\blacktriangle}\int_{\Gamma_\bullet} G(\mathbf{x},\mathbf{y})\,\frac{dg}{dt}(\mathbf{y})\,\frac{dv}{dt}(\mathbf{x})\,dS(\mathbf{y})dS(\mathbf{x}) \qquad\qquad (2D) \\ \qquad (g, v) \mapsto \displaystyle\int_{\Gamma_\blacktriangle}\int_{\Gamma_\bullet} G(\mathbf{x},\mathbf{y})\,\mathbf{curl}_\Gamma g(\mathbf{y})\cdot\mathbf{curl}_\Gamma v(\mathbf{x})\,dS(\mathbf{y})dS(\mathbf{x}) \qquad (3D). \end{cases}
$$

In the definition of $a_W^{\bullet,\blacktriangle}$, $\frac{d}{dt}$ denotes the arclength derivative along a curve and $\mathbf{curl}_\Gamma u(\mathbf{x}) := \mathbf{grad}_\Gamma u(\mathbf{x}) \times \mathbf{n}_e(\mathbf{x})$ is the vectorial surface curl operator. This notation allows us to rewrite (4.3.9) as

$$
a_{a_V}^{I,C}(\psi_I, \tilde{\phi}) + a_{a_V}^{C,C}(\psi, \tilde{\phi}) - a_{a_K}^{I,C}(u_I, \tilde{\phi}) - a_{a_K}^{C,C}(\mathfrak{u}, \tilde{\phi})
$$

$$
= \frac{1}{2}l^C(\mathfrak{g}_{ex}, \tilde{\phi}) - a_{a_V}^{C,C}(\eta_{ex}, \tilde{\phi}) + a_{a_K}^{C,C}(\mathfrak{g}_{ex}, \tilde{\phi}) \quad \forall\tilde{\phi}\in\tilde{H}^{-\frac{1}{2}}(\Gamma_D).
$$

Similarly, we test the second equation in (4.3.5) for $* = e$ with a function $\mathfrak{v} \in H^{\frac{1}{2}}(\partial\Omega_e)$, such that $\mathfrak{v}|_{\Gamma_C} = \tilde{\mathfrak{v}} \in \tilde{H}^{\frac{1}{2}}(\Gamma_N)$ and $\mathfrak{v}|_{\Gamma_I} \equiv 0$. This yields

$$\mathrm{a}_{a_W^{I,C}}(\mathfrak{u}_I, \tilde{\mathfrak{v}}) + \mathrm{a}_{a_W^{C,C}}(\mathfrak{u}, \tilde{\mathfrak{v}}) + \mathrm{a}_{a_K^{C,C}}(\tilde{\mathfrak{v}}, \psi) + \mathrm{a}_{a_K^{C,I}}(\tilde{\mathfrak{v}}, \psi_I)$$
$$= \frac{1}{2}\mathrm{l}^C(\tilde{\mathfrak{v}}, \eta_{ex}) - \mathrm{a}_{a_W^{C,C}}(\mathfrak{g}_{ex}, \tilde{\mathfrak{v}}) - \mathrm{a}_{a_K^{C,C}}(\tilde{\mathfrak{v}}, \eta_{ex}) \quad \forall \tilde{v} \in \tilde{H}^{\frac{1}{2}}(\Gamma_N).$$

Note that we write the bilinear form corresponding to K' in terms of $\mathrm{a}_K^{\bullet;\blacktriangle}$, exploiting the relation $\langle \mathrm{K}_* g, \phi \rangle_* = \langle g, \mathrm{K}'_* \phi \rangle_*$. Next, we obtain equations on Γ_I. We test the first equation in (4.3.5) for $* = i$ with $\phi_I \in H^{-\frac{1}{2}}(\Gamma_I)$:

$$\mathrm{a}_{\mathrm{V},i}(\gamma_i^N u_i, \phi_I) = \frac{1}{2}\left\langle \gamma_i^D u_i, \phi_I \right\rangle_i + \mathrm{a}_{\mathrm{K},i}(\gamma_i^D u_i, \phi_I) \quad \forall \phi_I \in H^{-\frac{1}{2}}(\Gamma_I). \tag{4.3.10}$$

From the transmission conditions (4.3.4) we know that $\varepsilon_i \gamma_i^N u_i + \varepsilon_e \gamma_e^N u_e = 0$ on Γ_I, which gives $\gamma_i^N u_i = -\frac{\varepsilon_e}{\varepsilon_i}\psi_I$, and that $\gamma_i^D u_i = \mathfrak{u}_I$. Using these relations we get

$$-\frac{\varepsilon_e}{\varepsilon_i}\int_{\Gamma_I}\int_{\Gamma_I} G(\mathbf{x}, \mathbf{y})\,\psi_I(\mathbf{y})\,\phi_I(\mathbf{x})\,dS(\mathbf{y})dS(\mathbf{x}) = \frac{1}{2}\int_{\Gamma_I} \mathfrak{u}_I(\mathbf{x})\,\phi_I(\mathbf{x})\,dS(\mathbf{x})$$
$$+ \int_{\Gamma_I}\int_{\Gamma_I} \nabla G(\mathbf{x}, \mathbf{y}) \cdot \mathbf{n}_i(\mathbf{y})\,\mathfrak{u}_I(\mathbf{y})\,\phi_I(\mathbf{x})\,dS(\mathbf{y})dS(\mathbf{x}) \quad \forall \phi_I \in H^{-\frac{1}{2}}(\Gamma_I). \tag{4.3.11}$$

This equation on Γ_I is not very useful by itself, as we do not know any traces on Γ_I. We combine it with the corresponding equation for Ω_e as follows: We test the first equation in (4.3.5) for $* = e$ with a function $\phi \in H^{-\frac{1}{2}}(\partial\Omega_e)$, such that $\phi|_{\Gamma_C} \equiv 0$ and $\phi|_{\Gamma_I} = \phi_I \in H^{-\frac{1}{2}}(\Gamma_I)$. Then subtracting (4.3.11) from it gives

$$\mathrm{a}_{a_V^{C,I}}(\psi, \phi_I) + (1 + \frac{\varepsilon_e}{\varepsilon_i})\mathrm{a}_{a_V^{I,I}}(\psi_I, \phi_I) - \mathrm{a}_{a_K^{C,I}}(\mathfrak{u}, \phi_I) - 2\mathrm{a}_{a_K^{I,I}}(\mathfrak{u}_I, \phi_I) =$$
$$- \mathrm{a}_{a_V^{C,I}}(\eta_{ex}, \phi_I) + \mathrm{a}_{a_K^{C,I}}(\mathfrak{g}_{ex}, \phi_I) \quad \forall \phi_I \in H^{-\frac{1}{2}}(\Gamma_I).$$

In the simplification above, we used the fact $\mathbf{n}_i = -\mathbf{n}_e|_{\Gamma_I}$. Combining the second equation in (4.3.5) for $* = i, e$ in a similar fashion, we obtain

$$\mathrm{a}_{a_W^{C,I}}(\mathfrak{u}, \mathfrak{v}_I) + (1 + \frac{\varepsilon_i}{\varepsilon_e})\mathrm{a}_{a_W^{I,I}}(\mathfrak{u}_I, \mathfrak{v}_I) + \mathrm{a}_{a_K^{I,C}}(\mathfrak{v}_I, \psi) + 2\mathrm{a}_{a_K^{I,I}}(\mathfrak{v}_I, \psi_I) =$$
$$- \mathrm{a}_{a_W^{C,I}}(\mathfrak{g}_{ex}, \mathfrak{v}_I) - \mathrm{a}_{a_K^{I,C}}(\mathfrak{v}_I, \eta_{ex}) \quad \forall \mathfrak{v}_I \in H^{\frac{1}{2}}(\Gamma_I).$$

In the combined system of equations we seek $\mathfrak{u} \in \tilde{H}^{\frac{1}{2}}(\Gamma_N)$, $\psi \in \tilde{H}^{-\frac{1}{2}}(\Gamma_D)$, $\mathfrak{u}_I \in H^{\frac{1}{2}}(\Gamma_I)$ and $\psi_I \in H^{-\frac{1}{2}}(\Gamma_I)$ such that

$$
\mathrm{a}_{a_W^{C,I}}(\mathfrak{u}, \mathfrak{v}_I) + (1 + \frac{\varepsilon_i}{\varepsilon_e})\mathrm{a}_{a_W^{I,I}}(\mathfrak{u}_I, \mathfrak{v}_I) + \mathrm{a}_{\mathrm{K}}^{\mathrm{I,C}}(\mathfrak{v}_I, \psi) + 2\mathrm{a}_{a_K^{I,I}}(\mathfrak{v}_I, \psi_I)
$$
$$
= -\mathrm{a}_{a_W^{C,I}}(\mathfrak{g}_{ex}, \mathfrak{v}_I) - \mathrm{a}_{a_K^{I,C}}(\mathfrak{v}_I, \eta_{ex}) \qquad \forall \mathfrak{v}_I \in H^{\frac{1}{2}}(\Gamma_I),
$$

$$
\mathrm{a}_{a_V^{C,I}}(\psi, \phi_I) + (1 + \frac{\varepsilon_e}{\varepsilon_i})\mathrm{a}_{a_V^{I,I}}(\psi_I, \phi_I) - \mathrm{a}_{\mathrm{K}}^{\mathrm{C,I}}(\mathfrak{u}, \phi_I) - 2\mathrm{a}_{a_K^{I,I}}(\mathfrak{u}_I, \phi_I)
$$
$$
= -\mathrm{a}_{a_V^{C,I}}(\eta_{ex}, \phi_I) + \mathrm{a}_{a_K^{C,I}}(\mathfrak{g}_{ex}, \phi_I) \qquad \forall \phi_I \in H^{-\frac{1}{2}}(\Gamma_I),
$$

$$
\mathrm{a}_{a_V^{I,C}}(\psi_I, \tilde{\phi}) + \mathrm{a}_{a_V^{C,C}}(\psi, \tilde{\phi}) - \mathrm{a}_{a_K^{I,C}}(u_I, \tilde{\phi}) - \mathrm{a}_{a_K^{C,C}}(\mathfrak{u}, \tilde{\phi})
$$
$$
= \frac{1}{2}\mathrm{l}^C(\mathfrak{g}_{ex}, \tilde{\phi}) - \mathrm{a}_{a_V^{C,C}}(\eta_{ex}, \tilde{\phi}) + \mathrm{a}_{a_K^{C,C}}(\mathfrak{g}_{ex}, \tilde{\phi}) \quad \forall \tilde{\phi} \in \tilde{H}^{-\frac{1}{2}}(\Gamma_D),
$$

$$
\mathrm{a}_{a_W^{I,C}}(\mathfrak{u}_I, \tilde{\mathfrak{v}}) + \mathrm{a}_{a_W^{C,C}}(\mathfrak{u}, \tilde{\mathfrak{v}}) + \mathrm{a}_{a_K^{C,C}}(\tilde{\mathfrak{v}}, \psi) + \mathrm{a}_{a_K^{C,I}}(\tilde{\mathfrak{v}}, \psi_I)
$$
$$
= \frac{1}{2}\mathrm{l}^C(\tilde{\mathfrak{v}}, \eta_{ex}) - \mathrm{a}_{a_W^{C,C}}(\mathfrak{g}_{ex}, \tilde{\mathfrak{v}}) - \mathrm{a}_{a_K^{C,C}}(\tilde{\mathfrak{v}}, \eta_{ex}) \quad \forall \tilde{v} \in \tilde{H}^{\frac{1}{2}}(\Gamma_N).
$$
$$
(4.3.12)
$$

Remark 1. *From our knowledge of the mapping properties of the layer potentials and boundary integral operators [54, Sec. 3.1.2] we know that all the bilinear forms on the LHS of (4.3.12) are bounded. Combining all the bilinear forms on the LHS and setting $(\tilde{\mathfrak{v}}, \tilde{\phi}, \mathfrak{v}_I, \phi_I) = (\mathfrak{u}, \psi, \mathfrak{u}_I, \psi_I)$ we get the ellipticity estimate*

$$
(1 + \frac{\varepsilon_i}{\varepsilon_e})\mathrm{a}_{a_W^{I,I}}(\mathfrak{u}_I, \mathfrak{u}_I) + (1 + \frac{\varepsilon_e}{\varepsilon_i})\mathrm{a}_{a_V^{I,I}}(\psi_I, \psi_I) + \mathrm{a}_{a_V^{C,C}}(\psi, \psi) + \mathrm{a}_{a_W^{C,C}}(\mathfrak{u}, \mathfrak{u}) + 2\mathrm{a}_{a_V^{I,C}}(\psi_I, \psi) + 2\mathrm{a}_{a_W^{I,C}}(\mathfrak{u}_I, \mathfrak{u})
$$
$$
\geq \mathrm{a}_{a_V^{I,I}}(\psi_I, \psi_I) + \mathrm{a}_{a_V^{C,C}}(\psi, \psi) + 2\mathrm{a}_{a_V^{I,C}}(\psi_I, \psi) + \mathrm{a}_{a_W^{C,C}}(\mathfrak{u}, \mathfrak{u}) + 2\mathrm{a}_{a_W^{I,C}}(\mathfrak{u}_I, \mathfrak{u}) + \mathrm{a}_{a_W^{I,I}}(\mathfrak{u}_I, \mathfrak{u}_I)
$$
$$
= \mathrm{a}_{\mathrm{V},e}(\psi', \psi') + \mathrm{a}_{\mathrm{W},e}(\mathfrak{u}', \mathfrak{u}')
$$
$$
\geq c \left(\|\psi\|^2_{\tilde{H}^{-\frac{1}{2}}(\Gamma_D)} + \|\psi_I\|^2_{H^{-\frac{1}{2}}(\Gamma_I)} + \|\mathfrak{u}_I\|^2_{H^{\frac{1}{2}}(\Gamma_I)} + \|\mathfrak{u}\|^2_{\tilde{H}^{\frac{1}{2}}(\Gamma_N)} \right),
$$

where $\psi' \in H^{-\frac{1}{2}}(\partial\Omega_e) : \psi'|_{\Gamma_I} = \psi_I, \psi'|_{\Gamma_C} = \psi$ and $\mathfrak{u}' \in H^{\frac{1}{2}}(\partial\Omega_e) : \mathfrak{u}'|_{\Gamma_I} = \mathfrak{u}_I, \mathfrak{u}'|_{\Gamma_C} = \mathfrak{u}$. For ellipticity results on the bilinear forms a_V and a_W we refer to [54, Sec. 3.5.2]. The existence of a unique solution for (4.3.12) is then guaranteed by the Lax-Milgram lemma [54, Lem. 2.1.51].

4.3.3 Variational Formulation on Deformed Domain

We start by denoting the reference configuration with superscript zero, that is Ω_i^0 and Ω_e^0 for the inner and outer dielectric materials, and $\Omega_c^0 = \overline{\Omega}_i^0 \cup \Omega_e^0$ for the capacitor domain. We denote by $\Gamma_I^0 := \partial\Omega_i^0$ the reference interface on which we wish to compute forces, and by $\Gamma_C^0 := \partial\Omega_c^0$ the outer boundary of the capacitor. We will only consider perturbations of the reference domain Ω_e^0 as it induces the perturbation of Ω_i^0. The perturbation map (3.0.1) then gives a set $\mathcal{A}_{\boldsymbol{\nu}}$ of admissible domains, $\mathcal{A}_{\boldsymbol{\nu}} := \{\Omega_e^s := \mathbf{T}_s^{\boldsymbol{\nu}}(\Omega_e^0), s \in (-\delta(\boldsymbol{\nu}), \delta(\boldsymbol{\nu}))\}$. In the spirit of the Virtual Work Principle, we consider the electrostatic setting from Sub-section 4.3 for this set of admissible domains. Temporarily we fix a velocity field $\boldsymbol{\mathcal{V}} \in C_0^\infty(D)$, which need not vanish on Γ_C^0. Dependence on $\boldsymbol{\mathcal{V}}$ will not always be indicated in notations.

For the "s" configuration, all the boundaries and interfaces are defined using the perturbation map, for example $\Gamma_I^s := \mathbf{T}_s^{\boldsymbol{\nu}}(\Gamma_I^0)$. The dielectric constant for the s-configuration is defined as $\varepsilon^s(\mathbf{x}) := \varepsilon_*$ for $\mathbf{x} \in \Omega_*^s$, $* \in \{i, e\}$. The boundary conditions for the s-configuration are denoted by $\mathfrak{g}_{ex}^s \in H^{\frac{1}{2}}(\Gamma_C^s)$ and $\eta_{ex}^s \in H^{-\frac{1}{2}}(\Gamma_C^s)$. To impose constant Dirichlet boundary conditions on the capacitor plates we need a voltage source which we will call the battery in the sequel. It needs to be included in the energy considerations because the battery supplies energy during shape deformations. We denote the total energy for the s-configuration by $\mathcal{J}(s)$, which is the sum of battery's energy $\mathcal{J}_B(s)$ and the electric field energy $\mathcal{J}_F(s)$, which are mappings $\mathcal{J}, \mathcal{J}_B, \mathcal{J}_F : (-\delta(\boldsymbol{\nu}), \delta(\boldsymbol{\nu})) \to \mathbb{R}$. The field energy is given as

$$
\begin{aligned}
\mathcal{J}_F(s) &:= \frac{1}{2} \int\limits_{\Omega_c^s} \varepsilon^s(\mathbf{x}) \nabla u^s(\mathbf{x}) \cdot \nabla u^s(\mathbf{x}) \, d\mathbf{x} \\
&= \frac{\varepsilon_i}{2} \int\limits_{\Omega_i^s} ||\nabla u_i^s(\mathbf{x})||^2 \, d\mathbf{x} + \frac{\varepsilon_e}{2} \int\limits_{\Omega_e^s} ||\nabla u_e^s(\mathbf{x})||^2 \, d\mathbf{x} \\
&= \frac{\varepsilon_e}{2} \int\limits_{\Gamma_C^s} \left(\mathfrak{u}^s(\mathbf{x}) + \mathfrak{g}_{ex}^s(\mathbf{x}) \right) \left(\eta_{ex}^s(\mathbf{x}) + \psi^s(\mathbf{x}) \right) \, d\mathrm{S}(\mathbf{x}),
\end{aligned} \tag{4.3.13}
$$

where $u^s : \Omega_c^s \to \mathbb{R}$ is the electrostatic potential in the s-configuration, and $u_e^s := u^s|_{\Omega_e^s}$, $u_i^s := u^s|_{\Omega_i^s}$. The Dirichlet and Neumann traces are denoted in a similar way using the superscript s where $\mathfrak{u}^s$ and ψ^s denote the traces on Γ_C^s, and $\mathfrak{u}_I^s$ and ψ_I^s denote the traces on Γ_I^s. The field energy expression for s-configuration motivates us to define

$$
J(s) : H^{\frac{1}{2}}(\Gamma_C^s) \times H^{-\frac{1}{2}}(\Gamma_C^s) \to \mathbb{R},
$$

$$
J(s)(\mathfrak{v}, \phi) := \frac{\varepsilon_e}{2} \int\limits_{\Gamma_C^s} \left(\mathfrak{v}(\mathbf{x}) + \mathfrak{g}_{ex}^s(\mathbf{x}) \right) \left(\eta_{ex}^s(\mathbf{x}) + \phi(\mathbf{x}) \right) \, d\mathrm{S}(\mathbf{x}). \tag{4.3.14}
$$

Remark 2. *The shape derivative of the battery energy is related to the shape derivative for the field energy by $\frac{d\mathcal{J}_B}{ds}(0) = -2\frac{d\mathcal{J}_F}{ds}(0)$. This holds because for a battery supplying a constant voltage $\frac{d\mathcal{J}_B}{ds}(0) = -\mathfrak{g}\frac{dQ}{ds}(0)$, where $Q(s)$ is the net charge on the outer boundary Γ_C^s, given as*

$$
Q(s) = \varepsilon_e \int_{\Gamma_D^s} (\psi^s + \eta_{ex}^s) \, d\mathrm{S}.
$$

Hence we only need to examine the shape derivative of the field energy which gives the negative force field.

Since the perturbation map is a C^∞ diffeomorphism for small enough s, the domains in $\mathcal{A}_{\boldsymbol{\nu}}$ will possess connected Lipschitz boundaries. Thus, we can augment the bilinear forms from (4.3.12) appropriately to get the variational formulation for the s-dependent problem.

The augmented bilinear forms are given as

$$a_V^{\bullet,\blacktriangle}(s) : \begin{cases} H^{-\frac{1}{2}}(\mathbf{T}_s^{\boldsymbol{\nu}}(\Gamma_\bullet^0)) \times H^{-\frac{1}{2}}(\mathbf{T}_s^{\boldsymbol{\nu}}(\Gamma_\blacktriangle^0)) \to \mathbb{R} \\ \quad (\psi, \phi) \mapsto \displaystyle\int\limits_{\mathbf{T}_s^{\boldsymbol{\nu}}(\Gamma_\blacktriangle^0)} \int\limits_{\mathbf{T}_s^{\boldsymbol{\nu}}(\Gamma_\bullet^0)} G(\mathbf{x}, \mathbf{y})\, \psi(\mathbf{y})\, \phi(\mathbf{x})\, dS(\mathbf{y}) dS(\mathbf{x}) \end{cases}$$

$$\mathrm{l}^\bullet(s) : \begin{cases} H^{\frac{1}{2}}(\mathbf{T}_s^{\boldsymbol{\nu}}(\Gamma_\bullet^0)) \times H^{-\frac{1}{2}}(\mathbf{T}_s^{\boldsymbol{\nu}}(\Gamma_\bullet^0)) \to \mathbb{R} \\ \quad (g, \phi) \mapsto \displaystyle\int\limits_{\mathbf{T}_s^{\boldsymbol{\nu}}(\Gamma_\bullet^0)} g(\mathbf{x})\, \phi(\mathbf{x})\, dS(\mathbf{x}) \end{cases}$$

$$a_K^{\bullet,\blacktriangle}(s) : \begin{cases} H^{\frac{1}{2}}(\mathbf{T}_s^{\boldsymbol{\nu}}(\Gamma_\bullet^0)) \times H^{-\frac{1}{2}}(\mathbf{T}_s^{\boldsymbol{\nu}}(\Gamma_\blacktriangle^0)) \to \mathbb{R} \\ \quad (g, \phi) \mapsto \displaystyle\int\limits_{\mathbf{T}_s^{\boldsymbol{\nu}}(\Gamma_\blacktriangle^0)} \int\limits_{\mathbf{T}_s^{\boldsymbol{\nu}}(\Gamma_\bullet^0)} \nabla_y G(\mathbf{x}, \mathbf{y}) \cdot \mathbf{n}_e^s(\mathbf{y})\, g(\mathbf{y})\, \phi(\mathbf{x})\, dS(\mathbf{y}) dS(\mathbf{x}) \end{cases}$$

$$a_W^{\bullet,\blacktriangle}(s) : \begin{cases} H^{\frac{1}{2}}(\mathbf{T}_s^{\boldsymbol{\nu}}(\Gamma_\bullet^0)) \times H^{\frac{1}{2}}(\mathbf{T}_s^{\boldsymbol{\nu}}(\Gamma_\blacktriangle^0)) \to \mathbb{R} \\ \quad (g, v) \mapsto \displaystyle\int\limits_{\mathbf{T}_s^{\boldsymbol{\nu}}(\Gamma_\blacktriangle^0)} \int\limits_{\mathbf{T}_s^{\boldsymbol{\nu}}(\Gamma_\bullet^0)} G(\mathbf{x}, \mathbf{y})\, \frac{dg}{dt}(\mathbf{y})\, \frac{dv}{dt}(\mathbf{x})\, dS(\mathbf{y}) dS(\mathbf{x}) \qquad \text{(2D)} \\ \quad (g, v) \mapsto \displaystyle\int\limits_{\mathbf{T}_s^{\boldsymbol{\nu}}(\Gamma_\blacktriangle^0)} \int\limits_{\mathbf{T}_s^{\boldsymbol{\nu}}(\Gamma_\bullet^0)} G(\mathbf{x}, \mathbf{y})\, \mathbf{curl}_\Gamma\, g(\mathbf{y}) \cdot \mathbf{curl}_\Gamma\, v(\mathbf{x})\, dS(\mathbf{y}) dS(\mathbf{x}) \qquad \text{(3D)}, \end{cases}$$

where $\bullet, \blacktriangle \in \{I, C\}$. Note that in the new s-dependent expressions, $\frac{dg}{dt}$ and $\mathbf{curl}_\Gamma$ denote the arclength derivative and the surface curl operator respectively on the perturbed boundaries. The symbol $\mathbf{n}_e^s$ denotes the normal vector on $\partial\Omega_e^s = \Gamma_C^s \cup \Gamma_I^s$. This notation allows us to write the s-dependent model problem in a similarly compact way. We seek $\mathfrak{u}^s \in \tilde{H}^{\frac{1}{2}}(\Gamma_N^s)$, $\psi^s \in \tilde{H}^{-\frac{1}{2}}(\Gamma_D^s)$, $\mathfrak{u}_I^s \in H^{\frac{1}{2}}(\Gamma_I^s)$ and $\psi_I^s \in H^{-\frac{1}{2}}(\Gamma_I^s)$ such that

$$a_W^{C,I}(s)(\mathfrak{u}^s, \mathfrak{v}_I) + (1 + \frac{\varepsilon_1}{\varepsilon_2})a_W^{I,I}(s)(\mathfrak{u}_I^s, \mathfrak{v}_I) + a_K^{I,C}(s)(\mathfrak{v}_I, \psi^s) + 2a_K^{I,I}(s)(\mathfrak{v}_I, \psi_I^s)$$
$$= -a_W^{C,I}(s)(\mathfrak{g}_{ex}^s, \mathfrak{v}_I) - a_K^{I,C}(s)(\mathfrak{v}_I, \eta_{ex}^s) \qquad \forall \mathfrak{v}_I \in H^{\frac{1}{2}}(\Gamma_I^s),$$

$$a_V^{C,I}(s)(\psi^s, \phi_I) + (1 + \frac{\varepsilon_2}{\varepsilon_1})a_V^{I,I}(s)(\psi_I^s, \phi_I) - a_K^{C,I}(s)(\mathfrak{u}^s, \phi_I) - 2a_K^{I,I}(s)(\mathfrak{u}_I^s, \phi_I)$$
$$= -a_V^{C,I}(s)(\eta_{ex}^s, \phi_I) + a_K^{C,I}(s)(\mathfrak{g}_{ex}^s, \phi_I) \qquad \forall \phi_I \in H^{-\frac{1}{2}}(\Gamma_I^s),$$

$$a_V^{I,C}(s)(\psi_I^s, \tilde{\phi}) + a_V^{C,C}(s)(\psi^s, \tilde{\phi}) - a_K^{I,C}(s)(\mathfrak{u}_I^s, \tilde{\phi}) - a_K^{C,C}(s)(\mathfrak{u}^s, \tilde{\phi})$$
$$= \frac{1}{2}\mathrm{l}^C(s)(\mathfrak{g}_{ex}^s, \tilde{\phi}) - a_V^{C,C}(s)(\eta_{ex}^s, \tilde{\phi}) + a_K^{C,C}(s)(\mathfrak{g}_{ex}^s, \tilde{\phi}) \quad \forall \tilde{\phi} \in \tilde{H}^{-\frac{1}{2}}(\Gamma_D^s),$$

$$a_W^{I,C}(s)(\mathfrak{u}_I^s, \tilde{\mathfrak{v}}) + a_W^{C,C}(s)(\mathfrak{u}^s, \tilde{\mathfrak{v}}) + a_K^{C,C}(s)(\tilde{\mathfrak{v}}, \psi^s) + a_K^{C,I}(s)(\tilde{\mathfrak{v}}, \psi_I^s)$$
$$= \frac{1}{2}\mathrm{l}^C(s)(\tilde{\mathfrak{v}}, \eta_{ex}^s) - a_W^{C,C}(s)(\mathfrak{g}_{ex}^s, \tilde{\mathfrak{v}}) - a_K^{C,C}(s)(\tilde{\mathfrak{v}}, \eta_{ex}^s) \quad \forall \tilde{\mathfrak{v}} \in \tilde{H}^{\frac{1}{2}}(\Gamma_N^s).$$
$$(4.3.15)$$

A possible way to choose these boundary conditions is by taking the trace of functions in the volume, for example $\mathfrak{g}_{ex}^s := f|_{\Gamma_C^s} \in H^{\frac{1}{2}}(\Gamma_C^s)$ for some $f \in H^1(\mathbb{R}^d)$.

4.3.4 Equivalent Formulation on Reference Domain

We begin by transforming the integrals back to the reference domain using the perturbation map. The objective is to write an equivalent problem to (4.3.15) on the reference domain.

$$
a_V^{\bullet;\blacktriangle}(s)(\psi,\phi) = \int_{\Gamma_\blacktriangle^0}\int_{\Gamma_\bullet^0} G(\mathbf{T}_s^{\boldsymbol{\nu}}(\mathbf{x}),\mathbf{T}_s^{\boldsymbol{\nu}}(\mathbf{y}))\,\psi(\mathbf{T}_s^{\boldsymbol{\nu}}(\mathbf{y}))\,\omega_s(\mathbf{y})\,\phi(\mathbf{T}_s^{\boldsymbol{\nu}}(\mathbf{x}))\,\omega_s(\mathbf{x})\,dS(\mathbf{y})dS(\mathbf{x}),
$$

$$
l^{\bullet}(s)(g,\phi) = \int_{\Gamma_\bullet^0} g(\mathbf{T}_s^{\boldsymbol{\nu}}(\mathbf{x}))\,\phi(\mathbf{T}_s^{\boldsymbol{\nu}}(\mathbf{x}))\,\omega_s(\mathbf{x})\,dS(\mathbf{x}),
$$

$$
a_K^{\bullet;\blacktriangle}(s)(g,\phi) = \int_{\Gamma_\blacktriangle^0}\int_{\Gamma_\bullet^0} \nabla_y G(\mathbf{T}_s^{\boldsymbol{\nu}}(\mathbf{x}),\mathbf{T}_s^{\boldsymbol{\nu}}(\mathbf{y}))\cdot\mathbf{C}(\mathsf{D}\mathbf{T}_s^{\boldsymbol{\nu}}(\mathbf{y}))\mathbf{n}_e^0(\mathbf{y})\,g(\mathbf{T}_s^{\boldsymbol{\nu}}(\mathbf{y}))\cdot
$$
$$
\phi(\mathbf{T}_s^{\boldsymbol{\nu}}(\mathbf{x}))\,\omega_s(\mathbf{x})\,dS(\mathbf{y})dS(\mathbf{x}),
$$

$$
a_W^{\bullet;\blacktriangle}(s)(g,v) =
\begin{cases}
\displaystyle\int_{\Gamma_\blacktriangle^0}\int_{\Gamma_\bullet^0} G(\mathbf{T}_s^{\boldsymbol{\nu}}(\mathbf{x}),\mathbf{T}_s^{\boldsymbol{\nu}}(\mathbf{y}))\,(\frac{dg}{dt})(\mathbf{T}_s^{\boldsymbol{\nu}}(\mathbf{y}))\,(\frac{dv}{dt})(\mathbf{T}_s^{\boldsymbol{\nu}}(\mathbf{x}))\cdot & \text{(2D)}, \\
\quad \omega_s(\mathbf{y})\,\omega_s(\mathbf{x})\,dS(\mathbf{y})dS(\mathbf{x}) & \\
\displaystyle\int_{\Gamma_\blacktriangle^0}\int_{\Gamma_\bullet^0} G(\mathbf{T}_s^{\boldsymbol{\nu}}(\mathbf{x}),\mathbf{T}_s^{\boldsymbol{\nu}}(\mathbf{y}))\,(\mathbf{curl}_\Gamma\,g)(\mathbf{T}_s^{\boldsymbol{\nu}}(\mathbf{y}))\cdot(\mathbf{curl}_\Gamma\,v)(\mathbf{T}_s^{\boldsymbol{\nu}}(\mathbf{x}))\cdot & \text{(3D)}, \\
\quad \omega_s(\mathbf{y})\,\omega_s(\mathbf{x})\,dS(\mathbf{y})dS(\mathbf{x}) &
\end{cases}
$$

(4.3.16)

where $\mathbf{n}_e^0$ is the unit normal vector field on the reference boundary $\partial\Omega_e^0$ and $\mathbf{C}(M)$ is the cofactor matrix of M. We have used the following identity for transforming surface integrals [18, Ch. 9, Sec. 4.2, eq. 4.9], [57, Sect. 2.17] from $\mathbf{T}_s^{\boldsymbol{\nu}}(\Gamma^0)$ to Γ^0:

$$
\int_{\mathbf{T}_s^{\boldsymbol{\nu}}(\Gamma^0)} f(\mathbf{x}')\,dS(\mathbf{x}') = \int_{\Gamma^0}(f\circ\mathbf{T}_s^{\boldsymbol{\nu}})(\mathbf{x})\,\omega_s(\mathbf{x})\,dS(\mathbf{x}), \quad \omega_s(\mathbf{x}) := \left\|\mathbf{C}(\mathsf{D}\mathbf{T}_s^{\boldsymbol{\nu}})(\mathbf{x})\,\mathbf{n}^0(\mathbf{x})\right\|, \; \mathbf{x}\in\Gamma^0,
$$

where $\mathbf{n}^s$ is the unit normal for $\mathbf{T}_s^{\boldsymbol{\nu}}(\Gamma^0)$. We have also used the following formula for the transformation of unit normal vector fields [18, Ch. 9, Thm. 4.4]

$$
\mathbf{n}^s(\mathbf{T}_s^{\boldsymbol{\nu}}(\mathbf{x})) = \frac{\mathbf{C}(\mathsf{D}\mathbf{T}_s^{\boldsymbol{\nu}}(\mathbf{x}))\mathbf{n}^0(\mathbf{x})}{\|\mathbf{C}(\mathsf{D}\mathbf{T}_s^{\boldsymbol{\nu}}(\mathbf{x}))\mathbf{n}^0(\mathbf{x})\|}, \; \mathbf{x}\in\Gamma^0.
$$

4.3.5 Pullback

The next step to achieve our objective of having an equivalent problem on the reference domain is the use of a pullback, which allows us to get rid of the s-dependence of the function spaces. We use a pullback of surface charge densities (2-forms in the language of exterior calculus) for functions in $H^{-\frac{1}{2}}(\Gamma_\bullet^s)$ and a pullback of potentials (0-forms from the perspective of exterior calculus) for functions in $H^{\frac{1}{2}}(\Gamma_\bullet^s)$, $\bullet\in\{I,C\}$:

$$
\hat\psi\in H^{-\frac{1}{2}}(\Gamma_\bullet^0): \quad \hat\psi := (\psi\circ\mathbf{T}_s^{\boldsymbol{\nu}})\,\omega_s, \quad \psi\in H^{-\frac{1}{2}}(\Gamma_\bullet^s), \tag{4.3.17}
$$

$$
\hat v\in H^{\frac{1}{2}}(\Gamma_\bullet^0): \quad \hat v := v\circ\mathbf{T}_s^{\boldsymbol{\nu}}, \qquad v\in H^{\frac{1}{2}}(\Gamma_\bullet^s). \tag{4.3.18}
$$

The pullback allows us to work with functions on the reference boundaries $\Gamma_\bullet^0$ which will be important in order to compute the energy shape derivative later. Since $\mathbf{T}_s^{\boldsymbol{\nu}}$ is a Lipschitz continuous mapping and $\omega_s \in L^\infty(\Gamma_\bullet^s)$, the trace spaces are preserved under pullback. We also need additional transformation rules for the hypersingular bilinear form $a_W^{\bullet,\blacktriangle}(s)(g,v)$. In 2D it involves the arclength derivative which transforms as

$$\left(\frac{dg}{dt}\right)(\mathbf{T}_s^{\boldsymbol{\nu}}(\mathbf{x})) = \lim_{\|\mathbf{y}-\mathbf{x}\|\to 0} \frac{g(\mathbf{T}_s^{\boldsymbol{\nu}}(\mathbf{x})) - g(\mathbf{T}_s^{\boldsymbol{\nu}}(\mathbf{y}))}{\|\mathbf{T}_s^{\boldsymbol{\nu}}(\mathbf{x}) - \mathbf{T}_s^{\boldsymbol{\nu}}(\mathbf{y})\|} = \lim_{\|\mathbf{y}-\mathbf{x}\|\to 0} \frac{g\circ\mathbf{T}_s^{\boldsymbol{\nu}}(\mathbf{x}) - g\circ\mathbf{T}_s^{\boldsymbol{\nu}}(\mathbf{y})}{\omega_s(\mathbf{x})\,\|\mathbf{y}-\mathbf{x}\|} = \frac{1}{\omega_s(\mathbf{x})}\left(\frac{d\hat{g}}{dt}\right)(\mathbf{x}),$$

where $\frac{d\hat{g}}{dt}$ is the arclength derivative of $\hat{g}$ which lies on the reference boundary.

In 3D we have to transform the surface curl operator. We begin by noting that $\mathbf{curl}_\Gamma u(\mathbf{x}) := \mathbf{grad}_\Gamma u(\mathbf{x}) \times \mathbf{n}(\mathbf{x}) = \nabla\tilde{u}(\mathbf{x}) \times \mathbf{n}(\mathbf{x})$, where $\tilde{u} : \mathbb{R}^3 \to \mathbb{R}$ is an extension of $u \in C^1(\Gamma)$ to a neighborhood of the surface Γ along the outward normal $\mathbf{n}(\mathbf{x})$. Using the transformation rules for the gradient and the normal we get

$$(\mathbf{curl}_\Gamma u)(\mathbf{T}_s^{\boldsymbol{\nu}}(\mathbf{x})) = \nabla\tilde{u}(\mathbf{T}_s^{\boldsymbol{\nu}}(\mathbf{x})) \times \mathbf{n}^s(\mathbf{T}_s^{\boldsymbol{\nu}}(\mathbf{x}))$$

$$= \mathsf{D}\mathbf{T}_s^{\boldsymbol{\nu}}(\mathbf{x})^{-T}\nabla(\tilde{u}\circ\mathbf{T}_s^{\boldsymbol{\nu}})(\mathbf{x}) \times \frac{\mathsf{D}\mathbf{T}_s^{\boldsymbol{\nu}}(\mathbf{x})^{-T}\,\mathbf{n}^0(\mathbf{x})}{\|\mathsf{D}\mathbf{T}_s^{\boldsymbol{\nu}}(\mathbf{x})^{-T}\,\mathbf{n}^0(\mathbf{x})\|}$$

$$= \frac{\det(\mathsf{D}\mathbf{T}_s^{\boldsymbol{\nu}}(\mathbf{x})^{-T})\mathsf{D}\mathbf{T}_s^{\boldsymbol{\nu}}(\mathbf{x})}{\|\mathsf{D}\mathbf{T}_s^{\boldsymbol{\nu}}(\mathbf{x})^{-T}\,\mathbf{n}^0(\mathbf{x})\|}\big(\nabla(\tilde{u}\circ\mathbf{T}_s^{\boldsymbol{\nu}})(\mathbf{x}) \times \mathbf{n}^0(\mathbf{x})\big) = \frac{\mathsf{D}\mathbf{T}_s^{\boldsymbol{\nu}}(\mathbf{x})}{\omega_s(\mathbf{x})}(\mathbf{curl}_\Gamma\,\hat{u})(\mathbf{x}),$$

where we used the identity $(\mathbf{M}\mathbf{a})\times(\mathbf{M}\mathbf{b}) = \det(\mathbf{M})\mathbf{M}^{-T}(\mathbf{a}\times\mathbf{b})$ for a regular matrix $\mathbf{M} \in \mathbb{R}^{3,3}$ and vectors $\mathbf{a}, \mathbf{b} \in \mathbb{R}^3$, and $\mathbf{n}^s(\mathbf{x})$ is the outward normal on the boundary $\mathbf{T}_s^{\boldsymbol{\nu}}(\Gamma^0)$.

Based on the pullbacks, we define bilinear forms that look similar to those of (4.3.16), but are defined on s-independent trace spaces on reference boundaries. Notice the difference in notation for these bilinear forms for which the parameter s is included as an independent variable, thanks to the spaces being independent of s.

$$\hat{a}_V^{\bullet,\blacktriangle} : \begin{cases} \big(-\delta(\boldsymbol{\mathcal{V}}),\delta(\boldsymbol{\mathcal{V}})\big) \times H^{-\frac{1}{2}}(\Gamma_\bullet^0) \times H^{-\frac{1}{2}}(\Gamma_\blacktriangle^0) \to \mathbb{R} \\ (s;\hat{\psi},\hat{\phi}) \mapsto \displaystyle\int_{\Gamma_\blacktriangle^0}\int_{\Gamma_\bullet^0} G(\mathbf{T}_s^{\boldsymbol{\nu}}(\mathbf{x}),\mathbf{T}_s^{\boldsymbol{\nu}}(\mathbf{y}))\,\hat{\psi}(\mathbf{y})\,\hat{\phi}(\mathbf{x})\,dS(\mathbf{y})dS(\mathbf{x}) \end{cases}$$

$$\hat{\imath}^\bullet : \begin{cases} \big(-\delta(\boldsymbol{\mathcal{V}}),\delta(\boldsymbol{\mathcal{V}})\big) \times H^{\frac{1}{2}}(\Gamma_\bullet^0) \times H^{-\frac{1}{2}}(\Gamma_\bullet^0) \to \mathbb{R} \\ (s;\hat{g},\hat{\phi}) \mapsto \displaystyle\int_{\Gamma_\bullet^0} \hat{g}(\mathbf{x})\,\hat{\phi}(\mathbf{x})\,dS(\mathbf{x}) \end{cases}$$

$$\hat{a}_K^{\bullet,\blacktriangle} : \begin{cases} \big(-\delta(\boldsymbol{\mathcal{V}}),\delta(\boldsymbol{\mathcal{V}})\big) \times H^{\frac{1}{2}}(\Gamma_\bullet^0) \times H^{-\frac{1}{2}}(\Gamma_\blacktriangle^0) \to \mathbb{R} \\ (s;\hat{g},\hat{\phi}) \mapsto \displaystyle\int_{\Gamma_\blacktriangle^0}\int_{\Gamma_\bullet^0} \nabla_y G(\mathbf{T}_s^{\boldsymbol{\nu}}(\mathbf{x}),\mathbf{T}_s^{\boldsymbol{\nu}}(\mathbf{y})) \cdot \mathbf{C}(\mathsf{D}\mathbf{T}_s^{\boldsymbol{\nu}}(\mathbf{y}))\mathbf{n}_e^0(\mathbf{y})\,\hat{g}(\mathbf{y})\,\hat{\phi}(\mathbf{x})\,dS(\mathbf{y})dS(\mathbf{x}) \end{cases}$$

$$\hat{a}_W^{\bullet,\blacktriangle} : \begin{cases} \big(-\delta(\boldsymbol{\mathcal{V}}),\delta(\boldsymbol{\mathcal{V}})\big) \times H^{\frac{1}{2}}(\Gamma_\bullet^0) \times H^{\frac{1}{2}}(\Gamma_\blacktriangle^0) \to \mathbb{R} \\ (s;\hat{g},\hat{v}) \mapsto \displaystyle\int_{\Gamma_\blacktriangle^0}\int_{\Gamma_\bullet^0} G(\mathbf{T}_s^{\boldsymbol{\nu}}(\mathbf{x}),\mathbf{T}_s^{\boldsymbol{\nu}}(\mathbf{y}))\,\left(\frac{d\hat{g}}{dt}\right)(\mathbf{y})\,\left(\frac{d\hat{v}}{dt}\right)(\mathbf{x})\,dS(\mathbf{y})dS(\mathbf{x}) \quad \text{(2D)}, \\ (s;\hat{g},\hat{v}) \mapsto \displaystyle\int_{\Gamma_\blacktriangle^0}\int_{\Gamma_\bullet^0} G(\mathbf{T}_s^{\boldsymbol{\nu}}(\mathbf{x}),\mathbf{T}_s^{\boldsymbol{\nu}}(\mathbf{y}))\,\big(\mathsf{D}\mathbf{T}_s^{\boldsymbol{\nu}}(\mathbf{y})(\mathbf{curl}_\Gamma\,\hat{g})(\mathbf{y})\big) \cdot \qquad \text{(3D)}. \\ \qquad\qquad\qquad \big(\mathsf{D}\mathbf{T}_s^{\boldsymbol{\nu}}(\mathbf{x})(\mathbf{curl}_\Gamma\,\hat{v})(\mathbf{x})\big)\,dS(\mathbf{y})dS(\mathbf{x}) \end{cases}$$

Using a similar procedure we can also get a transformed energy functional $\hat{J}$

$$\hat{J}: \begin{cases} (-\delta(\boldsymbol{\mathcal{V}}), \delta(\boldsymbol{\mathcal{V}})) \times H^{\frac{1}{2}}(\Gamma_C^0) \times H^{-\frac{1}{2}}(\Gamma_C^0) \to \mathbb{R}, \\[2mm] (s; \hat{\mathbf{u}}, \hat{\psi}) \mapsto \dfrac{\varepsilon_e}{2} \displaystyle\int_{\Gamma_C^0} (\hat{\mathbf{u}}(\mathbf{x}) + \hat{\mathfrak{g}}_{ex}^s(\mathbf{x}))\, (\hat{\eta}_{ex}^s(\mathbf{x}) + \hat{\psi}(\mathbf{x}))\, d\mathrm{S}(\mathbf{x}), \end{cases}$$

where $\hat{\mathfrak{g}}_{ex}^s$ and $\hat{\eta}_{ex}^s$ are the pullbacks of the extended Dirichlet and Neumann boundary data respectively. Finally our system of equations becomes: seek $\hat{\mathbf{u}}^s \in \tilde{H}^{\frac{1}{2}}(\Gamma_N^0)$, $\hat{\psi}^s \in \tilde{H}^{-\frac{1}{2}}(\Gamma_D^0)$, $\hat{\mathbf{u}}_I^s \in H^{\frac{1}{2}}(\Gamma_I^0)$ and $\hat{\psi}_I^s \in H^{-\frac{1}{2}}(\Gamma_I^0)$ such that

$$\hat{\mathrm{a}}_{\mathrm{W}}^{\mathrm{C,I}}(s; \hat{\mathbf{u}}^s, \hat{\mathbf{v}}_I) + (1 + \frac{\varepsilon_i}{\varepsilon_e})\hat{\mathrm{a}}_{\mathrm{W}}^{\mathrm{I,I}}(s; \hat{\mathbf{u}}_I^s, \hat{\mathbf{v}}_I) + \hat{\mathrm{a}}_{\mathrm{K}}^{\mathrm{I,C}}(s; \hat{\mathbf{v}}_I, \hat{\psi}^s) + 2\hat{\mathrm{a}}_{\mathrm{K}}^{\mathrm{I,I}}(s; \hat{\mathbf{v}}_I, \hat{\psi}_I^s)$$
$$= -\hat{\mathrm{a}}_{\mathrm{W}}^{\mathrm{C,I}}(s; \hat{\mathfrak{g}}_{ex}^s, \hat{\mathbf{v}}_I) - \hat{\mathrm{a}}_{\mathrm{K}}^{\mathrm{I,C}}(s; \hat{\mathbf{v}}_I, \hat{\eta}_{ex}^s) \qquad \forall \hat{\mathbf{v}}_I \in H^{\frac{1}{2}}(\Gamma_I^0),$$

$$\hat{\mathrm{a}}_{\mathrm{V}}^{\mathrm{C,I}}(s; \hat{\psi}^s, \hat{\phi}_I) + (1 + \frac{\varepsilon_2}{\varepsilon_1})\hat{\mathrm{a}}_{\mathrm{V}}^{\mathrm{I,I}}(s; \hat{\psi}_I^s, \hat{\phi}_I) - \hat{\mathrm{a}}_{\mathrm{K}}^{\mathrm{C,I}}(s; \hat{\mathbf{u}}^s, \hat{\phi}_I) - 2\hat{\mathrm{a}}_{\mathrm{K}}^{\mathrm{I,I}}(s; \hat{\mathbf{u}}_I^s, \hat{\phi}_I)$$
$$= -\hat{\mathrm{a}}_{\mathrm{V}}^{\mathrm{C,I}}(s; \hat{\eta}_{ex}^s, \hat{\phi}_I) + \hat{\mathrm{a}}_{\mathrm{K}}^{\mathrm{C,I}}(s; \hat{\mathfrak{g}}_{ex}^s, \hat{\phi}_I) \qquad \forall \hat{\phi}_I \in H^{-\frac{1}{2}}(\Gamma_I^0),$$

$$\hat{\mathrm{a}}_{\mathrm{V}}^{\mathrm{I,C}}(s; \hat{\psi}_I^s, \hat{\phi}) + \hat{\mathrm{a}}_{\mathrm{V}}^{\mathrm{C,C}}(s; \hat{\psi}^s, \hat{\phi}) - \hat{\mathrm{a}}_{\mathrm{K}}^{\mathrm{I,C}}(s; \hat{\mathbf{u}}_I^s, \hat{\phi}) - \hat{\mathrm{a}}_{\mathrm{K}}^{\mathrm{C,C}}(s; \hat{\mathbf{u}}^s, \hat{\phi})$$
$$= \frac{1}{2}\hat{\mathrm{l}}^C(s; \hat{\mathfrak{g}}_{ex}^s, \hat{\phi}) - \hat{\mathrm{a}}_{\mathrm{V}}^{\mathrm{C,C}}(s; \hat{\eta}_{ex}^s, \hat{\phi}) + \hat{\mathrm{a}}_{\mathrm{K}}^{\mathrm{C,C}}(s; \hat{\mathfrak{g}}_{ex}^s, \hat{\phi}) \quad \forall \hat{\phi} \in \tilde{H}^{-\frac{1}{2}}(\Gamma_D^0),$$

$$\hat{\mathrm{a}}_{\mathrm{W}}^{\mathrm{I,C}}(s; \hat{\mathbf{u}}_I^s, \tilde{\mathbf{v}}) + \hat{\mathrm{a}}_{\mathrm{W}}^{\mathrm{C,C}}(s; \hat{\mathbf{u}}^s, \hat{\mathbf{v}}) + \hat{\mathrm{a}}_{\mathrm{K}}^{\mathrm{C,C}}(s; \hat{\mathbf{v}}, \hat{\psi}^s) + \hat{\mathrm{a}}_{\mathrm{K}}^{\mathrm{C,I}}(s; \hat{\mathbf{v}}, \hat{\psi}_I^s)$$
$$= \frac{1}{2}\hat{\mathrm{l}}^C(s; \hat{\mathbf{v}}, \hat{\eta}_{ex}^s) - \hat{\mathrm{a}}_{\mathrm{W}}^{\mathrm{C,C}}(s; \hat{\mathfrak{g}}_{ex}^s, \hat{\mathbf{v}}) - \hat{\mathrm{a}}_{\mathrm{K}}^{\mathrm{C,C}}(s; \hat{\mathbf{v}}, \hat{\eta}_{ex}^s) \quad \forall \hat{\mathbf{v}} \in \tilde{H}^{\frac{1}{2}}(\Gamma_N^0).$$
$$(4.3.19)$$

At this point we make the assumption that $\boldsymbol{\mathcal{V}}|_{\Gamma_C^0} \equiv 0$. Consequently, the boundary Γ_C^0 does not change under the perturbation map, neither do the boundary conditions on Γ_C^0. Exploiting this we write $\hat{\eta}_{ex}^s = \eta_{ex}$ and $\hat{\mathfrak{g}}_{ex}^s = \mathfrak{g}_{ex}$ which will make easier computing partial derivatives with respect to s.

Introducing the notations

$$V := \tilde{H}^{-\frac{1}{2}}(\Gamma_D^0) \times \tilde{H}^{\frac{1}{2}}(\Gamma_N^0) \times H^{-\frac{1}{2}}(\Gamma_I^0) \times H^{\frac{1}{2}}(\Gamma_I^0),$$
$$\mathbf{X} := (\hat{\psi}, \hat{\mathbf{u}}, \hat{\psi}_I, \hat{\mathbf{u}}_I) \in V, \quad \mathbf{X}^s := (\hat{\psi}^s, \hat{\mathbf{u}}^s, \hat{\psi}_I^s, \hat{\mathbf{u}}_I^s) \in V, \quad \mathbf{Y} := (\hat{\phi}, \hat{\mathbf{v}}, \hat{\phi}_I, \hat{\mathbf{v}}_I) \in V,$$

the system of equations (4.3.19) can be written as

$$\boxed{\mathbf{X}^s \in V : \quad \mathrm{A}(s; \mathbf{X}^s, \mathbf{Y}) = \mathrm{L}(s; \mathbf{Y}) \quad \forall \mathbf{Y} \in V}, \qquad (4.3.20)$$

where the s dependent bilinear and linear forms A and L are given as

$$
A : \begin{cases}
\big(-\delta(\boldsymbol{\mathcal{V}}), \delta(\boldsymbol{\mathcal{V}})\big) \times V \times V \to \mathbb{R} \\
\quad (s; \mathbf{X}, \mathbf{Y}) \mapsto \hat{\mathrm{a}}_{\mathrm{W}}^{\mathrm{C,I}}(s; \hat{\mathfrak{u}}, \hat{\mathfrak{v}}_I) + (1 + \dfrac{\varepsilon_i}{\varepsilon_e})\hat{\mathrm{a}}_{\mathrm{W}}^{\mathrm{I,I}}(s; \hat{\mathfrak{u}}_I, \hat{\mathfrak{v}}_I) + \hat{\mathrm{a}}_{\mathrm{K}}^{\mathrm{I,C}}(s; \hat{\mathfrak{v}}_I, \hat{\psi}) + 2\hat{\mathrm{a}}_{\mathrm{K}}^{\mathrm{I,I}}(s; \hat{\mathfrak{v}}_I, \hat{\psi}_I) + \\
\qquad \hat{\mathrm{a}}_{\mathrm{V}}^{\mathrm{C,I}}(s; \hat{\psi}, \hat{\phi}_I) + (1 + \dfrac{\varepsilon_e}{\varepsilon_i})\hat{\mathrm{a}}_{\mathrm{V}}^{\mathrm{I,I}}(s; \hat{\psi}_I, \hat{\phi}_I) - \hat{\mathrm{a}}_{\mathrm{K}}^{\mathrm{C,I}}(s; \hat{\mathfrak{u}}, \hat{\phi}_I) - 2\hat{\mathrm{a}}_{\mathrm{K}}^{\mathrm{I,I}}(s; \hat{\mathfrak{u}}_I, \hat{\phi}_I) + \\
\qquad \hat{\mathrm{a}}_{\mathrm{V}}^{\mathrm{I,C}}(s; \hat{\psi}_I, \hat{\phi}) + \hat{\mathrm{a}}_{\mathrm{V}}^{\mathrm{C,C}}(s; \hat{\psi}, \hat{\phi}) - \hat{\mathrm{a}}_{\mathrm{K}}^{\mathrm{I,C}}(s; \hat{\mathfrak{u}}_I, \hat{\phi}) - \hat{\mathrm{a}}_{\mathrm{K}}^{\mathrm{C,C}}(s; \hat{\mathfrak{u}}, \hat{\phi}) + \\
\qquad \hat{\mathrm{a}}_{\mathrm{W}}^{\mathrm{I,C}}(s; \hat{\mathfrak{u}}_I, \hat{\mathfrak{v}}) + \hat{\mathrm{a}}_{\mathrm{W}}^{\mathrm{C,C}}(s; \hat{\mathfrak{u}}, \hat{\mathfrak{v}}) + \hat{\mathrm{a}}_{\mathrm{K}}^{\mathrm{C,C}}(s; \hat{\mathfrak{v}}, \hat{\psi}) + \hat{\mathrm{a}}_{\mathrm{K}}^{\mathrm{C,I}}(s; \hat{\mathfrak{v}}, \hat{\psi}_I),
\end{cases}
$$

$$
L : \begin{cases}
\big(-\delta(\boldsymbol{\mathcal{V}}), \delta(\boldsymbol{\mathcal{V}})\big) \times V \to \mathbb{R} \\
\quad (s; \mathbf{Y}) \mapsto -\hat{\mathrm{a}}_{\mathrm{W}}^{\mathrm{C,I}}(s; \mathfrak{g}_{ex}, \hat{\mathfrak{v}}_I) - \hat{\mathrm{a}}_{\mathrm{K}}^{\mathrm{I,C}}(s; \hat{\mathfrak{v}}_I, \eta_{ex}) - \hat{\mathrm{a}}_{\mathrm{V}}^{\mathrm{C,I}}(s; \eta_{ex}, \hat{\phi}_I) + \hat{\mathrm{a}}_{\mathrm{K}}^{\mathrm{C,I}}(s; \mathfrak{g}_{ex}, \hat{\phi}_I) + \\
\qquad \dfrac{1}{2}\hat{\mathrm{l}}^C(s; \mathfrak{g}_{ex}, \hat{\phi}) - \hat{\mathrm{a}}_{\mathrm{V}}^{\mathrm{C,C}}(s; \eta_{ex}, \hat{\phi}) + \hat{\mathrm{a}}_{\mathrm{K}}^{\mathrm{C,C}}(s; \mathfrak{g}_{ex}, \hat{\phi}) + \dfrac{1}{2}\hat{\mathrm{l}}^C(s; \hat{\mathfrak{v}}, \eta_{ex}) - \\
\qquad \hat{\mathrm{a}}_{\mathrm{W}}^{\mathrm{C,C}}(s; \mathfrak{g}_{ex}, \hat{\mathfrak{v}}) - \hat{\mathrm{a}}_{\mathrm{K}}^{\mathrm{C,C}}(s; \hat{\mathfrak{v}}, \eta_{ex}).
\end{cases}
$$

We call (4.3.20) the *"state (variational) equation"*. This formulation is equivalent to our s-dependent model problem as a solution of the original formulation (4.3.15) also solves this pulled-back formulation by definition. Conversely, if $\hat{\mathfrak{u}}^s \in \tilde{H}^{\frac{1}{2}}(\Gamma_N^0)$, $\hat{\psi}^s \in \tilde{H}^{-\frac{1}{2}}(\Gamma_D^0)$, $\hat{\mathfrak{u}}_I^s \in H^{\frac{1}{2}}(\Gamma_I^0)$ and $\hat{\psi}_I^s \in H^{-\frac{1}{2}}(\Gamma_I^0)$ solve (4.3.19) then using the fact that $\mathbf{T}_s^{\boldsymbol{\nu}}$ is a diffeomorphism and taking into account pullbacks, we recover the original formulation (4.3.15).

4.3.6 BIE Constrained Shape Derivative

While shape differentiating the field energy, we need to account for the constraint (4.3.19). We do this using the well-established adjoint approach [31, Sect. 1.6.4]. We start by defining the Lagrangian:

$$
\mathcal{L} : (-\delta(\boldsymbol{\mathcal{V}}), \delta(\boldsymbol{\mathcal{V}})) \times V \times V \to \mathbb{R}, \quad \mathcal{L}(s; \mathbf{X}, \mathbf{Y}) := A(s; \mathbf{X}, \mathbf{Y}) - L(s; \mathbf{Y}) + J(s; \mathbf{X}),
$$

where

$$
J : (-\delta(\boldsymbol{\mathcal{V}}), \delta(\boldsymbol{\mathcal{V}})) \times V \to \mathbb{R}, \quad J(s; \mathbf{X}) := \frac{\varepsilon_e}{2} \int_{\Gamma_C^0} (\hat{\mathfrak{u}}(\mathbf{x}) + \mathfrak{g}_{ex}(\mathbf{x}))\, (\eta_{ex}(\mathbf{x}) + \hat{\psi}(\mathbf{x}))\, d\mathrm{S}(\mathbf{x}).
$$

We recover the energy functional by plugging in the pulled-back solution $\mathbf{X}^s \in V$ of (4.3.20) into the Lagrangian,

$$
\mathcal{L}(s; \mathbf{X}^s, \mathbf{Y}) = J(s; \mathbf{X}^s) = \mathcal{J}_F(s).
$$

Differentiating with respect to s and using chain rule gives

$$
\frac{d\mathcal{J}_F}{ds}(0) = \frac{\partial \mathcal{L}}{\partial s}(0; \mathbf{X}^0, \mathbf{Y}) + \left\langle \frac{\partial \mathcal{L}}{\partial \mathbf{X}}(0; \mathbf{X}^0, \mathbf{Y}); \frac{d\mathbf{X}^s}{ds}(0) \right\rangle \quad \forall \mathbf{Y} \in V.
$$

Using the adjoint solution $\mathbf{P} \in V$, the Gateaux shape derivative in the direction of $\boldsymbol{\mathcal{V}}$ can be written as:

$$
\frac{d\mathcal{J}_F}{ds}(0) = \frac{\partial \mathcal{L}}{\partial s}(0; \mathbf{X}^0, \mathbf{P}).
$$

The adjoint solution $\mathbf{P} := (\hat{\rho}, \hat{p}, \hat{\rho}_I, \hat{p}_I) \in V$ solves the *adjoint variational equation*

$$\boxed{\left\langle \frac{\partial \mathcal{L}}{\partial \mathbf{X}}(0; \mathbf{X}^0, \mathbf{P}); \mathbf{Z} \right\rangle = 0 \quad \forall \mathbf{Z} \in V}, \tag{4.3.21}$$

where $\mathbf{Z} := (\beta, w, \beta_I, w_I)$, and the notation $\left\langle \frac{\partial \mathcal{L}}{\partial \mathbf{X}}(0; \mathbf{X}^0, \mathbf{P}); \mathbf{Z} \right\rangle$ means the derivative in the direction $\mathbf{Z}$. Written more explicitly, the adjoint variational equation is

$$\mathbf{P} \in V: \quad A(0; \mathbf{Z}, \mathbf{P}) = -\frac{\varepsilon_e}{2} \big(\hat{\mathrm{l}}^C(0; w, \eta_{ex} + \hat{\psi}^0) + \hat{\mathrm{l}}^C(0; \mathfrak{g}_{ex} + \hat{\mathfrak{u}}^0, \beta) \big) \quad \forall \mathbf{Z} \in V. \tag{4.3.22}$$

The adjoint equation involves a similar bilinear form as the state equation (4.3.20) and a modified RHS. The partial derivatives with respect to s are computed by differentiating with respect to s under the integral, using the chain rule and product rule:

$$\frac{\partial \hat{a}_V^{\bullet,\blacktriangle}}{\partial s}(0; \hat{\psi}, \hat{\phi}) = \int_{\Gamma_\blacktriangle^0} \int_{\Gamma_\bullet^0} (\nabla_x G(\mathbf{x}, \mathbf{y}) \cdot \boldsymbol{\nu}(\mathbf{x}) + \nabla_y G(\mathbf{x}, \mathbf{y}) \cdot \boldsymbol{\nu}(\mathbf{y})) \, \hat{\psi}(\mathbf{y}) \, \hat{\phi}(\mathbf{x}) \, dS(\mathbf{y}) dS(\mathbf{x}),$$

$$\frac{\partial \hat{\mathrm{l}}^\bullet}{\partial s}(0; \hat{g}, \hat{\phi}) = 0,$$

$$\frac{\partial \hat{a}_K^{\bullet,\blacktriangle}}{\partial s}(0; \hat{g}, \hat{\phi}) = \int_{\Gamma_\blacktriangle^0} \int_{\Gamma_\bullet^0} (\nabla_x(\nabla_y G(\mathbf{x}, \mathbf{y}))^T \cdot \boldsymbol{\nu}(\mathbf{x}) +$$
$$\nabla_y(\nabla_y G(\mathbf{x}, \mathbf{y}))^T \cdot \boldsymbol{\nu}(\mathbf{y})) \cdot \mathbf{n}_e^0(\mathbf{y}) \, \hat{g}(\mathbf{y}) \, \hat{\phi}(\mathbf{x}) \, dS(\mathbf{y}) dS(\mathbf{x})$$
$$+ \int_{\Gamma_\blacktriangle^0} \int_{\Gamma_\bullet^0} \nabla_y G(\mathbf{x}, \mathbf{y}) \cdot (\nabla \cdot \boldsymbol{\nu}(\mathbf{y}) \mathbf{n}_e^0(\mathbf{y}) - D\boldsymbol{\nu}^T(\mathbf{y}) \mathbf{n}_e^0(\mathbf{y})) \cdot$$
$$\hat{g}(\mathbf{y}) \, \hat{\phi}(\mathbf{x}) \, dS(\mathbf{y}) dS(\mathbf{x}),$$

$$\frac{\partial \hat{a}_W^{\bullet,\blacktriangle}}{\partial s}(0; \hat{g}, \hat{v}) = \begin{cases} \int_{\Gamma_\blacktriangle^0} \int_{\Gamma_\bullet^0} (\nabla_x G(\mathbf{x}, \mathbf{y}) \cdot \boldsymbol{\nu}(\mathbf{x}) + \nabla_y G(\mathbf{x}, \mathbf{y}) \cdot \boldsymbol{\nu}(\mathbf{y})) \cdot & \text{(2D)} \\ \qquad \frac{d\hat{g}}{d\hat{t}}(\mathbf{y}) \frac{d\hat{v}}{d\hat{t}}(\mathbf{x}) \, dS(\mathbf{y}) dS(\mathbf{x}), \\[2mm] \int_{\Gamma_\blacktriangle^0} \int_{\Gamma_\bullet^0} (\nabla_x G(\mathbf{x}, \mathbf{y}) \cdot \boldsymbol{\nu}(\mathbf{x}) + \nabla_y G(\mathbf{x}, \mathbf{y}) \cdot \boldsymbol{\nu}(\mathbf{y})) \cdot & \text{(3D)} \\ \qquad \mathbf{curl}_\Gamma \, \hat{g}(\mathbf{y}) \cdot \mathbf{curl}_\Gamma \, \hat{v}(\mathbf{x}) \, dS(\mathbf{y}) dS(\mathbf{x}) \\[2mm] + \int_{\Gamma_\blacktriangle^0} \int_{\Gamma_\bullet^0} G(\mathbf{x}, \mathbf{y}) \, ((D\boldsymbol{\mathcal{V}}(\mathbf{y}) \, \mathbf{curl}_\Gamma \, \hat{g}(\mathbf{y})) \cdot \mathbf{curl}_\Gamma \, \hat{v}(\mathbf{x}) + \\ \qquad \mathbf{curl}_\Gamma \, \hat{g}(\mathbf{y}) \cdot (D\boldsymbol{\mathcal{V}}(\mathbf{x}) \, \mathbf{curl}_\Gamma \, \hat{v}(\mathbf{x})) \, dS(\mathbf{y}) dS(\mathbf{x}), \end{cases}$$

$$\tag{4.3.23}$$

where we have used the identities [57, Sect. 2.13]

$$\frac{d(f \circ \mathbf{T}_s^{\boldsymbol{\nu}})}{ds}\Big|_{s=0} = \nabla f \cdot \boldsymbol{\nu}, \quad \frac{d(\mathbf{C}(D\mathbf{T}_s^{\boldsymbol{\nu}}))}{ds}\Big|_{s=0} = \nabla \cdot \boldsymbol{\nu} \, \mathbf{I}_d - (D\boldsymbol{\nu})^T, \quad \frac{d(D\mathbf{T}_s^{\boldsymbol{\nu}})}{ds}\Big|_{s=0} = D\boldsymbol{\mathcal{V}}.$$

The energy shape derivative is obtained by combining these partial derivatives. It seems that the integrands in $\frac{\partial \hat{a}_K^{\bullet,\blacktriangle}}{\partial s}(0; \hat{g}, \hat{\phi})$ feature strong singularities. However, after inserting a Taylor expansion of $\boldsymbol{\mathcal{V}}$ it turns out that these cancel and we end up with only weak singularities [48, Equation 4.37].

The final expression for the shape derivative of the field energy in the direction of $\mathcal{V}$ reads

$$
\begin{aligned}
\frac{d\mathcal{J}_F}{ds}(0;\mathcal{V})[\mathbf{X}_0,\mathbf{P}] =& \frac{\partial\mathcal{L}}{\partial s}(0;\mathbf{X}_0,\mathbf{P}) = \frac{\partial\mathrm{A}}{\partial s}(0;\mathbf{X}_0,\mathbf{P}) - \frac{\partial\mathrm{L}}{\partial s}(0;\mathbf{P}) + \frac{\partial\mathrm{J}}{\partial s}(0;\mathbf{X}_0) = \\
& \frac{\partial}{\partial s}\hat{\mathrm{a}}_\mathrm{W}^{\mathrm{C,I}}(0;\hat{\mathfrak{u}}^0,\hat{p}_I) + (1+\frac{\varepsilon_1}{\varepsilon_2})\frac{\partial}{\partial s}\hat{\mathrm{a}}_\mathrm{W}^{\mathrm{I,I}}(0;\hat{\mathfrak{u}}_I^0,\hat{p}_I) + \frac{\partial}{\partial s}\hat{\mathrm{a}}_\mathrm{K}^{\mathrm{I,C}}(0;\hat{p}_I,\hat{\psi}^0) + 2\frac{\partial}{\partial s}\hat{\mathrm{a}}_\mathrm{K}^{\mathrm{I,I}}(0;\hat{p}_I,\hat{\psi}_I^0) \\
& + \frac{\partial}{\partial s}\hat{\mathrm{a}}_\mathrm{V}^{\mathrm{C,I}}(0;\hat{\psi}^0,\hat{\rho}_I) + (1+\frac{\varepsilon_2}{\varepsilon_1})\frac{\partial}{\partial s}\hat{\mathrm{a}}_\mathrm{V}^{\mathrm{I,I}}(0;\hat{\psi}_I^0,\hat{\rho}_I) - \frac{\partial}{\partial s}\hat{\mathrm{a}}_\mathrm{K}^{\mathrm{C,I}}(0;\hat{\mathfrak{u}}^0,\hat{\rho}_I) - 2\frac{\partial}{\partial s}\hat{\mathrm{a}}_\mathrm{K}^{\mathrm{I,I}}(0;\hat{\mathfrak{u}}_I^0,\hat{\rho}_I) \\
& + \frac{\partial}{\partial s}\hat{\mathrm{a}}_\mathrm{V}^{\mathrm{I,C}}(0;\hat{\psi}_I^0,\hat{\rho}) + \frac{\partial}{\partial s}\hat{\mathrm{a}}_\mathrm{V}^{\mathrm{C,C}}(0;\hat{\psi}^0,\hat{\rho}) - \frac{\partial}{\partial s}\hat{\mathrm{a}}_\mathrm{K}^{\mathrm{I,C}}(0;\hat{\mathfrak{u}}_I^0,\hat{\rho}) - \frac{\partial}{\partial s}\hat{\mathrm{a}}_\mathrm{K}^{\mathrm{C,C}}(0;\hat{\mathfrak{u}}^0,\hat{\rho}) \\
& + \frac{\partial}{\partial s}\hat{\mathrm{a}}_\mathrm{W}^{\mathrm{I,C}}(0;\hat{\mathfrak{u}}_I^0,\hat{p}) + \frac{\partial}{\partial s}\hat{\mathrm{a}}_\mathrm{W}^{\mathrm{C,C}}(0;\hat{\mathfrak{u}}^0,\hat{p}) + \frac{\partial}{\partial s}\hat{\mathrm{a}}_\mathrm{K}^{\mathrm{C,C}}(0;\hat{p},\hat{\psi}^0) + \frac{\partial}{\partial s}\hat{\mathrm{a}}_\mathrm{K}^{\mathrm{C,I}}(0;\hat{p},\hat{\psi}_I^0) \\
& + \frac{\partial}{\partial s}\hat{\mathrm{a}}_\mathrm{W}^{\mathrm{C,I}}(0;\mathfrak{g}_{ex},\hat{p}_I) + \frac{\partial}{\partial s}\hat{\mathrm{a}}_\mathrm{K}^{\mathrm{I,C}}(0;\hat{p}_I,\eta_{ex}) + \frac{\partial}{\partial s}\hat{\mathrm{a}}_\mathrm{V}^{\mathrm{C,I}}(0;\eta_{ex},\hat{\rho}_I) - \frac{\partial}{\partial s}\hat{\mathrm{a}}_\mathrm{K}^{\mathrm{C,I}}(0;\mathfrak{g}_{ex},\hat{\rho}_I) \\
& - \frac{1}{2}\frac{\partial}{\partial s}\hat{\mathrm{l}}^C(0;\mathfrak{g}_{ex},\hat{\rho}) + \frac{\partial}{\partial s}\hat{\mathrm{a}}_\mathrm{V}^{\mathrm{C,C}}(0;\eta_{ex},\hat{\rho}) - \frac{\partial}{\partial s}\hat{\mathrm{a}}_\mathrm{K}^{\mathrm{C,C}}(0;\mathfrak{g}_{ex},\hat{\rho}) - \frac{1}{2}\frac{\partial}{\partial s}\hat{\mathrm{l}}^C(0;\hat{p},\eta_{ex}) \\
& + \frac{\partial}{\partial s}\hat{\mathrm{a}}_\mathrm{W}^{\mathrm{C,C}}(0;\mathfrak{g}_{ex},\hat{p}) + \frac{\partial}{\partial s}\hat{\mathrm{a}}_\mathrm{K}^{\mathrm{C,C}}(0;\hat{p},\eta_{ex}),
\end{aligned}
$$

$$(4.3.24)$$

because J does not depend on s. Now we will study the properties of the shape derivative expression.

4.3.7 Mapping Properties of the Shape Derivative Formula

We saw in the previous sub-section that the shape derivative formula (4.3.24) contains the expressions $\frac{\partial}{\partial s}\hat{\mathrm{a}}_\mathrm{V}^{\bullet,\blacktriangle}(0;\hat{\psi},\hat{\phi})$, $\frac{\partial}{\partial s}\hat{\mathrm{a}}_\mathrm{K}^{\bullet,\blacktriangle}(0;\hat{g},\hat{\phi})$ and $\frac{\partial}{\partial s}\hat{\mathrm{a}}_\mathrm{W}^{\bullet,\blacktriangle}(0;\hat{g},\hat{v})$ for $\bullet,\blacktriangle \in \{I,C\}$. In this sub-section, following [48, Section 4], we will briefly discuss the singularities of the kernels in these integrals which will determine the mapping properties of the related boundary integral operators. It is to be noted that when $\bullet \neq \blacktriangle$, the integrals are well defined as Lebesgue integrals since the singularity is never encountered in the double integral. So we will restrict the discussion to the case $\bullet = \blacktriangle$ and write Γ instead of Γ_*. We also drop the superscript notation for the sake of simplicity. For the analysis we assume $\boldsymbol{\nu} \in (C_0^\infty(\Omega_c))^d$ and $\mathfrak{g}_{ex} \in C^\infty(\Gamma_C)$.

Next, we focus on the terms $\frac{\partial\hat{\mathrm{a}}_\mathrm{V}}{\partial s}$ and $\frac{\partial\hat{\mathrm{a}}_\mathrm{W}}{\partial s}$ to demonstrate the analysis techniques, as they contain the same kernel. A similar analysis for $\frac{\partial\hat{\mathrm{a}}_\mathrm{K}}{\partial s}$ can be found in [48, Sec. 4.4]. Using the expression for the fundamental solution, we obtain its gradient:

$$
\nabla_y G(\mathbf{x},\mathbf{y}) = \frac{1}{2^{d-1}\pi}\frac{\mathbf{x}-\mathbf{y}}{\|\mathbf{x}-\mathbf{y}\|^d}, \quad d = 2,3.
$$

The boundary integral operator T_V at the core of $\frac{\partial \widehat{a_V}}{\partial s}$ and $\frac{\partial \widehat{a_W}}{\partial s}$ is

$$T_V \psi(\mathbf{x}) := \frac{1}{2^{d-1}\pi} \int_\Gamma \frac{\mathbf{x} - \mathbf{y}}{\|\mathbf{x} - \mathbf{y}\|^d} \cdot \big(\boldsymbol{\nu}(\mathbf{x}) - \boldsymbol{\nu}(\mathbf{y})\big) \, \psi(\mathbf{y}) \, dS(\mathbf{y}), \quad \mathbf{x} \in \Gamma \tag{4.3.25}$$

$$= \frac{1}{2^{d-1}\pi} \int_\Gamma K_V(\mathbf{x}, \mathbf{x} - \mathbf{y}) \, \psi(\mathbf{y}) \, dS(\mathbf{y}), \quad K_V(\mathbf{x}, \boldsymbol{z}) := \frac{\boldsymbol{z}}{\|\boldsymbol{z}\|^d} \cdot \big(\boldsymbol{\nu}(\mathbf{x}) - \boldsymbol{\nu}(\mathbf{x} - \boldsymbol{z})\big).$$

Thanks to the smoothness of the velocity field $\boldsymbol{\mathcal{V}}$, we can employ a local Taylor expansion

$$\boldsymbol{\mathcal{V}}(\mathbf{x}) - \boldsymbol{\mathcal{V}}(\mathbf{x} - \boldsymbol{z}) = \mathsf{D}\boldsymbol{\mathcal{V}}(\mathbf{x})\boldsymbol{z} - \frac{1}{2}\mathsf{D}^2\boldsymbol{\mathcal{V}}(\mathbf{x})(\boldsymbol{z}, \boldsymbol{z}) + O(\|\boldsymbol{z}\|^3) \quad \text{for } \boldsymbol{z} \to 0,$$

which gives us

$$K_V(\mathbf{x}, \boldsymbol{z}) = K_V^1(\mathbf{x}, \boldsymbol{z}) + K_V^2(\mathbf{x}, \boldsymbol{z}), \quad K_V^1(\mathbf{x}, \boldsymbol{z}) := \frac{\boldsymbol{z}^T \mathsf{D}\boldsymbol{\mathcal{V}}(\mathbf{x})\boldsymbol{z}}{\|\boldsymbol{z}\|^d}.$$

For $d = 2$ we observe that $K_V^1(\mathbf{x}, \boldsymbol{z})$ is a homogeneous kernel of class -1 according to the definition in [44, Sec. 4.3.3], as its first order derivatives in $\boldsymbol{z}$ are homogeneous with degree $-1 = -(d-1)$, and are odd. We also observe that $\boldsymbol{z} \mapsto K_V^2(\mathbf{x}, \boldsymbol{z}) \in W^{1,\infty}(\mathbb{R}^2)$ for all $\mathbf{x} \in \Omega$. Finally, the assumptions on $\boldsymbol{\mathcal{V}}$ give us regularity of $\mathbf{x} \mapsto K_V(\mathbf{x}, \boldsymbol{z})$. Thus $K_V(\mathbf{x}, \boldsymbol{z})$ is a pseudo-homogeneous kernel of class -1.

For $d = 3$ we first redefine the notations as

$$K_V(\mathbf{x}, \boldsymbol{z}) = K_V^1(\mathbf{x}, \boldsymbol{z}) + K_V^2(\mathbf{x}, \boldsymbol{z}) + K_V^3(\mathbf{x}, \boldsymbol{z}),$$

$$K_V^1(\mathbf{x}, \boldsymbol{z}) := \frac{\boldsymbol{z}^T \mathsf{D}\boldsymbol{\mathcal{V}}(\mathbf{x})\boldsymbol{z}}{\|\boldsymbol{z}\|^d}, \quad K_V^2(\mathbf{x}, \boldsymbol{z}) := \frac{1}{2}\frac{\boldsymbol{z}^T \mathsf{D}^2\boldsymbol{\mathcal{V}}(\mathbf{x})(\boldsymbol{z}, \boldsymbol{z})}{\|\boldsymbol{z}\|^d},$$

and see that the first order derivatives of $\boldsymbol{z} \mapsto K_V^1(\mathbf{x}, \boldsymbol{z})$ are homogeneous with degree $-2 = -(d-1)$ and are odd, making it pseudo homogeneous of class -1. The same holds true for the second order derivatives of $\boldsymbol{z} \mapsto K_V^2(\mathbf{x}, \boldsymbol{z})$ which makes it of class -2. The rest of the terms encapsulated in $\boldsymbol{z} \mapsto K_V^3(\mathbf{x}, \boldsymbol{z})$ belong to $W^{1,\infty}(\mathbb{R}^3)$. Using regularity of $\boldsymbol{\mathcal{V}}$ we conclude that $K_V(\mathbf{x}, \boldsymbol{z})$ is pseudo-homogeneous of class -1.

The pseudo-homogeneity discussed is enough to invoke [44, Thm. 4.3.2]. Combining it with results from [24, Sec. 1.3] on scales of Sobolev spaces $H^s(\Gamma)$ supported on boundaries of class $C^{r,1}, r \in \mathbb{N}_0$ [24, Def. 1.2.1.1], we get the mapping properties which are summarized in the following three lemmas, whose detailed proofs we skip, referring to [48, Section 4] instead.

Lemma 2. *Assuming $\boldsymbol{\mathcal{V}} \in (C_0^\infty(D))^d$ and Γ of class $C^{r,1}$, the boundary integral operator T_V defined in (4.3.25) is a bounded linear operator $T_V : H^{l-\frac{1}{2}}(\Gamma) \to H^{l+\frac{1}{2}}(\Gamma), -r-\frac{1}{2} \le l \le r+\frac{1}{2}$. Consequently $\frac{\partial \widehat{a_V}}{\partial s}$ provides a continuous bilinear form on $H^{l-\frac{1}{2}}(\Gamma) \times H^{-l-\frac{1}{2}}(\Gamma)$.*

Lemma 3. *Assuming $\boldsymbol{\mathcal{V}} \in (C_0^\infty(D))^d$ and Γ of class $C^{r,1}$, $\frac{\partial \widehat{a_W}}{\partial s} : H^{l+1}(\Gamma) \times H^{-l}(\Gamma) \to \mathbb{R}$ is a continuous bilinear form for $-r-1 \le l \le r$.*

73

This result is due to the special structure of $\frac{\partial \hat{a}_W}{\partial s}$. For $d = 2$, using integration by parts,

$$\frac{\partial \hat{a}_W}{\partial s}(0; u, v) = -\left(v, (\frac{d}{dt} \circ T_V \circ \frac{d}{dt})u\right)_{L^2(\Gamma)}. \tag{4.3.26}$$

Since $T_V : H^l(\Gamma) \to H^{l+1}(\Gamma), -r - 1 \le l \le r$, we have $\frac{d}{dt} \circ T_V \circ \frac{d}{dt} : H^{l+1}(\Gamma) \to H^l(\Gamma)$ and by duality the lemma follows.

For $d = 3$ the expression $\frac{\partial \hat{a}_W}{\partial s}(0; u, v)$ consists of two parts as seen in (4.3.23). Using integration by parts, the first term becomes

$$\int_\Gamma \int_\Gamma (\nabla_x G(\mathbf{x}, \mathbf{y}) \cdot \boldsymbol{\nu}(\mathbf{x}) + \nabla_y G(\mathbf{x}, \mathbf{y}) \cdot \boldsymbol{\nu}(\mathbf{y})) \, \mathbf{curl}_\Gamma \, u(\mathbf{y}) \cdot \mathbf{curl}_\Gamma \, v(\mathbf{x}) \, dS(\mathbf{y}) dS(\mathbf{x})$$

$$= -(v, (\mathrm{curl}_\Gamma \circ T_V \circ \mathbf{curl}_\Gamma)u)_{L^2(\Gamma)},$$

where curl_Γ is the scalar surface curl operator. For the second part of $\frac{\partial \hat{a}_W}{\partial s}(0; u, v)$ in (4.3.23), integration by parts gives

$$\int_\Gamma \int_\Gamma G(\mathbf{x}, \mathbf{y}) \left((D\boldsymbol{\mathcal{V}}(\mathbf{y}) \, \mathbf{curl}_\Gamma \, u(\mathbf{y})) \cdot \mathbf{curl}_\Gamma \, v(\mathbf{x}) + \mathbf{curl}_\Gamma \, u(\mathbf{y}) \cdot (D\boldsymbol{\mathcal{V}}(\mathbf{x}) \, \mathbf{curl}_\Gamma \, v(\mathbf{x}))\right) dS(\mathbf{y}) dS(\mathbf{x})$$

$$= -\left(v, (\mathrm{curl}_\Gamma \circ T_V \circ (D\boldsymbol{\mathcal{V}} + D\boldsymbol{\mathcal{V}}^T) \, \mathbf{curl}_\Gamma)u\right)_{L^2(\Gamma)}.$$

For $T_V : H^l(\Gamma) \to H^{l+1}(\Gamma), -r - 1 \le l \le r$, we have bounded operators

$$\mathrm{curl}_\Gamma \circ T_V \circ \mathbf{curl}_\Gamma : H^{l+1}(\Gamma) \to H^l(\Gamma),$$
$$\mathrm{curl}_\Gamma \circ T_V \circ (D\boldsymbol{\mathcal{V}} + D\boldsymbol{\mathcal{V}}^T) \, \mathbf{curl}_\Gamma : H^{l+1}(\Gamma) \to H^l(\Gamma),$$

and by duality the lemma follows.

Lemma 4. *[48, Sec. 4.4] Assuming $\boldsymbol{\mathcal{V}} \in (C_0^\infty(D))^d$ and Γ of class $C^{r,1}$, $\frac{\partial \hat{a}_K}{\partial s}$ provides a continuous bilinear form on $H^l(\Gamma) \times H^{-l}(\Gamma)$, $-r - 1 \le l \le r + 1$.*

The obtained mapping properties of the bilinear forms lead to the following Proposition

Proposition 2. The bilinear mapping $\frac{d\mathcal{J}_F}{ds}(0; \boldsymbol{\mathcal{V}}) : V \times V \to \mathbb{R}$, $(\mathbf{X_0}, \mathbf{P}) \mapsto \frac{d\mathcal{J}_F}{ds}(0; \boldsymbol{\mathcal{V}})[\mathbf{X_0}, \mathbf{P}]$, as defined in (4.3.24) is continuous.

This paves the way for invoking Proposition 1 to conclude superconvergence of the BEM approximation $\frac{d\mathcal{J}_F}{ds}(0; \boldsymbol{\mathcal{V}})[\mathbf{X}_{0,h}, \mathbf{P}_h]$, where $\mathbf{X}_{0,h}, \mathbf{P}_h$ are the boundary-element Galerkin solutions.

4.3.8 Numerical Experiments in 2D

This section is focused on demonstrating the numerical efficacy of the new shape derivative formula (4.3.24) by using it to compute forces and torques, and comparing it with the interface-based and volume-based methods obtained from the Maxwell Stress Tensor [23,

Section 8.2, Eq. 8.17]. Inside the linear, homogeneous and isotropic dielectric medium Ω_*, $* = i, e$, the Maxwell stress tensor is given as [10]

$$\mathbf{T}_*(u_*)(\mathbf{x}) := \varepsilon_* \left(\nabla u_*(\mathbf{x}) \nabla u_*(\mathbf{x})^\top - \frac{1}{2} \|\nabla u_*(\mathbf{x})\|^2 \mathbf{I}_d \right), \quad \mathbf{x} \in \Omega_*. \tag{4.3.27}$$

At the material interface Γ_I, the Maxwell stress tensor is discontinuous and the surface force density $\mathbf{f}_I$ is defined as $(\mathbf{T}_e(u_e) - \mathbf{T}_i(u_i))\mathbf{n}_i$ [28]. In our model problem, there are no residual charges inside Ω_i, hence it experiences only surface forces. The net force $\mathbf{F}$ on the interface Γ_I can be obtained by integrating the surface force density

$$\mathbf{F} := \int_{\Gamma_I} \mathbf{f}_I(\mathbf{x}) \, dS(\mathbf{x}) = \int_{\Gamma_I} (\mathbf{T}_e(u_e)(\mathbf{x}) - \mathbf{T}_i(u_i)(\mathbf{x})) \, \mathbf{n}_i(\mathbf{x}) \, dS(\mathbf{x}). \tag{4.3.28}$$

Note that the above expression for net force is an interface-based expression as it only involves integration on the boundary Γ_I. For $d = 2$ (4.3.28) can be simplified further using the transmission conditions, resulting in an expression containing only Dirichlet and Neumann traces,

$$\mathbf{F} = \frac{\varepsilon_i - \varepsilon_e}{2} \int_{\Gamma_I} \left(\left(\frac{d\mathfrak{u}_I}{dt}(\mathbf{x}) \right)^2 + \frac{\varepsilon_e}{\varepsilon_i} \psi_I^2(\mathbf{x}) \right) \mathbf{n}_i(\mathbf{x}) \, dS(\mathbf{x}), \tag{4.3.29}$$

where $\psi_I = \gamma_e^N u_e|_{\Gamma_I}$, $\mathfrak{u}_I = \gamma_e^D u_e|_{\Gamma_I}$, and $\frac{d\mathfrak{u}_I}{dt}$ represents the arclength derivative of $\mathfrak{u}_I$. Note that the expression (4.3.29) is not well defined on $H^{\frac{1}{2}}(\Gamma_I) \times H^{-\frac{1}{2}}(\Gamma_I)$.

4.3.8.1 Boundary-Element Galerkin Discretization

We start with mesh partitions $\mathcal{C}_h$ and $\mathcal{I}_h$ of the boundaries Γ_C and Γ_I respectively, whose cells consist of either straight line segments ($d = 2$) or flat triangular panels ($d = 3$). We perform a Galerkin discretization of (4.3.12) employing the lowest order boundary element spaces $S_0^{-1}(\mathcal{C}_h)$ and $S_0^{-1}(\mathcal{I}_h)$ for $H^{-\frac{1}{2}}(\Gamma_C)$ and $H^{-\frac{1}{2}}(\Gamma_I)$ respectively, and $S_1^0(\mathcal{C}_h)$ and $S_1^0(\mathcal{I}_h)$ for $H^{\frac{1}{2}}(\Gamma_C)$ and $H^{\frac{1}{2}}(\Gamma_I)$ respectively. S_0^{-1} is the space of functions that are piece-wise constant on the underlying mesh. S_1^0 is the space of functions which are continuous across the boundaries of the mesh elements and are polynomials of degree one when restricted to the elements (piece-wise linear functions). For more details about the construction of the spaces S_0^{-1} and S_1^0 we refer to [58, Ch. 10] or [54, Ch. 4]. The choice of basis functions and the computation of the Galerkin matrices is presented in [54, Ch. 5].

4.3.8.2 Implementation

The BEM solution for both state and adjoint problem is computed using 2DParametricBEM [11], a C++ library for BEM in 2D which uses exact parametrization for the boundaries. It evaluates the integrals with weakly singular kernels, like that of Single and Double layer potential, using log weighted Gauss quadrature (order 16) and regularization by transformation

---

[10]$\mathbf{I}_d$ stands for the $d \times d$ identity matrix, $\|.\|$ denotes the Euclidean norm
[11]Code available on Ning Ren's Github repository https://github.com/gninr/FCSCD

to polar coordinates [26, Section 9.4.5]. Galerkin boundary-element solutions of the state and adjoint equations, (4.3.20) and (4.3.22), are computed using lowest order BEM spaces $S_0^{-1}(\mathcal{C}_h), S_0^{-1}(\mathcal{I}_h), S_1^0(\mathcal{C}_h), S_1^0(\mathcal{I}_h)$ for a quasi-uniform sequence of mesh partitions $\mathcal{C}_h$ of Γ_C and $\mathcal{I}_h$ of Γ_I with decreasing meshwidth h. As pointed out in Section 4.3.8.1, S_0^{-1} is the space of piece-wise constants, and S_1^0 is the space of continuous piece-wise linear functions. In the implementation, the extended trace $\mathfrak{g}_{ex}$ is constructed using a smooth extension of $\mathfrak{g}$ by zero to Γ_C, which on the discrete level is implemented by forcing its finite element approximation to have zero coefficients on mesh nodes in the interior of Γ_N. η_{ex} is obtained from η by a trivial extension by 0.

The shape derivative formula (4.3.24) is also implemented in 2DParametricBEM using similar techniques to evaluate integrals with weakly singular kernels. For implementation we assume that the perturbation field $\boldsymbol{\nu}$ is available in a functional form along with its first and second derivatives. Smooth integrals are simply evaluated using Gauss quadrature of order 16.

Comparison with the volume formula is done using a FEM implementation. The solution for the potential u is computed using piece-wise linear finite elements on a quasi-uniform sequence of triangular meshes of Ω_c with decreasing mesh size h. A polygonal approximation of smooth curved boundaries is used.

4.3.8.3   Force Computation

For computing forces using the shape derivative formula, we use specific test vector fields $\boldsymbol{\mathcal{V}}$ as pointed out in (3.0.5). The cut-off function ξ we use is such that $\xi \in C_0^\infty(\Omega_c)$ and $\xi \equiv 1$ in a neighborhood of Γ_I[12]

The force evaluated using the above recipe is compared to the interface based formula from (4.3.28), which is evaluated using the BEM solution and the trace of the FEM solution. For the sake of completeness we also do a comparison with the volume based "egg-shell" formula [27], [28], [42] which is computed by plugging the FEM solution for u into

$$\mathbf{F} = -\int_{\Omega_c} \varepsilon(\mathbf{x}) \left(\nabla u(\mathbf{x}) \left(\nabla u(\mathbf{x}) \cdot \nabla w(\mathbf{x}) \right) - \frac{1}{2} \|\nabla u(\mathbf{x})\|^2 \nabla w(\mathbf{x}) \right) d\mathbf{x}, \qquad (4.3.30)$$

where $w \in W^{1,\infty}(\Omega_c)$ with $w|_{\Gamma_I} \equiv 1$ and $w|_{\Gamma_C} \equiv 0$. We perform numerical computations on two domains

- A square shaped $\Omega_c := (-2, 2)^2$ and a smooth kite-shaped Ω_i given by the parametrization

$$\gamma : [0, 2\pi] \to \mathbb{R}^2, \ t \mapsto \begin{bmatrix} 0.3 + 0.5 \ \cos(t) + 0.1625 \ \cos(2t) \\ 0.5 + 0.35 \ \sin(t) \end{bmatrix}.$$

- A square shaped $\Omega_c := (-2, 2)^2$ and a square-shaped $\Omega_i := (0, 1)^2$

The coarsest volume meshes can be seen in Figure 4.13 for both geometries. The Dirichlet boundary conditions in both cases are given as $\mathfrak{g}(-2, y) = 4, \mathfrak{g}(2, y) = 0, \ y \in [-2, 2]$ and the

---

[12]Only the values of ζ on $\Gamma_I(= 1)$ and on $\Gamma_C(= 0)$ are needed. Thus ζ need not be specified any further.

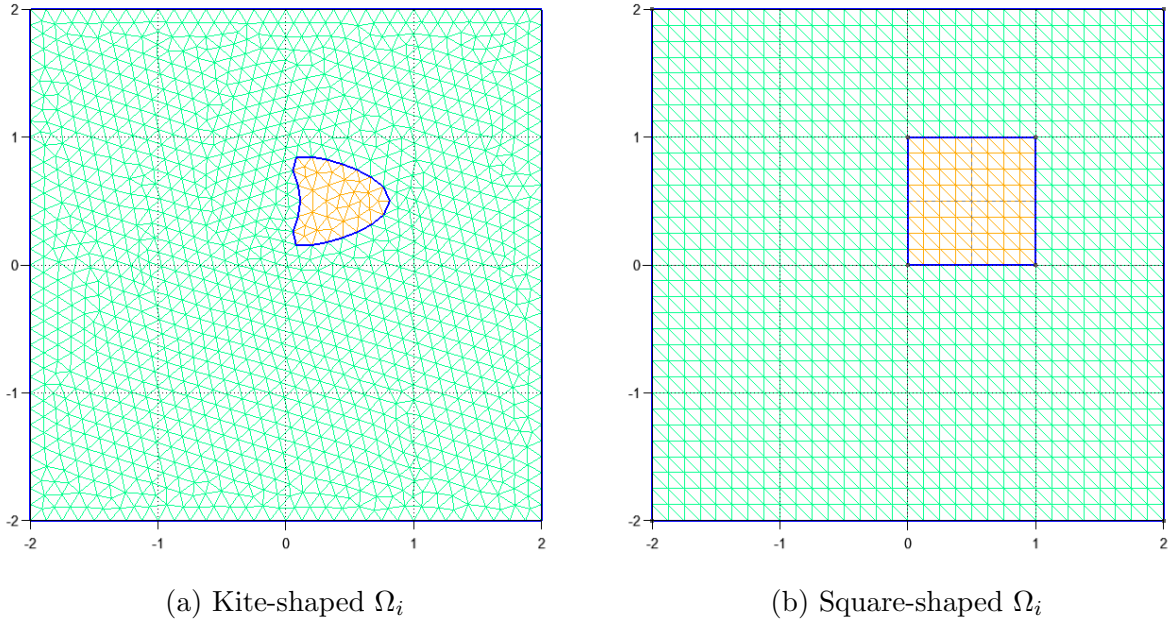(a) Kite-shaped Ω_i (b) Square-shaped Ω_i

Figure 4.13: Geometries for the numerical experiments

Neumann data $\eta = 0$. For the volume based formula (4.3.30), we use the cut-off function

$$w(\mathbf{x}) := \begin{cases} 1 & \text{for } \|\mathbf{x}\| < 1.4, \\ \cos^2\left(\frac{\|\mathbf{x}\|-1.4}{0.5}\frac{\pi}{2}\right) & \text{for } 1.4 \leq \|\mathbf{x}\| \leq 1.9, \\ 0 & \text{for } \|\mathbf{x}\| > 1.9. \end{cases}$$

The reference values are computed using the shape derivative formula at a refinement level of 4728 panels for the kite-shaped Ω_i and 5120 panels for the square-shaped Ω_i. Figure 4.14 shows the convergence plots for relative error of the computed net force $\left(\sum_{i=1}^{d} F_i^2\right)^{\frac{1}{2}}$ vs meshwidth h for both domains.

From the plots we can immediately see that the shape derivative formula outperforms other methods in terms of absolute accuracy as well as the asymptotic convergence rate, which are tabulated in Table 4.3. The worst formula in terms of performance is the interface-based formula from (4.3.28).

Table 4.3: Estimated asymptotic rates of algebraic convergence

Method	Kite-shaped Ω_i	Square-shaped Ω_i
Pullback approach (BEM)	2.96	1.76
Stress tensor (BEM)	1.76	0.648
Volume formula (FEM)	2.29	1.73
Stress tensor (FEM)	1.06	1.09

(a) Kite-shaped Ω_i (b) Square-shaped Ω_i
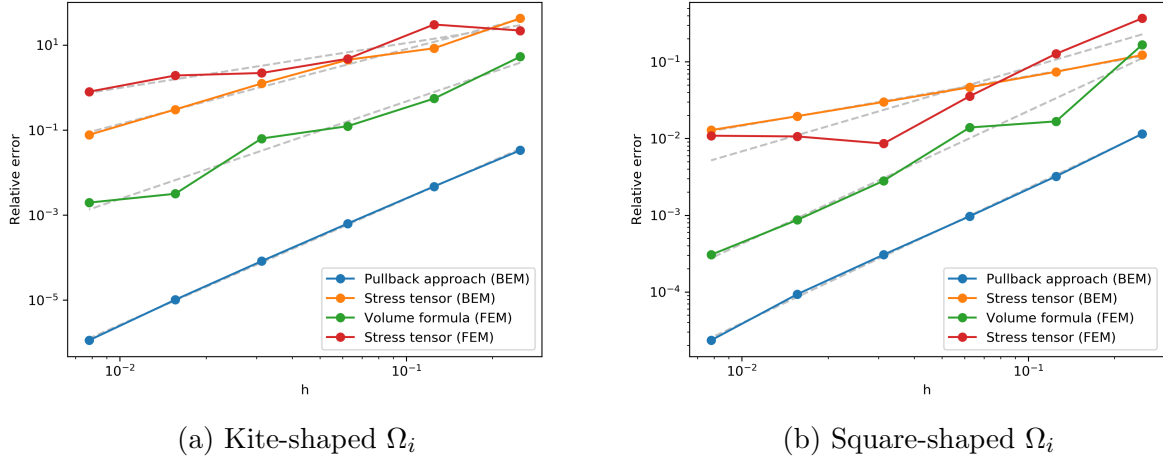
Figure 4.14: Error of total forces as a function of the meshwidth h. Dashed lines represent the linear regression fits.

4.3.8.4 Torque Computation

For computing the net torque about a point $\boldsymbol{c} \in \mathbb{R}^2$ using the shape derivative, we use a rotational test vector field $\boldsymbol{\mathcal{V}}$ around the point $\boldsymbol{c}$ as mentioned in (3.0.5). The net torque on Ω_i is given as

$$T = \frac{d\mathcal{J}_F}{ds}(0; \{\boldsymbol{x} \mapsto (\mathbf{x} - \boldsymbol{c})^{\perp}\xi(\mathbf{x})\}),$$

where $\xi \in C_0^{\infty}(\Omega_c)$ and $\xi \equiv 1$ in a neighborhood of Γ_I. This will be compared to torque computed using the surface force density $(\mathbf{T}_e(u_e) - \mathbf{T}_i(u_i)) \cdot \mathbf{n}_i$ at the interface Γ_I which is given as:

$$T = \int_{\Gamma_I} \det \left[\mathbf{x} - \boldsymbol{c}, \ \big(\mathbf{T}_e(u_e)(\mathbf{x}) - \mathbf{T}_i(u_i)(\mathbf{x})\big) \cdot \mathbf{n}_i(\mathbf{x})\right] \ d\mathrm{S}(\mathbf{x}).$$

The determinant is a simple way of computing a cross product in 2D. Numerical computations are done in the same experimental setting introduced in the previous subsection. As reference solution we use the torque evaluated using the shape derivative formula at a refinement level of 4728 panels for the kite-shaped Ω_i and 5120 panels for square-shaped Ω_i. Torque is computed about the point $\boldsymbol{c} = (0.3, 0.5)$ for square-shaped Ω_i and about $\boldsymbol{c} = (0.5, 0.5)$ for kite-shaped Ω_i. Figure 4.15 shows the plot of the relative errors in the computed torque vs the meshwidth h for both domains.

78
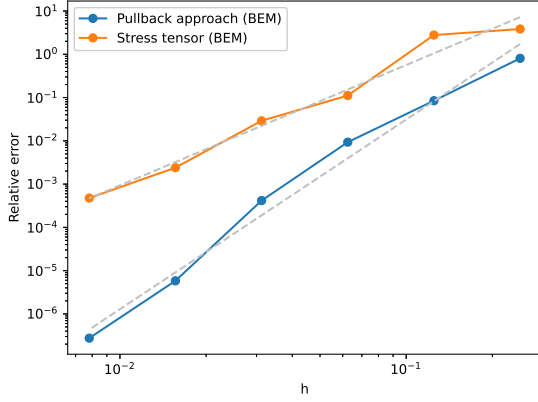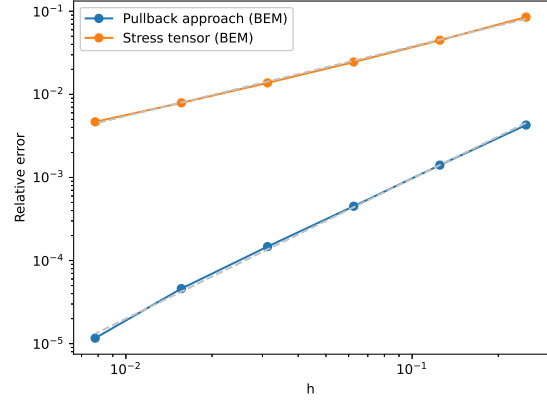
(a) Kite-shaped Ω_i (b) Square-shaped Ω_i

Figure 4.15: Error of net torque as a function of the meshwidth h. Dashed lines represent the linear regression fits.

Estimates of asymptotic convergence rates are given in Table 4.4.

Table 4.4: Asymptotic rate of algebraic convergence

Method	Kite-shaped Ω_i	Square-shaped Ω_i
Pullback approach (BEM)	4.38	1.69
Stress tensor (BEM)	2.78	0.84

4.4   Linear Dielectric With Source Charge Density

Consider a linear, homogeneous and isotropic dielectric material, occupying a bounded simply connected and open domain $\Omega \subset \mathbb{R}^3$ with C_{pw}^2 boundary, whose permittivity is given by $\epsilon \in \mathbb{R}^+$. The material is placed in a vaccum with permittivity $\epsilon_0 \in \mathbb{R}^+$. In the vicinity of the linear material, we have a continuous distribution of charges occupying $\Omega_{\mathrm{src}} \Subset \mathbb{R}^d$ whose charge density is given by $\rho(\mathbf{x})$, where for $\mathbf{x} \notin \Omega_{\mathrm{src}}$ $\rho(\mathbf{x}) \equiv 0$. The situation is depicted in Figure 4.16
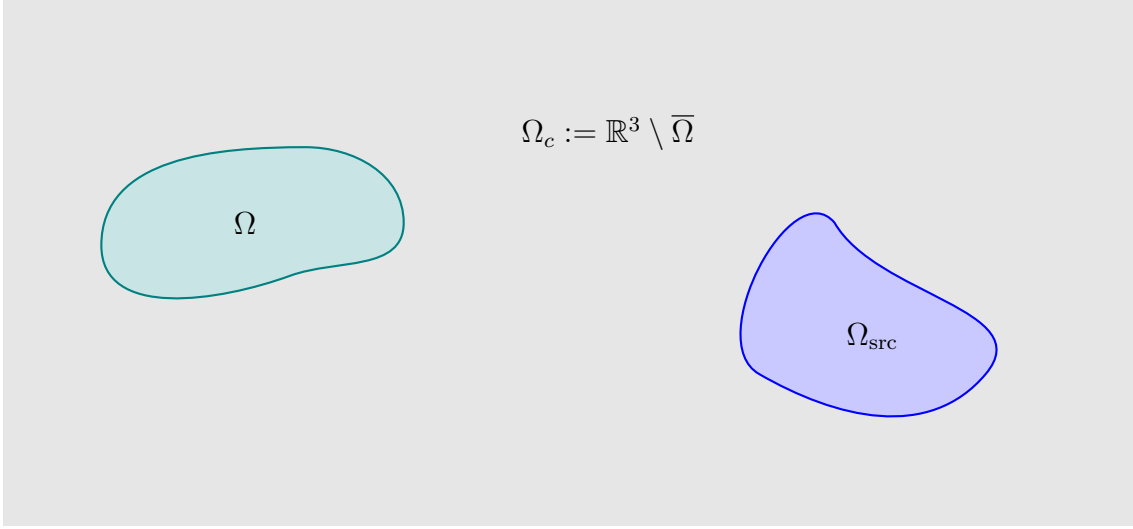
Figure 4.16: Geometric setting

The electrostatic potential u is described by the following transmission problem

$$
\begin{aligned}
- \operatorname{div}(\epsilon(\mathbf{x})\,\nabla u(\mathbf{x})) &= \rho(\mathbf{x}) && \text{in } \Omega \cup \Omega_c, \\
[\![\gamma_D u]\!]_\Gamma &= 0 && \text{on } \Gamma := \partial\Omega, \\
[\![\epsilon(\mathbf{x})\,\gamma_N u]\!]_\Gamma &= 0 && \text{on } \Gamma, \\
|u(\mathbf{x})| &= O(\|\mathbf{x}\|^{-1}) && \text{for } \|\mathbf{x}\| \to \infty.
\end{aligned}
\tag{4.4.1}
$$

4.4.1   Variational Boundary Integral Equations

The transmission problem 4.4.1 can be approximated using a boundary integral formulation. We start with the representation formulae 2.1.20 for u in the two subdomains.

For Ω:

$$
u(\mathbf{x}) = \Psi_{SL}(\gamma_N^- u)(\mathbf{x}) - \Psi_{DL}(\gamma_D^- u)(\mathbf{x}).
$$

For Ω_c:

$$
u(\mathbf{x}) = -\Psi_{SL}(\gamma_N^+ u)(\mathbf{x}) + \Psi_{DL}(\gamma_D^+ u)(\mathbf{x}) + \frac{1}{\epsilon_0}\mathrm{N}(\rho)(\mathbf{x}).
$$

where $\mathrm{N}(\rho)(\mathbf{x}) = \int\limits_{\Omega_{\mathrm{src}}} G(\mathbf{x},\mathbf{y})\,\rho(\mathbf{y})\,d\mathbf{y}$ is the Newton potential of the charge distribution ρ. Applying the Dirichlet and Neumann trace operators from both subdomains yields the boundary integral equations (2.1.21) and (2.1.22) which we use directly.

$$
\begin{bmatrix} V & -\tfrac{\mathsf{Id}}{2} - K \\ -\tfrac{\mathsf{Id}}{2} + K' & W \end{bmatrix}
\begin{bmatrix} \gamma_N^- u \\ \gamma_D^- u \end{bmatrix}
= \begin{bmatrix} 0 \\ 0 \end{bmatrix},
$$

$$
\begin{bmatrix} V & \tfrac{\mathsf{Id}}{2} - K \\ \tfrac{\mathsf{Id}}{2} + K' & W \end{bmatrix}
\begin{bmatrix} \gamma_N^+ u \\ \gamma_D^+ u \end{bmatrix}
= \frac{1}{\epsilon_0}\begin{bmatrix} \gamma_D^+\mathrm{N}(\rho) \\ \gamma_N^+\mathrm{N}(\rho) \end{bmatrix}.
$$

We use the notation $\psi := \gamma_N^+ u$ and $g := \gamma_D^+ u$ for the exterior traces. Using the transmission conditions, the interior traces are denoted as $\gamma_D^- u = g$ and $\gamma_N^- u = \frac{\epsilon_0}{\epsilon}\psi$. Inserting this notation into the equation for Ω gives us

$$\begin{bmatrix} V & -\frac{\mathrm{Id}}{2} - K \\ -\frac{\mathrm{Id}}{2} + K' & W \end{bmatrix} \begin{bmatrix} \frac{\epsilon_0}{\epsilon}\psi \\ g \end{bmatrix} = \begin{bmatrix} 0 \\ 0 \end{bmatrix},$$

which can be rescaled to get

$$\begin{bmatrix} \frac{\epsilon_0}{\epsilon} V & -\frac{\mathrm{Id}}{2} - K \\ -\frac{\mathrm{Id}}{2} + K' & \frac{\epsilon}{\epsilon_0} W \end{bmatrix} \begin{bmatrix} \psi \\ g \end{bmatrix} = \begin{bmatrix} 0 \\ 0 \end{bmatrix}.$$

Adding it to the equations for Ω_c gives us

$$\begin{bmatrix} (1 + \frac{\epsilon_0}{\epsilon}) V & -2\,K \\ 2\,K' & (1 + \frac{\epsilon}{\epsilon_0}) W \end{bmatrix} \begin{bmatrix} \psi \\ g \end{bmatrix} = \frac{1}{\epsilon_0} \begin{bmatrix} \gamma_D^+ N(\rho) \\ \gamma_N^+ N(\rho) \end{bmatrix}.$$

The first equation is in $H^{\frac{1}{2}}(\Gamma)$ and can be tested with $\phi \in H^{-\frac{1}{2}}(\Gamma)$ to get the variational equation

$$(1 + \frac{\epsilon_0}{\epsilon})b_V(\psi, \phi) - 2b_K(g, \phi) = \frac{1}{\epsilon_0} \left\langle \gamma_D^+ N(\rho), \phi \right\rangle \quad \forall \phi \in H^{-\frac{1}{2}}(\Gamma).$$

Similarly the second equation is tested with $w \in H^{\frac{1}{2}}(\Gamma)$ to get

$$(1 + \frac{\epsilon}{\epsilon_0})b_W(g, w) + 2b_{K'}(\psi, w) = \frac{1}{\epsilon_0} \left\langle \gamma_N^+ N(\rho), w \right\rangle \quad \forall w \in H^{\frac{1}{2}}(\Gamma).$$

We can combine the two equations into a single variational formulation. We seek the solution $\psi \in H^{-\frac{1}{2}}(\Gamma), g \in H^{\frac{1}{2}}(\Gamma)$ such that

$$(1 + \frac{\epsilon_0}{\epsilon})b_V(\psi, \phi) - 2b_K(g, \phi) + (1 + \frac{\epsilon}{\epsilon_0})b_W(g, w) + 2b_{K'}(\psi, w)$$

$$= \frac{1}{\epsilon_0} \left\langle \gamma_D^+ N(\rho), \phi \right\rangle + \frac{1}{\epsilon_0} \left\langle \gamma_N^+ N(\rho), w \right\rangle, \quad \forall \phi \in H^{-\frac{1}{2}}(\Gamma), w \in H^{\frac{1}{2}}(\Gamma). \quad (4.4.2)$$

Equation (4.4.2) is uniquely solvable as we will see next. We first note that the equation has a solution, which are the exterior traces of the potential u that solves the transmission problem (4.4.1). To show unique solvability, we require the solution of the homogeneous equation to be trivial.

Theorem 2. For $\epsilon, \epsilon_0 \in \mathbb{R}^+$, the homogeneous equation

$$(1 + \frac{\epsilon_0}{\epsilon})b_V(\psi, \phi) - 2b_K(g, \phi) + (1 + \frac{\epsilon}{\epsilon_0})b_W(g, w) + 2b_{K'}(\psi, w) = 0, \quad \forall \phi \in H^{-\frac{1}{2}}(\Gamma), w \in H^{\frac{1}{2}}(\Gamma),$$

$$(4.4.3)$$

has a trivial solution $\psi = 0 \in H^{-\frac{1}{2}}(\Gamma)$ and $g = 0 \in H^{\frac{1}{2}}(\Gamma)$.

Proof. Plugging in $\phi = \psi$ and $w = g$ into (4.4.3) we get

$$(1 + \frac{\epsilon_0}{\epsilon})\mathrm{b_V}(\psi, \psi) + (1 + \frac{\epsilon}{\epsilon_0})\mathrm{b_W}(g, g) = 0. \tag{4.4.4}$$

Writing $g_* := g - c$ where $c := \int_\Gamma g \, dS$, we see that

$$\mathrm{b_W}(g, g) = \mathrm{b_W}(g_* + c, g_* + c) = \mathrm{b_W}(g_*, g_*). \tag{4.4.5}$$

Obviously $g_* \in H_*^{\frac{1}{2}}(\Gamma) := \{u \in H^{\frac{1}{2}}(\Gamma) : \int_\Gamma u \, dS = 0\}$. Given the ellipticity of V on $H^{-\frac{1}{2}}(\Gamma)$ and W on $H_*^{\frac{1}{2}}(\Gamma)$ [58, Section 6.6.1, 6.6.2] we conclude that

$$\psi = 0, \quad g_* = 0.$$

Thus we have $g = c$. Testing the homogeneous equation with $w = 0$ and putting $\psi = 0$ we get

$$-2\mathrm{b_K}(c, \phi) = 0 \quad \forall \phi \in H^{-\frac{1}{2}}(\Gamma).$$

Since $\mathrm{K}\,\mathbb{1}_{\partial D} = -\frac{1}{2}$ as seen in (4.2.4), we get

$$c \int_\Gamma \phi \, dS = 0 \quad \forall \phi \in H^{-\frac{1}{2}}(\Gamma).$$

Thus we have $c = 0$ which implies $g = 0$. $\qquad\square$

The field energy is given as

$$\begin{aligned}
\mathcal{E}_F &= \frac{1}{2} \int_{\mathbb{R}^3} \epsilon(\mathbf{x}) \left\| \nabla u(\mathbf{x}) \right\|^2 \, d\mathbf{x} \\
&= \frac{\epsilon}{2} \int_\Omega \left\| \nabla u(\mathbf{x}) \right\|^2 \, d\mathbf{x} + \frac{\epsilon_0}{2} \int_{\Omega_c} \left\| \nabla u(\mathbf{x}) \right\|^2 \, d\mathbf{x} \\
&= \frac{\epsilon}{2} \int_\Gamma u \, \gamma_N^- u \, dS - \frac{\epsilon_0}{2} \int_\Gamma u \, \gamma_N^+ u \, dS + \frac{1}{2} \int_{\Omega_{\mathrm{src}}} \rho \, u \, d\mathbf{x} \\
&= \frac{1}{2} \int_{\Omega_{\mathrm{src}}} \rho \, u \, d\mathbf{x}, \quad \text{since } [\![\epsilon \gamma_N u]\!]_\Gamma = 0.
\end{aligned}$$

To get the energy in terms of traces, we insert the representation formula for u in the exterior domain and get

$$\mathcal{E}_F = \frac{1}{2} \int_{\Omega_{\mathrm{src}}} \rho(\mathbf{x}) \left(-\Psi_{SL}(\psi)(\mathbf{x}) + \Psi_{DL}(g)(\mathbf{x}) + \frac{1}{\epsilon_0} \mathrm{N}(\rho)(\mathbf{x}) \right) \, d\mathbf{x}.$$

We observe the following relations

$$\int_{\Omega_{src}} \rho(\mathbf{x}) \, \Psi_{SL}(\psi)(\mathbf{x}) \, d\mathbf{x} = \int_{\Omega_{src}} \rho(\mathbf{x}) \int_{\Gamma} G(\mathbf{x}, \mathbf{y}) \, \psi(\mathbf{y}) \, dS_{\mathbf{y}} \, d\mathbf{x}$$

$$= \int_{\Gamma} \psi(\mathbf{y}) \int_{\Omega_{src}} G(\mathbf{x}, \mathbf{y}) \, \rho(\mathbf{x}) \, d\mathbf{x} \, dS_{\mathbf{y}} = \langle \gamma_D^+ \mathrm{N}(\rho), \psi \rangle \, ,$$

and

$$\int_{\Omega_{src}} \rho(\mathbf{x}) \, \Psi_{DL}(g)(\mathbf{x}) \, d\mathbf{x} = \int_{\Omega_{src}} \rho(\mathbf{x}) \int_{\Gamma} \nabla_y G(\mathbf{x}, \mathbf{y}) \cdot \mathbf{n}(\mathbf{y}) \, g(\mathbf{y}) \, dS_{\mathbf{y}} \, d\mathbf{x}$$

$$= \int_{\Gamma} g(\mathbf{y}) \int_{\Omega_{src}} \nabla_y G(\mathbf{x}, \mathbf{y}) \cdot \mathbf{n}(\mathbf{y}) \, \rho(\mathbf{x}) \, d\mathbf{x} \, dS_{\mathbf{y}}$$

$$= \int_{\Gamma} g(\mathbf{x}) \int_{\Omega_{src}} \nabla_y G(\mathbf{y}, \mathbf{x}) \cdot \mathbf{n}(\mathbf{x}) \, \rho(\mathbf{y}) \, d\mathbf{y} \, dS_{\mathbf{x}}$$

$$= \int_{\Gamma} g(\mathbf{x}) \int_{\Omega_{src}} \nabla_x G(\mathbf{x}, \mathbf{y}) \cdot \mathbf{n}(\mathbf{x}) \, \rho(\mathbf{y}) \, d\mathbf{y} \, dS_{\mathbf{x}} = \langle \gamma_N^+ \mathrm{N}(\rho), g \rangle \, .$$

In the last step we used the fact $\nabla_y G(\mathbf{y}, \mathbf{x}) = -\nabla_y G(\mathbf{x}, \mathbf{y}) = \nabla_x G(\mathbf{x}, \mathbf{y})$. Using these relations, the energy can be written as

$$\mathcal{E}_F = -\frac{1}{2} \langle \gamma_D^+ \mathrm{N}(\rho), \psi \rangle + \frac{1}{2} \langle \gamma_N^+ \mathrm{N}(\rho), g \rangle + \frac{1}{2\epsilon_0} \int_{\Omega_{src}} \rho(\mathbf{x}) \, \mathrm{N}(\rho)(\mathbf{x}) \, d\mathbf{x}.$$

We notice that the first two terms of the energy expression (up to a scaling) correspond to the rhs of the variational formulation (4.4.2) with a flipped sign.

4.4.2 Variational Formulation on Deformed Domain

Let Ω^0 denote the reference domain and let $\Omega^s := \mathbf{T}_s^{\boldsymbol{\nu}}(\Omega^0)$ where $\mathbf{T}_s^{\boldsymbol{\nu}}$ is the perturbation map 3.0.1. The velocity field $\boldsymbol{\mathcal{V}}$ is such that $\boldsymbol{\mathcal{V}} = 0$ at the source domain Ω_{src}, leading to deformations of only the material occupying Ω^0. The variational formulation for the transmission problem posed on the deformed domain has a similar structure to 4.4.2: seek $\psi_s \in H^{-\frac{1}{2}}(\Gamma^s), g_s \in H^{\frac{1}{2}}(\Gamma^s)$ such that

$$(1 + \frac{\epsilon_0}{\epsilon}) b_V(s)(\psi_s, \phi) - 2 b_K(s)(g_s, \phi) + (1 + \frac{\epsilon}{\epsilon_0}) b_W(s)(g_s, w) + 2 b_{K'}(s)(\psi_s, w)$$

$$= \frac{1}{\epsilon_0} \langle \gamma_D^+ \mathrm{N}(\rho), \phi \rangle_{\Gamma^s} + \frac{1}{\epsilon_0} \langle \gamma_N^+ \mathrm{N}(\rho), w \rangle_{\Gamma^s}, \quad \forall \phi \in H^{-\frac{1}{2}}(\Gamma^s), w \in H^{\frac{1}{2}}(\Gamma^s), \quad (4.4.6)$$

where the bilinear forms $b_*(s), * \in \{V, K, K', W\}$ contain integrals on Γ^s and $\langle \cdot, \cdot \rangle_{\Gamma^s}$ represents the duality pairing for $H^{-\frac{1}{2}}(\Gamma^s)$ and $H^{\frac{1}{2}}(\Gamma^s)$.

4.4.3 Equivalent Formulation on Reference Domain

We start by transforming the integrals in the bilinear forms back to the reference boundary Γ^0 using the perturbation map.

$$
\begin{aligned}
b_V(s)(\psi,\phi) &= \int\limits_{\Gamma^s}\int\limits_{\Gamma^s} G(\mathbf{x},\mathbf{y})\,\psi(\mathbf{y})\,\phi(\mathbf{x})\,dS_{\mathbf{y}}\,dS_{\mathbf{x}} \\
&= \int\limits_{\Gamma^0}\int\limits_{\Gamma^0} G(\mathbf{T}^{\boldsymbol{\nu}}_s(\hat{\mathbf{x}}),\mathbf{T}^{\boldsymbol{\nu}}_s(\hat{\mathbf{y}}))\,\psi(\mathbf{T}^{\boldsymbol{\nu}}_s(\hat{\mathbf{y}}))\,\phi(\mathbf{T}^{\boldsymbol{\nu}}_s(\hat{\mathbf{y}}))\,\omega_s(\hat{\mathbf{x}})\,\omega_s(\hat{\mathbf{y}})\,dS_{\hat{\mathbf{y}}}\,dS_{\hat{\mathbf{x}}}, \\[4pt]
b_K(s)(g,\phi) &= \int\limits_{\Gamma^s}\int\limits_{\Gamma^s} \nabla_{\mathbf{y}} G(\mathbf{x},\mathbf{y})\cdot\mathbf{n}(\mathbf{y})\,g(\mathbf{y})\,\phi(\mathbf{x})\,dS_{\mathbf{y}}\,dS_{\mathbf{x}} \\
&= \int\limits_{\Gamma^0}\int\limits_{\Gamma^0} \nabla_{\mathbf{y}} G(\mathbf{T}^{\boldsymbol{\nu}}_s(\hat{\mathbf{x}}),\mathbf{T}^{\boldsymbol{\nu}}_s(\hat{\mathbf{y}}))\cdot\frac{\mathbf{C}(D\mathbf{T}^{\boldsymbol{\nu}}_s(\hat{\mathbf{y}}))\,\hat{\mathbf{n}}(\hat{\mathbf{y}})}{\omega_s(\hat{\mathbf{y}})}\,g(\mathbf{T}^{\boldsymbol{\nu}}_s(\hat{\mathbf{y}}))\,\phi(\mathbf{T}^{\boldsymbol{\nu}}_s(\hat{\mathbf{x}})) \\
&\qquad\qquad \omega_s(\hat{\mathbf{x}})\,\omega_s(\hat{\mathbf{y}})\,dS_{\hat{\mathbf{y}}}\,dS_{\hat{\mathbf{x}}}, \\[4pt]
b_W(s)(g,v) &= \int\limits_{\Gamma^s}\int\limits_{\Gamma^s} G(\mathbf{x},\mathbf{y})\,\mathbf{curl}_\Gamma\, g(\mathbf{y})\cdot\mathbf{curl}_\Gamma\, v(\mathbf{x})\,dS_{\mathbf{y}}\,dS_{\mathbf{x}} \\
&= \int\limits_{\Gamma^0}\int\limits_{\Gamma^0} G(\mathbf{T}^{\boldsymbol{\nu}}_s(\hat{\mathbf{x}}),\mathbf{T}^{\boldsymbol{\nu}}_s(\hat{\mathbf{y}}))\,\mathbf{curl}_\Gamma\, g(\mathbf{T}^{\boldsymbol{\nu}}_s(\hat{\mathbf{y}}))\cdot\mathbf{curl}_\Gamma\, v(\mathbf{T}^{\boldsymbol{\nu}}_s(\hat{\mathbf{x}}))\,\omega_s(\hat{\mathbf{x}})\,\omega_s(\hat{\mathbf{y}})\,dS_{\hat{\mathbf{y}}}\,dS_{\hat{\mathbf{x}}}.
\end{aligned}
$$

We don't explicitly mention $b_{K'}$ since it can be written in terms of its adjoint b_K. Transforming the terms appearing on the RHS of 4.4.6 we get

$$
\left\langle \gamma^+_D N(\rho),\phi \right\rangle_{\Gamma^s} = \int\limits_{\Gamma^0}\int\limits_{\Omega_{\text{src}}} G(\mathbf{T}^{\boldsymbol{\nu}}_s(\hat{\mathbf{x}}),\mathbf{y})\,\rho(\mathbf{y})\,\phi(\mathbf{T}^{\boldsymbol{\nu}}_s(\hat{\mathbf{x}}))\,\omega_s(\hat{\mathbf{x}})\,d\mathbf{y}\,dS_{\hat{\mathbf{x}}},
$$

$$
\left\langle \gamma^+_N N(\rho),u \right\rangle_{\Gamma^s} = \int\limits_{\Gamma^0}\int\limits_{\Omega_{\text{src}}} \nabla_{\mathbf{x}} G(\mathbf{T}^{\boldsymbol{\nu}}_s(\hat{\mathbf{x}}),\mathbf{y})\cdot\mathbf{n}(\mathbf{T}^{\boldsymbol{\nu}}_s(\hat{\mathbf{x}}))\,\rho(\mathbf{y})\,u(\mathbf{T}^{\boldsymbol{\nu}}_s(\hat{\mathbf{x}}))\,\omega_s(\hat{\mathbf{x}})\,d\mathbf{y}\,dS_{\hat{\mathbf{x}}}.
$$

Based on the pullbacks in Section 3.0.4.1 we have

$$
u(\mathbf{T}^{\boldsymbol{\nu}}_s(\hat{\mathbf{x}})) = \hat{u}(\hat{\mathbf{x}}),
$$

$$
\psi(\mathbf{T}^{\boldsymbol{\nu}}_s(\hat{\mathbf{x}})) = \frac{\hat{\psi}(\hat{\mathbf{x}})}{\omega_s(\hat{\mathbf{x}})},
$$

$$
\mathbf{curl}_\Gamma\, u(\mathbf{T}^{\boldsymbol{\nu}}_s(\hat{\mathbf{x}})) = \frac{D\mathbf{T}^{\boldsymbol{\nu}}_s(\hat{\mathbf{x}})}{\omega_s(\hat{\mathbf{x}})}\,\mathbf{curl}_\Gamma\, \hat{u}(\hat{\mathbf{x}}),
$$

we define new pulled back bilinear forms

$$\hat{\mathsf{b}}_{\mathrm{V}}(s;\hat{\psi},\hat{\phi}) := \int\limits_{\Gamma^0}\int\limits_{\Gamma^0} G(\mathbf{T}_s^{\boldsymbol{\nu}}(\hat{\mathbf{x}}), \mathbf{T}_s^{\boldsymbol{\nu}}(\hat{\mathbf{y}}))\, \hat{\psi}(\hat{\mathbf{y}})\, \hat{\phi}(\hat{\mathbf{x}})\, dS_{\hat{\mathbf{y}}}\, dS_{\hat{\mathbf{x}}},$$

$$\hat{\mathsf{b}}_{\mathrm{K}}(s;\hat{g},\hat{\phi}) := \int\limits_{\Gamma^0}\int\limits_{\Gamma^0} \nabla_{\mathbf{y}} G(\mathbf{T}_s^{\boldsymbol{\nu}}(\hat{\mathbf{x}}), \mathbf{T}_s^{\boldsymbol{\nu}}(\hat{\mathbf{y}})) \cdot \left(\mathbf{C}(\mathrm{D}\mathbf{T}_s^{\boldsymbol{\nu}}(\hat{\mathbf{y}}))\, \hat{\mathbf{n}}(\hat{\mathbf{y}})\right) \hat{g}(\hat{\mathbf{y}})\, \hat{\phi}(\hat{\mathbf{x}})\, dS_{\hat{\mathbf{y}}}\, dS_{\hat{\mathbf{x}}},$$

$$\hat{\mathsf{b}}_{\mathrm{W}}(s;\hat{g},\hat{v}) := \int\limits_{\Gamma^0}\int\limits_{\Gamma^0} G(\mathbf{T}_s^{\boldsymbol{\nu}}(\hat{\mathbf{x}}), \mathbf{T}_s^{\boldsymbol{\nu}}(\hat{\mathbf{y}})) \left(\mathrm{D}\mathbf{T}_s^{\boldsymbol{\nu}}(\hat{\mathbf{y}})\, \mathbf{curl}_\Gamma\, \hat{g}(\hat{\mathbf{y}})\right) \cdot \left(\mathrm{D}\mathbf{T}_s^{\boldsymbol{\nu}}(\hat{\mathbf{y}})\, \mathbf{curl}_\Gamma\, \hat{v}(\hat{\mathbf{y}})\right) dS_{\hat{\mathbf{y}}}\, dS_{\hat{\mathbf{x}}}.$$

Similarly we define the pulled back linear form

$$\hat{\ell}(s; \begin{bmatrix}\hat{\phi}\\\hat{u}\end{bmatrix}) := \frac{1}{\epsilon_0} \int\limits_{\Gamma^0}\int\limits_{\Omega_{\mathrm{src}}} G(\mathbf{T}_s^{\boldsymbol{\nu}}(\hat{\mathbf{x}}), \mathbf{y})\, \rho(\mathbf{y})\, \hat{\phi}(\hat{\mathbf{x}})\, d\mathbf{y}\, dS_{\hat{\mathbf{x}}}$$

$$+ \frac{1}{\epsilon_0} \int\limits_{\Gamma^0}\int\limits_{\Omega_{\mathrm{src}}} \nabla_{\mathbf{x}} G(\mathbf{T}_s^{\boldsymbol{\nu}}(\hat{\mathbf{x}}), \mathbf{y}) \cdot \left(\mathbf{C}(\mathrm{D}\mathbf{T}_s^{\boldsymbol{\nu}}(\hat{\mathbf{x}}))\, \hat{\mathbf{n}}(\hat{\mathbf{x}})\right) \rho(\mathbf{y})\, \hat{u}(\hat{\mathbf{x}})\, d\mathbf{y}\, dS_{\hat{\mathbf{x}}}.$$

The equivalent pulled back formulation reads: Seek $\hat{\psi}_s, \hat{g}_s \in V_0 := H^{-\frac{1}{2}}(\Gamma^0) \times H^{\frac{1}{2}}(\Gamma^0)$ such that

$$\hat{\mathsf{b}}(s; \begin{bmatrix}\hat{\psi}_s\\\hat{g}_s\end{bmatrix}, \begin{bmatrix}\hat{\phi}\\\hat{u}\end{bmatrix}) = \hat{\ell}(s; \begin{bmatrix}\hat{\phi}\\\hat{u}\end{bmatrix}) \quad \forall \begin{bmatrix}\hat{\phi}\\\hat{u}\end{bmatrix} \in V_0, \tag{4.4.7}$$

where

$$\hat{\mathsf{b}}(s; \begin{bmatrix}\hat{\psi}\\\hat{g}\end{bmatrix}, \begin{bmatrix}\hat{\phi}\\\hat{u}\end{bmatrix}) := (1 + \frac{\epsilon_0}{\epsilon})\hat{\mathsf{b}}_{\mathrm{V}}(s;\hat{\psi},\hat{\phi}) - 2\hat{\mathsf{b}}_{\mathrm{K}}(s;\hat{g},\hat{\phi}) + 2\hat{\mathsf{b}}_{\mathrm{K}'}(s;\hat{\psi},\hat{u}) + (1 + \frac{\epsilon}{\epsilon_0})\hat{\mathsf{b}}_{\mathrm{W}}(s;\hat{g},\hat{u}).$$

The energy for the deformed s configuration can be written as

$$\mathcal{E}_F(s) = \frac{\epsilon_0}{2}\, \hat{\ell}(s; \begin{bmatrix}-\hat{\psi}_s\\\hat{g}_s\end{bmatrix}) + \frac{1}{2\epsilon_0} \int\limits_{\Omega_{\mathrm{src}}} \rho(\mathbf{x})\, \mathrm{N}(\rho)(\mathbf{x})\, d\mathbf{x}.$$

Notice that the second contribution does not depend on s as the source charges don't move with the velocity field $\boldsymbol{\mathcal{V}}$.

4.4.4 BIE-Constrained Shape Derivative

We start by defining the Lagrangian $\mathcal{L} : \mathbb{R} \times V_0 \times V_0 \to \mathbb{R}$,

$$\mathcal{L}(s; \begin{bmatrix}\hat{\psi}\\\hat{g}\end{bmatrix}, \begin{bmatrix}\hat{\phi}\\\hat{u}\end{bmatrix}) := \hat{\mathsf{b}}(s; \begin{bmatrix}\hat{\psi}\\\hat{g}\end{bmatrix}, \begin{bmatrix}\hat{\phi}\\\hat{u}\end{bmatrix}) - \hat{\ell}(s; \begin{bmatrix}\hat{\phi}\\\hat{u}\end{bmatrix}) + \frac{\epsilon_0}{2}\, \hat{\ell}(s; \begin{bmatrix}-\hat{\psi}\\\hat{g}\end{bmatrix}) + \frac{1}{2\epsilon_0} \int\limits_{\Omega_{\mathrm{src}}} \rho(\mathbf{x})\, \mathrm{N}(\rho)(\mathbf{x})\, d\mathbf{x}.$$

Plugging in the pulled back state solution gives

$$\mathcal{E}_F(s) = \mathcal{L}(s; \begin{bmatrix}\hat{\psi}_s\\\hat{g}_s\end{bmatrix}, \begin{bmatrix}\hat{\phi}\\\hat{u}\end{bmatrix}) \quad \forall \begin{bmatrix}\hat{\phi}\\\hat{u}\end{bmatrix} \in V_0.$$

Differentiating with respect to s gives

$$\frac{d\mathcal{E}_F}{ds}(0) = \frac{\partial \mathcal{L}}{\partial s}\left(0; \begin{bmatrix} \hat{\psi}_0 \\ \hat{g}_0 \end{bmatrix}, \begin{bmatrix} \hat{\phi} \\ \hat{u} \end{bmatrix}\right) + \left\langle \frac{\partial \mathcal{L}}{\partial \begin{bmatrix} \hat{\psi} \\ \hat{g} \end{bmatrix}}\left(0; \begin{bmatrix} \hat{\psi}_0 \\ \hat{g}_0 \end{bmatrix}, \begin{bmatrix} \hat{\phi} \\ \hat{u} \end{bmatrix}\right); \frac{d}{ds}\begin{bmatrix} \hat{\psi}_s \\ \hat{g}_s \end{bmatrix}|_{s=0} \right\rangle \quad \forall \begin{bmatrix} \hat{\phi} \\ \hat{u} \end{bmatrix} \in V_0.$$

We use the freedom to choose the test functions such that the second term vanishes. This gives us the adjoint equation where we seek $\begin{bmatrix} \hat{\lambda} \\ \hat{p} \end{bmatrix} \in V_0$ such that

$$\left\langle \frac{\partial \mathcal{L}}{\partial \begin{bmatrix} \hat{\psi} \\ \hat{g} \end{bmatrix}}\left(0; \begin{bmatrix} \hat{\psi}_0 \\ \hat{g}_0 \end{bmatrix}, \begin{bmatrix} \hat{\lambda} \\ \hat{p} \end{bmatrix}\right); \begin{bmatrix} \hat{\phi} \\ \hat{u} \end{bmatrix} \right\rangle = 0 \quad \forall \begin{bmatrix} \hat{\phi} \\ \hat{u} \end{bmatrix} \in V_0.$$

Computing the partial derivative of the Lagrangian gives us

$$\hat{b}\left(0; \begin{bmatrix} \hat{\phi} \\ \hat{u} \end{bmatrix}, \begin{bmatrix} \hat{\lambda} \\ \hat{p} \end{bmatrix}\right) = \frac{\epsilon_0}{2} \hat{\ell}\left(0; \begin{bmatrix} \hat{\phi} \\ -\hat{u} \end{bmatrix}\right) \quad \forall \begin{bmatrix} \hat{\phi} \\ \hat{u} \end{bmatrix} \in V_0.$$

Flipping the sign of the test function $\hat{u}$ we get

$$\hat{b}\left(0; \begin{bmatrix} \hat{\phi} \\ -\hat{u} \end{bmatrix}, \begin{bmatrix} \hat{\lambda} \\ \hat{p} \end{bmatrix}\right) = \frac{\epsilon_0}{2} \hat{\ell}\left(0; \begin{bmatrix} \hat{\phi} \\ \hat{u} \end{bmatrix}\right) \quad \forall \begin{bmatrix} \hat{\phi} \\ \hat{u} \end{bmatrix} \in V_0.$$

Finally by noticing that

$$\hat{b}\left(s; \begin{bmatrix} \hat{\phi} \\ -\hat{u} \end{bmatrix}, \begin{bmatrix} \hat{\lambda} \\ \hat{p} \end{bmatrix}\right) = \hat{b}\left(s; \begin{bmatrix} \hat{\lambda} \\ -\hat{p} \end{bmatrix}, \begin{bmatrix} \hat{\phi} \\ \hat{u} \end{bmatrix}\right),$$

the adjoint equation reads

$$\begin{bmatrix} \hat{\lambda} \\ \hat{p} \end{bmatrix} \in V_0: \quad \hat{b}\left(0; \begin{bmatrix} \hat{\lambda} \\ -\hat{p} \end{bmatrix}, \begin{bmatrix} \hat{\phi} \\ \hat{u} \end{bmatrix}\right) = \frac{\epsilon_0}{2} \hat{\ell}\left(0; \begin{bmatrix} \hat{\phi} \\ \hat{u} \end{bmatrix}\right) \quad \forall \begin{bmatrix} \hat{\phi} \\ \hat{u} \end{bmatrix} \in V_0.$$

Comparing to the state equation 4.4.7 we conclude that

$$\begin{bmatrix} \hat{\lambda} \\ -\hat{p} \end{bmatrix} = \frac{\epsilon_0}{2} \begin{bmatrix} \hat{\psi}_0 \\ \hat{g}_0 \end{bmatrix} \implies \begin{bmatrix} \hat{\lambda} \\ \hat{p} \end{bmatrix} = \frac{\epsilon_0}{2} \begin{bmatrix} \hat{\psi}_0 \\ -\hat{g}_0 \end{bmatrix}.$$

Thus the shape derivative is given as

$$\frac{d\mathcal{E}_F}{ds}(0) = \frac{\partial \mathcal{L}}{\partial s}(0; \begin{bmatrix} \hat{\psi}_0 \\ \hat{g}_0 \end{bmatrix}, \frac{\epsilon_0}{2}\begin{bmatrix} \hat{\psi}_0 \\ -\hat{g}_0 \end{bmatrix})$$

$$= \frac{\partial \hat{\mathsf{b}}}{\partial s}(0; \begin{bmatrix} \hat{\psi}_0 \\ \hat{g}_0 \end{bmatrix}, \frac{\epsilon_0}{2}\begin{bmatrix} \hat{\psi}_0 \\ -\hat{g}_0 \end{bmatrix}) - \frac{\partial \hat{\ell}}{\partial s}(0; \frac{\epsilon_0}{2}\begin{bmatrix} \hat{\psi}_0 \\ -\hat{g}_0 \end{bmatrix}) + \frac{\epsilon_0}{2}\frac{\partial \hat{\ell}}{\partial s}(0; \begin{bmatrix} -\hat{\psi}_0 \\ \hat{g}_0 \end{bmatrix})$$

$$= \frac{\epsilon_0}{2}\frac{\partial \hat{\mathsf{b}}}{\partial s}(0; \begin{bmatrix} \hat{\psi}_0 \\ \hat{g}_0 \end{bmatrix}, \begin{bmatrix} \hat{\psi}_0 \\ -\hat{g}_0 \end{bmatrix}) - \epsilon_0\frac{\partial \hat{\ell}}{\partial s}(0; \begin{bmatrix} \hat{\psi}_0 \\ -\hat{g}_0 \end{bmatrix})$$

$$= \frac{\epsilon_0}{2}(1 + \frac{\epsilon_0}{\epsilon}) \int_{\Gamma^0} \int_{\Gamma^0} \left\{ \nabla_{\mathbf{x}} G(\mathbf{x},\mathbf{y}) \cdot \boldsymbol{\mathcal{V}}(\mathbf{x}) + \nabla_{\mathbf{y}} G(\mathbf{x},\mathbf{y}) \cdot \boldsymbol{\mathcal{V}}(\mathbf{y}) \right\} \hat{\psi}_0(\hat{\mathbf{y}}) \, \hat{\psi}_0(\hat{\mathbf{x}}) \, dS_{\hat{\mathbf{y}}} \, dS_{\hat{\mathbf{x}}}$$

$$- 2\epsilon_0 \int_{\Gamma^0} \int_{\Gamma^0} \nabla_{\mathbf{y}} G(\mathbf{x},\mathbf{y}) \cdot \left(\nabla \cdot \boldsymbol{\mathcal{V}}(\mathbf{y}) \, \hat{\mathbf{n}}(\mathbf{y}) - \mathsf{D}\boldsymbol{\mathcal{V}}(\mathbf{y})^T \, \hat{\mathbf{n}}(\mathbf{y}) \right) \hat{g}_0(\hat{\mathbf{y}}) \, \hat{\psi}_0(\hat{\mathbf{x}}) \, dS_{\hat{\mathbf{y}}} \, dS_{\hat{\mathbf{x}}}$$

$$- 2\epsilon_0 \int_{\Gamma^0} \int_{\Gamma^0} \frac{d\nabla_{\mathbf{y}} G(\mathbf{T}_s^{\boldsymbol{\nu}}(\hat{\mathbf{x}}), \mathbf{T}_s^{\boldsymbol{\nu}}(\hat{\mathbf{y}}))}{ds}\Big|_{s=0} \cdot \hat{\mathbf{n}}(\hat{\mathbf{y}}) \, \hat{g}_0(\hat{\mathbf{y}}) \, \hat{\psi}_0(\hat{\mathbf{x}}) \, dS_{\hat{\mathbf{y}}} \, dS_{\hat{\mathbf{x}}}$$

$$- \frac{\epsilon_0}{2}(1 + \frac{\epsilon}{\epsilon_0}) \int_{\Gamma^0} \int_{\Gamma^0} \left\{ \nabla_{\mathbf{x}} G(\mathbf{x},\mathbf{y}) \cdot \boldsymbol{\mathcal{V}}(\mathbf{x}) + \nabla_{\mathbf{y}} G(\mathbf{x},\mathbf{y}) \cdot \boldsymbol{\mathcal{V}}(\mathbf{y}) \right\} \mathbf{curl}_\Gamma \, \hat{g}_0(\hat{\mathbf{y}}) \cdot \mathbf{curl}_\Gamma \, \hat{g}_0(\hat{\mathbf{x}}) \, dS_{\hat{\mathbf{y}}} \, dS_{\hat{\mathbf{x}}}$$

$$- \frac{\epsilon_0}{2}(1 + \frac{\epsilon}{\epsilon_0}) \int_{\Gamma^0} \int_{\Gamma^0} G(\mathbf{x},\mathbf{y}) \left\{ \mathsf{D}\boldsymbol{\mathcal{V}}(\mathbf{y}) \, \mathbf{curl}_\Gamma \, \hat{g}_0(\hat{\mathbf{y}}) \cdot \mathbf{curl}_\Gamma \, \hat{g}_0(\hat{\mathbf{y}}) \right.$$

$$\left. + \mathsf{D}\boldsymbol{\mathcal{V}}(\mathbf{x}) \, \mathbf{curl}_\Gamma \, \hat{g}_0(\hat{\mathbf{x}}) \cdot \mathbf{curl}_\Gamma \, \hat{g}_0(\hat{\mathbf{y}}) \right\} dS_{\hat{\mathbf{y}}} \, dS_{\hat{\mathbf{x}}}$$

$$- \int_{\Gamma^0} \int_{\Omega_{\mathrm{src}}} \nabla_x G(\hat{\mathbf{x}},\mathbf{y}) \cdot \boldsymbol{\mathcal{V}}(\hat{\mathbf{x}}) \, \rho(\mathbf{y}) \, \hat{\psi}_0(\hat{\mathbf{x}}) \, d\mathbf{y} \, dS_{\hat{\mathbf{x}}}$$

$$+ \int_{\Gamma^0} \int_{\Omega_{\mathrm{src}}} \frac{d\nabla_{\mathbf{x}} G(\mathbf{T}_s^{\boldsymbol{\nu}}(\hat{\mathbf{x}}), \mathbf{y})}{ds} \cdot \hat{\mathbf{n}}(\hat{\mathbf{x}}) \, \rho(\mathbf{y}) \, \hat{g}_0(\hat{\mathbf{x}}) \, d\mathbf{y} \, dS_{\hat{\mathbf{x}}}$$

$$+ \int_{\Gamma^0} \int_{\Omega_{\mathrm{src}}} \nabla_{\mathbf{x}} G(\hat{\mathbf{x}},\mathbf{y}) \cdot \left(\nabla \cdot \boldsymbol{\mathcal{V}}(\hat{\mathbf{x}}) \, \hat{\mathbf{n}}(\hat{\mathbf{x}}) - \mathsf{D}\boldsymbol{\mathcal{V}}(\hat{\mathbf{x}})^T \, \hat{\mathbf{n}}(\hat{\mathbf{x}}) \right) \rho(\mathbf{y}) \, \hat{g}_0(\hat{\mathbf{x}}) \, d\mathbf{y} \, dS_{\hat{\mathbf{x}}}. \tag{4.4.8}$$

The derivative of $\nabla_{\mathbf{y}} G(\mathbf{T}_s^{\boldsymbol{\nu}}(\hat{\mathbf{x}}), \mathbf{T}_s^{\boldsymbol{\nu}}(\hat{\mathbf{y}}))$ with respect to s is given as

$$\frac{d\nabla_{\mathbf{y}} G(\mathbf{T}_s^{\boldsymbol{\nu}}(\hat{\mathbf{x}}), \mathbf{T}_s^{\boldsymbol{\nu}}(\hat{\mathbf{y}}))}{ds}\Bigg|_{s=0} = \mathsf{D}_x \nabla_y G(\hat{\mathbf{x}}, \hat{\mathbf{y}}) \, \boldsymbol{\mathcal{V}}(\hat{\mathbf{x}}) + \mathsf{D}_y \nabla_y G(\hat{\mathbf{x}}, \hat{\mathbf{y}}) \, \boldsymbol{\mathcal{V}}(\hat{\mathbf{y}}) \tag{4.4.9}$$

$$= \nabla_y \nabla_y G(\hat{\mathbf{x}}, \hat{\mathbf{y}}) \left(\boldsymbol{\mathcal{V}}(\hat{\mathbf{y}}) - \boldsymbol{\mathcal{V}}(\hat{\mathbf{x}}) \right), \tag{4.4.10}$$

where

$$\nabla_y \nabla_y G(\mathbf{x},\mathbf{y}) = \nabla_x \nabla_x G(\mathbf{x},\mathbf{y}) = \frac{3}{4\pi} \frac{(\mathbf{x}-\mathbf{y})(\mathbf{x}-\mathbf{y})^T}{\|\mathbf{x}-\mathbf{y}\|^5} - \frac{1}{4\pi}\frac{\mathsf{Id}}{\|\mathbf{x}-\mathbf{y}\|^3}. \tag{4.4.11}$$

87

4.4.5 Shape Derivative From Volume Based Variational Formulation

The transmission problem from (4.4.1) has a well posed variational formulation in the weighted Sobolev space $H^1(\Delta; \mathbb{R}^3) := \{u : \mathbb{R}^3 \to \mathbb{R} : \int_{\mathbb{R}^3} \|\nabla u\|^2 + \frac{u^2}{1+\|\mathbf{x}\|^2} \, d\mathbf{x} < \infty\}$ [54, Section 2.9.2.8]: seek $u \in H^1(\Delta; \mathbb{R}^3)$ such that

$$\int_{\mathbb{R}^3} \epsilon(\mathbf{x}) \, \nabla u(\mathbf{x}) \cdot \nabla v(\mathbf{x}) \, d\mathbf{x} = \int_{\Omega_{\mathrm{src}}} \rho(\mathbf{x}) \, v(\mathbf{x}) \, d\mathbf{x} \quad \forall v \in H^1(\Delta; \mathbb{R}^3). \qquad (4.4.12)$$

We deform the reference domain Ω^0 using a velocity field $\boldsymbol{\mathcal{V}}$ that is zero around the source charge. The resulting variational problem on the deformed domain $\Omega^s := \mathbf{T}_s^{\boldsymbol{\nu}}(\Omega^0)$ has a similar structure. Transforming the permittivity as a 0-form, we get the variational problem: seek $u_s \in H^1(\Delta; \mathbb{R}^3)$ such that

$$\int_{\mathbb{R}^3} \epsilon_s(\mathbf{x}) \, \nabla u_s(\mathbf{x}) \cdot \nabla v(\mathbf{x}) \, d\mathbf{x} = \int_{\Omega_{\mathrm{src}}} \rho(\mathbf{x}) \, v(\mathbf{x}) \, d\mathbf{x} \quad \forall v \in H^1(\Delta; \mathbb{R}^3).$$

The bilinear form on the LHS can be transformed using the perturbation map as

$$\int_{\mathbb{R}^3} \epsilon_s(\mathbf{x}) \, \nabla u_s(\mathbf{x}) \cdot \nabla v(\mathbf{x}) \, d\mathbf{x} = \int_{\mathbb{R}^3} \epsilon(\hat{\mathbf{x}}) \, \nabla u_s(\mathbf{T}_s^{\boldsymbol{\nu}}(\hat{\mathbf{x}})) \cdot \nabla v(\mathbf{T}_s^{\boldsymbol{\nu}}(\hat{\mathbf{x}})) \, \det \mathsf{D}\mathbf{T}_s^{\boldsymbol{\nu}}(\hat{\mathbf{x}}) \, d\hat{\mathbf{x}},$$

and using the pullback for a 1-form to transform the gradient $(\nabla u(\mathbf{T}_s^{\boldsymbol{\nu}}(\hat{\mathbf{x}})) = \mathsf{D}\mathbf{T}_s^{\boldsymbol{\nu}}(\hat{\mathbf{x}})^{-T} \nabla \hat{u}(\hat{\mathbf{x}}))$, we get the pulled back bilinear form

$$\hat{\mathsf{b}}(s; \hat{u}, \hat{v}) := \int_{\mathbb{R}^3} \epsilon(\hat{\mathbf{x}}) \left(\mathsf{D}\mathbf{T}_s^{\boldsymbol{\nu}}(\hat{\mathbf{x}})^{-T} \nabla \hat{u}(\hat{\mathbf{x}}) \right) \cdot \left(\mathsf{D}\mathbf{T}_s^{\boldsymbol{\nu}}(\hat{\mathbf{x}})^{-T} \nabla \hat{v}(\hat{\mathbf{x}}) \right) \, \det \mathsf{D}\mathbf{T}_s^{\boldsymbol{\nu}}(\hat{\mathbf{x}}) \, d\hat{\mathbf{x}}.$$

Since the velocity field is zero in Ω_{src}, the linear form on the RHS remains unchanged. So we define the pulled back linear form as

$$\hat{\ell}(\hat{v}) := \int_{\Omega_{\mathrm{src}}} \rho(\mathbf{x}) \, \hat{v}(\mathbf{x}) \, d\mathbf{x}.$$

The pulled back formulation reads: Seek $\hat{u}_s \in H^1(\Delta; \mathbb{R}^3)$ such that

$$\hat{\mathsf{b}}(s; \hat{u}_s, \hat{v}) = \hat{\ell}(\hat{v}) \quad \forall \hat{v} \in H^1(\Delta; \mathbb{R}^3). \qquad (4.4.13)$$

The field energy for the deformed configuration can be written in terms of the pulled back bilinear form and reads

$$\mathcal{E}_F(s) = \frac{1}{2} \hat{\mathsf{b}}(s; \hat{u}_s, \hat{u}_s).$$

To compute the shape derivative using the adjoint method, we define the Lagrangian $\mathcal{L}$: $\mathbb{R} \times H^1(\Delta; \mathbb{R}^3) \times H^1(\Delta; \mathbb{R}^3) \to \mathbb{R}$,

$$\mathcal{L}(s; \hat{u}, \hat{v}) := \hat{\mathsf{b}}(s; \hat{u}, \hat{v}) - \hat{\ell}(\hat{v}) + \frac{1}{2}\hat{\mathsf{b}}(s; \hat{u}, \hat{u}).$$

Plugging in $\hat{u} = \hat{u}_s$ gives the field energy

$$\mathcal{E}_F(s) = \mathcal{L}(s; \hat{u}_s, \hat{v}) \quad \hat{v} \in H^1(\Delta; \mathbb{R}^3).$$

The shape derivative can be computed as

$$\frac{d\mathcal{E}_F}{ds}(0) = \frac{\partial \mathcal{L}}{\partial s}(0; \hat{u}_0, \hat{p}),$$

where $\hat{p} \in H^1(\Delta; \mathbb{R}^3)$ solves the adjoint equation

$$\left\langle \frac{\partial \mathcal{L}}{\partial \hat{u}}(0; \hat{u}_0, \hat{p}); \hat{v} \right\rangle = 0 \quad \forall \hat{v} \in H_0^1(\mathbb{R}^3).$$

Simplifying the above and using the symmetry of the bilinear form we get

$$\hat{\mathsf{b}}(0; \hat{v}, \hat{p}) + \hat{\mathsf{b}}(0; \hat{v}, \hat{u}_0) = 0 \quad \forall \hat{v} \in H^1(\Delta; \mathbb{R}^3),$$

which immediately yields the adjoint solution as $\hat{p} = -\hat{u}_0$. Using (3.0.12) we compute the shape derivative as

$$\frac{d\mathcal{E}_F}{ds}(0) = \frac{\partial \mathcal{L}}{\partial s}(0; \hat{u}_0, -\hat{u}_0) = -\frac{1}{2}\frac{\partial \hat{\mathsf{b}}}{\partial s}(0; \hat{u}_0, \hat{u}_0)$$
$$= -\frac{1}{2}\int_{\mathbb{R}^3} \epsilon(\mathbf{x})\Big\{ -\nabla \hat{u}_0^T(\mathbf{x})\Big(\mathsf{D}\boldsymbol{\mathcal{V}}(\mathbf{x}) + \mathsf{D}\boldsymbol{\mathcal{V}}^T(\mathbf{x})\Big)\nabla \hat{u}_0 + \|\nabla \hat{u}_0(\mathbf{x})\|^2 \nabla \cdot \boldsymbol{\mathcal{V}}(\mathbf{x})\Big\} \, d\mathbf{x}.$$

$$(4.4.14)$$

We use the identity [2, Section 6]

$$\boldsymbol{\mathcal{V}} \cdot \nabla(\nabla u \cdot \nabla v) + \nabla u^T(\mathsf{D}\boldsymbol{\mathcal{V}} + \mathsf{D}\boldsymbol{\mathcal{V}}^T)\nabla v = \nabla v \cdot \nabla(\boldsymbol{\mathcal{V}} \cdot \nabla u) + \nabla u \cdot \nabla(\boldsymbol{\mathcal{V}} \cdot \nabla v).$$

For $u = v$ it becomes

$$\boldsymbol{\mathcal{V}} \cdot \nabla(\|\nabla u\|^2) - 2\nabla u \cdot \nabla(\boldsymbol{\mathcal{V}} \cdot \nabla u) = -\nabla u^T(\mathsf{D}\boldsymbol{\mathcal{V}} + \mathsf{D}\boldsymbol{\mathcal{V}}^T)\nabla u.$$

Using this the integrand in 4.4.14 becomes

$$-\nabla \hat{u}_0^T(\mathbf{x})\Big(\mathsf{D}\boldsymbol{\mathcal{V}}(\mathbf{x}) + \mathsf{D}\boldsymbol{\mathcal{V}}^T(\mathbf{x})\Big)\nabla \hat{u}_0(\mathbf{x}) + \|\nabla \hat{u}_0(\mathbf{x})\|^2 \nabla \cdot \boldsymbol{\mathcal{V}}(\mathbf{x})$$
$$= \boldsymbol{\mathcal{V}}(\mathbf{x}) \cdot \nabla(\|\nabla \hat{u}_0(\mathbf{x})\|^2) - 2\nabla \hat{u}_0(\mathbf{x}) \cdot \nabla(\boldsymbol{\mathcal{V}}(\mathbf{x}) \cdot \nabla \hat{u}_0(\mathbf{x})) + \|\nabla \hat{u}_0(\mathbf{x})\|^2 \nabla \cdot \boldsymbol{\mathcal{V}}(\mathbf{x})$$
$$= \nabla \cdot \Big(\|\nabla \hat{u}_0(\mathbf{x})\|^2 \boldsymbol{\mathcal{V}}(\mathbf{x})\Big) - 2\nabla \hat{u}_0(\mathbf{x}) \cdot \nabla(\boldsymbol{\mathcal{V}}(\mathbf{x}) \cdot \nabla \hat{u}_0(\mathbf{x})),$$

allowing us to write the shape derivative as

$$-\frac{1}{2}\int\limits_{\mathbb{R}^3}\epsilon(\mathbf{x})\Big\{\nabla\cdot\Big(\|\nabla\hat{u}_0(\mathbf{x})\|^2\,\boldsymbol{\mathcal{V}}(\mathbf{x})\Big)-2\,\nabla\hat{u}_0(\mathbf{x})\cdot\nabla(\boldsymbol{\mathcal{V}}(\mathbf{x})\cdot\nabla\hat{u}_0(\mathbf{x}))\Big\}\,d\mathbf{x}$$

$$=-\frac{1}{2}\int\limits_{\Omega}\epsilon\,\Big\{\nabla\cdot\Big(\|\nabla\hat{u}_0(\mathbf{x})\|^2\,\boldsymbol{\mathcal{V}}(\mathbf{x})\Big)-2\,\nabla\hat{u}_0(\mathbf{x})\cdot\nabla(\boldsymbol{\mathcal{V}}(\mathbf{x})\cdot\nabla\hat{u}_0(\mathbf{x}))\Big\}\,d\mathbf{x}$$

$$-\frac{1}{2}\int\limits_{\Omega_c}\epsilon_0\,\Big\{\nabla\cdot\Big(\|\nabla\hat{u}_0(\mathbf{x})\|^2\,\boldsymbol{\mathcal{V}}(\mathbf{x})\Big)-2\,\nabla\hat{u}_0(\mathbf{x})\cdot\nabla(\boldsymbol{\mathcal{V}}(\mathbf{x})\cdot\nabla\hat{u}_0(\mathbf{x}))\Big\}\,d\mathbf{x}.$$

The integrals on the two subdomains can be simplified further. We show the simplification for Ω and the other one follows in a similar fashion

$$\int\limits_{\Omega}\nabla u(\mathbf{x})\cdot\nabla(\boldsymbol{\mathcal{V}}(\mathbf{x})\cdot\nabla u(\mathbf{x}))\,d\mathbf{x}=\int\limits_{\Omega}\nabla\cdot\Big(\boldsymbol{\mathcal{V}}(\mathbf{x})\cdot\nabla u(\mathbf{x})\,\nabla u(\mathbf{x})\Big)-\int\limits_{\Omega}\boldsymbol{\mathcal{V}}(\mathbf{x})\cdot\nabla u(\mathbf{x})\,\Delta u(\mathbf{x})\,d\mathbf{x}.$$

We get

$$\frac{d\mathcal{E}_F}{ds}(0)=-\frac{1}{2}\int\limits_{\Omega}\epsilon\,\Big\{\nabla\cdot\Big(\|\nabla\hat{u}_0(\mathbf{x})\|^2\,\boldsymbol{\mathcal{V}}(\mathbf{x})-2\,\nabla\hat{u}_0(\mathbf{x})\nabla\hat{u}_0(\mathbf{x})^T\boldsymbol{\mathcal{V}}(\mathbf{x})\Big)\Big\}\,d\mathbf{x}$$

$$-\frac{1}{2}\int\limits_{\Omega_c}\epsilon_0\,\Big\{\nabla\cdot\Big(\|\nabla\hat{u}_0(\mathbf{x})\|^2\,\boldsymbol{\mathcal{V}}(\mathbf{x})-2\,\nabla\hat{u}_0(\mathbf{x})\nabla\hat{u}_0(\mathbf{x})^T\boldsymbol{\mathcal{V}}(\mathbf{x})\Big)-2\,\boldsymbol{\mathcal{V}}(\mathbf{x})\cdot\nabla\hat{u}_0(\mathbf{x})\frac{\rho(\mathbf{x})}{\epsilon_0}\Big\}\,d\mathbf{x}.$$

We see the appearance of the Maxwell Stress Tensor in the integrands and write the expressions as

$$\frac{d\mathcal{E}_F}{ds}(0)=-\int\limits_{\Omega}\epsilon\,\nabla\cdot\Big(\Big\{\frac{\|\nabla\hat{u}_0(\mathbf{x})\|^2}{2}\mathsf{Id}-\nabla\hat{u}_0(\mathbf{x})\nabla\hat{u}_0(\mathbf{x})^T\Big\}\boldsymbol{\mathcal{V}}(\mathbf{x})\Big)\,d\mathbf{x}$$

$$-\int\limits_{\Omega_c}\epsilon_0\,\nabla\cdot\Big(\Big\{\frac{\|\nabla\hat{u}_0(\mathbf{x})\|^2}{2}\mathsf{Id}-\nabla\hat{u}_0(\mathbf{x})\nabla\hat{u}_0(\mathbf{x})^T\Big\}\boldsymbol{\mathcal{V}}(\mathbf{x})\Big)\,d\mathbf{x}$$

$$+\int\limits_{\Omega_{\mathrm{src}}}\boldsymbol{\mathcal{V}}(\mathbf{x})\cdot\nabla\hat{u}_0(\mathbf{x})\,\rho(\mathbf{x})\,d\mathbf{x}.$$

The integral over Ω_{src} vanishes since the velocity field is chosen to be zero at the source charges. We look at the integrals with stress tensors and change them to boundary integrals using divergence theorem. This gives the jump of the stress tensor on the boundary. We write $\hat{u}_0^+$ for the potential in Ω_c and $\hat{u}_0^-$ for the potential in Ω and get the jump of stress tensor times the normal which resembles the force density reported in [28]

$$\frac{d\mathcal{E}_F}{ds}(0)=-\int\limits_{\Gamma}\epsilon\,\boldsymbol{\mathcal{V}}(\mathbf{x})^T\Big\{\frac{\|\nabla\hat{u}_0^-(\mathbf{x})\|^2}{2}\mathbf{n}(\mathbf{x})-\nabla\hat{u}_0^-(\mathbf{x})\nabla\hat{u}_0^-(\mathbf{x})\cdot\mathbf{n}(\mathbf{x})\Big\}\,d\mathbf{x}$$

$$+\int\limits_{\Gamma}\epsilon_0\,\boldsymbol{\mathcal{V}}(\mathbf{x})^T\Big\{\frac{\|\nabla\hat{u}_0^+(\mathbf{x})\|^2}{2}\mathbf{n}(\mathbf{x})-\nabla\hat{u}_0^+(\mathbf{x})\nabla\hat{u}_0^+(\mathbf{x})\cdot\mathbf{n}(\mathbf{x})\Big\}\,d\mathbf{x}.$$

Now we inspect the integrand closely. Skipping the hat and the zero subscript in the notation of potential u, we see that

$$\frac{\|\nabla u\|^2}{2}\mathbf{n} - (\nabla u \cdot \mathbf{n})\nabla u = \frac{(\nabla u \cdot \mathbf{n})^2 + \|\mathbf{grad}_\Gamma u\|^2}{2}\mathbf{n} - (\nabla u \cdot \mathbf{n})^2\mathbf{n} - (\nabla u \cdot \mathbf{n})\,\mathbf{grad}_\Gamma u$$

$$= -\frac{(\nabla u \cdot \mathbf{n})^2}{2}\mathbf{n} + \frac{\|\mathbf{grad}_\Gamma u\|^2}{2}\mathbf{n} - (\nabla u \cdot \mathbf{n})\,\mathbf{grad}_\Gamma u,$$

which allows us to simplify the jump as

$$\epsilon_0\Big(\frac{\|\nabla u^+\|^2}{2}\mathbf{n} - (\nabla u^+ \cdot \mathbf{n})\nabla u^+\Big) - \epsilon\Big(\frac{\|\nabla u^-\|^2}{2}\mathbf{n} - (\nabla u^- \cdot \mathbf{n})\nabla u^-\Big)$$

$$= \epsilon_0\Big(-\frac{(\gamma_N^+ u)^2}{2}\mathbf{n} + \frac{\|\mathbf{grad}_\Gamma \gamma_D^+ u\|^2}{2}\mathbf{n} - \gamma_N^+ u\,\mathbf{grad}_\Gamma \gamma_D^+ u\Big)$$

$$- \epsilon\Big(-\frac{(\gamma_N^- u)^2}{2}\mathbf{n} + \frac{\|\mathbf{grad}_\Gamma \gamma_D^- u\|^2}{2}\mathbf{n} - \gamma_N^- u\,\mathbf{grad}_\Gamma \gamma_D^- u\Big).$$

Using the transmission conditions and defining $\alpha := \epsilon_0\,\gamma_N^+ u = \epsilon\,\gamma_N^- u$, $g := \gamma_D^+ u = \gamma_D^- u$ we get a force density expression that resembles its magnetic counterpart reported in [6]

$$\Big(\llbracket\epsilon\rrbracket_\Gamma \|\mathbf{grad}_\Gamma g\|^2 - \llbracket\epsilon^{-1}\rrbracket_\Gamma \alpha^2\Big)\frac{\mathbf{n}}{2},$$

which finally allows us to express the shape derivative in Hadamard form

$$\frac{d\mathcal{E}_F}{ds}(0) = \frac{1}{2}\int_\Gamma \Big(\llbracket\epsilon\rrbracket_\Gamma \|\mathbf{grad}_\Gamma g(\mathbf{x})\|^2 - \llbracket\epsilon^{-1}\rrbracket_\Gamma \alpha(\mathbf{x})^2\Big)\boldsymbol{\mathcal{V}}(\mathbf{x}) \cdot \mathbf{n}(\mathbf{x})\, dS_\mathbf{x}. \qquad (4.4.15)$$

4.4.6 A Note on "Holding the Fluxes Constant"

Often in literature, the Virtual Work Principle is applied by computing the derivative of the energy with respect to geometric configuration while "holding the fluxes constant" [28, 52]. We would like to clarify that the approach we take is a fundamentally different one and is described by holding the charges constant. Nevertheless, we see that in the end we obtain the same result. We can see this by working backwards from the expression

$$\frac{d\mathcal{E}_F}{ds}(0) = -\frac{1}{2}\frac{\partial\hat{\mathbf{b}}}{\partial s}(0; \hat{u}_0, \hat{u}_0)$$

$$= -\frac{1}{2}\frac{d}{ds}\Big(\int_{\mathbb{R}^3} \epsilon(\hat{\mathbf{x}})\Big(\mathsf{D}\mathbf{T}_s^{\boldsymbol{\nu}}(\hat{\mathbf{x}})^{-T}\nabla\hat{u}_0(\hat{\mathbf{x}})\Big) \cdot \Big(\mathsf{D}\mathbf{T}_s^{\boldsymbol{\nu}}(\hat{\mathbf{x}})^{-T}\nabla\hat{u}_0(\hat{\mathbf{x}})\Big)\,\det\mathsf{D}\mathbf{T}_s^{\boldsymbol{\nu}}(\hat{\mathbf{x}})\,d\hat{\mathbf{x}}\Big)\Big|_{s=0}.$$

Now we imagine the potential $\hat{u}_0$ in the reference configuration transported by the perturbation map to u_s^*, for which we have the pullback relations

$$u_s^*(\mathbf{T}_s^{\boldsymbol{\nu}}(\hat{\mathbf{x}})) = \hat{u}_0(\hat{\mathbf{x}}), \quad \nabla u_s^*(\mathbf{T}_s^{\boldsymbol{\nu}}(\hat{\mathbf{x}})) = \mathsf{D}\mathbf{T}_s^{\boldsymbol{\nu}}(\hat{\mathbf{x}})^{-T}\nabla\hat{u}_0(\hat{\mathbf{x}}),$$

91

which allows us to write

$$\frac{d\mathcal{E}_F}{ds}(0) = -\frac{1}{2}\frac{d}{ds}\left(\int_{\mathbb{R}^3} \epsilon(\hat{\mathbf{x}}) \left(\nabla u_s^*(\mathbf{T}_s^{\boldsymbol{\nu}}(\hat{\mathbf{x}}))\right) \cdot \left(\nabla u_s^*(\mathbf{T}_s^{\boldsymbol{\nu}}(\hat{\mathbf{x}}))\right) \, \det \mathrm{D}\mathbf{T}_s^{\boldsymbol{\nu}}(\hat{\mathbf{x}}) \, d\hat{\mathbf{x}}\right)\Big|_{s=0}.$$

Transforming the integral using the inverse of the perturbation map gives us

$$\frac{d\mathcal{E}_F}{ds}(0) = -\frac{1}{2}\frac{d}{ds}\left(\int_{\mathbb{R}^3} \epsilon_s(\mathbf{x}) \, \|\nabla u_s^*(\mathbf{x})\|^2 \, d\mathbf{x}\right)\Big|_{s=0} = -\frac{d\mathcal{E}_F^*}{ds}(0),$$

where $\mathcal{E}_F^*(s)$ is the field energy obtained by simply transporting the reference solution $\hat{u}_0$ using the perturbation map. The left hand side contains the energy shape derivative computed by moving the charges in reference configuration as a 3-form, whereas the shape derivative on the RHS is computed by moving the potential in the reference configuration as a 0-form. By moving the potential a 0-form on the RHS, the commutative property of the exterior derivative and pullback [32, Equation 2.13] ensures that the electric field in the reference configuration (exterior derivative of the potential) moves as a 1-form, hence preserving its fluxes. This idea is also reported by the authors in [28] and we see both forms of the virtual work principle reported in [39]. Note that in both the cases, the permittivity is moved as a 0-form. This will also hold true for the magnetostatic case as we will see later.

4.4.7 Numerical Experiments

Now we compare the shape derivatives (4.4.15) (called "MST" in the plots) and (4.4.8) (called "BEM" in the plots) using numerical experiments. Discretizing the boundary with a triangular mesh of meshwidth h, we solve for the traces ψ_h and g_h by the Galerkin method, restricting the BIE formulation (4.4.2) to the discrete spaces S_1^0 for $H^{\frac{1}{2}}$ (piece-wise linear functions) and S_0^{-1} (piecewise constants) for $H^{-\frac{1}{2}}$. We compute the forces and torques for a sequence of meshes with decreasing meshwidth h using the recipe in (3.0.5) and plot the errors against h. Terms in the BEM based shape derivative (4.4.8) are computed using the Sauter and Schwab quadrature rule [54, Chapter 5] of order 5^4 whereas (4.4.15) is evaluated using a quadrature rule of order 3 per triangle element. The computations are done using Gysilab [13].

4.4.7.1 Dual Norm Error Computation

The shape derivative can be interpreted as a linear functional on test velocity fields $\boldsymbol{\mathcal{V}} \in \mathcal{X}$. Denoting the evaluation of the shape derivative for $\boldsymbol{\mathcal{V}}$ by $\frac{d\mathcal{E}_F}{ds}(0; \boldsymbol{\mathcal{V}})$, we can define the dual norm error as

$$\mathrm{err} := \sup_{\boldsymbol{\mathcal{V}} \in \mathcal{X}, \|\boldsymbol{\mathcal{V}}\|_{\mathcal{X}}=1} \left(\frac{d\mathcal{E}_F}{ds}(0; \boldsymbol{\mathcal{V}}) - \frac{d\mathcal{E}_F^h}{ds}(0; \boldsymbol{\mathcal{V}})\right), \tag{4.4.16}$$

---

[13]Code is available at https://github.com/piyushplcr7/gypsilab_forces

where $\frac{d\mathcal{E}_F^h}{ds}(0; \mathcal{V})$ denotes the evaluation by plugging in the Galerkin solution at a meshwidth h. The reference value $\frac{d\mathcal{E}_F}{ds}(0; \mathcal{V})$ is computed numerically at a high refinement level. To make the computation tractable [46], we choose $\mathcal{X}$ as the finite dimensional span of the orthogonal velocity fields

$$\boldsymbol{v}(a, b, c, k) : (-N\pi, N\pi)^3 \to \mathbb{R}^3, \quad N \in \mathbb{Z}^+, \ a, b, c \in \{0, 1, 2\}, \ k = 1, 2, 3,$$

$$\boldsymbol{v}(a, b, c, k)(\begin{bmatrix} x \\ y \\ z \end{bmatrix}) := \cos(ax) \ \cos(by) \ cos(cz) \ \mathbf{e}_k.$$

The size parameter N is chosen to be big enough such that $(-N\pi, N\pi)^3$ contains the domain of interest. Because of the ease of computation, we choose the H^1 norm for $\mathcal{X}$. The supremum can be explicitly computed. Consider the following abstract setting: we have a linear functional $l : \mathcal{X} \to \mathbb{R}$ where $\mathcal{X}$ is a Hilbert space with a finite dimensional basis. We want to maximize $l(\mathcal{V})$ such that $\|\mathcal{V}\|_{\mathcal{X}} = 1$. This can be done by introducing the Lagrange function

$$f : \mathbb{R} \times \mathcal{X} \to \mathbb{R}, \quad f(\lambda, \mathcal{V}) := l(\mathcal{V}) + \lambda\Big(\|\mathcal{V}\|_{\mathcal{X}}^2 - 1\Big).$$

The solution of the constrained maximization problem $\mathcal{V}_* \in \mathcal{X}$ satisfies

$$\Big\langle \frac{\partial f}{\partial \mathcal{V}}(\lambda, \mathcal{V}_*); \mathcal{V}' \Big\rangle = 0 \quad \forall \mathcal{V}' \in \mathcal{X},$$

which gives

$$l(\mathcal{V}') + 2\lambda \, (\mathcal{V}_*, \mathcal{V}')_{\mathcal{X}} = 0 \quad \forall \mathcal{V}' \in \mathcal{X}.$$

Writing $\mathcal{V}_* = \sum \alpha_j^* \, b_j$ and testing the above with b_i gives

$$\sum \alpha_j^* (b_j, b_i)_{\mathcal{X}} = -\frac{1}{2\lambda} l(b_i).$$

We can solve for $\boldsymbol{\alpha} := \alpha_1, \alpha_2, ...$ from the linear system

$$\mathbf{M}\boldsymbol{\alpha} = -\boldsymbol{l}, \quad \mathbf{M}_{ij} := (b_j, b_i)_{\mathcal{X}}, \ \boldsymbol{l}_i := l(b_i),$$

which gives $\alpha_j^* = \frac{1}{2\lambda}\alpha_j$. Using the constraint $\|\mathcal{V}_*\|_{\mathcal{X}}^2 = 1$ we get

$$\lambda = \sqrt{\frac{1}{2}\boldsymbol{\alpha}^T \mathbf{M} \, \boldsymbol{\alpha}} = \sqrt{-\frac{1}{2}\boldsymbol{\alpha}^T \boldsymbol{l}}.$$

Thus the constrained maxima for the linear functional is

$$l(\mathcal{V}_*) = l(\sum \alpha_j^* \, b_j) = \sum \alpha_j^* \, l(b_j) = \frac{1}{2\lambda}\boldsymbol{\alpha}^T \boldsymbol{l} = \frac{\boldsymbol{\alpha}^T \boldsymbol{l}}{\sqrt{-2\boldsymbol{\alpha}^T \boldsymbol{l}}} = \sqrt{-\frac{1}{2}\boldsymbol{\alpha}^T \boldsymbol{l}} = \sqrt{\frac{1}{2}\boldsymbol{l}^T \mathbf{M}^{-T} \boldsymbol{l}}.$$

Thus we need to evaluate the errors for different velocity fields and they can be combined using the formula above to get the dual norm. The matrix $\mathbf{M}$ can be computed explicitly for the chosen velocity fields. Since the velocity fields are orthogonal to each other, $\mathbf{M}$ is diagonal.

Experiment 7. In this experiment, Ω is a spherical domain of radius 1, centered at $(5, 5, 3)$, occupied by a linear material with $\epsilon = 4$, surrounded by a linear material with $\epsilon_0 = 2$. There is a spherical charge source of radius 1 centered at the origin, with a constant surface charge density equal to 15. The situation is depicted in Figure 4.17
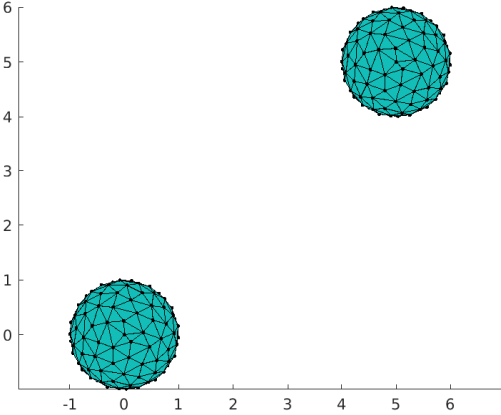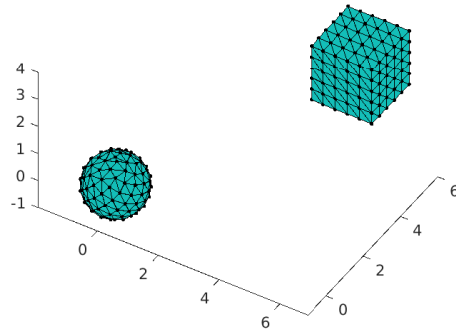

Figure 4.17: Spherical material with spherical charge

Total force and torque is computed using the shape derivatives (4.4.8) and (4.4.15) and the errors are plotted in Figure 4.18. As reference value, we use the BEM based computation at a refinement level of $h = 0.055$. Torque is computed about the point $(4, 0, 0)$. The convergence rates for the two methods are very similar as seen in the plot. They are also tabulated in Table 4.5.

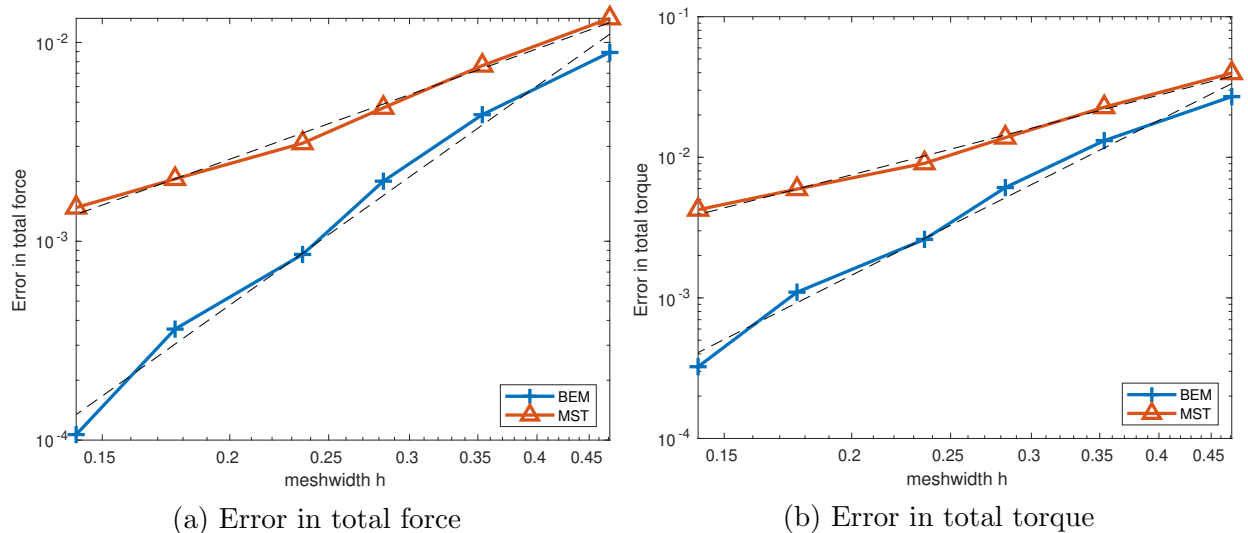(a) Error in total force

(b) Error in total torque
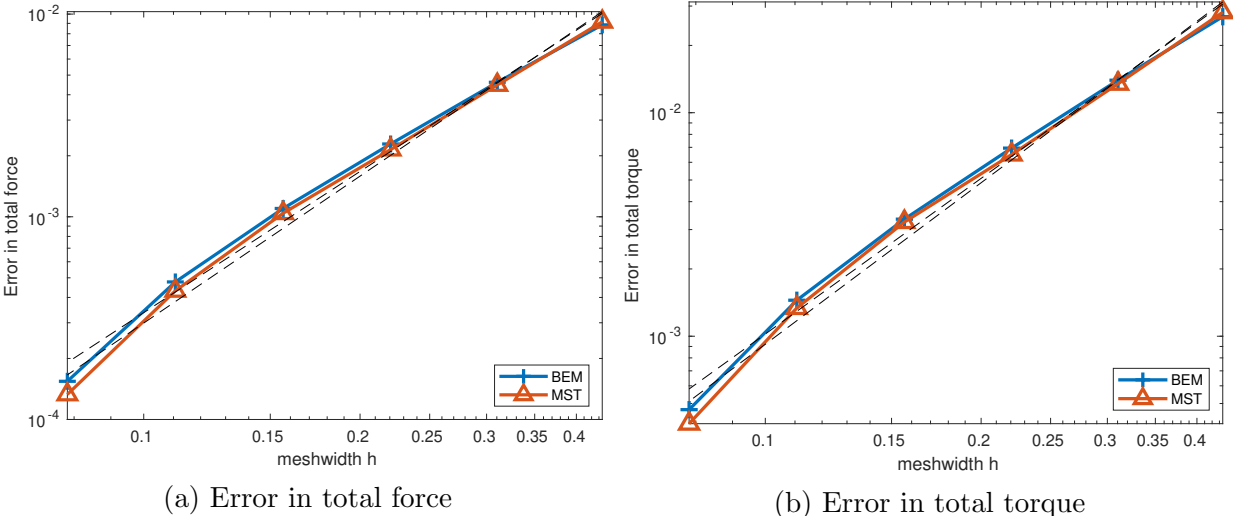
Figure 4.18: Error in force and torque computation for Experiment 7

Table 4.5: Asymptotic rate of algebraic convergence for Experiment 7

Method	Force	Torque
Pullback approach	2.31	2.31
Stress tensor	2.41	2.40

The methods can also be compared via dual norm error. The results for it are plotted in Figure 4.19 where we see similar convergence rates. The reference values for dual norm error computation are computed using the BEM based shape derivative at a refinement level of $h = 0.078$.
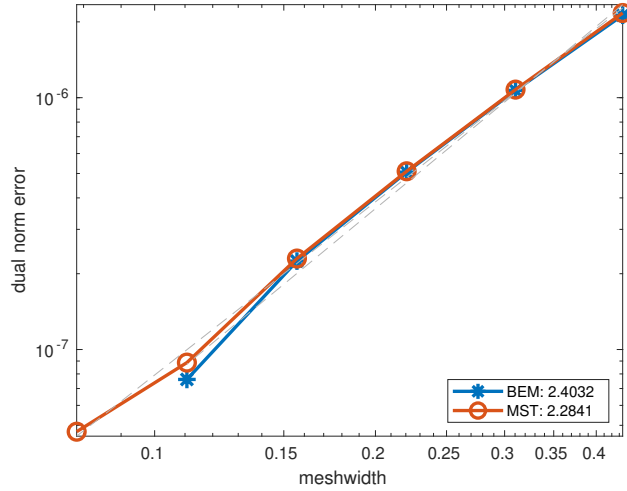
Figure 4.19: Dual norm error for Experiment 7

Experiment 8. Keeping the same spherical source charge as in the previous experiment, we now have Ω as a cube shaped domain of side 2 and centered at $(5, 5, 3)$, occupied by a linear material with $\epsilon = 4$, surrounded by a linear material with $\epsilon_0 = 2$. The situation is depicted in Figure 4.20
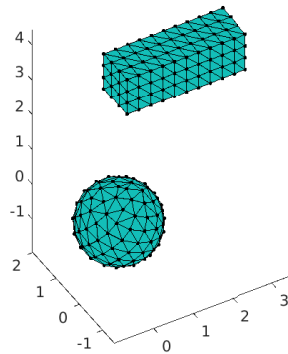

Figure 4.20: Cube shaped material with spherical charge

95

Total force and torque is computed using the shape derivatives (4.4.8) and (4.4.15) and the error plotted in Figure 4.21. Torque is computed about the point $(4, 0, 0)$. As reference value, we use the BEM based computation at a refinement level of $h = 0.108$. As seen in the plot, for this non-smooth setting the BEM based formula gives a higher convergence rate which is also tabulated in Table 4.6.
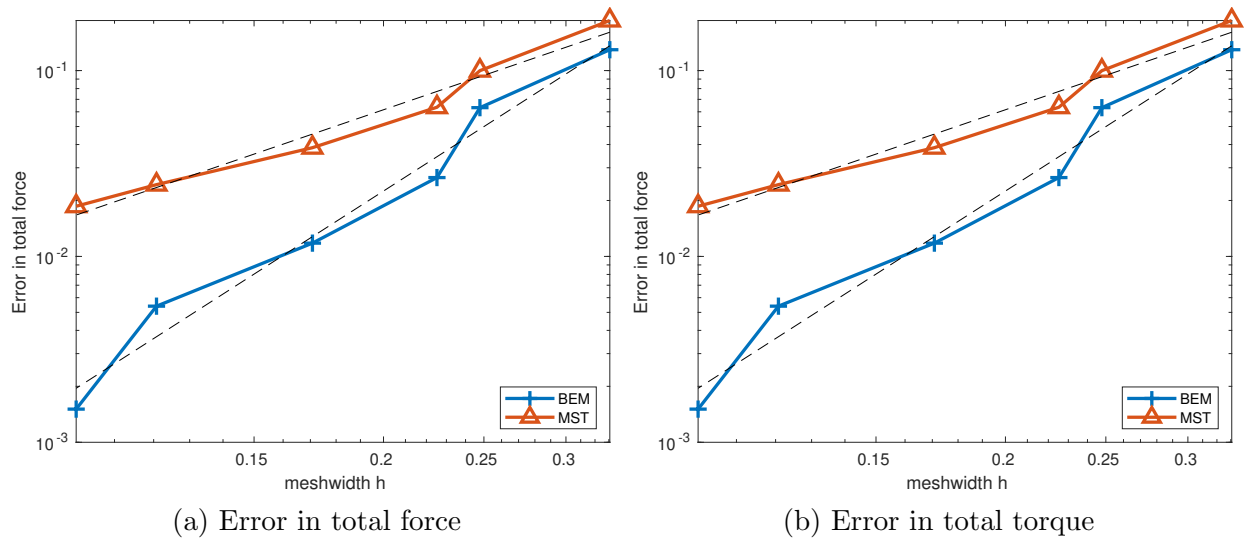

(a) Error in total force
(b) Error in total torque

Figure 4.21: Error in force and torque computation for Experiment 8

Table 4.6: Asymptotic rate of algebraic convergence for Experiment 8

Method	Force	Torque
Pullback approach	3.66	3.65
Stress tensor	1.84	1.88

The methods can also be compared via dual norm error. The results for it are plotted in Figure 4.22 where we get another confirmation of the superior convergence rate of the BEM based shape derivative. The reference values for dual norm error computation are obtained using the BEM based shape derivative at $h = 0.108$.
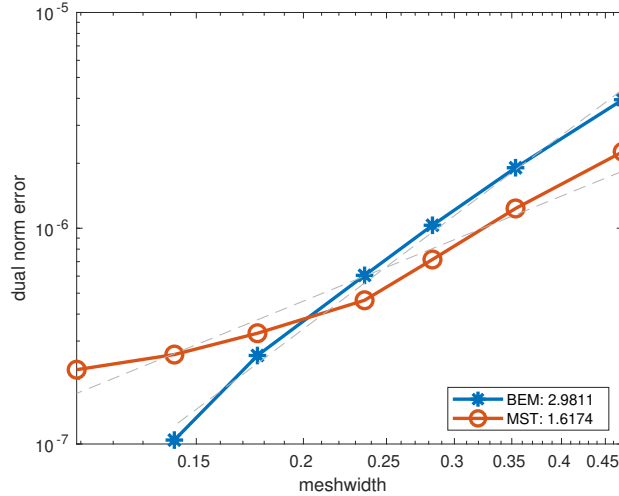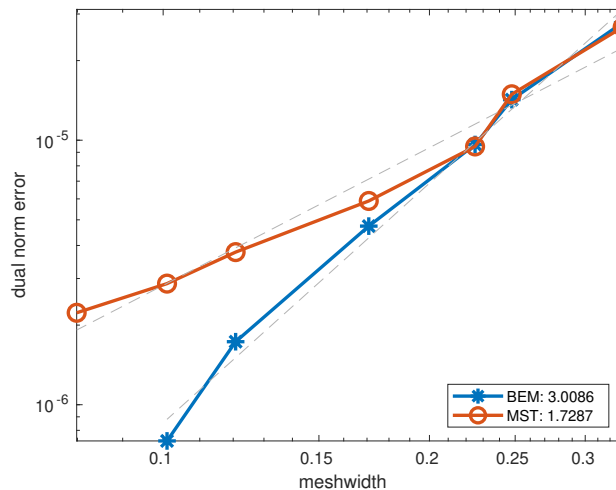
Figure 4.22: Dual norm error for Experiment 8

Experiment 9. Keeping the same spherical source charge, we make Ω a brick shaped domain with side lengths $(3,1,1)$ and centered at $(2,1,3)$, occupied by a linear material with $\epsilon = 4$, surrounded by a linear material with $\epsilon_0 = 2$. The situation is depicted in Figure 4.23
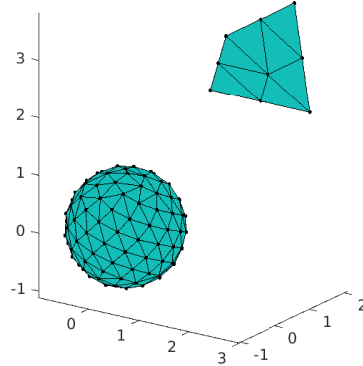

Figure 4.23: Brick shaped material with spherical charge

Total force and torque is computed using the shape derivatives (4.4.8) and (4.4.15) and the error plotted in Figure 4.24. Torque is computed about the point $(4, 0, 0)$. As reference value, we use the BEM based computation at a refinement level of $h = 0.079$. As seen in the plot, for this non-smooth setting the BEM based formula gives a higher convergence rate which is also tabulated in Table 4.7.

(a) Error in total force

(b) Error in total torque

Figure 4.24: Error in force and torque computation for Experiment 9

Table 4.7: Asymptotic rate of algebraic convergence for Experiment 9

Method	Force	Torque
Pullback approach	3.58	3.58
Stress tensor	1.91	1.88

The methods can also be compared via dual norm error. The results for it are plotted in Figure 4.25 where we get another confirmation of the superior convergence rate of the BEM based shape derivative. The reference values for dual norm error computation are obtained using the BEM based shape derivative at $h = 0.079$.

Figure 4.25: Dual norm error for Experiment 9

Experiment 10. Keeping the same spherical source charge, we make Ω a tetrahedral shaped domain with corners $(\pm 1, 0, -\frac{1}{\sqrt{2}})$ and $(0, \pm 1, \frac{1}{\sqrt{2}})$, translated by $(2,1,3)$, occupied by a linear

material with $\epsilon = 4$, surrounded by a linear material with $\epsilon_0 = 2$. The situation is depicted in Figure 4.26

Figure 4.26: Tetrahedral shaped material with spherical charge

Total force and torque is computed using the shape derivatives (4.4.8) and (4.4.15) and the error plotted in Figure 4.27. Torque is computed about the point $(4, 0, 0)$. As reference value, we use the BEM based computation at a refinement level of $h = 0.04$. As seen in the plot, for this non-smooth setting the BEM based formula gives a higher convergence rate which is also tabulated in Table 4.8.
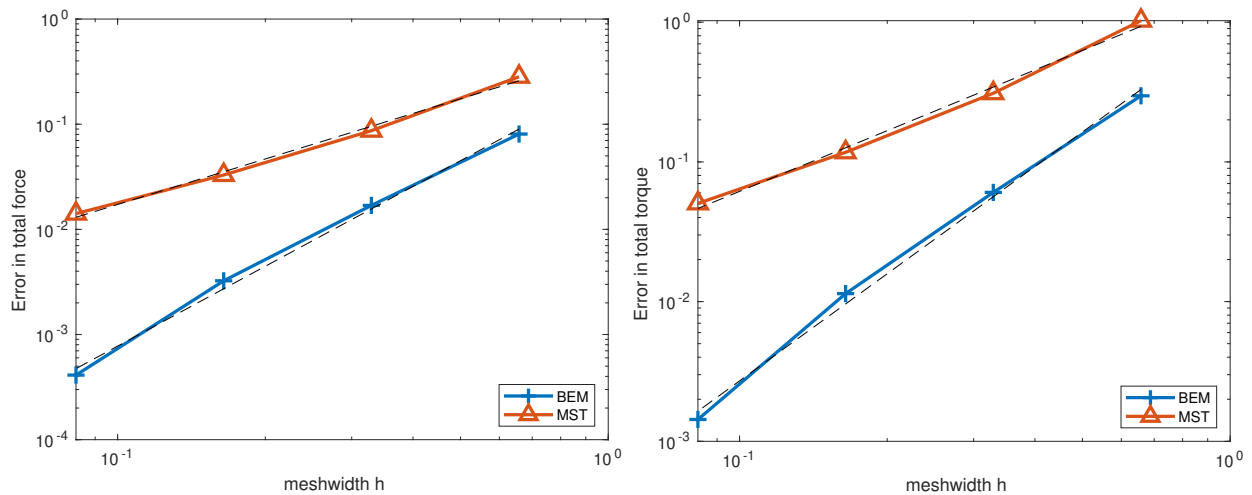
(a) Error in total force

(b) Error in total torque

Figure 4.27: Error in force and torque computation for Experiment 10

Table 4.8: Asymptotic rate of algebraic convergence for Experiment 10

Method	Force	Torque
Pullback approach	2.52	2.55
Stress tensor	1.44	1.44

The methods can also be compared via dual norm error. The results for it are plotted in Figure 4.28 where we get another confirmation of the superior convergence rate of the BEM based shape derivative. The reference values for dual norm error computation are obtained using the BEM based shape derivative at $h = 0.04$.
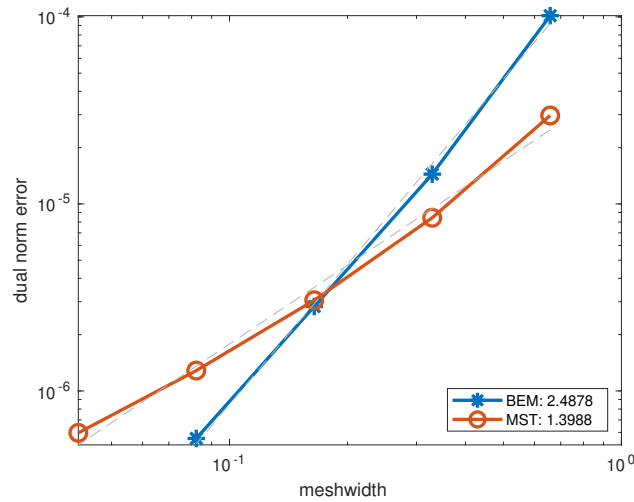
Figure 4.28: Dual norm error for Experiment 10

Chapter 5

Energy Shape Derivatives for Magnetostatic Models

In this section we apply the Virtual Work Principle via Shape Calculus to various magnetostatic settings, following a similar procedure to the electrostatics case in the previous chapter. In magnetostatics we can approach the model problem using either a scalar potential or a vector potential formulation. We will explore shape derivatives obtained using both formulations. In addition to that, we can also choose between a volume based or a BIE based variational formulation as a constraint. We will explore both choices, and similar to the electrostatics case, the volume based formulations will yield expressions based on Maxwell Stress Tensor, whereas the BIE based formulation will yield novel expressions for computing forces and torques.

5.1   Linear Magnetic Material - Transmission Problem
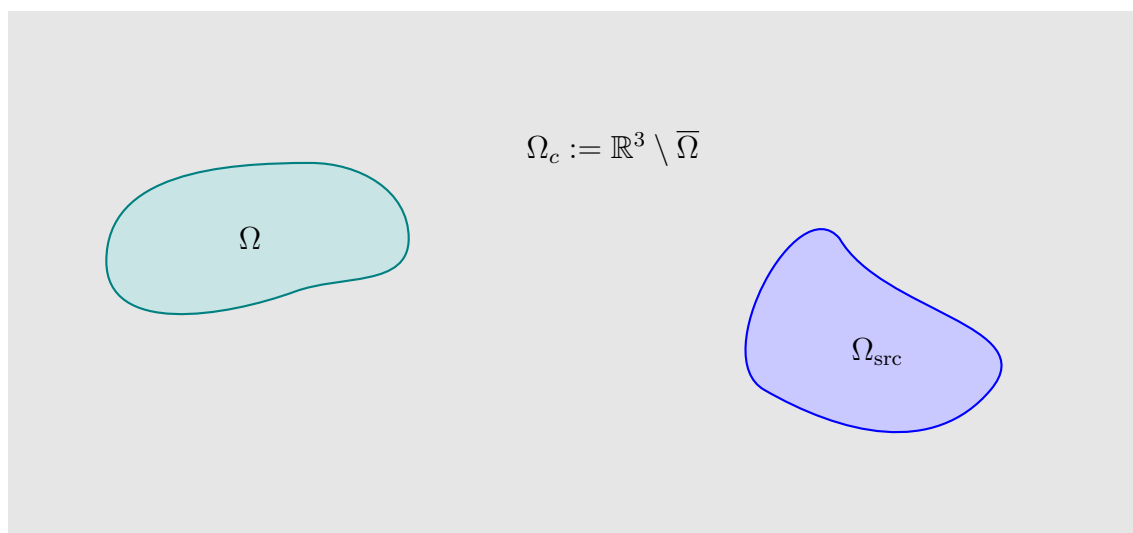
Figure 5.1: Geometric setting

We have a linear, isotropic and homogeneous material with permeability $\mu \in \mathbb{R}^+$ occupying the bounded, simply connected and open domain $\Omega \subset \mathbb{R}^3$ with C_{pw}^2 boundary. The exterior $\Omega_c := \mathbb{R}^3 \setminus \overline{\Omega}$ represents vacuum with permeability given as $\mu_0 \in \mathbb{R}^+, \mu_0 \neq \mu$. There is an external current source supplying the current density $\mathbf{J}$ which is compactly supported with $\mathrm{supp}(\mathbf{J}) \subset \Omega_{\mathrm{src}} \Subset \mathbb{R}^3$. The fields $\mathbf{B}$ and $\mathbf{H}$ are modelled by the Maxwell's equations

$$\mathrm{div}\,\mathbf{B} = 0 \quad \text{in } \mathbb{R}^3, \tag{5.1.1}$$

$$\mathbf{curl}\mathbf{H} = \mathbf{J} \quad \text{in } \mathbb{R}^3, \tag{5.1.2}$$

which are supplemented by the material law:

$$\mathbf{B}(\mathbf{x}) = \mu(\mathbf{x})\,\mathbf{H}(\mathbf{x}), \quad \mu(\mathbf{x}) = \begin{cases} \mu & \mathbf{x} \in \Omega \\ \mu_0 & \mathbf{x} \in \Omega_c \end{cases}. \tag{5.1.3}$$

The fields are discontinuous at the interface $\Gamma := \partial\Omega$ due to different material parameters and are coupled through the following transmission conditions:

$$[\![\mathbf{B}]\!]_\Gamma \cdot \mathbf{n} = 0, \quad [\![\mathbf{H}]\!]_\Gamma \times \mathbf{n} = 0, \tag{5.1.4}$$

where $[\![\cdot]\!]_\Gamma$ denotes the jump, defined earlier in Section 2.1.4. The fields can be obtained by solving a variational problem posed on the volume or the boundary. We will investigate formulations based on either a scalar/vector potential for the fields. The field energy stored in the magnetic field $\mathcal{E}_F$ we will shape differentiate is given as

$$\mathcal{E}_F := \frac{1}{2} \int_{\mathbb{R}^3} \mu^{-1}(\mathbf{x})\,\|\mathbf{B}(\mathbf{x})\|^2\;d\mathbf{x}. \tag{5.1.5}$$

5.1.1 Scalar Potential Formulation

We begin by defining $\tilde{\mathbf{H}} := \mathbf{H} - \mathbf{H_J}$ and noticing that

$$\mathbf{curl}\tilde{\mathbf{H}} = \mathbf{curl}(\mathbf{H} - \mathbf{H_J}) = 0 \quad \text{in } \mathbb{R}^3,$$

where

$$\mathbf{H_J}(\mathbf{x}) := \mathbf{curl} \int_{\Omega_{\mathrm{src}}} G(\mathbf{x}, \mathbf{y})\,\mathbf{J}(\mathbf{y})\,d\mathbf{y} \implies \mathbf{curl}\mathbf{H_J} = \mathbf{J},\; \mathrm{div}\,\mathbf{H_J} = 0. \tag{5.1.6}$$

This allows us to write $\tilde{\mathbf{H}} = \nabla u$ for a scalar potential u in $\Omega \cup \Omega_c$, which means $\mathbf{H} = \nabla u + \mathbf{H_J}$. Using the equation $\mathrm{div}\,\mathbf{B} = 0$ and the material law, we get

$$\mathrm{div}\,\tilde{\mathbf{H}} = \Delta u = \mathrm{div}\,\mathbf{H} - \mathrm{div}\,\mathbf{H_J} = \mathrm{div}(\mu(\mathbf{x})^{-1}\,\mathbf{B}(\mathbf{x})) = 0 \quad \text{in } \Omega \cup \Omega_c,$$

where we used the fact $\mathrm{div}\,\mathbf{H_J} = 0$, which holds for a divergence free source current density $\mathbf{J}$. The transmission conditions can be obtained as

$$[\![\mathbf{B}]\!]_\Gamma \cdot \mathbf{n} = 0 \implies [\![\mu(\nabla u + \mathbf{H_J})]\!]_\Gamma \cdot \mathbf{n} = 0.$$

Enforcing the continuity of the Dirichlet trace for the scalar potential u, that is $\gamma_D^+ u = \gamma_D^- u$ leads to the continuity of the surface curl of the traces, or

$$[\![\nabla u]\!]_\Gamma \times \mathbf{n} = 0 \implies [\![\mathbf{H}]\!]_\Gamma \times \mathbf{n} = 0. \tag{5.1.7}$$

Thus we have the transmission problem

$$
\begin{aligned}
\Delta u &= 0 && \text{in } \Omega \cup \Omega_c \\
[\![u]\!]_\Gamma &= 0 && \text{on } \Gamma \\
[\![\mu \, \nabla u]\!]_\Gamma \cdot \mathbf{n} &= -[\![\mu]\!]_\Gamma \mathbf{H_J} \cdot \mathbf{n} && \text{on } \Gamma \\
|u(\mathbf{x})| &= O(\|\mathbf{x}\|^{-1}) && \text{for } \|\mathbf{x}\| \to \infty
\end{aligned} \tag{5.1.8}
$$

5.1.1.1 Variational BIEs

The transmission problem at hand can be approached using boundary integral equations. We simply reuse the BIEs we derived for the Laplace equation in 2.1.22

$$\begin{bmatrix} -V & \frac{\mathsf{Id}}{2} + K \\ \frac{\mathsf{Id}}{2} - K' & -W \end{bmatrix} \begin{bmatrix} \gamma_N^- u \\ \gamma_D^- u \end{bmatrix} = \begin{bmatrix} 0 \\ 0 \end{bmatrix}, \tag{5.1.9}$$

$$\begin{bmatrix} -V & -\frac{\mathsf{Id}}{2} + K \\ -\frac{\mathsf{Id}}{2} - K' & -W \end{bmatrix} \begin{bmatrix} \gamma_N^+ u \\ \gamma_D^+ u \end{bmatrix} = \begin{bmatrix} 0 \\ 0 \end{bmatrix}. \tag{5.1.10}$$

We can test the above equations with $\phi \in H^{-\frac{1}{2}}(\Gamma)$ and $v \in H^{\frac{1}{2}}(\Gamma)$. The first set of equations gives

$$-\mathsf{b}_V(\gamma_N^- u, \phi) + \frac{1}{2}\left\langle \gamma_D^- u, \phi \right\rangle + \mathsf{b}_K(\gamma_D^- u, \phi) = 0 \quad \forall \phi \in H^{-\frac{1}{2}}(\Gamma), \tag{5.1.11}$$

$$\frac{1}{2}\left\langle \gamma_N^- u, v \right\rangle - \mathsf{b}_{K'}(\gamma_N^- u, v) - \mathsf{b}_W(\gamma_D^- u, v) = 0 \quad \forall v \in H^{\frac{1}{2}}(\Gamma), \tag{5.1.12}$$

and the second set of equations gives

$$-\mathsf{b}_V(\gamma_N^+ u, \phi) - \frac{1}{2}\left\langle \gamma_D^+ u, \phi \right\rangle + \mathsf{b}_K(\gamma_D^+ u, \phi) = 0 \quad \forall \phi \in H^{-\frac{1}{2}}(\Gamma), \tag{5.1.13}$$

$$-\frac{1}{2}\left\langle \gamma_N^+ u, v \right\rangle - \mathsf{b}_{K'}(\gamma_N^+ u, v) - \mathsf{b}_W(\gamma_D^+ u, v) = 0 \quad \forall v \in H^{\frac{1}{2}}(\Gamma). \tag{5.1.14}$$

We denote the exterior traces as $g := \gamma_D^+ u$ and $\psi := \gamma_N^+ u$. Based on this the interior traces have the notation $\gamma_D^- u = g$ and $\gamma_N^- u = \frac{\mu_0}{\mu}\psi + \frac{[\![\mu]\!]_\Gamma}{\mu}\mathbf{H_J} \cdot \mathbf{n}$. The two sets of equations can be combined together and we get the variational problem: seek $\psi \in H^{-\frac{1}{2}}(\Gamma)$, $g \in H^{\frac{1}{2}}(\Gamma)$ such that

$$(1 + \frac{\mu_0}{\mu}) \, \mathsf{b}_V(\psi, \phi) - 2 \, \mathsf{b}_K(g, \phi) + 2 \, \mathsf{b}_{K'}(\psi, v) + (1 + \frac{\mu}{\mu_0}) \, \mathsf{b}_W(g, v)$$

$$= -\frac{[\![\mu]\!]_\Gamma}{\mu}\mathsf{b}_V(\mathbf{H_J} \cdot \mathbf{n}, \phi) + \frac{[\![\mu]\!]_\Gamma}{2\mu_0}\left\langle \mathbf{H_J} \cdot \mathbf{n}, v \right\rangle - \frac{[\![\mu]\!]_\Gamma}{\mu_0}\mathsf{b}_{K'}(\mathbf{H_J} \cdot \mathbf{n}, v) \qquad \forall \phi \in H^{-\frac{1}{2}}(\Gamma), v \in H^{\frac{1}{2}}(\Gamma). \tag{5.1.15}$$

We know that the traces of the potential u satisfying (5.1.8) is a solution to (5.1.15). The solution is unique from Theorem 2. The field energy $\mathcal{E}_F$ in (5.1.5) can be written in terms of the scalar potential as

$$\mathcal{E}_F = \frac{1}{2}\int_{\mathbb{R}^3} \mu(\mathbf{x}) \|\nabla u(\mathbf{x})\|^2 \ d\mathbf{x} + \frac{1}{2}\int_{\mathbb{R}^3} \mu(\mathbf{x}) \|\mathbf{H_J}(\mathbf{x})\|^2 \ d\mathbf{x} + \int_{\mathbb{R}^3} \mu(\mathbf{x}) \, \nabla u(\mathbf{x}) \cdot \mathbf{H_J}(\mathbf{x}) \ d\mathbf{x}.$$

Applying Green's formula in Ω and Ω_c and using div $\mathbf{H_J} = 0$ we get

$$\mathcal{E}_F = \frac{1}{2}\int_{\mathbb{R}^3} \mu(\mathbf{x}) \|\nabla u(\mathbf{x})\|^2 \ d\mathbf{x} + \frac{1}{2}\int_{\mathbb{R}^3} \mu(\mathbf{x}) \|\mathbf{H_J}(\mathbf{x})\|^2 \ d\mathbf{x} - [\![\mu]\!]_\Gamma \int_\Gamma g \, \mathbf{H_J} \cdot \mathbf{n} \ dS$$

$$= \frac{1}{2}\int_\Omega \mu \|\nabla u(\mathbf{x})\|^2 \ d\mathbf{x} + \frac{1}{2}\int_{\Omega_c} \mu_0 \|\nabla u(\mathbf{x})\|^2 \ d\mathbf{x} + \frac{1}{2}\int_{\mathbb{R}^3} \mu(\mathbf{x}) \|\mathbf{H_J}(\mathbf{x})\|^2 \ d\mathbf{x} - [\![\mu]\!]_\Gamma \int_\Gamma g \, \mathbf{H_J} \cdot \mathbf{n} \ dS$$

$$= \frac{\mu}{2}\int_\Gamma \gamma_D^- u \, \gamma_N^- u \ dS - \frac{\mu_0}{2}\int_\Gamma \gamma_D^+ u \, \gamma_N^+ u \ dS + \frac{1}{2}\int_{\mathbb{R}^3} \mu(\mathbf{x}) \|\mathbf{H_J}(\mathbf{x})\|^2 \ d\mathbf{x} - [\![\mu]\!]_\Gamma \int_\Gamma g \, \mathbf{H_J} \cdot \mathbf{n} \ dS$$

$$= -\frac{[\![\mu]\!]_\Gamma}{2}\int_\Gamma g \, \mathbf{H_J} \cdot \mathbf{n} \ dS + \frac{1}{2}\int_{\mathbb{R}^3} \mu(\mathbf{x}) \|\mathbf{H_J}(\mathbf{x})\|^2 \ d\mathbf{x}.$$

To make the computation of shape derivative simpler, we express the field energy in terms of the linear form on the RHS of Equation (5.1.15), which is

$$\ell(\begin{bmatrix} \phi \\ v \end{bmatrix}) := -\frac{[\![\mu]\!]_\Gamma}{\mu}\mathsf{b}_V(\mathbf{H_J} \cdot \mathbf{n}, \phi) + \frac{[\![\mu]\!]_\Gamma}{2\mu_0} \langle \mathbf{H_J} \cdot \mathbf{n}, v \rangle - \frac{[\![\mu]\!]_\Gamma}{\mu_0}\mathsf{b}_{K'}(\mathbf{H_J} \cdot \mathbf{n}, v).$$

To see the connection with $\mathcal{E}_F$, we plug in $-\psi$ and g into the linear form to get

$$\ell(\begin{bmatrix} -\psi \\ g \end{bmatrix}) = \frac{[\![\mu]\!]_\Gamma}{\mu}\mathsf{b}_V(\mathbf{H_J} \cdot \mathbf{n}, \psi) + \frac{[\![\mu]\!]_\Gamma}{2\mu_0} \langle \mathbf{H_J} \cdot \mathbf{n}, g \rangle - \frac{[\![\mu]\!]_\Gamma}{\mu_0}\mathsf{b}_{K'}(\mathbf{H_J} \cdot \mathbf{n}, g)$$

$$= \frac{[\![\mu]\!]_\Gamma}{\mu_0}\left\{ \frac{\mu_0}{\mu} \, \mathsf{b}_V(\psi, \mathbf{H_J} \cdot \mathbf{n}) - \mathsf{b}_{K'}(\mathbf{H_J} \cdot \mathbf{n}, g) + \frac{1}{2} \langle \mathbf{H_J} \cdot \mathbf{n}, g \rangle \right\}. \qquad (5.1.16)$$

Testing (5.1.11) with $\mathbf{H_J} \cdot \mathbf{n}$ gives us

$$\frac{\mu_0}{\mu}\mathsf{b}_V(\psi, \mathbf{H_J} \cdot \mathbf{n}) - \mathsf{b}_{K'}(\mathbf{H_J} \cdot \mathbf{n}, g) = -\frac{[\![\mu]\!]_\Gamma}{\mu}\mathsf{b}_V(\mathbf{H_J} \cdot \mathbf{n}, \mathbf{H_J} \cdot \mathbf{n}) + \frac{1}{2} \langle g, \mathbf{H_J} \cdot \mathbf{n} \rangle,$$

which can be plugged into (5.1.16) to get the relation

$$\ell(\begin{bmatrix} -\psi \\ g \end{bmatrix}) = \frac{[\![\mu]\!]_\Gamma}{\mu_0}\left\{ -\frac{[\![\mu]\!]_\Gamma}{\mu}\mathsf{b}_V(\mathbf{H_J} \cdot \mathbf{n}, \mathbf{H_J} \cdot \mathbf{n}) + \langle \mathbf{H_J} \cdot \mathbf{n}, g \rangle \right\},$$

which finally yields the relation for the field energy

$$\mathcal{E}_F = -\frac{\mu_0}{2}\ell(\begin{bmatrix} -\psi \\ g \end{bmatrix}) - \frac{[\![\mu]\!]_\Gamma^2}{2\mu}\mathsf{b}_V(\mathbf{H_J} \cdot \mathbf{n}, \mathbf{H_J} \cdot \mathbf{n}) + \frac{1}{2}\int_{\mathbb{R}^3} \mu(\mathbf{x}) \|\mathbf{H_J}(\mathbf{x})\|^2 \ d\mathbf{x}. \qquad (5.1.17)$$

104

5.1.1.2 Variational Formulation on Deformed Domain

The reference domain Ω^0 is deformed using the perturbation map $\mathbf{T}^{\boldsymbol{\nu}}_s$, using a velocity field $\boldsymbol{\mathcal{V}}$ which is zero at the source current. In other words, we only deform the domain Ω^0. The permeability is transformed as a 0-form to μ_s such that $\mu_s(\mathbf{T}^{\boldsymbol{\nu}}_s(\hat{\mathbf{x}})) = \mu(\hat{\mathbf{x}})$. The variational formulation for this deformed s configuration has a similar structure to (5.1.15): Seek $\psi_s \in H^{-\frac{1}{2}}(\Gamma^s)$, $g_s \in H^{\frac{1}{2}}(\Gamma^s)$ such that

$$(1 + \frac{\mu_0}{\mu})\, \mathsf{b}_{\mathrm{V}}(s)(\psi_s, \phi) - 2\, \mathsf{b}_{\mathrm{K}}(s)(g_s, \phi) + 2\, \mathsf{b}_{\mathrm{K}'}(s)(\psi_s, v) + (1 + \frac{\mu}{\mu_0})\, \mathsf{b}_{\mathrm{W}}(s)(g_s, v)$$

$$= -\frac{[\![\mu]\!]_\Gamma}{\mu}\mathsf{b}_{\mathrm{V}}(s)(\mathbf{H_J}\cdot\mathbf{n}, \phi) + \frac{[\![\mu]\!]_\Gamma}{2\mu_0}\, \langle \mathbf{H_J} \cdot \mathbf{n}, v \rangle_{\Gamma^s} - \frac{[\![\mu]\!]_\Gamma}{\mu_0}\mathsf{b}_{\mathrm{K}'}(s)(\mathbf{H_J}\cdot\mathbf{n}, v) \quad \forall v \in H^{\frac{1}{2}}(\Gamma^s), \forall \phi \in H^{-\frac{1}{2}}(\Gamma^s),$$

where the bilinear forms $b_*(s)$ contain integrals on $\Gamma^s = \partial\Omega^s = \mathbf{T}^{\boldsymbol{\nu}}_s(\Gamma^0)$ and $\langle \cdot, \cdot \rangle_{\Gamma^s}$ denotes the duality pairing between $H^{-\frac{1}{2}}(\Gamma^s)$ and $H^{\frac{1}{2}}(\Gamma^s)$.

5.1.1.3 Equivalent Formulation on Reference Domain

Using the perturbation map $\mathbf{T}^{\boldsymbol{\nu}}_s$, we transform the integrals in the (bi)linear forms back to the reference boundary Γ^0, similar to Section 4.1.3 and Section 4.4.3

$$\mathsf{b}_{\mathrm{V}}(s)(\psi_s, \phi) = \int_{\Gamma^s}\int_{\Gamma^s} G(\mathbf{x}, \mathbf{y})\, \psi_s(\mathbf{y})\, \phi(\mathbf{x})\, dS_{\mathbf{y}}\, dS_{\mathbf{x}}$$

$$= \int_{\Gamma^0}\int_{\Gamma^0} G(\mathbf{T}^{\boldsymbol{\nu}}_s(\hat{\mathbf{x}}), \mathbf{T}^{\boldsymbol{\nu}}_s(\hat{\mathbf{y}}))\, \psi_s(\mathbf{T}^{\boldsymbol{\nu}}_s(\hat{\mathbf{y}}))\, \phi(\mathbf{T}^{\boldsymbol{\nu}}_s(\hat{\mathbf{y}}))\, \omega_s(\hat{\mathbf{x}})\, \omega_s(\hat{\mathbf{y}})\, dS_{\hat{\mathbf{y}}}\, dS_{\hat{\mathbf{x}}},$$

$$\mathsf{b}_{\mathrm{K}}(s)(g_s, \phi) = \int_{\Gamma^s}\int_{\Gamma^s} \nabla_{\mathbf{y}}G(\mathbf{x}, \mathbf{y}) \cdot \mathbf{n}(\mathbf{y})\, g_s(\mathbf{y})\, \phi(\mathbf{x})\, dS_{\mathbf{y}}\, dS_{\mathbf{x}}$$

$$= \int_{\Gamma^0}\int_{\Gamma^0} \nabla_{\mathbf{y}}G(\mathbf{T}^{\boldsymbol{\nu}}_s(\hat{\mathbf{x}}), \mathbf{T}^{\boldsymbol{\nu}}_s(\hat{\mathbf{y}})) \cdot \frac{\mathbf{C}(D\mathbf{T}^{\boldsymbol{\nu}}_s(\hat{\mathbf{y}}))\, \hat{\mathbf{n}}(\hat{\mathbf{y}})}{\omega_s(\hat{\mathbf{y}})}\, g_s(\mathbf{T}^{\boldsymbol{\nu}}_s(\hat{\mathbf{y}}))\, \phi(\mathbf{T}^{\boldsymbol{\nu}}_s(\hat{\mathbf{x}}))\, \omega_s(\hat{\mathbf{x}})\, \omega_s(\hat{\mathbf{y}})\, dS_{\hat{\mathbf{y}}}\, dS_{\hat{\mathbf{x}}},$$

$$\mathsf{b}_{\mathrm{W}}(s)(g_s, v) = \int_{\Gamma^s}\int_{\Gamma^s} G(\mathbf{x}, \mathbf{y})\, \mathbf{curl}_\Gamma\, g_s(\mathbf{y}) \cdot \mathbf{curl}_\Gamma\, v(\mathbf{x})\, dS_{\mathbf{y}}\, dS_{\mathbf{x}}$$

$$= \int_{\Gamma^0}\int_{\Gamma^0} G(\mathbf{T}^{\boldsymbol{\nu}}_s(\hat{\mathbf{x}}), \mathbf{T}^{\boldsymbol{\nu}}_s(\hat{\mathbf{y}}))\, \mathbf{curl}_\Gamma\, g_s(\mathbf{T}^{\boldsymbol{\nu}}_s(\hat{\mathbf{y}})) \cdot \mathbf{curl}_\Gamma\, v(\mathbf{T}^{\boldsymbol{\nu}}_s(\hat{\mathbf{x}}))\, \omega_s(\hat{\mathbf{x}})\, \omega_s(\hat{\mathbf{y}})\, dS_{\hat{\mathbf{y}}}\, dS_{\hat{\mathbf{x}}},$$

$$\ell_1(s)(\phi) = \mathsf{b}_{\mathrm{V}}(s)(\mathbf{H_J} \cdot \mathbf{n}, \phi) = \int_{\Gamma^s}\int_{\Gamma^s} G(\mathbf{x}, \mathbf{y})\, \mathbf{H_J}(\mathbf{y}) \cdot \mathbf{n}(\mathbf{y})\, \phi(\mathbf{x})\, dS_{\mathbf{y}}\, dS_{\mathbf{x}}$$

$$= \int_{\Gamma^0}\int_{\Gamma^0} G(\mathbf{T}^{\boldsymbol{\nu}}_s(\hat{\mathbf{x}}), \mathbf{T}^{\boldsymbol{\nu}}_s(\hat{\mathbf{y}}))\, \mathbf{H_J}(\mathbf{T}^{\boldsymbol{\nu}}_s(\hat{\mathbf{y}})) \cdot \frac{\mathbf{C}(D\mathbf{T}^{\boldsymbol{\nu}}_s(\hat{\mathbf{y}}))\, \hat{\mathbf{n}}(\hat{\mathbf{y}})}{\omega_s(\hat{\mathbf{y}})}\, \phi(\mathbf{T}^{\boldsymbol{\nu}}_s(\hat{\mathbf{y}}))\, \omega_s(\hat{\mathbf{x}})\, \omega_s(\hat{\mathbf{y}})\, dS_{\hat{\mathbf{y}}}\, dS_{\hat{\mathbf{x}}},$$

$$\ell_2(s)(v) := \langle \mathbf{H_J} \cdot \mathbf{n}, v \rangle_{\Gamma^s} = \int_{\Gamma^s} \mathbf{H_J}(\mathbf{x}) \cdot \mathbf{n}(\mathbf{x})\, v(\mathbf{x})\, dS_{\mathbf{x}}$$

$$= \int_{\Gamma^0} \mathbf{H_J}(\mathbf{T}_s^{\boldsymbol{\nu}}(\hat{\mathbf{x}})) \cdot \frac{\mathbf{C}(\mathsf{D}\mathbf{T}_s^{\boldsymbol{\nu}}(\hat{\mathbf{x}}))\,\hat{\mathbf{n}}(\hat{\mathbf{x}})}{\omega_s(\hat{\mathbf{x}})}\, v(\mathbf{T}_s^{\boldsymbol{\nu}}(\hat{\mathbf{x}}))\, \omega_s(\hat{\mathbf{x}})\, dS_{\hat{\mathbf{x}}},$$

$$\ell_3(s)(v) = \mathsf{b}_{\mathrm{K}'}(s)(\mathbf{H_J} \cdot \mathbf{n}, v) = \int_{\Gamma^s} \int_{\Gamma^s} \nabla_{\mathbf{y}} G(\mathbf{x}, \mathbf{y}) \cdot \mathbf{n}(\mathbf{y})\, v(\mathbf{y})\, \mathbf{H_J}(\mathbf{x}) \cdot \mathbf{n}(\mathbf{x})\, dS_{\mathbf{y}}\, dS_{\mathbf{x}}$$

$$= \int_{\Gamma^0} \int_{\Gamma^0} \nabla_{\mathbf{y}} G(\mathbf{T}_s^{\boldsymbol{\nu}}(\hat{\mathbf{x}}), \mathbf{T}_s^{\boldsymbol{\nu}}(\hat{\mathbf{x}})) \cdot \frac{\mathbf{C}(\mathsf{D}\mathbf{T}_s^{\boldsymbol{\nu}}(\hat{\mathbf{y}}))\,\hat{\mathbf{n}}(\hat{\mathbf{y}})}{\omega_s(\hat{\mathbf{y}})}$$

$$v(\mathbf{T}_s^{\boldsymbol{\nu}}(\hat{\mathbf{y}}))\, \mathbf{H_J}(\mathbf{T}_s^{\boldsymbol{\nu}}(\hat{\mathbf{x}})) \cdot \frac{\mathbf{C}(\mathsf{D}\mathbf{T}_s^{\boldsymbol{\nu}}(\hat{\mathbf{x}}))\,\hat{\mathbf{n}}(\hat{\mathbf{x}})}{\omega_s(\hat{\mathbf{x}})}\, \omega_s(\hat{\mathbf{y}})\, \omega_s(\hat{\mathbf{x}})\, dS_{\hat{\mathbf{y}}}\, dS_{\hat{\mathbf{x}}}.$$

We use the same pullbacks as in Section 4.4.3

$$u(\mathbf{T}_s^{\boldsymbol{\nu}}(\hat{\mathbf{x}})) = \hat{u}(\hat{\mathbf{x}}),$$

$$\psi(\mathbf{T}_s^{\boldsymbol{\nu}}(\hat{\mathbf{x}})) = \frac{\hat{\psi}(\hat{\mathbf{x}})}{\omega_s(\hat{\mathbf{x}})},$$

$$\mathbf{curl}_\Gamma\, u(\mathbf{T}_s^{\boldsymbol{\nu}}(\hat{\mathbf{x}})) = \frac{\mathsf{D}\mathbf{T}_s^{\boldsymbol{\nu}}(\hat{\mathbf{x}})}{\omega_s(\hat{\mathbf{x}})}\, \mathbf{curl}_\Gamma\, \hat{u}(\hat{\mathbf{x}}).$$

This leads us to the pulled back hat (bi)linear forms

$$\hat{\mathsf{b}}_{\mathrm{V}}(s; \hat{\psi}, \hat{\phi}) := \int_{\Gamma^0} \int_{\Gamma^0} G(\mathbf{T}_s^{\boldsymbol{\nu}}(\hat{\mathbf{x}}), \mathbf{T}_s^{\boldsymbol{\nu}}(\hat{\mathbf{y}}))\, \hat{\psi}(\hat{\mathbf{y}})\, \hat{\phi}(\hat{\mathbf{x}})\, dS_{\hat{\mathbf{y}}}\, dS_{\hat{\mathbf{x}}}$$

$$\hat{\mathsf{b}}_{\mathrm{K}}(s; \hat{g}, \hat{\phi}) = \int_{\Gamma^0} \int_{\Gamma^0} \nabla_{\mathbf{y}} G(\mathbf{T}_s^{\boldsymbol{\nu}}(\hat{\mathbf{x}}), \mathbf{T}_s^{\boldsymbol{\nu}}(\hat{\mathbf{y}})) \cdot \left(\mathbf{C}(\mathsf{D}\mathbf{T}_s^{\boldsymbol{\nu}}(\hat{\mathbf{y}}))\,\hat{\mathbf{n}}(\hat{\mathbf{y}})\right) \hat{g}(\hat{\mathbf{y}})\, \hat{\phi}(\hat{\mathbf{x}})\, dS_{\hat{\mathbf{y}}}\, dS_{\hat{\mathbf{x}}}$$

$$\hat{\mathsf{b}}_{\mathrm{W}}(s; \hat{g}, \hat{v}) = \int_{\Gamma^0} \int_{\Gamma^0} G(\mathbf{T}_s^{\boldsymbol{\nu}}(\hat{\mathbf{x}}), \mathbf{T}_s^{\boldsymbol{\nu}}(\hat{\mathbf{y}})) \left(\mathsf{D}\mathbf{T}_s^{\boldsymbol{\nu}}(\hat{\mathbf{y}})\, \mathbf{curl}_\Gamma\, \hat{g}(\hat{\mathbf{y}})\right) \cdot \left(\mathsf{D}\mathbf{T}_s^{\boldsymbol{\nu}}(\hat{\mathbf{y}})\, \mathbf{curl}_\Gamma\, \hat{v}(\hat{\mathbf{y}})\right) dS_{\hat{\mathbf{y}}}\, dS_{\hat{\mathbf{x}}}$$

$$\hat{\ell}_1(s; \hat{\phi}) = \int_{\Gamma^0} \int_{\Gamma^0} G(\mathbf{T}_s^{\boldsymbol{\nu}}(\hat{\mathbf{x}}), \mathbf{T}_s^{\boldsymbol{\nu}}(\hat{\mathbf{y}}))\, \mathbf{H_J}(\mathbf{T}_s^{\boldsymbol{\nu}}(\hat{\mathbf{y}})) \cdot \left(\mathbf{C}(\mathsf{D}\mathbf{T}_s^{\boldsymbol{\nu}}(\hat{\mathbf{y}}))\,\hat{\mathbf{n}}(\hat{\mathbf{y}})\right) \hat{\phi}(\hat{\mathbf{x}})\, dS_{\hat{\mathbf{y}}}\, dS_{\hat{\mathbf{x}}}$$

$$\hat{\ell}_2(s; \hat{v}) = \int_{\Gamma^0} \mathbf{H_J}(\mathbf{T}_s^{\boldsymbol{\nu}}(\hat{\mathbf{x}})) \cdot \left(\mathbf{C}(\mathsf{D}\mathbf{T}_s^{\boldsymbol{\nu}}(\hat{\mathbf{x}}))\,\hat{\mathbf{n}}(\hat{\mathbf{x}})\right) \hat{v}(\hat{\mathbf{x}})\, dS_{\hat{\mathbf{x}}}$$

$$\hat{\ell}_3(s; \hat{v}) = \int_{\Gamma^0} \int_{\Gamma^0} \nabla_{\mathbf{y}} G(\mathbf{T}_s^{\boldsymbol{\nu}}(\hat{\mathbf{x}}), \mathbf{T}_s^{\boldsymbol{\nu}}(\hat{\mathbf{x}})) \cdot \left(\mathbf{C}(\mathsf{D}\mathbf{T}_s^{\boldsymbol{\nu}}(\hat{\mathbf{y}}))\,\hat{\mathbf{n}}(\hat{\mathbf{y}})\right)$$

$$\hat{v}(\hat{\mathbf{y}})\, \mathbf{H_J}(\mathbf{T}_s^{\boldsymbol{\nu}}(\hat{\mathbf{x}})) \cdot \left(\mathbf{C}(\mathsf{D}\mathbf{T}_s^{\boldsymbol{\nu}}(\hat{\mathbf{x}}))\,\hat{\mathbf{n}}(\hat{\mathbf{x}})\right) dS_{\hat{\mathbf{y}}}\, dS_{\hat{\mathbf{x}}}.$$

Using the pulled back hat (bi)linear forms, we formulate the pulled back variational formulation: seek $\hat{\psi}_s, \hat{g}_s \in V_0 := H^{-\frac{1}{2}}(\Gamma^0) \times H^{\frac{1}{2}}(\Gamma^0)$ such that

$$\hat{\mathsf{b}}\left(s; \begin{bmatrix} \hat{\psi}_s \\ \hat{g}_s \end{bmatrix}, \begin{bmatrix} \hat{\phi} \\ \hat{v} \end{bmatrix}\right) = \hat{\ell}\left(s; \begin{bmatrix} \hat{\phi} \\ \hat{v} \end{bmatrix}\right) \quad \forall \begin{bmatrix} \hat{\phi} \\ \hat{v} \end{bmatrix} \in V_0,$$

where

$$\hat{\mathsf{b}}\left(s; \begin{bmatrix}\hat{\psi}\\\hat{g}\end{bmatrix}, \begin{bmatrix}\hat{\phi}\\\hat{v}\end{bmatrix}\right) := (1 + \frac{\mu_0}{\mu})\,\hat{\mathsf{b}}_{\mathrm{V}}(s; \hat{\psi}, \hat{\phi}) - 2\,\hat{\mathsf{b}}_{\mathrm{K}}(s; \hat{g}, \hat{\phi}) + 2\,\hat{\mathsf{b}}_{\mathrm{K}'}(s; \hat{\psi}, \hat{v}) + (1 + \frac{\mu}{\mu_0})\,\hat{\mathsf{b}}_{\mathrm{W}}(s; \hat{g}, \hat{v}),$$

$$\hat{\ell}\left(s; \begin{bmatrix}\hat{\phi}\\\hat{v}\end{bmatrix}\right) := -\frac{[\![\mu]\!]_\Gamma}{\mu}\,\hat{\ell}_1(s; \hat{\phi}) + \frac{[\![\mu]\!]_\Gamma}{2\mu_0}\,\hat{\ell}_2(s; \hat{v}) - \frac{[\![\mu]\!]_\Gamma}{\mu_0}\,\hat{\ell}_3(s; \hat{v}).$$

Following the structure in (5.1.17), field energy for the deformed s configuration can be expressed in terms of the pulled back linear form as

$$\mathcal{E}_F(s) = -\frac{\mu_0}{2}\hat{\ell}\left(s; \begin{bmatrix}-\hat{\psi}_s\\\hat{g}_s\end{bmatrix}\right) + \frac{1}{2}\int_{\mathbb{R}^3}\mu(\mathbf{x})\,\|\mathbf{H}_{\mathbf{J}}(\mathbf{T}_s^{\boldsymbol{\nu}}(\hat{\mathbf{x}}))\|^2\;\det \mathsf{D}\mathbf{T}_s^{\boldsymbol{\nu}}(\hat{\mathbf{x}})\,d\hat{\mathbf{x}}$$

$$-\frac{[\![\mu]\!]_\Gamma^2}{2\mu}\int_{\Gamma^0}\int_{\Gamma^0}G(\mathbf{T}_s^{\boldsymbol{\nu}}(\hat{\mathbf{x}}),\mathbf{T}_s^{\boldsymbol{\nu}}(\hat{\mathbf{y}}))\,\mathbf{H}_{\mathbf{J}}(\mathbf{T}_s^{\boldsymbol{\nu}}(\hat{\mathbf{y}}))\cdot\left(\mathbf{C}(\mathsf{D}\mathbf{T}_s^{\boldsymbol{\nu}}(\hat{\mathbf{y}}))\,\hat{\mathbf{n}}(\hat{\mathbf{y}})\right)$$

$$\mathbf{H}_{\mathbf{J}}(\mathbf{T}_s^{\boldsymbol{\nu}}(\hat{\mathbf{x}}))\cdot\left(\mathbf{C}(\mathsf{D}\mathbf{T}_s^{\boldsymbol{\nu}}(\hat{\mathbf{x}}))\,\hat{\mathbf{n}}(\hat{\mathbf{x}})\right)\,d\mathrm{S}_{\hat{\mathbf{y}}}\,d\mathrm{S}_{\hat{\mathbf{x}}}.$$

The integral over $\mathbb{R}^3$ is transformed using $\mu_s(\mathbf{T}_s^{\boldsymbol{\nu}}(\hat{\mathbf{x}})) = \mu(\hat{\mathbf{x}})$, leading to the expression above.

5.1.1.4 BIE-Constrained Shape Derivative

We start by defining the Lagrangian $\mathcal{L}: \mathbb{R} \times V_0 \times V_0 \to \mathbb{R}$,

$$\mathcal{L}\left(s; \begin{bmatrix}\hat{\psi}\\\hat{g}\end{bmatrix}, \begin{bmatrix}\hat{\phi}\\\hat{v}\end{bmatrix}\right) := \hat{\mathsf{b}}\left(s; \begin{bmatrix}\hat{\psi}\\\hat{g}\end{bmatrix}, \begin{bmatrix}\hat{\phi}\\\hat{v}\end{bmatrix}\right) - \hat{\ell}\left(s; \begin{bmatrix}\hat{\phi}\\\hat{v}\end{bmatrix}\right) - \frac{\mu_0}{2}\hat{\ell}\left(s; \begin{bmatrix}-\hat{\psi}\\\hat{g}\end{bmatrix}\right)$$

$$+ \frac{1}{2}\int_{\mathbb{R}^3}\mu(\hat{\mathbf{x}})\,\|\mathbf{H}_{\mathbf{J}}(\mathbf{T}_s^{\boldsymbol{\nu}}(\hat{\mathbf{x}}))\|^2\;\det \mathsf{D}\mathbf{T}_s^{\boldsymbol{\nu}}(\hat{\mathbf{x}})\,d\hat{\mathbf{x}}$$

$$-\frac{[\![\mu]\!]_\Gamma^2}{2\mu}\int_{\Gamma^0}\int_{\Gamma^0}G(\mathbf{T}_s^{\boldsymbol{\nu}}(\hat{\mathbf{x}}),\mathbf{T}_s^{\boldsymbol{\nu}}(\hat{\mathbf{y}}))\,\mathbf{H}_{\mathbf{J}}(\mathbf{T}_s^{\boldsymbol{\nu}}(\hat{\mathbf{y}}))\cdot\left(\mathbf{C}(\mathsf{D}\mathbf{T}_s^{\boldsymbol{\nu}}(\hat{\mathbf{y}}))\,\hat{\mathbf{n}}(\hat{\mathbf{y}})\right)$$

$$\mathbf{H}_{\mathbf{J}}(\mathbf{T}_s^{\boldsymbol{\nu}}(\hat{\mathbf{x}}))\cdot\left(\mathbf{C}(\mathsf{D}\mathbf{T}_s^{\boldsymbol{\nu}}(\hat{\mathbf{x}}))\,\hat{\mathbf{n}}(\hat{\mathbf{x}})\right)\,d\mathrm{S}_{\hat{\mathbf{y}}}\,d\mathrm{S}_{\hat{\mathbf{x}}}.$$

Plugging in the pulled back state solution $\begin{bmatrix}\hat{\psi}\\\hat{g}\end{bmatrix} = \begin{bmatrix}\hat{\psi}_s\\\hat{g}_s\end{bmatrix}$ gives

$$\mathcal{E}_F(s) = \mathcal{L}\left(s; \begin{bmatrix}\hat{\psi}_s\\\hat{g}_s\end{bmatrix}, \begin{bmatrix}\hat{\phi}\\\hat{v}\end{bmatrix}\right) \quad \forall \begin{bmatrix}\hat{\phi}\\\hat{v}\end{bmatrix} \in V_0.$$

The shape derivative can be computed as

$$\frac{d\mathcal{E}_F}{ds}(0) = \frac{\partial\mathcal{L}}{\partial s}\left(0; \begin{bmatrix}\hat{\psi}_0\\\hat{g}_0\end{bmatrix}, \begin{bmatrix}\hat{\lambda}\\\hat{p}\end{bmatrix}\right),$$

where the adjoint solution $\begin{bmatrix} \hat{\lambda} \\ \hat{p} \end{bmatrix} \in V_0$ solves the adjoint equation

$$\left\langle \frac{\partial \mathcal{L}}{\partial \begin{bmatrix} \hat{\psi} \\ \hat{g} \end{bmatrix}}(0; \begin{bmatrix} \hat{\psi}_0 \\ \hat{g}_0 \end{bmatrix}, \begin{bmatrix} \hat{\lambda} \\ \hat{p} \end{bmatrix}); \begin{bmatrix} \hat{\phi} \\ \hat{v} \end{bmatrix} \right\rangle = 0 \quad \begin{bmatrix} \hat{\phi} \\ \hat{v} \end{bmatrix} \in V_0.$$

Computing the partial derivative gives the adjoint equation in an explicit form

$$\hat{b}(0; \begin{bmatrix} \hat{\phi} \\ \hat{v} \end{bmatrix}, \begin{bmatrix} \hat{\lambda} \\ \hat{p} \end{bmatrix}) = \frac{\mu_0}{2}\hat{\ell}(0; \begin{bmatrix} -\hat{\phi} \\ \hat{v} \end{bmatrix}) \quad \forall \begin{bmatrix} \hat{\phi} \\ \hat{v} \end{bmatrix} \in V_0.$$

Flipping the sign of the test function $\hat{\phi}$ gives us

$$\hat{b}(0; \begin{bmatrix} -\hat{\phi} \\ \hat{v} \end{bmatrix}, \begin{bmatrix} \hat{\lambda} \\ \hat{p} \end{bmatrix}) = \frac{\mu_0}{2}\hat{\ell}(0; \begin{bmatrix} \hat{\phi} \\ \hat{v} \end{bmatrix}) \quad \forall \begin{bmatrix} \hat{\phi} \\ \hat{v} \end{bmatrix} \in V_0,$$

and finally using the property

$$\hat{b}(0; \begin{bmatrix} -\hat{\phi} \\ \hat{v} \end{bmatrix}, \begin{bmatrix} \hat{\lambda} \\ \hat{p} \end{bmatrix}) = \hat{b}(0; \begin{bmatrix} -\hat{\lambda} \\ \hat{p} \end{bmatrix}, \begin{bmatrix} \hat{\phi} \\ \hat{v} \end{bmatrix}),$$

we get

$$\hat{b}(0; \begin{bmatrix} -\hat{\lambda} \\ \hat{p} \end{bmatrix}, \begin{bmatrix} \hat{\phi} \\ \hat{v} \end{bmatrix}) = \frac{\mu_0}{2}\hat{\ell}(0; \begin{bmatrix} \hat{\phi} \\ \hat{v} \end{bmatrix}) \quad \forall \begin{bmatrix} \hat{\phi} \\ \hat{v} \end{bmatrix} \in V_0,$$

which yields the adjoint solution as

$$\begin{bmatrix} -\hat{\lambda} \\ \hat{p} \end{bmatrix} = \frac{\mu_0}{2} \begin{bmatrix} \hat{\psi}_0 \\ \hat{g}_0 \end{bmatrix} \implies \begin{bmatrix} \hat{\lambda} \\ \hat{p} \end{bmatrix} = \frac{\mu_0}{2} \begin{bmatrix} -\hat{\psi}_0 \\ \hat{g}_0 \end{bmatrix}.$$

Using this the energy shape derivative can be computed using the partial derivatives (3.0.11) and (3.0.13), and is expressed as

$$\frac{d\mathcal{E}_F}{ds}(0) = \frac{\partial \mathcal{L}}{\partial s}(0; \begin{bmatrix} \hat{\psi}_0 \\ \hat{g}_0 \end{bmatrix}, \frac{\mu_0}{2}\begin{bmatrix} -\hat{\psi}_0 \\ \hat{g}_0 \end{bmatrix})$$

$$= \frac{\mu_0}{2}\frac{\partial \hat{b}}{\partial s}(0; \begin{bmatrix} \hat{\psi}_0 \\ \hat{g}_0 \end{bmatrix}, \begin{bmatrix} -\hat{\psi}_0 \\ \hat{g}_0 \end{bmatrix}) - \mu_0 \frac{\partial \hat{\ell}}{\partial s}(0; \begin{bmatrix} -\hat{\psi}_0 \\ \hat{g}_0 \end{bmatrix})$$

$$- \frac{[\![\mu]\!]_\Gamma}{2}\int_{\Gamma^0} \|\mathbf{H_J}\|^2 \, \boldsymbol{\mathcal{V}} \cdot \mathbf{n} \, dS$$

$$- \frac{[\![\mu]\!]_\Gamma^2}{2\mu}\int_{\Gamma^0}\int_{\Gamma^0} \left\{ \nabla_{\mathbf{x}}G(\hat{\mathbf{x}}, \hat{\mathbf{y}}) \cdot \boldsymbol{\mathcal{V}}(\hat{\mathbf{x}}) + \nabla_{\mathbf{y}}G(\mathbf{x}, \mathbf{y}) \cdot \boldsymbol{\mathcal{V}}(\hat{\mathbf{y}}) \right\} \left(\mathbf{H_J}(\hat{\mathbf{y}}) \cdot \hat{\mathbf{n}}(\hat{\mathbf{y}}) \right) \left(\mathbf{H_J}(\hat{\mathbf{x}}) \cdot \hat{\mathbf{n}}(\hat{\mathbf{x}}) \right) dS_{\hat{\mathbf{y}}} \, dS_{\hat{\mathbf{x}}}$$

$$- \frac{[\![\mu]\!]_\Gamma^2}{2\mu}\int_{\Gamma^0}\int_{\Gamma^0} G(\hat{\mathbf{x}}, \hat{\mathbf{y}}) \left\{ \hat{\mathbf{n}}^T(\hat{\mathbf{y}}) \, \mathsf{D}\mathbf{H_J}(\hat{\mathbf{y}}) \, \boldsymbol{\mathcal{V}}(\hat{\mathbf{y}}) + \mathbf{H_J}(\hat{\mathbf{y}})^T \hat{\mathbf{n}}(\hat{\mathbf{y}}) \, \nabla \cdot \boldsymbol{\mathcal{V}}(\hat{\mathbf{y}}) \right.$$

$$\left. - \mathbf{H_J}(\hat{\mathbf{y}})^T \, \mathsf{D}\boldsymbol{\mathcal{V}}^T(\hat{\mathbf{y}}) \, \hat{\mathbf{n}}(\hat{\mathbf{y}}) \right\} \left(\mathbf{H_J}(\hat{\mathbf{x}}) \cdot \hat{\mathbf{n}}(\hat{\mathbf{x}}) \right) dS_{\hat{\mathbf{y}}} \, dS_{\hat{\mathbf{x}}}$$

$$-\frac{[\![\mu]\!]_\Gamma^2}{2\mu} \int_{\Gamma^0} \int_{\Gamma^0} G(\hat{\mathbf{x}}, \hat{\mathbf{y}}) \left\{ \hat{\mathbf{n}}^T(\hat{\mathbf{x}})\, \mathsf{D}\mathbf{H_J}(\hat{\mathbf{x}})\, \boldsymbol{\mathcal{V}}(\hat{\mathbf{x}}) + \mathbf{H_J}(\hat{\mathbf{x}})^T \hat{\mathbf{n}}(\hat{\mathbf{x}})\, \nabla \cdot \boldsymbol{\mathcal{V}}(\hat{\mathbf{x}}) \right. \tag{5.1.18}$$

$$\left. - \mathbf{H_J}(\hat{\mathbf{x}})^T\, \mathsf{D}\boldsymbol{\mathcal{V}}^T(\hat{\mathbf{x}})\, \hat{\mathbf{n}}(\hat{\mathbf{x}}) \right\} \left(\mathbf{H_J}(\hat{\mathbf{y}}) \cdot \hat{\mathbf{n}}(\hat{\mathbf{y}}) \right) dS_{\hat{\mathbf{y}}}\, dS_{\hat{\mathbf{x}}}.$$

The partial derivatives of the (bi)linear forms can be computed using formulas in (3.0.11) and (3.0.13), and are given as

$$\frac{\partial \hat{\mathsf{b}}_V}{\partial s}(0; \hat{\psi}, \hat{\phi}) := \int_{\Gamma^0} \int_{\Gamma^0} \left\{ \nabla_{\mathbf{x}} G(\mathbf{x}, \mathbf{y}) \cdot \boldsymbol{\mathcal{V}}(\mathbf{x}) + \nabla_{\mathbf{y}} G(\mathbf{x}, \mathbf{y}) \cdot \boldsymbol{\mathcal{V}}(\mathbf{y}) \right\} \hat{\psi}(\hat{\mathbf{y}})\, \hat{\phi}(\hat{\mathbf{x}})\, dS_{\hat{\mathbf{y}}}\, dS_{\hat{\mathbf{x}}},$$

$$\frac{\partial \hat{\mathsf{b}}_K}{\partial s}(0; \hat{g}, \hat{\phi}) = \int_{\Gamma^0} \int_{\Gamma^0} \nabla_{\mathbf{y}} G(\mathbf{x}, \mathbf{y}) \cdot \left(\nabla \cdot \boldsymbol{\mathcal{V}}(\mathbf{y})\, \hat{\mathbf{n}}(\mathbf{y}) - \mathsf{D}\boldsymbol{\mathcal{V}}(\mathbf{y})^T\, \hat{\mathbf{n}}(\mathbf{y}) \right) \hat{g}(\hat{\mathbf{y}})\, \hat{\phi}(\hat{\mathbf{x}})\, dS_{\hat{\mathbf{y}}}\, dS_{\hat{\mathbf{x}}}$$

$$+ \int_{\Gamma^0} \int_{\Gamma^0} \frac{d\nabla_{\mathbf{y}} G(\mathbf{T}_s^{\boldsymbol{\nu}}(\hat{\mathbf{x}}), \mathbf{T}_s^{\boldsymbol{\nu}}(\hat{\mathbf{y}}))}{ds}\bigg|_{s=0} \cdot \hat{\mathbf{n}}(\hat{\mathbf{y}})\, \hat{g}(\hat{\mathbf{y}})\, \hat{\phi}(\hat{\mathbf{x}})\, dS_{\hat{\mathbf{y}}}\, dS_{\hat{\mathbf{x}}},$$

$$\frac{\partial \hat{\mathsf{b}}_W}{\partial s}(0; \hat{g}, \hat{v}) = \int_{\Gamma^0} \int_{\Gamma^0} \left\{ \nabla_{\mathbf{x}} G(\mathbf{x}, \mathbf{y}) \cdot \boldsymbol{\mathcal{V}}(\mathbf{x}) + \nabla_{\mathbf{y}} G(\mathbf{x}, \mathbf{y}) \cdot \boldsymbol{\mathcal{V}}(\mathbf{y}) \right\} \mathbf{curl}_\Gamma\, \hat{g}(\hat{\mathbf{y}}) \cdot \mathbf{curl}_\Gamma\, \hat{v}(\hat{\mathbf{x}})\, dS_{\hat{\mathbf{y}}}\, dS_{\hat{\mathbf{x}}}$$

$$+ \int_{\Gamma^0} \int_{\Gamma^0} G(\mathbf{x}, \mathbf{y}) \left\{ \mathsf{D}\boldsymbol{\mathcal{V}}(\mathbf{y})\, \mathbf{curl}_\Gamma\, \hat{g}(\hat{\mathbf{y}}) \cdot \mathbf{curl}_\Gamma\, \hat{v}(\hat{\mathbf{y}}) + \right.$$

$$\left. \mathsf{D}\boldsymbol{\mathcal{V}}(\mathbf{x})\, \mathbf{curl}_\Gamma\, \hat{v}(\hat{\mathbf{x}}) \cdot \mathbf{curl}_\Gamma\, \hat{g}(\hat{\mathbf{y}}) \right\} dS_{\hat{\mathbf{y}}}\, dS_{\hat{\mathbf{x}}},$$

$$\frac{\partial \hat{\ell}_1}{\partial s}(0; \hat{\phi}) = \int_{\Gamma^0} \int_{\Gamma^0} \left\{ \nabla_{\mathbf{x}} G(\mathbf{x}, \mathbf{y}) \cdot \boldsymbol{\mathcal{V}}(\mathbf{x}) + \nabla_{\mathbf{y}} G(\mathbf{x}, \mathbf{y}) \cdot \boldsymbol{\mathcal{V}}(\mathbf{y}) \right\} \mathbf{H_J}(\mathbf{y}) \cdot \hat{\mathbf{n}}(\hat{\mathbf{y}})\, \hat{\phi}(\hat{\mathbf{x}})\, dS_{\hat{\mathbf{y}}}\, dS_{\hat{\mathbf{x}}}$$

$$+ \int_{\Gamma^0} \int_{\Gamma^0} G(\mathbf{x}, \mathbf{y})\, \hat{\mathbf{n}}(\mathbf{y})^T \left\{ \mathsf{D}\mathbf{H_J}\, \boldsymbol{\mathcal{V}} - \mathsf{D}\boldsymbol{\mathcal{V}}\, \mathbf{H_J} + \nabla \cdot \boldsymbol{\mathcal{V}}\, \mathbf{H_J} \right\}(\mathbf{y})\, \hat{\phi}(\hat{\mathbf{x}})\, dS_{\hat{\mathbf{y}}}\, dS_{\hat{\mathbf{x}}},$$

$$\frac{\partial \hat{\ell}_2}{\partial s}(0; \hat{v}) = \int_{\Gamma^0} \hat{\mathbf{n}}(\mathbf{x})^T \left\{ \mathsf{D}\mathbf{H_J}\, \boldsymbol{\mathcal{V}} - \mathsf{D}\boldsymbol{\mathcal{V}}\, \mathbf{H_J} + \nabla \cdot \boldsymbol{\mathcal{V}}\, \mathbf{H_J} \right\}(\mathbf{x})\, \hat{v}(\hat{\mathbf{x}})\, dS_{\hat{\mathbf{x}}}, \tag{5.1.19}$$

$$\frac{\partial \hat{\ell}_3}{\partial s}(0; \hat{v}) = \int_{\Gamma^0} \int_{\Gamma^0} \frac{d\nabla_{\mathbf{y}} G(\mathbf{T}_s^{\boldsymbol{\nu}}(\hat{\mathbf{x}}), \mathbf{T}_s^{\boldsymbol{\nu}}(\hat{\mathbf{x}}))}{ds}\bigg|_{s=0} \cdot \hat{\mathbf{n}}(\hat{\mathbf{y}})\, \hat{v}(\hat{\mathbf{y}})\, \mathbf{H_J}(\mathbf{x}) \cdot \hat{\mathbf{n}}(\hat{\mathbf{x}})\, dS_{\hat{\mathbf{y}}}\, dS_{\hat{\mathbf{x}}}$$

$$+ \int_{\Gamma^0} \int_{\Gamma^0} \nabla_{\mathbf{y}} G(\mathbf{x}, \mathbf{y}) \cdot \left(\nabla \cdot \boldsymbol{\mathcal{V}}(\mathbf{y})\, \hat{\mathbf{n}}(\mathbf{y}) - \mathsf{D}\boldsymbol{\mathcal{V}}(\mathbf{y})^T\, \hat{\mathbf{n}}(\mathbf{y}) \right) \hat{v}(\hat{\mathbf{y}})\, \mathbf{H_J}(\mathbf{x}) \cdot \hat{\mathbf{n}}(\hat{\mathbf{x}})\, dS_{\hat{\mathbf{y}}}\, dS_{\hat{\mathbf{x}}}$$

$$+ \int_{\Gamma^0} \int_{\Gamma^0} \nabla_{\mathbf{y}} G(\mathbf{x}, \mathbf{y}) \cdot \hat{\mathbf{n}}(\hat{\mathbf{y}})\, \hat{v}(\hat{\mathbf{y}})\, \hat{\mathbf{n}}(\mathbf{x})^T \left\{ \mathsf{D}\mathbf{H_J}\, \boldsymbol{\mathcal{V}} - \mathsf{D}\boldsymbol{\mathcal{V}}\, \mathbf{H_J} + \nabla \cdot \boldsymbol{\mathcal{V}}\, \mathbf{H_J} \right\}(\mathbf{x})\, dS_{\hat{\mathbf{y}}}\, dS_{\hat{\mathbf{x}}}.$$

$$\tag{5.1.20}$$

The derivative for $\nabla_{\mathbf{y}} G(\mathbf{T}_s^{\boldsymbol{\nu}}(\hat{\mathbf{x}}), \mathbf{T}_s^{\boldsymbol{\nu}}(\hat{\mathbf{y}}))$ is given in (4.1.18).

5.1.1.5 Shape Derivative From Volume Based Variational Formulation

The transmission problem 5.1.8 has a weak solution $u \in H^1(\Delta; \mathbb{R}^3)$ which solves the variational problem

$$\int_{\mathbb{R}^3} \mu(\mathbf{x}) \, \nabla u(\mathbf{x}) \cdot \nabla v(\mathbf{x}) \, d\mathbf{x} = \int_{\Gamma} v \, [\![\mu]\!]_{\Gamma} \, \mathbf{H_J} \cdot \mathbf{n} \, d\mathrm{S} \quad \forall v \in H^1(\Delta; \mathbb{R}^3). \tag{5.1.21}$$

We write the field energy (5.1.5) in terms of the bilinear form of the variational formulation above

$$\mathcal{E}_F = \frac{1}{2} \int_{\mathbb{R}^3} \mu^{-1}(\mathbf{x}) \, \|\mathbf{B}\|^2 \, d\mathbf{x}$$

$$= \frac{\mu}{2} \int_{\Omega} \|\nabla u + \mathbf{H_J}\|^2 \, d\mathbf{x} + \frac{\mu_0}{2} \int_{\Omega_c} \|\nabla u + \mathbf{H_J}\|^2 \, d\mathbf{x}$$

$$= \frac{1}{2} \int_{\mathbb{R}^3} \mu(\mathbf{x}) \, \|\nabla u(\mathbf{x})\|^2 \, d\mathbf{x} + \frac{1}{2} \int_{\mathbb{R}^3} \mu(\mathbf{x}) \, \|\mathbf{H_J}(\mathbf{x})\|^2 \, d\mathbf{x} + \mu_0 \int_{\Omega_c} \nabla u \cdot \mathbf{H_J} \, d\mathbf{x} + \mu \int_{\Omega} \nabla u \cdot \mathbf{H_J} \, d\mathbf{x}$$

$$= \frac{1}{2} \int_{\mathbb{R}^3} \mu(\mathbf{x}) \, \|\nabla u(\mathbf{x})\|^2 \, d\mathbf{x} + \frac{1}{2} \int_{\mathbb{R}^3} \mu(\mathbf{x}) \, \|\mathbf{H_J}(\mathbf{x})\|^2 \, d\mathbf{x} - [\![\mu]\!]_{\Gamma} \int_{\Gamma} u \, \mathbf{H_J} \cdot \mathbf{n} \, d\mathrm{S}$$

$$= -\frac{1}{2} \int_{\mathbb{R}^3} \mu(\mathbf{x}) \, \|\nabla u(\mathbf{x})\|^2 \, d\mathbf{x} + \frac{1}{2} \int_{\mathbb{R}^3} \mu(\mathbf{x}) \, \|\mathbf{H_J}(\mathbf{x})\|^2 \, d\mathbf{x}.$$

In the above manipulations we used the fact that $\operatorname{div} \mathbf{H_J} = 0$ and the variational equation (5.1.21).

5.1.1.6 Variational Formulation on Deformed Domain

We use the perturbation map $\mathbf{T}_s^{\boldsymbol{\nu}}$ from 3.0.1 with velocity field $\boldsymbol{\mathcal{V}}$ such that $\boldsymbol{\mathcal{V}} \equiv 0$ around the source. This leads to deformations of only the reference domain Ω^0. The permeability $\mu(\mathbf{x})$ is transformed as a 0-form to $\mu_s(\mathbf{x})$ such that $\mu_s(\mathbf{T}_s^{\boldsymbol{\nu}}(\hat{\mathbf{x}})) = \mu(\hat{\mathbf{x}})$. The variational formulation has a structure similar to 5.1.21 and reads: seek $u_s \in H^1(\Delta; \mathbb{R}^3)$ such that

$$\int_{\mathbb{R}^3} \mu_s(\mathbf{x}) \, \nabla u_s(\mathbf{x}) \cdot \nabla v(\mathbf{x}) \, d\mathbf{x} = [\![\mu]\!]_{\Gamma} \int_{\Gamma^s} v \, \mathbf{H_J} \cdot \mathbf{n} \, d\mathrm{S} \quad \forall v \in H^1(\Delta; \mathbb{R}^3).$$

5.1.1.7 Transformation and Pullback

Transforming the integrals using the perturbation map and using the pullback $\nabla u(\mathbf{T}_s^{\boldsymbol{\nu}}(\hat{\mathbf{x}})) = \mathrm{D}\mathbf{T}_s^{\boldsymbol{\nu}}(\hat{\mathbf{x}})^{-T} \nabla \hat{u}(\hat{\mathbf{x}})$, we get

$$\int_{\mathbb{R}^3} \mu_s(\mathbf{x}) \, \nabla u_s(\mathbf{x}) \cdot \nabla v(\mathbf{x}) \, d\mathbf{x} = \int_{\mathbb{R}^3} \mu_s(\mathbf{T}_s^{\boldsymbol{\nu}}(\hat{\mathbf{x}})) \, \nabla u_s(\mathbf{T}_s^{\boldsymbol{\nu}}(\hat{\mathbf{x}})) \cdot \nabla v(\mathbf{T}_s^{\boldsymbol{\nu}}(\hat{\mathbf{x}})) \, \det \mathrm{D}\mathbf{T}_s^{\boldsymbol{\nu}}(\hat{\mathbf{x}}) \, d\mathbf{x}$$

$$= \int\limits_{\mathbb{R}^3} \mu(\hat{\mathbf{x}}) \, \nabla u_s(\mathbf{T}_s^{\boldsymbol{\nu}}(\hat{\mathbf{x}})) \cdot \nabla v(\mathbf{T}_s^{\boldsymbol{\nu}}(\hat{\mathbf{x}})) \, \det \mathsf{D}\mathbf{T}_s^{\boldsymbol{\nu}}(\hat{\mathbf{x}}) \, d\hat{\mathbf{x}}$$

$$= \int\limits_{\mathbb{R}^3} \mu(\hat{\mathbf{x}}) \left(\mathsf{D}\mathbf{T}_s^{\boldsymbol{\nu}}(\hat{\mathbf{x}})^{-T} \nabla \hat{u}_s(\hat{\mathbf{x}}) \right) \cdot \left(\mathsf{D}\mathbf{T}_s^{\boldsymbol{\nu}}(\hat{\mathbf{x}})^{-T} \nabla \hat{v}(\hat{\mathbf{x}}) \right) \, \det \mathsf{D}\mathbf{T}_s^{\boldsymbol{\nu}}(\hat{\mathbf{x}}) \, d\hat{\mathbf{x}},$$

$$[\![\mu]\!]_\Gamma \int\limits_{\Gamma^s} v \, \mathbf{H_J} \cdot \mathbf{n} \, dS = [\![\mu]\!]_\Gamma \int\limits_{\Gamma^0} v(\mathbf{T}_s^{\boldsymbol{\nu}}(\hat{\mathbf{x}})) \, \mathbf{H_J}(\mathbf{T}_s^{\boldsymbol{\nu}}(\hat{\mathbf{x}})) \cdot \frac{\mathbf{C}(\mathsf{D}\mathbf{T}_s^{\boldsymbol{\nu}}(\hat{\mathbf{x}})) \, \hat{\mathbf{n}}(\hat{\mathbf{x}})}{\omega_s(\hat{\mathbf{x}})} \, \omega_s(\hat{\mathbf{x}}) \, dS_{\hat{\mathbf{x}}}$$

$$= [\![\mu]\!]_\Gamma \int\limits_{\Gamma^0} \hat{v}(\hat{\mathbf{x}}) \, \mathbf{H_J}(\mathbf{T}_s^{\boldsymbol{\nu}}(\hat{\mathbf{x}})) \cdot \left(\mathbf{C}(\mathsf{D}\mathbf{T}_s^{\boldsymbol{\nu}}(\hat{\mathbf{x}})) \, \hat{\mathbf{n}}(\hat{\mathbf{x}}) \right) \, dS_{\hat{\mathbf{x}}}.$$

Based on these expressions we define the pulled back hat (bi)linear forms:

$$\hat{\mathsf{b}}(s; \hat{u}, \hat{v}) := \int\limits_{\mathbb{R}^3} \mu(\hat{\mathbf{x}}) \left(\mathsf{D}\mathbf{T}_s^{\boldsymbol{\nu}}(\hat{\mathbf{x}})^{-T} \nabla \hat{u}(\hat{\mathbf{x}}) \right) \cdot \left(\mathsf{D}\mathbf{T}_s^{\boldsymbol{\nu}}(\hat{\mathbf{x}})^{-T} \nabla \hat{v}(\hat{\mathbf{x}}) \right) \, \det \mathsf{D}\mathbf{T}_s^{\boldsymbol{\nu}}(\hat{\mathbf{x}}) \, d\hat{\mathbf{x}},$$

$$\hat{\ell}(s; \hat{v}) := [\![\mu]\!]_\Gamma \int\limits_{\Gamma^0} \hat{v}(\hat{\mathbf{x}}) \, \mathbf{H_J}(\mathbf{T}_s^{\boldsymbol{\nu}}(\hat{\mathbf{x}})) \cdot \left(\mathbf{C}(\mathsf{D}\mathbf{T}_s^{\boldsymbol{\nu}}(\hat{\mathbf{x}})) \, \hat{\mathbf{n}}(\hat{\mathbf{x}}) \right) \, dS_{\hat{\mathbf{x}}},$$

which allows us to write the equivalent pulled back formulation: seek $\hat{u}_s \in H^1(\Delta; \mathbb{R}^3)$ such that

$$\hat{\mathsf{b}}(s; \hat{u}_s, \hat{v}) = \hat{\ell}(s; \hat{v}) \quad \hat{v} \in H^1(\Delta; \mathbb{R}^3).$$

The field energy for the deformed configuration s can be written in terms of the pulled back bilinear form as

$$\mathcal{E}_F(s) = -\frac{1}{2} \hat{\mathsf{b}}(s; \hat{u}_s, \hat{u}_s) + \frac{1}{2} \int\limits_{\mathbb{R}^3} \mu(\hat{\mathbf{x}}) \, \|\mathbf{H_J}(\mathbf{T}_s^{\boldsymbol{\nu}}(\hat{\mathbf{x}}))\|^2 \, \det \mathsf{D}\mathbf{T}_s^{\boldsymbol{\nu}}(\hat{\mathbf{x}}) \, d\hat{\mathbf{x}}.$$

5.1.1.8 Adjoint Method

We start by defining the Lagrangian $\mathcal{L} : \mathbb{R} \times H^1(\Delta; \mathbb{R}^3) \times H^1(\Delta; \mathbb{R}^3) \to \mathbb{R}$,

$$\mathcal{L}(s; \hat{u}, \hat{v}) := \hat{\mathsf{b}}(s; \hat{u}, \hat{v}) - \hat{\ell}(s; \hat{v}) - \frac{1}{2} \hat{\mathsf{b}}(s; \hat{u}, \hat{u}) + \frac{1}{2} \int\limits_{\mathbb{R}^3} \mu(\hat{\mathbf{x}}) \, \|\mathbf{H_J}(\mathbf{T}_s^{\boldsymbol{\nu}}(\hat{\mathbf{x}}))\|^2 \, \det \mathsf{D}\mathbf{T}_s^{\boldsymbol{\nu}}(\hat{\mathbf{x}}) \, d\hat{\mathbf{x}}.$$

Plugging in $\hat{u} = \hat{u}_s$ gives the field energy

$$\mathcal{L}(s; \hat{u}_s, \hat{v}) = \mathcal{E}_F(s) \quad \forall \hat{v} \in H^1(\Delta; \mathbb{R}^3).$$

The shape derivative can be computed as

$$\frac{d\mathcal{E}_F}{ds}(0) = \frac{\partial \mathcal{L}}{\partial s}(0; \hat{u}_0, \hat{p}),$$

where $\hat{p} \in H^1(\Delta; \mathbb{R}^3)$ solves the adjoint equation

$$\left\langle \frac{\partial \mathcal{L}}{\partial \hat{u}}(0; \hat{u}_0, \hat{p}); \hat{v} \right\rangle = 0 \quad \forall \hat{v} \in H^1(\Delta; \mathbb{R}^3).$$

111

Computing the partial derivatives gives the adjoint equation in an explicit form

$$\hat{\mathsf{b}}(s; \hat{p}, \hat{v}) - \hat{\mathsf{b}}(s; \hat{u}_0, \hat{v}) = 0 \quad \forall \hat{v} \in H^1(\Delta; \mathbb{R}^3),$$

which gives the adjoint solution as $\hat{p} = \hat{u}_0$. Using the partial derivatives from (3.0.11), (3.0.13), and $\frac{d}{ds}\mathbf{H_J}(\mathbf{T}_s^{\boldsymbol{\nu}}(\hat{\mathbf{x}}))|_{s=0} = \mathsf{D}\mathbf{H_J}(\hat{\mathbf{x}})\,\boldsymbol{\mathcal{V}}(\hat{\mathbf{x}})$, the shape derivative is expressed as

$$
\begin{aligned}
\frac{d\mathcal{E}_F}{ds}(0) &= \frac{\partial \mathcal{L}}{\partial s}(0; \hat{u}_0, \hat{u}_0) \\
&= \frac{1}{2}\frac{\partial \hat{\mathsf{b}}}{\partial s}(0; \hat{u}_0, \hat{u}_0) - \frac{\partial \hat{\ell}}{\partial s}(0; \hat{u}_0) \\
&\quad + \frac{1}{2}\int_{\mathbb{R}^3} \mu(\mathbf{x})\Big\{ \|\mathbf{H_J}(\mathbf{x})\|^2\,\nabla\cdot\boldsymbol{\mathcal{V}}(\mathbf{x}) + 2\,\big(\mathsf{D}\mathbf{H_J}(\mathbf{x})\,\boldsymbol{\mathcal{V}}(\mathbf{x})\big)\cdot\mathbf{H_J}(\mathbf{x})\Big\}\,d\mathbf{x}. \\
&= \frac{1}{2}\int_{\mathbb{R}^3} \mu(\mathbf{x})\Big\{ -\nabla\hat{u}_0^T(\mathbf{x})\big(\mathsf{D}\boldsymbol{\mathcal{V}}(\mathbf{x}) + \mathsf{D}\boldsymbol{\mathcal{V}}^T(\mathbf{x})\big)\nabla\hat{u}_0(\mathbf{x}) + \|\nabla\hat{u}_0(\mathbf{x})\|^2\,\nabla\cdot\boldsymbol{\mathcal{V}}(\mathbf{x})\Big\}\,d\mathbf{x} \\
&\quad - [\![\mu]\!]_\Gamma \int_{\Gamma^0} \hat{u}_0(\mathbf{x})\Big\{\big(\mathsf{D}\mathbf{H_J}(\mathbf{x})\,\boldsymbol{\mathcal{V}}(\mathbf{x})\big)\cdot\hat{\mathbf{n}}(\mathbf{x}) + \mathbf{H_J}(\mathbf{x})\cdot\big(\nabla\cdot\boldsymbol{\mathcal{V}}(\mathbf{x})\,\hat{\mathbf{n}}(\mathbf{x}) - \mathsf{D}\boldsymbol{\mathcal{V}}^T(\mathbf{x})\,\hat{\mathbf{n}}(\mathbf{x})\big)\Big\}dS_\mathbf{x} \\
&\quad + \frac{1}{2}\int_{\mathbb{R}^3} \mu(\mathbf{x})\Big\{ \|\mathbf{H_J}(\mathbf{x})\|^2\,\nabla\cdot\boldsymbol{\mathcal{V}}(\mathbf{x}) + \boldsymbol{\mathcal{V}}(\mathbf{x})\cdot\nabla\big(\mathbf{H_J}(\mathbf{x})\cdot\mathbf{H_J}(\mathbf{x})\big)\Big\}\,d\mathbf{x}.
\end{aligned}
$$

The expressions can be simplified further. We observe that

$$\int_{\mathbb{R}^3} \mu(\mathbf{x})\Big\{ \|\mathbf{H_J}(\mathbf{x})\|^2\,\nabla\cdot\boldsymbol{\mathcal{V}}(\mathbf{x}) + \boldsymbol{\mathcal{V}}(\mathbf{x})\cdot\nabla\big(\mathbf{H_J}(\mathbf{x})\cdot\mathbf{H_J}(\mathbf{x})\big)\Big\}\,d\mathbf{x}.$$

$$= \int_{\Omega} \mu\,\mathrm{div}(\|\mathbf{H_J}\|^2\,\boldsymbol{\mathcal{V}})\,d\mathbf{x} + \int_{\Omega_c} \mu_0\,\mathrm{div}(\|\mathbf{H_J}\|^2\,\boldsymbol{\mathcal{V}})\,d\mathbf{x} = -[\![\mu]\!]_\Gamma \int_{\Gamma} \|\mathbf{H_J}(\mathbf{x})\|^2\,\boldsymbol{\mathcal{V}}(\mathbf{x})\cdot\mathbf{n}(\mathbf{x})\,dS_\mathbf{x}.$$

We also have the identity [2, Section 6]

$$\boldsymbol{\mathcal{V}}\cdot\nabla(\nabla u\cdot\nabla v) + \nabla u^T(\mathsf{D}\boldsymbol{\mathcal{V}} + \mathsf{D}\boldsymbol{\mathcal{V}}^T)\,\nabla v = \nabla v\cdot\nabla(\boldsymbol{\mathcal{V}}\cdot\nabla u) + \nabla u\cdot\nabla(\boldsymbol{\mathcal{V}}\cdot\nabla v).$$

Thus we have

$$\boldsymbol{\mathcal{V}}\cdot\nabla(\|\nabla u\|^2) - 2\,\nabla u\cdot\nabla(\boldsymbol{\mathcal{V}}\cdot\nabla u) = -\nabla u^T(\mathsf{D}\boldsymbol{\mathcal{V}} + \mathsf{D}\boldsymbol{\mathcal{V}}^T)\,\nabla u,$$

which helps us simplify the expression

$$\int_{\mathbb{R}^3} \mu(\mathbf{x})\Big\{ -\nabla\hat{u}_0^T(\mathbf{x})\big(\mathsf{D}\boldsymbol{\mathcal{V}}(\mathbf{x}) + \mathsf{D}\boldsymbol{\mathcal{V}}^T(\mathbf{x})\big)\nabla\hat{u}_0 + \|\nabla\hat{u}_0(\mathbf{x})\|^2\,\nabla\cdot\boldsymbol{\mathcal{V}}(\mathbf{x})\Big\}\,d\mathbf{x}$$

$$= \int_{\Omega} \mu\Big\{ \boldsymbol{\mathcal{V}}(\mathbf{x})\cdot\nabla(\|\nabla\hat{u}_0(\mathbf{x})\|^2) - 2\,\nabla\hat{u}_0(\mathbf{x})\cdot\nabla(\boldsymbol{\mathcal{V}}(\mathbf{x})\cdot\nabla\hat{u}_0(\mathbf{x})) + \|\nabla\hat{u}_0(\mathbf{x})\|^2\,\nabla\cdot\boldsymbol{\mathcal{V}}(\mathbf{x})\Big\}\,d\mathbf{x}$$

$$+ \int_{\Omega_c} \mu_0 \Big\{ \boldsymbol{\mathcal{V}}(\mathbf{x}) \cdot \nabla(\|\nabla \hat{u}_0(\mathbf{x})\|^2) - 2\, \nabla \hat{u}_0(\mathbf{x}) \cdot \nabla(\boldsymbol{\mathcal{V}}(\mathbf{x}) \cdot \nabla \hat{u}_0(\mathbf{x})) + \|\nabla \hat{u}_0(\mathbf{x})\|^2 \, \nabla \cdot \boldsymbol{\mathcal{V}}(\mathbf{x}) \Big\}\, d\mathbf{x}$$

$$= 2 \int_{\Omega} \mu \, \nabla \cdot \Big\{ \frac{\|\nabla u\|^2}{2} \boldsymbol{\mathcal{V}} - \nabla u \, \nabla u^T \, \boldsymbol{\mathcal{V}} \Big\}\, d\mathbf{x} + 2 \int_{\Omega_c} \mu_0 \, \nabla \cdot \Big\{ \frac{\|\nabla u\|^2}{2} \boldsymbol{\mathcal{V}} - \nabla u \, \nabla u^T \, \boldsymbol{\mathcal{V}} \Big\}\, d\mathbf{x}.$$

$$(5.1.22)$$

Using the following notation for the Maxwell Stress Tensor

$$\overleftrightarrow{\mathbf{T}}(u) = \epsilon \left(\nabla u \, \nabla u^T - \frac{\mathbf{Id}}{2} \, \|\nabla u\|^2 \right),$$

the above expression can be written as

$$2 \int_{\Gamma} \boldsymbol{\mathcal{V}}^T \, \Big[\!\!\Big[\mu \, \overleftrightarrow{\mathbf{T}}(u) \Big]\!\!\Big]_{\Gamma} \, \mathbf{n} \, dS.$$

We try to simplify $\Big[\!\!\Big[\mu \, \overleftrightarrow{\mathbf{T}}(u) \Big]\!\!\Big]_{\Gamma} \mathbf{n}$. We start by writing

$$\Big[\!\!\Big[\mu \, \overleftrightarrow{\mathbf{T}}(u) \Big]\!\!\Big]_{\Gamma} \mathbf{n} = \mu_0 (\gamma_N^+ u)^2 \frac{\mathbf{n}}{2} + \mu_0 \, \gamma_N^+ u \, \mathbf{grad}_{\Gamma} \, \gamma_D^+ u - \mu_0 \frac{\|\mathbf{grad}_{\Gamma} \, \gamma_D^+ u\|^2}{2} \mathbf{n}$$

$$- \mu (\gamma_N^- u)^2 \frac{\mathbf{n}}{2} - \mu \, \gamma_N^- u \, \mathbf{grad}_{\Gamma} \, \gamma_D^- u + \mu \frac{\|\mathbf{grad}_{\Gamma} \, \gamma_D^- u\|^2}{2} \mathbf{n}.$$

Since $[\![\gamma_D u]\!]_{\Gamma} = 0$, we write the Dirichlet trace as g. The expression above becomes

$$= \Big(\mu_0 (\gamma_N^+ u)^2 - \mu (\gamma_N^- u)^2 \Big) \frac{\mathbf{n}}{2} + [\![\mu \, \gamma_N u]\!]_{\Gamma} \, \mathbf{grad}_{\Gamma} \, g - \frac{[\![\mu]\!]_{\Gamma}}{2} \|\mathbf{grad}_{\Gamma} \, g\|^2 \, \mathbf{n}$$

$$= \Big(\mu_0 (\gamma_N^+ u)^2 - \mu (\gamma_N^- u)^2 \Big) \frac{\mathbf{n}}{2} - [\![\mu]\!]_{\Gamma} \, \mathbf{H_J} \cdot \mathbf{n} \, \mathbf{grad}_{\Gamma} \, g - \frac{[\![\mu]\!]_{\Gamma}}{2} \|\mathbf{grad}_{\Gamma} \, g\|^2 \, \mathbf{n}.$$

We know that $[\![\mathbf{B}]\!]_{\Gamma} \cdot \mathbf{n} = 0$. We denote the normal trace of $\mathbf{B}$ as B_n which allows us to write the relations

$$\gamma_N^- u = \mu^{-1} B_n - \mathbf{H_J} \cdot \mathbf{n}, \quad \gamma_N^+ u = \mu_0^{-1} B_n - \mathbf{H_J} \cdot \mathbf{n}.$$

Thus we get

$$\mu_0 (\gamma_N^+ u)^2 - \mu (\gamma_N^- u)^2 = \mu_0 (\mu_0^{-1} B_n - \mathbf{H_J} \cdot \mathbf{n})^2 - \mu (\mu^{-1} B_n - \mathbf{H_J} \cdot \mathbf{n})^2$$

$$= \mu_0 \Big(\frac{B_n^2}{\mu_0^2} + (\mathbf{H_J} \cdot \mathbf{n})^2 - 2 \frac{B_n}{\mu_0} \mathbf{H_J} \cdot \mathbf{n} \Big) - \mu \Big(\frac{B_n^2}{\mu^2} + (\mathbf{H_J} \cdot \mathbf{n})^2 - 2 \frac{B_n}{\mu} \mathbf{H_J} \cdot \mathbf{n} \Big)$$

$$= [\![\nu]\!]_{\Gamma} \, B_n^2 + [\![\mu]\!]_{\Gamma} \, (\mathbf{H_J} \cdot \mathbf{n})^2$$

The remaining expression to be simplified in the shape derivative is

$$- [\![\mu]\!]_{\Gamma} \int_{\Gamma^0} \hat{u}_0(\mathbf{x}) \Big\{ \Big(\mathsf{D} \mathbf{H_J}(\mathbf{x}) \, \boldsymbol{\mathcal{V}}(\mathbf{x}) \Big) \cdot \hat{\mathbf{n}}(\mathbf{x}) + \mathbf{H_J}(\mathbf{x}) \cdot \Big(\nabla \cdot \boldsymbol{\mathcal{V}}(\mathbf{x}) \, \hat{\mathbf{n}}(\mathbf{x}) - \mathsf{D}\boldsymbol{\mathcal{V}}^T(\mathbf{x}) \, \hat{\mathbf{n}}(\mathbf{x}) \Big) \Big\} dS_{\mathbf{x}}.$$

To simplify it, we rely on the identity

$$\nabla \cdot (\boldsymbol{\mathcal{V}} \, \mathbf{H}^T) = (\nabla \cdot \boldsymbol{\mathcal{V}}) \, \mathbf{H} + (\mathrm{D}\mathbf{H}) \, \boldsymbol{\mathcal{V}}. \tag{5.1.23}$$

Interchanging $\boldsymbol{\mathcal{V}}$ and $\mathbf{H}$ in the above gives (for $\operatorname{div} \mathbf{H} = 0$)

$$\nabla \cdot (\mathbf{H} \, \boldsymbol{\mathcal{V}}^T) = (\nabla \cdot \mathbf{H}) \, \boldsymbol{\mathcal{V}} + (\mathrm{D}\boldsymbol{\mathcal{V}}) \, \mathbf{H} = (\mathrm{D}\boldsymbol{\mathcal{V}}) \, \mathbf{H}.$$

The two identities allow the simplification

$$
\begin{aligned}
&\Big(\mathsf{D}\mathbf{H}_{\mathbf{J}}(\mathbf{x}) \, \boldsymbol{\mathcal{V}}(\mathbf{x})\Big) \cdot \hat{\mathbf{n}}(\mathbf{x}) + \mathbf{H}_{\mathbf{J}}(\mathbf{x}) \cdot \Big(\nabla \cdot \boldsymbol{\mathcal{V}}(\mathbf{x}) \, \hat{\mathbf{n}}(\mathbf{x}) - \mathsf{D}\boldsymbol{\mathcal{V}}^T(\mathbf{x}) \, \hat{\mathbf{n}}(\mathbf{x})\Big) \\
&= \hat{\mathbf{n}}^T(\mathbf{x}) \, \mathsf{D}\mathbf{H}_{\mathbf{J}}(\mathbf{x}) \, \boldsymbol{\mathcal{V}}(\mathbf{x}) + \hat{\mathbf{n}}^T(\mathbf{x}) \, \mathbf{H}_{\mathbf{J}}(\mathbf{x}) \, \nabla \cdot \boldsymbol{\mathcal{V}}(\mathbf{x}) - \hat{\mathbf{n}}^T(\mathbf{x}) \, \mathsf{D}\boldsymbol{\mathcal{V}}(\mathbf{x}) \, \mathbf{H}_{\mathbf{J}}(\mathbf{x}) \\
&= \hat{\mathbf{n}}^T(\mathbf{x}) \Big(\mathsf{D}\mathbf{H}_{\mathbf{J}}(\mathbf{x}) \, \boldsymbol{\mathcal{V}}(\mathbf{x}) + \mathbf{H}_{\mathbf{J}}(\mathbf{x}) \, \nabla \cdot \boldsymbol{\mathcal{V}}(\mathbf{x}) - \mathsf{D}\boldsymbol{\mathcal{V}}(\mathbf{x}) \, \mathbf{H}_{\mathbf{J}}(\mathbf{x})\Big) \\
&= \hat{\mathbf{n}}^T(\mathbf{x}) \, \nabla \cdot \Big(\boldsymbol{\mathcal{V}}(\mathbf{x}) \, \mathbf{H}_{\mathbf{J}}^T(\mathbf{x}) - \mathbf{H}_{\mathbf{J}}(\mathbf{x}) \, \boldsymbol{\mathcal{V}}^T(\mathbf{x})\Big) \\
&= \hat{\mathbf{n}}(\mathbf{x}) \cdot \nabla \times \Big(\mathbf{H}_{\mathbf{J}}(\mathbf{x}) \times \boldsymbol{\mathcal{V}}(\mathbf{x})\Big). \tag{5.1.24}
\end{aligned}
$$

Thus we have

$$
\begin{aligned}
&- [\![\mu]\!]_\Gamma \int_{\Gamma^0} \hat{u}_0(\mathbf{x}) \Big\{\Big(\mathsf{D}\mathbf{H}_{\mathbf{J}}(\mathbf{x}) \, \boldsymbol{\mathcal{V}}(\mathbf{x})\Big) \cdot \hat{\mathbf{n}}(\mathbf{x}) + \mathbf{H}_{\mathbf{J}}(\mathbf{x}) \cdot \Big(\nabla \cdot \boldsymbol{\mathcal{V}}(\mathbf{x}) \, \hat{\mathbf{n}}(\mathbf{x}) - \mathsf{D}\boldsymbol{\mathcal{V}}^T(\mathbf{x}) \, \hat{\mathbf{n}}(\mathbf{x})\Big)\Big\} dS_{\mathbf{x}} \\
&= - [\![\mu]\!]_\Gamma \int_{\Gamma^0} \hat{u}_0(\mathbf{x}) \, \hat{\mathbf{n}}(\mathbf{x}) \cdot \nabla \times \Big(\mathbf{H}_{\mathbf{J}}(\mathbf{x}) \times \boldsymbol{\mathcal{V}}(\mathbf{x})\Big) \, dS_{\mathbf{x}} \\
&= - [\![\mu]\!]_\Gamma \int_{\Gamma^0} \mathbf{curl}_\Gamma \, \hat{u}_0(\mathbf{x}) \cdot \Big(\mathbf{H}_{\mathbf{J}}(\mathbf{x}) \times \boldsymbol{\mathcal{V}}(\mathbf{x})\Big) \, dS_{\mathbf{x}} \\
&= - [\![\mu]\!]_\Gamma \int_{\Gamma^0} \boldsymbol{\mathcal{V}}(\mathbf{x}) \cdot \Big(\mathbf{curl}_\Gamma \, \hat{u}_0(\mathbf{x}) \times \mathbf{H}_{\mathbf{J}}(\mathbf{x})\Big) \, dS_{\mathbf{x}},
\end{aligned}
$$

where in the last step we used the identity from [9, Definition 2.3]. Denoting the tangential component of $\mathbf{H}$ and $\mathbf{H}_{\mathbf{J}}$ as $\mathbf{H}^\tau$ and $\mathbf{H}_{\mathbf{J}}^\tau$ respectively, we get the force distribution

$$
\begin{aligned}
&\Big([\![\nu]\!]_\Gamma B_n^2 + [\![\mu]\!]_\Gamma (\mathbf{H}_{\mathbf{J}} \cdot \mathbf{n})^2\Big) \frac{\mathbf{n}}{2} - [\![\mu]\!]_\Gamma \, \mathbf{H}_{\mathbf{J}} \cdot \mathbf{n} \, \mathbf{grad}_\Gamma \, g - \frac{[\![\mu]\!]_\Gamma}{2} \|\mathbf{grad}_\Gamma \, g\|^2 \, \mathbf{n} \\
&\quad - [\![\mu]\!]_\Gamma \, \mathbf{curl}_\Gamma \, g \times \mathbf{H}_{\mathbf{J}} - \frac{[\![\mu]\!]_\Gamma}{2} \|\mathbf{H}_{\mathbf{J}}\|^2 \, \mathbf{n} \\
&= \Big([\![\nu]\!]_\Gamma B_n^2 + [\![\mu]\!]_\Gamma (\mathbf{H}_{\mathbf{J}} \cdot \mathbf{n})^2\Big) \frac{\mathbf{n}}{2} - [\![\mu]\!]_\Gamma \, \mathbf{H}_{\mathbf{J}} \cdot \mathbf{n} \, \mathbf{grad}_\Gamma \, g - \frac{[\![\mu]\!]_\Gamma}{2} \|\mathbf{grad}_\Gamma \, g\|^2 \, \mathbf{n} \\
&\quad + [\![\mu]\!]_\Gamma \, \mathbf{H}_{\mathbf{J}} \times (\mathbf{grad}_\Gamma \, g \times \mathbf{n}) - \frac{[\![\mu]\!]_\Gamma}{2} (\mathbf{H}_{\mathbf{J}} \cdot \mathbf{n})^2 \mathbf{n} - \frac{[\![\mu]\!]_\Gamma}{2} \|\mathbf{H}_{\mathbf{J}}^\tau\|^2 \, \mathbf{n} \\
&= [\![\nu]\!]_\Gamma B_n^2 \frac{\mathbf{n}}{2} - \frac{[\![\mu]\!]_\Gamma}{2} \|\mathbf{grad}_\Gamma \, g\|^2 \, \mathbf{n} - [\![\mu]\!]_\Gamma \, \mathbf{H}_{\mathbf{J}} \cdot \mathbf{grad}_\Gamma \, g \, \mathbf{n} - \frac{[\![\mu]\!]_\Gamma}{2} \|\mathbf{H}_{\mathbf{J}}^\tau\|^2 \mathbf{n} \\
&= [\![\nu]\!]_\Gamma B_n^2 \frac{\mathbf{n}}{2} - [\![\mu]\!]_\Gamma \|\mathbf{grad}_\Gamma \, g + \mathbf{H}_{\mathbf{J}}^\tau\|^2 \frac{\mathbf{n}}{2}
\end{aligned}
$$

114

$$= [\![\nu]\!]_\Gamma \, B_n^2 \frac{\mathbf{n}}{2} - [\![\mu]\!]_\Gamma \, \|\mathbf{H}^\tau\|^2 \, \frac{\mathbf{n}}{2}.$$

We recover the classical formula for the force distribution at the interface of a linear material [6], and the shape derivative is reduced to the Hadamard form

$$\frac{d\mathcal{E}_F}{ds}(0) = \frac{1}{2} \int_{\Gamma^0} \left([\![\nu]\!]_\Gamma \, B_n^2 - [\![\mu]\!]_\Gamma \, \|\mathbf{H}^\tau\|^2 \right) \boldsymbol{\mathcal{V}} \cdot \mathbf{n} \, d\mathrm{S}. \tag{5.1.25}$$

5.1.1.9 Numerical Experiments

In this section we evaluate the shape derivative formulas (5.1.18) (called "BEM" in the plots) and (5.1.25) (called "MST" in the plots) numerically. Since both formulas are entirely boundary-based, we use the boundary element method based on a discretization of (5.1.15) to solve for the required boundary data. The geometries in our numerical experiments are discretized with a triangular boundary mesh and we use the discrete spaces S_1^0 for $H^{\frac{1}{2}}$ and S_0^{-1} for $H^{-\frac{1}{2}}$. The Galerkin approximation of the boundary data is then plugged into the shape derivative formulas which are evaluated on the discretized geometry using numerical quadrature. For evaluating the MST like shape derivative, we use 3 quadrature points per triangle and for evaluating the BIE based shape derivative we use the Sauter and Schwab quadrature rule which is described in [54]. The integral over the four dimensional unit cube is computed using a tensorized quadrature rule of 5^4 points, obtained using 5 Gauss Legendre quadrature points in one dimension. All the terms that appear in the BIE based shape derivative resemble the electrostatic case where we also dealt with a BIE constraint arising from a Laplace problem. To study convergence of the two methods, we use the values obtained using the BIE based shape derivative at a high refinement level as the reference. The shape derivatives can also be compared using the dual norm error computation. The procedure for that is outlined in Section 4.4.7.1.

Experiment 11. We have a linear material in the shape of a cube which is in presence of a source current of unit strength running along the surface of a torus. The cube has sides of length 2 and center at (5,5,3) and the torus is centered at the origin, with a distance of 2 betwen the origin and the center of the tube which has a radius of 0.5. The material parameters are chosen as $\mu = 4$ and $\mu_0 = 2$.
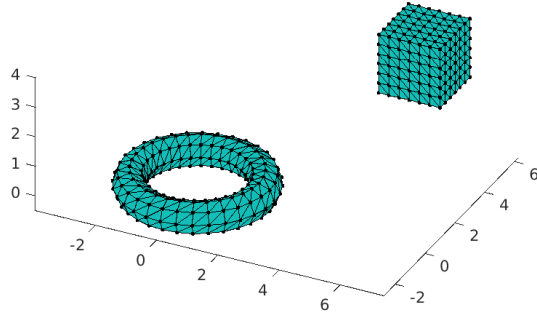
Figure 5.2: Cube and Torus geometry

The results for total force and torque computation are presented in Figure 5.3. As reference values, we use the force/torque obtained from the average of (5.1.18) and (5.1.35) at a refinement level of $h = 0.088$. Torque is computed about the point (4,0,0). We see the superiority of the BEM based shape derivative. The asymptotic convergence rates are tabulated in Table 5.1.
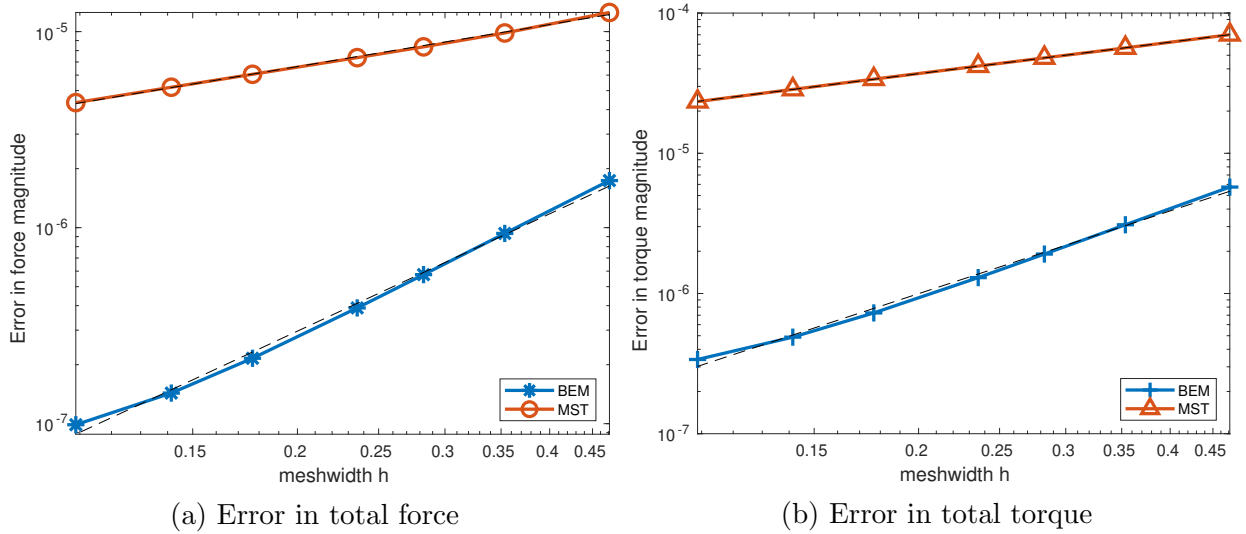

(a) Error in total force

(b) Error in total torque
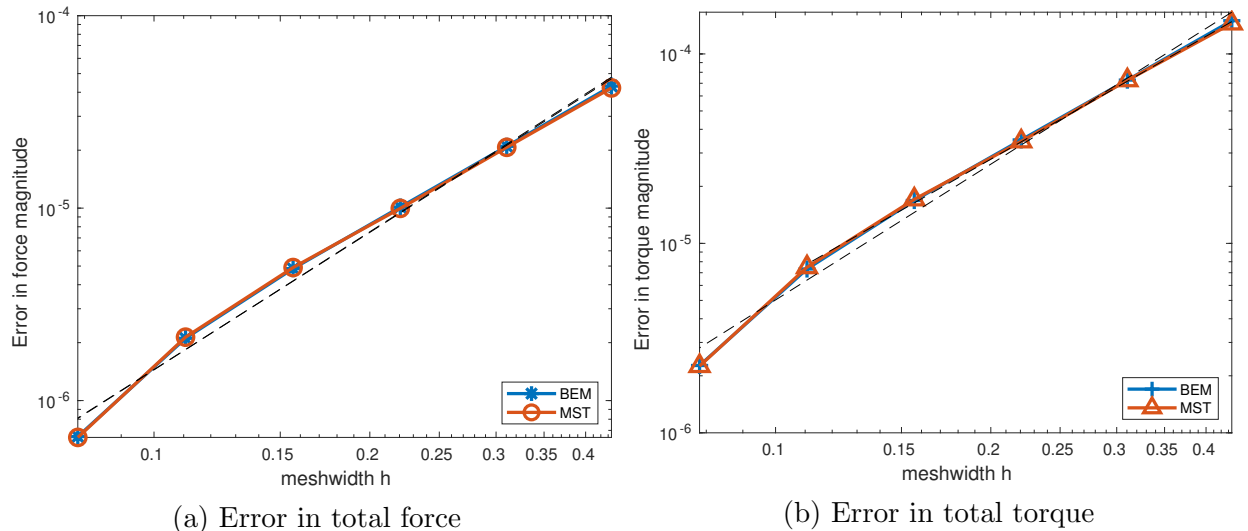
Figure 5.3: Error in force and torque computation for cube torus (Experiment 11)

Table 5.1: Asymptotic rate of algebraic convergence for Experiment 11

Method	Force	Torque
Pullback approach	1.98	1.96
Stress tensor	0.71	0.74

116

We also compare the shape derivative in terms of dual norm errors, which are plotted in the Figure 5.4, confirming the slight edge of the BEM based formula. For dual norm computations, the reference values are computed using the BEM based shape derivative at a refinement level of $h = 0.088$.
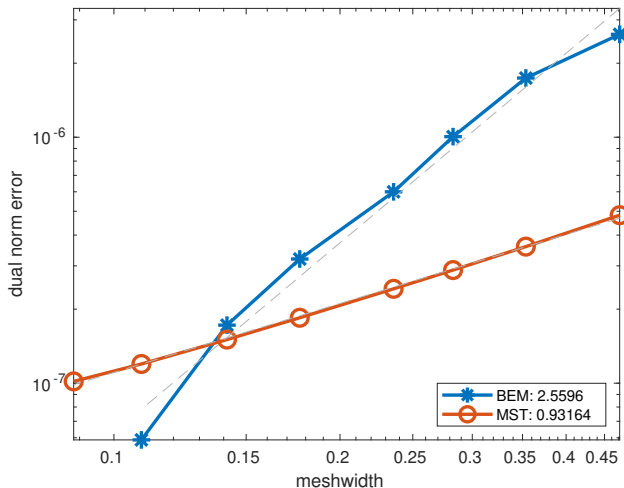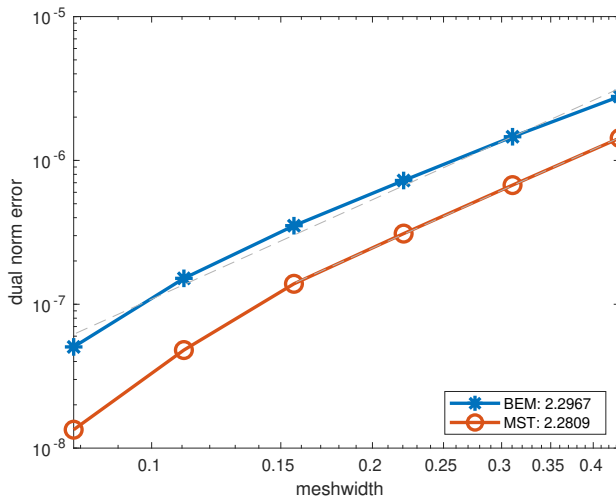

Figure 5.4: Dual norm error for Experiment 11

Experiment 12. In this experiment we consider a spherical shaped linear material in presence of a torus shaped source current. The sphere is of radius 1 and centered at $(5,5,3)$, whereas the torus is the same shape and at the same location as in Experiment 11 with a unit tangential current. We choose the parameters $\mu = 4$ and $\mu_0 = 2$.
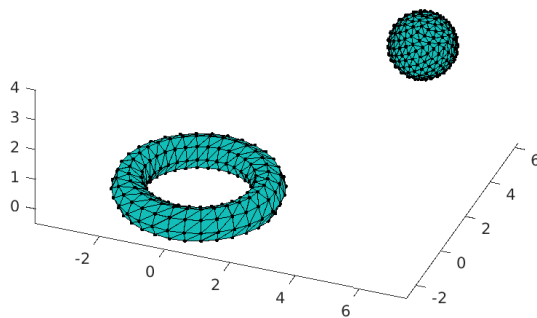
Figure 5.5: Sphere torus geometry

The results for total force and torque computation are shown in Experiment 12. As reference values, we use the force/torque obtained from the average of (5.1.18) and (5.1.35) at a refinement level of $h = 0.055$. Torque is computed about the point (4,0,0). We see that the two methods have identical performance which is in contrast with the results from

117

Experiment 11. This is in alignment with the results we have seen for a smooth domain in other experiments. The asymptotic convergence rates are reported in Table 5.2.

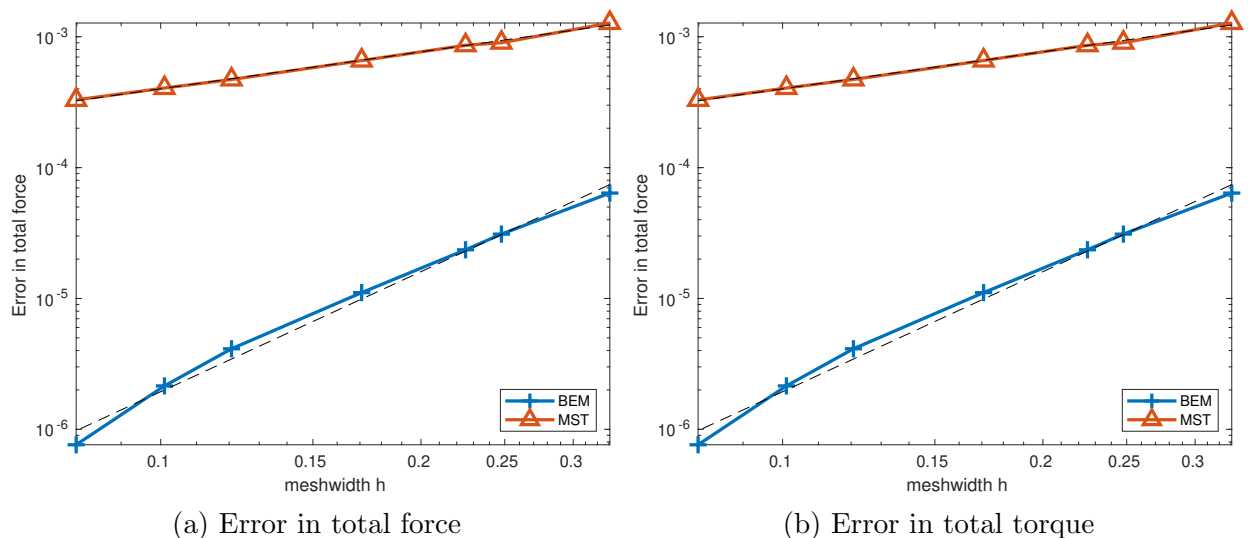(a) Error in total force

(b) Error in total torque

Figure 5.6: Error in force and torque computation for sphere and torus (Experiment 12)

Table 5.2: Asymptotic rate of algebraic convergence for Experiment 12

Method	Force	Torque
Pullback approach	2.38	2.38
Stress tensor	2.37	2.36

The shape derivatives can be compared using dual norm error computed for cosine velocity fields as mentioned in Section 4.4.7.1, the results of which are plotted in Figure 5.7. As in the force and torque error computations, the reference values are obtained using the BEM based shape derivative formula at a refinement level of $h = 0.055$.

Figure 5.7: Dual norm error for Experiment 12

Experiment 13. In this experiment we consider a brick shaped linear material with permeability $\mu = 4$ placed near the torus shaped current source from Experiment 11. We use $\mu_0 = 2$ for the external medium. The cuboid has sides of length 3,1,1 and is centered at (2,1,3).
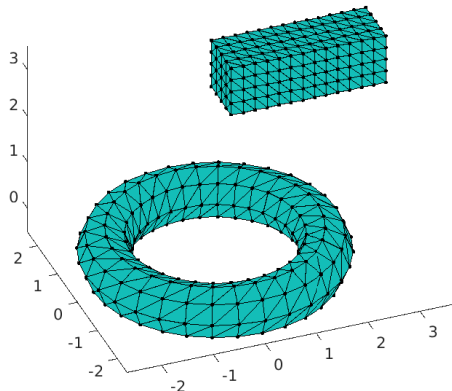
Figure 5.8: Cuboid torus geometry

The results for total force and torque computation are shown in Experiment 13. For error computation we use the BEM shape derivative based values at a refinement level $h = 0.064$ as the reference value. Torque is computed about the point (4,0,0). We observe a superior performance from the BEM based shape derivative. The asymptotic convergence rates are tabulated in Table 5.3

(a) Error in total force

(b) Error in total torque

Figure 5.9: Error in force and torque computation for cuboid and torus (Experiment 13)

Table 5.3: Asymptotic rate of algebraic convergence for Experiment 13

Method	Force	Torque
Pullback approach	3.05	3.11
Stress tensor	0.94	0.79

The dualnorm errors are computed using the BEM based shape derivative as the reference value at $h = 0.064$ and are plotted in Figure 5.10. It confirms the superiority of the BEM based shape derivative.
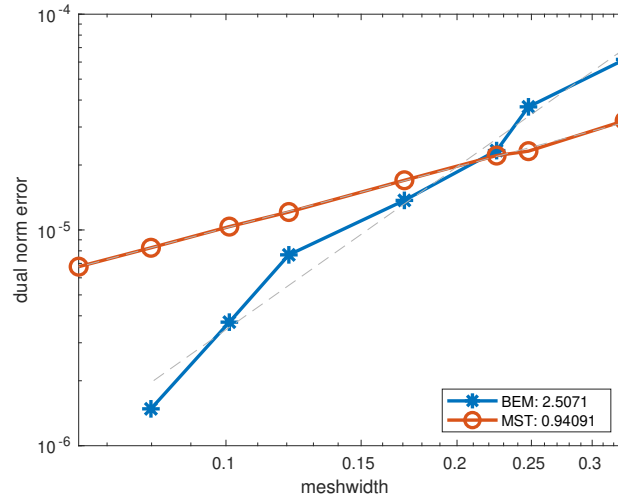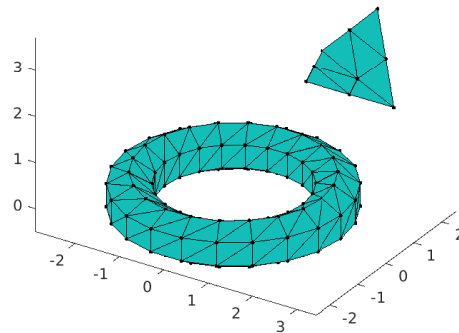

Figure 5.10: Dual norm error for Experiment 13

Experiment 14. In this experiment we consider a tetrahedral shaped linear material with permeability $\mu = 4$ placed near the torus shaped current source from Experiment 11. We use $\mu_0 = 2$ for the external medium. The tetrahedron has corners at $(\pm 1, 0, -\frac{1}{\sqrt{2}})$ and $(0, \pm 1, \frac{1}{\sqrt{2}})$ is translated by $(2,1,3)$.

Figure 5.11: Tetrahedron torus geometry

120

The results for total force and torque computation are shown in Experiment 14. For error computation we use the BEM shape derivative based values at a refinement level $h = 0.041$ as the reference value. Torque is computed about the point (4,0,0). We observe a superior performance from the BEM based shape derivative. The asymptotic convergence rates are tabulated in Table 5.4
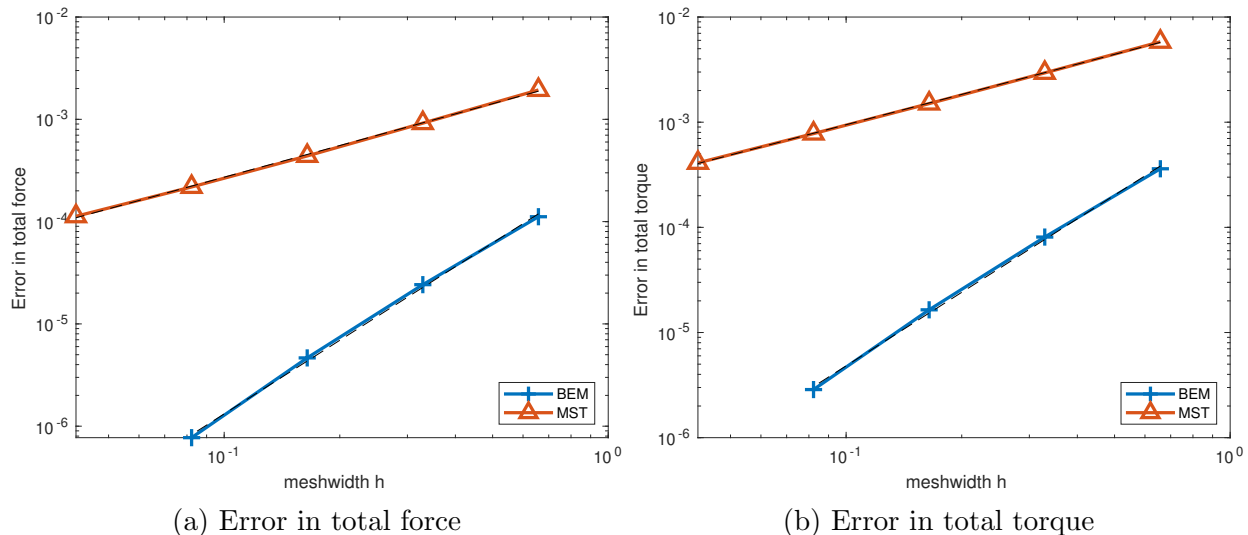

(a) Error in total force   (b) Error in total torque

Figure 5.12: Error in force and torque computation for tetrahedron and torus (Experiment 14)

Table 5.4: Asymptotic rate of algebraic convergence for Experiment 14

Method	Force	Torque
Pullback approach	2.39	2.32
Stress tensor	1.02	0.96

The dualnorm errors are computed using the BEM based shape derivative as the reference value at $h = 0.041$ and are plotted in Figure 5.13. We see a superior performance from the BEM based shape derivative.
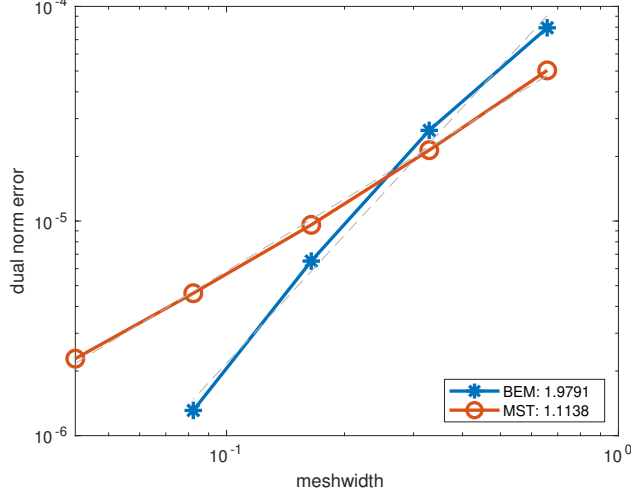
Figure 5.13: Dual norm error for Experiment 14

5.1.2 Vector Potential Formulation

The divergence equation in 5.1.2 allows us to write $\mathbf{B} = \mathbf{curl A}$ in $\Omega \cup \Omega_c$. Enforcing the jump condition $[\![\mathbf{A}]\!]_\Gamma \times \mathbf{n} = 0$ leads to

$$0 = \mathbf{curl}_\Gamma(\mathbf{n} \times ([\![\mathbf{A}]\!]_\Gamma \times \mathbf{n})) = \mathbf{curl}\,[\![\mathbf{A}]\!]_\Gamma \cdot \mathbf{n} = [\![\mathbf{B}]\!]_\Gamma \cdot \mathbf{n}. \tag{5.1.26}$$

The other jump condition is obtained from the jump condition for $\mathbf{H}$

$$[\![\mu^{-1}\,\mathbf{curl A}]\!]_\Gamma \times \mathbf{n} = 0. \tag{5.1.27}$$

Combining it with the equation for $\mathbf{H}$ in 5.1.2 and the material law 5.1.3 we get

$$
\begin{aligned}
\mathbf{curl}(\mu^{-1}(\mathbf{x})\,\mathbf{curl A}(\mathbf{x})) &= \mathbf{J}(\mathbf{x}) && \text{in } \Omega \cup \Omega_c, \\
[\![\mu^{-1}\,\gamma_\mathbf{M}\mathbf{A}]\!]_\Gamma &= 0 && \text{on } \Gamma, \\
[\![\gamma_\mathbf{t}\mathbf{A}]\!]_\Gamma &= 0 && \text{on } \Gamma, \\
\|\mathbf{A}(\mathbf{x})\| &= O(\|\mathbf{x}\|^{-1}) && \text{at } \infty.
\end{aligned} \tag{5.1.28}
$$

The solution the to the above problem is still not unique, we take care of that by using the Coulomb gauge:

$$\operatorname{div}\mathbf{A} = 0 \quad \text{in } \Omega \cup \Omega_c, \quad [\![\mathbf{A}]\!]_\Gamma \cdot \mathbf{n} = 0 \quad \text{on } \Gamma.$$

5.1.2.1 Variational Boundary Integral Equations

We approach 5.1.28 with a BIE based formulation. We can use the boundary integral equations derived in (2.2.23) for the interior and exterior traces

$$
\begin{bmatrix} \mathcal{A} & -\frac{\mathsf{Id}}{2} - \mathcal{C} \\ -\frac{\mathsf{Id}}{2} + \mathcal{B} & -\mathcal{N} \end{bmatrix}
\begin{bmatrix} \gamma_\mathbf{M}^-\mathbf{A} \\ \gamma_\mathbf{t}^-\mathbf{A} \end{bmatrix}
+ \begin{bmatrix} \operatorname{grad}_\Gamma \Psi_V(\gamma_n^-\mathbf{A}) \\ 0 \end{bmatrix}
= \begin{bmatrix} 0 \\ 0 \end{bmatrix},
$$

$$
\begin{bmatrix} \mathcal{A} & \frac{\mathsf{Id}}{2} - \mathcal{C} \\ \frac{\mathsf{Id}}{2} + \mathcal{B} & -\mathcal{N} \end{bmatrix}
\begin{bmatrix} \gamma_\mathbf{M}^+\mathbf{A} \\ \gamma_\mathbf{t}^+\mathbf{A} \end{bmatrix}
+ \begin{bmatrix} \operatorname{grad}_\Gamma \Psi_V(\gamma_n^+\mathbf{A}) \\ 0 \end{bmatrix}
= \mu_0 \begin{bmatrix} \gamma_\mathbf{t}^+\mathrm{N}(\mathbf{J}) \\ \gamma_\mathbf{M}^+\mathrm{N}(\mathbf{J}) \end{bmatrix}.
$$

Since there are no surface currents at the interface $\Gamma := \partial\Omega$, the magnetic trace $\gamma_{\mathbf{M}}^- \mathbf{A} \in \boldsymbol{H}^{-\frac{1}{2}}(\operatorname{div}_\Gamma 0, \Gamma)$ and the first equation can be tested with a test function $\boldsymbol{\zeta} \in \boldsymbol{H}^{-\frac{1}{2}}(\operatorname{div}_\Gamma 0, \Gamma)$, leading to a meaningful variational formulation [33]. The second equation for interior and exterior traces is tested with test function $\mathbf{u} \in \boldsymbol{H}^{-\frac{1}{2}}(\mathbf{curl}_\Gamma, \Gamma)$. We get the equations

$$\mathsf{b}_\mathcal{A}(\gamma_{\mathbf{M}}^- \mathbf{A}, \boldsymbol{\zeta}) - \frac{1}{2}\left\langle \gamma_{\mathbf{t}}^- \mathbf{A}, \boldsymbol{\zeta} \right\rangle - \mathsf{b}_\mathcal{C}(\gamma_{\mathbf{t}}^- \mathbf{A}, \boldsymbol{\zeta}) = 0 \qquad \forall \boldsymbol{\zeta} \in \boldsymbol{H}^{-\frac{1}{2}}(\operatorname{div}_\Gamma 0, \Gamma),$$

$$-\mathsf{b}_\mathcal{N}(\gamma_{\mathbf{t}}^- \mathbf{A}, \mathbf{u}) - \frac{1}{2}\left\langle \gamma_{\mathbf{M}}^- \mathbf{A}, \mathbf{u} \right\rangle + \mathsf{b}_\mathcal{B}(\gamma_{\mathbf{M}}^- \mathbf{A}, \mathbf{u}) = 0 \qquad \forall \mathbf{u} \in \boldsymbol{H}^{-\frac{1}{2}}(\mathbf{curl}_\Gamma, \Gamma),$$

$$\mathsf{b}_\mathcal{A}(\gamma_{\mathbf{M}}^+ \mathbf{A}, \boldsymbol{\zeta}) + \frac{1}{2}\left\langle \gamma_{\mathbf{t}}^+ \mathbf{A}, \boldsymbol{\zeta} \right\rangle - \mathsf{b}_\mathcal{C}(\gamma_{\mathbf{t}}^+ \mathbf{A}, \boldsymbol{\zeta}) = \mu_0 \left\langle \gamma_{\mathbf{t}}^+ \mathrm{N}(\mathbf{J}), \boldsymbol{\zeta} \right\rangle \qquad \forall \boldsymbol{\zeta} \in \boldsymbol{H}^{-\frac{1}{2}}(\operatorname{div}_\Gamma 0, \Gamma),$$

$$-\mathsf{b}_\mathcal{N}(\gamma_{\mathbf{t}}^+ \mathbf{A}, \mathbf{u}) + \frac{1}{2}\left\langle \gamma_{\mathbf{M}}^+ \mathbf{A}, \mathbf{u} \right\rangle + \mathsf{b}_\mathcal{B}(\gamma_{\mathbf{M}}^+ \mathbf{A}, \mathbf{u}) = \mu_0 \left\langle \gamma_{\mathbf{M}}^+ \mathrm{N}(\mathbf{J}), \mathbf{u} \right\rangle \qquad \forall \mathbf{u} \in \boldsymbol{H}^{-\frac{1}{2}}(\mathbf{curl}_\Gamma, \Gamma).$$

Using the notation $< \cdot, \cdot >$ for the duality pairing between $\boldsymbol{H}^{-\frac{1}{2}}(\operatorname{div}_\Gamma, \Gamma)$ and $\boldsymbol{H}^{-\frac{1}{2}}(\mathbf{curl}_\Gamma, \Gamma)$, the bilinear forms used in the above equations are defined as

$$\mathsf{b}_\mathcal{A}(\boldsymbol{\psi}, \boldsymbol{\zeta}) := \langle \mathcal{A}(\boldsymbol{\psi}), \boldsymbol{\zeta} \rangle, \quad \mathsf{b}_\mathcal{C}(\mathbf{g}, \boldsymbol{\zeta}) := \langle \mathcal{C}(\mathbf{g}), \boldsymbol{\zeta} \rangle, \tag{5.1.29}$$

$$\mathsf{b}_\mathcal{B}(\boldsymbol{\psi}, \mathbf{u}) := \langle \mathcal{B}(\boldsymbol{\psi}), \mathbf{u} \rangle, \quad \mathsf{b}_\mathcal{N}(\mathbf{g}, \mathbf{u}) := \langle \mathcal{N}(\mathbf{g}), \mathbf{u} \rangle. \tag{5.1.30}$$

The variational equations can be combined using the transmission conditions to get a single-trace formulation. We use the notation $\mathbf{g} := \gamma_{\mathbf{t}}^+ \mathbf{A}$ and $\boldsymbol{\psi} := \gamma_{\mathbf{M}}^+ \mathbf{A}$ for the exterior tangential and magnetic traces respectively. The interior traces can then be written as $\gamma_{\mathbf{t}}^- \mathbf{A} = \mathbf{g}$ and $\gamma_{\mathbf{M}}^- \mathbf{A} = \frac{\mu}{\mu_0}\boldsymbol{\psi}$. Substituting the notation for traces and combining the variational equations gives the variational formulation. To ensure its unique solvability, we need the space $\boldsymbol{V} := \{\mathbf{u} \in \boldsymbol{H}^{-\frac{1}{2}}(\mathbf{curl}_\Gamma, \Gamma) : (\mathbf{u}, \mathbf{grad}_\Gamma v)_{-\frac{1}{2}, \Gamma} = 0 \quad \forall v \in H_*^{\frac{1}{2}}(\Gamma)\}$, where $(\cdot, \cdot)_{-\frac{1}{2}, \Gamma}$ is the $\boldsymbol{H}^{-\frac{1}{2}}$ inner product which essentially ensures orthogonality to the kernel of $\mathcal{N}$ which is $\mathbf{grad}_\Gamma H_*^{\frac{1}{2}}(\Gamma)$. This works for simple topologies as mentioned in Remark 2. We seek $\boldsymbol{\psi} \in \boldsymbol{H}^{-\frac{1}{2}}(\operatorname{div}_\Gamma 0, \Gamma), \mathbf{g} \in \boldsymbol{V}$ such that

$$(1 + \frac{\mu}{\mu_0})\mathsf{b}_\mathcal{A}(\boldsymbol{\psi}, \boldsymbol{\zeta}) - 2\,\mathsf{b}_\mathcal{C}(\mathbf{g}, \boldsymbol{\zeta}) - (1 + \frac{\mu_0}{\mu})\mathsf{b}_\mathcal{N}(\mathbf{g}, \mathbf{u}) + 2\,\mathsf{b}_\mathcal{B}(\boldsymbol{\psi}, \mathbf{u})$$

$$= \mu_0 \left\langle \gamma_{\mathbf{t}}^+ \mathrm{N}(\mathbf{J}), \boldsymbol{\zeta} \right\rangle + \mu_0 \left\langle \gamma_{\mathbf{M}}^+ \mathrm{N}(\mathbf{J}), \mathbf{u} \right\rangle \quad \forall \boldsymbol{\zeta} \in \boldsymbol{H}^{-\frac{1}{2}}(\operatorname{div}_\Gamma 0, \Gamma), \forall \mathbf{u} \in \boldsymbol{V}. \tag{5.1.31}$$

The unique solvability can be seen by plugging in $\boldsymbol{\zeta} = \boldsymbol{\psi}$ and $\mathbf{u} = \mathbf{g}$ on the LHS which gives

$$(1 + \frac{\mu}{\mu_0})\mathsf{b}_\mathcal{A}(\boldsymbol{\psi}, \boldsymbol{\zeta}) - (1 + \frac{\mu_0}{\mu})\mathsf{b}_\mathcal{N}(\mathbf{g}, \mathbf{u}).$$

We conclude the ellipticity based on the ellipticity of $\mathsf{b}_\mathcal{A}$ [33] and $-\mathsf{b}_\mathcal{N}$ which can be concluded by combining the closed range of operator $\operatorname{curl}_\Gamma$ [13, Lemma 9] and the result [33, Lemma 6.3]. The field energy can be written in terms of traces. Starting with the expression for field energy

$$\mathcal{E}_F := \frac{1}{2}\int_{\mathbb{R}^3} \mu^{-1}(\mathbf{x})\,\|\mathbf{curl}\mathbf{A}(\mathbf{x})\|^2\,d\mathbf{x}$$

$$= \frac{\mu^{-1}}{2} \int_{\Omega} \|\mathbf{curl A(x)}\|^2 \ d\mathbf{x} + \frac{\mu_0^{-1}}{2} \int_{\Omega_c} \|\mathbf{curl A(x)}\|^2 \ d\mathbf{x}$$

$$= \frac{\mu^{-1}}{2} \left\langle \gamma_{\mathbf{M}}^- \mathbf{A}, \gamma_{\mathbf{t}}^- \mathbf{A} \right\rangle - \frac{\mu_0^{-1}}{2} \left\langle \gamma_{\mathbf{M}}^+ \mathbf{A}, \gamma_{\mathbf{t}}^+ \mathbf{A} \right\rangle + \frac{1}{2} \int_{\Omega_{\mathrm{src}}} \mathbf{A} \cdot \mathbf{J} \ d\mathbf{x}.$$

Due to the transmission conditions, the first two terms cancel each other. To write the energy expression purely in terms of traces, we use the representation formula for $\mathbf{A}$ in the exterior domain Ω_c (2.2.22). This gives us

$$\mathcal{E}_F = \frac{1}{2} \int_{\Omega_{\mathrm{src}}} \left(\boldsymbol{\Psi_M}(\mathbf{g}) - \boldsymbol{\Psi_A}(\boldsymbol{\psi}) - \mathrm{grad}_{\mathbf{x}} \, \Psi_V(\gamma_n^+ \mathbf{A}) + \mu_0 \mathrm{N}(\mathbf{J}) \right) \cdot \mathbf{J} \ d\mathbf{x}.$$

The third term in the representation formula drops out since we assume $\mathrm{div} \, \mathbf{J} = 0$ in Ω_{src} and $\mathbf{J} \cdot \mathbf{n} = 0$ on $\partial\Omega_{\mathrm{src}}$. This gives

$$\mathcal{E}_F = \frac{1}{2} \int_{\Omega_{\mathrm{src}}} \left(\boldsymbol{\Psi_M}(\mathbf{g}) - \boldsymbol{\Psi_A}(\boldsymbol{\psi}) + \mu_0 \mathrm{N}(\mathbf{J}) \right) \cdot \mathbf{J} \ d\mathbf{x}$$

$$= \frac{1}{2} \int_{\Omega_{\mathrm{src}}} \int_{\Gamma} \left(\nabla_{\mathbf{x}} G(\mathbf{x}, \mathbf{y}) \times (\mathbf{n} \times \mathbf{g})(\mathbf{y}) \right) \cdot \mathbf{J}(\mathbf{x}) \ d\mathbf{x} \ d\mathrm{S}_{\mathbf{y}}$$

$$- \frac{1}{2} \int_{\Omega_{\mathrm{src}}} \int_{\Gamma} G(\mathbf{x}, \mathbf{y}) \, \boldsymbol{\psi}(\mathbf{y}) \cdot \mathbf{J}(\mathbf{x}) \ d\mathrm{S}_{\mathbf{y}} \ d\mathbf{x} + \frac{\mu_0}{2} \int_{\Omega_{\mathrm{src}}} \int_{\Omega_{\mathrm{src}}} G(\mathbf{x}, \mathbf{y}) \, \mathbf{J}(\mathbf{y}) \cdot \mathbf{J}(\mathbf{x}) \ d\mathbf{y} \ d\mathbf{x}.$$

Swapping the variables $\mathbf{x}$ and $\mathbf{y}$ in the first two terms and using the fact that $\nabla_{\mathbf{x}} G(\mathbf{x}, \mathbf{y}) = -\nabla_{\mathbf{x}} G(\mathbf{y}, \mathbf{x})$ we get the field energy in terms of traces

$$\mathcal{E}_F = \frac{1}{2} \left\langle \gamma_{\mathbf{M}}^+ \mathrm{N}(\mathbf{J}), \mathbf{g} \right\rangle - \frac{1}{2} \left\langle \gamma_{\mathbf{t}}^+ \mathrm{N}(\mathbf{J}), \boldsymbol{\psi} \right\rangle + \frac{\mu_0}{2} \int_{\Omega_{\mathrm{src}}} \int_{\Omega_{\mathrm{src}}} G(\mathbf{x}, \mathbf{y}) \, \mathbf{J}(\mathbf{y}) \cdot \mathbf{J}(\mathbf{x}) \ d\mathbf{y} \ d\mathbf{x}. \qquad (5.1.32)$$

5.1.2.2 Variational Formulation on Deformed Domain

We consider a deformation using $\boldsymbol{\mathcal{V}}$ such that $\boldsymbol{\mathcal{V}} \equiv 0$ at Ω_{src}. Thus only the domain Ω^0 is deformed. The variational formulation for the deformed s configuration has the same structure as 5.1.31: seek $\boldsymbol{\psi}_s \in \boldsymbol{H}^{-\frac{1}{2}}(\mathrm{div}_{\Gamma} \, 0, \Gamma^s)$, $\mathbf{g}_s \in \boldsymbol{V}_s := \{ \mathbf{u} \in \boldsymbol{H}^{-\frac{1}{2}}(\mathbf{curl}_{\Gamma}, \Gamma^s) : (\mathbf{u}, \mathbf{grad}_{\Gamma} \, v)_{-\frac{1}{2}, \Gamma^s} = 0 \quad \forall v \in H_*^{\frac{1}{2}}(\Gamma^s) \}$ such that

$$(1 + \frac{\mu}{\mu_0}) \mathsf{b}_{\mathcal{A}}(s)(\boldsymbol{\psi}_s, \boldsymbol{\zeta}) - 2 \, \mathsf{b}_{\mathcal{C}}(s)(\mathbf{g}_s, \boldsymbol{\zeta}) + 2 \, \mathsf{b}_{\mathcal{B}}(s)(\boldsymbol{\psi}_s, \mathbf{u}) - (1 + \frac{\mu_0}{\mu}) \mathsf{b}_{\mathcal{N}}(s)(\mathbf{g}_s, \mathbf{u})$$

$$= \mu_0 \left\langle \gamma_{\mathbf{t}}^+ \mathrm{N}(\mathbf{J}), \boldsymbol{\zeta} \right\rangle_{\Gamma^s} + \mu_0 \left\langle \gamma_{\mathbf{M}}^+ \mathrm{N}(\mathbf{J}), \mathbf{u} \right\rangle_{\Gamma^s} \quad \forall \boldsymbol{\zeta} \in \boldsymbol{H}^{-\frac{1}{2}}(\mathrm{div}_{\Gamma} \, 0, \Gamma^s), \forall \mathbf{u} \in \boldsymbol{V}_s.$$

In the variational formulation above, the bilinear forms $\mathsf{b}_*(s)$ represent integrals on $\Gamma^s := \partial\Omega^s$ and $\langle \cdot, \cdot \rangle_{\Gamma^s}$ represents the duality pairing between $\boldsymbol{H}^{-\frac{1}{2}}(\mathbf{curl}_{\Gamma}, \Gamma^s)$ and $\boldsymbol{H}^{-\frac{1}{2}}(\mathrm{div}_{\Gamma}, \Gamma^s)$.

5.1.2.3 Equivalent Formulation on Reference Domain

We transform integrals in the (bi)linear forms back to the reference boundary Γ^0 using the perturbation map

$$
\begin{aligned}
\mathsf{b}_{\mathcal{A}}(s)(\boldsymbol{\psi},\boldsymbol{\zeta}) &= \int_{\Gamma^s}\int_{\Gamma^s} G(\mathbf{x},\mathbf{y})\,\boldsymbol{\psi}(\mathbf{y})\cdot\boldsymbol{\zeta}(\mathbf{x})\,dS_{\mathbf{y}}dS_{\mathbf{x}} \\
&= \int_{\Gamma^0}\int_{\Gamma^0} G(\mathbf{T}_s^{\boldsymbol{\nu}}(\hat{\mathbf{x}}),\mathbf{T}_s^{\boldsymbol{\nu}}(\hat{\mathbf{y}}))\,\boldsymbol{\psi}(\mathbf{T}_s^{\boldsymbol{\nu}}(\hat{\mathbf{y}}))\cdot\boldsymbol{\zeta}(\mathbf{T}_s^{\boldsymbol{\nu}}(\hat{\mathbf{x}}))\,\omega_s(\hat{\mathbf{x}})\,\omega_s(\hat{\mathbf{y}})\,dS_{\hat{\mathbf{y}}}dS_{\hat{\mathbf{x}}}, \\
\mathsf{b}_{\mathcal{C}}(s)(\mathbf{g},\boldsymbol{\zeta}) &= \int_{\Gamma^s}\int_{\Gamma^s} (\nabla_{\mathbf{x}}G(\mathbf{x},\mathbf{y})\times(\mathbf{n}\times\mathbf{g})(\mathbf{y}))\cdot\boldsymbol{\zeta}(\mathbf{x})\,dS_{\mathbf{y}}\,dS_{\mathbf{x}} \\
&= \int_{\Gamma^0}\int_{\Gamma^0}\left(\nabla_{\mathbf{x}}G(\mathbf{T}_s^{\boldsymbol{\nu}}(\hat{\mathbf{x}}),\mathbf{T}_s^{\boldsymbol{\nu}}(\hat{\mathbf{y}}))\times\left(\frac{\mathbf{C}(\mathsf{D}\mathbf{T}_s^{\boldsymbol{\nu}})(\hat{\mathbf{y}})\,\hat{\mathbf{n}}(\hat{\mathbf{y}})}{\omega_s(\hat{\mathbf{y}})}\times\mathbf{g}(\mathbf{T}_s^{\boldsymbol{\nu}}(\hat{\mathbf{y}}))\right)\right) \\
&\qquad\cdot\boldsymbol{\zeta}(\mathbf{T}_s^{\boldsymbol{\nu}}(\hat{\mathbf{x}}))\,\omega_s(\hat{\mathbf{x}})\,\omega_s(\hat{\mathbf{y}})\,dS_{\hat{\mathbf{y}}}\,dS_{\hat{\mathbf{x}}}, \\
\mathsf{b}_{\mathcal{N}}(s)(\mathbf{g},\mathbf{u}) &= -\int_{\Gamma^s}\int_{\Gamma^s} G(\mathbf{x},\mathbf{y})\,\operatorname{curl}_{\Gamma}\mathbf{g}(\mathbf{y})\,\operatorname{curl}_{\Gamma}\mathbf{u}(\mathbf{x})\,dS_{\mathbf{y}}\,dS_{\mathbf{x}} \\
&= -\int_{\Gamma^0}\int_{\Gamma^0} G(\mathbf{T}_s^{\boldsymbol{\nu}}(\hat{\mathbf{x}}),\mathbf{T}_s^{\boldsymbol{\nu}}(\hat{\mathbf{y}}))\,\operatorname{curl}_{\Gamma}\mathbf{g}(\mathbf{T}_s^{\boldsymbol{\nu}}(\hat{\mathbf{y}}))\,\operatorname{curl}_{\Gamma}\mathbf{u}(\mathbf{T}_s^{\boldsymbol{\nu}}(\hat{\mathbf{x}}))\,\omega_s(\hat{\mathbf{y}})\,\omega_s(\hat{\mathbf{x}})\,dS_{\hat{\mathbf{y}}}\,dS_{\hat{\mathbf{x}}}, \\
\ell_1(s)(\boldsymbol{\zeta}) &= \left\langle\gamma_{\mathbf{t}}^{+}\mathrm{N}(\mathbf{J}),\boldsymbol{\zeta}\right\rangle_{\Gamma^s} = \int_{\Gamma^s}\int_{\Omega_{\mathrm{src}}} G(\mathbf{x},\mathbf{y})\,\mathbf{J}(\mathbf{y})\cdot\boldsymbol{\zeta}(\mathbf{x})\,d\mathbf{y}\,dS_{\mathbf{x}} \\
&= \int_{\Gamma^0}\int_{\Omega_{\mathrm{src}}} G(\mathbf{T}_s^{\boldsymbol{\nu}}(\hat{\mathbf{x}}),\mathbf{y})\,\mathbf{J}(\mathbf{y})\cdot\boldsymbol{\zeta}(\mathbf{T}_s^{\boldsymbol{\nu}}(\hat{\mathbf{x}}))\,\omega_s(\hat{\mathbf{x}})\,d\mathbf{y}\,dS_{\hat{\mathbf{x}}}, \\
\ell_2(s)(\mathbf{u}) &= \left\langle\gamma_{\mathbf{M}}^{+}\mathrm{N}(\mathbf{J}),\mathbf{u}\right\rangle_{\Gamma^s} = \int_{\Gamma^s}\int_{\Omega_{\mathrm{src}}}\left(\nabla_{\mathbf{x}}G(\mathbf{x},\mathbf{y})\times\mathbf{J}(\mathbf{y})\right)\cdot(\mathbf{n}(\mathbf{x})\times\mathbf{u}(\mathbf{x}))\,d\mathbf{y}\,dS_{\mathbf{x}} \\
&= \int_{\Gamma^0}\int_{\Omega_{\mathrm{src}}}\left(\nabla_{\mathbf{x}}G(\mathbf{T}_s^{\boldsymbol{\nu}}(\hat{\mathbf{x}}),\mathbf{y})\times\mathbf{J}(\mathbf{y})\right)\cdot\left(\frac{\mathbf{C}(\mathsf{D}\mathbf{T}_s^{\boldsymbol{\nu}})(\hat{\mathbf{x}})\,\hat{\mathbf{n}}(\hat{\mathbf{x}})}{\omega_s(\hat{\mathbf{x}})}\times\mathbf{u}(\mathbf{T}_s^{\boldsymbol{\nu}}(\hat{\mathbf{x}}))\right)\omega_s(\hat{\mathbf{x}})\,d\mathbf{y}\,dS_{\hat{\mathbf{x}}}.
\end{aligned}
$$

The vector potential $\mathbf{A}$ in our considerations is a 1-form and its tangential trace ($\gamma_{\mathbf{t}}$) would be a 1-form as well. So for functions associated with the space $\boldsymbol{H}^{-\frac{1}{2}}(\mathbf{curl}_{\Gamma},\Gamma)$ we use a pullback for 1-forms. The Neumann trace is a twisted tangential trace of a 1-form and we will use the following pullback derived using the duality pairing of these traces

$$
\boldsymbol{\psi}\in\boldsymbol{H}^{-\frac{1}{2}}(\operatorname{div}_{\Gamma}0,\Gamma^s),\ \hat{\boldsymbol{\psi}}\in\boldsymbol{H}^{-\frac{1}{2}}(\operatorname{div}_{\Gamma}0,\Gamma^0):\quad\boldsymbol{\psi}(\mathbf{T}_s^{\boldsymbol{\nu}}(\hat{\mathbf{x}}))=\frac{\mathsf{D}\mathbf{T}_s^{\boldsymbol{\nu}}(\hat{\mathbf{x}})}{\omega_s(\hat{x})}\,\hat{\boldsymbol{\psi}}(\hat{\mathbf{x}}),
$$

$$
\mathbf{g}\in\boldsymbol{H}^{-\frac{1}{2}}(\mathbf{curl}_{\Gamma},\Gamma^s),\ \hat{\mathbf{g}}\in\boldsymbol{H}^{-\frac{1}{2}}(\mathbf{curl}_{\Gamma},\Gamma^0):\quad\mathbf{g}(\mathbf{T}_s^{\boldsymbol{\nu}}(\hat{\mathbf{x}}))=\mathsf{D}\mathbf{T}_s^{\boldsymbol{\nu}}(\hat{\mathbf{x}})^{-T}\,\hat{\mathbf{g}}(\hat{\mathbf{x}}).
$$

We will also need a pullback for the scalar surface curl operator that appears in $\mathsf{b}_{\mathcal{N}}$

$$
\operatorname{curl}_{\Gamma}\mathbf{g}(\mathbf{T}_s^{\boldsymbol{\nu}}(\hat{\mathbf{x}}))=\frac{\operatorname{curl}_{\Gamma}\hat{\mathbf{g}}(\hat{\mathbf{x}})}{\omega_s(\hat{\mathbf{x}})}.
$$

Based on the transformed integrals and pullbacks, we define the pulled back hat (bi)linear forms:

$$\hat{\mathsf{b}}_{\mathcal{A}}(s;\hat{\boldsymbol{\psi}},\hat{\boldsymbol{\zeta}}) = \int_{\Gamma^0}\int_{\Gamma^0} G(\mathbf{T}_s^{\boldsymbol{\nu}}(\hat{\mathbf{x}}),\mathbf{T}_s^{\boldsymbol{\nu}}(\hat{\mathbf{y}}))\Big(D\mathbf{T}_s^{\boldsymbol{\nu}}(\hat{\mathbf{y}})\,\hat{\boldsymbol{\psi}}(\hat{\mathbf{y}})\Big)\cdot\Big(D\mathbf{T}_s^{\boldsymbol{\nu}}(\hat{\mathbf{x}})\,\hat{\boldsymbol{\zeta}}(\hat{\mathbf{x}})\Big)dS_{\hat{\mathbf{y}}}\,dS_{\hat{\mathbf{x}}},$$

$$\hat{\mathsf{b}}_{\mathcal{C}}(s;\hat{\mathbf{g}},\hat{\boldsymbol{\zeta}}) = \int_{\Gamma^0}\int_{\Gamma^0}\Big(\nabla_{\mathbf{x}}G(\mathbf{T}_s^{\boldsymbol{\nu}}(\hat{\mathbf{x}}),\mathbf{T}_s^{\boldsymbol{\nu}}(\hat{\mathbf{y}}))\times\Big(D\mathbf{T}_s^{\boldsymbol{\nu}}(\hat{\mathbf{y}})\,\{\hat{\mathbf{n}}(\hat{\mathbf{y}})\times\hat{\mathbf{g}}(\hat{\mathbf{y}})\}\Big)\Big)\cdot\Big(D\mathbf{T}_s^{\boldsymbol{\nu}}(\hat{\mathbf{x}})\,\hat{\boldsymbol{\zeta}}(\hat{\mathbf{x}})\Big)\,dS_{\hat{\mathbf{y}}}\,dS_{\hat{\mathbf{x}}},$$

$$\hat{\mathsf{b}}_{\mathcal{N}}(s;\hat{\mathbf{g}},\hat{\mathbf{u}}) = -\int_{\Gamma^0}\int_{\Gamma^0} G(\mathbf{T}_s^{\boldsymbol{\nu}}(\hat{\mathbf{x}}),\mathbf{T}_s^{\boldsymbol{\nu}}(\hat{\mathbf{y}}))\ \mathrm{curl}_{\Gamma}\,\hat{\mathbf{g}}(\hat{\mathbf{y}})\ \mathrm{curl}_{\Gamma}\,\hat{\mathbf{u}}(\hat{\mathbf{x}})\,dS_{\hat{\mathbf{y}}}\,dS_{\hat{\mathbf{x}}},$$

$$\hat{\ell}_1(s;\hat{\boldsymbol{\zeta}}) = \int_{\Gamma^0}\int_{\Omega_{\mathrm{src}}} G(\mathbf{T}_s^{\boldsymbol{\nu}}(\hat{\mathbf{x}}),\mathbf{y})\,\mathbf{J}(\mathbf{y})\cdot\Big(D\mathbf{T}_s^{\boldsymbol{\nu}}(\hat{\mathbf{x}})\,\hat{\boldsymbol{\zeta}}(\hat{\mathbf{x}})\Big)\,d\mathbf{y}\,dS_{\hat{\mathbf{x}}},$$

$$\hat{\ell}_2(s;\hat{\mathbf{u}}) = \int_{\Gamma^0}\int_{\Omega_{\mathrm{src}}}\Big(\nabla_{\mathbf{x}}G(\mathbf{T}_s^{\boldsymbol{\nu}}(\hat{\mathbf{x}}),\mathbf{y})\times\mathbf{J}(\mathbf{y})\Big)\cdot\Big(D\mathbf{T}_s^{\boldsymbol{\nu}}(\hat{\mathbf{x}})\{\hat{\mathbf{n}}(\hat{\mathbf{x}})\times\hat{\mathbf{u}}(\hat{\mathbf{x}})\}\Big)\,d\mathbf{y}\,dS_{\hat{\mathbf{x}}}.$$

We don't explicitly mention the bilinear form $\mathsf{b}_{\mathcal{B}}$ since it can be written in terms of the bilinear form related to $\mathsf{b}_{\mathcal{C}}$. For the pulled back bilinear form we have the relation $\hat{\mathsf{b}}_{\mathcal{B}}(s;\hat{\boldsymbol{\psi}},\hat{\mathbf{u}}) = \hat{\mathsf{b}}_{\mathcal{C}}(s;\hat{\mathbf{u}},\hat{\boldsymbol{\psi}})$. For $\boldsymbol{\mathcal{X}}_0 := \boldsymbol{H}^{-\frac{1}{2}}(\mathrm{div}_{\Gamma}\,0,\Gamma^0)\times\boldsymbol{V}_0$ the pulled back formulation reads

$$\begin{bmatrix}\hat{\boldsymbol{\psi}}_s\\\hat{\mathbf{g}}_s\end{bmatrix}\in\boldsymbol{\mathcal{X}}_0:\quad \hat{\mathsf{b}}(s;\begin{bmatrix}\hat{\boldsymbol{\psi}}_s\\\hat{\mathbf{g}}_s\end{bmatrix},\begin{bmatrix}\hat{\boldsymbol{\zeta}}\\\hat{\mathbf{u}}\end{bmatrix}) = \hat{\ell}(s;\begin{bmatrix}\hat{\boldsymbol{\zeta}}\\\hat{\mathbf{u}}\end{bmatrix})\quad\forall\begin{bmatrix}\hat{\boldsymbol{\zeta}}\\\hat{\mathbf{u}}\end{bmatrix}\in\boldsymbol{\mathcal{X}}_0, \tag{5.1.33}$$

where

$$\hat{\mathsf{b}}(s;\begin{bmatrix}\hat{\boldsymbol{\psi}}\\\hat{\mathbf{g}}\end{bmatrix},\begin{bmatrix}\hat{\boldsymbol{\zeta}}\\\hat{\mathbf{u}}\end{bmatrix}) := (1+\frac{\mu}{\mu_0})\hat{\mathsf{b}}_{\mathcal{A}}(s;\hat{\boldsymbol{\psi}},\hat{\boldsymbol{\zeta}}) - 2\,\hat{\mathsf{b}}_{\mathcal{C}}(s;\hat{\mathbf{g}},\hat{\boldsymbol{\zeta}}) + 2\,\hat{\mathsf{b}}_{\mathcal{B}}(s;\hat{\boldsymbol{\psi}},\hat{\mathbf{u}}) - (1+\frac{\mu_0}{\mu})\hat{\mathsf{b}}_{\mathcal{N}}(s;\hat{\mathbf{g}},\hat{\mathbf{u}}),$$

$$\hat{\ell}(s;\begin{bmatrix}\hat{\boldsymbol{\zeta}}\\\hat{\mathbf{u}}\end{bmatrix}) := \mu_0\,\hat{\ell}_1(s;\hat{\boldsymbol{\zeta}}) + \mu_0\,\hat{\ell}_2(s;\hat{\mathbf{u}}).$$

Following the expression in (5.1.32), the field energy for the deformed configuration can be written in terms of the pulled back linear form as

$$\mathcal{E}_F(s) = -\frac{1}{2}\hat{\ell}_1(s;\hat{\boldsymbol{\psi}}_s) + \frac{1}{2}\hat{\ell}_2(s;\hat{\mathbf{g}}_s) + \frac{\mu_0}{2}\int_{\Omega_{\mathrm{src}}}\int_{\Omega_{\mathrm{src}}} G(\mathbf{x},\mathbf{y})\,\mathbf{J}(\mathbf{y})\cdot\mathbf{J}(\mathbf{x})\,d\mathbf{y}\,d\mathbf{x}.$$

Using the variational equation (5.1.33) we can write it as

$$\mathcal{E}_F(s) = \frac{1}{2\mu_0}\hat{\mathsf{b}}(s;\begin{bmatrix}\hat{\boldsymbol{\psi}}_s\\\hat{\mathbf{g}}_s\end{bmatrix},\begin{bmatrix}-\hat{\boldsymbol{\psi}}_s\\\hat{\mathbf{g}}_s\end{bmatrix}) + \frac{\mu_0}{2}\int_{\Omega_{\mathrm{src}}}\int_{\Omega_{\mathrm{src}}} G(\mathbf{x},\mathbf{y})\,\mathbf{J}(\mathbf{y})\cdot\mathbf{J}(\mathbf{x})\,d\mathbf{y}\,d\mathbf{x}.$$

5.1.2.4 BIE-Constrained Shape Derivative

To compute the shape derivative, we start by introducing the Lagrangian $\mathcal{L}:\mathbb{R}\times\boldsymbol{\mathcal{X}}_0\times\boldsymbol{\mathcal{X}}_0\to\mathbb{R}$,

$$\mathcal{L}(s;\begin{bmatrix}\hat{\boldsymbol{\psi}}\\\hat{\mathbf{g}}\end{bmatrix},\begin{bmatrix}\hat{\boldsymbol{\zeta}}\\\hat{\mathbf{u}}\end{bmatrix}) := \hat{\mathsf{b}}(s;\begin{bmatrix}\hat{\boldsymbol{\psi}}\\\hat{\mathbf{g}}\end{bmatrix},\begin{bmatrix}\hat{\boldsymbol{\zeta}}\\\hat{\mathbf{u}}\end{bmatrix}) - \hat{\ell}(s;\begin{bmatrix}\hat{\boldsymbol{\zeta}}\\\hat{\mathbf{u}}\end{bmatrix})$$

$$+ \frac{1}{2\mu_0} \hat{\mathsf{b}}(s; \begin{bmatrix} \hat{\boldsymbol{\psi}} \\ \hat{\mathbf{g}} \end{bmatrix}, \begin{bmatrix} -\hat{\boldsymbol{\psi}} \\ \hat{\mathbf{g}} \end{bmatrix}) + \frac{\mu_0}{2} \int\limits_{\Omega_{\text{src}}} \int\limits_{\Omega_{\text{src}}} G(\mathbf{x}, \mathbf{y}) \, \mathbf{J}(\mathbf{y}) \cdot \mathbf{J}(\mathbf{x}) \, d\mathbf{y} \, d\mathbf{x}.$$

Plugging in the state solution gives the field energy

$$\mathcal{L}(s; \begin{bmatrix} \hat{\boldsymbol{\psi}}_s \\ \hat{\mathbf{g}}_s \end{bmatrix}, \begin{bmatrix} \hat{\boldsymbol{\zeta}} \\ \hat{\mathbf{u}} \end{bmatrix}) = \mathcal{E}_F(s) \quad \forall \begin{bmatrix} \hat{\boldsymbol{\zeta}} \\ \hat{\mathbf{u}} \end{bmatrix} \in \boldsymbol{\mathcal{X}}_0.$$

This allows us to compute the shape derivative as

$$\frac{d\mathcal{E}_F}{ds}(0) = \frac{\partial \mathcal{L}}{\partial s}(0; \begin{bmatrix} \hat{\boldsymbol{\psi}}_0 \\ \hat{\mathbf{g}}_0 \end{bmatrix}, \begin{bmatrix} \hat{\boldsymbol{\lambda}} \\ \hat{\mathbf{p}} \end{bmatrix}),$$

where $\begin{bmatrix} \hat{\boldsymbol{\lambda}} \\ \hat{\mathbf{p}} \end{bmatrix} \in \boldsymbol{\mathcal{X}}_0$ solves the adjoint equation

$$\left\langle \frac{\partial \mathcal{L}}{\partial \begin{bmatrix} \hat{\boldsymbol{\psi}} \\ \hat{\mathbf{g}} \end{bmatrix}}(0; \begin{bmatrix} \hat{\boldsymbol{\psi}}_0 \\ \hat{\mathbf{g}}_0 \end{bmatrix}, \begin{bmatrix} \hat{\boldsymbol{\lambda}} \\ \hat{\mathbf{p}} \end{bmatrix}); \begin{bmatrix} \hat{\boldsymbol{\zeta}} \\ \hat{\mathbf{u}} \end{bmatrix} \right\rangle = 0 \quad \forall \begin{bmatrix} \hat{\boldsymbol{\zeta}} \\ \hat{\mathbf{u}} \end{bmatrix} \in \boldsymbol{\mathcal{X}}_0.$$

Computing the partial derivatives gives us the adjoint equation in an explicit form

$$\hat{\mathsf{b}}(0; \begin{bmatrix} \hat{\boldsymbol{\zeta}} \\ \hat{\mathbf{u}} \end{bmatrix}, \begin{bmatrix} \hat{\boldsymbol{\lambda}} \\ \hat{\mathbf{p}} \end{bmatrix}) + \frac{1}{2\mu_0} \hat{\mathsf{b}}(0; \begin{bmatrix} \hat{\boldsymbol{\psi}}_0 \\ \hat{\mathbf{g}}_0 \end{bmatrix}, \begin{bmatrix} -\hat{\boldsymbol{\zeta}} \\ \hat{\mathbf{u}} \end{bmatrix}) + \frac{1}{2\mu_0} \hat{\mathsf{b}}(0; \begin{bmatrix} \hat{\boldsymbol{\zeta}} \\ \hat{\mathbf{u}} \end{bmatrix}, \begin{bmatrix} -\hat{\boldsymbol{\psi}}_0 \\ \hat{\mathbf{g}}_0 \end{bmatrix}) = 0 \quad \forall \begin{bmatrix} \hat{\boldsymbol{\zeta}} \\ \hat{\mathbf{u}} \end{bmatrix} \in \boldsymbol{\mathcal{X}}_0.$$

To simplify the adjoint equation we observe the relation

$$\hat{\mathsf{b}}(0; \begin{bmatrix} \hat{\boldsymbol{\psi}}_0 \\ \hat{\mathbf{g}}_0 \end{bmatrix}, \begin{bmatrix} -\hat{\boldsymbol{\zeta}} \\ \hat{\mathbf{u}} \end{bmatrix}) = -(1 + \frac{\mu}{\mu_0}) \hat{\mathsf{b}}_{\mathcal{A}}(0; \hat{\boldsymbol{\psi}}_0, \hat{\boldsymbol{\zeta}}) + 2\, \hat{\mathsf{b}}_{\mathcal{C}}(0; \hat{\mathbf{g}}_0, \hat{\boldsymbol{\zeta}}) + 2\, \hat{\mathsf{b}}_{\mathcal{B}}(0; \hat{\boldsymbol{\psi}}_0, \hat{\mathbf{u}}) - (1 + \frac{\mu_0}{\mu}) \hat{\mathsf{b}}_{\mathcal{N}}(0; \hat{\mathbf{g}}_0, \hat{\mathbf{u}})$$

$$= \hat{\mathsf{b}}(0; \begin{bmatrix} \hat{\boldsymbol{\zeta}} \\ \hat{\mathbf{u}} \end{bmatrix}, \begin{bmatrix} -\hat{\boldsymbol{\psi}}_0 \\ \hat{\mathbf{g}}_0 \end{bmatrix}),$$

where we used the symmetry of $\hat{\mathsf{b}}_{\mathcal{A}}$ and $\hat{\mathsf{b}}_{\mathcal{N}}$. The adjoint equation then reduces to the simple form

$$\hat{\mathsf{b}}(0; \begin{bmatrix} \hat{\boldsymbol{\zeta}} \\ \hat{\mathbf{u}} \end{bmatrix}, \begin{bmatrix} \hat{\boldsymbol{\lambda}} \\ \hat{\mathbf{p}} \end{bmatrix}) + \hat{\mathsf{b}}(0; \begin{bmatrix} \hat{\boldsymbol{\zeta}} \\ \hat{\mathbf{u}} \end{bmatrix}, \frac{1}{\mu_0} \begin{bmatrix} -\hat{\boldsymbol{\psi}}_0 \\ \hat{\mathbf{g}}_0 \end{bmatrix}) = 0 \quad \forall \begin{bmatrix} \hat{\boldsymbol{\zeta}} \\ \hat{\mathbf{u}} \end{bmatrix} \in \boldsymbol{\mathcal{X}}_0. \tag{5.1.34}$$

We get the adjoint solution in an explicit form as

$$\begin{bmatrix} \hat{\boldsymbol{\lambda}} \\ \hat{\mathbf{p}} \end{bmatrix} = \frac{1}{\mu_0} \begin{bmatrix} \hat{\boldsymbol{\psi}}_0 \\ -\hat{\mathbf{g}}_0 \end{bmatrix}.$$

The shape derivative can be written as

$$\frac{d\mathcal{E}_F}{ds}(0) = \frac{\partial \mathcal{L}}{\partial s}(0; \begin{bmatrix} \hat{\boldsymbol{\psi}}_0 \\ \hat{\mathbf{g}}_0 \end{bmatrix}, \frac{1}{\mu_0} \begin{bmatrix} \hat{\boldsymbol{\psi}}_0 \\ -\hat{\mathbf{g}}_0 \end{bmatrix})$$

$$= \frac{1}{\mu_0} \frac{\partial \hat{\mathsf{b}}}{\partial s}(0; \begin{bmatrix} \hat{\boldsymbol{\psi}}_0 \\ \hat{\mathbf{g}}_0 \end{bmatrix}, \begin{bmatrix} \hat{\boldsymbol{\psi}}_0 \\ -\hat{\mathbf{g}}_0 \end{bmatrix}) - \frac{1}{\mu_0} \frac{\partial \hat{\ell}}{\partial s}(0; \begin{bmatrix} \hat{\boldsymbol{\psi}}_0 \\ -\hat{\mathbf{g}}_0 \end{bmatrix}) + \frac{1}{2\mu_0} \frac{\partial \hat{\mathsf{b}}}{\partial s}(0; \begin{bmatrix} \hat{\boldsymbol{\psi}}_0 \\ \hat{\mathbf{g}}_0 \end{bmatrix}, \begin{bmatrix} -\hat{\boldsymbol{\psi}}_0 \\ \hat{\mathbf{g}}_0 \end{bmatrix})$$

$$= \frac{1}{2\mu_0} \frac{\partial \hat{\mathsf{b}}}{\partial s}(0; \begin{bmatrix} \hat{\boldsymbol{\psi}}_0 \\ \hat{\mathbf{g}}_0 \end{bmatrix}, \begin{bmatrix} \hat{\boldsymbol{\psi}}_0 \\ -\hat{\mathbf{g}}_0 \end{bmatrix}) - \frac{1}{\mu_0} \frac{\partial \hat{\ell}}{\partial s}(0; \begin{bmatrix} \hat{\boldsymbol{\psi}}_0 \\ -\hat{\mathbf{g}}_0 \end{bmatrix})$$

$$= \frac{1}{2\mu_0} \left\{ (1 + \frac{\mu}{\mu_0}) \frac{\partial \hat{\mathsf{b}}_{\mathcal{A}}}{\partial s}(0; \hat{\boldsymbol{\psi}}_0, \hat{\boldsymbol{\psi}}_0) - 2 \frac{\partial \hat{\mathsf{b}}_{\mathcal{C}}}{\partial s}(0; \hat{\mathbf{g}}_0, \hat{\boldsymbol{\psi}}_0) - 2 \frac{\partial \hat{\mathsf{b}}_{\mathcal{B}}}{\partial s}(0; \hat{\boldsymbol{\psi}}_0, \hat{\mathbf{g}}_0) + (1 + \frac{\mu_0}{\mu}) \frac{\partial \hat{\mathsf{b}}_{\mathcal{N}}}{\partial s}(0; \hat{\mathbf{g}}_0, \hat{\mathbf{g}}_0) \right\}$$

$$- \left\{ \frac{\partial \hat{\ell}_1}{\partial s}(0; \hat{\boldsymbol{\psi}}_0) - \frac{\partial \hat{\ell}_2}{\partial s}(0; \hat{\mathbf{g}}_0) \right\}. \tag{5.1.35}$$

We list all the partial derivatives with respect to s which will be used in evaluating the above expression

$$\frac{\partial \hat{\mathsf{b}}_{\mathcal{A}}}{\partial s}(0; \hat{\boldsymbol{\psi}}, \hat{\boldsymbol{\zeta}}) = \int_{\Gamma^0} \int_{\Gamma^0} \{\nabla_{\mathbf{x}} G(\mathbf{x}, \mathbf{y}) \cdot \boldsymbol{\mathcal{V}}(\mathbf{x}) + \nabla_{\mathbf{y}} G(\mathbf{x}, \mathbf{y}) \cdot \boldsymbol{\mathcal{V}}(\mathbf{y})\} \, \hat{\boldsymbol{\psi}}(\mathbf{y}) \cdot \hat{\boldsymbol{\zeta}}(\mathbf{x}) \, d\mathrm{S}_{\mathbf{y}} \, d\mathrm{S}_{\mathbf{x}}$$

$$+ \int_{\Gamma^0} \int_{\Gamma^0} G(\mathbf{x}, \mathbf{y}) \left\{ (\mathsf{D}\boldsymbol{\mathcal{V}}(\mathbf{y}) \, \hat{\boldsymbol{\psi}}(\mathbf{y})) \cdot \hat{\boldsymbol{\zeta}}(\mathbf{x}) + \hat{\boldsymbol{\psi}}(\mathbf{y}) \cdot (\mathsf{D}\boldsymbol{\mathcal{V}}(\mathbf{x}) \, \hat{\boldsymbol{\zeta}}(\mathbf{x})) \right\} d\mathrm{S}_{\mathbf{y}} \, d\mathrm{S}_{\mathbf{x}},$$

$$\frac{\partial \hat{\mathsf{b}}_{\mathcal{C}}}{\partial s}(0; \hat{\mathbf{g}}, \hat{\boldsymbol{\zeta}}) = \int_{\Gamma^0} \int_{\Gamma^0} \left(\nabla_{\mathbf{x}} G(\mathbf{x}, \mathbf{y}) \times \left(\mathsf{D}\boldsymbol{\mathcal{V}}(\mathbf{y})\{\hat{\mathbf{n}}(\mathbf{y}) \times \hat{\mathbf{g}}(\mathbf{y})\} \right) \right) \cdot \hat{\boldsymbol{\zeta}}(\mathbf{x}) \, d\mathrm{S}_{\mathbf{y}} \, d\mathrm{S}_{\mathbf{x}}$$

$$+ \int_{\Gamma^0} \int_{\Gamma^0} \left(\nabla_{\mathbf{x}} G(\mathbf{x}, \mathbf{y}) \times \left(\hat{\mathbf{n}}(\mathbf{y}) \times \hat{\mathbf{g}}(\mathbf{y}) \right) \right) \cdot \left(\mathsf{D}\boldsymbol{\mathcal{V}}(\mathbf{x}) \, \hat{\boldsymbol{\zeta}}(\mathbf{x}) \right) d\mathrm{S}_{\mathbf{y}} \, d\mathrm{S}_{\mathbf{x}}$$

$$+ \int_{\Gamma^0} \int_{\Gamma^0} \left(\frac{d\nabla_{\mathbf{x}} G(\mathbf{T}_s^{\boldsymbol{\nu}}(\mathbf{x}), \mathbf{T}_s^{\boldsymbol{\nu}}(\mathbf{y}))}{ds} \Big|_{s=0} \times \left(\hat{\mathbf{n}}(\mathbf{y}) \times \hat{\mathbf{g}}(\mathbf{y}) \right) \right) \cdot \hat{\boldsymbol{\zeta}}(\mathbf{x}) \, d\mathrm{S}_{\mathbf{y}} \, d\mathrm{S}_{\mathbf{x}}, \tag{5.1.36}$$

$$\frac{\partial \hat{\mathsf{b}}_{\mathcal{N}}}{\partial s}(0; \hat{\mathbf{g}}, \hat{\mathbf{u}}) = - \int_{\Gamma^0} \int_{\Gamma^0} \{\nabla_{\mathbf{x}} G(\mathbf{x}, \mathbf{y}) \cdot \boldsymbol{\mathcal{V}}(\mathbf{x}) + \nabla_{\mathbf{y}} G(\mathbf{x}, \mathbf{y}) \cdot \boldsymbol{\mathcal{V}}(\mathbf{y})\} \, \mathrm{curl}_{\Gamma} \, \hat{\mathbf{g}}(\mathbf{y}) \, \mathrm{curl}_{\Gamma} \, \hat{\mathbf{u}}(\mathbf{x}) \, d\mathrm{S}_{\mathbf{y}} \, d\mathrm{S}_{\mathbf{x}},$$

$$\frac{\partial \hat{\ell}_1}{\partial s}(0; \hat{\boldsymbol{\zeta}}) = \int_{\Gamma^0} \int_{\Omega_{\mathrm{src}}} G(\mathbf{x}, \mathbf{y}) \, \mathbf{J}(\mathbf{y}) \cdot \left(\mathsf{D}\boldsymbol{\mathcal{V}}(\mathbf{x}) \, \hat{\boldsymbol{\zeta}}(\mathbf{x}) \right) d\mathbf{y} \, d\mathrm{S}_{\mathbf{x}}$$

$$+ \int_{\Gamma^0} \int_{\Omega_{\mathrm{src}}} \nabla_{\mathbf{x}} G(\mathbf{x}, \mathbf{y}) \cdot \boldsymbol{\mathcal{V}}(\mathbf{x}) \, \mathbf{J}(\mathbf{y}) \cdot \hat{\boldsymbol{\zeta}}(\mathbf{x}) \, d\mathbf{y} \, d\mathrm{S}_{\mathbf{x}},$$

$$\frac{\partial \hat{\ell}_2}{\partial s}(0; \hat{\mathbf{u}}) = \int_{\Gamma^0} \int_{\Omega_{\mathrm{src}}} \left(\nabla_{\mathbf{x}} G(\mathbf{x}, \mathbf{y}) \times \mathbf{J}(\mathbf{y}) \right) \cdot \left(\mathsf{D}\boldsymbol{\mathcal{V}}(\mathbf{x})\{\hat{\mathbf{n}}(\mathbf{x}) \times \hat{\mathbf{u}}(\mathbf{x})\} \right) d\mathbf{y} \, d\mathrm{S}_{\mathbf{x}}$$

$$+ \int_{\Gamma^0} \int_{\Omega_{\mathrm{src}}} \left(\frac{d\nabla_{\mathbf{x}} G(\mathbf{T}_s^{\boldsymbol{\nu}}(\mathbf{x}), \mathbf{y})}{ds} \Big|_{s=0} \times \mathbf{J}(\mathbf{y}) \right) \cdot \left(\hat{\mathbf{n}}(\mathbf{x}) \times \hat{\mathbf{u}}(\mathbf{x}) \right) d\mathbf{y} \, d\mathrm{S}_{\mathbf{x}}.$$

The partial derivative for $\nabla_x G(\mathbf{T}_s^{\boldsymbol{\nu}}(\hat{\mathbf{x}}), \mathbf{T}_s^{\boldsymbol{\nu}}(\hat{\mathbf{y}}))$ with respect to s is given as

$$\frac{d\nabla_{\boldsymbol{x}} G(\mathbf{T}_s^{\boldsymbol{\nu}}(\hat{\mathbf{x}}), \mathbf{T}_s^{\boldsymbol{\nu}}(\hat{\boldsymbol{y}}))}{ds} \bigg|_{s=0} = \mathsf{D}_x \nabla_x G(\hat{\mathbf{x}}, \hat{\mathbf{y}}) \, \boldsymbol{\mathcal{V}}(\hat{\mathbf{x}}) + \mathsf{D}_y \nabla_x G(\hat{\mathbf{x}}, \hat{\mathbf{y}}) \, \boldsymbol{\mathcal{V}}(\hat{\mathbf{y}}) \tag{5.1.37}$$

$$= \nabla_x \nabla_x G(\hat{\mathbf{x}}, \hat{\mathbf{y}}) \Big(\boldsymbol{\mathcal{V}}(\hat{\mathbf{x}}) - \boldsymbol{\mathcal{V}}(\hat{\mathbf{y}}) \Big), \tag{5.1.38}$$

where

$$\nabla_y \nabla_y G(\mathbf{x}, \mathbf{y}) = \nabla_x \nabla_x G(\mathbf{x}, \mathbf{y}) = \frac{3}{4\pi} \frac{(\mathbf{x} - \mathbf{y})(\mathbf{x} - \mathbf{y})^T}{\|\mathbf{x} - \mathbf{y}\|^5} - \frac{1}{4\pi} \frac{\mathsf{Id}}{\|\mathbf{x} - \mathbf{y}\|^3}. \tag{5.1.39}$$

Similarly

$$\frac{d \nabla_{\mathbf{x}} G(\mathbf{T}_s^{\boldsymbol{\nu}}(\mathbf{x}), \mathbf{y})}{ds} \Big|_{s=0} = \mathsf{D}_x \nabla_x G(\mathbf{x}, \mathbf{y}) \, \boldsymbol{\mathcal{V}}(\mathbf{x}) = \nabla_x \nabla_x G(\mathbf{x}, \mathbf{y}) \, \boldsymbol{\mathcal{V}}(\mathbf{x}). \tag{5.1.40}$$

5.1.2.5 Shape Derivative From Volume Based Variational Formulation

We need the following weighted Sobolev space for physical vector potential solutions in the whole space $\mathbb{R}^3$ [33]

$$\boldsymbol{V}(\mathbb{R}^3) := \{ \mathbf{u} \in \boldsymbol{\mathcal{D}}(\mathbb{R}^3)', \ \frac{\mathbf{u}(\mathbf{x})}{\sqrt{1 + \|\mathbf{x}\|^2}} \in \boldsymbol{L}^2(\mathbb{R}^3), \ \mathbf{curl u} \in \boldsymbol{L}^2(\mathbb{R}^3), \ \text{div } \mathbf{u} = 0 \text{ in } \mathbb{R}^3 \}.$$

Writing $\boldsymbol{V} = \boldsymbol{V}(\mathbb{R}^3)$, the transmission problem (5.1.28) has a weak solution that satisfies the following variational formulation

$$\mathbf{A} \in \boldsymbol{V} : \quad \int_{\mathbb{R}^3} \mu^{-1}(\mathbf{x}) \, \mathbf{curl A}(\mathbf{x}) \cdot \mathbf{curl A}'(\mathbf{x}) \, d\mathbf{x} = \int_{\Omega_{\mathrm{src}}} \mathbf{J}(\mathbf{x}) \cdot \mathbf{A}'(\mathbf{x}) \, d\mathbf{x} \quad \forall \mathbf{A}' \in \boldsymbol{V}. \tag{5.1.41}$$

The field energy expression can be written in terms of the vector potential

$$\mathcal{E}_F = \frac{1}{2} \int_{\mathbb{R}^3} \mu^{-1}(\mathbf{x}) \, \|\mathbf{curl A}(\mathbf{x})\|^2 \, d\mathbf{x}.$$

5.1.2.6 Energy Shape Derivative

We deform the system using $\boldsymbol{\mathcal{V}}$ such that $\boldsymbol{\mathcal{V}} \equiv 0$ around the source current. So we deform only the material occupying Ω^0. The permeability is transformed like a 0-form: permeability for the s configuration is $\mu_s(\mathbf{x})$ and satisfies $\mu(\hat{\mathbf{x}}) = \mu_s(\mathbf{T}_s^{\boldsymbol{\nu}}(\hat{\mathbf{x}}))$. The variational formulation for the s configuration is similar to (5.1.41) in structure

$$\mathbf{A}_s \in \boldsymbol{V} : \quad \int_{\mathbb{R}^3} \mu_s^{-1}(\mathbf{x}) \, \mathbf{curl A}_s(\mathbf{x}) \cdot \mathbf{curl A}'(\mathbf{x}) \, d\mathbf{x} = \int_{\Omega_{\mathrm{src}}} \mathbf{J}(\mathbf{x}) \cdot \mathbf{A}'(\mathbf{x}) \, d\mathbf{x} \quad \forall \mathbf{A}' \in \boldsymbol{V}.$$

Transforming the integral on the LHS using the perturbation map gives us:

$$\int_{\mathbb{R}^3} \mu_s^{-1}(\mathbf{T}_s^{\boldsymbol{\nu}}(\hat{\mathbf{x}})) \, (\mathbf{curl A}_s)(\mathbf{T}_s^{\boldsymbol{\nu}}(\hat{\mathbf{x}})) \cdot (\mathbf{curl A}')(\mathbf{T}_s^{\boldsymbol{\nu}}(\hat{\mathbf{x}})) \, | \det \mathsf{D}\mathbf{T}_s^{\boldsymbol{\nu}}(\hat{\mathbf{x}})| \, d\hat{\mathbf{x}} = \int_{\Omega_{\mathrm{src}}} \mathbf{J}(\hat{\mathbf{x}}) \cdot \mathbf{A}'(\hat{\mathbf{x}}) \, d\hat{\mathbf{x}}.$$

The right-hand side remains unchanged since the velocity field is zero around Ω_{src}. We use the following pullback for the curl of the vector potential which transforms like 2-forms:

$$(\mathbf{curl\,A})(\mathbf{T}_s^{\boldsymbol{\nu}}(\hat{\mathbf{x}})) = \frac{1}{\det \mathsf{DT}_s^{\boldsymbol{\nu}}(\hat{\mathbf{x}})} \mathsf{DT}_s^{\boldsymbol{\nu}}(\hat{\mathbf{x}}) \, \mathbf{curl}\hat{\mathbf{A}}(\hat{\mathbf{x}}).$$

Denoting the pullback of $\mathbf{A}_s$ by $\hat{\mathbf{A}}_s$, using the pullback relation $\mathbf{A}(\mathbf{T}_s^{\boldsymbol{\nu}}(\hat{\mathbf{x}})) = \mathsf{DT}_s^{\boldsymbol{\nu}}(\hat{\mathbf{x}})^{-T}\hat{\mathbf{A}}(\hat{\mathbf{x}})$ from Section 3.0.4.2, we get the pulled back variational formulation: seek $\hat{\mathbf{A}}_s \in \boldsymbol{V}$ such that

$$\int\limits_{\mathbb{R}^3} \mu^{-1}(\hat{\mathbf{x}}) \, (\mathsf{DT}_s^{\boldsymbol{\nu}}(\hat{\mathbf{x}}) \, \mathbf{curl}\hat{\mathbf{A}}_s(\hat{\mathbf{x}})) \cdot (\mathsf{DT}_s^{\boldsymbol{\nu}}(\hat{\mathbf{x}}) \, \mathbf{curl}\hat{\mathbf{A}}'(\hat{\mathbf{x}})) \, \frac{1}{|\det \mathsf{DT}_s^{\boldsymbol{\nu}}(\hat{\mathbf{x}})|} \, d\hat{\mathbf{x}}$$

$$= \int\limits_{\Omega_{\text{src}}} \mathbf{J}(\hat{\mathbf{x}}) \cdot \mathbf{A}'(\hat{\mathbf{x}}) \, d\hat{\mathbf{x}} \quad \forall \mathbf{A}' \in \boldsymbol{V}. \quad (5.1.42)$$

To write things compactly we introduce the (bi)linear forms

$$\hat{\mathrm{b}}(s; \hat{\mathbf{A}}, \hat{\mathbf{A}}') := \int\limits_{\mathbb{R}^3} \mu^{-1}(\hat{\mathbf{x}}) \, (\mathsf{DT}_s^{\boldsymbol{\nu}}(\hat{\mathbf{x}}) \, \mathbf{curl}\hat{\mathbf{A}}(\hat{\mathbf{x}})) \cdot (\mathsf{DT}_s^{\boldsymbol{\nu}}(\hat{\mathbf{x}}) \, \mathbf{curl}\hat{\mathbf{A}}'(\hat{\mathbf{x}})) \, \frac{1}{|\det \mathsf{DT}_s^{\boldsymbol{\nu}}(\hat{\mathbf{x}})|} \, d\hat{\mathbf{x}},$$

$$\hat{\mathrm{l}}(s; \hat{\mathbf{A}}') := \int\limits_{\Omega_{\text{src}}} \mathbf{J}(\hat{\mathbf{x}}) \cdot \hat{\mathbf{A}}'(\hat{\mathbf{x}}) \, d\hat{\mathbf{x}}.$$

The pulled back variational formulation can be written as

$$\hat{\mathbf{A}}_s \in \boldsymbol{V} : \quad \hat{\mathrm{b}}(s; \hat{\mathbf{A}}_s, \hat{\mathbf{A}}') = \hat{\mathrm{l}}(s; \hat{\mathbf{A}}') \quad \forall \hat{\mathbf{A}}' \in \boldsymbol{V}.$$

The field energy for the deformed s configuration $\mathcal{E}_F(s)$ can be written in terms of the pulled back bilinear form $\hat{\mathrm{b}}$ as

$$\mathcal{E}_F(s) = \frac{1}{2}\hat{\mathrm{b}}(s; \hat{\mathbf{A}}_s, \hat{\mathbf{A}}_s).$$

For using the adjoint method, we start by defining the Lagrangian $\mathcal{L} : \mathbb{R} \times \boldsymbol{V} \times \boldsymbol{V} \to \mathbb{R}$,

$$\mathcal{L}(s; \hat{\mathbf{A}}, \hat{\mathbf{A}}') := \hat{\mathrm{b}}(s; \hat{\mathbf{A}}, \hat{\mathbf{A}}') - \hat{\mathrm{l}}(s; \hat{\mathbf{A}}') + \frac{1}{2}\hat{\mathrm{b}}(s; \hat{\mathbf{A}}, \hat{\mathbf{A}}).$$

Plugging in the state solution gives us

$$\mathcal{L}(s; \hat{\mathbf{A}}_s, \hat{\mathbf{A}}') = \mathcal{E}_F(s) \quad \forall \hat{\mathbf{A}}' \in \boldsymbol{V}.$$

The shape derivative can be computed as

$$\frac{d\mathcal{E}_F}{ds}(0) = \frac{\partial \mathcal{L}}{\partial s}(0; \hat{\mathbf{A}}_0, \hat{\mathbf{P}}),$$

where $\hat{\mathbf{P}} \in \boldsymbol{V}$ solves the adjoint equation

$$\left\langle \frac{\partial \mathcal{L}}{\partial \hat{\mathbf{A}}}(0; \hat{\mathbf{A}}_0, \hat{\mathbf{P}}); \hat{\mathbf{A}}' \right\rangle = 0 \quad \forall \hat{\mathbf{A}}' \in \boldsymbol{V}.$$

The adjoint equation can be written explicitly as

$$\hat{b}(0; \hat{\mathbf{P}}, \hat{\mathbf{A}}') + \hat{b}(0; \hat{\mathbf{A}}_0, \hat{\mathbf{A}}') = 0 \quad \forall \hat{\mathbf{A}}' \in \mathbf{V},$$

which yields the adjoint solution $\hat{\mathbf{P}} = -\hat{\mathbf{A}}_0$. Thus the energy shape derivative is

$$\frac{d\mathcal{E}_F}{ds}(0) = -\frac{1}{2} \int_{\mathbb{R}^3} \mu^{-1}(\hat{\mathbf{x}}) \left\{ \begin{array}{l} \mathsf{D}\boldsymbol{\mathcal{V}}(\hat{\mathbf{x}}) \mathbf{curl}\hat{\mathbf{A}}_0 \cdot \mathbf{curl}\hat{\mathbf{A}}_0(\hat{\mathbf{x}}) + \mathbf{curl}\hat{\mathbf{A}}_0(\hat{\mathbf{x}}) \cdot \mathsf{D}\boldsymbol{\mathcal{V}}(\hat{\mathbf{x}}) \mathbf{curl}\hat{\mathbf{A}}_0 \\ - \mathbf{curl}\hat{\mathbf{A}}_0(\hat{\mathbf{x}}) \cdot \mathbf{curl}\hat{\mathbf{A}}_0(\hat{\mathbf{x}}) \, \nabla \cdot \boldsymbol{\mathcal{V}}(\hat{\mathbf{x}}) \end{array} \right\} d\hat{\mathbf{x}}.$$

$$(5.1.43)$$

The shape derivative can be simplified further. The integral can be split into integrals over $\mathbb{R}^3$ into Ω and Ω_c. Writing the magnetic flux intensity $\mathbf{B}$ in place of $\mathbf{curl A}_0$ we get

$$\frac{d\mathcal{E}_F}{ds}(0) = -\frac{\mu^{-1}}{2} \int_\Omega \{\mathbf{B}^T(\mathsf{D}\boldsymbol{\mathcal{V}} + \mathsf{D}\boldsymbol{\mathcal{V}}^T)\mathbf{B} - \|\mathbf{B}\|^2 \, \nabla \cdot \boldsymbol{\mathcal{V}}\} \, d\mathbf{x}$$

$$- \frac{\mu_0^{-1}}{2} \int_{\Omega_c} \{\mathbf{B}^T(\mathsf{D}\boldsymbol{\mathcal{V}} + \mathsf{D}\boldsymbol{\mathcal{V}}^T)\mathbf{B} - \|\mathbf{B}\|^2 \, \nabla \cdot \boldsymbol{\mathcal{V}}\} \, d\mathbf{x}.$$

The expression $\mathbf{B}^T(\mathsf{D}\boldsymbol{\mathcal{V}} + \mathsf{D}\boldsymbol{\mathcal{V}})\mathbf{B}$ in the integrands above can be simplified further as

$$\mathbf{B}^T(\mathsf{D}\boldsymbol{\mathcal{V}} + \mathsf{D}\boldsymbol{\mathcal{V}}^T)\mathbf{B} = 2\mathbf{B}^T \, \nabla\boldsymbol{\mathcal{V}} \, \mathbf{B} = 2\mathbf{B}^T(\nabla(\mathbf{B} \cdot \boldsymbol{\mathcal{V}}) - \nabla\mathbf{B} \, \boldsymbol{\mathcal{V}}) = 2\mathbf{B}^T\nabla(\mathbf{B} \cdot \boldsymbol{\mathcal{V}}) - 2\mathbf{B}^T\nabla\mathbf{B} \, \boldsymbol{\mathcal{V}}$$

$$= 2\operatorname{div}((\mathbf{B} \cdot \boldsymbol{\mathcal{V}}) \, \mathbf{B}) - 2\mathbf{B}^T\nabla\mathbf{B} \, \boldsymbol{\mathcal{V}} = 2\operatorname{div}(\mathbf{B}\mathbf{B}^T \, \boldsymbol{\mathcal{V}}) - 2\mathbf{B}^T\nabla\mathbf{B} \, \boldsymbol{\mathcal{V}}.$$

The expression $\|\mathbf{B}\|^2 \, \nabla \cdot \boldsymbol{\mathcal{V}}$ can be replaced using the following relation

$$\operatorname{div}(\|\mathbf{B}\|^2 \, \boldsymbol{\mathcal{V}}) = 2 \, \boldsymbol{\mathcal{V}}^T\nabla\mathbf{B} \, \mathbf{B} + \|\mathbf{B}\|^2 \, \nabla \cdot \boldsymbol{\mathcal{V}}.$$

The whole integrand then becomes

$$2\operatorname{div}(\mathbf{B}\mathbf{B}^T \, \boldsymbol{\mathcal{V}} - \frac{\|\mathbf{B}\|^2}{2} \, \boldsymbol{\mathcal{V}}) + 2 \, \boldsymbol{\mathcal{V}}^T(\nabla\mathbf{B} \, - \nabla\mathbf{B}^T)\mathbf{B}.$$

The above expression can be simplified further by observing that

$$\nabla\mathbf{B} - \nabla\mathbf{B}^T = \begin{bmatrix} \partial_1 B_1 & \partial_1 B_2 & \partial_1 B_3 \\ \partial_2 B_1 & \partial_2 B_2 & \partial_2 B_3 \\ \partial_3 B_1 & \partial_3 B_2 & \partial_3 B_3 \end{bmatrix} - \begin{bmatrix} \partial_1 B_1 & \partial_2 B_1 & \partial_3 B_1 \\ \partial_1 B_2 & \partial_2 B_2 & \partial_3 B_2 \\ \partial_1 B_3 & \partial_2 B_3 & \partial_3 B_3 \end{bmatrix}$$

$$= \begin{bmatrix} 0 & \partial_1 B_2 - \partial_2 B_1 & \partial_1 B_3 - \partial_3 B_1 \\ \partial_2 B_1 - \partial_1 B_2 & 0 & \partial_2 B_3 - \partial_3 B_2 \\ \partial_3 B_1 - \partial_1 B_3 & \partial_3 B_2 - \partial_2 B_3 & 0 \end{bmatrix}.$$

Thus the product $(\nabla\mathbf{B} - \nabla\mathbf{B}^T)\mathbf{B}$ becomes

$$\begin{bmatrix} 0 & \partial_1 B_2 - \partial_2 B_1 & \partial_1 B_3 - \partial_3 B_1 \\ \partial_2 B_1 - \partial_1 B_2 & 0 & \partial_2 B_3 - \partial_3 B_2 \\ \partial_3 B_1 - \partial_1 B_3 & \partial_3 B_2 - \partial_2 B_3 & 0 \end{bmatrix} \begin{bmatrix} B_1 \\ B_2 \\ B_3 \end{bmatrix}$$

131

$$
= \begin{bmatrix} (\partial_1 B_2 - \partial_2 B_1)B_2 + (\partial_1 B_3 - \partial_3 B_1)B_3 \\ (\partial_2 B_1 - \partial_1 B_2)B_1 + (\partial_2 B_3 - \partial_3 B_2)B_3 \\ (\partial_3 B_1 - \partial_1 B_3)B_1 + (\partial_3 B_2 - \partial_2 B_3)B_2 \end{bmatrix} = \begin{bmatrix} (\mathbf{curlB})_3 B_2 - (\mathbf{curlB})_2 B_3 \\ (\mathbf{curlB})_1 B_3 - (\mathbf{curlB})_3 B_1 \\ (\mathbf{curlB})_2 B_1 - (\mathbf{curlB})_1 B_2 \end{bmatrix} = \mathbf{B} \times \mathbf{curlB}.
$$

$$(5.1.44)$$

Combining all these simplifications, the shape derivative reduces to

$$
= -\mu^{-1} \int_\Omega \operatorname{div}(\mathbf{B}\mathbf{B}^T \, \boldsymbol{\mathcal{V}} - \frac{\|\mathbf{B}\|^2}{2} \, \boldsymbol{\mathcal{V}}) \, d\mathbf{x} - \mu_0^{-1} \int_{\Omega_c} \operatorname{div}(\mathbf{B}\mathbf{B}^T \, \boldsymbol{\mathcal{V}} - \frac{\|\mathbf{B}\|^2}{2} \, \boldsymbol{\mathcal{V}}) - \int_{\Omega_{\mathrm{src}}} \boldsymbol{\mathcal{V}} \cdot (\mathbf{B} \times \mathbf{J}) \, d\mathbf{x}
$$

$$
= -\mu^{-1} \int_\Omega \operatorname{div}(\mathbf{B}\mathbf{B}^T \, \boldsymbol{\mathcal{V}} - \frac{\|\mathbf{B}\|^2}{2} \, \boldsymbol{\mathcal{V}}) \, d\mathbf{x} - \mu_0^{-1} \int_{\Omega_c} \operatorname{div}(\mathbf{B}\mathbf{B}^T \, \boldsymbol{\mathcal{V}} - \frac{\|\mathbf{B}\|^2}{2} \, \boldsymbol{\mathcal{V}}).
$$

Using divergence theorem, the formula reduces to

$$
\int_{\Gamma^0} \boldsymbol{\mathcal{V}}^T \left[\!\!\left[\overleftrightarrow{\mathbf{T}}(\mathbf{B}) \right]\!\!\right]_\Gamma \mathbf{n} \, d\mathrm{S},
$$

where we have the Maxwell Stress Tensor

$$
\overleftrightarrow{\mathbf{T}}(\mathbf{B})(\mathbf{x}) := \mu(\mathbf{x})^{-1} \Big\{ \mathbf{B}\mathbf{B}^T - \frac{\|\mathbf{B}\|^2}{2} \mathsf{Id} \Big\}.
$$

Finally using the transmission conditions, the shape derivative reduces to the Hadamard form and we recover the same expression obtained using the scalar potential formulation in (5.1.25)

$$
\frac{d\mathcal{E}_F}{ds}(0) = \int_{\Gamma^0} \left\{ \frac{B_n^2 \, [\![\mu^{-1}]\!]_\Gamma}{2} - \frac{H_\tau^2 \, [\![\mu]\!]_\Gamma}{2} \right\} \boldsymbol{\mathcal{V}} \cdot \mathbf{n} \, d\mathrm{S}. \tag{5.1.45}
$$

where B_n is the normal component of $\mathbf{B}$ and H_τ is the tangential component of $\mathbf{H}$. Notice that this formula matches with the force formula in literature [6].

5.1.2.7 Note on "Holding the Fluxes Constant"

We inspect the shape derivative in 5.1.43 which is given as

$$
\frac{d\mathcal{E}_F}{ds}(0) = -\frac{1}{2} \frac{d}{ds} \Big(\int_{\mathbb{R}^3} \mu^{-1}(\hat{\mathbf{x}}) \left\| \mathsf{D}\mathbf{T}_s^{\boldsymbol{\nu}}(\hat{\mathbf{x}}) \, \mathbf{curl}\hat{\mathbf{A}}_0(\hat{\mathbf{x}}) \right\|^2 \frac{1}{\det \mathsf{D}\mathbf{T}_s^{\boldsymbol{\nu}}(\hat{\mathbf{x}})} \, d\hat{\mathbf{x}} \Big).
$$

Consider that the vector potential $\hat{\mathbf{A}}_0$ in the reference configuration is moved by $\mathbf{T}_s^{\boldsymbol{\nu}}$ as a 1-form to $\mathbf{A}_s^*$ such that $\mathbf{A}_s^*(\mathbf{T}_s^{\boldsymbol{\nu}}(\hat{\mathbf{x}})) = \mathsf{D}\mathbf{T}_s^{\boldsymbol{\nu}}(\hat{\mathbf{x}})^{-T} \hat{\mathbf{A}}_0(\hat{\mathbf{x}})$. For its curl, a 2-form, we have the pullback relation

$$
\mathbf{curl}\mathbf{A}_s^*(\mathbf{T}_s^{\boldsymbol{\nu}}(\hat{\mathbf{x}})) = \frac{\mathsf{D}\mathbf{T}_s^{\boldsymbol{\nu}}(\hat{\mathbf{x}}) \, \mathbf{curl}\hat{\mathbf{A}}_0(\hat{\mathbf{x}})}{\det \mathsf{D}\mathbf{T}_s^{\boldsymbol{\nu}}(\hat{\mathbf{x}})}.
$$

Thus we can write

$$\frac{d\mathcal{E}_F}{ds}(0) = -\frac{1}{2}\frac{d}{ds}\left(\int_{\mathbb{R}^3} \mu^{-1}(\hat{\mathbf{x}})\left\|\mathsf{D}\mathbf{T}_s^{\boldsymbol{\nu}}(\hat{\mathbf{x}})\,\mathbf{curl}\hat{\mathbf{A}}_0(\hat{\mathbf{x}})\right\|^2\,\frac{1}{\det\mathsf{D}\mathbf{T}_s^{\boldsymbol{\nu}}(\hat{\mathbf{x}})}\,d\hat{\mathbf{x}}\right)\Big|_{s=0}$$

$$= -\frac{1}{2}\frac{d}{ds}\left(\int_{\mathbb{R}^3} \mu_s^{-1}(\mathbf{T}_s^{\boldsymbol{\nu}}(\hat{\mathbf{x}}))\,\|\mathbf{curl}\mathbf{A}_s^*(\mathbf{T}_s^{\boldsymbol{\nu}}(\hat{\mathbf{x}}))\|^2\,\det\mathsf{D}\mathbf{T}_s^{\boldsymbol{\nu}}(\hat{\mathbf{x}})\,d\hat{\mathbf{x}}\right)\Big|_{s=0}$$

$$= -\frac{d}{ds}\left(\frac{1}{2}\int_{\mathbb{R}^3} \mu_s^{-1}(\mathbf{x})\,\|\mathbf{curl}\mathbf{A}_s^*(\mathbf{x})\|^2\,d\mathbf{x}\right)\Big|_{s=0}$$

$$= -\frac{d\mathcal{E}_F^*}{ds}(0),\quad \mathcal{E}_F^*(s) := \frac{1}{2}\int_{\mathbb{R}^3} \mu_s^{-1}(\mathbf{x})\,\|\mathbf{curl}\mathbf{A}_s^*(\mathbf{x})\|^2\,d\mathbf{x}.$$

In the last step we transformed the integral back using the perturbation map. The expression in the brackets is the energy of the magnetic vector potential obtained by dragging the vector potential in the reference configuration as the appropriate differential form, denoted by $\mathcal{E}_F^*(s)$. This dragging of fields as the appropriate differential form is what constitutes holding the flux constant, also mentioned in [28]. We obtain a relation similar to the one we saw in 4.4.16

$$\frac{d\mathcal{E}_F}{ds}(0) = -\frac{d\mathcal{E}_F^*}{ds}(0).$$

5.1.2.8   Numerical Experiments

Now we compute the shape derivatives and evaluate their performance numerically. Since both the shape derivative formulas (5.1.35) (called "BEM" in the plots) and (5.1.45) (called "MST" in the plots) are purely boundary based, we directly solve for the boundary data using a discretization of (5.1.31). Discretizing the boundary Γ with a mesh $\mathcal{M}_h$ consisting of triangular elements, we use the space $\mathbf{n} \times \nabla P_*^1(\mathcal{M}_h)$ to discretize $\boldsymbol{H}^{-\frac{1}{2}}(\mathrm{div}_\Gamma\,0, \Gamma)$ which was the zero surface divergence constraint built into the equation [33]. The space $P_*^1(\mathcal{M}_h)$ is the space $P^1(\mathcal{M}_h)$ with the constants removed, which can be implemented by enforcing zero mean on the elements of P_1. For the tangential trace the relevant continuous space is $V :=$ $\{\mathbf{u} \in \boldsymbol{H}^{-\frac{1}{2}}(\mathbf{curl}_\Gamma, \Gamma) : (\mathbf{u}, \mathbf{grad}_\Gamma\, v)_{-\frac{1}{2}} = 0 \quad \forall v \in H_*^{\frac{1}{2}}(\Gamma)\}$ (for trivial topology), as explained in Remark 2, which is discretized using the lowest order Nedelec edge elements and enforcing the orthogonality constraint to the elements of $P_*^1(\mathcal{M}_h)$ space. In the discrete system, these constraints are applied through a mixed formulation following the ideas mentioned in [58, Section 3.5, Chapter 3]. For the computation of the BEM based shape derivative, we use the Sauter and Schwab quadrature rule [54] of order 5^4. For evaluating the partial derivative $\frac{\partial\hat{\mathbf{b}}_{\mathcal{C}}}{\partial s}$, we simply use the singular quadrature rule for evaluation even though we do not have a proof that the integrals exist as weakly singular integrals, like we had in the case of electrostatics as seen in Section 4.1.7. Surprisingly, the numerical performance seems very good as we will see next. The shape derivatives are also compared using the dual norm error computation, the procedure for which was outlined in Section 4.4.7.1.

Experiment 15. We have the same experimental setting as in Experiment 11 (cubic Ω), now approached using a BIE formulation based on the vector potential. The strategy for computing force and torque remains the same, as mentioned in Section 3.0.2. As reference values, we use the force/torque obtained from the average of (5.1.18) and (5.1.35) at a refinement level of $h = 0.088$. Torque is computed about the point (4,0,0). The errors are plotted in Figure 5.14 and their asymptotic convergence rates are reported in Table 5.5. We can see the superior asymptotic convergence rate of the BEM based shape derivative formula.


(a) Error in total force   (b) Error in total torque
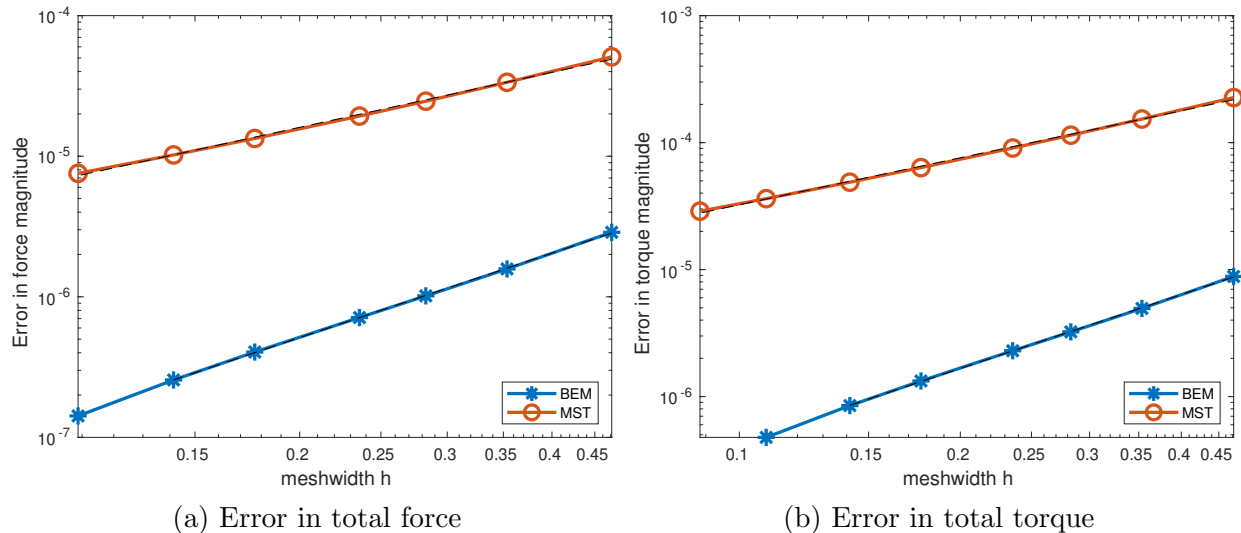
Figure 5.14: Error in force and torque computation for cube torus (Experiment 15)

Table 5.5: Asymptotic rate of algebraic convergence (Experiment 15)

Method	Force	Torque
Pullback approach	2.00	1.93
Stress tensor	1.30	1.23

The shape derivatives can also be compared via dual norm computations for cosine velocity fields mentioned in Section 4.4.7.1. The results for that are plotted in Figure 5.15 which confirms the superiority of the BEM based shape derivative formula.
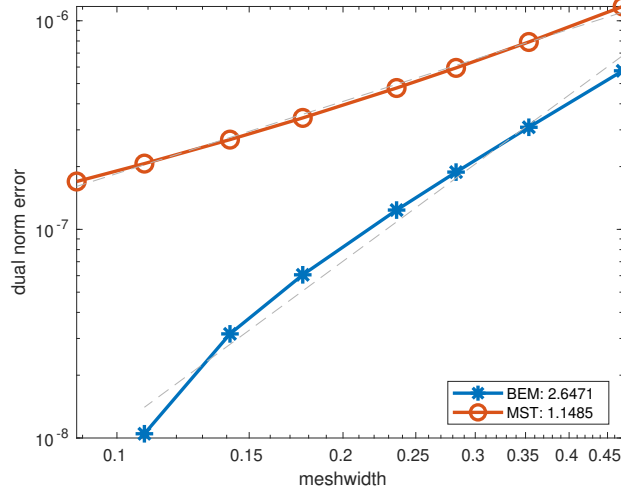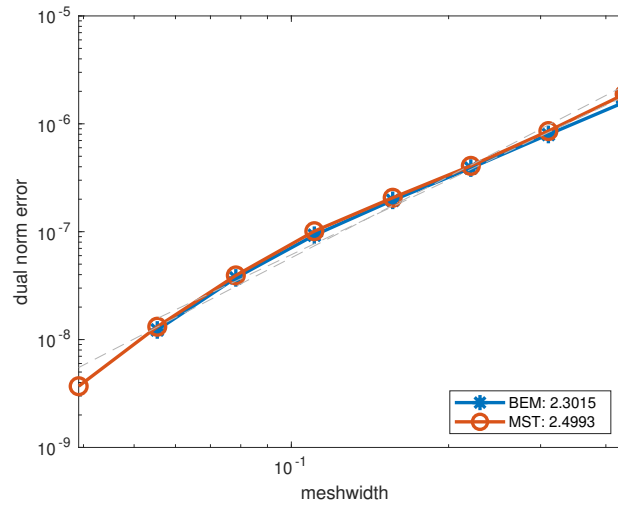
Figure 5.15: Dual norm error for Experiment 15

Experiment 16. We have the same experimental setting as in Experiment 12 (spherical Ω), now approached via a vector potential formulation. As reference values, we use the force/torque obtained from the average of (5.1.18) and (5.1.35) at a refinement level of $h = 0.055$. The errors are plotted in Figure 5.16. Torque is computed about the point $(4,0,0)$. The asymptotic convergence rates are reported in Table 5.6. We see a similar performance from the two methods for this smooth case.

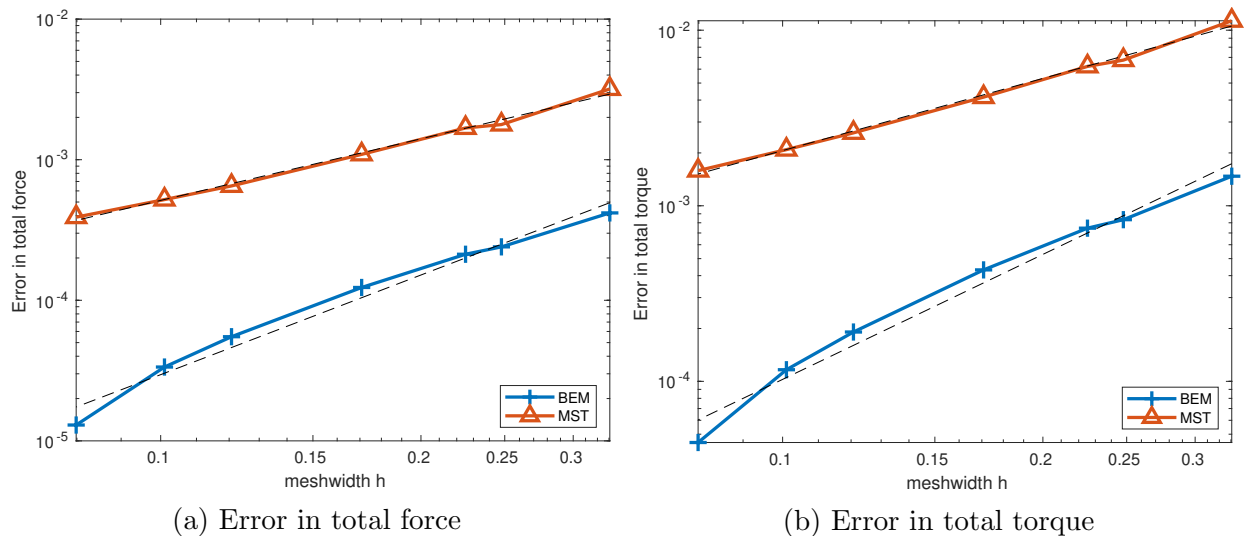(a) Error in total force

(b) Error in total torque
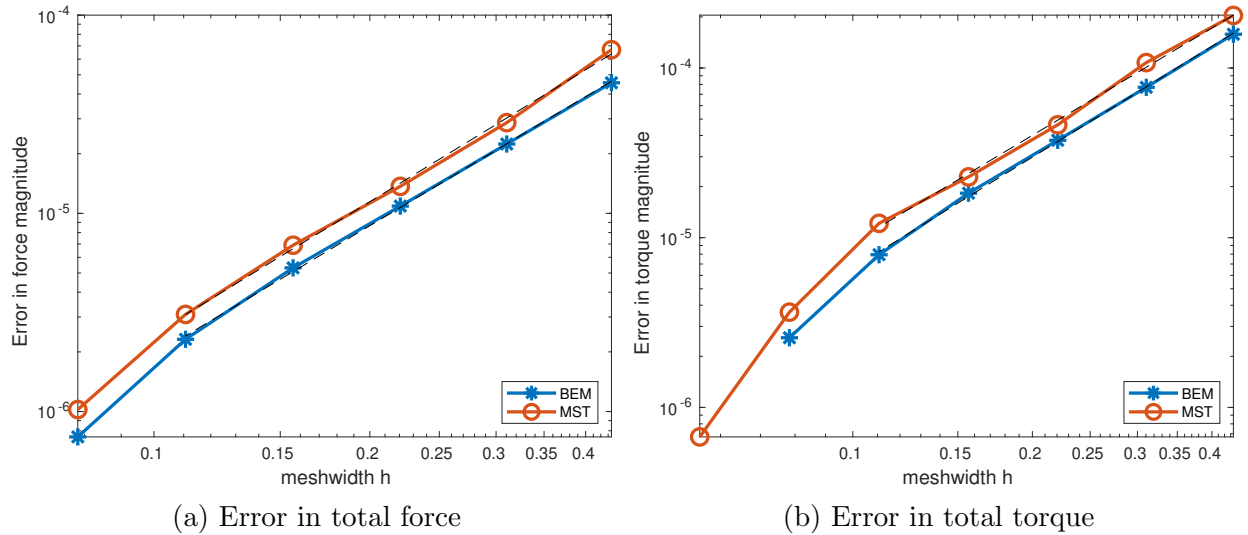
Figure 5.16: Error in force and torque computation for sphere and torus (Experiment 16)

Table 5.6: Asymptotic rate of algebraic convergence for Experiment 16

Method	Force	Torque
Pullback approach	2.16	2.17
Stress tensor	2.21	2.10

135

The shape derivatives are also compared via a dual norm error computation which is plotted in Figure 5.17. It confirms the similar performance for this smooth case.
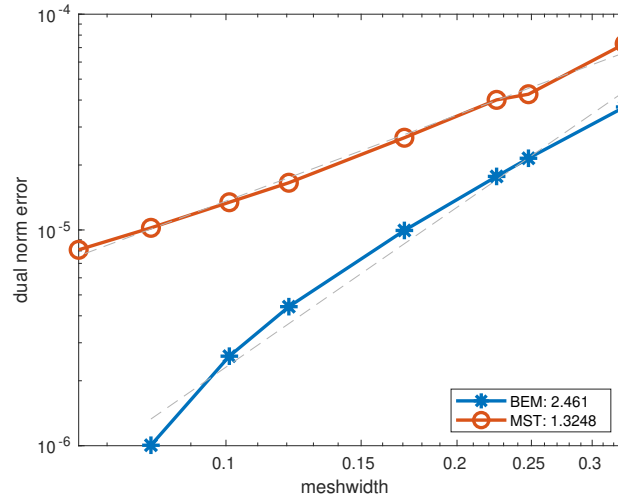

Figure 5.17: Dual norm error for Experiment 16

Experiment 17. We have the same experimental setting as in Experiment 13 (cuboidal Ω) now approached via a vector potential formulation. The errors are computed using the BEM based shape derivatives as the reference value obtained at a refinement level of $h = 0.064$ and plotted in Figure 5.18. Torque is computed about the point (4,0,0). We see that the BEM based shape derivative gives a higher convergence rate which is also tabulated in Table 5.7
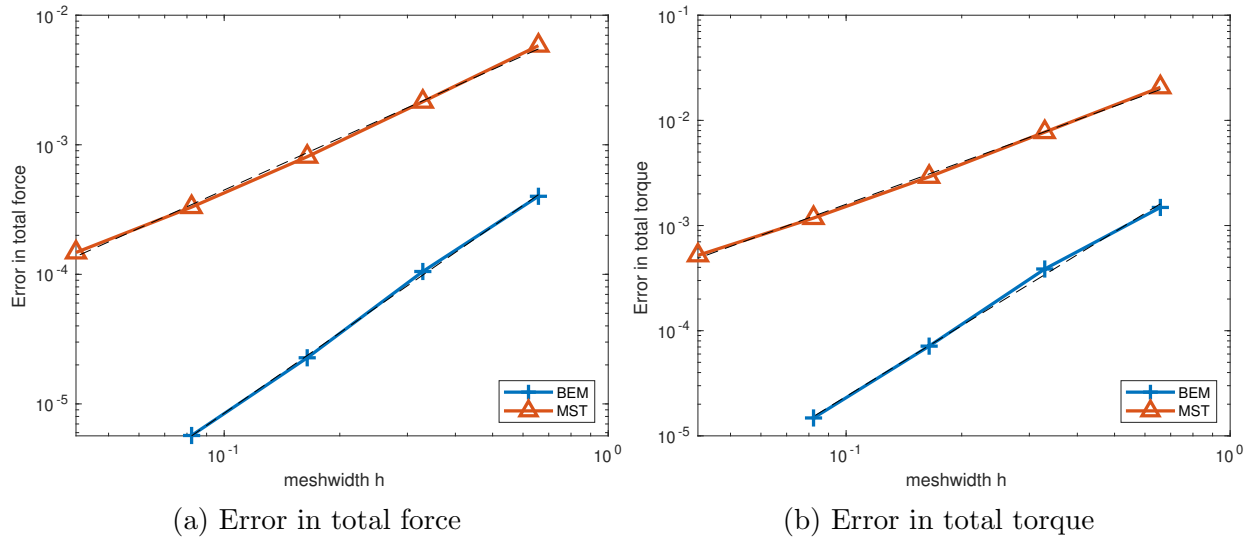

(a) Error in total force

(b) Error in total torque

Figure 5.18: Error in force and torque computation for cuboid and torus (Experiment 17)

Table 5.7: Asymptotic rate of algebraic convergence for Experiment 17

Method	Force	Torque
Pullback approach	2.35	2.36
Stress tensor	1.46	1.37

The dual norm errors are also computed for the shape derivatives which are reported in Figure 5.19. The reference values are again computed using the BEM shape derivative at $h = 0.064$. The superiority of the BEM based shape derivative is confirmed.

Figure 5.19: Dual norm error for Experiment 17

Experiment 18. We have the same experimental setting as in Experiment 14 (tetrahedral Ω) now approached via a vector potential formulation. The errors are computed using the BEM based shape derivatives as the reference value obtained at a refinement level of $h = 0.041$ and plotted in Figure 5.20. Torque is computed about the point (4,0,0). We see that the BEM based shape derivative gives a higher convergence rate which is also tabulated in Table 5.8

(a) Error in total force

(b) Error in total torque

Figure 5.20: Error in force and torque computation for tetrahedron and torus (Experiment 18)

Table 5.8: Asymptotic rate of algebraic convergence for Experiment 18

Method	Force	Torque
Pullback approach	2.06	2.24
Stress tensor	1.33	1.33

The dual norm errors are also computed for the shape derivatives which are reported in Figure 5.21. The reference values are again computed using the BEM shape derivative at $h = 0.041$. The dual norm computation confirms the superior performance of the BEM based shape derivative.
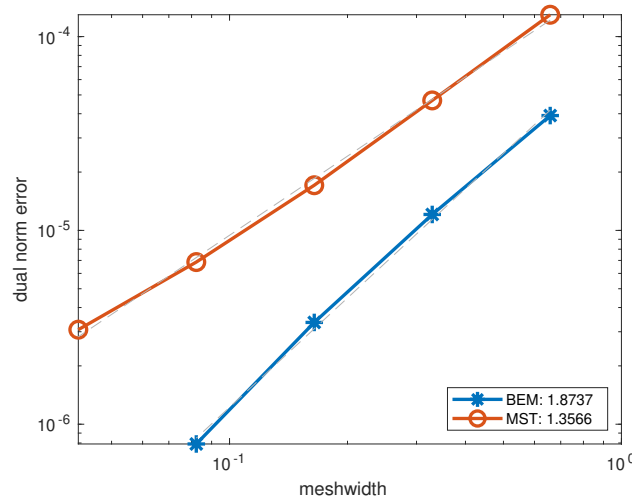
Figure 5.21: Dual norm error for Experiment 18

5.2 Linear Material Inside a Constant Field
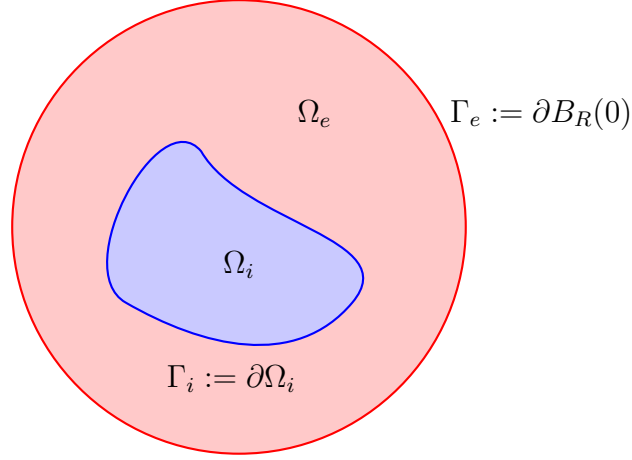
Figure 5.22: Geometric setting

Consider a linear, isotropic and homogeneous material with permeability $\mu \in \mathbb{R}^+$ occupying the bounded, simply connected and open domain $\Omega_i \subset \mathbb{R}^3$ with C_{pw}^2 boundary. This domain is entirely enclosed by a ball $B_R(0)$ centered at the origin and with radius R. The domain $\Omega_e := B_R(0) \setminus \overline{\Omega_i}$ denotes the space in between, which is occupied by a linear, isotropic and homogeneous material of permeability $\mu_0 \in \mathbb{R}^+$. Our motivation is to model a case where a linear material is placed inside a constant field. The total fields $\mathbf{B}_{tot}, \mathbf{H}_{tot}$ inside the domain obey the magnetostatic equations

$$\operatorname{div} \mathbf{B}_{tot} = 0, \quad \mathbf{curl} \mathbf{H}_{tot} = 0,$$

which are complemented by the material law

$$\mathbf{B}_{tot} = \mu(\mathbf{x})\mathbf{H}_{tot}, \quad \mu(\mathbf{x}) := \begin{cases} \mu & \mathbf{x} \in \Omega_i, \\ \mu_0 & \mathbf{x} \in \Omega_e. \end{cases}$$

5.2.1 Vector Potential Formulation

The divergence constraint on $\mathbf{B}_{tot}$ allows us to use a vector potential ansatz $\mathbf{B}_{tot} = \mathbf{curl} \mathbf{A}_{tot}$. In an attempt to model a constant field at Γ_e, we enforce the Dirichlet boundary condition $\gamma_{\mathbf{t}} \mathbf{A}_{tot} = \gamma_{\mathbf{t}} \mathbf{A}_{const}$ where $\mathbf{A}_{const}$ is a vector potential such that $\mathbf{curl} \mathbf{A}_{const} = \mathbf{B}_0$, $\mathbf{B}_0 \in \mathbb{R}^3$ being the constant field. Notice that we can find an explicit form for $\mathbf{A}_{const} = \frac{1}{2}\mathbf{B}_0 \times \mathbf{x}$ but we won't need it. We can do the decomposition $\mathbf{A}_{tot} = \mathbf{A} + \mathbf{A}_{const}$ and writing the transmission conditions for $\mathbf{A}_{tot}$ in terms of $\mathbf{A}$ we get the transmission problem

$$\begin{aligned}
\mathbf{curl}(\mu^{-1}(\mathbf{x}) \, \mathbf{curl} \mathbf{A}) &= 0 & &\text{in } \Omega_i \cup \Omega_e, \\
\llbracket \mu^{-1} \gamma_{\mathbf{M}} \mathbf{A} \rrbracket_\Gamma &= - \llbracket \mu^{-1} \rrbracket_\Gamma \mathbf{B}_0 \times \mathbf{n} & &\text{on } \Gamma_i, \\
\llbracket \gamma_{\mathbf{t}} \mathbf{A} \rrbracket_\Gamma &= 0 & &\text{on } \Gamma_i, \\
\gamma_{\mathbf{t}} \mathbf{A} &= 0 & &\text{on } \Gamma_e.
\end{aligned} \quad (5.2.1)$$

To render the above transmission problem uniquely solvable, we enforce the coulomb gauge $\operatorname{div} \mathbf{A} = 0$.

5.2.1.1 Variational Boundary Integral Equations

The transmission problem can be approached using a BIE based formulation. We start by inspecting the BIEs for $\partial\Omega_e$ in the variational form. Since Ω_e is bounded we use the first set of BIEs in (2.2.23) and denote the BIOs on $\partial\Omega_e$ with a subscript e. For the vector potential $\mathbf{A}$ in Ω_e, we denote its magnetic trace as $\boldsymbol{\psi}$ and its tangential trace as $\mathbf{g}$. Thus we have

$$-b_{\mathcal{A}_e}(\boldsymbol{\psi},\boldsymbol{\zeta}) + b_{\mathcal{C}_e}(\mathbf{g},\boldsymbol{\zeta}) + \frac{1}{2}\langle\mathbf{g},\boldsymbol{\zeta}\rangle_{\partial\Omega_e} = 0 \quad \forall\boldsymbol{\zeta}\in\boldsymbol{H}^{-\frac{1}{2}}(\mathrm{div}_\Gamma\, 0,\partial\Omega_e),$$

$$-b_{\mathcal{B}_e}(\boldsymbol{\psi},\mathbf{u}) + \frac{1}{2}\langle\boldsymbol{\psi},\mathbf{u}\rangle_{\partial\Omega_e} + b_{\mathcal{N}_e}(\mathbf{g},\mathbf{u}) = 0 \quad \forall\mathbf{u}\in\boldsymbol{H}^{-\frac{1}{2}}(\mathbf{curl}_\Gamma,\partial\Omega_e). \qquad (5.2.2)$$

Since $\partial\Omega_e = \Gamma_i\cup\Gamma_e$, the integrals in the bilinear forms can be decomposed, which are written compactly using the notation

$$b_{\mathcal{A}}^{\bullet;\blacktriangle} : \boldsymbol{H}^{-\frac{1}{2}}(\mathrm{div}_\Gamma\, 0,\Gamma_\bullet)\times\boldsymbol{H}^{-\frac{1}{2}}(\mathrm{div}_\Gamma\, 0,\Gamma_\blacktriangle)\to\mathbb{R},$$

$$b_{\mathcal{A}}^{\bullet;\blacktriangle}(\boldsymbol{\psi},\boldsymbol{\zeta}) := \int_{\Gamma_\blacktriangle}\int_{\Gamma_\bullet} G(\mathbf{x},\mathbf{y})\,\boldsymbol{\psi}(\mathbf{y})\cdot\boldsymbol{\zeta}(\mathbf{x})\,dS_\mathbf{y}\,dS_\mathbf{x},$$

$$b_{\mathcal{C}}^{\bullet;\blacktriangle} : \boldsymbol{H}^{-\frac{1}{2}}(\mathbf{curl}_\Gamma,\Gamma_\bullet)\times\boldsymbol{H}^{-\frac{1}{2}}(\mathrm{div}_\Gamma\, 0,\Gamma_\blacktriangle)\to\mathbb{R},$$

$$b_{\mathcal{C}}^{\bullet;\blacktriangle}(\mathbf{g},\boldsymbol{\zeta}) := \int_{\Gamma_\blacktriangle}\int_{\Gamma_\bullet}\left(\nabla_x G(\mathbf{x},\mathbf{y})\times(\mathbf{n}(\mathbf{y})\times\mathbf{g}(\mathbf{y}))\right)\cdot\boldsymbol{\zeta}(\mathbf{x})\,dS_\mathbf{y}\,dS_\mathbf{x},$$

$$b_{\mathcal{N}}^{\bullet;\blacktriangle} : \boldsymbol{H}^{-\frac{1}{2}}(\mathbf{curl}_\Gamma,\Gamma_\bullet)\times\boldsymbol{H}^{-\frac{1}{2}}(\mathbf{curl}_\Gamma,\Gamma_\blacktriangle)\to\mathbb{R},$$

$$b_{\mathcal{N}}^{\bullet;\blacktriangle}(\mathbf{g},\mathbf{u}) := -\int_{\Gamma_\blacktriangle}\int_{\Gamma_\bullet} G(\mathbf{x},\mathbf{y})\,\mathrm{curl}_\Gamma\,\mathbf{g}(\mathbf{y})\,\mathrm{curl}_\Gamma\,\mathbf{u}(\mathbf{x})\,dS_\mathbf{y}\,dS_\mathbf{x}. \qquad (5.2.3)$$

The bilinear form $b_{\mathcal{B}}^{\bullet;\blacktriangle}(\boldsymbol{\psi},\mathbf{u}) := b_{\mathcal{C}}^{\blacktriangle;\bullet}(\mathbf{u},\boldsymbol{\psi})$. In the above definitions, $\mathbf{n}$ represents the exterior unit normal on both Γ_i and Γ_e. The duality pairing over $\partial\Omega_e$ can be easily split into duality pairings over Γ_i and Γ_e. Denoting $\boldsymbol{\psi}_* = \boldsymbol{\psi}|_{\Gamma_*}, \mathbf{g}_* = \mathbf{g}|_{\Gamma_*}, \boldsymbol{\zeta}_* = \boldsymbol{\zeta}|_{\Gamma_*}, \mathbf{u}_* = \mathbf{u}|_{\Gamma_*}, *\in\{i,e\}$, we can write the equations in (5.2.2) as

$$-b_{\mathcal{A}}^{i,i}(\boldsymbol{\psi}_i,\boldsymbol{\zeta}_i) - b_{\mathcal{A}}^{i,e}(\boldsymbol{\psi}_i,\boldsymbol{\zeta}_e) - b_{\mathcal{A}}^{e,i}(\boldsymbol{\psi}_e,\boldsymbol{\zeta}_i) - b_{\mathcal{A}}^{e,e}(\boldsymbol{\psi}_e,\boldsymbol{\zeta}_e)$$

$$-b_{\mathcal{C}}^{i,i}(\mathbf{g}_i,\boldsymbol{\zeta}_i) - b_{\mathcal{C}}^{i,e}(\mathbf{g}_i,\boldsymbol{\zeta}_e) + b_{\mathcal{C}}^{e,i}(\mathbf{g}_e,\boldsymbol{\zeta}_i) + b_{\mathcal{C}}^{e,e}(\mathbf{g}_e,\boldsymbol{\zeta}_e) + \frac{1}{2}\langle\mathbf{g}_i,\boldsymbol{\zeta}_i\rangle_{\Gamma_i} + \frac{1}{2}\langle\mathbf{g}_e,\boldsymbol{\zeta}_e\rangle_{\Gamma_e} = 0,$$

$$b_{\mathcal{B}}^{i,i}(\boldsymbol{\psi}_i,\mathbf{u}_i) + b_{\mathcal{B}}^{e,i}(\boldsymbol{\psi}_e,\mathbf{u}_i) - b_{\mathcal{B}}^{i,e}(\boldsymbol{\psi}_i,\mathbf{u}_e) - b_{\mathcal{B}}^{e,e}(\boldsymbol{\psi}_e,\mathbf{u}_e)$$

$$+b_{\mathcal{N}}^{i,i}(\mathbf{g}_i,\mathbf{u}_i) + b_{\mathcal{N}}^{e,i}(\mathbf{g}_e,\mathbf{u}_i) + b_{\mathcal{N}}^{i,e}(\mathbf{g}_i,\mathbf{u}_e) + b_{\mathcal{N}}^{e,e}(\mathbf{g}_e,\mathbf{u}_e) + \frac{1}{2}\langle\boldsymbol{\psi}_i,\mathbf{u}_i\rangle_{\Gamma_i} + \frac{1}{2}\langle\boldsymbol{\psi}_e,\mathbf{u}_e\rangle_{\Gamma_e} = 0.$$

Notice the sign flip in the bilinear form related to $\mathcal{C}$. This arises from the fact that the external unit normal $\mathbf{n}_e$ on $\partial\Omega_e$ satisfies $\mathbf{n}_e|_{\Gamma_i} = -\mathbf{n}$. From the Dirichlet boundary condition at Γ_e, we have $\mathbf{g}_e = 0$. We first set $\boldsymbol{\zeta}_e = 0, \mathbf{u}_e = 0$ which gives us

$$-b_{\mathcal{A}}^{i,i}(\boldsymbol{\psi}_i,\boldsymbol{\zeta}_i) - b_{\mathcal{A}}^{e,i}(\boldsymbol{\psi}_e,\boldsymbol{\zeta}_i) - b_{\mathcal{C}}^{i,i}(\mathbf{g}_i,\boldsymbol{\zeta}_i) + \frac{1}{2}\langle\mathbf{g}_i,\boldsymbol{\zeta}_i\rangle_{\Gamma_i} = 0 \quad \forall\boldsymbol{\zeta}_i\in\boldsymbol{H}^{-\frac{1}{2}}(\mathrm{div}_\Gamma\, 0,\Gamma_i), \qquad (5.2.4)$$

$$b_{\mathcal{B}}^{i,i}(\boldsymbol{\psi}_i,\mathbf{u}_i) + b_{\mathcal{B}}^{e,i}(\boldsymbol{\psi}_e,\mathbf{u}_i) + b_{\mathcal{N}}^{i,i}(\mathbf{g}_i,\mathbf{u}_i) + \frac{1}{2}\langle\boldsymbol{\psi}_i,\mathbf{u}_i\rangle_{\Gamma_i} = 0 \quad \forall\mathbf{u}_i\in\boldsymbol{H}^{-\frac{1}{2}}(\mathbf{curl}_\Gamma,\Gamma_i). \qquad (5.2.5)$$

Setting $\boldsymbol{\zeta}_i = 0, \mathbf{u}_i = 0$ instead gives us

$$-\mathsf{b}_{\mathcal{A}}^{i;e}(\boldsymbol{\psi}_i, \boldsymbol{\zeta}_e) - \mathsf{b}_{\mathcal{A}}^{e;e}(\boldsymbol{\psi}_e, \boldsymbol{\zeta}_e) - \mathsf{b}_{\mathcal{C}}^{i;e}(\mathbf{g}_i, \boldsymbol{\zeta}_e) = 0 \quad \forall \boldsymbol{\zeta}_e \in \boldsymbol{H}^{-\frac{1}{2}}(\mathrm{div}_\Gamma\, 0, \Gamma_e), \quad (5.2.6)$$

$$-\mathsf{b}_{\mathcal{B}}^{i;e}(\boldsymbol{\psi}_i, \mathbf{u}_e) - \mathsf{b}_{\mathcal{B}}^{e;e}(\boldsymbol{\psi}_e, \mathbf{u}_e) + \mathsf{b}_{\mathcal{N}}^{i;e}(\mathbf{g}_i, \mathbf{u}_e) + \frac{1}{2}\langle \boldsymbol{\psi}_e, \mathbf{u}_e \rangle_{\Gamma_e} = 0 \quad \forall \mathbf{u}_e \in \boldsymbol{H}^{-\frac{1}{2}}(\mathbf{curl}_\Gamma, \Gamma_e). \quad (5.2.7)$$

Now we have a look at the BIEs on $\Gamma_i = \partial\Omega_i$. Denoting the interior traces as $\boldsymbol{\psi}_I, \mathbf{g}_I$ we get the variational equations by testing the interior BIEs in (2.2.23) with $\boldsymbol{\zeta}_i \in \boldsymbol{H}^{-\frac{1}{2}}(\mathrm{div}_\Gamma\, 0, \Gamma_i), \mathbf{u}_i \in \boldsymbol{H}^{-\frac{1}{2}}(\mathbf{curl}_\Gamma, \Gamma_i)$. Thus we have

$$-\mathsf{b}_{\mathcal{A}}^{i;i}(\boldsymbol{\psi}_I, \boldsymbol{\zeta}_i) + \mathsf{b}_{\mathcal{C}}^{i;i}(\mathbf{g}_I, \boldsymbol{\zeta}_i) + \frac{1}{2}\langle \mathbf{g}_I, \boldsymbol{\zeta}_i \rangle_{\Gamma_i} = 0 \quad \forall \boldsymbol{\zeta}_i \in \boldsymbol{H}^{-\frac{1}{2}}(\mathrm{div}_\Gamma\, 0, \Gamma_i), \quad (5.2.8)$$

$$-\mathsf{b}_{\mathcal{B}}^{i;i}(\boldsymbol{\psi}_I, \mathbf{u}_i) + \frac{1}{2}\langle \boldsymbol{\psi}_I, \mathbf{u}_i \rangle_{\Gamma_i} + \mathsf{b}_{\mathcal{N}}^{i;i}(\mathbf{g}_I, \mathbf{u}_i) = 0 \quad \forall \mathbf{u}_i \in \boldsymbol{H}^{-\frac{1}{2}}(\mathbf{curl}_\Gamma, \Gamma_i). \quad (5.2.9)$$

Using the transmission conditions we have the relations

$$\mathbf{g}_I = \mathbf{g}_i, \quad \boldsymbol{\psi}_I = \mu \left[\!\left[\mu^{-1} \right]\!\right]_\Gamma \mathbf{B}_0 \times \mathbf{n} - \frac{\mu}{\mu_0}\boldsymbol{\psi}_i,$$

allowing us to write the above equations as

$$\frac{\mu}{\mu_0}\mathsf{b}_{\mathcal{A}}^{i;i}(\boldsymbol{\psi}_i, \boldsymbol{\zeta}_i) + \mathsf{b}_{\mathcal{C}}^{i;i}(\mathbf{g}_i, \boldsymbol{\zeta}_i) + \frac{1}{2}\langle \mathbf{g}_i, \boldsymbol{\zeta}_i \rangle_{\Gamma_i} = \mu \left[\!\left[\mu^{-1} \right]\!\right]_\Gamma \mathsf{b}_{\mathcal{A}}^{i;i}(\mathbf{B}_0 \times \mathbf{n}, \boldsymbol{\zeta}_i), \quad (5.2.10)$$

$$\mathsf{b}_{\mathcal{B}}^{i;i}(\boldsymbol{\psi}_i, \mathbf{u}_i) - \frac{1}{2}\langle \boldsymbol{\psi}_i, \mathbf{u}_i \rangle_{\Gamma_i} + \frac{\mu_0}{\mu}\mathsf{b}_{\mathcal{N}}^{i;i}(\mathbf{g}_i, \mathbf{u}_i)$$
$$= \mu_0 \left[\!\left[\mu^{-1} \right]\!\right]_\Gamma \mathsf{b}_{\mathcal{B}}^{i;i}(\mathbf{B}_0 \times \mathbf{n}, \mathbf{u}_i) - \frac{\mu_0 \left[\!\left[\mu^{-1} \right]\!\right]_\Gamma}{2}\langle \mathbf{B}_0 \times \mathbf{n}, \mathbf{u}_i \rangle_{\Gamma_i}. \quad (5.2.11)$$

Subtracting (5.2.4) from (5.2.10) we get

$$(1 + \frac{\mu}{\mu_0})\mathsf{b}_{\mathcal{A}}^{i;i}(\boldsymbol{\psi}_i, \boldsymbol{\zeta}_i) + 2\mathsf{b}_{\mathcal{C}}^{i;i}(\mathbf{g}_i, \boldsymbol{\zeta}_i) + \mathsf{b}_{\mathcal{A}}^{e;i}(\boldsymbol{\psi}_e, \boldsymbol{\zeta}_i) = \mu \left[\!\left[\mu^{-1} \right]\!\right]_\Gamma \mathsf{b}_{\mathcal{A}}^{i;i}(\mathbf{B}_0 \times \mathbf{n}, \boldsymbol{\zeta}_i),$$

adding (5.2.11) and (5.2.5) we get

$$2\mathsf{b}_{\mathcal{B}}^{i;i}(\boldsymbol{\psi}_i, \mathbf{u}_i) + \mathsf{b}_{\mathcal{B}}^{e;i}(\boldsymbol{\psi}_e, \mathbf{u}_i) + (1 + \frac{\mu_0}{\mu})\mathsf{b}_{\mathcal{N}}^{i;i}(\mathbf{g}_i, \mathbf{u}_i)$$
$$= \mu_0 \left[\!\left[\mu^{-1} \right]\!\right]_\Gamma \mathsf{b}_{\mathcal{B}}^{i;i}(\mathbf{B}_0 \times \mathbf{n}, \mathbf{u}_i) - \frac{\mu_0 \left[\!\left[\mu^{-1} \right]\!\right]_\Gamma}{2}\langle \mathbf{B}_0 \times \mathbf{n}, \mathbf{u}_i \rangle_{\Gamma_i}.$$

Using (5.2.6) as the third equation, we get an elliptic system if we look for $\mathbf{g}_i \in \boldsymbol{V}_i :=$ $\{\mathbf{u} \in \boldsymbol{H}^{-\frac{1}{2}}(\mathbf{curl}_\Gamma, \Gamma_i) : (\mathbf{u}, \mathbf{grad}_\Gamma\, v)_{-\frac{1}{2}, \Gamma_i} = 0 \quad \forall v \in H_*^{\frac{1}{2}}(\Gamma_i)\}$, where $(\cdot, \cdot)_{-\frac{1}{2}, \Gamma_i}$ is the $-\frac{1}{2}$ inner product for function spaces associated with Γ_i. The variational problem is then : seek $\boldsymbol{\psi}_i \in \boldsymbol{H}^{-\frac{1}{2}}(\mathrm{div}_\Gamma\, 0, \Gamma_i), \mathbf{g}_i \in \boldsymbol{V}_i, \boldsymbol{\psi}_e \in \boldsymbol{H}^{-\frac{1}{2}}(\mathrm{div}_\Gamma\, 0, \Gamma_e)$ such that

$$(1 + \frac{\mu}{\mu_0})\mathsf{b}_{\mathcal{A}}^{i;i}(\boldsymbol{\psi}_i, \boldsymbol{\zeta}_i) + 2\mathsf{b}_{\mathcal{C}}^{i;i}(\mathbf{g}_i, \boldsymbol{\zeta}_i) + \mathsf{b}_{\mathcal{A}}^{e;i}(\boldsymbol{\psi}_e, \boldsymbol{\zeta}_i) =$$
$$\mu \left[\!\left[\mu^{-1} \right]\!\right]_\Gamma \mathsf{b}_{\mathcal{A}}^{i;i}(\mathbf{B}_0 \times \mathbf{n}, \boldsymbol{\zeta}_i) \qquad \forall \boldsymbol{\zeta}_i \in \boldsymbol{H}^{-\frac{1}{2}}(\mathrm{div}_\Gamma\, 0, \Gamma_i),$$

141

$$- 2b_{\mathcal{B}}^{i,i}(\boldsymbol{\psi}_i, \mathbf{u}_i) - (1 + \frac{\mu_0}{\mu})b_{\mathcal{N}}^{i,i}(\mathbf{g}_i, \mathbf{u}_i) - b_{\mathcal{B}}^{e,i}(\boldsymbol{\psi}_e, \mathbf{u}_i) =$$

$$- \mu_0 [\![\mu^{-1}]\!]_\Gamma \, b_{\mathcal{B}}^{i,i}(\mathbf{B}_0 \times \mathbf{n}, \mathbf{u}_i) + \frac{\mu_0 [\![\mu^{-1}]\!]_\Gamma}{2} \langle \mathbf{B}_0 \times \mathbf{n}, \mathbf{u}_i \rangle_{\Gamma_i} \quad \forall \mathbf{u}_i \in \boldsymbol{V}_i,$$

$$b_{\mathcal{A}}^{i,e}(\boldsymbol{\psi}_i, \boldsymbol{\zeta}_e) + b_{\mathcal{C}}^{i,e}(\mathbf{g}_i, \boldsymbol{\zeta}_e) + b_{\mathcal{A}}^{e,e}(\boldsymbol{\psi}_e, \boldsymbol{\zeta}_e) = 0 \qquad\qquad \forall \boldsymbol{\zeta}_e \in \boldsymbol{H}^{-\frac{1}{2}}(\mathrm{div}_\Gamma\, 0, \Gamma_e).$$

Defining the space $\boldsymbol{\mathcal{X}} := \boldsymbol{H}^{-\frac{1}{2}}(\mathrm{div}_\Gamma\, 0, \Gamma_i) \times \boldsymbol{V}_i \times \boldsymbol{H}^{-\frac{1}{2}}(\mathrm{div}_\Gamma\, 0, \Gamma_e)$, the above system can be written compactly as

$$\begin{bmatrix} \boldsymbol{\psi}_i \\ \mathbf{g}_i \\ \boldsymbol{\psi}_e \end{bmatrix} \in \boldsymbol{\mathcal{X}}: \quad b\left(\begin{bmatrix} \boldsymbol{\psi}_i \\ \mathbf{g}_i \\ \boldsymbol{\psi}_e \end{bmatrix}, \begin{bmatrix} \boldsymbol{\zeta}_i \\ \mathbf{u}_i \\ \boldsymbol{\zeta}_e \end{bmatrix}\right) = \ell\left(\begin{bmatrix} \boldsymbol{\zeta}_i \\ \mathbf{u}_i \\ \boldsymbol{\zeta}_e \end{bmatrix}\right) \quad \forall \begin{bmatrix} \boldsymbol{\zeta}_i \\ \mathbf{u}_i \\ \boldsymbol{\zeta}_e \end{bmatrix} \in \boldsymbol{\mathcal{X}}, \qquad (5.2.12)$$

where

$$b\left(\begin{bmatrix} \boldsymbol{\psi}_i \\ \mathbf{g}_i \\ \boldsymbol{\psi}_e \end{bmatrix}, \begin{bmatrix} \boldsymbol{\zeta}_i \\ \mathbf{u}_i \\ \boldsymbol{\zeta}_e \end{bmatrix}\right) := (1 + \frac{\mu}{\mu_0})b_{\mathcal{A}}^{i,i}(\boldsymbol{\psi}_i, \boldsymbol{\zeta}_i) + 2b_{\mathcal{C}}^{i,i}(\mathbf{g}_i, \boldsymbol{\zeta}_i) + b_{\mathcal{A}}^{e,i}(\boldsymbol{\psi}_e, \boldsymbol{\zeta}_i)$$

$$- 2b_{\mathcal{B}}^{i,i}(\boldsymbol{\psi}_i, \mathbf{u}_i) - (1 + \frac{\mu_0}{\mu})b_{\mathcal{N}}^{i,i}(\mathbf{g}_i, \mathbf{u}_i) - b_{\mathcal{B}}^{e,i}(\boldsymbol{\psi}_e, \mathbf{u}_i)$$

$$+ b_{\mathcal{A}}^{i,e}(\boldsymbol{\psi}_i, \boldsymbol{\zeta}_e) + b_{\mathcal{C}}^{i,e}(\mathbf{g}_i, \boldsymbol{\zeta}_e) + b_{\mathcal{A}}^{e,e}(\boldsymbol{\psi}_e, \boldsymbol{\zeta}_e),$$

$$\ell\left(\begin{bmatrix} \boldsymbol{\zeta}_i \\ \mathbf{u}_i \\ \boldsymbol{\zeta}_e \end{bmatrix}\right) := \mu [\![\mu^{-1}]\!]_\Gamma \, b_{\mathcal{A}}^{i,i}(\mathbf{B}_0 \times \mathbf{n}, \boldsymbol{\zeta}_i)$$

$$- \mu_0 [\![\mu^{-1}]\!]_\Gamma \, b_{\mathcal{B}}^{i,i}(\mathbf{B}_0 \times \mathbf{n}, \mathbf{u}_i) + \frac{\mu_0 [\![\mu^{-1}]\!]_\Gamma}{2} \langle \mathbf{B}_0 \times \mathbf{n}, \mathbf{u}_i \rangle_{\Gamma_i}.$$

It is easy to see that the bilinear form is elliptic. Putting $\boldsymbol{\zeta}_i = \boldsymbol{\psi}_i, \mathbf{u}_i = \mathbf{g}_i, \boldsymbol{\zeta}_e = \boldsymbol{\psi}_e$ we get

$$(1 + \frac{\mu}{\mu_0})b_{\mathcal{A}}^{i,i}(\boldsymbol{\psi}_i, \boldsymbol{\psi}_i) + b_{\mathcal{A}}^{e,i}(\boldsymbol{\psi}_e, \boldsymbol{\psi}_i) + b_{\mathcal{A}}^{i,e}(\boldsymbol{\psi}_i, \boldsymbol{\psi}_e) + b_{\mathcal{A}}^{e,e}(\boldsymbol{\psi}_e, \boldsymbol{\zeta}_e) - (1 + \frac{\mu_0}{\mu})b_{\mathcal{N}}^{i,i}(\mathbf{g}_i, \mathbf{g}_i)$$

$$\geq b_{\mathcal{A}_e}(\boldsymbol{\psi}, \boldsymbol{\psi}) - (1 + \frac{\mu_0}{\mu})b_{\mathcal{N}}^{i,i}(\mathbf{g}_i, \mathbf{g}_i)$$

$$\geq c_1 \|\boldsymbol{\psi}\|_{\boldsymbol{H}^{-\frac{1}{2}}(\mathrm{div}_\Gamma, \partial\Omega_e)}^2 + c_2 \|\mathbf{g}_i\|_{\boldsymbol{H}^{-\frac{1}{2}}(\mathbf{curl}_\Gamma, \Gamma_i)}^2$$

$$= c_1 \|\boldsymbol{\psi}_i\|_{\boldsymbol{H}^{-\frac{1}{2}}(\mathrm{div}_\Gamma, \Gamma_i)}^2 + c_1 \|\boldsymbol{\psi}_e\|_{\boldsymbol{H}^{-\frac{1}{2}}(\mathrm{div}_\Gamma, \Gamma_e)}^2 + c_2 \|\mathbf{g}_i\|_{\boldsymbol{H}^{-\frac{1}{2}}(\mathbf{curl}_\Gamma, \Gamma_i)}^2$$

$$\geq C\left(\|\boldsymbol{\psi}_i\|_{\boldsymbol{H}^{-\frac{1}{2}}(\mathrm{div}_\Gamma, \Gamma_i)}^2 + \|\boldsymbol{\psi}_e\|_{\boldsymbol{H}^{-\frac{1}{2}}(\mathrm{div}_\Gamma, \Gamma_e)}^2 + \|\mathbf{g}_i\|_{\boldsymbol{H}^{-\frac{1}{2}}(\mathbf{curl}_\Gamma, \Gamma_i)}^2\right).$$

We concluded the ellipticity for $-\mathcal{N}$ using the closed range of the operator curl_Γ from [13, Lemma 9] and the result [33, Lemma 6.3]. Now we try to express the field energy in terms of the linear form. We focus on the field energy inside $B_R(0)$ since the chosen deformation fields will not affect the exterior or the Dirichlet boundary Γ_e. The field energy is given as

$$\mathcal{E}_F = \int_{B_R(0)} \mu^{-1}(\mathbf{x}) \, \|\mathbf{curl A}(\mathbf{x}) + \mathbf{B}_0\|^2 \, d\mathbf{x}.$$

Splitting the integrand, using integration by parts and transmission conditions, we get

$$\mathcal{E}_F = -\frac{[\![\mu]\!]_\Gamma^{-1}}{2}\langle \mathbf{g}_i, \mathbf{B}_0 \times \mathbf{n}\rangle_{\Gamma_i} + \frac{\|\mathbf{B}_0\|^2}{2}\int\limits_{B_R(0)} \mu^{-1}(\mathbf{x})\,d\mathbf{x}.$$

To get the desired relation we start by observing that

$$\frac{1}{[\![\mu^{-1}]\!]_\Gamma\,\mu_0}\ell(\begin{bmatrix}\boldsymbol{\psi}_i\\-\mathbf{g}_i\\\boldsymbol{\psi}_e\end{bmatrix}) = \frac{\mu}{\mu_0}\mathsf{b}_\mathcal{A}^{i,i}(\mathbf{B}_0 \times \mathbf{n}, \boldsymbol{\psi}_i) + \mathsf{b}_\mathcal{B}^{i,i}(\mathbf{B}_0 \times \mathbf{n}, \mathbf{g}_i) - \frac{1}{2}\langle\mathbf{B}_0 \times \mathbf{n}, \mathbf{g}_i\rangle_{\Gamma_i}.$$

Testing (5.2.10) with $\mathbf{B}_0 \times \mathbf{n}$ we get

$$\frac{\mu}{\mu_0}\mathsf{b}_\mathcal{A}^{i,i}(\boldsymbol{\psi}_i, \mathbf{B}_0 \times \mathbf{n}) + \mathsf{b}_\mathcal{C}^{i,i}(\mathbf{g}_i, \mathbf{B}_0 \times \mathbf{n}) + \frac{1}{2}\langle\mathbf{g}_i, \mathbf{B}_0 \times \mathbf{n}\rangle_{\Gamma_i} = \mu\,[\![\mu^{-1}]\!]_\Gamma\,\mathsf{b}_\mathcal{A}^{i,i}(\mathbf{B}_0 \times \mathbf{n}, \mathbf{B}_0 \times \mathbf{n}),$$

which can be plugged into the relation above to get

$$\frac{1}{[\![\mu^{-1}]\!]_\Gamma\,\mu_0}\ell(\begin{bmatrix}\boldsymbol{\psi}_i\\-\mathbf{g}_i\\\boldsymbol{\psi}_e\end{bmatrix}) = \mu\,[\![\mu^{-1}]\!]_\Gamma\,\mathsf{b}_\mathcal{A}^{i,i}(\mathbf{B}_0 \times \mathbf{n}, \mathbf{B}_0 \times \mathbf{n}) - \langle\mathbf{B}_0 \times \mathbf{n}, \mathbf{g}_i\rangle_{\Gamma_i}.$$

Comparing with the expression for the energy, we finally get the relation

$$\mathcal{E}_F = \frac{1}{2\mu_0}\ell(\begin{bmatrix}\boldsymbol{\psi}_i\\-\mathbf{g}_i\\\boldsymbol{\psi}_e\end{bmatrix}) - \frac{\mu\,[\![\mu^{-1}]\!]_\Gamma^2}{2}\mathsf{b}_\mathcal{A}^{i,i}(\mathbf{B}_0 \times \mathbf{n}, \mathbf{B}_0 \times \mathbf{n}) + \frac{\|\mathbf{B}_0\|^2}{2}\int\limits_{B_R(0)}\mu^{-1}(\mathbf{x})\,d\mathbf{x}. \qquad (5.2.13)$$

5.2.1.2 Variational BIEs on Deformed Boundary

The configuration is deformed using the perturbation map $\mathbf{T}_s^\nu$ from (3.0.1) with a velocity field $\boldsymbol{\mathcal{V}} \in (C_0^\infty(B_R(0)))^3$ which leaves the outer boundary unperturbed. For the deformed configuration, the Dirichlet boundary condition at the outer boundary remains unchanged. The material parameter μ_s in the deformed configuration is obtained by transforming the reference values as a 0-form. We denote the deformed boundaries with a superscript s, for example Γ_i^s, Γ_e^s and so on. The variational BIEs for the deformed configuration have a similar structure to (5.2.12). Defining the relevant function space $\boldsymbol{\mathcal{X}}_s := \boldsymbol{H}^{-\frac{1}{2}}(\mathrm{div}_\Gamma\,0, \Gamma_i^s) \times \boldsymbol{V}_i^s \times \boldsymbol{H}^{-\frac{1}{2}}(\mathrm{div}_\Gamma\,0, \Gamma_e^s)$, where $\boldsymbol{V}_i^s := \{\mathbf{u} \in \boldsymbol{H}^{-\frac{1}{2}}(\mathbf{curl}_\Gamma, \Gamma_i^s) : (\mathbf{u}, \mathbf{grad}_\Gamma\,v)_{-\frac{1}{2},\Gamma_i^s} = 0 \quad \forall v \in H_*^{\frac{1}{2}}(\Gamma_i^s)\}$, we have the variational problem

$$\begin{bmatrix}\boldsymbol{\psi}_i^s\\\mathbf{g}_i^s\\\boldsymbol{\psi}_e^s\end{bmatrix} \in \boldsymbol{\mathcal{X}}_s: \quad \mathsf{b}(s)(\begin{bmatrix}\boldsymbol{\psi}_i^s\\\mathbf{g}_i^s\\\boldsymbol{\psi}_e^s\end{bmatrix}, \begin{bmatrix}\boldsymbol{\zeta}_i\\\mathbf{u}_i\\\boldsymbol{\zeta}_e\end{bmatrix}) = \ell(s)(\begin{bmatrix}\boldsymbol{\zeta}_i\\\mathbf{u}_i\\\boldsymbol{\zeta}_e\end{bmatrix}) \quad \forall \begin{bmatrix}\boldsymbol{\zeta}_i\\\mathbf{u}_i\\\boldsymbol{\zeta}_e\end{bmatrix} \in \boldsymbol{\mathcal{X}}_s, \qquad (5.2.14)$$

where

$$\mathsf{b}(s)(\begin{bmatrix}\boldsymbol{\psi}_i\\\mathbf{g}_i\\\boldsymbol{\psi}_e\end{bmatrix}, \begin{bmatrix}\boldsymbol{\zeta}_i\\\mathbf{u}_i\\\boldsymbol{\zeta}_e\end{bmatrix}) := (1 + \frac{\mu}{\mu_0})\mathsf{b}_\mathcal{A}^{i,i}(s)(\boldsymbol{\psi}_i, \boldsymbol{\zeta}_i) + 2\mathsf{b}_\mathcal{C}^{i,i}(s)(\mathbf{g}_i, \boldsymbol{\zeta}_i) + \mathsf{b}_\mathcal{A}^{e,i}(s)(\boldsymbol{\psi}_e, \boldsymbol{\zeta}_i)$$

$$- 2\mathsf{b}_{\mathcal{B}}^{i,i}(s)(\boldsymbol{\psi}_i, \mathbf{u}_i) - (1 + \frac{\mu_0}{\mu})\mathsf{b}_{\mathcal{N}}^{i,i}(s)(\mathbf{g}_i, \mathbf{u}_i) - \mathsf{b}_{\mathcal{B}}^{e,i}(s)(\boldsymbol{\psi}_e, \mathbf{u}_i)$$

$$+ \mathsf{b}_{\mathcal{A}}^{i,e}(s)(\boldsymbol{\psi}_i, \boldsymbol{\zeta}_e) + \mathsf{b}_{\mathcal{C}}^{i,e}(s)(\mathbf{g}_i, \boldsymbol{\zeta}_e) + \mathsf{b}_{\mathcal{A}}^{e,e}(s)(\boldsymbol{\psi}_e, \boldsymbol{\zeta}_e),$$

$$\ell(s)(\begin{bmatrix} \boldsymbol{\zeta}_i \\ \mathbf{u}_i \\ \boldsymbol{\zeta}_e \end{bmatrix}) := \mu \, [\![\mu^{-1}]\!]_\Gamma \, \mathsf{b}_{\mathcal{A}}^{i,i}(s)(\mathbf{B}_0 \times \mathbf{n}, \boldsymbol{\zeta}_i)$$

$$- \mu_0 \, [\![\mu^{-1}]\!]_\Gamma \, \mathsf{b}_{\mathcal{B}}^{i,i}(s)(\mathbf{B}_0 \times \mathbf{n}, \mathbf{u}_i) + \frac{\mu_0 \, [\![\mu^{-1}]\!]_\Gamma}{2} \, \langle \mathbf{B}_0 \times \mathbf{n}, \mathbf{u}_i \rangle_{\Gamma_i^s} \,.$$

The definitions for the s bilinear forms are analogous to (5.2.3), with integrals on $\Gamma_\bullet^s$ and $\Gamma_\blacktriangle^s$.

5.2.1.3 Equivalent Formulation on Reference Boundary

For computing the shape derivative, we require the pulled back version of the bilinear forms. The procedure of transformation and pullbacks mirrors the one outlined in 5.1.2.3. Here we directly mention the pulled back bilinear forms. We skip the sub/superscript s when it is zero.

$$\hat{\mathsf{b}}_{\mathcal{A}}^{\bullet;\blacktriangle} : \mathbb{R} \times \boldsymbol{H}^{-\frac{1}{2}}(\text{div}_\Gamma \, 0, \Gamma_\bullet^0) \times \boldsymbol{H}^{-\frac{1}{2}}(\text{div}_\Gamma \, 0, \Gamma_\blacktriangle^0) \to \mathbb{R},$$

$$\hat{\mathsf{b}}_{\mathcal{A}}^{\bullet;\blacktriangle}(s; \hat{\boldsymbol{\psi}}, \hat{\boldsymbol{\zeta}}) := \int_{\Gamma_\blacktriangle^0} \int_{\Gamma_\bullet^0} G(\mathbf{T}_s^\nu(\hat{\mathbf{x}}), \mathbf{T}_s^\nu(\hat{\mathbf{y}})) \left(\mathsf{DT}_s^\nu(\hat{\mathbf{y}}) \, \hat{\boldsymbol{\psi}}(\hat{\mathbf{y}})\right) \cdot \left(\mathsf{DT}_s^\nu(\hat{\mathbf{x}}) \, \hat{\boldsymbol{\zeta}}(\hat{\mathbf{x}})\right) dS_{\hat{\mathbf{y}}} \, dS_{\hat{\mathbf{x}}},$$

$$\hat{\mathsf{b}}_{\mathcal{C}}^{\bullet;\blacktriangle} : \mathbb{R} \times \boldsymbol{H}^{-\frac{1}{2}}(\mathbf{curl}_\Gamma, \Gamma_\bullet^0) \times \boldsymbol{H}^{-\frac{1}{2}}(\text{div}_\Gamma \, 0, \Gamma_\blacktriangle^0) \to \mathbb{R},$$

$$\hat{\mathsf{b}}_{\mathcal{C}}^{\bullet;\blacktriangle}(s; \hat{\mathbf{g}}, \hat{\boldsymbol{\zeta}}) := \int_{\Gamma_\blacktriangle^0} \int_{\Gamma_\bullet^0} \left(\nabla_x G(\mathbf{T}_s^\nu(\hat{\mathbf{x}}), \mathbf{T}_s^\nu(\hat{\mathbf{y}})) \times \left(\mathsf{DT}_s^\nu(\hat{\mathbf{y}})\{\hat{\mathbf{n}}(\hat{\mathbf{y}}) \times \hat{\mathbf{g}}(\hat{\mathbf{y}})\}\right)\right) \cdot \left(\mathsf{DT}_s^\nu(\hat{\mathbf{x}}) \, \hat{\boldsymbol{\zeta}}(\hat{\mathbf{x}})\right) dS_{\hat{\mathbf{y}}} \, dS_{\hat{\mathbf{x}}},$$

$$\hat{\mathsf{b}}_{\mathcal{N}}^{\bullet;\blacktriangle} : \mathbb{R} \times \boldsymbol{H}^{-\frac{1}{2}}(\mathbf{curl}_\Gamma, \Gamma_\bullet^0) \times \boldsymbol{H}^{-\frac{1}{2}}(\mathbf{curl}_\Gamma, \Gamma_\blacktriangle^0) \to \mathbb{R},$$

$$\hat{\mathsf{b}}_{\mathcal{N}}^{\bullet;\blacktriangle}(s; \hat{\mathbf{g}}, \hat{\mathbf{u}}) := - \int_{\Gamma_\blacktriangle^0} \int_{\Gamma_\bullet^0} G(\mathbf{T}_s^\nu(\hat{\mathbf{x}}), \mathbf{T}_s^\nu(\hat{\mathbf{y}})) \, \text{curl}_\Gamma \, \hat{\mathbf{g}}(\hat{\mathbf{y}}) \, \text{curl}_\Gamma \, \hat{\mathbf{u}}(\hat{\mathbf{x}}) \, dS_{\hat{\mathbf{y}}} \, dS_{\hat{\mathbf{x}}}. \tag{5.2.15}$$

We define $\hat{\mathsf{b}}_{\mathcal{B}}^{\bullet;\blacktriangle}(s; \hat{\boldsymbol{\zeta}}, \hat{\mathbf{g}}) := \hat{\mathsf{b}}_{\mathcal{C}}^{\blacktriangle;\bullet}(s; \hat{\mathbf{g}}, \hat{\boldsymbol{\zeta}})$. Notice that on the outer boundary Γ_e, $\mathbf{T}_s^\nu(\hat{\mathbf{x}}) \equiv \hat{\mathbf{x}}$ and $\mathsf{DT}_s^\nu(\hat{\mathbf{x}}) \equiv \mathsf{Id}$. We need to do similar transformations for the terms appearing on the RHS to get a pulled back linear form. We skip the details and mention the expression for it

$$\hat{\ell}(s; \begin{bmatrix} \hat{\boldsymbol{\zeta}}_i \\ \hat{\mathbf{u}}_i \\ \hat{\boldsymbol{\zeta}}_e \end{bmatrix}) :=$$

$$\mu \, [\![\mu^{-1}]\!]_\Gamma \int_{\Gamma_i^0} \int_{\Gamma_i^0} G(\mathbf{T}_s^\nu(\hat{\mathbf{x}}), \mathbf{T}_s^\nu(\hat{\mathbf{y}})) \left(\mathbf{B}_0 \times \{\mathbf{C}(\mathsf{DT}_s^\nu)(\hat{\mathbf{y}}) \, \hat{\mathbf{n}}(\hat{\mathbf{y}})\}\right) \cdot \left(\mathsf{DT}_s^\nu(\hat{\mathbf{x}}) \, \hat{\boldsymbol{\zeta}}_i(\hat{\mathbf{x}})\right) dS_{\hat{\mathbf{y}}} \, dS_{\hat{\mathbf{x}}}$$

$$- \mu_0 \, [\![\mu^{-1}]\!]_\Gamma \int_{\Gamma_i^0} \int_{\Gamma_i^0} \left(\nabla_x G(\mathbf{T}_s^\nu(\hat{\mathbf{x}}), \mathbf{T}_s^\nu(\hat{\mathbf{y}})) \times \left(\mathsf{DT}_s^\nu(\hat{\mathbf{y}})\{\hat{\mathbf{n}}(\hat{\mathbf{y}}) \times \hat{\mathbf{u}}_i(\hat{\mathbf{y}})\}\right)\right) \cdot$$

$$\left(\mathbf{B}_0 \times \{\mathbf{C}(\mathsf{DT}_s^\nu)(\hat{\mathbf{x}}) \, \hat{\mathbf{n}}(\hat{\mathbf{x}})\}\right) dS_{\hat{\mathbf{y}}} \, dS_{\hat{\mathbf{x}}}$$

$$+ \frac{\mu_0 \, [\![\mu^{-1}]\!]_\Gamma}{2} \int_{\Gamma_i^0} \left(\mathsf{D}\mathbf{T}_s^{\boldsymbol{\nu}}(\hat{\mathbf{x}})\{\hat{\mathbf{n}}(\hat{\mathbf{x}}) \times \hat{\mathbf{u}}_i(\hat{\mathbf{x}})\} \right) \cdot \mathbf{B}_0 \; dS_{\hat{\mathbf{x}}}.$$

We have the pulled back state equation:

$$\begin{bmatrix} \hat{\boldsymbol{\psi}}_i^s \\ \hat{\mathbf{g}}_i^s \\ \hat{\boldsymbol{\psi}}_e^s \end{bmatrix} \in \boldsymbol{\mathcal{X}}: \quad \hat{\mathsf{b}}(s; \begin{bmatrix} \hat{\boldsymbol{\psi}}_i^s \\ \hat{\mathbf{g}}_i^s \\ \hat{\boldsymbol{\psi}}_e^s \end{bmatrix}, \begin{bmatrix} \hat{\boldsymbol{\zeta}}_i \\ \hat{\mathbf{u}}_i \\ \hat{\boldsymbol{\zeta}}_e \end{bmatrix}) = \hat{\ell}(s; \begin{bmatrix} \hat{\boldsymbol{\zeta}}_i \\ \hat{\mathbf{u}}_i \\ \hat{\boldsymbol{\zeta}}_e \end{bmatrix}) \quad \forall \begin{bmatrix} \hat{\boldsymbol{\zeta}}_i \\ \hat{\mathbf{u}}_i \\ \hat{\boldsymbol{\zeta}}_e \end{bmatrix} \in \boldsymbol{\mathcal{X}},$$

where

$$\hat{\mathsf{b}}(s; \begin{bmatrix} \hat{\boldsymbol{\psi}}_i \\ \hat{\mathbf{g}}_i \\ \hat{\boldsymbol{\psi}}_e \end{bmatrix}, \begin{bmatrix} \hat{\boldsymbol{\zeta}}_i \\ \hat{\mathbf{u}}_i \\ \hat{\boldsymbol{\zeta}}_e \end{bmatrix}) := (1 + \frac{\mu}{\mu_0}) \hat{\mathsf{b}}_{\mathcal{A}}^{i,i}(s; \hat{\boldsymbol{\psi}}_i, \hat{\boldsymbol{\zeta}}_i) + 2\hat{\mathsf{b}}_{\mathcal{C}}^{i,i}(s; \hat{\mathbf{g}}_i, \hat{\boldsymbol{\zeta}}_i) + \hat{\mathsf{b}}_{\mathcal{A}}^{e,i}(s; \hat{\boldsymbol{\psi}}_e, \hat{\boldsymbol{\zeta}}_i)$$
$$- 2\hat{\mathsf{b}}_{\mathcal{B}}^{i,i}(s; \hat{\boldsymbol{\psi}}_i, \hat{\mathbf{u}}_i) - (1 + \frac{\mu_0}{\mu}) \hat{\mathsf{b}}_{\mathcal{N}}^{i,i}(s; \hat{\mathbf{g}}_i, \hat{\mathbf{u}}_i) - \hat{\mathsf{b}}_{\mathcal{B}}^{e,i}(s; \hat{\boldsymbol{\psi}}_e, \hat{\mathbf{u}}_i)$$
$$+ \hat{\mathsf{b}}_{\mathcal{A}}^{i,e}(s; \hat{\boldsymbol{\psi}}_i, \hat{\boldsymbol{\zeta}}_e) + \hat{\mathsf{b}}_{\mathcal{C}}^{i,e}(s; \hat{\mathbf{g}}_i, \hat{\boldsymbol{\zeta}}_e) + \hat{\mathsf{b}}_{\mathcal{A}}^{e,e}(s; \hat{\boldsymbol{\psi}}_e, \hat{\boldsymbol{\zeta}}_e). \qquad (5.2.16)$$

5.2.1.4 BIE-Constrained Shape Derivative

The transformations are also carried out for the additional terms appearing in the relation between the field energy and the linear form (5.2.13). Again, we skip the details and include the transformed expressions in the definition of the Lagrangian $\mathcal{L}: \mathbb{R} \times \boldsymbol{\mathcal{X}} \times \boldsymbol{\mathcal{X}} \to \mathbb{R}$

$$\mathcal{L}(s; \begin{bmatrix} \hat{\boldsymbol{\psi}}_i \\ \hat{\mathbf{g}}_i \\ \hat{\boldsymbol{\psi}}_e \end{bmatrix}, \begin{bmatrix} \hat{\boldsymbol{\zeta}}_i \\ \hat{\mathbf{u}}_i \\ \hat{\boldsymbol{\zeta}}_e \end{bmatrix}) := \hat{\mathsf{b}}(s; \begin{bmatrix} \hat{\boldsymbol{\psi}}_i \\ \hat{\mathbf{g}}_i \\ \hat{\boldsymbol{\psi}}_e \end{bmatrix}, \begin{bmatrix} \hat{\boldsymbol{\zeta}}_i \\ \hat{\mathbf{u}}_i \\ \hat{\boldsymbol{\zeta}}_e \end{bmatrix}) - \hat{\ell}(s; \begin{bmatrix} \hat{\boldsymbol{\zeta}}_i \\ \hat{\mathbf{u}}_i \\ \hat{\boldsymbol{\zeta}}_e \end{bmatrix}) + \frac{1}{2\mu_0} \hat{\ell}(s; \begin{bmatrix} \hat{\boldsymbol{\psi}}_i \\ -\hat{\mathbf{g}}_i \\ \hat{\boldsymbol{\psi}}_e \end{bmatrix})$$

$$- \frac{\mu \, [\![\mu^{-1}]\!]_\Gamma^2}{2} \int_{\Gamma_i^0} \int_{\Gamma_i^0} G(\mathbf{T}_s^{\boldsymbol{\nu}}(\hat{\mathbf{x}}), \mathbf{T}_s^{\boldsymbol{\nu}}(\hat{\mathbf{y}})) \left(\mathbf{B}_0 \times \{\mathbf{C}(\mathsf{D}\mathbf{T}_s^{\boldsymbol{\nu}})(\hat{\mathbf{y}}) \, \hat{\mathbf{n}}(\hat{\mathbf{y}})\} \right) \cdot \left(\mathbf{B}_0 \times \{\mathbf{C}(\mathsf{D}\mathbf{T}_s^{\boldsymbol{\nu}})(\hat{\mathbf{x}}) \, \hat{\mathbf{n}}(\hat{\mathbf{x}})\} \right) dS_{\hat{\mathbf{y}}} \, dS_{\hat{\mathbf{x}}}$$

$$+ \frac{\|\mathbf{B}_0\|^2}{2} \int_{B_R(0)} \mu^{-1}(\hat{\mathbf{x}}) \, \det \mathsf{D}\mathbf{T}_s^{\boldsymbol{\nu}}(\hat{\mathbf{x}}) \, d\hat{\mathbf{x}}.$$

Plugging in the pulled back state solution gives the relation

$$\mathcal{E}_F(s) = \mathcal{L}(s; \begin{bmatrix} \hat{\boldsymbol{\psi}}_i^s \\ \hat{\mathbf{g}}_i^s \\ \hat{\boldsymbol{\psi}}_e^s \end{bmatrix}, \begin{bmatrix} \hat{\boldsymbol{\zeta}}_i \\ \hat{\mathbf{u}}_i \\ \hat{\boldsymbol{\zeta}}_e \end{bmatrix}) \quad \forall \begin{bmatrix} \hat{\boldsymbol{\zeta}}_i \\ \hat{\mathbf{u}}_i \\ \hat{\boldsymbol{\zeta}}_e \end{bmatrix} \in \boldsymbol{\mathcal{X}},$$

which allows us to compute the shape derivative as

$$\frac{d\mathcal{E}_F}{ds}(0) = \frac{\partial \mathcal{L}}{\partial s}(0; \begin{bmatrix} \hat{\boldsymbol{\psi}}_i^0 \\ \hat{\mathbf{g}}_i^0 \\ \hat{\boldsymbol{\psi}}_e^0 \end{bmatrix}, \begin{bmatrix} \hat{\boldsymbol{\lambda}}_i \\ \hat{\mathbf{p}}_i \\ \hat{\boldsymbol{\lambda}}_e \end{bmatrix}),$$

using the adjoint solution

$$
\begin{bmatrix} \hat{\boldsymbol{\lambda}}_i \\ \hat{\mathbf{p}}_i \\ \hat{\boldsymbol{\lambda}}_e \end{bmatrix} \in \boldsymbol{\mathcal{X}}: \quad \left\langle \frac{\partial \mathcal{L}}{\partial \begin{bmatrix} \hat{\boldsymbol{\psi}}_i \\ \hat{\mathbf{g}}_i \\ \hat{\boldsymbol{\psi}}_e \end{bmatrix}}(0; \begin{bmatrix} \hat{\boldsymbol{\psi}}_i^0 \\ \hat{\mathbf{g}}_i^0 \\ \hat{\boldsymbol{\psi}}_e^0 \end{bmatrix}, \begin{bmatrix} \hat{\boldsymbol{\lambda}}_i \\ \hat{\mathbf{p}}_i \\ \hat{\boldsymbol{\lambda}}_e \end{bmatrix}); \begin{bmatrix} \hat{\boldsymbol{\zeta}}_i \\ \hat{\mathbf{u}}_i \\ \hat{\boldsymbol{\zeta}}_e \end{bmatrix} \right\rangle = 0 \quad \forall \begin{bmatrix} \hat{\boldsymbol{\zeta}}_i \\ \hat{\mathbf{u}}_i \\ \hat{\boldsymbol{\zeta}}_e \end{bmatrix} \in \boldsymbol{\mathcal{X}}.
$$

Computing the partial derivative reduces the above expression to an explicit variational equation

$$
\hat{\mathsf{b}}(0; \begin{bmatrix} \hat{\boldsymbol{\zeta}}_i \\ \hat{\mathbf{u}}_i \\ \hat{\boldsymbol{\zeta}}_e \end{bmatrix}, \begin{bmatrix} \hat{\boldsymbol{\lambda}}_i \\ \hat{\mathbf{p}}_i \\ \hat{\boldsymbol{\lambda}}_e \end{bmatrix}) + \frac{1}{2\mu_0} \hat{\ell}(0; \begin{bmatrix} \hat{\boldsymbol{\zeta}}_i \\ -\hat{\mathbf{u}}_i \\ \hat{\boldsymbol{\zeta}}_e \end{bmatrix}) = 0 \quad \forall \begin{bmatrix} \hat{\boldsymbol{\zeta}}_i \\ \hat{\mathbf{u}}_i \\ \hat{\boldsymbol{\zeta}}_e \end{bmatrix} \in \boldsymbol{\mathcal{X}}.
$$

Changing the sign of the test function $\hat{u}_i$ we get

$$
\hat{\mathsf{b}}(0; \begin{bmatrix} \hat{\boldsymbol{\zeta}}_i \\ -\hat{\mathbf{u}}_i \\ \hat{\boldsymbol{\zeta}}_e \end{bmatrix}, \begin{bmatrix} \hat{\boldsymbol{\lambda}}_i \\ \hat{\mathbf{p}}_i \\ \hat{\boldsymbol{\lambda}}_e \end{bmatrix}) = \hat{\mathsf{b}}(0; \begin{bmatrix} \hat{\boldsymbol{\lambda}}_i \\ -\hat{\mathbf{p}}_i \\ \hat{\boldsymbol{\lambda}}_e \end{bmatrix}, \begin{bmatrix} \hat{\boldsymbol{\zeta}}_i \\ \hat{\mathbf{u}}_i \\ \hat{\boldsymbol{\zeta}}_e \end{bmatrix}) = -\frac{1}{2\mu_0} \hat{\ell}(0; \begin{bmatrix} \hat{\boldsymbol{\zeta}}_i \\ \hat{\mathbf{u}}_i \\ \hat{\boldsymbol{\zeta}}_e \end{bmatrix}) \quad \forall \begin{bmatrix} \hat{\boldsymbol{\zeta}}_i \\ \hat{\mathbf{u}}_i \\ \hat{\boldsymbol{\zeta}}_e \end{bmatrix} \in \boldsymbol{\mathcal{X}}.
$$

Comparing with the state equation we get

$$
\begin{bmatrix} \hat{\boldsymbol{\lambda}}_i \\ \hat{\mathbf{p}}_i \\ \hat{\boldsymbol{\lambda}}_e \end{bmatrix} = \frac{1}{2\mu_0} \begin{bmatrix} -\hat{\boldsymbol{\psi}}_i^0 \\ \hat{\mathbf{g}}_i^0 \\ -\hat{\boldsymbol{\psi}}_e^0 \end{bmatrix}.
$$

The shape derivative can then be computed using (3.0.11), (3.0.13), and is given as

$$
\frac{d\mathcal{E}_F}{ds}(0) = \frac{\partial \mathcal{L}}{\partial s}(0; \begin{bmatrix} \hat{\boldsymbol{\psi}}_i^0 \\ \hat{\mathbf{g}}_i^0 \\ \hat{\boldsymbol{\psi}}_e^0 \end{bmatrix}, \frac{1}{2\mu_0} \begin{bmatrix} -\hat{\boldsymbol{\psi}}_i^0 \\ \hat{\mathbf{g}}_i^0 \\ -\hat{\boldsymbol{\psi}}_e^0 \end{bmatrix})
$$

$$
= -\frac{1}{2\mu_0} \frac{\partial \hat{\mathsf{b}}}{\partial s}(0; \begin{bmatrix} \hat{\boldsymbol{\psi}}_i^0 \\ \hat{\mathbf{g}}_i^0 \\ \hat{\boldsymbol{\psi}}_e^0 \end{bmatrix}, \begin{bmatrix} \hat{\boldsymbol{\psi}}_i^0 \\ -\hat{\mathbf{g}}_i^0 \\ \hat{\boldsymbol{\psi}}_e^0 \end{bmatrix}) + \frac{1}{\mu_0} \frac{\partial \hat{\ell}}{\partial s}(0; \begin{bmatrix} \hat{\boldsymbol{\psi}}_i^0 \\ -\hat{\mathbf{g}}_i^0 \\ \hat{\boldsymbol{\psi}}_e^0 \end{bmatrix})
$$

$$
- \frac{\mu \, [\![\mu^{-1}]\!]_\Gamma^2}{2} \int_{\Gamma_i^0} \int_{\Gamma_i^0} \left(\nabla_x G(\hat{\mathbf{x}}, \hat{\mathbf{y}}) \cdot \boldsymbol{\mathcal{V}}(\hat{\mathbf{x}}) + \nabla_y G(\hat{\mathbf{x}}, \hat{\mathbf{y}}) \cdot \boldsymbol{\mathcal{V}}(\hat{\mathbf{y}}) \right) \left(\mathbf{B}_0 \times \hat{\mathbf{n}}(\hat{\mathbf{y}}) \right) \cdot \left(\mathbf{B}_0 \times \hat{\mathbf{n}}(\hat{\mathbf{x}}) \right) dS_{\hat{\mathbf{y}}} \, dS_{\hat{\mathbf{x}}}
$$

$$
- \frac{\mu \, [\![\mu^{-1}]\!]_\Gamma^2}{2} \int_{\Gamma_i^0} \int_{\Gamma_i^0} G(\hat{\mathbf{x}}, \hat{\mathbf{y}}) \left(\mathbf{B}_0 \times \{ \nabla \cdot \boldsymbol{\mathcal{V}}(\hat{\mathbf{y}}) \, \hat{\mathbf{n}}(\hat{\mathbf{y}}) - \mathsf{D}\boldsymbol{\mathcal{V}}^T(\hat{\mathbf{y}}) \hat{\mathbf{n}}(\hat{\mathbf{y}}) \} \right) \cdot \left(\mathbf{B}_0 \times \hat{\mathbf{n}}(\hat{\mathbf{x}}) \right) dS_{\hat{\mathbf{y}}} \, dS_{\hat{\mathbf{x}}}
$$

$$
- \frac{\mu \, [\![\mu^{-1}]\!]_\Gamma^2}{2} \int_{\Gamma_i^0} \int_{\Gamma_i^0} G(\hat{\mathbf{x}}, \hat{\mathbf{y}}) \left(\mathbf{B}_0 \times \hat{\mathbf{n}}(\hat{\mathbf{y}}) \right) \cdot \left(\mathbf{B}_0 \times \{ \nabla \cdot \boldsymbol{\mathcal{V}}(\hat{\mathbf{x}}) \, \hat{\mathbf{n}}(\hat{\mathbf{x}}) - \mathsf{D}\boldsymbol{\mathcal{V}}^T(\hat{\mathbf{x}}) \hat{\mathbf{n}}(\hat{\mathbf{x}}) \} \right) dS_{\hat{\mathbf{y}}} \, dS_{\hat{\mathbf{x}}}
$$

$$-\frac{[\![\mu^{-1}]\!]_\Gamma \, \|\mathbf{B}_0\|^2}{2} \int\limits_{\Gamma_i^0} \boldsymbol{\mathcal{V}}(\hat{\mathbf{x}}) \cdot \hat{\mathbf{n}}(\hat{\mathbf{x}}) \, dS_{\hat{\mathbf{x}}}, \tag{5.2.17}$$

where the partial derivative of the bilinear form can be computed using the definition (5.2.16) and the partial derivatives of its constituents

$$\frac{\partial \hat{\mathsf{b}}_{\mathcal{A}}^{\bullet;\blacktriangle}}{\partial s}(0; \hat{\boldsymbol{\psi}}, \hat{\boldsymbol{\zeta}}) := \int\limits_{\Gamma_{\blacktriangle}^0} \int\limits_{\Gamma_{\bullet}^0} \left(\nabla_x G(\hat{\mathbf{x}}, \hat{\mathbf{y}}) \cdot \boldsymbol{\mathcal{V}}(\hat{\mathbf{x}}) + \nabla_y G(\hat{\mathbf{x}}, \hat{\mathbf{y}}) \cdot \boldsymbol{\mathcal{V}}(\hat{\mathbf{y}}) \right) \hat{\boldsymbol{\psi}}(\hat{\mathbf{y}}) \cdot \hat{\boldsymbol{\zeta}}(\hat{\mathbf{x}}) \, dS_{\hat{\mathbf{y}}} \, dS_{\hat{\mathbf{x}}}$$

$$+ \int\limits_{\Gamma_{\blacktriangle}^0} \int\limits_{\Gamma_{\bullet}^0} G(\hat{\mathbf{x}}, \hat{\mathbf{y}}) \left(\mathsf{D}\boldsymbol{\mathcal{V}}(\hat{\mathbf{y}}) \, \hat{\boldsymbol{\psi}}(\hat{\mathbf{y}}) \right) \cdot \hat{\boldsymbol{\zeta}}(\hat{\mathbf{x}}) \, dS_{\hat{\mathbf{y}}} \, dS_{\hat{\mathbf{x}}}$$

$$+ \int\limits_{\Gamma_{\blacktriangle}^0} \int\limits_{\Gamma_{\bullet}^0} G(\hat{\mathbf{x}}, \hat{\mathbf{y}}) \, \hat{\boldsymbol{\psi}}(\hat{\mathbf{y}}) \cdot \left(\mathsf{D}\boldsymbol{\mathcal{V}}(\hat{\mathbf{x}}) \, \hat{\boldsymbol{\zeta}}(\hat{\mathbf{x}}) \right) \, dS_{\hat{\mathbf{y}}} \, dS_{\hat{\mathbf{x}}},$$

$$\frac{\partial \hat{\mathsf{b}}_{\mathcal{C}}^{\bullet;\blacktriangle}}{\partial s}(0; \hat{\mathbf{g}}, \hat{\boldsymbol{\zeta}}) := \int\limits_{\Gamma_{\blacktriangle}^0} \int\limits_{\Gamma_{\bullet}^0} \left(\frac{d\nabla_x G(\mathbf{T}_s^{\boldsymbol{\nu}}(\hat{\mathbf{x}}), \mathbf{T}_s^{\boldsymbol{\nu}}(\hat{\mathbf{y}}))}{ds}\Big|_{s=0} \times \left(\hat{\mathbf{n}}(\hat{\mathbf{y}}) \times \hat{\mathbf{g}}(\hat{\mathbf{y}}) \right) \right) \cdot \hat{\boldsymbol{\zeta}}(\hat{\mathbf{x}}) \, dS_{\hat{\mathbf{y}}} \, dS_{\hat{\mathbf{x}}}$$

$$+ \int\limits_{\Gamma_{\blacktriangle}^0} \int\limits_{\Gamma_{\bullet}^0} \left(\nabla_x G(\hat{\mathbf{x}}, \hat{\mathbf{y}}) \times \left(\mathsf{D}\boldsymbol{\mathcal{V}}(\hat{\mathbf{y}})\{\hat{\mathbf{n}}(\hat{\mathbf{y}}) \times \hat{\mathbf{g}}(\hat{\mathbf{y}})\} \right) \right) \cdot \hat{\boldsymbol{\zeta}}(\hat{\mathbf{x}}) \, dS_{\hat{\mathbf{y}}} \, dS_{\hat{\mathbf{x}}}$$

$$+ \int\limits_{\Gamma_{\blacktriangle}^0} \int\limits_{\Gamma_{\bullet}^0} \left(\nabla_x G(\hat{\mathbf{x}}, \hat{\mathbf{y}}) \times \left(\hat{\mathbf{n}}(\hat{\mathbf{y}}) \times \hat{\mathbf{g}}(\hat{\mathbf{y}}) \right) \right) \cdot \left(\mathsf{D}\boldsymbol{\mathcal{V}}(\hat{\mathbf{x}}) \, \hat{\boldsymbol{\zeta}}(\hat{\mathbf{x}}) \right) \, dS_{\hat{\mathbf{y}}} \, dS_{\hat{\mathbf{x}}},$$

$$\frac{\partial \hat{\mathsf{b}}_{\mathcal{N}}^{\bullet;\blacktriangle}}{\partial s}(0; \hat{\mathbf{g}}, \hat{\mathbf{u}}) := - \int\limits_{\Gamma_{\blacktriangle}^0} \int\limits_{\Gamma_{\bullet}^0} \left(\nabla_x G(\hat{\mathbf{x}}, \hat{\mathbf{y}}) \cdot \boldsymbol{\mathcal{V}}(\hat{\mathbf{x}}) + \nabla_y G(\hat{\mathbf{x}}, \hat{\mathbf{y}}) \cdot \boldsymbol{\mathcal{V}}(\hat{\mathbf{y}}) \right) \, \mathrm{curl}_\Gamma \, \hat{\mathbf{g}}(\hat{\mathbf{y}}) \, \mathrm{curl}_\Gamma \, \hat{\mathbf{u}}(\hat{\mathbf{x}}) \, dS_{\hat{\mathbf{y}}} \, dS_{\hat{\mathbf{x}}}.$$

$$\tag{5.2.18}$$

The partial derivative for $\nabla_x G(\mathbf{T}_s^{\boldsymbol{\nu}}(\hat{\mathbf{x}}), \mathbf{T}_s^{\boldsymbol{\nu}}(\hat{\mathbf{y}}))$ with respect to s is computed in (5.1.38). The partial derivative for the linear form is given as

$$\frac{\partial \hat{\ell}}{\partial s}\left(0; \begin{bmatrix} \hat{\boldsymbol{\zeta}}_i \\ \hat{\mathbf{u}}_i \\ \hat{\boldsymbol{\zeta}}_e \end{bmatrix}\right) :=$$

$$\mu \, [\![\mu^{-1}]\!]_\Gamma \int\limits_{\Gamma_i^0} \int\limits_{\Gamma_i^0} \left(\nabla_x G(\hat{\mathbf{x}}, \hat{\mathbf{y}}) \cdot \boldsymbol{\mathcal{V}}(\hat{\mathbf{x}}) + \nabla_y G(\hat{\mathbf{x}}, \hat{\mathbf{y}}) \cdot \boldsymbol{\mathcal{V}}(\hat{\mathbf{y}}) \right) \left(\mathbf{B}_0 \times \hat{\mathbf{n}}(\hat{\mathbf{y}}) \right) \cdot \hat{\boldsymbol{\zeta}}_i(\hat{\mathbf{x}}) \, dS_{\hat{\mathbf{y}}} \, dS_{\hat{\mathbf{x}}}$$

$$+ \mu \, [\![\mu^{-1}]\!]_\Gamma \int\limits_{\Gamma_i^0} \int\limits_{\Gamma_i^0} G(\hat{\mathbf{x}}, \hat{\mathbf{y}}) \left(\mathbf{B}_0 \times \{\nabla \cdot \boldsymbol{\mathcal{V}}(\hat{\mathbf{y}}) \, \hat{\mathbf{n}}(\hat{\mathbf{y}}) - \mathsf{D}\boldsymbol{\mathcal{V}}^T(\hat{\mathbf{y}})\hat{\mathbf{n}}(\hat{\mathbf{y}})\} \right) \cdot \hat{\boldsymbol{\zeta}}_i(\hat{\mathbf{x}}) \, dS_{\hat{\mathbf{y}}} \, dS_{\hat{\mathbf{x}}}$$

$$+ \mu \, [\![\mu^{-1}]\!]_\Gamma \int\limits_{\Gamma_i^0} \int\limits_{\Gamma_i^0} G(\hat{\mathbf{x}}, \hat{\mathbf{y}}) \left(\mathbf{B}_0 \times \hat{\mathbf{n}}(\hat{\mathbf{y}}) \right) \cdot \left(\mathsf{D}\boldsymbol{\mathcal{V}}(\hat{\mathbf{x}}) \, \hat{\boldsymbol{\zeta}}_i(\hat{\mathbf{x}}) \right) \, dS_{\hat{\mathbf{y}}} \, dS_{\hat{\mathbf{x}}}$$

$$
- \mu_0 \left[\!\left[\mu^{-1} \right]\!\right]_\Gamma \int_{\Gamma_i^0} \int_{\Gamma_i^0} \left(\frac{d\nabla_x G(\mathbf{T}_s^\nu(\hat{\mathbf{x}}), \mathbf{T}_s^\nu(\hat{\mathbf{y}}))}{ds} \bigg|_{s=0} \times \left(\hat{\mathbf{n}}(\hat{\mathbf{y}}) \times \hat{\mathbf{u}}_i(\hat{\mathbf{y}}) \right) \right) \cdot \left(\mathbf{B}_0 \times \hat{\mathbf{n}}(\hat{\mathbf{x}}) \right) \, dS_{\hat{\mathbf{y}}} \, dS_{\hat{\mathbf{x}}}
$$

$$
- \mu_0 \left[\!\left[\mu^{-1} \right]\!\right]_\Gamma \int_{\Gamma_i^0} \int_{\Gamma_i^0} \left(\nabla_x G(\hat{\mathbf{x}}, \hat{\mathbf{y}}) \times \left(\mathsf{D}\boldsymbol{\mathcal{V}}(\hat{\mathbf{y}}) \{ \hat{\mathbf{n}}(\hat{\mathbf{y}}) \times \hat{\mathbf{u}}_i(\hat{\mathbf{y}}) \} \right) \right) \cdot \left(\mathbf{B}_0 \times \hat{\mathbf{n}}(\hat{\mathbf{x}}) \right) \, dS_{\hat{\mathbf{y}}} \, dS_{\hat{\mathbf{x}}}
$$

$$
- \mu_0 \left[\!\left[\mu^{-1} \right]\!\right]_\Gamma \int_{\Gamma_i^0} \int_{\Gamma_i^0} \left(\nabla_x G(\hat{\mathbf{x}}, \hat{\mathbf{y}}) \times \left(\hat{\mathbf{n}}(\hat{\mathbf{y}}) \times \hat{\mathbf{u}}_i(\hat{\mathbf{y}}) \right) \right) \cdot \left(\mathbf{B}_0 \times \{ \nabla \cdot \boldsymbol{\mathcal{V}}(\hat{\mathbf{x}}) \, \hat{\mathbf{n}}(\hat{\mathbf{x}}) - \mathsf{D}\boldsymbol{\mathcal{V}}^T(\hat{\mathbf{x}}) \hat{\mathbf{n}}(\hat{\mathbf{x}}) \} \right) \, dS_{\hat{\mathbf{y}}} \, dS_{\hat{\mathbf{x}}}
$$

$$
+ \frac{\mu_0 \left[\!\left[\mu^{-1} \right]\!\right]_\Gamma}{2} \int_{\Gamma_i^0} \left(\mathsf{D}\boldsymbol{\mathcal{V}}(\hat{\mathbf{x}}) \{ \hat{\mathbf{n}}(\hat{\mathbf{x}}) \times \hat{\mathbf{u}}_i(\hat{\mathbf{x}}) \} \right) \cdot \mathbf{B}_0 \, dS_{\hat{\mathbf{x}}}.
$$

5.2.1.5   Numerical Experiments

In this section we evaluate the shape derivatives numerically and gauge their performance. The BEM based shape derivative (5.2.17) (denoted "BEM" in plots) is compared with (5.1.45) (denoted "MST" in plots). Note that "MST" is exactly the expression obtained via a volume based variational constraint, also obtained using the Maxwell Stress Tensor. Discretizing the boundary Γ with a triangular mesh $\mathcal{M}_h$, we use the space $\mathbf{n} \times \nabla P_*^1(\mathcal{M}_h)$ to discretize $\boldsymbol{H}^{-\frac{1}{2}}(\mathrm{div}_\Gamma\, 0, \Gamma)$, where P_*^1 is the space of piece-wise linear functions with a zero mean. For the tangential trace the relevant continuous space is $V := \{ \mathbf{u} \in \boldsymbol{H}^{-\frac{1}{2}}(\mathbf{curl}_\Gamma, \Gamma) : (\mathbf{u}, \mathbf{grad}_\Gamma\, v)_{-\frac{1}{2}} = 0 \quad \forall v \in H_*^{\frac{1}{2}}(\Gamma) \}$ (for trivial topology), as explained in Remark 2, which is discretized using the lowest order Nedelec edge elements and enforcing the orthogonality constraint to the elements of $P_*^1(\mathcal{M}_h)$ space. In the discrete system, these constraints are applied through a mixed formulation following the ideas mentioned in [58, Section 3.5, Chapter 3]. For the computation of the BEM based shape derivative, we use the Sauter and Schwab quadrature rule [54] of order 5^4. For evaluating the partial derivative $\frac{\partial \hat{\mathbf{b}}_c^{i,i}}{\partial s}$, we simply use the singular quadrature rule for evaluation even though we do not have a proof that the integrals exist as weakly singular integrals, exactly as done in Section 5.1.2.8.

Experiment 19. We have a spherical domain Ω_i with radius 2.5, centered at $(1, 0, 0)$ occupied by a linear material with $\mu = 4$. It is surrounded by a ball of radius 4 centered at $(0, 0, 0)$ and the space in between is occupied by a linear material with $\mu_0 = 2$. The setting is depicted in Figure 5.23. We use the value $\mathbf{B}_0 = (1, 1, 1)$.
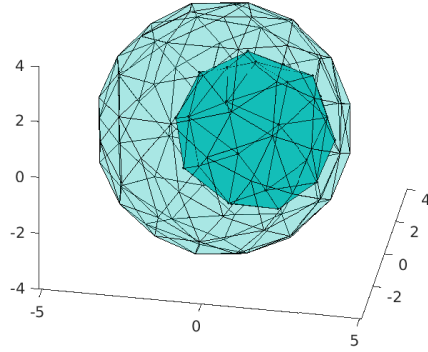
Figure 5.23: Geometrical setting

The total force and torques are computed using the shape derivative formulas (5.2.17) ("BEM") and (5.1.45) ("MST") and the errors are plotted in Figure 5.24. We see similar convergence rates for this smooth spherical setting which are also reported in Table 5.9. The reference values for force and torque are computed using the BEM based shape derivative at a refinement level of $h = 0.138$.
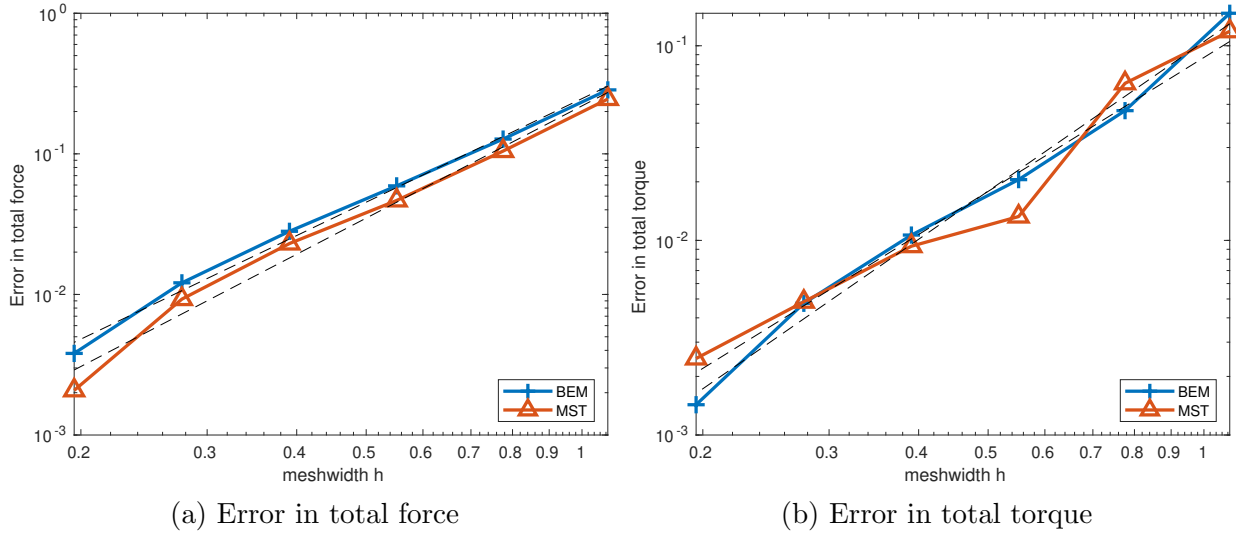

(a) Error in total force

(b) Error in total torque

Figure 5.24: Error in force and torque computation for Sphere (Experiment 19)

Table 5.9: Asymptotic rate of algebraic convergence for Experiment 19

Method	Force	Torque
Pullback approach	2.44	2.55
Stress tensor	2.65	2.28

The dual norm computations are presented in Figure 5.25 where the reference values are again computed using the BEM based shape derivative at a refinement level of $h = 0.196$.
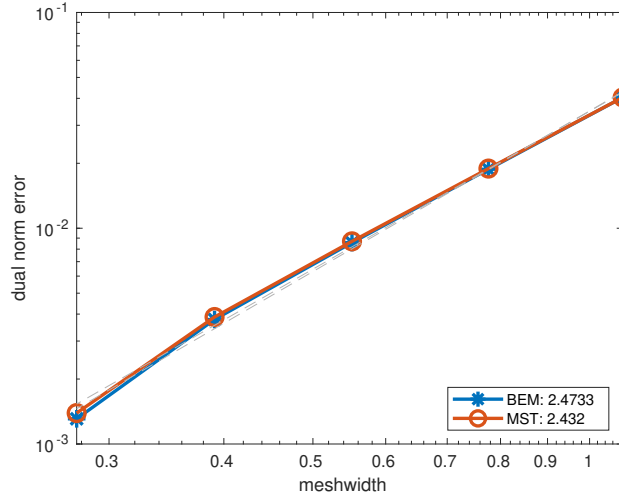
Figure 5.25: Dual norm error for Experiment 19

Experiment 20. We have a cubic domain Ω_i with side length 2, centered at $(1, 0.5, 1)$ occupied by a linear material with $\mu = 4$. It is surrounded by a ball of radius 4 centered at $(0, 0, 0)$ and the space in between is occupied by a linear material with $\mu_0 = 2$. The setting is depicted in Figure 5.26. We use the value $\mathbf{B}_0 = (1, 1, 1)$.
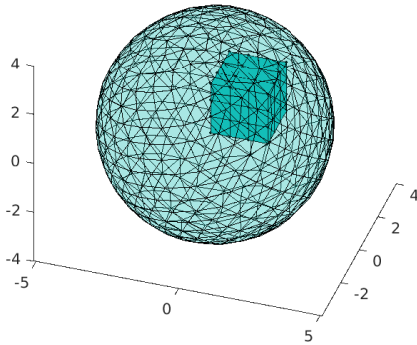

Figure 5.26: Geometrical setting

The total force and torques are computed using the shape derivative formulas (5.2.17) ("BEM") and (5.1.45) ("MST") and the errors are plotted in Figure 5.27. We see similar convergence rates for this smooth spherical setting which are also reported in Table 5.10. The reference values for force and torque are computed using the BEM based shape derivative at a refinement level of $h = 0.108$.
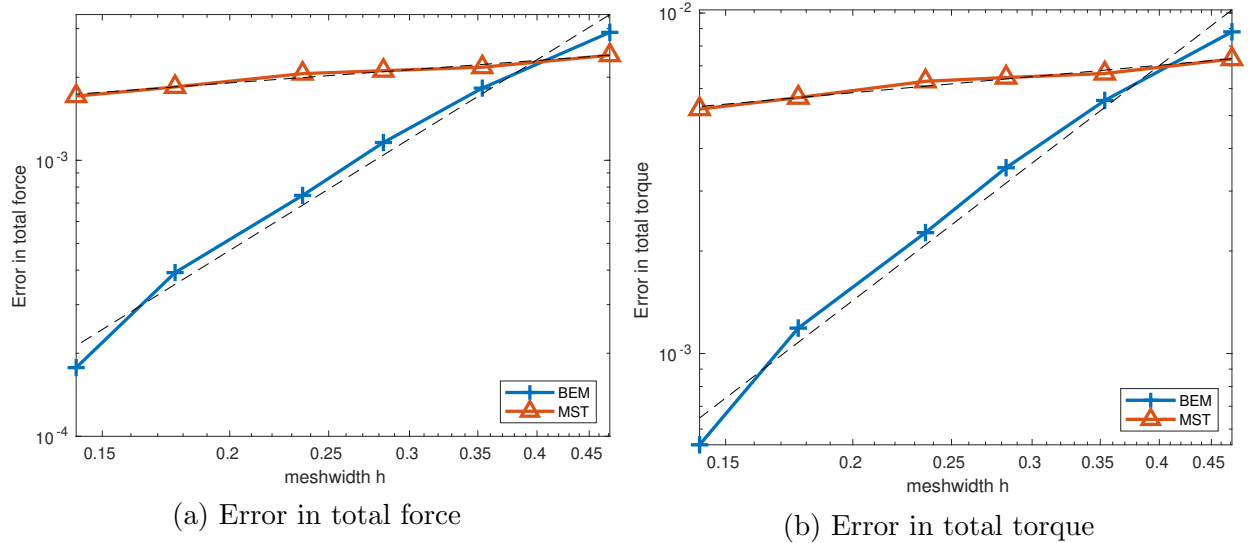
(a) Error in total force

(b) Error in total torque

Figure 5.27: Error in force and torque computation for Cube (Experiment 20)

Table 5.10: Asymptotic rate of algebraic convergence for Experiment 20

Method	Force	Torque
Pullback approach	2.29	2.29
Stress tensor	0.27	0.27

The dual norm computations are presented in Figure 5.28 where the reference values are again computed using the BEM based shape derivative at a refinement level of $h = 0.108$.
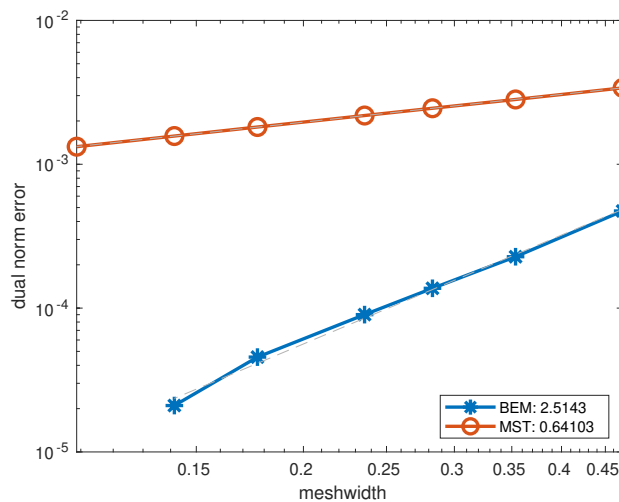

Figure 5.28: Dual norm error for Experiment 20

Experiment 21. We have a cuboidal shaped domain Ω_i with sides $(3,1,1)$, centered at $(1, 0.5, 1)$ occupied by a linear material with $\mu = 4$. It is surrounded by a ball of radius 4

centered at $(0,0,0)$ and the space in between is occupied by a linear material with $\mu_0 = 2$. The setting is depicted in Figure 5.29. We use the value $\mathbf{B}_0 = (1,1,1)$.
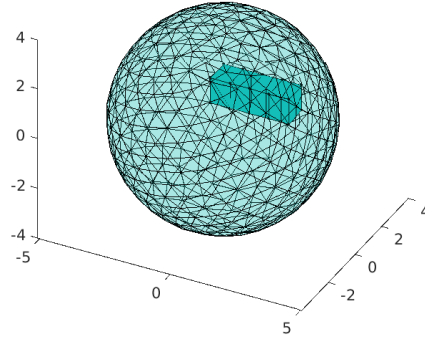

Figure 5.29: Geometrical setting

The total force and torques are computed using the shape derivative formulas (5.2.17) ("BEM") and (5.1.45) ("MST") and the errors are plotted in Figure 5.30. We see similar convergence rates for this smooth spherical setting which are also reported in Table 5.11. The reference values for force and torque are computed using the BEM based shape derivative at a refinement level of $h = 0.118$.

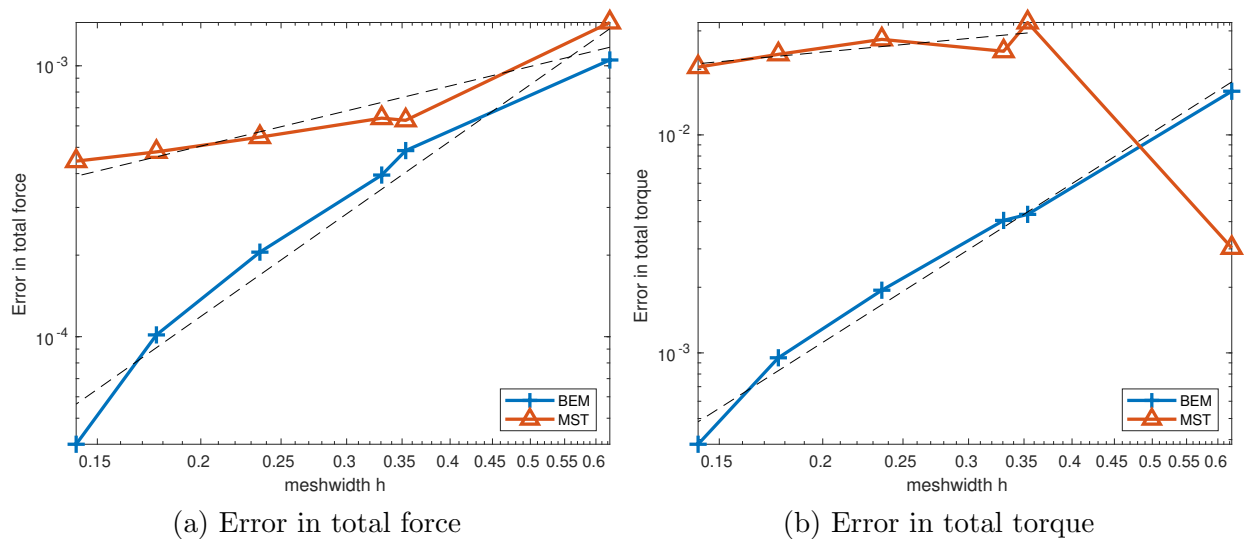(a) Error in total force

(b) Error in total torque

Figure 5.30: Error in force and torque computation for Cuboid (Experiment 21)

Table 5.11: Asymptotic rate of algebraic convergence for Experiment 21

Method	Force	Torque
Pullback approach	2.15	2.42
Stress tensor	0.74	0.35

The dual norm computations are presented in Figure 5.31 where the reference values are again computed using the BEM based shape derivative at a refinement level of $h = 0.118$.

Figure 5.31: Dual norm error for Experiment 21

Experiment 22. We have a tetrahedral shaped domain Ω_i with corners $(\pm 1, 0, -\frac{1}{\sqrt{2}})$ and $(0, \pm 1, \frac{1}{\sqrt{2}})$, translated by $(2, 1, 3)$ occupied by a linear material with $\mu = 4$. It is surrounded by a ball of radius 2 centered at $(2.3, 1.5, 3.1)$ and the space in between is occupied by a linear material with $\mu_0 = 2$. The setting is depicted in Figure 5.32. We use the value $\mathbf{B}_0 = (1, 0, 0)$.
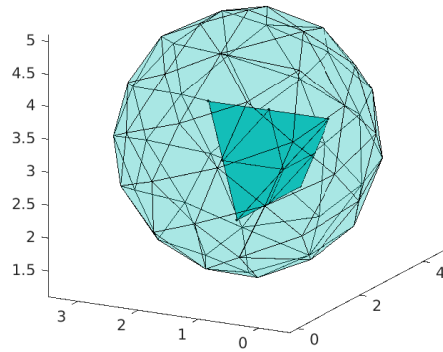
Figure 5.32: Geometrical setting

153

The total force and torques are computed using the shape derivative formulas (5.2.17) ("BEM") and (5.1.45) ("MST") and the errors are plotted in Figure 5.33. We see similar convergence rates for this smooth spherical setting which are also reported in Table 5.12. The reference values for force and torque are computed using the BEM based shape derivative at a refinement level of $h = 0.082$.

(a) Error in total force (b) Error in total torque
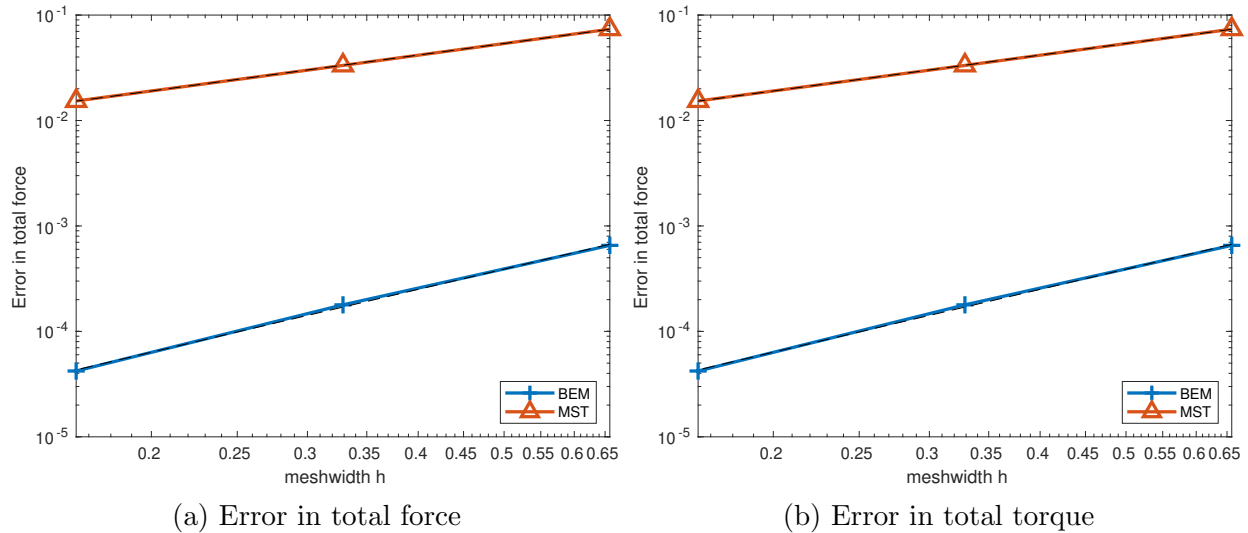
Figure 5.33: Error in force and torque computation for Tetrahedron (Experiment 22)

Table 5.12: Asymptotic rate of algebraic convergence for Experiment 22

Method	Force	Torque
Pullback approach	1.98	1.96
Stress tensor	1.13	1.13

The dual norm computations are presented in Figure 5.34 where the reference values are again computed using the BEM based shape derivative at a refinement level of $h = 0.082$.
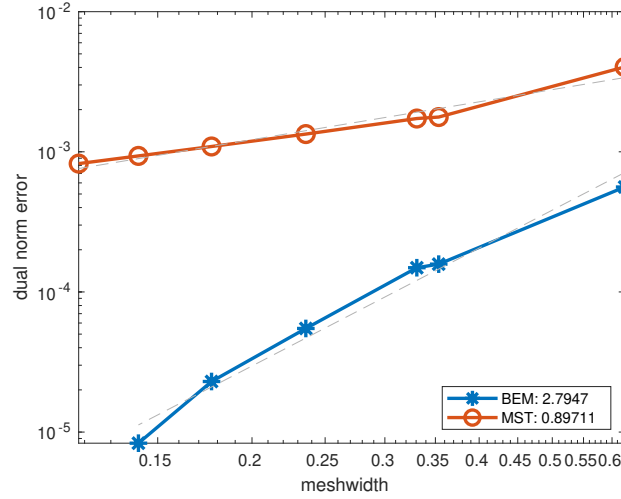
Figure 5.34: Dual norm error for Experiment 22
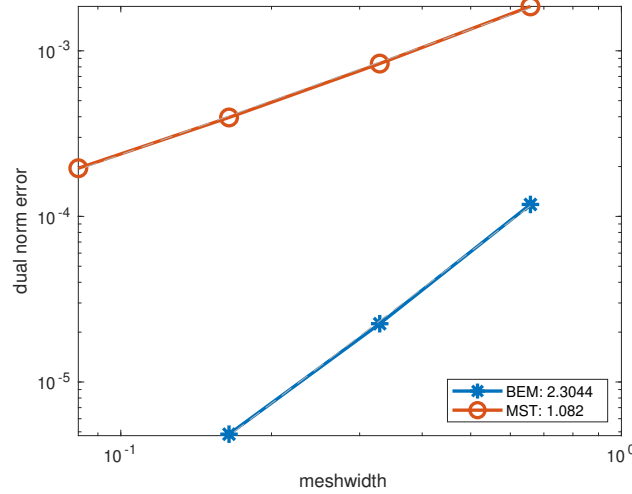
5.2.2 Scalar Potential Formulation

Instead of using the divergence constraint to introduce a vector potential ansatz, we use $\mathbf{curl}\,\mathbf{H}_{tot} = 0$ to write $\mathbf{H}_{tot} = \nabla u$. We enforce the Dirichlet boundary condition $\gamma_D u = \gamma_D u_{const}$ at the outer boundary Γ_e where $u_{const} = \mathbf{H}_0 \cdot \mathbf{x}$ such that $\nabla u_{const} = \mathbf{H}_0$. Coupling the scalar potential ansatz with the divergence equation for $\mathbf{B}_{tot}$ and the material law we get the transmission problem

$$
\begin{aligned}
\operatorname{div}(\mu(\mathbf{x})\,\nabla u) &= 0 && \text{in } \Omega_i \cup \Omega_e, \\
[\![\mu\gamma_N u]\!]_\Gamma &= 0 && \text{at } \Gamma_i, \\
[\![\gamma_D u]\!]_\Gamma &= 0 && \text{at } \Gamma_i, \\
\gamma_D u &= \mathbf{H}_0 \cdot \mathbf{x} && \text{at } \Gamma_e.
\end{aligned}
\tag{5.2.19}
$$

The transmission conditions are Γ_i are obtained from the transmission conditons for $\mathbf{B}_{tot}$ ($[\![\mathbf{B}_{tot}]\!]_\Gamma \cdot \mathbf{n} = 0$) and $\mathbf{H}_{tot}$ ($[\![\mathbf{H}_{tot}]\!]_\Gamma \times \mathbf{n} = 0$) expressed in terms of u.

5.2.2.1 Variational Boundary Integral Equations

We derive the BIE based variational formulation for (5.2.19). We start with BIEs for $\partial\Omega_e$ in variational form. Since Ω_e is bounded, we can use the equations for the bounded domain from (2.1.22). Denoting the Neumann and Dirichlet traces of u on $\partial\Omega_e$ by ψ and g respectively and denoting the BIOs with sub-script e we have

$$
\mathsf{b}_{\mathrm{V}_e}(\psi, \phi) - \mathsf{b}_{\mathrm{K}_e}(g, \phi) - \frac{1}{2}\langle g, \phi\rangle_{\partial\Omega_e} = 0 \quad \forall \phi \in H^{-\frac{1}{2}}(\partial\Omega_e),
$$

$$
-\frac{1}{2}\langle \psi, u\rangle_{\partial\Omega_e} + \mathsf{b}_{\mathrm{K}'_e}(\psi, u) + \mathsf{b}_{\mathrm{W}_e}(g, u) = 0 \quad \forall u \in H^{\frac{1}{2}}(\partial\Omega_e).
$$

Since $\partial\Omega_e = \Gamma_i \cup \Gamma_e$ we can split the integrals in the bilinear forms. The resulting equations can be written compactly using the following notation:

$$
\mathsf{b}_{\mathrm{V}}^{\bullet;\blacktriangle} : H^{-\frac{1}{2}}(\Gamma_\bullet) \times H^{-\frac{1}{2}}(\Gamma_\blacktriangle),
$$

155

$$\mathsf{b}_V^{\bullet;\blacktriangle}(\psi,\phi) := \int\limits_{\Gamma_\blacktriangle} \int\limits_{\Gamma_\bullet} G(\mathbf{x},\mathbf{y})\,\psi(\mathbf{y})\,\phi(\mathbf{x})\,dS_\mathbf{y}\,dS_\mathbf{x},$$

$$\mathsf{b}_K^{\bullet;\blacktriangle} : H^{\frac{1}{2}}(\Gamma_\bullet) \times H^{-\frac{1}{2}}(\Gamma_\blacktriangle),$$

$$\mathsf{b}_K^{\bullet;\blacktriangle}(g,\phi) := \int\limits_{\Gamma_\blacktriangle} \int\limits_{\Gamma_\bullet} \nabla_y G(\mathbf{x},\mathbf{y}) \cdot \mathbf{n}(\mathbf{y})\,g(\mathbf{y})\,\phi(\mathbf{x})\,dS_\mathbf{y}\,dS_\mathbf{x},$$

$$\mathsf{b}_W^{\bullet;\blacktriangle} : H^{\frac{1}{2}}(\Gamma_\bullet) \times H^{\frac{1}{2}}(\Gamma_\blacktriangle),$$

$$\mathsf{b}_W^{\bullet;\blacktriangle}(g,u) := \int\limits_{\Gamma_\blacktriangle} \int\limits_{\Gamma_\bullet} G(\mathbf{x},\mathbf{y})\,\mathbf{curl}_\Gamma\, g(\mathbf{y}) \cdot \mathbf{curl}_\Gamma\, u(\mathbf{x})\,dS_\mathbf{y}\,dS_\mathbf{x}. \tag{5.2.20}$$

Bilinear form for K′ is defined as $\mathsf{b}_{K'}^{\bullet;\blacktriangle}(\psi,u) := \mathsf{b}_K^{\blacktriangle;\bullet}(u,\psi)$. In the above definition, $\mathbf{n}$ denotes the exterior unit normal for both $\bullet, \blacktriangle \in \{i,e\}$. Writing $\psi_* := \psi|_{\Gamma_*}, g_* := g|_{\Gamma_*}, \phi_* = \phi|_{\Gamma_*}, u_* = u|_{\Gamma_*}, * \in \{i,e\}$ and the introduced notation, we can write the above equations as

$$\mathsf{b}_V^{i,i}(\psi_i,\phi_i) + \mathsf{b}_V^{i,e}(\psi_i,\phi_e) + \mathsf{b}_V^{e,i}(\psi_e,\phi_i) + \mathsf{b}_V^{e,e}(\psi_e,\phi_e)$$
$$+\mathsf{b}_K^{i,i}(g_i,\phi_i) + \mathsf{b}_K^{i,e}(g_i,\phi_e) - \mathsf{b}_K^{e,i}(g_e,\phi_i) - \mathsf{b}_K^{e,e}(g_e,\phi_e)$$
$$-\frac{1}{2}\langle g_i,\phi_i\rangle_{\Gamma_i} - \frac{1}{2}\langle g_e,\phi_e\rangle_{\Gamma_e} = 0,$$
$$\mathsf{b}_W^{i,i}(g_i,u_i) - \mathsf{b}_W^{i,e}(g_i,u_e) - \mathsf{b}_W^{e,i}(g_e,u_i) + \mathsf{b}_W^{e,e}(g_e,u_e)$$
$$-\mathsf{b}_K^{i,i}(u_i,\psi_i) - \mathsf{b}_K^{i,e}(u_i,\psi_e) + \mathsf{b}_K^{e,i}(u_e,\psi_i) + \mathsf{b}_K^{e,e}(u_e,\psi_e)$$
$$-\frac{1}{2}\langle \psi_i,u_i\rangle_{\Gamma_i} - \frac{1}{2}\langle \psi_e,u_e\rangle_{\Gamma_e} = 0.$$

Dirichlet boundary condition at Γ_e gives us $g_e(\mathbf{x}) = \mathbf{H}_0 \cdot \mathbf{x}$. Putting $\phi_e = u_e = 0$ gives us

$$\mathsf{b}_V^{i,i}(\psi_i,\phi_i) + \mathsf{b}_V^{e,i}(\psi_e,\phi_i) + \mathsf{b}_K^{i,i}(g_i,\phi_i) - \frac{1}{2}\langle g_i,\phi_i\rangle_{\Gamma_i} = \mathsf{b}_K^{e,i}(g_e,\phi_i) \quad \forall \phi_i \in H^{-\frac{1}{2}}(\Gamma_i), \quad (5.2.21)$$

$$\mathsf{b}_W^{i,i}(g_i,u_i) - \mathsf{b}_K^{i,i}(u_i,\psi_i) - \mathsf{b}_K^{i,e}(u_i,\psi_e) - \frac{1}{2}\langle \psi_i,u_i\rangle_{\Gamma_i} = \mathsf{b}_W^{e,i}(g_e,u_i) \quad \forall u_i \in H^{\frac{1}{2}}(\Gamma_i). \quad (5.2.22)$$

Putting $\phi_i = u_i = 0$ gives us

$$\mathsf{b}_V^{i,e}(\psi_i,\phi_e) + \mathsf{b}_V^{e,e}(\psi_e,\phi_e) + \mathsf{b}_K^{i,e}(g_i,\phi_e) = \mathsf{b}_K^{e,e}(g_e,\phi_e) + \frac{1}{2}\langle \phi_e,g_e\rangle_{\Gamma_e} \quad \forall \phi_e \in H^{-\frac{1}{2}}(\Gamma_e),$$
$$(5.2.23)$$

$$-\mathsf{b}_W^{i,e}(g_i,u_e) + \mathsf{b}_K^{e,i}(u_e,\psi_i) + \mathsf{b}_K^{e,e}(u_e,\psi_e) = \frac{1}{2}\langle \psi_e,u_e\rangle_{\Gamma_e} - \mathsf{b}_W^{e,e}(g_e,u_e) \quad \forall u_e \in H^{\frac{1}{2}}(\Gamma_e).$$
$$(5.2.24)$$

Now we write the variational BIEs for $\partial\Omega_i$, for which we can use the BIEs for a bounded domain again. They can be written in terms of the introduced notation. Denoting the interior Neumann and Dirichlet traces of u on $\partial\Omega_i$ as ψ_I and g_I respectively, we get

$$\mathsf{b}_V^{i,i}(\psi_I,\phi_i) - \mathsf{b}_K^{i,i}(g_I,\phi_i) - \frac{1}{2}\langle g_I,\phi_i\rangle_{\Gamma_i} = 0 \quad \forall \phi_i \in H^{-\frac{1}{2}}(\Gamma_i),$$

$$-\frac{1}{2}\langle\psi_I,u_i\rangle_{\Gamma_i}+\mathsf{b}_{\mathrm{K'}}^{i,i}(\psi_I,u_i)+\mathsf{b}_{\mathrm{W}}^{i,i}(g_I,u_i)=0 \quad \forall u_i\in H^{\frac{1}{2}}(\Gamma_i).$$

Transmission conditions at Γ_i allow us to write

$$g_I=g_i, \quad \psi_I=-\frac{\mu_0}{\mu}\psi_i.$$

Thus the variational equations for $\partial\Omega_i$ become

$$\frac{\mu_0}{\mu}\mathsf{b}_{\mathrm{V}}^{i,i}(\psi_i,\phi_i)+\mathsf{b}_{\mathrm{K}}^{i,i}(g_i,\phi_i)+\frac{1}{2}\langle g_i,\phi_i\rangle_{\Gamma_i}=0 \quad \forall\phi_i\in H^{-\frac{1}{2}}(\Gamma_i), \tag{5.2.25}$$

$$\frac{1}{2}\langle\psi_i,u_i\rangle_{\Gamma_i}-\mathsf{b}_{\mathrm{K'}}^{i,i}(\psi_i,u_i)+\frac{\mu}{\mu_0}\mathsf{b}_{\mathrm{W}}^{i,i}(g_i,u_i)=0 \quad \forall u_i\in H^{\frac{1}{2}}(\Gamma_i). \tag{5.2.26}$$

To get the variational problem we combine equations (5.2.25) and (5.2.21), and (5.2.26) and (5.2.22). The third equation we use is (5.2.23). Defining $\mathcal{X}:=H^{-\frac{1}{2}}(\Gamma_i)\times H^{\frac{1}{2}}(\Gamma_i)\times H^{-\frac{1}{2}}(\Gamma_e)$, we seek

$$\begin{bmatrix}\psi_i\\g_i\\\psi_e\end{bmatrix}\in\mathcal{X}: \quad \mathsf{b}(\begin{bmatrix}\psi_i\\g_i\\\psi_e\end{bmatrix},\begin{bmatrix}\phi_i\\u_i\\\phi_e\end{bmatrix})=\ell(\begin{bmatrix}\phi_i\\u_i\\\phi_e\end{bmatrix}) \quad \forall\begin{bmatrix}\phi_i\\u_i\\\phi_e\end{bmatrix}\in\mathcal{X}, \tag{5.2.27}$$

where

$$\mathsf{b}(\begin{bmatrix}\psi_i\\g_i\\\psi_e\end{bmatrix},\begin{bmatrix}\phi_i\\u_i\\\phi_e\end{bmatrix}):=(1+\frac{\mu_0}{\mu})\mathsf{b}_{\mathrm{V}}^{i,i}(\psi_i,\phi_i)+2\mathsf{b}_{\mathrm{K}}^{i,i}(g_i,\phi_i)+\mathsf{b}_{\mathrm{V}}^{e,i}(\psi_e,\phi_i)$$

$$-2\mathsf{b}_{\mathrm{K'}}^{i,i}(\psi_i,u_i)+(1+\frac{\mu}{\mu_0})\mathsf{b}_{\mathrm{W}}^{i,i}(g_i,u_i)-\mathsf{b}_{\mathrm{K'}}^{e,i}(\psi_e,u_i)$$

$$+\mathsf{b}_{\mathrm{V}}^{i,e}(\psi_i,\phi_e)+\mathsf{b}_{\mathrm{K}}^{i,e}(g_i,\phi_e)+\mathsf{b}_{\mathrm{V}}^{e,e}(\psi_e,\phi_e),$$

$$\ell(\begin{bmatrix}\phi_i\\u_i\\\phi_e\end{bmatrix}):=\mathsf{b}_{\mathrm{K}}^{e,i}(g_e,\phi_i)+\mathsf{b}_{\mathrm{W}}^{e,i}(g_e,u_i)+\mathsf{b}_{\mathrm{K}}^{e,e}(g_e,\phi_e)+\frac{1}{2}\langle\phi_e,g_e\rangle_{\Gamma_e}.$$

Obviously the traces of potential u satisfying (5.2.19) satisfy (5.2.27). To show that the solution is unique, we consider the solution to the homogeneous equation

$$\begin{bmatrix}\psi_i\\g_i\\\psi_e\end{bmatrix}\in\mathcal{X}: \quad \mathsf{b}(\begin{bmatrix}\psi_i\\g_i\\\psi_e\end{bmatrix},\begin{bmatrix}\phi_i\\u_i\\\phi_e\end{bmatrix})=0 \quad \forall\begin{bmatrix}\phi_i\\u_i\\\phi_e\end{bmatrix}\in\mathcal{X}. \tag{5.2.28}$$

Plugging in $\phi_i=\psi_i$, $u_i=g_i$ and $\phi_e=\psi_e$ we get

$$(1+\frac{\mu_0}{\mu})\mathsf{b}_{\mathrm{V}}^{i,i}(\psi_i,\psi_i)+(1+\frac{\mu}{\mu_0})\mathsf{b}_{\mathrm{W}}^{i,i}(g_i,g_i)+\mathsf{b}_{\mathrm{V}}^{e,e}(\psi_e,\psi_e)=0.$$

Similar to the proof of Theorem 2 we conclude that the solution to the homogeneous equation is trivial. Thus we have a unique solution to Equation (5.2.27).

For shape differentiation, we try to express the energy in terms of the linear form appearing in the variational formulation (5.2.27). We will focus on the energy inside $B_R(0)$.

$$\mathcal{E}_F = \frac{1}{2} \int\limits_{B_R(0)} \mu(\mathbf{x}) \, \|\mathbf{H}_{tot}(\mathbf{x})\|^2 \; d\mathbf{x} = \frac{1}{2} \int\limits_{B_R(0)} \mu(\mathbf{x}) \, \|\nabla u(\mathbf{x})\|^2 \; d\mathbf{x}.$$

The expression can be converted to a boundary based form using integration by parts and transmission conditions which yields

$$\mathcal{E}_F = \frac{\mu_0}{2} \, \langle g_e, \psi_e \rangle_{\Gamma_e} \,. \tag{5.2.29}$$

To relate the linear form with the energy expression, we begin by noting that

$$\frac{\mu_0}{[\![\mu]\!]_\Gamma} \ell(\begin{bmatrix} \psi_i \\ -g_i \\ \psi_e \end{bmatrix}) = \mathsf{b}_{\mathrm{K}}^{e,i}(g_e, \psi_i) - \mathsf{b}_{\mathrm{W}}^{e,i}(g_e, g_i) + \mathsf{b}_{\mathrm{K}}^{e,e}(g_e, \psi_e) + \frac{1}{2} \, \langle \psi_e, g_e \rangle_{\Gamma_e} \,.$$

Testing (5.2.24) with $u_e = g_e$ gives us

$$-\mathsf{b}_{\mathrm{W}}^{i,e}(g_i, g_e) + \mathsf{b}_{\mathrm{K}}^{e,i}(g_e, \psi_i) + \mathsf{b}_{\mathrm{K}}^{e,e}(g_e, \psi_e) = \frac{1}{2} \, \langle \psi_e, g_e \rangle_{\Gamma_e} - \mathsf{b}_{\mathrm{W}}^{e,e}(g_e, g_e) \quad \forall u_e \in H^{\frac{1}{2}}(\Gamma_e). \tag{5.2.30}$$

Thus we have the relation

$$\frac{\mu_0}{2} \ell(\begin{bmatrix} \psi_i \\ -g_i \\ \psi_e \end{bmatrix}) = \frac{\mu_0}{2} \, \langle \psi_e, g_e \rangle_{\Gamma_e} - \frac{\mu_0}{2} \mathsf{b}_{\mathrm{W}}^{e,e}(g_e, g_e).$$

Comparing with the energy expression in (5.2.29) we get the desired relation

$$\mathcal{E}_F = \frac{\mu_0}{2} \ell(\begin{bmatrix} \psi_i \\ -g_i \\ \psi_e \end{bmatrix}) + \frac{\mu_0}{2} \mathsf{b}_{\mathrm{W}}^{e,e}(g_e, g_e). \tag{5.2.31}$$

5.2.2.2 Variational Formulation on Deformed Domain

Similar to the vector potential case, we carry out deformations using a velocity field $\boldsymbol{\mathcal{V}} \in (C_0^\infty(B_R(0)))^3$ which only deforms the interior of the ball $B_R(0)$. For the deformed configuration, we move the permeability to μ_s as a 0-form while keeping the boundary condition at $\partial B_R(0)$ fixed to zero. Thus we have a similar variational problem to (5.2.27). Denoting the deformed boundaries and the corresponding solutions with a superscript s, we define the relevant space $\mathcal{X}_s := H^{-\frac{1}{2}}(\Gamma_i^s) \times H^{\frac{1}{2}}(\Gamma_i^s) \times H^{-\frac{1}{2}}(\Gamma_e^s)$. We have the variational problem

$$\begin{bmatrix} \psi_i^s \\ g_i^s \\ \psi_e^s \end{bmatrix} \in \mathcal{X}_s : \quad \mathsf{b}(s)(\begin{bmatrix} \psi_i^s \\ g_i^s \\ \psi_e^s \end{bmatrix}, \begin{bmatrix} \phi_i \\ u_i \\ \phi_e \end{bmatrix}) = \ell(s)(\begin{bmatrix} \phi_i \\ u_i \\ \phi_e \end{bmatrix}) \quad \forall \begin{bmatrix} \phi_i \\ u_i \\ \phi_e \end{bmatrix} \in \mathcal{X}_s,$$

where

$$\mathsf{b}(s)(\begin{bmatrix} \psi_i \\ g_i \\ \psi_e \end{bmatrix}, \begin{bmatrix} \phi_i \\ u_i \\ \phi_e \end{bmatrix}) := (1 + \frac{\mu_0}{\mu})\mathsf{b}_V^{i,i}(s)(\psi_i, \phi_i) + 2\mathsf{b}_K^{i,i}(s)(g_i, \phi_i) + \mathsf{b}_V^{e,i}(s)(\psi_e, \phi_i)$$

$$- 2\mathsf{b}_{K'}^{i,i}(s)(\psi_i, u_i) + (1 + \frac{\mu}{\mu_0})\mathsf{b}_W^{i,i}(s)(g_i, u_i) - \mathsf{b}_{K'}^{e,i}(s)(\psi_e, u_i)$$

$$+ \mathsf{b}_V^{i,e}(s)(\psi_i, \phi_e) + \mathsf{b}_K^{i,e}(s)(g_i, \phi_e) + \mathsf{b}_V^{e,e}(s)(\psi_e, \phi_e),$$

$$\ell(s)(\begin{bmatrix} \phi_i \\ u_i \\ \phi_e \end{bmatrix}) := \mathsf{b}_K^{e,i}(s)(g_e, \phi_i) + \mathsf{b}_W^{e,i}(s)(g_e, u_i) + \mathsf{b}_K^{e,e}(s)(g_e, \phi_e) + \frac{1}{2}\langle \phi_e, g_e \rangle_{\Gamma_e^s}.$$

The bilinear forms $\mathsf{b}_*^{\bullet,\blacktriangle}(s)$ are defined exactly like (5.2.20) but with integrals on $\Gamma_\bullet^s, \Gamma_\blacktriangle^s$ instead. Note that $\Gamma_e^s = \Gamma_e$. These integrals can be transformed back to the reference boundaries using the perturbation map and then using pullbacks, the arguments can be pulled back to function spaces associated with the reference boundaries.

5.2.2.3 Equivalent Formulation on Reference Boundary

We skip the derivation here as it mirrors the one shown in Section 5.1.1.3 and mention the definition of the pulled back bilinear forms.

$$\hat{\mathsf{b}}_V^{\bullet,\blacktriangle} : \mathbb{R} \times H^{-\frac{1}{2}}(\Gamma_\bullet^0) \times H^{-\frac{1}{2}}(\Gamma_\blacktriangle^0),$$

$$\hat{\mathsf{b}}_V^{\bullet,\blacktriangle}(s; \hat{\psi}, \hat{\phi}) := \int_{\Gamma_\blacktriangle^0} \int_{\Gamma_\bullet^0} G(\mathbf{T}_s^{\boldsymbol{\nu}}(\hat{\mathbf{x}}), \mathbf{T}_s^{\boldsymbol{\nu}}(\hat{\mathbf{y}}))\, \hat{\psi}(\hat{\mathbf{y}})\, \hat{\phi}(\hat{\mathbf{x}})\, dS_{\hat{\mathbf{y}}}\, dS_{\hat{\mathbf{x}}},$$

$$\hat{\mathsf{b}}_K^{\bullet,\blacktriangle} : \mathbb{R} \times H^{\frac{1}{2}}(\Gamma_\bullet^0) \times H^{-\frac{1}{2}}(\Gamma_\blacktriangle^0),$$

$$\hat{\mathsf{b}}_K^{\bullet,\blacktriangle}(s; \hat{g}, \hat{\phi}) := \int_{\Gamma_\blacktriangle^0} \int_{\Gamma_\bullet^0} \nabla_y G(\mathbf{T}_s^{\boldsymbol{\nu}}(\hat{\mathbf{x}}), \mathbf{T}_s^{\boldsymbol{\nu}}(\hat{\mathbf{y}})) \cdot \left(\mathbf{C}(\mathsf{D}\mathbf{T}_s^{\boldsymbol{\nu}}(\hat{\mathbf{y}})\, \hat{\mathbf{n}}(\hat{\mathbf{y}}))\right) \hat{g}(\hat{\mathbf{y}})\, \hat{\phi}(\hat{\mathbf{x}})\, dS_{\hat{\mathbf{y}}}\, dS_{\hat{\mathbf{x}}},$$

$$\hat{\mathsf{b}}_W^{\bullet,\blacktriangle} : \mathbb{R} \times H^{\frac{1}{2}}(\Gamma_\bullet^0) \times H^{\frac{1}{2}}(\Gamma_\blacktriangle^0),$$

$$\hat{\mathsf{b}}_W^{\bullet,\blacktriangle}(s; \hat{g}, \hat{u}) := \int_{\Gamma_\blacktriangle^0} \int_{\Gamma_\bullet^0} G(\mathbf{T}_s^{\boldsymbol{\nu}}(\hat{\mathbf{x}}), \mathbf{T}_s^{\boldsymbol{\nu}}(\hat{\mathbf{y}})) \left(\mathsf{D}\mathbf{T}_s^{\boldsymbol{\nu}}(\hat{\mathbf{y}})\, \mathbf{curl}_\Gamma\, \hat{g}(\hat{\mathbf{y}})\right) \cdot \left(\mathsf{D}\mathbf{T}_s^{\boldsymbol{\nu}}(\hat{\mathbf{x}})\, \mathbf{curl}_\Gamma\, \hat{u}(\hat{\mathbf{x}})\right) dS_{\hat{\mathbf{y}}}\, dS_{\hat{\mathbf{x}}}.$$

$$(5.2.32)$$

The pulled back bilinear form $\hat{\mathsf{b}}_{K'}^{\bullet,\blacktriangle}$ is defined as $\hat{\mathsf{b}}_{K'}^{\bullet,\blacktriangle}(s; \hat{\psi}, \hat{g}) := \hat{\mathsf{b}}_K^{\blacktriangle,\bullet}(s; \hat{g}, \hat{\psi})$. We carry out similar transformations for the RHS of the variational problem to get the pulled back linear form

$$\hat{\ell}(s; \begin{bmatrix} \hat{\phi}_i \\ \hat{u}_i \\ \hat{\phi}_e \end{bmatrix}) :=$$

$$\int_{\Gamma_i^0} \int_{\Gamma_e^0} \nabla_y G(\mathbf{T}_s^{\boldsymbol{\nu}}(\hat{\mathbf{x}}), \hat{\mathbf{y}}) \cdot \mathbf{n}(\hat{\mathbf{y}})\, \mathbf{H}_0 \cdot \hat{\mathbf{y}}\, \hat{\phi}(\hat{\mathbf{x}})\, dS_{\hat{\mathbf{y}}}\, dS_{\hat{\mathbf{x}}}$$

$$+ \int\limits_{\Gamma_i^0} \int\limits_{\Gamma_e^0} G(\mathbf{T}_s^{\boldsymbol{\nu}}(\hat{\mathbf{x}}), \hat{\mathbf{y}}) \left(\mathbf{H}_0 \times \mathbf{n}(\hat{\mathbf{y}}) \right) \cdot \left(\mathsf{D}\mathbf{T}_s^{\boldsymbol{\nu}}(\hat{\mathbf{x}}) \; \mathbf{curl}_\Gamma \, \hat{u}_i(\hat{\mathbf{x}}) \right) dS_{\hat{\mathbf{y}}} \, dS_{\hat{\mathbf{x}}}$$

$$+ \int\limits_{\Gamma_e^0} \int\limits_{\Gamma_e^0} \nabla_y G(\hat{\mathbf{x}}, \hat{\mathbf{y}}) \cdot \mathbf{n}(\hat{\mathbf{y}}) \, \mathbf{H}_0 \cdot \hat{\mathbf{y}} \, \hat{\hat{\phi}}_e(\hat{\mathbf{x}}) \, dS_{\hat{\mathbf{y}}} \, dS_{\hat{\mathbf{x}}}$$

$$+ \frac{1}{2} \int\limits_{\Gamma_e^0} \mathbf{H}_0 \cdot \hat{\mathbf{y}} \, \hat{\hat{\phi}}_e(\hat{\mathbf{y}}) \, dS_{\hat{\mathbf{y}}}.$$

Writing $\mathcal{X} = \mathcal{X}_0$ the pulled back state problem can be formulated as

$$\begin{bmatrix} \hat{\psi}_i^s \\ \hat{g}_i^s \\ \hat{\psi}_e^s \end{bmatrix} \in \mathcal{X}: \quad \hat{\mathsf{b}}(s; \begin{bmatrix} \hat{\psi}_i^s \\ \hat{g}_i^s \\ \hat{\psi}_e^s \end{bmatrix}, \begin{bmatrix} \hat{\phi}_i \\ \hat{u}_i \\ \hat{\phi}_e \end{bmatrix}) = \hat{\ell}(s; \begin{bmatrix} \hat{\phi}_i \\ \hat{u}_i \\ \hat{\phi}_e \end{bmatrix}) \quad \forall \begin{bmatrix} \hat{\phi}_i \\ \hat{u}_i \\ \hat{\phi}_e \end{bmatrix} \in \mathcal{X},$$

where

$$\hat{\mathsf{b}}(s; \begin{bmatrix} \hat{\psi}_i \\ \hat{g}_i \\ \hat{\psi}_e \end{bmatrix}, \begin{bmatrix} \hat{\phi}_i \\ \hat{u}_i \\ \hat{\phi}_e \end{bmatrix}) := (1 + \frac{\mu_0}{\mu}) \hat{\mathsf{b}}_V^{i,i}(s; \hat{\psi}_i, \hat{\phi}_i) + 2\hat{\mathsf{b}}_K^{i,i}(s; \hat{g}_i, \hat{\phi}_i) + \hat{\mathsf{b}}_V^{e,i}(s; \hat{\psi}_e, \hat{\phi}_i)$$

$$- 2\hat{\mathsf{b}}_{K'}^{i,i}(s; \hat{\psi}_i, \hat{u}_i) + (1 + \frac{\mu}{\mu_0}) \hat{\mathsf{b}}_W^{i,i}(s; \hat{g}_i, \hat{u}_i) - \hat{\mathsf{b}}_{K'}^{e,i}(s; \hat{\psi}_e, \hat{u}_i)$$

$$+ \hat{\mathsf{b}}_V^{i,e}(s; \hat{\psi}_i, \hat{\phi}_e) + \hat{\mathsf{b}}_K^{i,e}(s; \hat{g}_i, \hat{\phi}_e) + \hat{\mathsf{b}}_V^{e,e}(s; \hat{\psi}_e, \hat{\phi}_e). \qquad (5.2.33)$$

5.2.2.4 BIE-Constrained Shape Derivative

To compute the shape derivative we start by defining the Lagrangian $\mathcal{L} : \mathbb{R} \times \mathcal{X} \times \mathcal{X} \to \mathbb{R}$. Transformation for the additional terms in (5.2.31) is included in the definition of the Lagrangian.

$$\mathcal{L}(s; \begin{bmatrix} \hat{\psi}_i \\ \hat{g}_i \\ \hat{\psi}_e \end{bmatrix}, \begin{bmatrix} \hat{\phi}_i \\ \hat{u}_i \\ \hat{\phi}_e \end{bmatrix}) := \hat{\mathsf{b}}(s; \begin{bmatrix} \hat{\psi}_i \\ \hat{g}_i \\ \hat{\psi}_e \end{bmatrix}, \begin{bmatrix} \hat{\phi}_i \\ \hat{u}_i \\ \hat{\phi}_e \end{bmatrix}) - \hat{\ell}(s; \begin{bmatrix} \hat{\phi}_i \\ \hat{u}_i \\ \hat{\phi}_e \end{bmatrix}) + \frac{\mu_0}{2} \hat{\ell}(s; \begin{bmatrix} \hat{\psi}_i \\ -\hat{g}_i \\ \hat{\psi}_e \end{bmatrix}) + \frac{\mu_0}{2} \mathsf{b}_W^{e,e}(g_e, g_e).$$

By plugging in the pulled back state solution we see that

$$\mathcal{E}_F(s) = \mathcal{L}(s; \begin{bmatrix} \hat{\psi}_i^s \\ \hat{g}_i^s \\ \hat{\psi}_e^s \end{bmatrix}, \begin{bmatrix} \hat{\phi}_i \\ \hat{u}_i \\ \hat{\phi}_e \end{bmatrix}) \quad \forall \begin{bmatrix} \hat{\phi}_i \\ \hat{u}_i \\ \hat{\phi}_e \end{bmatrix} \in \mathcal{X}.$$

The shape derivative can then be computed as

$$\frac{d\mathcal{E}_F}{ds}(0) = \frac{\partial \mathcal{L}}{\partial s}(0; \begin{bmatrix} \hat{\psi}_i^0 \\ \hat{g}_i^0 \\ \hat{\psi}_e^0 \end{bmatrix}, \begin{bmatrix} \hat{\lambda}_i \\ \hat{p}_i \\ \hat{\lambda}_e \end{bmatrix}),$$

where the adjoint solution

$$\begin{bmatrix}\hat{\lambda}_i\\\hat{p}_i\\\hat{\lambda}_e\end{bmatrix}\in\mathcal{X}:\quad\left\langle\frac{\partial\mathcal{L}}{\partial\begin{bmatrix}\hat{\psi}_i\\\hat{g}_i\\\hat{\psi}_e\end{bmatrix}}(0;\begin{bmatrix}\hat{\psi}_i^0\\\hat{g}_i^0\\\hat{\psi}_e^0\end{bmatrix},\begin{bmatrix}\hat{\lambda}_i\\\hat{p}_i\\\hat{\lambda}_e\end{bmatrix});\begin{bmatrix}\hat{\phi}_i\\\hat{u}_i\\\hat{\phi}_e\end{bmatrix}\right\rangle=0\quad\forall\begin{bmatrix}\hat{\phi}_i\\\hat{u}_i\\\hat{\phi}_e\end{bmatrix}\in\mathcal{X}.$$

Computing the above partial derivative yields the adjoint equation in an explicit form

$$\hat{\mathsf{b}}(0;\begin{bmatrix}\hat{\phi}_i\\\hat{u}_i\\\hat{\phi}_e\end{bmatrix},\begin{bmatrix}\hat{\lambda}_i\\\hat{p}_i\\\hat{\lambda}_e\end{bmatrix})+\frac{\mu_0}{2}\hat{\ell}(0;\begin{bmatrix}\hat{\phi}_i\\-\hat{u}_i\\\hat{\phi}_e\end{bmatrix})=0\quad\forall\begin{bmatrix}\hat{\phi}_i\\\hat{u}_i\\\hat{\phi}_e\end{bmatrix}\in\mathcal{X}.$$

Changing the sign of the test function $\hat{u}_i$ yields

$$\hat{\mathsf{b}}(0;\begin{bmatrix}\hat{\phi}_i\\-\hat{u}_i\\\hat{\phi}_e\end{bmatrix},\begin{bmatrix}\hat{\lambda}_i\\\hat{p}_i\\\hat{\lambda}_e\end{bmatrix})=\hat{\mathsf{b}}(0;\begin{bmatrix}\hat{\lambda}_i\\-\hat{p}_i\\\hat{\lambda}_e\end{bmatrix},\begin{bmatrix}\hat{\phi}_i\\\hat{u}_i\\\hat{\phi}_e\end{bmatrix})=-\frac{\mu_0}{2}\hat{\ell}(0;\begin{bmatrix}\hat{\phi}_i\\\hat{u}_i\\\hat{\phi}_e\end{bmatrix})\quad\forall\begin{bmatrix}\hat{\phi}_i\\\hat{u}_i\\\hat{\phi}_e\end{bmatrix}\in\mathcal{X}.$$

Comparing with the state equation we get the adjoint solution in an explicit form

$$\begin{bmatrix}\hat{\lambda}_i\\\hat{p}_i\\\hat{\lambda}_e\end{bmatrix}=\frac{\mu_0}{2}\begin{bmatrix}-\hat{\psi}_i^0\\\hat{g}_i^0\\-\hat{\psi}_e^0\end{bmatrix}.$$

The shape derivative can then be computed as

$$\begin{aligned}\frac{d\mathcal{E}_F}{ds}(0)&=\frac{\partial\mathcal{L}}{\partial s}(0;\begin{bmatrix}\hat{\psi}_i^0\\\hat{g}_i^0\\\hat{\psi}_e^0\end{bmatrix},\frac{\mu_0}{2}\begin{bmatrix}-\hat{\psi}_i^0\\\hat{g}_i^0\\-\hat{\psi}_e^0\end{bmatrix})\\&=-\frac{\mu_0}{2}\frac{\partial\hat{\mathsf{b}}}{\partial s}(0;\begin{bmatrix}\hat{\psi}_i^0\\\hat{g}_i^0\\\hat{\psi}_e^0\end{bmatrix},\begin{bmatrix}\hat{\psi}_i^0\\-\hat{g}_i^0\\\hat{\psi}_e^0\end{bmatrix})+\mu_0\frac{\partial\hat{\ell}}{\partial s}(0;\begin{bmatrix}\hat{\psi}_i^0\\-\hat{g}_i^0\\\hat{\psi}_e^0\end{bmatrix}).\end{aligned}\qquad(5.2.34)$$

The partial derivative for the bilinear form can be computed based on the definition (5.2.33) and the partial derivatives

$$\frac{\partial\hat{\mathsf{b}}_{\mathrm{V}}^{\bullet;\blacktriangle}}{\partial s}(0;\hat{\psi},\hat{\phi})=\int_{\Gamma_{\blacktriangle}^0}\int_{\Gamma_{\bullet}^0}\Big(\nabla_x G(\hat{\mathbf{x}},\hat{\mathbf{y}})\cdot\boldsymbol{\mathcal{V}}(\hat{\mathbf{x}})+\nabla_y G(\hat{\mathbf{x}},\hat{\mathbf{y}})\cdot\boldsymbol{\mathcal{V}}(\hat{\mathbf{y}})\Big)\hat{\psi}(\hat{\mathbf{y}})\,\hat{\phi}(\hat{\mathbf{x}})\,dS_{\hat{\mathbf{y}}}\,dS_{\hat{\mathbf{x}}},$$

$$\begin{aligned}\frac{\partial\hat{\mathsf{b}}_{\mathrm{K}}^{\bullet;\blacktriangle}}{\partial s}(0;\hat{g},\hat{\phi})&=\int_{\Gamma_{\blacktriangle}^0}\int_{\Gamma_{\bullet}^0}\frac{d\nabla_y G(\mathbf{T}_s^{\boldsymbol{\nu}}(\hat{\mathbf{x}}),\mathbf{T}_s^{\boldsymbol{\nu}}(\hat{\mathbf{y}}))}{ds}\Big|_{s=0}\cdot\hat{\mathbf{n}}(\hat{\mathbf{y}})\,\hat{g}(\hat{\mathbf{y}})\,\hat{\phi}(\hat{\mathbf{x}})\,dS_{\hat{\mathbf{y}}}\,dS_{\hat{\mathbf{x}}}\\&\quad+\int_{\Gamma_{\blacktriangle}^0}\int_{\Gamma_{\bullet}^0}\nabla_y G(\hat{\mathbf{x}},\hat{\mathbf{y}})\cdot\Big(\nabla\cdot\boldsymbol{\mathcal{V}}(\hat{\mathbf{y}})\,\hat{\mathbf{n}}(\hat{\mathbf{y}})-\mathsf{D}\boldsymbol{\mathcal{V}}^T(\hat{\mathbf{y}})\,\hat{\mathbf{n}}(\hat{\mathbf{y}})\Big)\hat{g}(\hat{\mathbf{y}})\,\hat{\phi}(\hat{\mathbf{x}})\,dS_{\hat{\mathbf{y}}}\,dS_{\hat{\mathbf{x}}},\end{aligned}$$

$$\frac{\partial \hat{\mathsf{b}}_{\mathrm{W}}^{\bullet,\blacktriangle}}{\partial s}(0;\hat{g},\hat{u}) = \int\limits_{\Gamma_\blacktriangle^0} \int\limits_{\Gamma_\bullet^0} \Big(\nabla_x G(\hat{\mathbf{x}},\hat{\mathbf{y}}) \cdot \boldsymbol{\mathcal{V}}(\hat{\mathbf{x}}) + \nabla_y G(\hat{\mathbf{x}},\hat{\mathbf{y}}) \cdot \boldsymbol{\mathcal{V}}(\hat{\mathbf{y}})\Big)\ \mathbf{curl}_\Gamma\, \hat{g}(\hat{\mathbf{y}}) \cdot \mathbf{curl}_\Gamma\, \hat{u}(\hat{\mathbf{x}})\ dS_{\hat{\mathbf{y}}}\ dS_{\hat{\mathbf{x}}}$$

$$+ \int\limits_{\Gamma_\blacktriangle^0} \int\limits_{\Gamma_\bullet^0} G(\hat{\mathbf{x}},\hat{\mathbf{y}}) \Big(\mathsf{D}\boldsymbol{\mathcal{V}}(\hat{\mathbf{y}})\ \mathbf{curl}_\Gamma\, \hat{g}(\hat{\mathbf{y}})\Big) \cdot \mathbf{curl}_\Gamma\, \hat{u}(\hat{\mathbf{x}})\ dS_{\hat{\mathbf{y}}}\ dS_{\hat{\mathbf{x}}}$$

$$+ \int\limits_{\Gamma_\blacktriangle^0} \int\limits_{\Gamma_\bullet^0} G(\hat{\mathbf{x}},\hat{\mathbf{y}})\ \mathbf{curl}_\Gamma\, \hat{g}(\hat{\mathbf{y}}) \cdot \Big(\mathsf{D}\boldsymbol{\mathcal{V}}(\hat{\mathbf{x}})\ \mathbf{curl}_\Gamma\, \hat{u}(\hat{\mathbf{x}})\Big)\ dS_{\hat{\mathbf{y}}}\ dS_{\hat{\mathbf{x}}}. \qquad (5.2.35)$$

The derivative for $\nabla_y G(\mathbf{T}_s^{\boldsymbol{\nu}}(\hat{\mathbf{x}}), \mathbf{T}_s^{\boldsymbol{\nu}}(\hat{\mathbf{y}}))$ is given in (4.1.18). Partial derivative of the linear form is given as

$$\frac{\partial \hat{\ell}}{\partial s}\left(0; \begin{bmatrix} \hat{\phi}_i \\ \hat{u}_i \\ \hat{\phi}_e \end{bmatrix}\right) =$$

$$\int\limits_{\Gamma_i} \int\limits_{\Gamma_e} \Big(\mathsf{D}_x \nabla_y G(\hat{\mathbf{x}},\hat{\mathbf{y}})\boldsymbol{\mathcal{V}}(\hat{\mathbf{x}})\Big) \cdot \mathbf{n}(\hat{\mathbf{y}})\ \mathbf{H}_0 \cdot \hat{\mathbf{y}}\ \hat{\phi}(\hat{\mathbf{x}})\ dS_{\hat{\mathbf{y}}}\ dS_{\hat{\mathbf{x}}}$$

$$+ \int\limits_{\Gamma_i} \int\limits_{\Gamma_e} \nabla_x G(\hat{\mathbf{x}},\hat{\mathbf{y}}) \cdot \boldsymbol{\mathcal{V}}(\hat{\mathbf{x}}) \Big(\mathbf{H}_0 \times \mathbf{n}(\hat{\mathbf{y}})\Big) \cdot \mathbf{curl}_\Gamma\, \hat{u}_i(\hat{\mathbf{x}})\ dS_{\hat{\mathbf{y}}}\ dS_{\hat{\mathbf{x}}}$$

$$+ \int\limits_{\Gamma_i} \int\limits_{\Gamma_e} G(\hat{\mathbf{x}},\hat{\mathbf{y}}) \Big(\mathbf{H}_0 \times \mathbf{n}(\hat{\mathbf{y}})\Big) \cdot \Big(\mathsf{D}\boldsymbol{\mathcal{V}}(\hat{\mathbf{x}})\ \mathbf{curl}_\Gamma\, \hat{u}_i(\hat{\mathbf{x}})\Big)\ dS_{\hat{\mathbf{y}}}\ dS_{\hat{\mathbf{x}}}.$$

We have the relation

$$\mathsf{D}_x \nabla_y G(\hat{\mathbf{x}},\hat{\mathbf{y}})\boldsymbol{\mathcal{V}}(\hat{\mathbf{x}}) = -\nabla_x \nabla_x G(\hat{\mathbf{x}},\hat{\mathbf{y}})\ \boldsymbol{\mathcal{V}}(\hat{\mathbf{x}}), \qquad (5.2.36)$$

where $\nabla_x \nabla_x G(\hat{\mathbf{x}},\hat{\mathbf{y}})$ is given in (4.1.19).

5.2.2.5   Numerical Experiments

Now we compare the shape derivative formulas (5.2.34) and (5.1.45) using numerical experiments. We discretize the geometry with a triangular mesh and solve for the boundary data using a Galerkin method based on the BIE formulation (5.2.27). The discrete spaces used are S_1^0 (piece wise linear functions) and S_0^{-1} (piece wise constants) for $H^{\frac{1}{2}}$ and $H^{-\frac{1}{2}}$ respectively. The computed solution is plugged directly into the shape derivative formulas for evaluation. The terms in the BEM based shape derivative (5.2.34) are computed using Sauter and Schwab quadrature rule of order 5^4 whereas (5.1.45) is calculated using a quadrature rule of order 3 per triangle. The shape derivatives are computed for a sequence of uniformly refined meshes with decreasing meshwidth h. The computations are done using Gypsilab [1].

---

[1] Code is available at https://github.com/piyushplcr7/gypsilab_forces

Experiment 23. We have a spherical domain Ω_i with radius 2.5, centered at $(1, 0, 0)$ occupied by a linear material with $\mu = 4$. It is surrounded by a ball of radius 4 centered at $(0, 0, 0)$ and the space in between is occupied by a linear material with $\mu_0 = 2$. The setting is depicted in Figure 5.35. We use the value $\mathbf{H}_0 = (10, 3, 1)$.

Figure 5.35: Geometrical setting

The total force and torques are computed using the shape derivative formulas (5.2.34) and (5.1.45) and the errors are plotted in Figure 5.36. We see similar convergence rates for this smooth spherical setting which are also reported in Table 5.13. The reference values for force and torque are computed using the BEM based shape derivative at a refinement level of $h = 0.196$.

(a) Error in total force

(b) Error in total torque

Figure 5.36: Error in force and torque computation for Sphere (Experiment 23)

Table 5.13: Asymptotic rate of algebraic convergence for Experiment 23

Method	Force	Torque
Pullback approach	2.72	3.55
Stress tensor	2.69	2.85

The dual norm computations are presented in Figure 5.37 where the reference values are again computed using the BEM based shape derivative at a refinement level of $h = 0.138$.

Figure 5.37: Dual norm error for Experiment 23

Experiment 24. We have a cubic domain Ω_i with side length 2, centered at $(1, 0.5, 1)$ occupied by a linear material with $\mu = 4$. It is surrounded by a ball of radius 4 centered at $(0, 0, 0)$ and the space in between is occupied by a linear material with $\mu_0 = 2$. The setting is depicted in Figure 5.38. We use the value $\mathbf{H}_0 = (10, 3, 1)$.
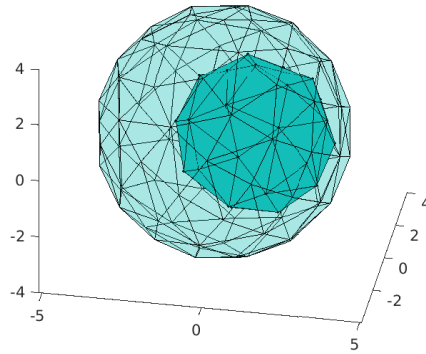

Figure 5.38: Geometrical setting

The total force and torques are computed using the shape derivative formulas (5.2.34)

and (5.1.45) and the errors are plotted in Figure 5.39. We see similar convergence rates for this smooth spherical setting which are also reported in Table 5.14. The reference values for force and torque are computed using the BEM based shape derivative at a refinement level of $h = 0.108$.
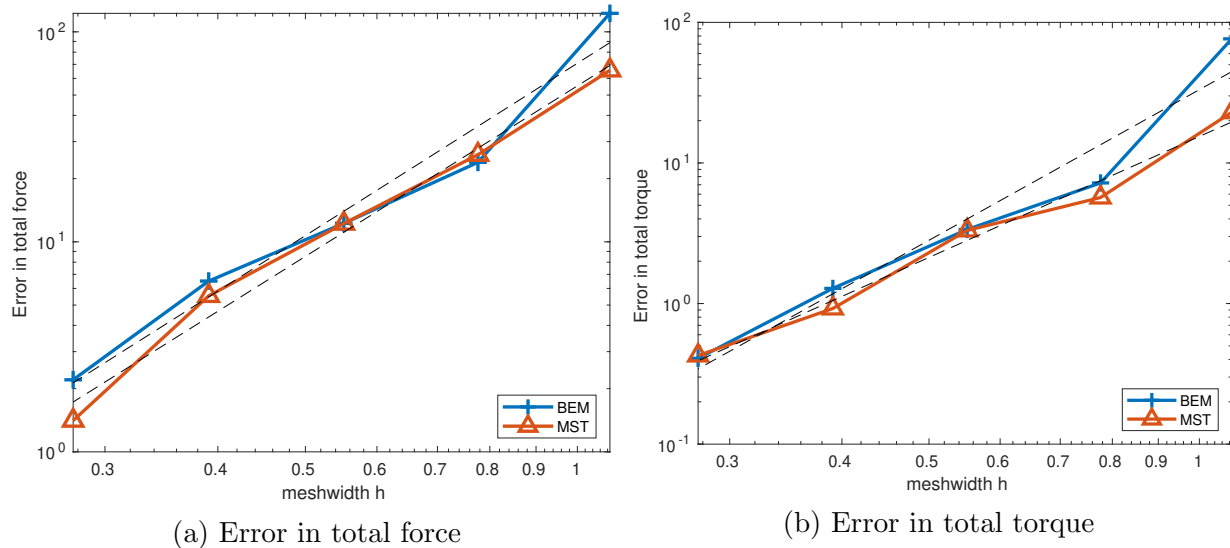

(a) Error in total force

(b) Error in total torque
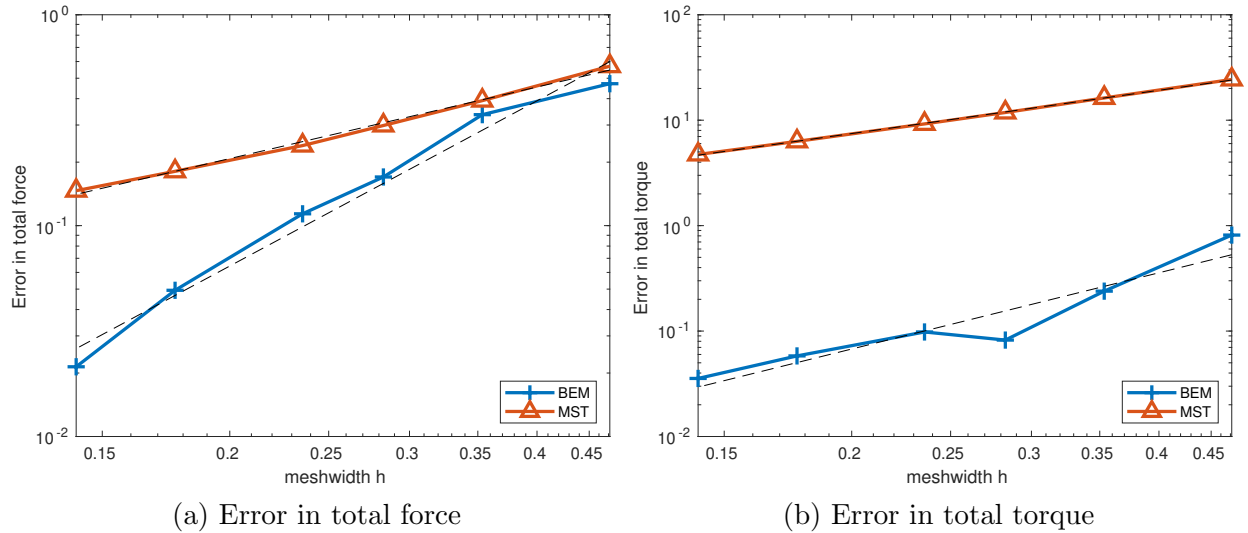
Figure 5.39: Error in force and torque computation for Cube (Experiment 24)

Table 5.14: Asymptotic rate of algebraic convergence for Experiment 24

Method	Force	Torque
Pullback approach	2.6	2.40
Stress tensor	1.12	1.36

The dual norm computations are presented in Figure 5.40 where the reference values are again computed using the BEM based shape derivative at a refinement level of $h = 0.108$.

Figure 5.40: Dual norm error for Experiment 24

Experiment 25. We have a cuboidal shaped domain Ω_i with sides (3,1,1), centered at $(1, 0.5, 1)$ occupied by a linear material with $\mu = 4$. It is surrounded by a ball of radius 4 centered at $(0,0,0)$ and the space in between is occupied by a linear material with $\mu_0 = 2$. The setting is depicted in Figure 5.41. We use the value $\mathbf{H}_0 = (10, 3, 1)$.
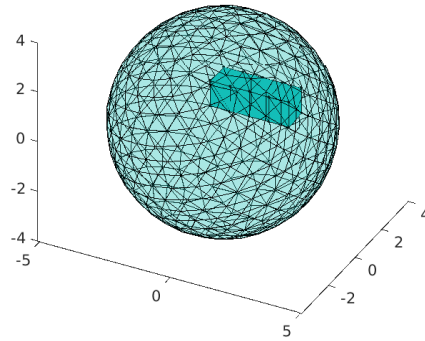
Figure 5.41: Geometrical setting

The total force and torques are computed using the shape derivative formulas (5.2.34) and (5.1.45) and the errors are plotted in Figure 5.42. We see similar convergence rates for this smooth spherical setting which are also reported in Table 5.15. The reference values for force and torque are computed using the BEM based shape derivative at a refinement level of $h = 0.118$.

(a) Error in total force

(b) Error in total torque
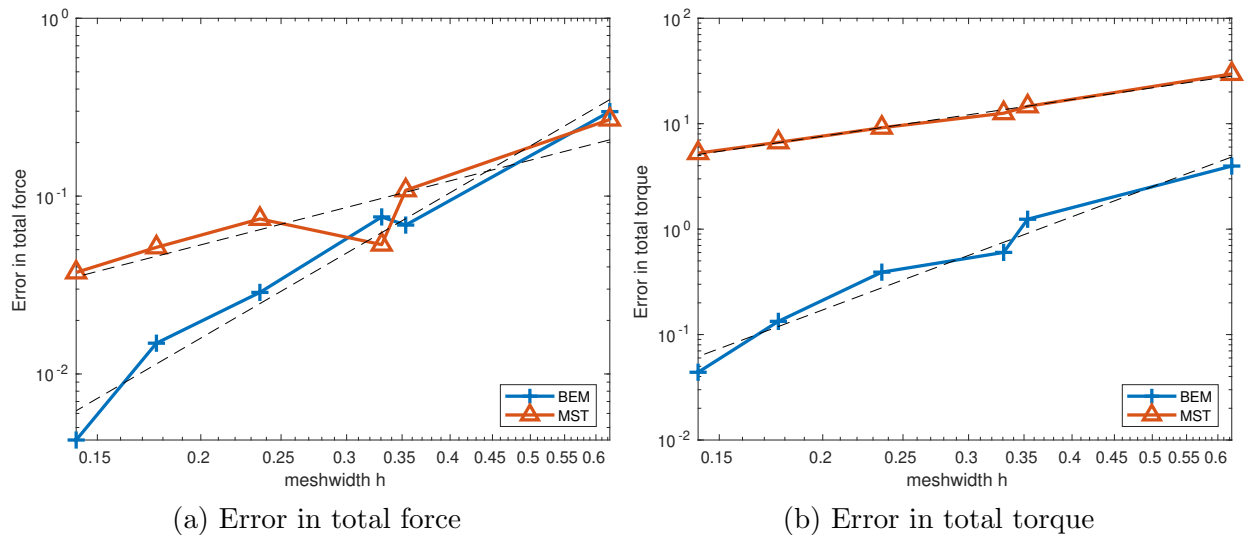
Figure 5.42: Error in force and torque computation for Cuboid (Experiment 25)

166

Table 5.15: Asymptotic rate of algebraic convergence for Experiment 25

Method	Force	Torque
Pullback approach	2.71	2.93
Stress tensor	1.2	1.15

The dual norm computations are presented in Figure 5.43 where the reference values are again computed using the BEM based shape derivative at a refinement level of $h = 0.118$.
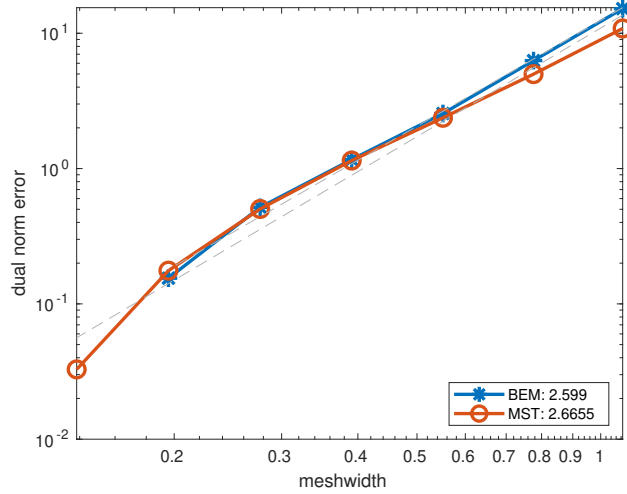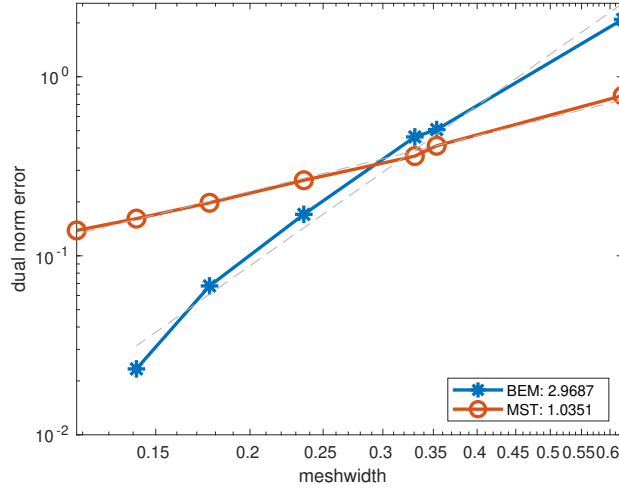

Figure 5.43: Dual norm error for Experiment 25

Experiment 26. We have a tetrahedral shaped domain Ω_i with corners $(\pm 1, 0, -\frac{1}{\sqrt{2}})$ and $(0, \pm 1, \frac{1}{\sqrt{2}})$, translated by $(2, 1, 3)$ occupied by a linear material with $\mu = 4$. It is surrounded by a ball of radius 2 centered at $(2.3, 1.5, 3.1)$ and the space in between is occupied by a linear material with $\mu_0 = 2$. The setting is depicted in Figure 5.44. We use the value $\mathbf{H}_0 = (10, 3, 1)$.
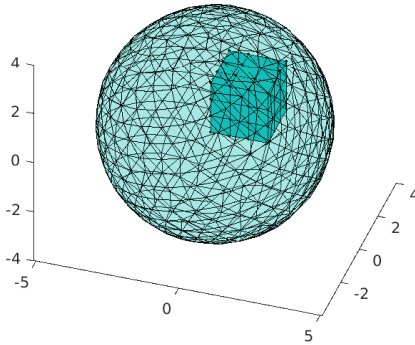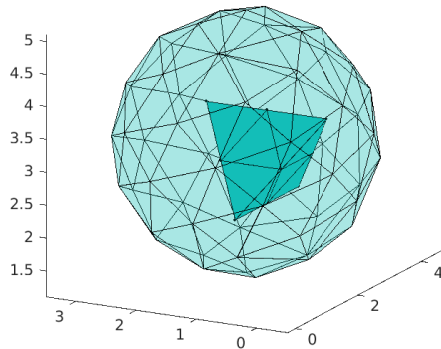

Figure 5.44: Geometrical setting

167

The total force and torques are computed using the shape derivative formulas (5.2.34) and (5.1.45) and the errors are plotted in Figure 5.45. We see similar convergence rates for this smooth spherical setting which are also reported in Table 5.16. The reference values for force and torque are computed using the BEM based shape derivative at a refinement level of $h = 0.082$.


(a) Error in total force   (b) Error in total torque
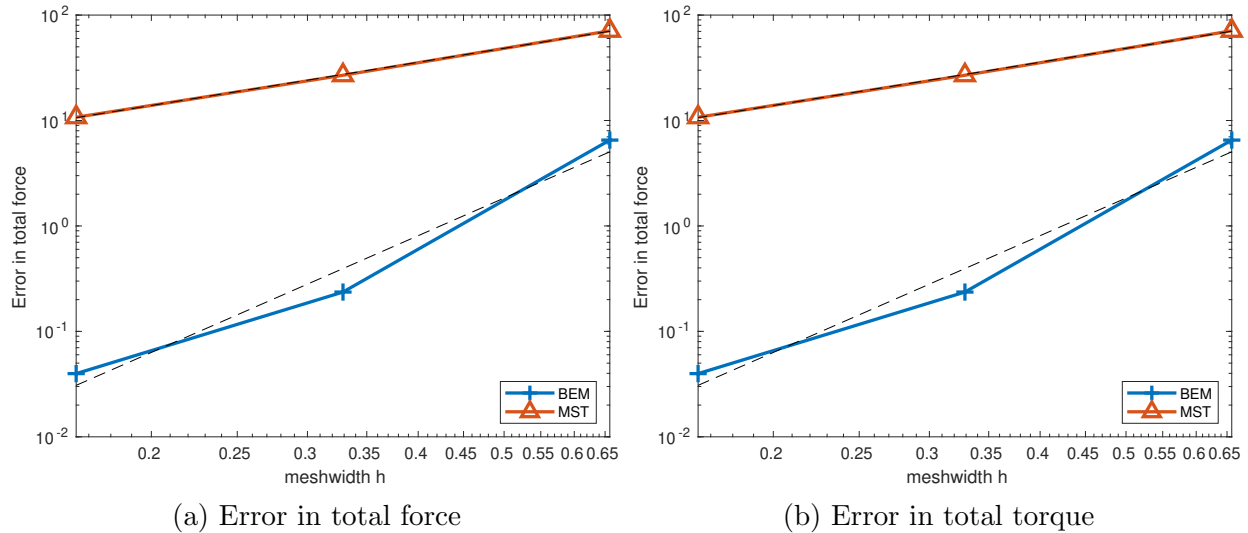
Figure 5.45: Error in force and torque computation for Tetrahedron (Experiment 26)

Table 5.16: Asymptotic rate of algebraic convergence for Experiment 26

Method	Force	Torque
Pullback approach	3.67	3.69
Stress tensor	1.36	1.37

The dual norm computations are presented in Figure 5.46 where the reference values are again computed using the BEM based shape derivative at a refinement level of $h = 0.082$.
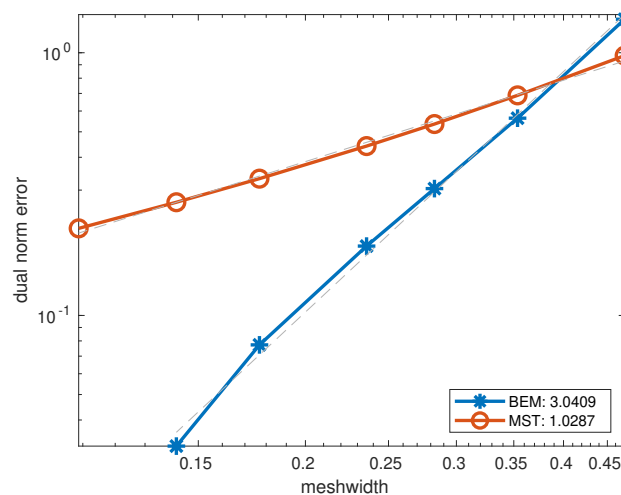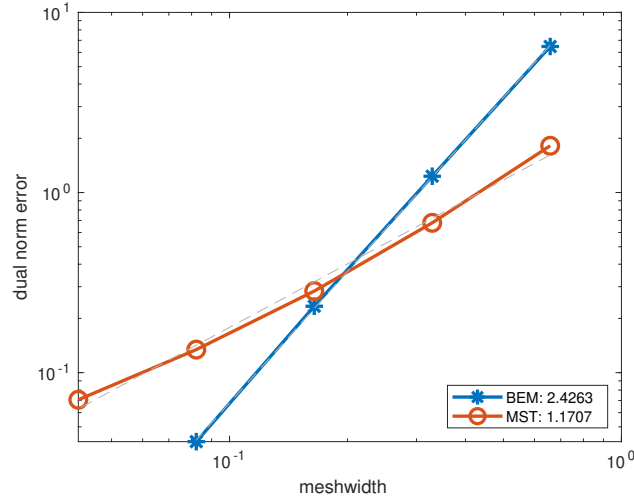
Figure 5.46: Dual norm error for Experiment 26

5.3 Dirichlet BVP (Superconductor)

$$\Omega_c := \mathbb{R}^3 \setminus \overline{\Omega}$$

$$\Omega$$

$$\Omega_{\mathrm{src}}$$
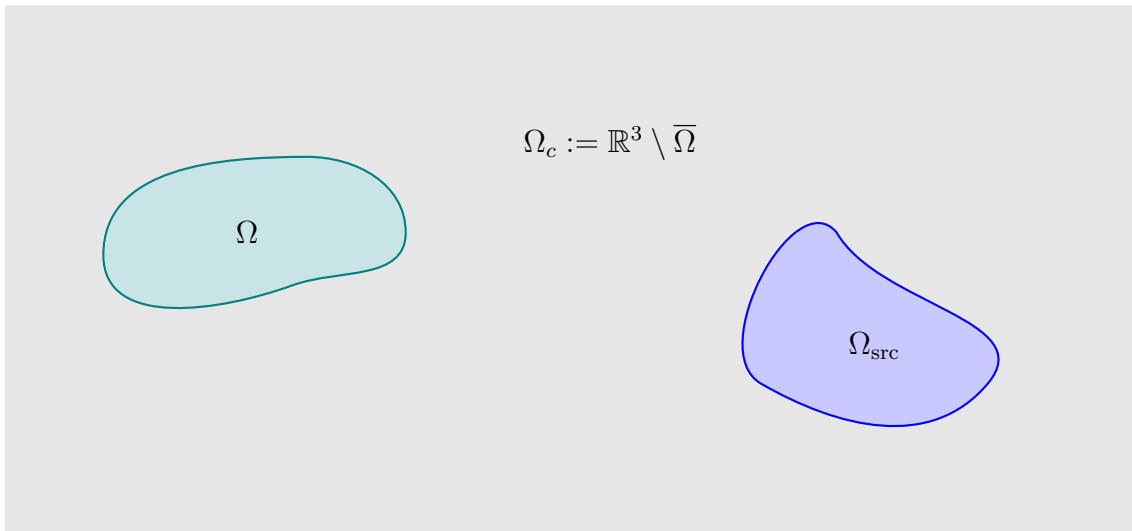
Figure 5.47: Geometric setting

We have a superconducting material occupying the bounded, simply connected and open $\Omega \subset \mathbb{R}^3$ with C^2_{pw} boundary. The exterior $\Omega_c := \mathbb{R}^3 \setminus \overline{\Omega}$ represents vacuum with permeability $\mu_0 \in \mathbb{R}^+$. There is an external current source supplying the current density $\mathbf{J}$ which is compactly supported with $\mathrm{supp}(\mathbf{J}) \subset \Omega_{\mathrm{src}} \Subset \mathbb{R}^3$. The fields $\mathbf{B}$ and $\mathbf{H}$ are modelled by the Maxwell's equations

$$\operatorname{div} \mathbf{B} = 0 \quad \text{in } \mathbb{R}^3,$$
$$\mathbf{curlH} = \mathbf{J} \quad \text{in } \mathbb{R}^3.$$

Since superconducting materials expel magnetic field, we have $\mathbf{B} = 0$ inside Ω and the boundary condition $\mathbf{B} \cdot \mathbf{n} = 0$ on $\Gamma := \partial\Omega$. In the exterior domain Ω_c we have a linear relationship between $\mathbf{B}$ and $\mathbf{H}$ given as

$$\mathbf{B} = \mu_0 \, \mathbf{H}.$$

The energy stored in the magnetic field $\mathcal{E}_F$ is given as

$$\mathcal{E}_F := \frac{\mu_0^{-1}}{2} \int\limits_{\Omega^c} \|\mathbf{B}(\mathbf{x})\|^2 \; d\mathbf{x}.$$

5.3.1 Vector Potential

Since $\operatorname{div} \mathbf{B} = 0$, we introduce the vector potential $\mathbf{A}$ such that $\mathbf{B} = \mathbf{curl}\mathbf{A}$. Using the material law and the equation for $\mathbf{H}$, we get the boundary value problem

$$
\begin{aligned}
\mu_0^{-1}\mathbf{curl}\mathbf{curl}\mathbf{A} &= \mathbf{J} && \text{in } \Omega_c, \\
\gamma_{\mathbf{t}}^+ \mathbf{A} &= 0 && \text{on } \Gamma := \partial\Omega, \\
\operatorname{div} \mathbf{A} &= 0 && \text{in } \Omega_c, \\
\|\mathbf{A}(\mathbf{x})\| &= O(\|\mathbf{x}\|^{-1}) && \text{for } \|\mathbf{x}\| \to \infty.
\end{aligned}
\tag{5.3.1}
$$

Note that we choose the Coulomb gauge $\operatorname{div} \mathbf{A} = 0$ to ensure uniqueness of the solution. The Dirichlet condition $\gamma_{\mathbf{t}}^+ \mathbf{A} = 0$ implies $\mathbf{curl}_\Gamma \, \gamma_{\mathbf{t}}^+ \mathbf{A} = \mathbf{curl}\mathbf{A} \cdot \mathbf{n} = \mathbf{B} \cdot \mathbf{n} = 0$, or in other words, the body Ω expells the magnetic field.

5.3.1.1 Variational BIEs

We approach the exterior Dirichlet BVP (5.3.1) using boundary integral formulation. Putting the Dirichlet trace to zero in the first equation for the exterior traces in (2.2.23) gives us

$$\mathcal{A}(\gamma_{\mathbf{M}}^+ \mathbf{A}) = -\operatorname{grad}_\Gamma \Psi_V(\gamma_n^+ \mathbf{A}) + \mu_0 \, \gamma_{\mathbf{t}}^+ \mathrm{N}(\mathbf{J}).$$

Denoting the unknown magnetic trace by $\boldsymbol{\psi}$ and testing with $\boldsymbol{\zeta} \in \boldsymbol{H}^{-\frac{1}{2}}(\operatorname{div}_\Gamma 0, \Gamma)$ gives the variational problem: seek $\boldsymbol{\psi} \in \boldsymbol{H}^{-\frac{1}{2}}(\operatorname{div}_\Gamma 0, \Gamma)$ such that

$$\boldsymbol{\psi} \in \boldsymbol{H}^{-\frac{1}{2}}(\operatorname{div}_\Gamma 0, \Gamma): \quad \mathsf{b}_{\mathcal{A}}(\boldsymbol{\psi}, \boldsymbol{\zeta}) = \ell(\boldsymbol{\zeta}) \quad \forall \boldsymbol{\zeta} \in \boldsymbol{H}^{-\frac{1}{2}}(\operatorname{div}_\Gamma 0, \Gamma), \tag{5.3.2}$$

where the bilinear form was defined in 5.1.30 and the linear form is defined as

$$\ell(\boldsymbol{\zeta}) := \mu_0 \left\langle \gamma_{\mathbf{t}}^+ \mathrm{N}(\mathbf{J}), \boldsymbol{\zeta} \right\rangle = \mu_0 \int\limits_{\Gamma} \int\limits_{\Omega_{\mathrm{src}}} G(\mathbf{x}, \mathbf{y}) \, \boldsymbol{\zeta}(\mathbf{x}) \cdot \mathbf{J}(\mathbf{y}) \; d\mathbf{y} \; dS_{\mathbf{x}}.$$

We keep the notation $\langle \cdot, \cdot \rangle$ for the duality pairing between $\boldsymbol{H}^{-\frac{1}{2}}(\operatorname{div}_\Gamma, \Gamma)$ and $\boldsymbol{H}^{-\frac{1}{2}}(\mathbf{curl}_\Gamma, \Gamma)$. The variational problem is well posed because of the ellipticity of the bilinear form $\mathsf{b}_{\mathcal{A}}$

on $\boldsymbol{H}^{-\frac{1}{2}}(\mathrm{div}_\Gamma\, 0, \Gamma)$. The field energy can be obtained in terms of the traces by using the representation formula.

$$
\begin{aligned}
\mathcal{E}_F &= \frac{1}{2}\int\limits_{\Omega_{\mathrm{src}}} \mathbf{A}\cdot\mathbf{J}\, d\mathbf{x} \\
&= \frac{1}{2}\int\limits_{\Omega_{\mathrm{src}}} \left\{ -\boldsymbol{\Psi}_{\mathbf{A}}(\boldsymbol{\psi})(\mathbf{x}) - \mathrm{grad}_{\mathbf{x}}\,\Psi_V(\gamma_n^+\mathbf{A})(\mathbf{x}) + \mu_0\int\limits_{\Omega_{\mathrm{src}}} G(\mathbf{x},\mathbf{y})\,\mathbf{J}(\mathbf{y})\, \mathrm{d}\mathbf{y} \right\}\cdot\mathbf{J}(\mathbf{x})\, d\mathbf{x} \\
&= \frac{1}{2}\int\limits_{\Omega_{\mathrm{src}}} \left\{ -\boldsymbol{\Psi}_{\mathbf{A}}(\boldsymbol{\psi})(\mathbf{x}) + \mu_0\int\limits_{\Omega_{\mathrm{src}}} G(\mathbf{x},\mathbf{y})\,\mathbf{J}(\mathbf{y})\, \mathrm{d}\mathbf{y} \right\}\cdot\mathbf{J}(\mathbf{x})\, d\mathbf{x} \\
&= -\frac{1}{2}\int\limits_{\Omega_{\mathrm{src}}}\int\limits_{\Gamma} G(\mathbf{x},\mathbf{y})\,\boldsymbol{\psi}(\mathbf{y})\cdot\mathbf{J}(\mathbf{x})\, dS_{\mathbf{y}}\, d\mathbf{x} + \frac{\mu_0}{2}\int\limits_{\Omega_{\mathrm{src}}}\int\limits_{\Omega_{\mathrm{src}}} G(\mathbf{x},\mathbf{y})\,\mathbf{J}(\mathbf{y})\cdot\mathbf{J}(\mathbf{x})\, \mathrm{d}\mathbf{y}\, d\mathbf{x} \\
&= -\frac{1}{2\mu_0}\ell(\boldsymbol{\psi}) + \frac{\mu_0}{2}\int\limits_{\Omega_{\mathrm{src}}}\int\limits_{\Omega_{\mathrm{src}}} G(\mathbf{x},\mathbf{y})\,\mathbf{J}(\mathbf{y})\cdot\mathbf{J}(\mathbf{x})\, \mathrm{d}\mathbf{y}\, d\mathbf{x}.
\end{aligned}
$$

5.3.1.2 Variational BIEs on Deformed Domain

We consider deformations with a velocity field $\boldsymbol{\mathcal{V}}$ that is zero around Ω_{src}. Thus, the velocity field only deforms the superconducting material. The variational formulation for the deformed s domain $\Omega^s := \mathbf{T}_s^{\boldsymbol{\nu}}(\Omega^0)$ has a similar structure to 5.3.2: seek $\boldsymbol{\psi}_s \in \boldsymbol{H}^{-\frac{1}{2}}(\mathrm{div}_\Gamma\, 0, \Gamma^s)$ such that

$$
\mathsf{b}_{\mathcal{A}}(s)(\boldsymbol{\psi}_s,\boldsymbol{\zeta}) = \ell(s)(\boldsymbol{\zeta}) \quad \forall \boldsymbol{\zeta}\in\boldsymbol{H}^{-\frac{1}{2}}(\mathrm{div}_\Gamma\, 0, \Gamma^s),
$$

where the bilinear form $\mathsf{b}_{\mathcal{A}}(s)$ contains integrals on $\Gamma^s := \mathbf{T}_s^{\boldsymbol{\nu}}(\Gamma^0)$ and the linear form is given as

$$
\ell(s)(\boldsymbol{\zeta}) := \mu_0 \left\langle \gamma_{\mathbf{t}}^+ \mathrm{N}(\mathbf{J}), \boldsymbol{\zeta} \right\rangle_{\Gamma^s},
$$

where $\langle\cdot,\cdot\rangle_{\Gamma^s}$ represents the duality pairing between $\boldsymbol{H}^{-\frac{1}{2}}(\mathrm{div}_\Gamma, \Gamma^s)$ and $\boldsymbol{H}^{-\frac{1}{2}}(\mathbf{curl}_\Gamma, \Gamma^s)$.

5.3.1.3 Equivalent Formulation on Reference Domain

The integrals are transformed back to the reference boundary Γ^0 using the perturbation map. This gives

$$
\begin{aligned}
\mathsf{b}_{\mathcal{A}}(s)(\boldsymbol{\psi}_s,\boldsymbol{\zeta}) &= \int\limits_{\Gamma^s}\int\limits_{\Gamma^s} G(\mathbf{x},\mathbf{y})\,\boldsymbol{\psi}_s(\mathbf{y})\cdot\boldsymbol{\zeta}(\mathbf{x})\, dS_{\mathbf{y}}\, dS_{\mathbf{x}} \\
&= \int\limits_{\Gamma^0}\int\limits_{\Gamma^0} G(\mathbf{T}_s^{\boldsymbol{\nu}}(\hat{\mathbf{x}}), \mathbf{T}_s^{\boldsymbol{\nu}}(\hat{\mathbf{y}}))\,\boldsymbol{\psi}_s(\mathbf{T}_s^{\boldsymbol{\nu}}(\hat{\mathbf{y}}))\cdot\boldsymbol{\zeta}(\mathbf{T}_s^{\boldsymbol{\nu}}(\hat{\mathbf{x}}))\,\omega_s(\hat{\mathbf{y}})\,\omega_s(\hat{\mathbf{x}})\, dS_{\hat{\mathbf{y}}}\, dS_{\hat{\mathbf{x}}}, \\
\ell(s)(\boldsymbol{\zeta}) &= \mu_0\int\limits_{\Gamma^s}\int\limits_{\Omega_{\mathrm{src}}} G(\mathbf{x},\mathbf{y})\,\boldsymbol{\zeta}(\mathbf{x})\cdot\mathbf{J}(\mathbf{y})\, \mathrm{d}\mathbf{y}\, dS_{\mathbf{x}}
\end{aligned}
$$

$$= \mu_0 \int\limits_{\Gamma^0} \int\limits_{\Omega_{\mathrm{src}}} G(\mathbf{T}_s^{\boldsymbol{\nu}}(\hat{\mathbf{x}}), \mathbf{y}) \, \boldsymbol{\zeta}(\mathbf{T}_s^{\boldsymbol{\nu}}(\hat{\mathbf{x}})) \cdot \mathbf{J}(\mathbf{y}) \, \omega_s(\hat{\mathbf{x}}) \, d\mathbf{y} \, dS_{\hat{\mathbf{x}}}.$$

Using the pullback

$$\boldsymbol{\psi} \in \boldsymbol{H}^{-\frac{1}{2}}(\mathrm{div}_\Gamma \, 0, \Gamma^s), \; \hat{\boldsymbol{\psi}} \in \boldsymbol{H}^{-\frac{1}{2}}(\mathrm{div}_\Gamma \, 0, \Gamma^0) : \quad \boldsymbol{\psi}(\mathbf{T}_s^{\boldsymbol{\nu}}(\hat{\mathbf{x}})) = \frac{\mathsf{D}\mathbf{T}_s^{\boldsymbol{\nu}}(\hat{\mathbf{x}})}{\omega_s(\hat{\mathbf{x}})} \, \hat{\boldsymbol{\psi}}(\hat{\mathbf{x}}),$$

we define the pulled back hat (bi)linear forms:

$$\hat{\mathsf{b}}_{\mathcal{A}}(s; \hat{\boldsymbol{\psi}}, \hat{\boldsymbol{\zeta}}) := \int\limits_{\Gamma^0} \int\limits_{\Gamma^0} G(\mathbf{T}_s^{\boldsymbol{\nu}}(\hat{\mathbf{x}}), \mathbf{T}_s^{\boldsymbol{\nu}}(\hat{\mathbf{y}})) \left(\mathsf{D}\mathbf{T}_s^{\boldsymbol{\nu}}(\hat{\mathbf{y}}) \, \hat{\boldsymbol{\psi}}(\hat{\mathbf{y}}) \right) \cdot \left(\mathsf{D}\mathbf{T}_s^{\boldsymbol{\nu}}(\hat{\mathbf{x}}) \, \hat{\boldsymbol{\zeta}}(\hat{\mathbf{x}}) \right) dS_{\hat{\mathbf{y}}} \, dS_{\hat{\mathbf{x}}},$$

$$\hat{\ell}(s; \hat{\boldsymbol{\zeta}}) := \mu_0 \int\limits_{\Gamma^0} \int\limits_{\Omega_{\mathrm{src}}} G(\mathbf{T}_s^{\boldsymbol{\nu}}(\hat{\mathbf{x}}), \mathbf{y}) \left(\mathsf{D}\mathbf{T}_s^{\boldsymbol{\nu}}(\hat{\mathbf{x}}) \, \hat{\boldsymbol{\zeta}}(\hat{\mathbf{x}}) \right) \cdot \mathbf{J}(\mathbf{y}) \, d\mathbf{y} \, dS_{\hat{\mathbf{x}}}.$$

We can now write the equivalent pulled back variational problem: seek $\hat{\boldsymbol{\psi}}_s \in V_0 := \boldsymbol{H}^{-\frac{1}{2}}(\mathrm{div}_\Gamma \, 0, \Gamma^0)$ such that

$$\hat{\mathsf{b}}_{\mathcal{A}}(s; \hat{\boldsymbol{\psi}}_s, \hat{\boldsymbol{\zeta}}) = \hat{\ell}(s; \hat{\boldsymbol{\zeta}}) \quad \forall \hat{\boldsymbol{\zeta}} \in V_0.$$

Field energy for the deformed s-configuration can be expressed in terms of the pulled back linear form as

$$\mathcal{E}_F(s) = -\frac{1}{2\mu_0} \hat{\ell}(s; \hat{\boldsymbol{\psi}}_s) + \frac{\mu_0}{2} \int\limits_{\Omega_{\mathrm{src}}} \int\limits_{\Omega_{\mathrm{src}}} G(\mathbf{x}, \mathbf{y}) \, \mathbf{J}(\mathbf{y}) \cdot \mathbf{J}(\mathbf{x}) \, d\mathbf{y} \, d\mathbf{x}.$$

5.3.1.4 BIE-Constrained Shape Derivative

We start by defining the Lagrangian $\mathcal{L} : \mathbb{R} \times V_0 \times V_0 \to \mathbb{R}$,

$$\mathcal{L}(s; \hat{\boldsymbol{\psi}}, \hat{\boldsymbol{\zeta}}) := \hat{\mathsf{b}}_{\mathcal{A}}(s; \hat{\boldsymbol{\psi}}, \hat{\boldsymbol{\zeta}}) - \hat{\ell}(s; \hat{\boldsymbol{\zeta}}) - \frac{1}{2\mu_0} \hat{\ell}(s; \hat{\boldsymbol{\psi}}) + \frac{\mu_0}{2} \int\limits_{\Omega_{\mathrm{src}}} \int\limits_{\Omega_{\mathrm{src}}} G(\mathbf{x}, \mathbf{y}) \, \mathbf{J}(\mathbf{y}) \cdot \mathbf{J}(\mathbf{x}) \, d\mathbf{y} \, d\mathbf{x}$$

We recover the field energy after plugging in $\hat{\boldsymbol{\psi}} = \hat{\boldsymbol{\psi}}_s$

$$\mathcal{E}_F(s) = \mathcal{L}(s; \hat{\boldsymbol{\psi}}_s, \hat{\boldsymbol{\zeta}}) \quad \forall \hat{\boldsymbol{\zeta}} \in V_0.$$

The energy shape derivative can be computed as

$$\frac{d\mathcal{E}_F}{ds}(0) = \frac{\partial \mathcal{L}}{\partial s}(0; \hat{\boldsymbol{\psi}}_0, \hat{\boldsymbol{\lambda}}),$$

where $\hat{\boldsymbol{\lambda}} \in V_0$ solves the adjoint equation

$$\left\langle \frac{\partial \mathcal{L}}{\partial \hat{\boldsymbol{\psi}}}(0; \hat{\boldsymbol{\psi}}_0, \hat{\boldsymbol{\lambda}}); \hat{\boldsymbol{\zeta}} \right\rangle = 0 \quad \forall \hat{\boldsymbol{\zeta}} \in V_0.$$

Simplifying the above expression gives the adjoint equation in an explicit form.

$$\hat{\mathsf{b}}_{\mathcal{A}}(0;\hat{\boldsymbol{\zeta}},\hat{\boldsymbol{\lambda}}) - \frac{1}{2\mu_0}\hat{\ell}(0;\hat{\boldsymbol{\zeta}}) = 0 \quad \forall \hat{\boldsymbol{\zeta}} \in V_0.$$

Given the symmetry of the bilinear form, the adjoint solution is given as $\hat{\boldsymbol{\lambda}} = \frac{1}{2\mu_0}\hat{\boldsymbol{\psi}}_0$, allowing us to write the shape derivative as

$$
\begin{aligned}
\frac{d\mathcal{E}_F}{ds}(0) &= \frac{\partial\mathcal{L}}{\partial s}(0;\hat{\boldsymbol{\psi}}_0, \frac{1}{2\mu_0}\hat{\boldsymbol{\psi}}_0) \\
&= \frac{\hat{\mathsf{b}}_{\mathcal{A}}}{\partial s}(0;\hat{\boldsymbol{\psi}}_0, \frac{1}{2\mu_0}\hat{\boldsymbol{\psi}}_0) - \frac{\partial\hat{\ell}}{\partial s}(0;\frac{1}{2\mu_0}\hat{\boldsymbol{\psi}}_0) - \frac{1}{2\mu_0}\frac{\partial\hat{\ell}}{\partial s}(0;\hat{\boldsymbol{\psi}}_0) \\
&= \frac{1}{2\mu_0}\frac{\hat{\mathsf{b}}_{\mathcal{A}}}{\partial s}(0;\hat{\boldsymbol{\psi}}_0,\hat{\boldsymbol{\psi}}_0) - \frac{1}{\mu_0}\frac{\partial\hat{\ell}}{\partial s}(0;\hat{\boldsymbol{\psi}}_0) \\
&= \frac{1}{2\mu_0}\int_{\Gamma^0}\int_{\Gamma^0}\left(\nabla_{\mathbf{x}}G(\mathbf{x},\mathbf{y})\cdot\boldsymbol{\mathcal{V}}(\mathbf{x}) + \nabla_{\mathbf{y}}G(\mathbf{x},\mathbf{y})\cdot\boldsymbol{\mathcal{V}}(\mathbf{y})\right)\hat{\boldsymbol{\psi}}_0(\mathbf{y})\cdot\hat{\boldsymbol{\psi}}_0(\mathbf{x})\,dS_{\mathbf{y}}\,dS_{\mathbf{x}} \\
&\quad + \frac{1}{2\mu_0}\int_{\Gamma^0}\int_{\Gamma^0}G(\mathbf{x},\mathbf{y})\left\{\left(\mathsf{D}\boldsymbol{\mathcal{V}}(\mathbf{y})\,\hat{\boldsymbol{\psi}}_0(\mathbf{y})\right)\cdot\hat{\boldsymbol{\psi}}_0(\mathbf{x}) + \hat{\boldsymbol{\psi}}_0(\mathbf{y})\cdot\left(\mathsf{D}\boldsymbol{\mathcal{V}}(\mathbf{x})\,\hat{\boldsymbol{\psi}}_0(\mathbf{x})\right)\right\}dS_{\mathbf{y}}\,dS_{\mathbf{x}} \\
&\quad - \int_{\Gamma^0}\int_{\Omega_{\text{src}}}\nabla_{\mathbf{x}}G(\mathbf{x},\mathbf{y})\cdot\boldsymbol{\mathcal{V}}(\mathbf{x})\left(\hat{\boldsymbol{\psi}}_0(\mathbf{x})\cdot\mathbf{J}(\mathbf{y})\right)d\mathbf{y}\,dS_{\mathbf{x}} \\
&\quad - \int_{\Gamma^0}\int_{\Omega_{\text{src}}}G(\mathbf{x},\mathbf{y})\left(\mathsf{D}\boldsymbol{\mathcal{V}}(\mathbf{x})\,\hat{\boldsymbol{\psi}}_0(\mathbf{x})\right)\cdot\mathbf{J}(\mathbf{y})\,d\mathbf{y}\,dS_{\mathbf{x}}. \quad (5.3.3)
\end{aligned}
$$

5.3.1.5 Shape Derivative From Volume Based Variational Formulation

We start by defining the relevant space for vector potentials on the exterior domain Ω^c [33]

$$\boldsymbol{V}(\Omega_c) := \{\mathbf{u} \in \boldsymbol{\mathcal{D}}(\Omega_c)', \frac{\mathbf{u}(\mathbf{x})}{\sqrt{1+\|\mathbf{x}\|^2}} \in \boldsymbol{L}^2(\Omega_c), \ \mathbf{curl}\,\mathbf{u} \in \boldsymbol{L}^2(\Omega_c), \ \text{div}\,\mathbf{u} = 0 \text{ in } \Omega_c\}.$$

The boundary value problem 5.3.1 has a weak solution which satisfies the variational problem: seek $\mathbf{A} \in \boldsymbol{V}(\Omega_c)$ such that

$$\mu_0^{-1}\int_{\Omega_c}\mathbf{curl}\mathbf{A}\cdot\mathbf{curl}\mathbf{A}'\,d\mathbf{x} = \int_{\Omega_{\text{src}}}\mathbf{J}\cdot\mathbf{A}'\,d\mathbf{x} \quad \forall\mathbf{A}' \in \boldsymbol{V}(\Omega_c). \quad (5.3.4)$$

The field energy can be expressed in terms of the bilinear form as

$$\mathcal{E}_F = \frac{\mu_0^{-1}}{2}\int_{\Omega_c}\|\mathbf{curl}\mathbf{A}(\mathbf{x})\|^2\,d\mathbf{x}.$$

5.3.1.6 Perturbed Problem

As in our approach with BIEs, we only consider deformations of the superconducting material. The variational formulation for the deformed s-configuration resembles 5.3.4: seek $\mathbf{A}_s \in \boldsymbol{V}(\Omega_c^s)$ such that

$$\mathbf{A}_s \in \boldsymbol{V}(\Omega_c^s): \quad \mu_0^{-1} \int_{\Omega_c^s} \mathbf{curl}\mathbf{A}_s \cdot \mathbf{curl}\mathbf{A}' \, d\mathbf{x} = \int_{\Omega_{\text{src}}} \mathbf{J} \cdot \mathbf{A}' \, d\mathbf{x} \quad \forall \mathbf{A}' \in \boldsymbol{V}(\Omega_c^s),$$

where $\boldsymbol{V}(\Omega_c^s)$ is defined in an analogous way as $\boldsymbol{V}(\Omega_c)$.

5.3.1.7 Transformation + Pullback

We transform the integrals back to the reference domain using the perturbation map. This gives us

$$\int_{\Omega_c^s} \mathbf{curl}\mathbf{A}_s \cdot \mathbf{curl}\mathbf{A}' \, d\mathbf{x} = \int_{\Omega_c^0} \mathbf{curl}\mathbf{A}_s(\mathbf{T}_s^{\boldsymbol{\nu}}(\hat{\mathbf{x}})) \cdot \mathbf{curl}\mathbf{A}'(\mathbf{T}_s^{\boldsymbol{\nu}}(\hat{\mathbf{x}})) \, \det \mathsf{D}\mathbf{T}_s^{\boldsymbol{\nu}}(\hat{\mathbf{x}}) \, d\hat{\mathbf{x}}.$$

Since the vector potential $\mathbf{A}$ is a 1-form, we use the pullback of a 2-form for its curl

$$(\mathbf{curl}\mathbf{A})(\mathbf{T}_s^{\boldsymbol{\nu}}(\hat{\mathbf{x}})) = \frac{1}{\det \mathsf{D}\mathbf{T}_s^{\boldsymbol{\nu}}(\hat{\mathbf{x}})} \mathsf{D}\mathbf{T}_s^{\boldsymbol{\nu}}(\hat{\mathbf{x}}) \, \mathbf{curl}\hat{\mathbf{A}}(\hat{\mathbf{x}}).$$

Based on the pullback we define the pulled back (bi)linear forms. The linear form remains unchanged in structure because the deformations don't affect Ω_{src}

$$\hat{\mathsf{b}}(s; \hat{\mathbf{A}}, \hat{\mathbf{A}}') := \mu_0^{-1} \int_{\Omega_c^0} \left(\mathsf{D}\mathbf{T}_s^{\boldsymbol{\nu}}(\hat{\mathbf{x}}) \, \mathbf{curl}\hat{\mathbf{A}}_s(\hat{\mathbf{x}}) \right) \cdot \left(\mathsf{D}\mathbf{T}_s^{\boldsymbol{\nu}}(\hat{\mathbf{x}}) \, \mathbf{curl}\hat{\mathbf{A}}'(\hat{\mathbf{x}}) \right) \frac{1}{\det \mathsf{D}\mathbf{T}_s^{\boldsymbol{\nu}}(\hat{\mathbf{x}})} \, d\hat{\mathbf{x}},$$

$$\hat{\ell}(s; \hat{\mathbf{A}}') := \int_{\Omega_{\text{src}}} \mathbf{J} \cdot \hat{\mathbf{A}}' \, d\mathbf{x}.$$

The equivalent pulled back variational formulation reads: seek $\hat{\mathbf{A}}_s \in V_0 := \boldsymbol{V}(\Omega_c^0)$ such that

$$\hat{\mathsf{b}}(s; \hat{\mathbf{A}}_s, \hat{\mathbf{A}}') = \hat{\ell}(s; \hat{\mathbf{A}}') \quad \forall \mathbf{A}' \in V_0.$$

Energy for the deformed s-configuration can be expressed in terms of the pulled back bilinear form as

$$\mathcal{E}_F(s) = \frac{1}{2}\hat{\mathsf{b}}(s; \hat{\mathbf{A}}_s, \hat{\mathbf{A}}_s).$$

5.3.1.8 Adjoint Method

We start by defining the Lagrangian $\mathcal{L} : \mathbb{R} \times V_0 \times V_0 \to \mathbb{R}$,

$$\mathcal{L}(s; \hat{\mathbf{A}}, \hat{\mathbf{A}}') := \hat{\mathsf{b}}(s; \hat{\mathbf{A}}, \hat{\mathbf{A}}') - \hat{\ell}(s; \hat{\mathbf{A}}') + \frac{1}{2}\hat{\mathsf{b}}(s; \hat{\mathbf{A}}, \hat{\mathbf{A}}).$$

Plugging in the state solution gives

$$\mathcal{E}_F(s) = \mathcal{L}(s; \hat{\mathbf{A}}_s, \hat{\mathbf{A}}') \quad \forall \hat{\mathbf{A}}' \in V_0.$$

The energy shape derivative can be computed as

$$\frac{d\mathcal{E}_F}{ds}(0) = \frac{\partial \mathcal{L}}{\partial s}(0; \hat{\mathbf{A}}_0, \hat{\mathbf{P}}),$$

where $\hat{\mathbf{P}} \in V_0$ solves the adjoint equation

$$\left\langle \frac{\partial \mathcal{L}}{\partial \hat{\mathbf{A}}}(0; \hat{\mathbf{A}}_0, \hat{\mathbf{P}}); \hat{\mathbf{A}}' \right\rangle = 0 \quad \forall \hat{\mathbf{A}}' \in V_0.$$

Simplifying the above expression yields the adjoint equation in an explicit form

$$\hat{\mathsf{b}}(0; \hat{\mathbf{A}}', \hat{\mathbf{P}}) + \hat{\mathsf{b}}(0; \hat{\mathbf{A}}', \hat{\mathbf{A}}_0) = 0 \quad \forall \hat{\mathbf{A}}' \in V_0,$$

which gives the adjoint solution as $\hat{\mathbf{P}} = -\hat{\mathbf{A}}_0$. The shape derivative can then be written as

$$
\begin{aligned}
\frac{d\mathcal{E}_F}{ds}(0) &= \frac{\partial \mathcal{L}}{\partial s}(0; \hat{\mathbf{A}}_0, -\hat{\mathbf{A}}_0) \\
&= \frac{\partial \hat{\mathsf{b}}}{\partial s}(s; \hat{\mathbf{A}}_0, -\hat{\mathbf{A}}_0) - \frac{\partial \hat{\ell}}{\partial s}(0; -\hat{\mathbf{A}}_0) + \frac{1}{2}\frac{\partial \hat{\mathsf{b}}}{\partial s}(0; \hat{\mathbf{A}}_0, \hat{\mathbf{A}}_0) \\
&= -\frac{1}{2}\frac{\partial \hat{\mathsf{b}}}{\partial s}(0; \hat{\mathbf{A}}_0, \hat{\mathbf{A}}_0) \\
&= -\frac{\mu_0^{-1}}{2}\int_{\Omega_c^0} \left\{ \mathbf{curl}\hat{\mathbf{A}}_0^T(\mathsf{D}\boldsymbol{\mathcal{V}} + \mathsf{D}\boldsymbol{\mathcal{V}}^T)\mathbf{curl}\hat{\mathbf{A}}_0 - \left\|\mathbf{curl}\hat{\mathbf{A}}_0\right\|^2 \nabla \cdot \boldsymbol{\mathcal{V}} \right\} d\hat{\mathbf{x}}.
\end{aligned}
$$

The shape derivative can be simplified as we saw earlier in the arguments following 5.1.43. Since the velocity field $\boldsymbol{\mathcal{V}}$ is zero at Ω_{src} we get

$$
\begin{aligned}
\frac{d\mathcal{E}_F}{ds}(0) &= -\mu_0^{-1}\int_{\Omega_c} \mathrm{div}\left(\left\{ \mathbf{B}\mathbf{B}^T - \frac{\|\mathbf{B}\|^2}{2}\mathsf{Id} \right\}\boldsymbol{\mathcal{V}}\right) d\mathbf{x} \\
&= \mu_0^{-1}\int_{\Gamma} \boldsymbol{\mathcal{V}} \cdot \left\{ \mathbf{B}(\mathbf{B}\cdot\mathbf{n}) - \frac{\|\mathbf{B}\|^2}{2}\mathbf{n} \right\} dS. \quad\quad (5.3.5)
\end{aligned}
$$

As expected, we see the appearance of the Maxwell Stress Tensor.

5.3.1.9   Numerical Experiments

In this section we evaluate the shape derivative formulas numerically. Since the formulas (5.3.3) (called "BEM" in the plots) and (5.3.5) (called "MST" in the plots) are purely boundary based, we solve for the boundary data via a discretization of (5.3.2). We discretize the superconductor boundary Γ with a boundary mesh $\mathcal{M}_h$, consisting of triangular elements. As in the transmission problem case, we discretize $\boldsymbol{H}^{-\frac{1}{2}}(\mathrm{div}_\Gamma 0, \Gamma)$ using $\mathbf{n} \times \nabla S_1^0(\mathcal{M}_h)$,

enforcing a zero mean constraint for S_1^0 via a mixed formulation approach. The Galerkin solution is then plugged into the shape derivative formulas and evaluated using quadrature. For (5.3.5) we use a quadrature of order 3 on one triangle whereas for (5.3.3) we evaluate using the Sauter and Schwab quadrature of order 5^4 for each interaction. The computations are done for a series of meshes with decreasing meshwidth h. Forces and torques are evaluated using the procedure mentioned in Section 3.0.2 and the dual norm error is computed with the procedure mentioned in Section 4.4.7.1.

Experiment 27. We have the same geometrical setting as in Experiment 11 (cube shaped Ω), shown in Figure 5.2. The cube in this case represents the superconducting object whereas the torus carries a unit surface current. We choose $\mu_0 = 1$ and compute the error in force and torque computation. The reference value is obtained via the BEM based shape derivative at a refinement level of $h = 0.0707$. Torque is computed about the point (4,0,0). The errors are plotted in Figure 5.48 and their asymptotic convergence rates are reported in Table 5.17. We can see the superiority of the BEM based formula for this case of a cube shaped domain.

(a) Error in total force   (b) Error in total torque

Figure 5.48: Error in force and torque computation for cube torus (Experiment 27)

Table 5.17: Asymptotic rate of algebraic convergence (Experiment 27)

Method	Force	Torque
Pullback approach	2.892	2.897
Stress tensor	1.109	1.144

The shape derivatives are also compared via a dual norm computation which is plotted in Figure 5.49, confirming the superior performance of the BEM based shape derivative.

Figure 5.49: Dual norm error for Experiment 27

Experiment 28. Choosing $\mu_0 = 1$, we work with the geometrical setting introduced in Experiment 12 (spherical Ω), depicted in Figure 5.5. The sphere assumes the role of the superconductor whereas the torus carries a unit surface current density. For plotting the error in force and torque, we use a reference value obtained using the BEM based shape derivative at a refinement level of $h = 0.0392$. Torque is computed about the point $(4,0,0)$. The errors are plotted in Figure 5.50 along with their asymptotic convergence rates which are tabulated in Table 5.18. We see that for a smooth spherical domain, the performance of the two methods is identical. This is in line with our earlier observations with smooth domains.

(a) Error in total force

(b) Error in total torque

Figure 5.50: Error in force and torque computation for sphere and torus (Experiment 28)

Table 5.18: Asymptotic rate of algebraic convergence for Experiment 28

Method	Force	Torque
Pullback approach	1.976	1.981
Stress tensor	2.0335	1.981

The shape derivatives can also be compared in terms of the dual norm errors which is plotted in Figure 5.51
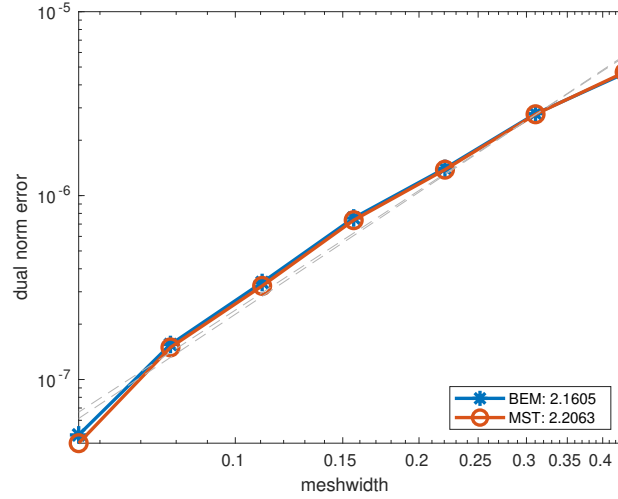
Figure 5.51: Dual norm error for Experiment 28

Experiment 29. Choosing $\mu_0 = 1$, we work with the geometrical setting introduced in Experiment 13 (brick shaped Ω), depicted in Experiment 13. The brick shaped domain assumes the role of the superconductor whereas the torus carries a unit surface current density. For plotting the error in force and torque, we use a reference value obtained using the BEM based shape derivative at a refinement level of $h = 0.064$. Torque is computed about the point (4,0,0). The errors are plotted in Figure 5.50 along with their asymptotic convergence rates which are tabulated in Table 5.19. Similar to the case of a cube shaped domain, we see a superior performance from the BEM based shape derivative.

(a) Error in total force
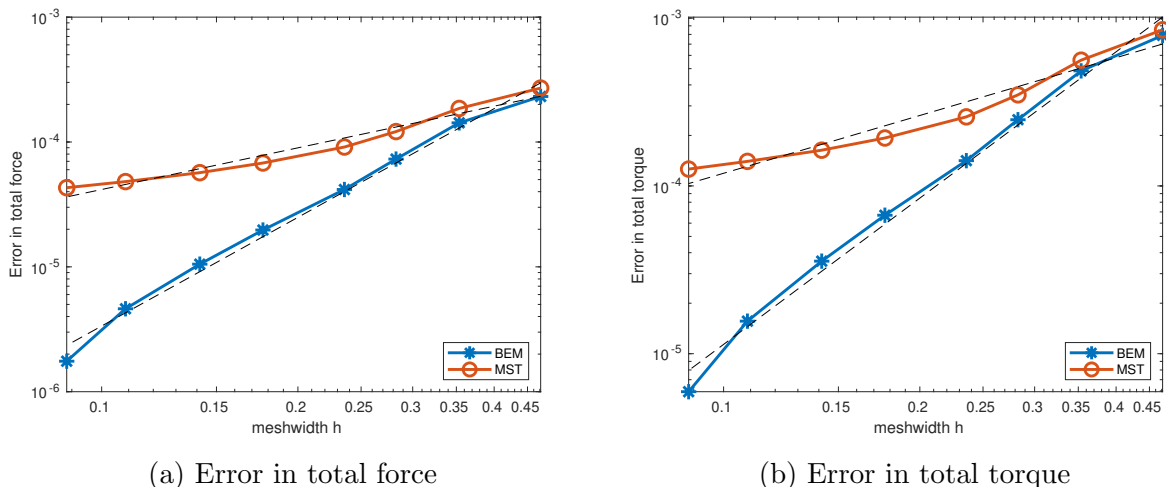
(b) Error in total torque
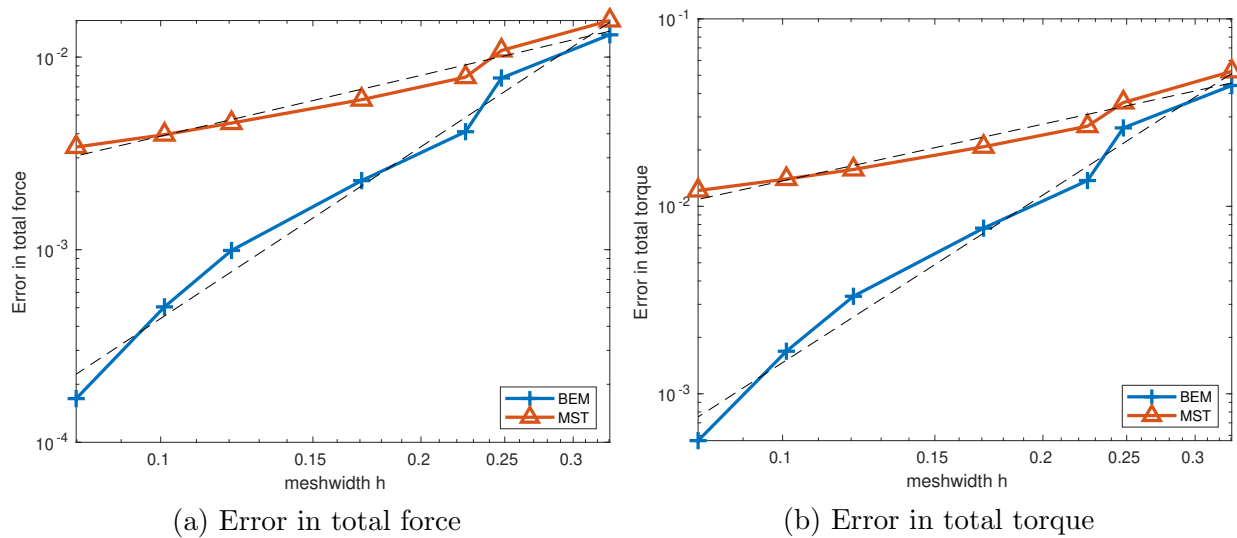
Figure 5.52: Error in force and torque computation for cuboid and torus (Experiment 29)

Table 5.19: Asymptotic rate of algebraic convergence for Experiment 29

Method	Force	Torque
Pullback approach	2.96	2.97
Stress tensor	1.05	1.00

The shape derivatives can also be compared in terms of the dual norm errors which is plotted in Figure 5.53. It confirms the superiority of the BEM based shape derivative.
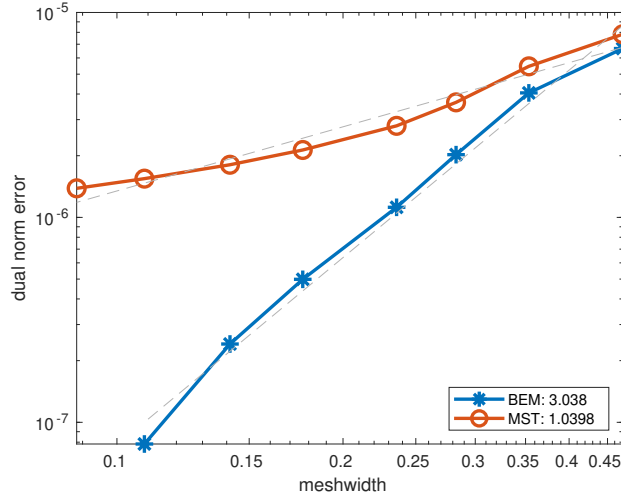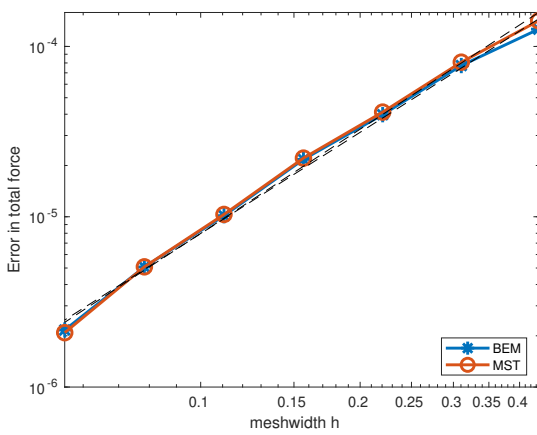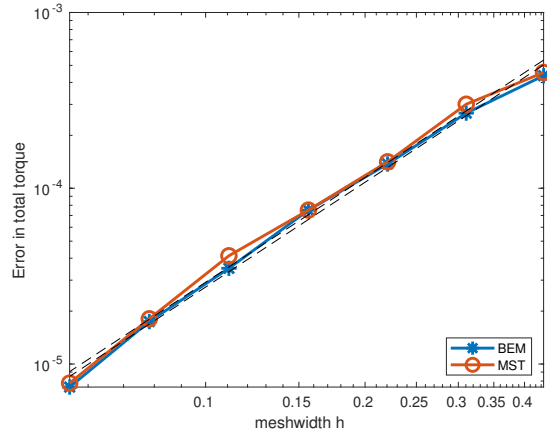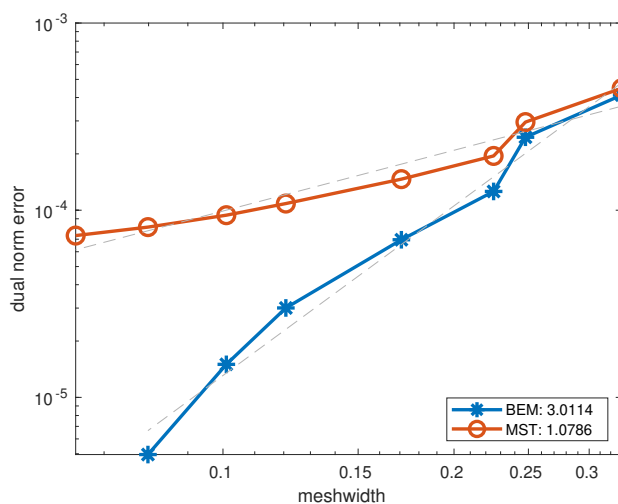

Figure 5.53: Dual norm error for Experiment 29

Experiment 30. Choosing $\mu_0 = 1$, we work with the geometrical setting introduced in Experiment 14 (tetrahedral Ω), depicted in Experiment 14. The tetrahedral domain assumes the role of the superconductor whereas the torus carries a unit surface current density. For

179

plotting the error in force and torque, we use a reference value obtained using the BEM based shape derivative at a refinement level of $h = 0.041$. Torque is computed about the point $(4,0,0)$. The errors are plotted in Figure 5.54 along with their asymptotic convergence rates which are tabulated in Table 5.20. We again see a superior performance from the BEM based shape derivative.

(a) Error in total force (b) Error in total torque
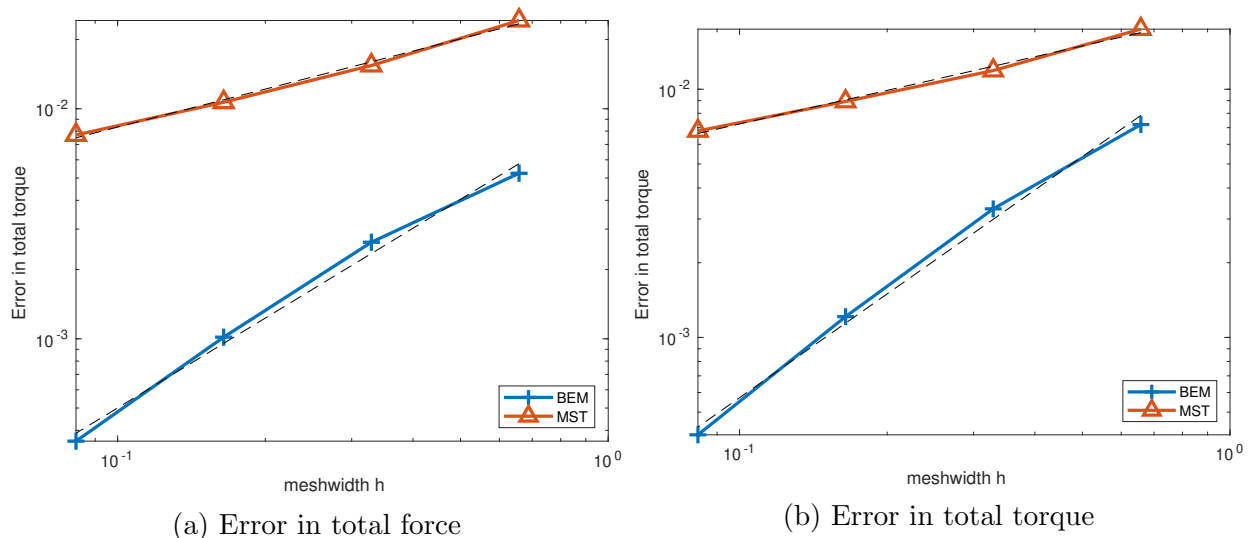
Figure 5.54: Error in force and torque computation for tetrahedron and torus (Experiment 30)

Table 5.20: Asymptotic rate of algebraic convergence for Experiment 30

Method	Force	Torque
Pullback approach	1.39	1.39
Stress tensor	0.53	0.45

The shape derivatives can also be compared in terms of the dual norm errors which is plotted in Figure 5.55, confirming the superiority of the BEM based shape derivative.
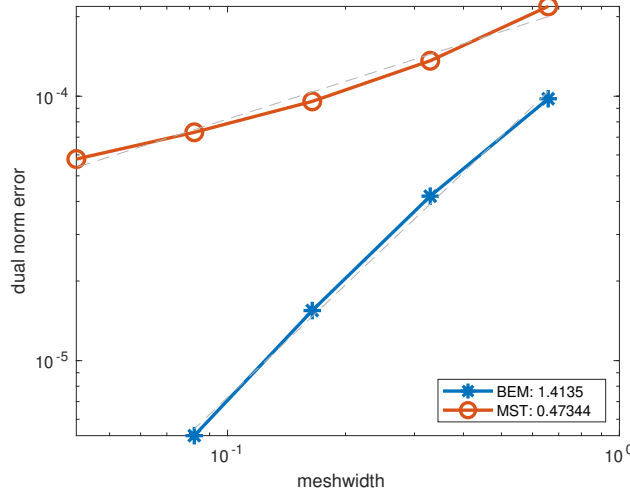
Figure 5.55: Dual norm error for Experiment 30

5.3.2 Scalar Potential

Similar to our approach to the transmission problem case using scalar potential, we use the equation

$$\mathbf{curl}\,\mathbf{H} = \mathbf{J},$$

to write

$$\mathbf{curl}\,\tilde{\mathbf{H}} = \mathbf{curl}(\mathbf{H} - \mathbf{H_J}) = 0$$

where $\mathbf{H_J}$ is defined in 5.1.6. The above equation allows us to introduce the scalar potential u such that $\tilde{\mathbf{H}} = \nabla u$ and div $\mathbf{B} = 0$ gives us

$$\Delta u = 0 \quad \text{in } \Omega_c. \tag{5.3.6}$$

The potential u decays as $O(\|\mathbf{x}\|^{-1})$ at ∞. At the boundary $\Gamma := \partial\Omega$, due to the linear material law $\mathbf{B} = \mu_0 \mathbf{H}$, we have the condition $\mathbf{H} \cdot \mathbf{n} = 0$ which translates to a Neumann boundary condition for u

$$(\tilde{\mathbf{H}} + \mathbf{H_J}) \cdot \mathbf{n} = 0 \implies \nabla u \cdot \mathbf{n} = -\mathbf{H_J} \cdot \mathbf{n} \quad \text{on } \Gamma. \tag{5.3.7}$$

Thus we have the boundary value problem

$$\Delta u = 0 \qquad \text{in } \Omega_c, \tag{5.3.8}$$

$$\nabla u \cdot \mathbf{n} = -\mathbf{H_J} \cdot \mathbf{n} \quad \text{on } \Gamma, \tag{5.3.9}$$

$$u(\mathbf{x}) = O(\|\mathbf{x}\|^{-1}) \quad \text{for } \|\mathbf{x}\| \to \infty. \tag{5.3.10}$$

5.3.2.1 Variational BIEs

The boundary value problem 5.3.10 has a unique solution because of the decay condition at infinity. We use the second boundary integral equation for the exterior traces 2.1.22

$$\mathrm{W}(\gamma_D^+ u) + \left(\frac{\mathsf{Id}}{2} + \mathrm{K}'\right)(\gamma_N^+ u) = 0.$$

Denoting the Dirichlet trace of u by g and plugging in the known Neumann trace, we get the relation

$$W(g) = \left(\frac{\mathsf{Id}}{2} + K'\right)(\mathbf{H_J} \cdot \mathbf{n})$$

Testing with $v \in H^{\frac{1}{2}}(\Gamma)$ gives

$$\mathsf{b}_W(g, v) = \frac{1}{2}\langle \mathbf{H_J} \cdot \mathbf{n}, v\rangle + \mathsf{b}_{K'}(\mathbf{H_J} \cdot \mathbf{n}, v) \quad v \in H^{\frac{1}{2}}(\Gamma). \tag{5.3.11}$$

Here $\langle \cdot, \cdot \rangle$ denotes the duality pairing between $H^{-\frac{1}{2}}(\Gamma)$ and $H^{\frac{1}{2}}(\Gamma)$. We know that the bilinear form on the left hand side has a kernel which is the constant functions [58, Section 6.6]. Thus solving for g using the above equation will not give a unique solution. To make the above variational equation uniquely solvable, we restrict ourselves to the space $V(\Gamma) := H_*^{\frac{1}{2}}(\Gamma)$. The variational problem reads: seek $\tilde{g} \in V(\Gamma)$ such that

$$\tilde{g} \in V(\Gamma): \quad \mathsf{b}_W(\tilde{g}, v) = l(v) \quad v \in V(\Gamma), \tag{5.3.12}$$

where

$$l(v) := \frac{1}{2}\langle \mathbf{H_J} \cdot \mathbf{n}, v\rangle + \mathsf{b}_{K'}(\mathbf{H_J} \cdot \mathbf{n}, v).$$

Note that the solution of the variational problem $\tilde{g}$ does not necessarily coincide with the Dirichlet trace of the potential u in the exterior domain, which we denote by g. The field energy is given as

$$\mathcal{E}_F = -\frac{\mu_0}{2}\int_{\Omega_c} \|\nabla u\|^2 \, d\mathbf{x} + \frac{\mu_0}{2}\int_{\Omega_c} \|\mathbf{H_J}\|^2 \, d\mathbf{x}$$

$$= -\frac{\mu_0}{2}\int_{\Gamma} g \, \mathbf{H_J} \cdot \mathbf{n} \, d\mathrm{S} + \frac{\mu_0}{2}\int_{\Omega_c} \|\mathbf{H_J}\|^2 \, d\mathbf{x}.$$

We notice that in the energy expression, we require the Dirichlet trace g. To express it using the solution $\tilde{g}$ of the variational BIE, we use the representation formula:

$$u(\mathbf{x}) = \psi_{\mathrm{SL}}(\mathbf{H_J} \cdot \mathbf{n})(\mathbf{x}) + \psi_{\mathrm{DL}}(\tilde{g})(\mathbf{x}) \quad \mathbf{x} \in \Omega_c.$$

Taking the Dirichlet trace gives us the desired relation

$$g = V(\mathbf{H_J} \cdot \mathbf{n}) + \frac{\tilde{g}}{2} + K(\tilde{g}).$$

Inserting the above expression into the field energy expression gives us

$$\mathcal{E}_F = -\frac{\mu_0}{2}\int_{\Gamma} \left(V(\mathbf{H_J} \cdot \mathbf{n}) + \frac{\tilde{g}}{2} + K(\tilde{g})\right) \mathbf{H_J} \cdot \mathbf{n} \, d\mathrm{S} + \frac{\mu_0}{2}\int_{\Omega_c} \|\mathbf{H_J}\|^2 \, d\mathbf{x}$$

$$= -\frac{\mu_0}{2}\left(\mathsf{b}_V(\mathbf{H_J} \cdot \mathbf{n}, \mathbf{H_J} \cdot \mathbf{n}) + \frac{1}{2}\langle \tilde{g}, \mathbf{H_J} \cdot \mathbf{n}\rangle + \mathsf{b}_K(\tilde{g}, \mathbf{H_J} \cdot \mathbf{n})\right) + \frac{\mu_0}{2}\int_{\Omega_c} \|\mathbf{H_J}\|^2 \, d\mathbf{x}$$

$$= -\frac{\mu_0}{2}\ell(\tilde{g}) - \frac{\mu_0}{2}\mathsf{b}_V(\mathbf{H_J} \cdot \mathbf{n}, \mathbf{H_J} \cdot \mathbf{n}) + \frac{\mu_0}{2}\int_{\Omega_c} \|\mathbf{H_J}\|^2 \, d\mathbf{x}.$$

5.3.2.2 Variational BIEs on Deformed Domain

As in the vector potential formulation, we deform only the superconducting object. To simplify the notation, we will denote the Dirichlet trace solution without a tilde symbol. Variational formulation for the deformed s-configuration has a similar structure to 5.3.12: seek $g_s \in V(\Gamma^s)$ such that

$$\mathsf{b}_W(s)(g_s, v) = l(s)(v) \quad \forall v \in V(\Gamma^s),$$

where $V(\Gamma^s) := H_*^{\frac{1}{2}}(\Gamma^s)$,

$$l(s)(v) := \frac{1}{2} \langle \mathbf{H_J} \cdot \mathbf{n}, v \rangle_{\Gamma^s} + \mathsf{b}_{K'}(s)(\mathbf{H_J} \cdot \mathbf{n}, v),$$

and the bilinear forms $b_*(s)$ are given in Section 4.4.3.

5.3.2.3 Equivalent Formulation on Reference Domain

The integrals can be transformed back to the reference boundary using the perturbation map. This gives

$$\mathsf{b}_W(s)(g_s, v) = \int_{\Gamma^s} \int_{\Gamma^s} G(\mathbf{x}, \mathbf{y}) \ \mathbf{curl}_\Gamma g_s(\mathbf{y}) \cdot \mathbf{curl}_\Gamma v(\mathbf{x}) \ dS_{\mathbf{y}} \ dS_{\mathbf{x}}$$

$$= \int_{\Gamma^0} \int_{\Gamma^0} G(\mathbf{T}_s^{\boldsymbol{\nu}}(\hat{\mathbf{x}}), \mathbf{T}_s^{\boldsymbol{\nu}}(\hat{\mathbf{y}})) \ \mathbf{curl}_\Gamma g_s(\mathbf{T}_s^{\boldsymbol{\nu}}(\hat{\mathbf{y}})) \cdot \mathbf{curl}_\Gamma v(\mathbf{T}_s^{\boldsymbol{\nu}}(\hat{\mathbf{x}})) \ \omega_s(\hat{\mathbf{y}}) \ \omega_s(\hat{\mathbf{x}}) \ dS_{\hat{\mathbf{y}}} \ dS_{\hat{\mathbf{x}}},$$

$$l(s)(v) = \frac{1}{2} \int_{\Gamma^s} \mathbf{H_J} \cdot \mathbf{n} \ v \ dS + \int_{\Gamma^s} \int_{\Gamma^s} \nabla_{\mathbf{y}} G(\mathbf{x}, \mathbf{y}) \cdot \mathbf{n}(\mathbf{y}) \ v(\mathbf{y}) \ \mathbf{H_J}(\mathbf{x}) \cdot \mathbf{n}(\mathbf{x}) \ dS_{\mathbf{y}} \ dS_{\mathbf{x}}$$

$$= \frac{1}{2} \int_{\Gamma^0} \mathbf{H_J}(\mathbf{T}_s^{\boldsymbol{\nu}}(\hat{\mathbf{x}})) \cdot \frac{\mathcal{C}(\mathsf{D}\mathbf{T}_s^{\boldsymbol{\nu}}(\hat{\mathbf{x}})) \ \hat{\mathbf{n}}(\hat{\mathbf{x}})}{\omega_s(\hat{\mathbf{x}})} \ v(\mathbf{T}_s^{\boldsymbol{\nu}}(\hat{\mathbf{x}})) \ \omega_s(\hat{\mathbf{x}}) \ dS_{\hat{\mathbf{x}}}$$

$$+ \int_{\Gamma^0} \int_{\Gamma^0} \nabla_{\mathbf{y}} G(\mathbf{T}_s^{\boldsymbol{\nu}}(\hat{\mathbf{x}}), \mathbf{T}_s^{\boldsymbol{\nu}})(\hat{\mathbf{y}})) \cdot \frac{\mathcal{C}(\mathsf{D}\mathbf{T}_s^{\boldsymbol{\nu}}(\hat{\mathbf{y}})) \ \hat{\mathbf{n}}(\hat{\mathbf{y}})}{\omega_s(\hat{\mathbf{y}})} \ v(\mathbf{T}_s^{\boldsymbol{\nu}}(\hat{\mathbf{y}}))$$

$$\mathbf{H_J}(\mathbf{T}_s^{\boldsymbol{\nu}}(\hat{\mathbf{x}})) \cdot \frac{\mathcal{C}(\mathsf{D}\mathbf{T}_s^{\boldsymbol{\nu}}(\hat{\mathbf{x}})) \ \hat{\mathbf{n}}(\hat{\mathbf{x}})}{\omega_s(\hat{\mathbf{x}})} \ \omega_s(\hat{\mathbf{y}}) \ \omega_s(\hat{\mathbf{x}}) \ dS_{\hat{\mathbf{y}}} \ dS_{\hat{\mathbf{x}}}.$$

We use the pullbacks

$$u(\mathbf{T}_s^{\boldsymbol{\nu}}(\hat{\mathbf{x}})) = \hat{u}(\hat{\mathbf{x}}),$$

$$\mathbf{curl}_\Gamma u(\mathbf{T}_s^{\boldsymbol{\nu}}(\hat{\mathbf{x}})) = \frac{\mathsf{D}\mathbf{T}_s^{\boldsymbol{\nu}}(\hat{\mathbf{x}})}{\omega_s(\hat{\mathbf{x}})} \ \mathbf{curl}_\Gamma \hat{u}(\hat{\mathbf{x}}),$$

while lead to the following definition of the pulled back hat (bi)linear forms

$$\hat{\mathsf{b}}_W(s; \hat{g}, \hat{v}) := \int_{\Gamma^0} \int_{\Gamma^0} G(\mathbf{T}_s^{\boldsymbol{\nu}}(\hat{\mathbf{x}}), \mathbf{T}_s^{\boldsymbol{\nu}}(\hat{\mathbf{y}})) \left(\mathsf{D}\mathbf{T}_s^{\boldsymbol{\nu}}(\hat{\mathbf{y}}) \ \mathbf{curl}_\Gamma \hat{g}(\hat{\mathbf{y}}) \right) \cdot \left(\mathsf{D}\mathbf{T}_s^{\boldsymbol{\nu}}(\hat{\mathbf{x}}) \ \mathbf{curl}_\Gamma \hat{v}(\hat{\mathbf{x}}) \right) \ dS_{\hat{\mathbf{y}}} \ dS_{\hat{\mathbf{x}}},$$

$$\hat{\ell}(s; \hat{v}) := \frac{1}{2} \int_{\Gamma^0} \mathbf{H_J}(\mathbf{T}_s^{\boldsymbol{\nu}}(\hat{\mathbf{x}})) \cdot \left(\mathcal{C}(\mathsf{D}\mathbf{T}_s^{\boldsymbol{\nu}}(\hat{\mathbf{x}}) \, \hat{\mathbf{n}}(\hat{\mathbf{x}})) \right) \hat{v}(\hat{\mathbf{x}}) \, dS_{\hat{\mathbf{x}}}$$

$$+ \int_{\Gamma^0} \int_{\Gamma^0} \nabla_{\mathbf{y}} G(\mathbf{T}_s^{\boldsymbol{\nu}}(\hat{\mathbf{x}}), \mathbf{T}_s^{\boldsymbol{\nu}}(\hat{\mathbf{y}})) \cdot \left(\mathcal{C}(\mathsf{D}\mathbf{T}_s^{\boldsymbol{\nu}}(\hat{\mathbf{y}}) \, \hat{\mathbf{n}}(\hat{\mathbf{y}})) \right) \hat{v}(\hat{\mathbf{y}})$$

$$\mathbf{H_J}(\mathbf{T}_s^{\boldsymbol{\nu}}(\hat{\mathbf{x}})) \cdot \left(\mathcal{C}(\mathsf{D}\mathbf{T}_s^{\boldsymbol{\nu}}(\hat{\mathbf{x}})) \, \hat{\mathbf{n}}(\hat{\mathbf{x}}) \right) \, dS_{\hat{\mathbf{y}}} \, dS_{\hat{\mathbf{x}}}.$$

The pulled back variational formulation reads: seek $\hat{g}_s \in V_0 := V(\Gamma^0)$ such that

$$\hat{\mathsf{b}}_{\mathrm{W}}(s; \hat{g}_s, \hat{v}) = \hat{\ell}(s; \hat{v}) \quad \hat{v} \in V_0.$$

Field energy for the deformed s-configuration can be written in terms of the pulled back linear form as

$$\mathcal{E}_F(s) = -\frac{\mu_0}{2} \hat{\ell}(s; \hat{g}_s)$$

$$- \frac{\mu_0}{2} \int_{\Gamma^0} \int_{\Gamma^0} G(\mathbf{T}_s^{\boldsymbol{\nu}}(\hat{\mathbf{x}}), \mathbf{T}_s^{\boldsymbol{\nu}}(\hat{\mathbf{y}})) \, \mathbf{H_J}(\mathbf{T}_s^{\boldsymbol{\nu}}(\hat{\mathbf{y}})) \cdot \left(\mathcal{C}(\mathsf{D}\mathbf{T}_s^{\boldsymbol{\nu}}(\hat{\mathbf{y}})) \, \hat{\mathbf{n}}(\hat{\mathbf{y}}) \right)$$

$$\mathbf{H_J}(\mathbf{T}_s^{\boldsymbol{\nu}}(\hat{\mathbf{x}})) \cdot \left(\mathcal{C}(\mathsf{D}\mathbf{T}_s^{\boldsymbol{\nu}}(\hat{\mathbf{x}})) \, \hat{\mathbf{n}}(\hat{\mathbf{x}}) \right) \, dS_{\mathbf{y}} \, dS_{\mathbf{x}}$$

$$+ \frac{\mu_0}{2} \int_{\Omega_c^0} \|\mathbf{H_J}(\mathbf{T}_s^{\boldsymbol{\nu}}(\hat{\mathbf{x}}))\|^2 \, \det \mathsf{D}\mathbf{T}_s^{\boldsymbol{\nu}}(\hat{\mathbf{x}}) \, d\hat{\mathbf{x}}.$$

5.3.2.4 BIE-Constrained Shape Derivative

We start by defining the Lagrangian $\mathcal{L} : \mathbb{R} \times V_0 \times V_0 \to \mathbb{R}$,

$$\mathcal{L}(s; \hat{g}, \hat{v}) := \hat{\mathsf{b}}_{\mathrm{W}}(s; \hat{g}, \hat{v}) - \hat{\ell}(s; \hat{v}) - \frac{\mu_0}{2} \hat{\ell}(s; \hat{g})$$

$$- \frac{\mu_0}{2} \int_{\Gamma^0} \int_{\Gamma^0} G(\mathbf{T}_s^{\boldsymbol{\nu}}(\hat{\mathbf{x}}), \mathbf{T}_s^{\boldsymbol{\nu}}(\hat{\mathbf{y}})) \, \mathbf{H_J}(\mathbf{T}_s^{\boldsymbol{\nu}}(\hat{\mathbf{y}})) \cdot \left(\mathcal{C}(\mathsf{D}\mathbf{T}_s^{\boldsymbol{\nu}}(\hat{\mathbf{y}})) \, \hat{\mathbf{n}}(\hat{\mathbf{y}}) \right)$$

$$\mathbf{H_J}(\mathbf{T}_s^{\boldsymbol{\nu}}(\hat{\mathbf{x}})) \cdot \left(\mathcal{C}(\mathsf{D}\mathbf{T}_s^{\boldsymbol{\nu}}(\hat{\mathbf{x}})) \, \hat{\mathbf{n}}(\hat{\mathbf{x}}) \right) \, dS_{\mathbf{y}} \, dS_{\mathbf{x}}$$

$$+ \frac{\mu_0}{2} \int_{\Omega_c^0} \|\mathbf{H_J}(\mathbf{T}_s^{\boldsymbol{\nu}}(\hat{\mathbf{x}}))\|^2 \, \det \mathsf{D}\mathbf{T}_s^{\boldsymbol{\nu}}(\hat{\mathbf{x}}) \, d\hat{\mathbf{x}}.$$

Plugging in the state solution gives the field energy

$$\mathcal{E}_F(s) = \mathcal{L}(s; \hat{g}_s, \hat{v}) \quad \forall \hat{v} \in V_0.$$

The energy shape derivative can be computed as

$$\frac{d\mathcal{E}_F}{ds}(0) = \frac{\partial \mathcal{L}}{\partial s}(0; \hat{g}_0, \hat{p}),$$

where $\hat{p} \in V_0$ solves the adjoint equation

$$\left\langle \frac{\partial \mathcal{L}}{\partial \hat{g}}(0; \hat{g}_0, \hat{p}); \hat{v} \right\rangle = 0 \quad \forall \hat{v} \in V_0.$$

Simplifying the above expression gives the adjoint equation in an explicit form

$$\hat{\mathsf{b}}_\mathrm{W}(0; \hat{p}, \hat{v}) - \frac{\mu_0}{2}\hat{\ell}(0; \hat{v}) = 0 \quad \hat{v} \in V_0.$$

The adjoint solution is given as $\hat{p} = \frac{\mu_0}{2}\hat{g}_0$, giving the energy shape derivative

$$
\begin{aligned}
\frac{d\mathcal{E}_F}{ds}(0) &= \frac{\partial \mathcal{L}}{\partial s}\left(0; \hat{g}_0, \frac{\mu_0}{2}\hat{g}_0\right)\\
&= \frac{\mu_0}{2}\int_{\Gamma^0}\int_{\Gamma^0}\left(\nabla_\mathbf{x}G(\mathbf{x},\mathbf{y})\cdot\boldsymbol{\mathcal{V}}(\mathbf{x}) + \nabla_\mathbf{y}G(\mathbf{x},\mathbf{y})\cdot\boldsymbol{\mathcal{V}}(\mathbf{y})\right)\,\mathbf{curl}_\Gamma\,\hat{g}_0(\mathbf{y})\cdot\mathbf{curl}_\Gamma\,\hat{g}_0(\mathbf{x})\,d\mathrm{S_y}\,d\mathrm{S_x}\\
&\quad + \frac{\mu_0}{2}\int_{\Gamma^0}\int_{\Gamma^0}G(\mathbf{x},\mathbf{y})\left(\mathsf{D}\boldsymbol{\mathcal{V}}(\mathbf{y})\,\mathbf{curl}_\Gamma\,\hat{g}(\mathbf{y})\right)\cdot\mathbf{curl}_\Gamma\,\hat{g}(\mathbf{x})\,d\mathrm{S_y}\,d\mathrm{S_x}\\
&\quad + \frac{\mu_0}{2}\int_{\Gamma^0}\int_{\Gamma^0}G(\mathbf{x},\mathbf{y})\left(\mathsf{D}\boldsymbol{\mathcal{V}}(\mathbf{x})\,\mathbf{curl}_\Gamma\,\hat{g}(\mathbf{x})\right)\cdot\mathbf{curl}_\Gamma\,\hat{g}(\mathbf{y})\,d\mathrm{S_y}\,d\mathrm{S_x}\\
&\quad - \frac{\mu_0}{2}\int_{\Gamma^0}\hat{g}_0\left\{\hat{\mathbf{n}}^T\mathsf{D}\mathbf{H_J}\,\boldsymbol{\mathcal{V}} + \mathbf{H_J}^T\left(\nabla\cdot\boldsymbol{\mathcal{V}}\,\hat{\mathbf{n}} - \mathsf{D}\boldsymbol{\mathcal{V}}^T\,\hat{\mathbf{n}}\right)\right\}\,d\mathrm{S}\\
&\quad - \mu_0\int_{\Gamma^0}\int_{\Gamma^0}\nabla_\mathbf{y}G(\mathbf{x},\mathbf{y})\cdot\hat{\mathbf{n}}(\mathbf{y})\,\hat{g}_0(\mathbf{y})\left\{\hat{\mathbf{n}}^T\mathsf{D}\mathbf{H_J}\,\boldsymbol{\mathcal{V}} + \mathbf{H_J}^T\left(\nabla\cdot\boldsymbol{\mathcal{V}}\,\hat{\mathbf{n}} - \mathsf{D}\boldsymbol{\mathcal{V}}^T\,\hat{\mathbf{n}}\right)\right\}(\mathbf{x})\,d\mathrm{S_y}\,d\mathrm{S_x}\\
&\quad - \mu_0\int_{\Gamma^0}\int_{\Gamma^0}\nabla_\mathbf{y}G(\mathbf{x},\mathbf{y})\cdot\left(\nabla\cdot\boldsymbol{\mathcal{V}}\,\hat{\mathbf{n}} - \mathsf{D}\boldsymbol{\mathcal{V}}^T\,\hat{\mathbf{n}}\right)(\mathbf{y})\,\hat{g}_0(\mathbf{y})\,\mathbf{H_J}(\mathbf{x})\cdot\hat{\mathbf{n}}(\mathbf{x})\,d\mathrm{S_y}\,d\mathrm{S_x}\\
&\quad - \mu_0\int_{\Gamma^0}\int_{\Gamma^0}\frac{d\nabla_\mathbf{y}G(\mathbf{T}_s^\nu(\mathbf{x}),\mathbf{T}_s^\nu(\mathbf{y}))}{ds}\cdot\hat{\mathbf{n}}(\mathbf{y})\,\hat{g}_0(\mathbf{y})\,\mathbf{H_J}(\mathbf{x})\cdot\hat{\mathbf{n}}(\mathbf{x})\,d\mathrm{S_y}\,d\mathrm{S_x}\\
&\quad - \frac{\mu_0}{2}\int_{\Gamma^0}\int_{\Gamma^0}\left(\nabla_\mathbf{x}G(\mathbf{x},\mathbf{y})\cdot\boldsymbol{\mathcal{V}}(\mathbf{x}) + \nabla_\mathbf{y}G(\mathbf{x},\mathbf{y})\cdot\boldsymbol{\mathcal{V}}(\mathbf{y})\right)(\mathbf{H_J}\cdot\hat{\mathbf{n}})(\mathbf{y})\,(\mathbf{H_J}\cdot\hat{\mathbf{n}})(\mathbf{x})\,d\mathrm{S_y}\,d\mathrm{S_x}\\
&\quad - \frac{\mu_0}{2}\int_{\Gamma^0}\int_{\Gamma^0}G(\mathbf{x},\mathbf{y})\left(\hat{\mathbf{n}}^T\mathsf{D}\mathbf{H_J}\,\boldsymbol{\mathcal{V}} + \mathbf{n}^T\mathbf{H_J}\,\nabla\cdot\boldsymbol{\mathcal{V}} - \mathbf{H_J}^T\,\mathsf{D}\boldsymbol{\mathcal{V}}\,\hat{\mathbf{n}}\right)(\mathbf{y})\left(\mathbf{H_J}\cdot\hat{\mathbf{n}}\right)(\mathbf{x})\,d\mathrm{S_y}\,d\mathrm{S_x}\\
&\quad - \frac{\mu_0}{2}\int_{\Gamma^0}\int_{\Gamma^0}G(\mathbf{x},\mathbf{y})\left(\hat{\mathbf{n}}^T\mathsf{D}\mathbf{H_J}\,\boldsymbol{\mathcal{V}} + \mathbf{n}^T\mathbf{H_J}\,\nabla\cdot\boldsymbol{\mathcal{V}} - \mathbf{H_J}^T\,\mathsf{D}\boldsymbol{\mathcal{V}}\,\hat{\mathbf{n}}\right)(\mathbf{x})\left(\mathbf{H_J}\cdot\hat{\mathbf{n}}\right)(\mathbf{y})\,d\mathrm{S_y}\,d\mathrm{S_x}\\
&\quad - \frac{\mu_0}{2}\int_{\Gamma^0}\|\mathbf{H_J}\|^2\,\boldsymbol{\mathcal{V}}\cdot\mathbf{n}\,d\mathrm{S}. \tag{5.3.13}
\end{aligned}
$$

5.3.2.5 Shape Derivative From Volume Based Variational Formulation

We begin by defining the relevant space for potentials in the unbounded domain

$$V(\Omega_c) := \{u : \Omega_c \to \mathbb{R} : \int_{\Omega_c} \|\nabla u\|^2 + \frac{u^2}{1 + \|\mathbf{x}\|^2} \, d\mathbf{x} < \infty\}.$$

The BVP (5.3.10) admits a weak solution in the space $V(\Omega_c)$ which solves the variational problem: seek $u \in V(\Omega_c)$ such that

$$\int_{\Omega_c} \nabla u \cdot \nabla v \, d\mathbf{x} = \int_{\Gamma} v \, \mathbf{H_J} \cdot \mathbf{n} \, dS \quad \forall v \in V(\Omega_c). \tag{5.3.14}$$

The field energy can be written in terms of the bilinear form as

$$\begin{aligned}
\mathcal{E}_F &= \frac{\mu_0}{2} \int_{\Omega_c} \|\nabla u + \mathbf{H_J}\|^2 \, d\mathbf{x} \\
&= \frac{\mu_0}{2} \int_{\Omega_c} \|\nabla u\|^2 \, d\mathbf{x} + \mu_0 \int_{\Omega_c} \nabla u \cdot \mathbf{H_J} \, d\mathbf{x} + \frac{\mu_0}{2} \int_{\Omega_c} \|\mathbf{H_J}\|^2 \, d\mathbf{x} \\
&= \frac{\mu_0}{2} \int_{\Omega_c} \|\nabla u\|^2 \, d\mathbf{x} - \mu_0 \int_{\Gamma} u \, \mathbf{H_J} \cdot \mathbf{n} \, d\mathbf{x} + \frac{\mu_0}{2} \int_{\Omega_c} \|\mathbf{H_J}\|^2 \, d\mathbf{x} \\
&= -\frac{\mu_0}{2} \int_{\Omega_c} \|\nabla u\|^2 \, d\mathbf{x} + \frac{\mu_0}{2} \int_{\Omega_c} \|\mathbf{H_J}\|^2 \, d\mathbf{x}.
\end{aligned}$$

5.3.2.6 Variational Formulation for Deformed Domain

Considering deformations of only the superconducting material, the deformed s-configuration has the variational problem with a similar structure to (5.3.14): seek $u_s \in V(\Omega_c^s)$ such that

$$\int_{\Omega_c^s} \nabla u_s \cdot \nabla v \, d\mathbf{x} = \int_{\Gamma^s} v \, \mathbf{H_J} \cdot \mathbf{n} \, dS \quad \forall v \in V(\Omega_c^s).$$

The space $V(\Omega_c^s)$ is defined in an analogous way as $V(\Omega_c)$.

5.3.2.7 Transformation + Pullback

The integrals in the variational formulation above are transformed back to the reference domain using the perturbation map which gives

$$\int_{\Omega_c^s} \nabla u_s \cdot \nabla v \, d\mathbf{x} = \int_{\Omega_c^0} \nabla u_s(\mathbf{T}_s^{\boldsymbol{\nu}}(\hat{\mathbf{x}})) \cdot \nabla v(\mathbf{T}_s^{\boldsymbol{\nu}}(\hat{\mathbf{x}})) \, \det \mathsf{D}\mathbf{T}_s^{\boldsymbol{\nu}}(\hat{\mathbf{x}}) \, d\hat{\mathbf{x}},$$

$$\int_{\Gamma^s} v \, \mathbf{H_J} \cdot \mathbf{n} \, dS = \int_{\Gamma^0} v(\mathbf{T}_s^{\boldsymbol{\nu}}(\hat{\mathbf{x}})) \, \mathbf{H_J}(\mathbf{T}_s^{\boldsymbol{\nu}}(\hat{\mathbf{x}})) \cdot \frac{\mathbf{C}(\mathsf{D}\mathbf{T}_s^{\boldsymbol{\nu}}(\hat{\mathbf{x}})) \, \hat{\mathbf{n}}(\hat{\mathbf{x}})}{\omega_s(\hat{\mathbf{x}})} \, \omega_s(\hat{\mathbf{x}}) \, dS_{\hat{\mathbf{x}}}.$$

We use the pullbacks

$$v(\mathbf{T}_s^{\boldsymbol{\nu}}(\hat{\mathbf{x}})) = \hat{v}(\hat{\mathbf{x}}),$$
$$\nabla v(\mathbf{T}_s^{\boldsymbol{\nu}}(\hat{\mathbf{x}})) = \mathsf{D}\mathbf{T}_s^{\boldsymbol{\nu}}(\hat{\mathbf{x}})^{-T}\,\nabla\hat{v}(\hat{\mathbf{x}}),$$

using which we define the pulled back hat (bi)linear forms

$$\hat{\mathsf{b}}(s;\hat{u},\hat{v}) := \int\limits_{\Omega_c^0} \left(\mathsf{D}\mathbf{T}_s^{\boldsymbol{\nu}}(\hat{\mathbf{x}})^{-T}\,\nabla\hat{u}(\hat{\mathbf{x}})\right)\cdot\left(\mathsf{D}\mathbf{T}_s^{\boldsymbol{\nu}}(\hat{\mathbf{x}})^{-T}\,\nabla\hat{v}(\hat{\mathbf{x}})\right)\,\det\mathsf{D}\mathbf{T}_s^{\boldsymbol{\nu}}(\hat{\mathbf{x}})\,d\hat{\mathbf{x}},$$

$$\hat{\ell}(s;\hat{v}) := \int\limits_{\Gamma^0} \hat{v}(\hat{\mathbf{x}})\,\mathbf{H_J}(\mathbf{T}_s^{\boldsymbol{\nu}}(\hat{\mathbf{x}}))\cdot\left(\mathbf{C}(\mathsf{D}\mathbf{T}_s^{\boldsymbol{\nu}}(\hat{\mathbf{x}}))\,\hat{\mathbf{n}}(\hat{\mathbf{x}})\right)\,dS_{\hat{\mathbf{x}}}.$$

The pulled back variational formulation is then given as: seek $\hat{u}_s \in V_0 := V(\Omega_c^0)$ such that

$$\hat{\mathsf{b}}(s;\hat{u}_s,\hat{v}) = \hat{\ell}(s;\hat{v}) \quad \hat{v}\in V_0.$$

Field energy for the deformed s-configuration can be expressed in terms of the pulled back bilinear form as

$$\mathcal{E}_F(s) = -\frac{\mu_0}{2}\hat{\mathsf{b}}(s;\hat{u}_s,\hat{u}_s) + \frac{\mu_0}{2}\int\limits_{\Omega_c^0}\|\mathbf{H_J}(\mathbf{T}_s^{\boldsymbol{\nu}}(\hat{\mathbf{x}}))\|^2\,\det\mathsf{D}\mathbf{T}_s^{\boldsymbol{\nu}}(\hat{\mathbf{x}})\,d\hat{\mathbf{x}}.$$

5.3.2.8   Adjoint Approach

We start with defining the Lagrangian $\mathcal{L}:\mathbb{R}\times V_0\times V_0\to\mathbb{R}$,

$$\mathcal{L}(s;\hat{u},\hat{v}) := \hat{\mathsf{b}}(s;\hat{u},\hat{v}) - \hat{\ell}(s;\hat{v}) - \frac{\mu_0}{2}\hat{\mathsf{b}}(s;\hat{u},\hat{u}) + \frac{\mu_0}{2}\int\limits_{\Omega_c^0}\|\mathbf{H_J}(\mathbf{T}_s^{\boldsymbol{\nu}}(\hat{\mathbf{x}}))\|^2\,\det\mathsf{D}\mathbf{T}_s^{\boldsymbol{\nu}}(\hat{\mathbf{x}})\,d\hat{\mathbf{x}}.$$

Plugging in the state solution gives the field energy

$$\mathcal{E}_F(s) = \mathcal{L}(s;\hat{u}_s,\hat{v}) \quad \forall\hat{v}\in V_0,$$

which can be shape differentiated as

$$\frac{d\mathcal{E}_F}{ds}(0) = \frac{\partial\mathcal{L}}{\partial s}(0;\hat{u}_0,\hat{p}),$$

where $\hat{p}\in V_0$ solves the adjoint equation given as

$$\left\langle\frac{\partial\mathcal{L}}{\partial\hat{u}}(0;\hat{u}_0,\hat{p});\hat{v}\right\rangle = 0 \quad \forall\hat{v}\in V_0.$$

On simplification, the adjoint equation can be written explicitly as

$$\hat{\mathsf{b}}(0;\hat{p},\hat{v}) - \mu_0\hat{\mathsf{b}}(0;\hat{u}_0,\hat{v}) = 0 \quad \forall\hat{v}\in V_0,$$

from which we can read the adjoint solution as $\hat{p} = \mu_0 \, \hat{u}_0$. The shape derivative is then

$$
\begin{aligned}
\frac{d\mathcal{E}_F}{ds}(0) &= \frac{\partial \mathcal{L}}{\partial s}(0; \hat{u}_0, \mu_0 \, \hat{u}_0) \\[2mm]
&= \frac{\mu_0}{2} \frac{\partial \hat{\mathbf{b}}}{\partial s}(0; \hat{u}_0, \hat{u}_0) - \mu_0 \frac{\partial \hat{\ell}}{\partial s}(0; \hat{u}_0) + \frac{\mu_0}{2} \int_{\Omega_c^0} \left\{ \|\mathbf{H_J}\|^2 \, \nabla \cdot \boldsymbol{\mathcal{V}} + \boldsymbol{\mathcal{V}} \cdot \nabla(\|\mathbf{H_J}\|^2) \right\} d\hat{\mathbf{x}} \\[2mm]
&= \frac{\mu_0}{2} \int_{\Omega_c^0} \left\{ - \nabla \hat{u}_0^T (\mathsf{D}\boldsymbol{\mathcal{V}} + \mathsf{D}\boldsymbol{\mathcal{V}}^T) \, \nabla \hat{u}_0 + \|\nabla \hat{u}_0\|^2 \, \nabla \cdot \boldsymbol{\mathcal{V}} \right\} d\mathbf{x} \\[2mm]
&\quad - \mu_0 \int_{\Gamma^0} \hat{u}_0 \left\{ \hat{\mathbf{n}}^T \mathsf{D}\mathbf{H_J} \, \boldsymbol{\mathcal{V}} + \mathbf{H_J} \cdot \hat{\mathbf{n}} \, (\nabla \cdot \boldsymbol{\mathcal{V}}) - \mathbf{H_J}^T \mathsf{D}\boldsymbol{\mathcal{V}}^T \, \hat{\mathbf{n}} \right\} d\mathrm{S} \\[2mm]
&\quad - \frac{\mu_0}{2} \int_{\Gamma^0} \|\mathbf{H_J}\|^2 \, \boldsymbol{\mathcal{V}} \cdot \mathbf{n} \, d\mathrm{S}.
\end{aligned}
\tag{5.3.15}
$$

The shape derivative can be simplified further using the simplification ideas shown in (5.1.22) and (5.1.24). Writing $g = \hat{u}_0|_\Gamma$, we have

$$
\begin{aligned}
\frac{d\mathcal{E}_F}{ds}(0) &= -\mu_0 \int_\Gamma \boldsymbol{\mathcal{V}} \cdot \left\{ \frac{\|\nabla \hat{u}_0\|^2}{2} \, \mathbf{n} - \nabla \hat{u}_0 \, \hat{u}_0 \cdot \mathbf{n} \right\} d\mathrm{S} \\[2mm]
&\quad - \mu_0 \int_\Gamma \boldsymbol{\mathcal{V}} \cdot \left(\mathbf{curl}_\Gamma \, g \times \mathbf{H_J} \right) d\mathrm{S} \\[2mm]
&\quad - \frac{\mu_0}{2} \int_{\Gamma^0} \|\mathbf{H_J}\|^2 \, \boldsymbol{\mathcal{V}} \cdot \mathbf{n} \, d\mathrm{S}.
\end{aligned}
$$

Inserting the Neumann trace allows further simplification and in the end we get

$$
\frac{d\mathcal{E}_F}{ds}(0) = -\frac{\mu_0}{2} \int_\Gamma \|\mathbf{H}_{tot}^\tau\|^2 \, \boldsymbol{\mathcal{V}} \cdot \mathbf{n} \, d\mathrm{S},
$$

where $\mathbf{H}_{tot}^\tau$ is the tangential component of the total $\mathbf{H}$ field at the interface Γ.

5.3.2.9 Numerical Experiments

Now we evaluate the shape derivative formulas (5.3.13) (called "BEM" in the plots) and (5.3.15) (called "MST" in the plots) numerically. Since both formulas are purely boundary based, we opt for a BEM solution using a discretization of (5.3.12). We discretize the superconductor boundary Γ with a triangular mesh $\mathcal{M}_h$. The space $H^{\frac{1}{2}}(\Gamma) \setminus \mathbb{R}$ is discretized using $P_*^1(\mathcal{M}_h)$, where the zero mean constraint is added via a mixed formulation. The galerkin solution is then plugged into both the shape derivative formulas and evaluated using numerical quadrature. The boundary based formula is evaluated using a quadrature rule of 3 points per triangle, whereas the BEM based shape derivative formula is evaluated using the Sauter and Schwab quadrature rule of 5^4 for each interaction. These computations are

done for a series of meshes with decreasing meshwidth h. Forces and torques are computed using the procedure mentioned in Section 3.0.2 and the dual norm error is computed using the procedure mentioned in Section 4.4.7.1.

Experiment 31. We have the same experimental setting as in Experiment 27 (cube shaped Ω), now approached via a scalar potential formulation. The error for force and torque computation is done using a reference solution obtained using the BEM based shape derivative evaluated at a refinement level of $h = 0.0707$. Torque is computed about the point $(4,0,0)$. The errors are plotted in Figure 5.56 and the rates of convergence are tabulated in Table 5.21. We again see the superiority of the BEM based shape derivative for the cube shaped superconductor.

(a) Error in total force   (b) Error in total torque

Figure 5.56: Error in force and torque computation for cube torus (Experiment 31)

Table 5.21: Asymptotic rate of algebraic convergence for Experiment 31

Method	Force	Torque
Pullback approach	2.922	2.926
Stress tensor	1.013	0.965

The shape derivative formulas are also compared via dual norm computations which are presented in Figure 5.57, confirming the superiority of the BEM based shape derivative.
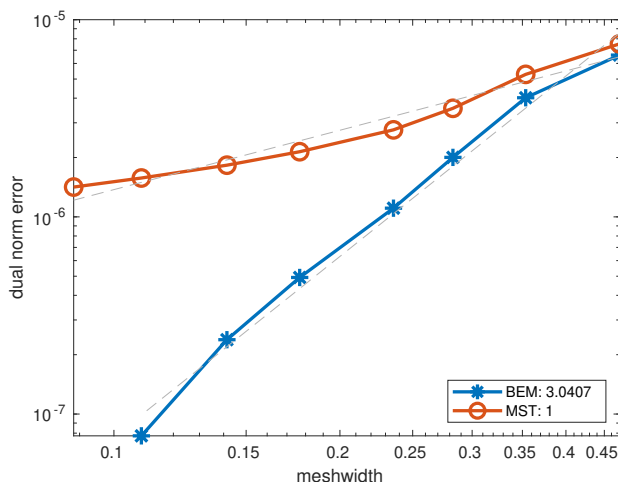
Figure 5.57: Dual norm error for Experiment 31

Experiment 32. We approach the experimental setting from Experiment 28 (spherical Ω) using a scalar potential formulation. Computing the reference force and torque values using the BEM based shape derivative at a refinement level of $h = 0.0277$, we get the error plots in Figure 5.58. Torque is computed about the point (4,0,0). The convergence rates are tabulated in Table 5.22. For the case of a smooth domain we see that the two formulas have identical performance which is not a surprising result for a smooth domain.

(a) Error in total force

(b) Error in total torque
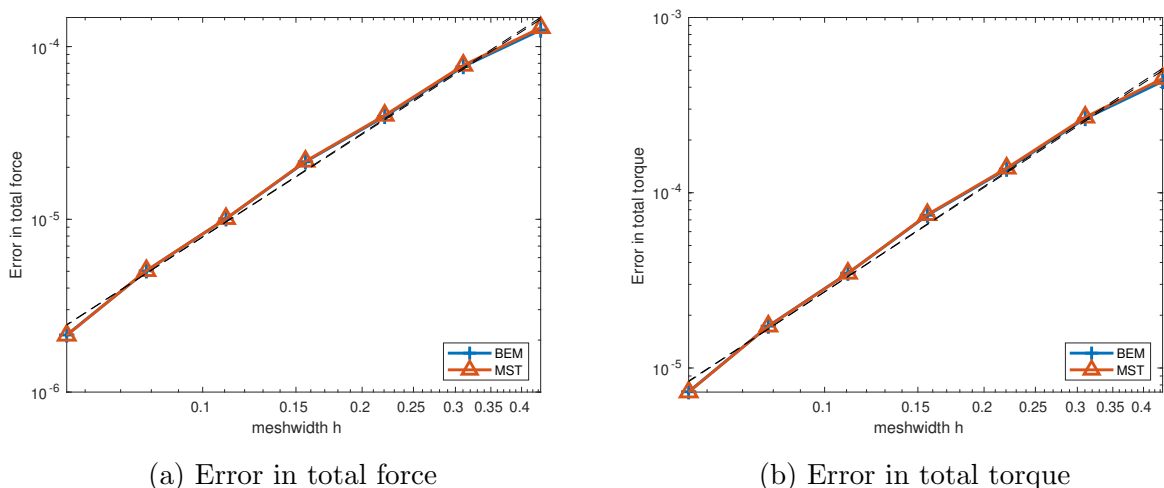
Figure 5.58: Error in force and torque computation for sphere and torus (Experiment 32)

Table 5.22: Asymptotic rate of algebraic convergence for Experiment 32

Method	Force	Torque
Pullback approach	1.975	1.980
Stress tensor	1.990	1.998

Comparison of the shape derivatives via dual norm computations results in identical performance as reported in Figure 5.59
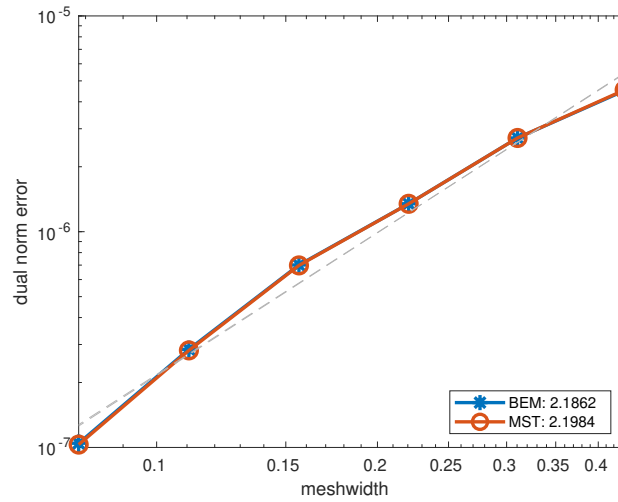
Figure 5.59: Dual norm error for Experiment 32

Experiment 33. We approach the experimental setting from Experiment 30 (tetrahedral shaped Ω) using a scalar potential formulation. Computing the reference force and torque values using the BEM based shape derivative at a refinement level of $h = 0.041$, we get the error plots in Figure 5.60. Torque is computed about the point (4,0,0). The convergence rates are tabulated in Table 5.23. We see superior performance from the BEM based shape derivative.

(a) Error in total force

(b) Error in total torque
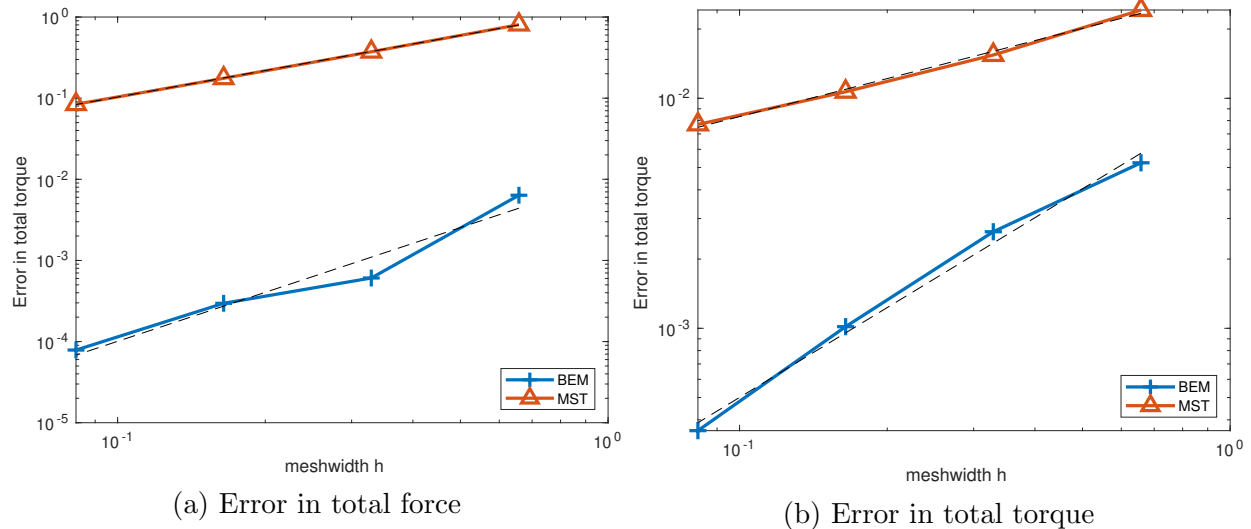
Figure 5.60: Error in force and torque computation for tetrahedron and torus (Experiment 33)

Table 5.23: Asymptotic rate of algebraic convergence for Experiment 33

Method	Force	Torque
Pullback approach	1.30	1.30
Stress tensor	0.54	0.55

Dual norm computation results as reported in Figure 5.61 which confirms the superiority of the BEM based shape derivative.
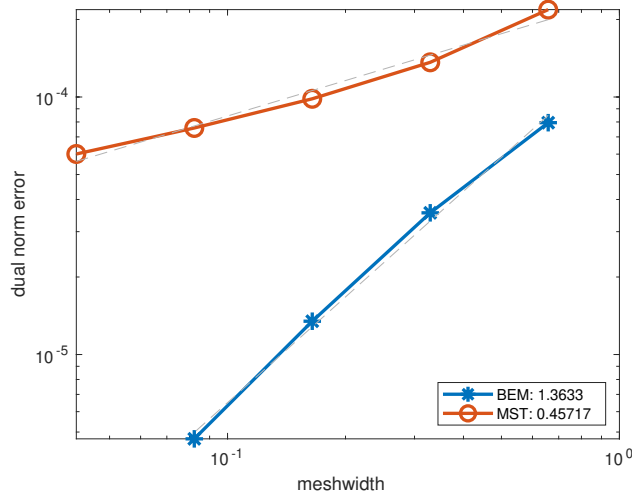
Figure 5.61: Dual norm error for Experiment 33

Experiment 34. We approach the experimental setting from Experiment 29 (brick shaped Ω) using a scalar potential formulation. Computing the reference force and torque values using the BEM based shape derivative at a refinement level of $h = 0.064$, we get the error plots in Figure 5.62. Torque is computed about the point (4,0,0). The convergence rates are tabulated in Table 5.24. We see a superior performance from the BEM based shape derivative.

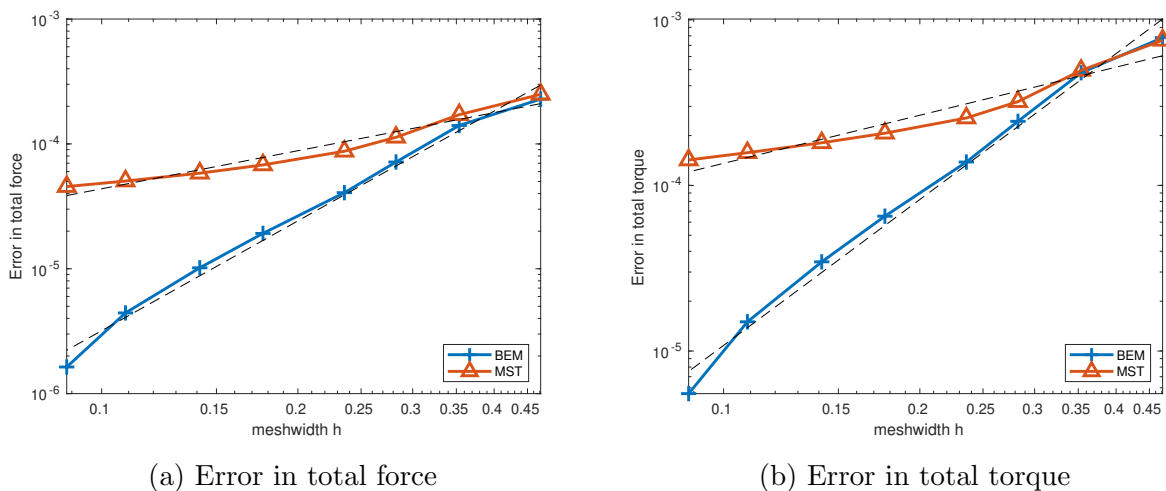(a) Error in total force (b) Error in total torque
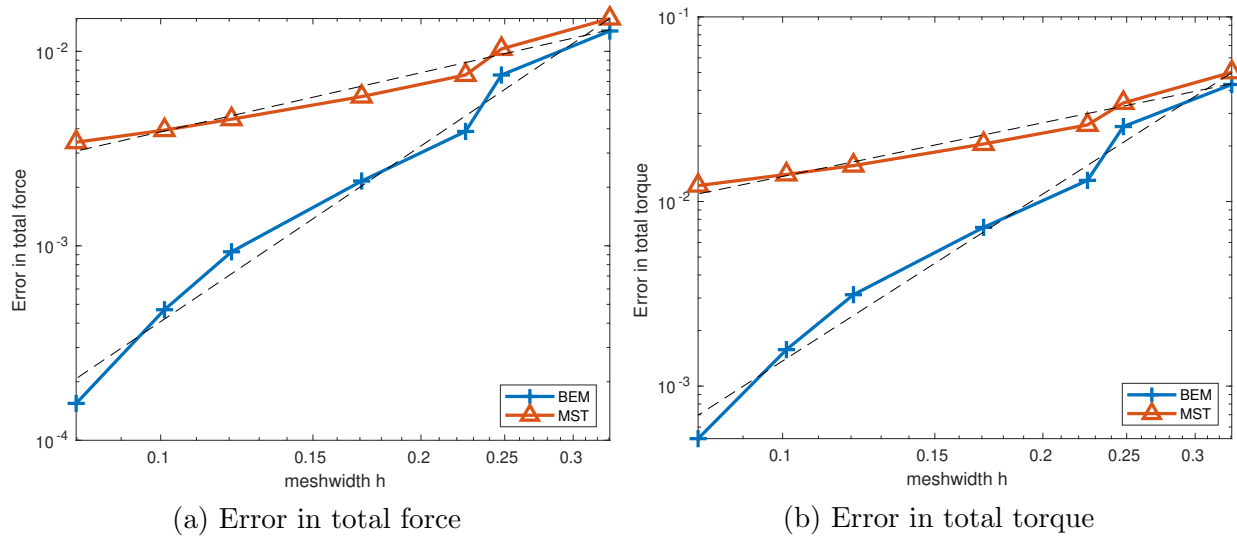
Figure 5.62: Error in force and torque computation for cuboid and torus (Experiment 34)

Table 5.24: Asymptotic rate of algebraic convergence for Experiment 34

Method	Force	Torque
Pullback approach	3.00	3.00
Stress tensor	1.01	0.97

Comparison of the shape derivatives via dual norm computations shows superior performance of the BEM based shape derivative as seen in Figure 5.63.
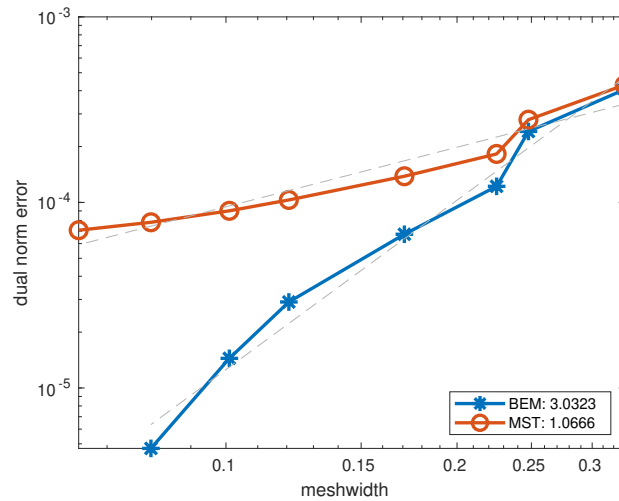
Figure 5.63: Dual norm error for Experiment 34

5.4 Permanent Magnet

In this section we look at the model for a permanent magnet where the relation between $\mathbf{B}$ and $\mathbf{H}$ fields is affine and is given as

$$\mathbf{B}(\mathbf{x}) = \mu_0(\mathbf{H}(\mathbf{x}) + \mathbf{M}(\mathbf{x})), \quad \mu_0 \in \mathbb{R}^+, \ \mathbf{x} \in \mathbb{R}^3.$$

This model is not new and has been used in the works [6, 7, 37, 39, 51]. In contrast to a linear material where we saw a linear relation, we can see that the magnetic flux density $\mathbf{B}$ does not go to zero when the externally applied magnetic field $\mathbf{H}$ is set to zero. This is in accordance with the physical concept of a permanent magnet where we don't necessarily need external current sources for magnetic effects. Note that it is the simplest model of a permanent magnet and does not consider effects like hysteresis. We take for granted the existence of a magnetized piece of material with the magnetization $\mathbf{M}$. In other words, we don't consider the energy expended to magnetize the permanent magnet.

In our concrete setting, we consider a permanent magnet with magnetization $\mathbf{M}$ occupying the bounded, simply connected and open domain Ω with C_{pw}^2 boundary, which is surrounded by vacuum (permeability $= \mu_0$). We assume $\mathbf{M}|_\Omega \in \boldsymbol{H}(\mathbf{curl}, \Omega)$, $\mathbf{curl}\mathbf{M} \in \boldsymbol{H}(\mathrm{div}; \mathbb{R}^3)$ and $\mathbf{M}(\mathbf{x}) \equiv 0$, $\mathbf{x} \in \Omega_c$. There is an exterior divergence free source current $\mathbf{J}$ with support in $\Omega_{\mathrm{src}} \Subset \mathbb{R}^3$, such that $\overline{\Omega}_{\mathrm{src}} \cap \overline{\Omega} = \phi$ and $\mathbf{J}|_{\partial\Omega_{\mathrm{src}}} \cdot \mathbf{n} = 0$. We have the magnetostatic equations

$$\mathrm{div}\,\mathbf{B}(\mathbf{x}) = 0 \quad \text{in } \mathbb{R}^3,$$
$$\mathbf{curl}\mathbf{H}(\mathbf{x}) = \mathbf{J}(\mathbf{x}) \quad \text{in } \mathbb{R}^3,$$

which are supplemented by the material law

$$\mathbf{B}(\mathbf{x}) = \mu\Big(\mathbf{H}(\mathbf{x}) + \mathbf{M}(\mathbf{x})\Big) \quad \mathbf{x} \in \Omega, \quad \mathbf{B}(\mathbf{x}) = \mu_0\,\mathbf{H}(\mathbf{x}) \quad \mathbf{x} \in \Omega_c. \tag{5.4.1}$$

Due to different material properties, the fields are discontinuous at the interface $\Gamma := \partial\Omega$, but nevertheless satisfy the following transmission conditions

$$[\![\mathbf{B}]\!]_\Gamma \cdot \mathbf{n} = 0, \quad [\![\mathbf{H}]\!]_\Gamma \times \mathbf{n} = 0.$$

For the case of permanent magnets, we will see that the choice of the energy or co-energy used to compute the shape derivative formula is important and is related to whether we use a $\mathbf{H}$ based (scalar potential) or a $\mathbf{B}$ based (vector potential) description.

5.4.1 Magnetic Field Energy and Co-Energy

The field energy is defined as the work done to create the given configuration. From the considerations in [38, Section 6.2] we see that for the incremental change $\delta\mathbf{B}$ in the magnetic flux density, the change in magnetic field energy is given by the expression

$$\delta W = \int_{\mathbb{R}^3} \mathbf{H} \cdot \delta\mathbf{B} \ d\mathbf{x}.$$
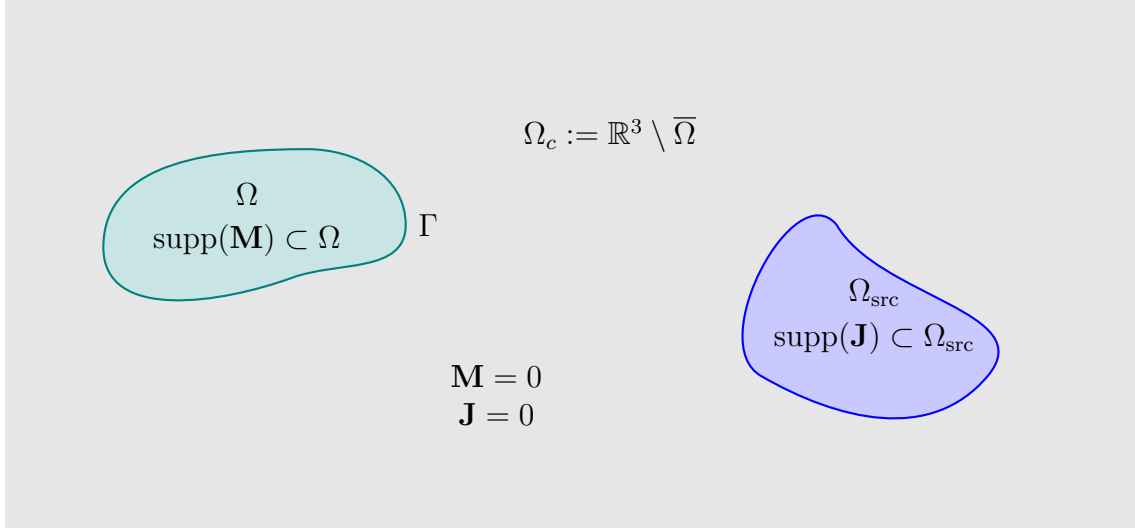
Figure 5.64: Geometric setting

The expression for co-energy is analogous, where a change $\delta\mathbf{H}$ is considered and it leads to

$$\delta U = \int_{\mathbb{R}^3} \mathbf{B} \cdot \delta\mathbf{H} \, d\mathbf{x}.$$

The expressions above suggest that we use energy with a vector potential formulation which models $\mathbf{B}$ and use co-energy with a scalar potential formulation which models $\mathbf{H}$, an idea which is well known [29, 39, 40, 51, 52]. The expressions above can be integrated to obtain the expressions for the energy and co-energy. Using the material law for the permanent magnet

$$\boldsymbol{B} = \mu_0(\mathbf{H} + \mathbf{M}),$$

where $\mathbf{M}$ is compactly supported, we get

$$W = \int_{\mathbf{B}=\mathbf{B}_r}^{\mathbf{B}} \int_{\mathbb{R}^3} \left(\mu_0^{-1}\mathbf{B} - \mathbf{M} \right) d\mathbf{x} \cdot d\mathbf{B}$$

$$= \int_{\mathbb{R}^3} \int_{\mathbf{B}=\mathbf{B}_r}^{\mathbf{B}} \mu_0^{-1}\mathbf{B} \cdot d\mathbf{B} \, d\mathbf{x} - \int_{\mathbb{R}^3} \int_{\mathbf{B}=\mathbf{B}_r}^{\mathbf{B}} \mathbf{M} \cdot d\mathbf{B} \, d\mathbf{x}$$

$$= \frac{\mu_0^{-1}}{2} \int_{\mathbb{R}^3} \left(\|\mathbf{B}\|^2 - \|\mathbf{B}_r\|^2 \right) d\mathbf{x} - \int_{\mathbb{R}^3} \mathbf{M} \cdot \left(\mathbf{B} - \mathbf{B}_r \right) d\mathbf{x}.$$

Choosing $\mathbf{B}_r = 0$ gives us the energy expression which matches with the expression reported in literature [7, 40, 51]. A similar integration of the co-energy expression gives

$$U = \int_{\mathbf{H}=\mathbf{H}_r}^{\mathbf{H}} \int_{\mathbb{R}^3} \mu_0 \left(\mathbf{H} + \mathbf{M} \right) d\mathbf{x} \cdot d\mathbf{H}$$

195

$$\int\limits_{\mathbf{H}=\mathbf{H}_r}^{\mathbf{H}} \int\limits_{\mathbb{R}^3} \mu_0 \mathbf{H} \, d\mathbf{x} \cdot d\mathbf{H} + \int\limits_{\mathbf{H}=\mathbf{H}_r}^{\mathbf{H}} \int\limits_{\mathbb{R}^3} \mu_0 \mathbf{M} \, d\mathbf{x} \cdot d\mathbf{H}$$

$$= \frac{\mu_0}{2} \int\limits_{\mathbb{R}^3} \left(\|\mathbf{H}\|^2 - \|\mathbf{H}_r\|^2 \right) d\mathbf{x} + \mu_0 \int\limits_{\mathbb{R}^3} \mathbf{M} \cdot \left(\mathbf{H} - \mathbf{H}_r \right) d\mathbf{x}.$$

Choosing $\mathbf{H}_r = 0$ gives us another familiar expression [40], where the authors also report two other expressions for energy and co-energy using different integration limits $\mathbf{B}_r$ and $\mathbf{H}_r$. Thus, we will consider the shape derivatives for the two energy shape functionals $\mathcal{E}_F, \mathcal{E}_F'$ and two co-energy shape functionals $\mathcal{J}_F$ and $\mathcal{J}_F'$, which are given as

$$\mathcal{E}_F := \frac{\mu_0^{-1}}{2} \int\limits_{\mathbb{R}^3} \|\mathbf{B}\|^2 \, d\mathbf{x}, \tag{5.4.2}$$

$$\mathcal{E}_F' := \frac{\mu_0^{-1}}{2} \int\limits_{\mathbb{R}^3} \|\mathbf{B}\|^2 \, d\mathbf{x} - \int\limits_{\mathbb{R}^3} \mathbf{B} \cdot \mathbf{M} \, d\mathbf{x}, \tag{5.4.3}$$

$$\mathcal{J}_F' := \frac{\mu_0}{2} \int\limits_{\mathbb{R}^3} \|\mathbf{H}\|^2 \, d\mathbf{x}, \tag{5.4.4}$$

$$\mathcal{J}_F := \frac{\mu_0}{2} \int\limits_{\mathbb{R}^3} \|\mathbf{H}\|^2 \, d\mathbf{x} + \mu_0 \int\limits_{\mathbb{R}^3} \mathbf{H} \cdot \mathbf{M} \, d\mathbf{x}. \tag{5.4.5}$$

Using the material law we can easily see the relations

$$\mathcal{J}_F' = \mathcal{E}_F' + \frac{\mu_0}{2} \int\limits_{\Omega} \|\mathbf{M}\|^2 \, d\mathbf{x}, \quad \mathcal{J}_F = \mathcal{E}_F - \frac{\mu_0}{2} \int\limits_{\Omega} \|\mathbf{M}\|^2 \, d\mathbf{x}. \tag{5.4.6}$$

Remark 11. We use these four different expressions because it is unclear what is the right one to use for the case of a permanent magnet. We simply compute the shape derivatives for these expressions and determine which ones make physical sense.

5.4.2 Vector Potential Formulation

Based on $\mathrm{div}\, \mathbf{B} = 0$ we express the magnetic flux as $\mathbf{B} = \mathbf{curl}\mathbf{A}$. Using the material law (5.4.1), we get

$$\mathbf{curl}\mathbf{A} = \mu_0(\mathbf{H} + \mathbf{M}) \quad \text{in } \Omega, \quad \mathbf{curl}\mathbf{A} = \mu_0 \mathbf{H} \quad \text{in } \Omega_c.$$

Combining this with the equation for $\mathbf{H}$ gives us

$$\mu_0^{-1}\mathbf{curl}\mathbf{curl}\mathbf{A} = \mathbf{curl}\mathbf{M} \quad \text{in } \Omega,$$
$$\mu_0^{-1}\mathbf{curl}\mathbf{curl}\mathbf{A} = \mathbf{J} \qquad \text{in } \Omega_c.$$

The vector potential satisfies the transmission conditions

$$[\![\mathbf{H}]\!]_\Gamma \times \mathbf{n} = 0 \implies \mu_0^{-1} [\![\gamma_\mathbf{M}\mathbf{A}]\!]_\Gamma = -\mathbf{M} \times \mathbf{n}.$$

196

By setting the jump of Dirichlet trace of $\mathbf{A}$ to zero, we get

$$[\![\gamma_{\mathbf{t}}\mathbf{A}]\!]_\Gamma = 0 \implies [\![\mathbf{curl}_\Gamma\,\gamma_{\mathbf{t}}\mathbf{A}]\!]_\Gamma = 0 \implies [\![\mathbf{curl}\mathbf{A}]\!]_\Gamma \cdot \mathbf{n} = 0 \implies [\![\mathbf{B}]\!]_\Gamma \cdot \mathbf{n} = 0.$$

Thus we have the transmission problem

$$\begin{aligned}
\mu_0^{-1}\mathbf{curl}\mathbf{curl}\mathbf{A} &= \mathbf{curl}\mathbf{M} && \text{in } \Omega, \\
\mu_0^{-1}\mathbf{curl}\mathbf{curl}\mathbf{A} &= \mathbf{J} && \text{in } \Omega_c, \\
[\![\gamma_{\mathbf{t}}\mathbf{A}]\!]_\Gamma &= 0 && \text{on } \Gamma, \\
\mu_0^{-1}[\![\gamma_{\mathbf{M}}\mathbf{A}]\!]_\Gamma &= -\mathbf{M} \times \mathbf{n} && \text{on } \Gamma, \\
\|\mathbf{A}(\mathbf{x})\| &= O(\|\mathbf{x}\|^{-1}) && \text{for } \|\mathbf{x}\| \to \infty.
\end{aligned} \tag{5.4.7}$$

To ensure uniqueness of the above problem, we enforce the Coulomb gauge, that is $\operatorname{div}\mathbf{A} = 0$ in $\Omega \cup \Omega_c$ and $[\![\mathbf{A}]\!]_\Gamma \cdot \mathbf{n} = 0$ on Γ.

5.4.2.1 Shape Derivative From Volume Based Variational Formulation

We define the following function space for physical vector potential solutions in $\mathbb{R}^3$ [33]

$$\mathbf{V}(\mathbb{R}^3) := \left\{ \mathbf{u} \in \mathcal{D}(\mathbb{R}^3)',\ \frac{\mathbf{u}(\mathbf{x})}{\sqrt{1+\|\mathbf{x}\|^2}} \in \mathbf{L}^2(\mathbb{R}^3),\ \mathbf{curl}\mathbf{u} \in \mathbf{L}^2(\mathbb{R}^3),\ \operatorname{div}\mathbf{u} = 0 \text{ in } \mathbb{R}^3 \right\}.$$

The transmission problem (5.4.7) has a weak solution $\mathbf{A}$ which solves the variational problem: seek $\mathbf{A} \in \mathbf{V}(\mathbb{R}^3)$ such that

$$\int_{\mathbb{R}^3} \mu_0^{-1}\,\mathbf{curl}\mathbf{A}\cdot\mathbf{curl}\mathbf{A}'\,d\mathbf{x} = \int_\Gamma (\mathbf{M}\times\mathbf{n})\cdot\mathbf{A}'\,dS + \int_\Omega \mathbf{curl}\mathbf{M}\cdot\mathbf{A}'\,d\mathbf{x} + \int_{\Omega_{\text{src}}} \mathbf{J}\cdot\mathbf{A}'\,d\mathbf{x} \quad \forall \mathbf{A}' \in \mathbf{V}(\mathbb{R}^3).$$

$$\tag{5.4.8}$$

The field energy $\mathcal{E}_F$ can be expressed in terms of the bilinear form as

$$\mathcal{E}_F = \frac{1}{2}\int_{\mathbb{R}^3} \mu_0^{-1}\,\|\mathbf{curl}\mathbf{A}(\mathbf{x})\|^2\,d\mathbf{x}.$$

Notice that it is also equal to half of the linear form in (5.4.8) with $\mathbf{A}' = \mathbf{A}$. We will also compute the shape derivative for

$$\begin{aligned}
\mathcal{E}_F' &= \frac{1}{2}\int_{\mathbb{R}^3} \mu_0^{-1}\,\|\mathbf{curl}\mathbf{A}(\mathbf{x})\|^2\,d\mathbf{x} - \int_\Omega \mathbf{curl}\mathbf{A}(\mathbf{x}) \cdot \mathbf{M}\,d\mathbf{x} \\
&= -\frac{1}{2}\int_\Gamma (\mathbf{M}\times\mathbf{n})\cdot\mathbf{A}\,dS - \frac{1}{2}\int_\Omega \mathbf{curl}\mathbf{M}\cdot\mathbf{A}\,d\mathbf{x} + \frac{1}{2}\int_{\Omega_{\text{src}}} \mathbf{J}\cdot\mathbf{A}'\,d\mathbf{x}. \tag{5.4.9}
\end{aligned}$$

5.4.2.2 Variational Formulation on Deformed Domain

The velocity field $\boldsymbol{\mathcal{V}}$ doesn't affect the source current and deforms only the magnet, whose magnetization is transformed like a 1-form to $\mathbf{M}_s$ such that $\mathbf{M}_s(\mathbf{T}_s^{\boldsymbol{\nu}}(\hat{\mathbf{x}})) := \mathsf{D}\mathbf{T}_s^{\boldsymbol{\nu}}(\hat{\mathbf{x}})^{-T}\,\mathbf{M}(\hat{\mathbf{x}})$. The variational formulation for the deformed s-configuration reads: seek $\mathbf{A}_s \in \boldsymbol{V}(\mathbb{R}^3)$ such that

$$\mathsf{b}(s)(\mathbf{A}_s, \mathbf{A}') = \ell(s)(\mathbf{A}') \quad \mathbf{A}' \in \boldsymbol{V}(\mathbb{R}^3),$$

where the (bi)linear forms are defined as

$$\mathsf{b}(s)(\mathbf{A}, \mathbf{A}') := \int_{\mathbb{R}^3} \mu_0^{-1}\, \mathbf{curl}\mathbf{A} \cdot \mathbf{curl}\mathbf{A}'\, d\mathbf{x},$$

$$\ell(s)(\mathbf{A}') := \ell_1(s)(\mathbf{A}') + \ell_2(s)(\mathbf{A}') + \ell_3(s)(\mathbf{A}'),$$

$$\ell_1(s)(\mathbf{A}') := \int_{\Gamma^s} (\mathbf{M}_s \times \mathbf{n}) \cdot \mathbf{A}'\, dS,$$

$$\ell_2(s)(\mathbf{A}') := \int_{\Omega^s} \mathbf{curl}\mathbf{M}_s \cdot \mathbf{A}'\, d\mathbf{x},$$

$$\ell_3(s)(\mathbf{A}') := \int_{\Omega_{\mathrm{src}}} \mathbf{J} \cdot \mathbf{A}'\, d\mathbf{x}.$$

The integrals are transformed using the perturbation map to get

$$\mathsf{b}(s)(\mathbf{A}, \mathbf{A}') = \int_{\mathbb{R}^3} \mu_0^{-1}\, \mathbf{curl}\mathbf{A} \cdot \mathbf{curl}\mathbf{A}'\, d\mathbf{x}$$

$$= \int_{\mathbb{R}^3} \mu_0^{-1}\, \mathbf{curl}\mathbf{A}(\mathbf{T}_s^{\boldsymbol{\nu}}(\hat{\mathbf{x}})) \cdot \mathbf{curl}\mathbf{A}'(\mathbf{T}_s^{\boldsymbol{\nu}}(\hat{\mathbf{x}}))\, \det \mathsf{D}\mathbf{T}_s^{\boldsymbol{\nu}}(\hat{\mathbf{x}})\, d\hat{\mathbf{x}},$$

$$\ell_1(s)(\mathbf{A}') = \int_{\Gamma^s} (\mathbf{M}_s \times \mathbf{n}) \cdot \mathbf{A}'\, dS$$

$$= \int_{\Gamma^0} \left(\mathbf{M}_s(\mathbf{T}_s^{\boldsymbol{\nu}}(\hat{\mathbf{x}})) \times \frac{\mathcal{C}(\mathsf{D}\mathbf{T}_s^{\boldsymbol{\nu}}(\hat{\mathbf{x}}))\, \hat{\mathbf{n}}(\mathbf{x})}{\omega_s(\hat{\mathbf{x}})} \right) \cdot \mathbf{A}'(\mathbf{T}_s^{\boldsymbol{\nu}}(\hat{\mathbf{x}}))\, \omega_s(\hat{\mathbf{x}})\, dS_{\hat{\mathbf{x}}},$$

$$\ell_2(s)(\mathbf{A}') = \int_{\Omega^s} \mathbf{curl}\mathbf{M}_s \cdot \mathbf{A}'\, d\mathbf{x}$$

$$= \int_{\Omega^0} \mathbf{curl}\mathbf{M}_s(\mathbf{T}_s^{\boldsymbol{\nu}}(\hat{\mathbf{x}})) \cdot \mathbf{A}'(\mathbf{T}_s^{\boldsymbol{\nu}}(\hat{\mathbf{x}}))\, \det \mathsf{D}\mathbf{T}_s^{\boldsymbol{\nu}}(\hat{\mathbf{x}})\, d\hat{\mathbf{x}},$$

$$\ell_3(s)(\mathbf{A}') = \int_{\Omega_{\mathrm{src}}} \mathbf{J} \cdot \mathbf{A}'\, d\mathbf{x}.$$

The vector potential $\mathbf{A}$ and the magnetization $\mathbf{M}$ are 1-forms. We use the following pullback for 1-forms and their **curl**

$$\mathbf{A}(\mathbf{T}_s^{\boldsymbol{\nu}}(\hat{\mathbf{x}})) = \mathsf{D}\mathbf{T}_s^{\boldsymbol{\nu}}(\hat{\mathbf{x}})^{-T}\, \hat{\mathbf{A}}(\hat{\mathbf{x}}), \qquad\qquad \mathbf{M}_s(\mathbf{T}_s^{\boldsymbol{\nu}}(\hat{\mathbf{x}})) = \mathsf{D}\mathbf{T}_s^{\boldsymbol{\nu}}(\hat{\mathbf{x}})^{-T}\, \mathbf{M}(\hat{\mathbf{x}}),$$

$$\mathbf{curlA}(\mathbf{T}_s^{\nu}(\hat{\mathbf{x}})) = \frac{\mathsf{D}\mathbf{T}_s^{\nu}(\hat{\mathbf{x}})}{\det \mathsf{D}\mathbf{T}_s^{\nu}(\hat{\mathbf{x}})}\, \mathbf{curl}\hat{\mathbf{A}}(\hat{\mathbf{x}}), \qquad \mathbf{curlM}_s(\mathbf{T}_s^{\nu}(\hat{\mathbf{x}})) = \frac{\mathsf{D}\mathbf{T}_s^{\nu}(\hat{\mathbf{x}})}{\det \mathsf{D}\mathbf{T}_s^{\nu}(\hat{\mathbf{x}})}\, \mathbf{curl}\hat{\mathbf{M}}(\hat{\mathbf{x}}).$$

Using the pullbacks we define the pulled-back hat (bi)linear forms

$$\hat{\mathsf{b}}(s; \hat{\mathbf{A}}, \hat{\mathbf{A}}') := \int_{\mathbb{R}^3} \mu_0^{-1} \left(\mathsf{D}\mathbf{T}_s^{\nu}(\hat{\mathbf{x}})\, \mathbf{curl}\hat{\mathbf{A}}(\hat{\mathbf{x}}) \right) \cdot \left(\mathsf{D}\mathbf{T}_s^{\nu}(\hat{\mathbf{x}})\, \mathbf{curl}\hat{\mathbf{A}}'(\hat{\mathbf{x}}) \right) \frac{1}{|\det \mathsf{D}\mathbf{T}_s^{\nu}(\hat{\mathbf{x}})|}\, d\hat{\mathbf{x}},$$

$$\hat{\ell}_1(s; \hat{\mathbf{A}}') := \int_{\Gamma^0} (\hat{\mathbf{M}} \times \hat{\mathbf{n}}) \cdot \hat{\mathbf{A}}'\, dS,$$

$$\hat{\ell}_2(s; \hat{\mathbf{A}}') := \int_{\Omega^0} \mathbf{curl}\hat{\mathbf{M}} \cdot \hat{\mathbf{A}}'\, d\mathbf{x},$$

$$\hat{\ell}_3(s; \hat{\mathbf{A}}') := \int_{\Omega_{\mathrm{src}}} \mathbf{J} \cdot \hat{\mathbf{A}}'\, d\mathbf{x}.$$

The pulled back variational formulation is then given as: seek $\hat{\mathbf{A}}_s \in V_0 := \mathbf{V}(\mathbb{R}^3)$ such that

$$\hat{\mathsf{b}}(s; \hat{\mathbf{A}}_s, \hat{\mathbf{A}}') = \hat{\ell}(s; \hat{\mathbf{A}}') \quad \forall \hat{\mathbf{A}}' \in V_0,$$

where

$$\hat{\ell}(s; \hat{\mathbf{A}}') := \hat{\ell}_1(s; \hat{\mathbf{A}}') + \hat{\ell}_2(s; \hat{\mathbf{A}}') + \hat{\ell}_3(s; \hat{\mathbf{A}}').$$

The energy $\mathcal{E}_F$ for the deformed s-configuration can be written as

$$\mathcal{E}_F(s) = \frac{1}{2}\hat{\mathsf{b}}(s; \hat{\mathbf{A}}_s, \hat{\mathbf{A}}_s).$$

5.4.2.3 Adjoint Method

To compute the shape derivative using the adjoint method, we start by defining the Lagrangian $\mathcal{L} : \mathbb{R} \times V_0 \times V_0 \to \mathbb{R}$,

$$\mathcal{L}(s; \hat{\mathbf{A}}, \hat{\mathbf{A}}') := \hat{\mathsf{b}}(s; \hat{\mathbf{A}}, \hat{\mathbf{A}}') - \hat{\ell}(s; \hat{\mathbf{A}}') + \frac{1}{2}\hat{\mathsf{b}}(s; \hat{\mathbf{A}}, \hat{\mathbf{A}}).$$

Plugging in the state solution gives

$$\mathcal{E}_F(s) = \mathcal{L}(s; \hat{\mathbf{A}}_s, \hat{\mathbf{A}}') \quad \hat{\mathbf{A}} \in V_0.$$

The energy shape derivative is then computed as

$$\frac{d\mathcal{E}_F}{ds}(0) = \frac{\partial \mathcal{L}}{\partial s}(0; \hat{\mathbf{A}}_0, \hat{\mathbf{P}}),$$

where $\hat{\mathbf{P}} \in V_0$ solves the adjoint equation

$$\left\langle \frac{\partial \mathcal{L}}{\partial \hat{\mathbf{A}}}(0; \hat{\mathbf{A}}_0, \hat{\mathbf{P}}); \hat{\mathbf{A}}' \right\rangle = 0 \quad \forall \hat{\mathbf{A}}' \in V_0.$$

The above expression simplifies to

$$\hat{\mathsf{b}}(0; \hat{\mathbf{P}}, \hat{\mathbf{A}}') + \hat{\mathsf{b}}(0; \hat{\mathbf{A}}_0, \hat{\mathbf{A}}') = 0 \quad \forall \hat{\mathbf{A}}' \in V_0,$$

which yields the adjoint solution as

$$\hat{\mathbf{P}} = -\hat{\mathbf{A}}_0.$$

The energy shape derivative is given as

$$\frac{d\mathcal{E}_F}{ds}(0) = \frac{\partial \mathcal{L}}{\partial s}(0; \hat{\mathbf{A}}_0, \hat{\mathbf{P}}) = -\frac{1}{2}\frac{\partial \hat{\mathsf{b}}}{\partial s}(0; \hat{\mathbf{A}}_0, \hat{\mathbf{A}}_0). \tag{5.4.10}$$

Note this is same as the expression Equation (5.1.43) derived in the transmission problem case which is computed using the identities in (3.0.11). It can be simplified further to get

$$\frac{d\mathcal{E}_F}{ds}(0) = -\frac{\mu_0^{-1}}{2} \int_{\mathbb{R}^3} \left\{ \mathbf{B}^T(\mathsf{D}\boldsymbol{\mathcal{V}} + \mathsf{D}\boldsymbol{\mathcal{V}}^T)\, \mathbf{B} - \|\mathbf{B}\|^2\, \nabla \cdot \boldsymbol{\mathcal{V}} \right\} d\mathbf{x}$$

$$= -\frac{\mu_0^{-1}}{2} \left(\int_{\Omega} \left\{ \mathbf{B}^T(\mathsf{D}\boldsymbol{\mathcal{V}} + \mathsf{D}\boldsymbol{\mathcal{V}}^T)\, \mathbf{B} - \|\mathbf{B}\|^2\, \nabla \cdot \boldsymbol{\mathcal{V}} \right\} d\mathbf{x} \right.$$

$$\left. + \int_{\Omega_c} \left\{ \mathbf{B}^T(\mathsf{D}\boldsymbol{\mathcal{V}} + \mathsf{D}\boldsymbol{\mathcal{V}}^T)\, \mathbf{B} - \|\mathbf{B}\|^2\, \nabla \cdot \boldsymbol{\mathcal{V}} \right\} d\mathbf{x} \right)$$

$$= \int_{\Omega} \boldsymbol{\mathcal{V}} \cdot \left(\mathbf{curl}\mathbf{M} \times \mathbf{B} \right) d\mathbf{x} + \mu_0^{-1} \int_{\Gamma} \boldsymbol{\mathcal{V}}^T \left[\!\!\left[\overset{\leftrightarrow}{\mathbf{T}}\, \mathbf{n} \right]\!\!\right]_{\Gamma} dS \tag{5.4.11}$$

where

$$\overset{\leftrightarrow}{\mathbf{T}}(\mathbf{B}) = \left(\mathbf{B}\,\mathbf{B}^T - \frac{\mathbf{Id}}{2}\,\|\mathbf{B}\|^2 \right).$$

By writing out the jump of the stress tensor using the transmission conditions, we finally get the equivalent current model which is known in literature [29, Example 2, Section 5], [39, Section 2.A], [45, Section 2.A], [56, Equation 6], [60, Section 2.1]

$$\frac{d\mathcal{E}_F}{ds}(0) = \int_{\Omega} \boldsymbol{\mathcal{V}} \cdot \left(\mathbf{curl}\mathbf{M} \times \mathbf{B} \right) d\mathbf{x} + \int_{\Gamma} \left((\mathbf{M} \times \mathbf{n}) \times \{\mathbf{B}\} \right) \cdot \boldsymbol{\mathcal{V}}\, dS. \tag{5.4.12}$$

For computing the total force $\mathbf{F}$, we plug constant velocity fields into (5.4.11). They can be taken out of the integral and we can write the vectorial form of the total force

$$\mathbf{F} = \int_{\Omega} \mathbf{curl}\mathbf{M} \times \mathbf{B}\, d\mathbf{x} + \mu_0^{-1} \int_{\Gamma} \left[\!\!\left[\overset{\leftrightarrow}{\mathbf{T}}\, \mathbf{n} \right]\!\!\right]_{\Gamma} dS \tag{5.4.13}$$

$$= \int_{\Omega} \mathbf{curl}\mathbf{M} \times \mathbf{B}\, d\mathbf{x} + \int_{\Gamma} (\mathbf{M} \times \mathbf{n}) \times \{\mathbf{B}\}\, dS. \tag{5.4.14}$$

Using (5.1.23), (5.1.44) and div $\mathbf{B} = 0$, we notice that

$$\nabla \cdot \overleftrightarrow{\mathbf{T}} = \mathrm{D}\mathbf{B}\,\mathbf{B} - \nabla\mathbf{B}\,\mathbf{B} = \mathbf{curlB} \times \mathbf{B}. \tag{5.4.15}$$

Inside Ω the material law gives us $\mathbf{curlB} = \mu_0\,\mathbf{curlM}$. Thus we can write (5.4.13) as

$$\mathbf{F} = \int_\Omega \mathbf{curlM} \times \mathbf{B}\,d\mathbf{x} + \mu_0^{-1} \int_\Gamma \left[\!\left[\overleftrightarrow{\mathbf{T}}\,\mathbf{n} \right]\!\right]_\Gamma dS. \tag{5.4.16}$$

$$= \mu_0^{-1} \int_\Omega \nabla \cdot \overleftrightarrow{\mathbf{T}}\,d\mathbf{x} + \mu_0^{-1} \int_\Gamma \left[\!\left[\overleftrightarrow{\mathbf{T}}\,\mathbf{n} \right]\!\right]_\Gamma dS. \tag{5.4.17}$$

Using the divergence theorem, we can write the expression purely in terms of the stress tensor from the outside $\overleftrightarrow{\mathbf{T}}^+$. We get

$$\mathbf{F} = \mu_0^{-1} \int_\Gamma \overleftrightarrow{\mathbf{T}}^+\,\mathbf{n}\,dS. \tag{5.4.18}$$

Now imagine a domain $\Omega_m \Subset \mathbb{R}^3$ such that $\Omega \Subset \Omega_m$. It is clear that $\operatorname{div} \overleftrightarrow{\mathbf{T}} = 0$ inside $\Omega_m \setminus \overline{\Omega}$ since there is no magnet or source current there. Integrating $\nabla \cdot \overleftrightarrow{\mathbf{T}}$ on this domain and using the divergence theorem gives us the result

$$\mathbf{F} = \int_\Omega \mathbf{curlM} \times \mathbf{B}\,d\mathbf{x} + \int_\Gamma (\mathbf{M} \times \mathbf{n}) \times \{\mathbf{B}\}\,dS = \mu_0^{-1} \int_\Gamma \overleftrightarrow{\mathbf{T}}^+\mathbf{n}\,dS = \mu_0^{-1} \int_{\partial\Omega_m} \overleftrightarrow{\mathbf{T}}^+\mathbf{n}\,dS. \tag{5.4.19}$$

Note that the above holds true for any arbitrary surface which doesn't intersect Ω and Ω_{src}.

Now we compute the shape derivative for $\mathcal{E}'_F$. From Equation (5.4.9) we see that it can be expressed in terms of the linear form. Thus, for the deformed configuration, we have

$$\mathcal{E}'_F(s) = -\frac{1}{2}\hat{\ell}_1(s; \hat{\mathbf{A}}_s) - \frac{1}{2}\hat{\ell}_2(s; \hat{\mathbf{A}}_s) + \frac{1}{2}\hat{\ell}_3(s; \hat{\mathbf{A}}_s).$$

Using the adjoint method again, we define the Lagrangian $\mathcal{L}' : \mathbb{R} \times V_0 \times V_0 \to \mathbb{R}$,

$$\mathcal{L}'(s; \hat{\mathbf{A}}, \hat{\mathbf{A}}') := \hat{\mathsf{b}}(s; \hat{\mathbf{A}}, \hat{\mathbf{A}}') - \hat{\ell}(s; \hat{\mathbf{A}}') - \frac{1}{2}\hat{\ell}_1(s; \hat{\mathbf{A}}) - \frac{1}{2}\hat{\ell}_2(s; \hat{\mathbf{A}}) + \frac{1}{2}\hat{\ell}_3(s; \hat{\mathbf{A}}).$$

Plugging in the pulled back state solution gives us

$$\mathcal{E}'_F(s) = \mathcal{L}'(s; \hat{\mathbf{A}}_s, \hat{\mathbf{A}}') \quad \forall \hat{\mathbf{A}}' \in V_0.$$

The shape derivative can be computed as

$$\frac{d\mathcal{E}'_F}{ds}(0) = \frac{\partial\mathcal{L}'}{\partial s}(0; \hat{\mathbf{A}}_0, \hat{\mathbf{P}}'),$$

where $\mathbf{P}' \in V_0$ solves the adjoint equation

$$\frac{\partial \mathcal{L}'}{\partial \hat{\mathbf{A}}}(0; \hat{\mathbf{A}}_0; \hat{\mathbf{P}}')(\hat{\mathbf{A}}') = 0 \quad \forall \hat{\mathbf{A}}' \in V_0.$$

The expression above simplifies to

$$\hat{\mathsf{b}}(0; \hat{\mathbf{A}}', \hat{\mathbf{P}}') = \frac{1}{2}\hat{\ell}_1(0; \hat{\mathbf{A}}') + \frac{1}{2}\hat{\ell}_2(0; \hat{\mathbf{A}}') - \frac{1}{2}\hat{\ell}_3(0; \hat{\mathbf{A}}') \quad \forall \hat{\mathbf{A}}' \in V_0.$$

We notice that the state solution $\hat{\mathbf{A}}_0 \in V_0$ solves the state equation

$$\hat{\mathsf{b}}(0; \hat{\mathbf{A}}_0, \hat{\mathbf{A}}') = \hat{\ell}_1(0; \hat{\mathbf{A}}') + \hat{\ell}_2(0; \hat{\mathbf{A}}') + \hat{\ell}_3(0; \hat{\mathbf{A}}') \quad \forall \hat{\mathbf{A}}' \in V_0.$$

To obtain the adjoint solution explicitly, we consider the state solution to be the sum $\hat{\mathbf{A}}_0 = \mathbf{A_M} + \mathbf{A_J}$, where the components solve the variational problems

$$\hat{\mathsf{b}}(0; \hat{\mathbf{A}}_{\mathbf{M}}, \hat{\mathbf{A}}') = \hat{\ell}_1(0; \hat{\mathbf{A}}') + \hat{\ell}_2(0; \hat{\mathbf{A}}') \qquad \forall \hat{\mathbf{A}}' \in V_0,$$
$$\hat{\mathsf{b}}(0; \hat{\mathbf{A}}_{\mathbf{J}}, \hat{\mathbf{A}}') = \hat{\ell}_3(0; \hat{\mathbf{A}}') \qquad \forall \hat{\mathbf{A}}' \in V_0.$$

The solution $\mathbf{A_J}$ is the vector potential for the magnetic flux density corresponding to zero magnetization $\mathbf{M}$, whereas $\mathbf{A_M}$ is the vector potential for the magnetic flux density for zero source current $\mathbf{J}$. Based on this the adjoint solution can be expressed as

$$\hat{\mathbf{P}}' = \frac{\mathbf{A_M} - \mathbf{A_J}}{2}.$$

The shape derivative is then given as

$$\frac{d\mathcal{E}_F'}{ds}(0) = \frac{\partial \mathcal{L}'}{\partial s}(0; \hat{\mathbf{A}}_0, \hat{\mathbf{P}}') = \frac{\partial \hat{\mathsf{b}}}{\partial s}(0; \hat{\mathbf{A}}_0, \hat{\mathbf{P}}')$$

$$= \frac{1}{2}\frac{\partial \hat{\mathsf{b}}}{\partial s}(0; \mathbf{A_M} + \mathbf{A_J}, \mathbf{A_M} - \mathbf{A_J}) = \frac{1}{2}\frac{\partial \hat{\mathsf{b}}}{\partial s}(0; \mathbf{A_M}, \mathbf{A_M}) - \frac{1}{2}\frac{\partial \hat{\mathsf{b}}}{\partial s}(0; \mathbf{A_J}, \mathbf{A_J})$$

$$= \frac{1}{2}\int_{\Omega} \mu_0^{-1} \left\{ \mathbf{B_M}^T \left(\mathsf{D}\boldsymbol{\mathcal{V}} + \mathsf{D}\boldsymbol{\mathcal{V}}^T\right) \mathbf{B_M} - \|\mathbf{B_M}\|^2 \ \nabla \cdot \boldsymbol{\mathcal{V}} \right\} d\mathbf{x}$$

$$+ \frac{1}{2}\int_{\Omega_c} \mu_0^{-1} \left\{ \mathbf{B_M}^T \left(\mathsf{D}\boldsymbol{\mathcal{V}} + \mathsf{D}\boldsymbol{\mathcal{V}}^T\right) \mathbf{B_M} - \|\mathbf{B_M}\|^2 \ \nabla \cdot \boldsymbol{\mathcal{V}} \right\} d\mathbf{x}$$

$$- \frac{1}{2}\int_{\Omega} \mu_0^{-1} \left\{ \mathbf{B_J}^T \left(\mathsf{D}\boldsymbol{\mathcal{V}} + \mathsf{D}\boldsymbol{\mathcal{V}}^T\right) \mathbf{B_J} - \|\mathbf{B_J}\|^2 \ \nabla \cdot \boldsymbol{\mathcal{V}} \right\} d\mathbf{x}$$

$$- \frac{1}{2}\int_{\Omega_c} \mu_0^{-1} \left\{ \mathbf{B_J}^T \left(\mathsf{D}\boldsymbol{\mathcal{V}} + \mathsf{D}\boldsymbol{\mathcal{V}}^T\right) \mathbf{B_J} - \|\mathbf{B_J}\|^2 \ \nabla \cdot \boldsymbol{\mathcal{V}} \right\} d\mathbf{x}.$$

It can be simplified further to get

$$= \mu_0^{-1}\int_{\Omega} \mathrm{div}\left(\left\{ \mathbf{B_M} \ \mathbf{B_M}^T - \frac{\mathsf{Id}}{2}\|\mathbf{B_M}\|^2 \right\}\boldsymbol{\mathcal{V}} \right) + \boldsymbol{\mathcal{V}} \cdot \left(\mathbf{B_M} \times \mathbf{curl B_M} \right) d\mathbf{x}$$

$$+ \mu_0^{-1} \int_{\Omega_c} \mathrm{div} \left(\left\{ \mathbf{B_M} \, \mathbf{B_M}^T - \frac{\mathsf{Id}}{2} \| \mathbf{B_M} \|^2 \right\} \boldsymbol{\mathcal{V}} \right) + \boldsymbol{\mathcal{V}} \cdot \left(\mathbf{B_M} \times \mathbf{curl B_M} \right) d\mathbf{x}$$

$$- \mu_0^{-1} \int_{\Omega} \mathrm{div} \left(\left\{ \mathbf{B_J} \, \mathbf{B_J}^T - \frac{\mathsf{Id}}{2} \| \mathbf{B_J} \|^2 \right\} \boldsymbol{\mathcal{V}} \right) + \boldsymbol{\mathcal{V}} \cdot \left(\mathbf{B_J} \times \mathbf{curl B_J} \right) d\mathbf{x}$$

$$- \mu_0^{-1} \int_{\Omega_c} \mathrm{div} \left(\left\{ \mathbf{B_J} \, \mathbf{B_J}^T - \frac{\mathsf{Id}}{2} \| \mathbf{B_J} \|^2 \right\} \boldsymbol{\mathcal{V}} \right) + \boldsymbol{\mathcal{V}} \cdot \left(\mathbf{B_J} \times \mathbf{curl B_J} \right) d\mathbf{x}$$

$$= \mu_0^{-1} \int_{\Omega} \mathrm{div} \left(\left\{ \mathbf{B_M} \, \mathbf{B_M}^T - \frac{\mathsf{Id}}{2} \| \mathbf{B_M} \|^2 \right\} \boldsymbol{\mathcal{V}} \right) d\mathbf{x} + \int_{\Omega} \boldsymbol{\mathcal{V}} \cdot \left(\mathbf{B_M} \times \mathbf{curl M} \right) d\mathbf{x}$$

$$+ \mu_0^{-1} \int_{\Omega_c} \mathrm{div} \left(\left\{ \mathbf{B_M} \, \mathbf{B_M}^T - \frac{\mathsf{Id}}{2} \| \mathbf{B_M} \|^2 \right\} \boldsymbol{\mathcal{V}} \right) d\mathbf{x}$$

$$- \mu_0^{-1} \int_{\Omega} \mathrm{div} \left(\left\{ \mathbf{B_J} \, \mathbf{B_J}^T - \frac{\mathsf{Id}}{2} \| \mathbf{B_J} \|^2 \right\} \boldsymbol{\mathcal{V}} \right) d\mathbf{x}$$

$$- \mu_0^{-1} \int_{\Omega_c} \mathrm{div} \left(\left\{ \mathbf{B_J} \, \mathbf{B_J}^T - \frac{\mathsf{Id}}{2} \| \mathbf{B_J} \|^2 \right\} \boldsymbol{\mathcal{V}} \right) d\mathbf{x}.$$

Jump of the stress tensor corresponding to $\mathbf{B_J}$ is zero since it arises for the case $\mathbf{M} = 0$ and the permeability is μ_0 everywhere. As we saw in the simplification for the shape derivative of $\mathcal{E}_F$, jump of the stress tensor with $\mathbf{B}_M$ gives the surface part of the equivalent current model. Thus we are left with

$$\frac{d\mathcal{E}_F'}{ds}(0) = \int_{\Gamma} \left(\{\mathbf{B_M}\}_\Gamma \times (\mathbf{M} \times \mathbf{n}) \right) \cdot \boldsymbol{\mathcal{V}} \, d\mathrm{S} + \int_{\Omega} \boldsymbol{\mathcal{V}} \cdot \left(\mathbf{B_M} \times \mathbf{curl M} \right) d\mathbf{x}. \tag{5.4.20}$$

The peculiar thing about the above expression is that it completely ignores the existence of the source current, since $\mathbf{B_M}$ is the magnetic field in absence of the source current. Using the shape derivatives of $\mathcal{E}_F$ and $\mathcal{E}_F'$, we can easily compute the shape derivatives for $\mathcal{J}_F$ and $\mathcal{J}_F'$ using the relations (5.4.6). We just need to compute the shape derivative of

$$\frac{\mu_0}{2} \int_{\Omega^s} \| \mathbf{M}_s \|^2 \, d\mathbf{x}.$$

For the vector potential case where $\mathbf{M}$ transforms as a 1-form, we get the following shape derivative

$$\frac{d}{ds} \left(\frac{\mu_0}{2} \int_{\Omega^s} \| \mathbf{M}_s \|^2 \, d\mathbf{x} \right) \Big|_{s=0} = \frac{\mu_0}{2} \int_{\Omega^0} \left\{ - \mathbf{M}^T \left(\mathsf{D} \boldsymbol{\mathcal{V}}(\hat{\mathbf{x}}) + \mathsf{D} \boldsymbol{\mathcal{V}}(\hat{\mathbf{x}})^T \right) \mathbf{M} + \| \mathbf{M} \|^2 \, \nabla \cdot \boldsymbol{\mathcal{V}}(\hat{\mathbf{x}}) \right\} d\hat{\mathbf{x}}.$$

The shape derivatives that emerge for $\mathcal{J}_F$ and $\mathcal{J}_F'$ are summarized in Table 5.29.

5.4.2.4 A Note on "Holding the Fluxes Constant"

Inspecting the shape derivative for $\mathcal{E}_F$ in (5.4.10) we see that we can use the same arguments as in Section 5.1.2.7 to conclude that we can recover the same force distribution by performing

differentiation while holding the fluxes of the $\mathbf{B}$ field constant, that is transforming the $\mathbf{B}$ field in the reference configuration as a 2-form. We would also get the same derivative for $\mathcal{E}_F'$ if we transform $\mathbf{B}$ as a 2-form and $\mathbf{M}$ as a 1-form. This holds because the additional term in $\mathcal{E}_F'$

$$-\int_\Omega \mathbf{B} \cdot \mathbf{M}\, d\mathbf{x},$$

would not change if we transformed the $\mathbf{B}$ field in the reference configuration as a 2-form to $\mathbf{B}_s^*$ and $\mathbf{M}$ as a 1-form to $\mathbf{M}_s$. We can easily verify it by seeing

$$\int_{\Omega^s} \mathbf{B}_s^*(\mathbf{x}) \cdot \mathbf{M}_s(\mathbf{x})\, d\mathbf{x} = \int_{\Omega^0} \frac{\mathbf{DT}_s^{\boldsymbol{\nu}}(\hat{\mathbf{x}})\, \mathbf{B}(\hat{\mathbf{x}})}{\det \mathbf{DT}_s^{\boldsymbol{\nu}}(\hat{\mathbf{x}})} \cdot \left(\mathbf{DT}_s^{\boldsymbol{\nu}}(\hat{\mathbf{x}})^{-T}\, \mathbf{M}(\hat{\mathbf{x}}) \right)\, \det \mathbf{DT}_s^{\boldsymbol{\nu}}(\hat{\mathbf{x}})\, d\hat{\mathbf{x}}$$

$$= \int_{\Omega^0} \mathbf{B} \cdot \mathbf{M}\, d\hat{\mathbf{x}}.$$

This is why differentiating the expression $\mathcal{E}_F'$ while holding the fluxes constant gives the expected force distribution as seen in [20, 29]. But we can clearly see from our computation of the shape derivative for $\mathcal{E}_F'$ that we get a different result. So the relation of energy shape derivatives computed by our approach and "holding the fluxes constant" remains intact for $\mathcal{E}_F$, but breaks down for $\mathcal{E}_F'$.

5.4.2.5 Variational BIEs

We approach the transmission problem (5.4.7) using boundary integral equations. We use the BIEs given in (2.2.23)

$$\begin{bmatrix} -\mathcal{A} & \frac{\mathsf{Id}}{2} + \mathcal{C} \\ \frac{\mathsf{Id}}{2} - \mathcal{B} & \mathcal{N} \end{bmatrix} \begin{bmatrix} \gamma_{\mathbf{M}}^- \mathbf{A} \\ \gamma_{\mathbf{t}}^- \mathbf{A} \end{bmatrix} - \begin{bmatrix} \mathrm{grad}_\Gamma\, \Psi_V(\gamma_n^- \mathbf{A}) \\ 0 \end{bmatrix} = \mu_0 \begin{bmatrix} \gamma_{\mathbf{t}}^-\, \mathrm{N}(\mathbf{curlM}) \\ \gamma_{\mathbf{M}}^- \mathrm{N}(\mathbf{curlM}) \end{bmatrix}, \tag{5.4.21}$$

$$\begin{bmatrix} \mathcal{A} & \frac{\mathsf{Id}}{2} - \mathcal{C} \\ \frac{\mathsf{Id}}{2} + \mathcal{B} & -\mathcal{N} \end{bmatrix} \begin{bmatrix} \gamma_{\mathbf{M}}^+ \mathbf{A} \\ \gamma_{\mathbf{t}}^+ \mathbf{A} \end{bmatrix} + \begin{bmatrix} \mathrm{grad}_\Gamma\, \Psi_V(\gamma_n^+ \mathbf{A}) \\ 0 \end{bmatrix} = \mu_0 \begin{bmatrix} \gamma_{\mathbf{t}}^+ \mathrm{N}(\mathbf{J}) \\ \gamma_{\mathbf{M}}^+ \mathrm{N}(\mathbf{J}) \end{bmatrix}, \tag{5.4.22}$$

where

$$\mathrm{N}(\mathbf{curlM}) := \int_\Omega G(\mathbf{x}, \mathbf{y})\, \mathbf{curlM}(\mathbf{y})\, d\mathbf{y}, \quad \mathrm{N}(\mathbf{J}) := \int_{\Omega_{\mathrm{src}}} G(\mathbf{x}, \mathbf{y})\, \mathbf{J}(\mathbf{y})\, d\mathbf{y}. \tag{5.4.23}$$

We denote the exterior traces as

$$\mathbf{g} = \gamma_{\mathbf{t}}^+ \mathbf{A}, \quad \boldsymbol{\psi} = \gamma_{\mathbf{M}}^+ \mathbf{A},$$

allowing us to express the interior traces using the transmission conditions as

$$\gamma_{\mathbf{t}}^- \mathbf{A} = \mathbf{g}, \quad \gamma_{\mathbf{M}}^- \mathbf{A} = \boldsymbol{\psi} + \mu_0\, \mathbf{M} \times \mathbf{n}.$$

Plugging this notation into the (5.4.21) and (5.4.22) and flipping the signs in (5.4.21) gives

$$\begin{bmatrix} \mathcal{A} & -\frac{\mathrm{Id}}{2} - \mathcal{C} \\ -\frac{\mathrm{Id}}{2} + \mathcal{B} & -\mathcal{N} \end{bmatrix} \begin{bmatrix} \boldsymbol{\psi} + \mu_0 \, \mathbf{M} \times \mathbf{n} \\ \mathbf{g} \end{bmatrix} + \begin{bmatrix} \mathrm{grad}_\Gamma \, \Psi_V(\gamma_n^- \mathbf{A}) \\ 0 \end{bmatrix} = -\mu_0 \begin{bmatrix} \gamma_\mathbf{t}^- \mathrm{N}(\mathbf{curlM}) \\ \gamma_\mathbf{M}^- \mathrm{N}(\mathbf{curlM}) \end{bmatrix},$$

$$\begin{bmatrix} \mathcal{A} & \frac{\mathrm{Id}}{2} - \mathcal{C} \\ \frac{\mathrm{Id}}{2} + \mathcal{B} & -\mathcal{N} \end{bmatrix} \begin{bmatrix} \boldsymbol{\psi} \\ \mathbf{g} \end{bmatrix} + \begin{bmatrix} \mathrm{grad}_\Gamma \, \Psi_V(\gamma_n^+ \mathbf{A}) \\ 0 \end{bmatrix} = \mu_0 \begin{bmatrix} \gamma_\mathbf{t}^+ \mathrm{N}(\mathbf{J}) \\ \gamma_\mathbf{M}^+ \mathrm{N}(\mathbf{J}) \end{bmatrix}. \qquad (5.4.24)$$

The first set of BIEs for the interior traces can be rearranged to get

$$\begin{bmatrix} \mathcal{A} & -\frac{\mathrm{Id}}{2} - \mathcal{C} \\ -\frac{\mathrm{Id}}{2} + \mathcal{B} & -\mathcal{N} \end{bmatrix} \begin{bmatrix} \boldsymbol{\psi} \\ \mathbf{g} \end{bmatrix} + \begin{bmatrix} \mathrm{grad}_\Gamma \, \Psi_V(\gamma_n^- \mathbf{A}) \\ 0 \end{bmatrix} = -\mu_0 \begin{bmatrix} \gamma_\mathbf{t}^- \mathrm{N}(\mathbf{curlM}) \\ \gamma_\mathbf{M}^- \mathrm{N}(\mathbf{curlM}) \end{bmatrix} - \mu_0 \begin{bmatrix} \mathcal{A}(\mathbf{M} \times \mathbf{n}) \\ -\frac{1}{2} \, \mathbf{M} \times \mathbf{n} + \mathcal{B}(\mathbf{M} \times \mathbf{n}) \end{bmatrix}.$$
$$(5.4.25)$$

Summing (5.4.24) and (5.4.25) we get

$$\begin{bmatrix} 2\mathcal{A} & -2\mathcal{C} \\ 2\mathcal{B} & -2\mathcal{N} \end{bmatrix} \begin{bmatrix} \boldsymbol{\psi} \\ \mathbf{g} \end{bmatrix} + \begin{bmatrix} \mathrm{grad}_\Gamma \, \Psi_V(\gamma_n^- \mathbf{A} + \gamma_n^+ \mathbf{A}) \\ 0 \end{bmatrix}$$
$$= -\mu_0 \begin{bmatrix} \gamma_\mathbf{t}^- \mathrm{N}(\mathbf{curlM}) \\ \gamma_\mathbf{M}^- \mathrm{N}(\mathbf{curlM}) \end{bmatrix} - \mu_0 \begin{bmatrix} \mathcal{A}(\mathbf{M} \times \mathbf{n}) \\ -\frac{1}{2} \, \mathbf{M} \times \mathbf{n} + \mathcal{B}(\mathbf{M} \times \mathbf{n}) \end{bmatrix} + \mu_0 \begin{bmatrix} \gamma_\mathbf{t}^+ \mathrm{N}(\mathbf{J}) \\ \gamma_\mathbf{M}^+ \mathrm{N}(\mathbf{J}) \end{bmatrix}.$$

We see that $\gamma_\mathbf{M}^+ \mathbf{A} \in \boldsymbol{H}^{-\frac{1}{2}}(\mathrm{div}_\Gamma \, 0, \Gamma)$ because from the outside, near Γ using the identity [14, Equation 2.75]

$$\mathrm{div}_\Gamma(\mathbf{curlA} \times \mathbf{n}) = \mathbf{curlcurlA} \cdot \mathbf{n} = 0.$$

This will allow us to test with functions in $\boldsymbol{H}^{-\frac{1}{2}}(\mathrm{div}_\Gamma \, 0, \Gamma)$ and get rid of the normal trace of $\mathbf{A}$, a strategy employed in [33]. Testing the first equation with $\boldsymbol{\zeta} \in \boldsymbol{H}^{-\frac{1}{2}}(\mathrm{div}_\Gamma \, 0, \Gamma)$ gives us

$$2\mathsf{b}_\mathcal{A}(\boldsymbol{\psi}, \boldsymbol{\zeta}) - 2\mathsf{b}_\mathcal{C}(\mathbf{g}, \boldsymbol{\zeta})$$
$$= \mu_0 \left\langle \gamma_\mathbf{t}^+ \mathrm{N}(\mathbf{J}), \boldsymbol{\zeta} \right\rangle - \mu_0 \left\langle \gamma_\mathbf{t}^- \mathrm{N}(\mathbf{curlM}), \boldsymbol{\zeta} \right\rangle - \mu_0 \, \mathsf{b}_\mathcal{A}(\mathbf{M} \times \mathbf{n}, \boldsymbol{\zeta}) \quad \forall \boldsymbol{\zeta} \in \boldsymbol{H}^{-\frac{1}{2}}(\mathrm{div}_\Gamma \, 0, \Gamma),$$

where the bilinear forms are defined as in (5.1.30) and $\langle \cdot, \cdot \rangle$ represents the duality pairing between $\boldsymbol{H}^{-\frac{1}{2}}(\mathrm{div}_\Gamma, \Gamma)$ and $\boldsymbol{H}^{-\frac{1}{2}}(\mathbf{curl}_\Gamma, \Gamma)$. Testing the second equation with $\mathbf{u} \in \boldsymbol{H}^{-\frac{1}{2}}(\mathbf{curl}_\Gamma, \Gamma)$ gives us

$$-2\mathsf{b}_\mathcal{N}(\mathbf{g}, \mathbf{u}) + 2\mathsf{b}_\mathcal{B}(\boldsymbol{\psi}, \mathbf{u})$$
$$= \mu_0 \left\langle \gamma_\mathbf{M}^+ \mathrm{N}(\mathbf{J}), \mathbf{u} \right\rangle - \mu_0 \left\langle \gamma_\mathbf{M}^- \mathrm{N}(\mathbf{curlM}), \mathbf{u} \right\rangle + \frac{\mu_0}{2} \left\langle \mathbf{M} \times \mathbf{n}, \mathbf{u} \right\rangle - \mu_0 \, \mathsf{b}_\mathcal{B}(\mathbf{M} \times \mathbf{n}, \mathbf{u}) \quad \forall \mathbf{u} \in \boldsymbol{H}^{-\frac{1}{2}}(\mathbf{curl}_\Gamma, \Gamma).$$

We combine the two equations to get a variational problem. To ensure unique solvability we require the space $\boldsymbol{V} := \{\mathbf{u} \in \boldsymbol{H}^{-\frac{1}{2}}(\mathbf{curl}_\Gamma, \Gamma) : (\mathbf{u}, \mathbf{grad}_\Gamma \, v)_{-\frac{1}{2}, \Gamma} = 0 \quad \forall v \in H_*^{\frac{1}{2}}(\Gamma)\}$ as explained in Section 5.1.2. We have a variational problem posed in the space $\boldsymbol{\mathcal{X}} := \boldsymbol{H}^{-\frac{1}{2}}(\mathrm{div}_\Gamma \, 0, \Gamma) \times \boldsymbol{V}(\Gamma)$: seek $\begin{bmatrix} \boldsymbol{\psi} \\ \mathbf{g} \end{bmatrix} \in \boldsymbol{\mathcal{X}}$ such that

$$\mathsf{b}\left(\begin{bmatrix} \boldsymbol{\psi} \\ \mathbf{g} \end{bmatrix}, \begin{bmatrix} \boldsymbol{\zeta} \\ \mathbf{u} \end{bmatrix}\right) = \ell\left(\begin{bmatrix} \boldsymbol{\zeta} \\ \mathbf{u} \end{bmatrix}\right) \quad \forall \begin{bmatrix} \boldsymbol{\zeta} \\ \mathbf{u} \end{bmatrix} \in \boldsymbol{\mathcal{X}}, \qquad (5.4.26)$$

where

$$\mathsf{b}\left(\begin{bmatrix}\boldsymbol{\psi}\\\mathbf{g}\end{bmatrix},\begin{bmatrix}\boldsymbol{\zeta}\\\mathbf{u}\end{bmatrix}\right) := 2\mathsf{b}_{\mathcal{A}}(\boldsymbol{\psi},\boldsymbol{\zeta}) - 2\mathsf{b}_{\mathcal{C}}(\mathbf{g},\boldsymbol{\zeta}) + 2\mathsf{b}_{\mathcal{B}}(\boldsymbol{\psi},\mathbf{u}) - 2\mathsf{b}_{\mathcal{N}}(\mathbf{g},\mathbf{u}),$$

and

$$\ell\left(\begin{bmatrix}\boldsymbol{\zeta}\\\mathbf{u}\end{bmatrix}\right) := \mu_0\left\langle\gamma_{\mathbf{t}}^+\mathrm{N}(\mathbf{J}),\boldsymbol{\zeta}\right\rangle - \mu_0\left\langle\gamma_{\mathbf{t}}^-\mathrm{N}(\mathbf{curlM}),\boldsymbol{\zeta}\right\rangle - \mu_0\,\mathsf{b}_{\mathcal{A}}(\mathbf{M}\times\mathbf{n},\boldsymbol{\zeta})$$
$$+ \mu_0\left\langle\gamma_{\mathbf{M}}^+\mathrm{N}(\mathbf{J}),\mathbf{u}\right\rangle - \mu_0\left\langle\gamma_{\mathbf{M}}^-\mathrm{N}(\mathbf{curlM}),\mathbf{u}\right\rangle + \frac{\mu_0}{2}\left\langle\mathbf{M}\times\mathbf{n},\mathbf{u}\right\rangle - \mu_0\,\mathsf{b}_{\mathcal{B}}(\mathbf{M}\times\mathbf{n},\mathbf{u}).$$

We focus on the expression $\mathcal{E}_F$ as we observed in (5.4.12) that we recover the equivalent current model from its shape derivative. $\mathcal{E}_F$ can be written in terms of traces of the vector potential $\mathbf{A}$ as

$$\mathcal{E}_F = \frac{1}{2}\int_\Omega \mathbf{A}\cdot\mathbf{curlM}\,d\mathbf{x} + \frac{1}{2}\int_\Gamma(\mathbf{M}\times\mathbf{n})\cdot\mathbf{A}\,dS + \frac{1}{2}\int_{\Omega_{\mathrm{src}}}\mathbf{J}\cdot\mathbf{A}\,d\mathbf{x}$$

$$= \frac{1}{2}\int_\Omega\left(-\boldsymbol{\Psi}_{\mathbf{M}}(\mathbf{g}) + \boldsymbol{\Psi}_{\mathbf{A}}(\boldsymbol{\psi} + \mu_0\,\mathbf{M}\times\mathbf{n}) + \mathrm{grad}_{\mathbf{x}}\,\Psi_V(\gamma_n^-\mathbf{A}) + \mu_0\,\mathrm{N}(\mathbf{curlM})\right)\cdot\mathbf{curlM}\,d\mathbf{x}$$

$$+ \frac{1}{2}\int_\Gamma(\mathbf{M}\times\mathbf{n})\cdot\mathbf{g}\,dS$$

$$+ \frac{1}{2}\int_{\Omega_{\mathrm{src}}}\left(\boldsymbol{\Psi}_{\mathbf{M}}(\mathbf{g}) - \boldsymbol{\Psi}_{\mathbf{A}}(\boldsymbol{\psi}) - \mathrm{grad}_{\mathbf{x}}\,\Psi_V(\gamma_n^+\mathbf{A}) + \mu_0\,\mathrm{N}(\mathbf{J})\right)\cdot\mathbf{J}\,d\mathbf{x}.$$

Assumption 2. Magnetization $\mathbf{M}$ is such that $\mathbf{curlM}|_\Gamma\cdot\mathbf{n} = \mathbf{curl}_\Gamma\,\gamma_{\mathbf{t}}\mathbf{M} = \mathrm{div}_\Gamma(\mathbf{M}\times\mathbf{n}) = 0$ on Γ, or equivalently $\mathbf{curlM}\in\boldsymbol{H}(\mathrm{div};\mathbb{R}^3)$.

Assumption 2 can be interpreted as conservation of charge for the equivalent current. It allows us to get rid of the normal trace of $\mathbf{A}$. Using $\mathbf{J}\cdot\mathbf{n}|_{\partial\Omega_{\mathrm{src}}} = 0$ and $\mathrm{div}\,\mathbf{J} = 0$, the energy expression becomes

$$= -\frac{1}{2}\int_\Omega\boldsymbol{\Psi}_{\mathbf{M}}(\mathbf{g})\cdot\mathbf{curlM}\,d\mathbf{x} + \frac{1}{2}\int_\Omega\boldsymbol{\Psi}_{\mathbf{A}}(\boldsymbol{\psi})\cdot\mathbf{curlM}\,d\mathbf{x} + \frac{\mu_0}{2}\int_\Omega\boldsymbol{\Psi}_{\mathbf{A}}(\mathbf{M}\times\mathbf{n})\cdot\mathbf{curlM}\,d\mathbf{x}$$

$$+ \frac{1}{2}\int_\Gamma(\mathbf{M}\times\mathbf{n})\cdot\mathbf{g}\,dS$$

$$+ \frac{1}{2}\int_{\Omega_{\mathrm{src}}}\boldsymbol{\Psi}_{\mathbf{M}}(\mathbf{g})\cdot\mathbf{J}\,d\mathbf{x} - \frac{1}{2}\int_{\Omega_{\mathrm{src}}}\boldsymbol{\Psi}_{\mathbf{A}}(\boldsymbol{\psi})\cdot\mathbf{J}\,d\mathbf{x}$$

$$+ \frac{\mu_0}{2}\int_\Omega\mathrm{N}(\mathbf{curlM})\cdot\mathbf{curlM}\,d\mathbf{x} + \frac{\mu_0}{2}\int_{\Omega_{\mathrm{src}}}\mathrm{N}(\mathbf{J})\cdot\mathbf{J}\,d\mathbf{x}.$$

The integrals which contain layer potentials can be written in terms of duality pairings.

$$\int_\Omega\boldsymbol{\Psi}_{\mathbf{M}}(\mathbf{g})(\mathbf{x})\cdot\mathbf{curlM}(\mathbf{x})\,d\mathbf{x} = \int_\Omega\mathbf{curlM}(\mathbf{x})\cdot\int_\Gamma\nabla_x G(\mathbf{x},\mathbf{y})\times(\mathbf{n}(\mathbf{y})\times\mathbf{g}(\mathbf{y}))\,dS_{\mathbf{y}}\,d\mathbf{x}$$

$$= \int_\Omega \int_\Gamma \left\{ \nabla_x G(\mathbf{x}, \mathbf{y}) \times (\mathbf{n}(\mathbf{y}) \times \mathbf{g}(\mathbf{y})) \right\} \cdot \mathbf{curlM}(\mathbf{x}) \, dS_\mathbf{y} \, d\mathbf{x}$$

$$\overset{\mathbf{x} \leftrightarrow \mathbf{y}}{=} \int_\Omega \int_\Gamma \left\{ \nabla_x G(\mathbf{y}, \mathbf{x}) \times (\mathbf{n}(\mathbf{x}) \times \mathbf{g}(\mathbf{x})) \right\} \cdot \mathbf{curlM}(\mathbf{y}) \, dS_\mathbf{x} \, d\mathbf{y}$$

$$= \int_\Gamma \int_\Omega \left\{ \nabla_x G(\mathbf{x}, \mathbf{y}) \times \mathbf{curlM}(\mathbf{y}) \right\} \cdot (\mathbf{n}(\mathbf{x}) \times \mathbf{g}(\mathbf{x})) \, d\mathbf{y} \, dS_\mathbf{x}$$

$$= \int_\Gamma \left\{ \mathbf{curl} \int_\Omega G(\mathbf{x}, \mathbf{y}) \, \mathbf{curlM}(\mathbf{y}) \, d\mathbf{y} \right\} \cdot (\mathbf{n}(\mathbf{x}) \times \mathbf{g}(\mathbf{x})) \, dS_\mathbf{x}$$

$$= \left\langle \gamma_\mathbf{M}^- \mathrm{N}(\mathbf{curlM}), \mathbf{g} \right\rangle,$$

$$\int_\Omega \boldsymbol{\Psi}_\mathbf{A}(\boldsymbol{\psi}) \cdot \mathbf{curlM} \, d\mathbf{x} = \int_\Omega \mathbf{curlM}(\mathbf{x}) \cdot \int_\Gamma G(\mathbf{x}, \mathbf{y}) \, \boldsymbol{\psi}(\mathbf{y}) \, dS_\mathbf{y} \, d\mathbf{x}$$

$$\overset{\mathbf{x} \leftrightarrow \mathbf{y}}{=} \int_\Omega \int_\Gamma G(\mathbf{y}, \mathbf{x}) \, \mathbf{curlM}(\mathbf{y}) \cdot \boldsymbol{\psi}(\mathbf{x}) \, dS_\mathbf{x} \, d\mathbf{y}$$

$$= \int_\Gamma \boldsymbol{\psi}(\mathbf{x}) \cdot \int_\Omega G(\mathbf{x}, \mathbf{y}) \, \mathbf{curlM}(\mathbf{y}) \, d\mathbf{y} \, dS_\mathbf{x}$$

$$= \left\langle \gamma_\mathbf{t}^- \mathrm{N}(\mathbf{curlM}), \boldsymbol{\psi} \right\rangle.$$

The same procedure applies for double integrals with Ω_{src} and Γ. Thus we get

$$\mathcal{E}_F = -\frac{1}{2} \left\langle \gamma_\mathbf{M}^- \mathrm{N}(\mathbf{curlM}), \mathbf{g} \right\rangle + \frac{1}{2} \left\langle \gamma_\mathbf{t}^- \mathrm{N}(\mathbf{curlM}), \boldsymbol{\psi} \right\rangle + \frac{\mu_0}{2} \left\langle \gamma_\mathbf{t}^- \mathrm{N}(\mathbf{curlM}), \mathbf{M} \times \mathbf{n} \right\rangle$$

$$+ \frac{1}{2} \int_\Gamma (\mathbf{M} \times \mathbf{n}) \cdot \mathbf{g} \, dS$$

$$+ \frac{1}{2} \left\langle \gamma_\mathbf{M}^+ \mathrm{N}(\mathbf{J}), \mathbf{g} \right\rangle - \frac{1}{2} \left\langle \gamma_\mathbf{t}^+ \mathrm{N}(\mathbf{J}), \boldsymbol{\psi} \right\rangle$$

$$+ \frac{\mu_0}{2} \int_\Omega \mathrm{N}(\mathbf{curlM}) \cdot \mathbf{curlM} \, d\mathbf{x} + \frac{\mu_0}{2} \int_{\Omega_{\mathrm{src}}} \mathrm{N}(\mathbf{J}) \cdot \mathbf{J} \, d\mathbf{x}.$$

Having a relation between the energy expression $\mathcal{E}_F$ and the linear form makes the computation of energy shape derivative simpler as we get the adjoint solution in an explicit form. We observe that

$$\frac{1}{2\mu_0} \ell \left(\begin{bmatrix} -\boldsymbol{\psi} \\ \mathbf{g} \end{bmatrix} \right) = -\frac{1}{2} \left\langle \gamma_\mathbf{t}^+ \mathrm{N}(\mathbf{J}), \boldsymbol{\psi} \right\rangle + \frac{1}{2} \left\langle \gamma_\mathbf{t}^- \mathrm{N}(\mathbf{curlM}), \boldsymbol{\psi} \right\rangle + \frac{1}{2} \, \mathsf{b}_\mathcal{A}(\mathbf{M} \times \mathbf{n}, \boldsymbol{\psi})$$

$$+ \frac{1}{2} \left\langle \gamma_\mathbf{M}^+ \mathrm{N}(\mathbf{J}), \mathbf{g} \right\rangle - \frac{1}{2} \left\langle \gamma_\mathbf{M}^- \mathrm{N}(\mathbf{curlM}), \mathbf{g} \right\rangle + \frac{1}{4} \left\langle \mathbf{M} \times \mathbf{n}, \mathbf{g} \right\rangle - \frac{1}{2} \, \mathsf{b}_\mathcal{B}(\mathbf{M} \times \mathbf{n}, \mathbf{g}).$$

Comparing with the expression for $\mathcal{E}_F$ above we get

$$\frac{1}{2\mu_0} \ell \left(\begin{bmatrix} -\boldsymbol{\psi} \\ \mathbf{g} \end{bmatrix} \right) = \mathcal{E}_F - \frac{\mu_0}{2} \left\langle \gamma_\mathbf{t}^- \mathrm{N}(\mathbf{curlM}), \mathbf{M} \times \mathbf{n} \right\rangle - \frac{1}{2} \left\langle \mathbf{M} \times \mathbf{n}, \mathbf{g} \right\rangle$$

$$-\frac{\mu_0}{2} \int_{\Omega} \mathrm{N}(\mathbf{curlM}) \cdot \mathbf{curlM} \, d\mathbf{x} - \frac{\mu_0}{2} \int_{\Omega_{\mathrm{src}}} \mathrm{N}(\mathbf{J}) \cdot \mathbf{J} \, d\mathbf{x}$$

$$+\frac{1}{2} \, \mathsf{b}_{\mathcal{A}}(\mathbf{M} \times \mathbf{n}, \boldsymbol{\psi}) + \frac{1}{4} \langle \mathbf{M} \times \mathbf{n}, \mathbf{g} \rangle - \frac{1}{2} \, \mathsf{b}_{\mathcal{B}}(\mathbf{M} \times \mathbf{n}, \mathbf{g}).$$

Since $\mathrm{div}_{\Gamma}(\mathbf{M} \times \mathbf{n}) = 0$ on Γ by Assumption 2, we can test the first BIE in Ω with $\mathbf{M} \times \mathbf{n}$ which gives

$$\mathsf{b}_{\mathcal{A}}(\boldsymbol{\psi}, \mathbf{M} \times \mathbf{n}) + \mu_0 \, \mathsf{b}_{\mathcal{A}}(\mathbf{M} \times \mathbf{n}, \mathbf{M} \times \mathbf{n}) - \frac{1}{2} \langle \mathbf{M} \times \mathbf{n}, \mathbf{g} \rangle - \mathsf{b}_{\mathcal{C}}(\mathbf{g}, \mathbf{M} \times \mathbf{n})$$
$$= -\mu_0 \langle \gamma_{\mathbf{t}}^{-} \mathrm{N}(\mathbf{curlM}), \mathbf{M} \times \mathbf{n} \rangle,$$

which can scaled to get

$$-\frac{1}{2} \mathsf{b}_{\mathcal{A}}(\boldsymbol{\psi}, \mathbf{M} \times \mathbf{n}) + \frac{1}{2} \mathsf{b}_{\mathcal{B}}(\mathbf{M} \times \mathbf{n}, \mathbf{g})$$
$$= \frac{\mu_0}{2} \langle \gamma_{\mathbf{t}}^{-} \mathrm{N}(\mathbf{curlM}), \mathbf{M} \times \mathbf{n} \rangle + \frac{\mu_0}{2} \, \mathsf{b}_{\mathcal{A}}(\mathbf{M} \times \mathbf{n}, \mathbf{M} \times \mathbf{n}) - \frac{1}{4} \langle \mathbf{M} \times \mathbf{n}, \mathbf{g} \rangle.$$

This allows us to write the relation between $\mathcal{E}_F$ and the linear form as

$$\mathcal{E}_F = \frac{1}{2\mu_0} \ell(\begin{bmatrix} -\boldsymbol{\psi} \\ \mathbf{g} \end{bmatrix}) + \mu_0 \langle \gamma_{\mathbf{t}}^{-} \mathrm{N}(\mathbf{curlM}), \mathbf{M} \times \mathbf{n} \rangle + \frac{\mu_0}{2} \, \mathsf{b}_{\mathcal{A}}(\mathbf{M} \times \mathbf{n}, \mathbf{M} \times \mathbf{n})$$
$$+ \frac{\mu_0}{2} \int_{\Omega} \mathrm{N}(\mathbf{curlM}) \cdot \mathbf{curlM} \, d\mathbf{x} + \frac{\mu_0}{2} \int_{\Omega_{\mathrm{src}}} \mathrm{N}(\mathbf{J}) \cdot \mathbf{J} \, d\mathbf{x}. \tag{5.4.27}$$

5.4.2.6 Variational BIEs on Deformed Domain

We consider deformations using $\boldsymbol{\mathcal{V}}$ such that $\boldsymbol{\mathcal{V}} = 0$ around the source current. Thus we only deform the permanent magnet whose magnetization is transformed like a 1-form to $\mathbf{M}_s$ such that $\mathbf{M}_s(\mathbf{T}_s^{\boldsymbol{\nu}}(\hat{\mathbf{x}})) := \mathsf{D}\mathbf{T}_s^{\boldsymbol{\nu}}(\hat{\mathbf{x}})^{-T} \, \mathbf{M}(\hat{\mathbf{x}})$. Variational formulation for the deformed s-configuration has a similar structure to (5.4.26). Defining $\boldsymbol{V}_s := \{\mathbf{u} \in \boldsymbol{H}^{-\frac{1}{2}}(\mathbf{curl}_{\Gamma}, \Gamma^s) : (\mathbf{u}, \mathbf{grad}_{\Gamma} v)_{-\frac{1}{2}, \Gamma^s} = 0 \quad \forall v \in H_*^{\frac{1}{2}}(\Gamma^s)\}$ we have: seek $\boldsymbol{\psi}_s, \mathbf{g}_s \in \boldsymbol{\mathcal{X}}_s := \boldsymbol{H}^{-\frac{1}{2}}(\mathrm{div}_{\Gamma} \, 0, \Gamma^s) \times \boldsymbol{V}_s$ such that

$$\mathsf{b}(s)(\begin{bmatrix} \boldsymbol{\psi}_s \\ \mathbf{g}_s \end{bmatrix}, \begin{bmatrix} \boldsymbol{\zeta} \\ \mathbf{u} \end{bmatrix}) = \ell(s)(\begin{bmatrix} \boldsymbol{\zeta} \\ \mathbf{u} \end{bmatrix}) \quad \forall \begin{bmatrix} \boldsymbol{\zeta} \\ \mathbf{u} \end{bmatrix} \in \boldsymbol{\mathcal{X}}_s,$$

where

$$\mathsf{b}(s)(\begin{bmatrix} \boldsymbol{\psi} \\ \mathbf{g} \end{bmatrix}, \begin{bmatrix} \boldsymbol{\zeta} \\ \mathbf{u} \end{bmatrix}) := 2\mathsf{b}_{\mathcal{A}}(s)(\boldsymbol{\psi}, \boldsymbol{\zeta}) - 2\mathsf{b}_{\mathcal{C}}(s)(\mathbf{g}, \boldsymbol{\zeta}) + 2\mathsf{b}_{\mathcal{B}}(s)(\boldsymbol{\psi}, \mathbf{u}) - 2\mathsf{b}_{\mathcal{N}}(s)(\mathbf{g}, \mathbf{u}),$$

using the bilinear forms $b(s)$ contain integrals over Γ^s and the linear form is split into a source current and permanent magnet part as

$$\ell(s)(\begin{bmatrix} \boldsymbol{\zeta} \\ \mathbf{u} \end{bmatrix}) := \ell_{\mathbf{J}}(s)(\begin{bmatrix} \boldsymbol{\zeta} \\ \mathbf{u} \end{bmatrix}) + \ell_{\mathbf{M}}(s)(\begin{bmatrix} \boldsymbol{\zeta} \\ \mathbf{u} \end{bmatrix}),$$

where

$$\ell_{\mathbf{J}}(s)(\begin{bmatrix} \boldsymbol{\zeta} \\ \mathbf{u} \end{bmatrix}) := \mu_0 \left\langle \gamma_{\mathbf{t}}^+ \mathrm{N}(\mathbf{J}), \boldsymbol{\zeta} \right\rangle_{\Gamma^s} + \mu_0 \left\langle \gamma_{\mathbf{M}}^+ \mathrm{N}(\mathbf{J}), \mathbf{u} \right\rangle_{\Gamma^s},$$

$$\ell_{\mathbf{M}}(s)(\begin{bmatrix} \boldsymbol{\zeta} \\ \mathbf{u} \end{bmatrix}) := -\mu_0 \left\langle \gamma_{\mathbf{t}}^- \mathrm{N}(\mathbf{curl}\mathbf{M}_s), \boldsymbol{\zeta} \right\rangle_{\Gamma^s} - \mu_0 \left\langle \gamma_{\mathbf{M}}^- \mathrm{N}(\mathbf{curl}\mathbf{M}_s), \mathbf{u} \right\rangle_{\Gamma^s}$$

$$+ \frac{\mu_0}{2} \left\langle \mathbf{M}_s \times \mathbf{n}, \mathbf{u} \right\rangle_{\Gamma^s} - \mu_0 \, \mathsf{b}_{\mathcal{A}}(s)(\mathbf{M}_s \times \mathbf{n}, \boldsymbol{\zeta}) - \mu_0 \, \mathsf{b}_{\mathcal{B}}(s)(\mathbf{M}_s \times \mathbf{n}, \mathbf{u}).$$

In the expressions above, $\langle \cdot, \cdot \rangle_{\Gamma^s}$ denotes the duality pairing between $\boldsymbol{H}^{-\frac{1}{2}}(\mathrm{div}_\Gamma, \Gamma^s)$ and $\boldsymbol{H}^{-\frac{1}{2}}(\mathbf{curl}_\Gamma, \Gamma^s)$.

5.4.2.7   Equivalent BIEs on Reference Domain

The integrals in the (bi)linear forms can be transformed back to the reference boundary using the perturbation map. This has already been done for the bilinear forms in 5.1.2.3 so we only mention the linear forms

$$\ell_{\mathbf{J}}(s)(\begin{bmatrix} \boldsymbol{\zeta} \\ \mathbf{u} \end{bmatrix}) = \mu_0 \left\langle \gamma_{\mathbf{t}}^+ \mathrm{N}(\mathbf{J}), \boldsymbol{\zeta} \right\rangle_{\Gamma^s} + \mu_0 \left\langle \gamma_{\mathbf{M}}^+ \mathrm{N}(\mathbf{J}), \mathbf{u} \right\rangle_{\Gamma^s}$$

$$= \mu_0 \int_{\Gamma^s} \int_{\Omega_{\mathrm{src}}} G(\mathbf{x}, \mathbf{y}) \, \mathbf{J}(\mathbf{y}) \cdot \boldsymbol{\zeta}(\mathbf{x}) \, d\mathbf{y} \, dS_{\mathbf{x}}$$

$$+ \mu_0 \int_{\Gamma^s} \int_{\Omega_{\mathrm{src}}} \left(\nabla_{\mathbf{x}} G(\mathbf{x}, \mathbf{y}) \times \mathbf{J}(\mathbf{y}) \right) \cdot (\mathbf{n}(\mathbf{x}) \times \mathbf{u}(\mathbf{x})) \, d\mathbf{y} \, dS_{\mathbf{x}}$$

$$= \mu_0 \int_{\Gamma^0} \int_{\Omega_{\mathrm{src}}} G(\mathbf{T}_s^{\boldsymbol{\nu}}(\hat{\mathbf{x}}), \mathbf{y}) \, \mathbf{J}(\mathbf{y}) \cdot \boldsymbol{\zeta}(\mathbf{T}_s^{\boldsymbol{\nu}}(\hat{\mathbf{x}})) \, \omega_s(\hat{\mathbf{x}}) \, d\mathbf{y} \, dS_{\hat{\mathbf{x}}}$$

$$+ \mu_0 \int_{\Gamma^0} \int_{\Omega_{\mathrm{src}}} \left(\nabla_{\mathbf{x}} G(\mathbf{T}_s^{\boldsymbol{\nu}}(\hat{\mathbf{x}}), \mathbf{y}) \times \mathbf{J}(\mathbf{y}) \right) \cdot \left(\frac{\mathbf{C}(\mathrm{D}\mathbf{T}_s^{\boldsymbol{\nu}})(\hat{\mathbf{x}}) \, \hat{\mathbf{n}}(\hat{\mathbf{x}})}{\omega_s(\hat{\mathbf{x}})} \times \mathbf{u}(\mathbf{T}_s^{\boldsymbol{\nu}}(\hat{\mathbf{x}})) \right) \omega_s(\hat{\mathbf{x}}) \, d\mathbf{y} \, dS_{\hat{\mathbf{x}}},$$

$$\ell_{\mathbf{M}}(s)(\begin{bmatrix} \boldsymbol{\zeta} \\ \mathbf{u} \end{bmatrix}) = -\mu_0 \left\langle \gamma_{\mathbf{t}}^- \mathrm{N}(\mathbf{curl}\mathbf{M}_s), \boldsymbol{\zeta} \right\rangle_{\Gamma^s} - \mu_0 \left\langle \gamma_{\mathbf{M}}^- \mathrm{N}(\mathbf{curl}\mathbf{M}_s), \mathbf{u} \right\rangle_{\Gamma^s}$$

$$+ \frac{\mu_0}{2} \left\langle \mathbf{M}_s \times \mathbf{n}, \mathbf{u} \right\rangle_{\Gamma^s} - \mu_0 \, \mathsf{b}_{\mathcal{A}}(s)(\mathbf{M}_s \times \mathbf{n}, \boldsymbol{\zeta}) - \mu_0 \, \mathsf{b}_{\mathcal{B}}(s)(\mathbf{M}_s \times \mathbf{n}, \mathbf{u})$$

$$= -\mu_0 \int_{\Gamma^s} \int_{\Omega^s} G(\mathbf{x}, \mathbf{y}) \, \mathbf{curl}\mathbf{M}_s(\mathbf{y}) \cdot \boldsymbol{\zeta}(\mathbf{x}) \, d\mathbf{y} \, dS_{\mathbf{x}}$$

$$- \mu_0 \int_{\Gamma^s} \int_{\Omega^s} \left(\nabla_{\mathbf{x}} G(\mathbf{x}, \mathbf{y}) \times \mathbf{curl}\mathbf{M}_s(\mathbf{y}) \right) \cdot (\mathbf{n}(\mathbf{x}) \times \mathbf{u}(\mathbf{x})) \, d\mathbf{y} \, dS_{\mathbf{x}}$$

$$+ \frac{\mu_0}{2} \int_{\Gamma^s} \left(\mathbf{M}_s(\mathbf{x}) \times \mathbf{n}(\mathbf{x}) \right) \cdot \mathbf{u}(\mathbf{x}) \, dS_{\mathbf{x}}$$

$$- \mu_0 \int_{\Gamma^s} \int_{\Gamma^s} G(\mathbf{x}, \mathbf{y}) \left(\mathbf{M}_s(\mathbf{y}) \times \mathbf{n}(\mathbf{y}) \right) \cdot \boldsymbol{\zeta}(\mathbf{x}) \, dS_{\mathbf{y}} dS_{\mathbf{x}}$$

$$-\mu_0 \int_{\Gamma^s} \int_{\Gamma^s} (\nabla_{\mathbf{x}} G(\mathbf{x},\mathbf{y}) \times (\mathbf{n} \times \mathbf{u})(\mathbf{y})) \cdot \Big(\mathbf{M}_s(\mathbf{x}) \times \mathbf{n}(\mathbf{x})\Big) \, dS_{\mathbf{y}} \, dS_{\mathbf{x}}$$

$$= -\mu_0 \int_{\Gamma^0} \int_{\Omega^0} G(\mathbf{T}_s^{\boldsymbol{\nu}}(\hat{\mathbf{x}}), \mathbf{T}_s^{\boldsymbol{\nu}}(\hat{\mathbf{y}})) \, \mathbf{curl}\mathbf{M}_s(\mathbf{T}_s^{\boldsymbol{\nu}}(\hat{\mathbf{y}})) \cdot \boldsymbol{\zeta}(\mathbf{T}_s^{\boldsymbol{\nu}}(\hat{\mathbf{x}})) \, \omega_s(\hat{\mathbf{x}}) \, \det \mathsf{D}\mathbf{T}_s^{\boldsymbol{\nu}}(\hat{\mathbf{y}}) \, d\hat{\mathbf{y}} \, dS_{\hat{\mathbf{x}}}$$

$$- \mu_0 \int_{\Gamma^0} \int_{\Omega^0} \Big(\nabla_{\mathbf{x}} G(\mathbf{T}_s^{\boldsymbol{\nu}}(\hat{\mathbf{x}}), \mathbf{T}_s^{\boldsymbol{\nu}}(\hat{\mathbf{y}})) \times \mathbf{curl}\mathbf{M}_s(\mathbf{T}_s^{\boldsymbol{\nu}}(\hat{\mathbf{y}}))\Big) \cdot$$

$$(\mathbf{n}(\mathbf{T}_s^{\boldsymbol{\nu}}(\hat{\mathbf{x}})) \times \mathbf{u}(\mathbf{T}_s^{\boldsymbol{\nu}}(\hat{\mathbf{x}}))) \, \omega_s(\hat{\mathbf{x}}) \, \det \mathsf{D}\mathbf{T}_s^{\boldsymbol{\nu}}(\hat{\mathbf{y}}) \, d\hat{\mathbf{y}} \, dS_{\hat{\mathbf{x}}}$$

$$+ \frac{\mu_0}{2} \int_{\Gamma^0} \Big(\mathbf{M}_s(\mathbf{T}_s^{\boldsymbol{\nu}}(\hat{\mathbf{x}})) \times \mathbf{n}(\mathbf{T}_s^{\boldsymbol{\nu}}(\hat{\mathbf{x}}))\Big) \cdot \mathbf{u}(\mathbf{T}_s^{\boldsymbol{\nu}}(\hat{\mathbf{x}})) \, \omega_s(\hat{\mathbf{x}}) \, dS_{\hat{\mathbf{x}}}$$

$$- \mu_0 \int_{\Gamma^0} \int_{\Gamma^0} G(\mathbf{T}_s^{\boldsymbol{\nu}}(\hat{\mathbf{x}}), \mathbf{T}_s^{\boldsymbol{\nu}}(\hat{\mathbf{y}})) \, \Big(\mathbf{M}_s(\mathbf{T}_s^{\boldsymbol{\nu}}(\hat{\mathbf{y}})) \times \mathbf{n}(\mathbf{T}_s^{\boldsymbol{\nu}}(\hat{\mathbf{y}}))\Big) \cdot \boldsymbol{\zeta}(\mathbf{T}_s^{\boldsymbol{\nu}}(\hat{\mathbf{x}})) \, \omega_s(\hat{\mathbf{y}}) \, \omega_s(\hat{\mathbf{x}}) \, dS_{\hat{\mathbf{y}}} dS_{\hat{\mathbf{x}}}$$

$$- \mu_0 \int_{\Gamma^0} \int_{\Gamma^0} \Big(\nabla_{\mathbf{x}} G(\mathbf{T}_s^{\boldsymbol{\nu}}(\hat{\mathbf{x}}), \mathbf{T}_s^{\boldsymbol{\nu}}(\hat{\mathbf{y}})) \times (\mathbf{n}(\mathbf{T}_s^{\boldsymbol{\nu}}(\hat{\mathbf{y}})) \times \mathbf{u}(\mathbf{T}_s^{\boldsymbol{\nu}}(\hat{\mathbf{y}})))\Big) \cdot$$

$$\Big(\mathbf{M}_s(\mathbf{T}_s^{\boldsymbol{\nu}}(\hat{\mathbf{x}})) \times \mathbf{n}(\mathbf{T}_s^{\boldsymbol{\nu}}(\hat{\mathbf{x}}))\Big) \, \omega_s(\hat{\mathbf{y}}) \, \omega_s(\hat{\mathbf{x}}) \, dS_{\hat{\mathbf{y}}} dS_{\hat{\mathbf{x}}}.$$

We use the following pullbacks for 1-forms and their curl

$$\mathbf{A}(\mathbf{T}_s^{\boldsymbol{\nu}}(\hat{\mathbf{x}})) = \mathsf{D}\mathbf{T}_s^{\boldsymbol{\nu}}(\hat{\mathbf{x}})^{-T} \, \hat{\mathbf{A}}(\hat{\mathbf{x}}),$$

$$\mathbf{curl}\mathbf{A}(\mathbf{T}_s^{\boldsymbol{\nu}}(\hat{\mathbf{x}})) = \frac{\mathsf{D}\mathbf{T}_s^{\boldsymbol{\nu}}(\hat{\mathbf{x}})}{\det \mathsf{D}\mathbf{T}_s^{\boldsymbol{\nu}}(\hat{\mathbf{x}})} \, \mathbf{curl}\hat{\mathbf{A}}(\hat{\mathbf{x}}).$$

For the traces and the corresponding test functions, we use the pullbacks

$$\boldsymbol{\psi} \in \boldsymbol{H}^{-\frac{1}{2}}(\mathrm{div}_\Gamma\, 0, \Gamma^s), \; \hat{\boldsymbol{\psi}} \in \boldsymbol{H}^{-\frac{1}{2}}(\mathrm{div}_\Gamma\, 0, \Gamma^0): \quad \boldsymbol{\psi}(\mathbf{T}_s^{\boldsymbol{\nu}}(\hat{\mathbf{x}})) = \frac{\mathsf{D}\mathbf{T}_s^{\boldsymbol{\nu}}(\hat{\mathbf{x}})}{\omega_s(\hat{x})} \, \hat{\boldsymbol{\psi}}(\hat{\mathbf{x}}),$$

$$\mathbf{g} \in \boldsymbol{H}^{-\frac{1}{2}}(\mathbf{curl}_\Gamma, \Gamma^s), \; \hat{\mathbf{g}} \in \boldsymbol{H}^{-\frac{1}{2}}(\mathbf{curl}_\Gamma, \Gamma^0): \quad \mathbf{g}(\mathbf{T}_s^{\boldsymbol{\nu}}(\hat{\mathbf{x}})) = \mathsf{D}\mathbf{T}_s^{\boldsymbol{\nu}}(\hat{\mathbf{x}})^{-T} \, \hat{\mathbf{g}}(\hat{\mathbf{x}}).$$

Using the transformations above, we define the pulled back hat (bi)linear forms. Here we only mention the linear forms since the bilinear forms are exactly like the ones defined in 5.1.2.3.

$$\hat{\ell}_{\mathbf{J}}\Big(s; \begin{bmatrix} \hat{\boldsymbol{\zeta}} \\ \hat{\mathbf{u}} \end{bmatrix}\Big) := \mu_0 \int_{\Gamma^0} \int_{\Omega_{\mathrm{src}}} G(\mathbf{T}_s^{\boldsymbol{\nu}}(\hat{\mathbf{x}}), \mathbf{y}) \, \mathbf{J}(\mathbf{y}) \cdot \Big(\mathsf{D}\mathbf{T}_s^{\boldsymbol{\nu}}(\hat{\mathbf{x}}) \, \hat{\boldsymbol{\zeta}}(\hat{\mathbf{x}})\Big) \, d\mathbf{y} \, dS_{\hat{\mathbf{x}}}$$

$$+ \mu_0 \int_{\Gamma^0} \int_{\Omega_{\mathrm{src}}} \Big(\nabla_{\mathbf{x}} G(\mathbf{T}_s^{\boldsymbol{\nu}}(\hat{\mathbf{x}}), \mathbf{y}) \times \mathbf{J}(\mathbf{y})\Big) \cdot \Big(\mathsf{D}\mathbf{T}_s^{\boldsymbol{\nu}}(\hat{\mathbf{x}})\{\hat{\mathbf{n}}(\hat{\mathbf{x}}) \times \hat{\mathbf{u}}(\hat{\mathbf{x}})\}\Big) \, d\mathbf{y} \, dS_{\hat{\mathbf{x}}},$$

$$\hat{\ell}_{\mathbf{M}}\Big(s; \begin{bmatrix} \hat{\boldsymbol{\zeta}} \\ \hat{\mathbf{u}} \end{bmatrix}\Big) := -\mu_0 \int_{\Gamma^0} \int_{\Omega^0} G(\mathbf{T}_s^{\boldsymbol{\nu}}(\hat{\mathbf{x}}), \mathbf{T}_s^{\boldsymbol{\nu}}(\hat{\mathbf{y}})) \, \Big(\mathsf{D}\mathbf{T}_s^{\boldsymbol{\nu}}(\hat{\mathbf{y}}) \, \mathbf{curl}\mathbf{M}(\hat{\mathbf{y}})\Big) \cdot \Big(\mathsf{D}\mathbf{T}_s^{\boldsymbol{\nu}}(\hat{\mathbf{x}}) \, \hat{\boldsymbol{\zeta}}(\hat{\mathbf{x}})\Big) \, d\hat{\mathbf{y}} \, dS_{\hat{\mathbf{x}}}$$

$$- \mu_0 \int\limits_{\Gamma^0} \int\limits_{\Omega^0} \left(\nabla_{\mathbf{x}} G(\mathbf{T}_s^{\boldsymbol{\nu}}(\hat{\mathbf{x}}), \mathbf{T}_s^{\boldsymbol{\nu}}(\hat{\mathbf{y}})) \times \left(D\mathbf{T}_s^{\boldsymbol{\nu}}(\hat{\mathbf{y}}) \, \mathbf{curl M}(\hat{\mathbf{y}}) \right) \right) \cdot$$

$$\left(D\mathbf{T}_s^{\boldsymbol{\nu}}(\hat{\mathbf{x}}) \{ \hat{\mathbf{n}}(\hat{\mathbf{x}}) \times \hat{\mathbf{u}}(\hat{\mathbf{x}}) \} \right) \, d\hat{\mathbf{y}} \, dS_{\hat{\mathbf{x}}}$$

$$+ \frac{\mu_0}{2} \int\limits_{\Gamma^0} \left(\mathbf{M}(\hat{\mathbf{x}}) \times \hat{\mathbf{n}}(\hat{\mathbf{x}}) \right) \cdot \hat{\mathbf{u}}(\hat{\mathbf{x}}) \, dS_{\hat{\mathbf{x}}}$$

$$- \mu_0 \int\limits_{\Gamma^0} \int\limits_{\Gamma^0} G(\mathbf{T}_s^{\boldsymbol{\nu}}(\hat{\mathbf{x}}), \mathbf{T}_s^{\boldsymbol{\nu}}(\hat{\mathbf{y}})) \left(D\mathbf{T}_s^{\boldsymbol{\nu}}(\hat{\mathbf{y}}) \left\{ \mathbf{M}(\hat{\mathbf{y}}) \times \hat{\mathbf{n}}(\hat{\mathbf{y}}) \right\} \right) \cdot \left(D\mathbf{T}_s^{\boldsymbol{\nu}}(\hat{\mathbf{x}}) \, \hat{\boldsymbol{\zeta}}(\hat{\mathbf{x}}) \right) \, dS_{\hat{\mathbf{y}}} \, dS_{\hat{\mathbf{x}}}$$

$$- \mu_0 \int\limits_{\Gamma^0} \int\limits_{\Gamma^0} \left(\nabla_{\mathbf{x}} G(\mathbf{T}_s^{\boldsymbol{\nu}}(\hat{\mathbf{x}}), \mathbf{T}_s^{\boldsymbol{\nu}}(\hat{\mathbf{y}})) \times \left(D\mathbf{T}_s^{\boldsymbol{\nu}}(\hat{\mathbf{y}}) \left\{ \hat{\mathbf{n}}(\hat{\mathbf{y}}) \times \hat{\mathbf{u}}(\hat{\mathbf{y}}) \right\} \right) \right) \cdot$$

$$\left(D\mathbf{T}_s^{\boldsymbol{\nu}}(\hat{\mathbf{x}}) \left\{ \mathbf{M}(\hat{\mathbf{x}}) \times \hat{\mathbf{n}}(\hat{\mathbf{x}}) \right\} \right) \, dS_{\hat{\mathbf{y}}} \, dS_{\hat{\mathbf{x}}}.$$

The equivalent pulled back formulation reads: seek $\begin{bmatrix} \hat{\boldsymbol{\psi}}_s \\ \hat{\mathbf{g}}_s \end{bmatrix} \in \boldsymbol{\mathcal{X}}_0$ such that

$$\hat{\mathsf{b}}\left(s; \begin{bmatrix} \hat{\boldsymbol{\psi}}_s \\ \hat{\mathbf{g}}_s \end{bmatrix}, \begin{bmatrix} \hat{\boldsymbol{\zeta}} \\ \hat{\mathbf{u}} \end{bmatrix}\right) = \hat{\ell}\left(s; \begin{bmatrix} \hat{\boldsymbol{\zeta}} \\ \hat{\mathbf{u}} \end{bmatrix}\right) \quad \forall \begin{bmatrix} \hat{\boldsymbol{\zeta}} \\ \hat{\mathbf{u}} \end{bmatrix} \in \boldsymbol{\mathcal{X}}_0,$$

where

$$\hat{\mathsf{b}}\left(s; \begin{bmatrix} \hat{\boldsymbol{\psi}}_s \\ \hat{\mathbf{g}}_s \end{bmatrix}, \begin{bmatrix} \hat{\boldsymbol{\zeta}} \\ \hat{\mathbf{u}} \end{bmatrix}\right) := 2\hat{\mathsf{b}}_{\mathcal{A}}(s; \hat{\boldsymbol{\psi}}, \hat{\boldsymbol{\zeta}}) - 2\hat{\mathsf{b}}_{\mathcal{C}}(s; \hat{\mathbf{g}}, \hat{\boldsymbol{\zeta}}) + 2\hat{\mathsf{b}}_{\mathcal{B}}(s; \hat{\boldsymbol{\psi}}, \hat{\mathbf{u}}) - 2\hat{\mathsf{b}}_{\mathcal{N}}(s; \hat{\mathbf{g}}, \hat{\mathbf{u}}),$$

and

$$\hat{\ell}\left(s; \begin{bmatrix} \hat{\boldsymbol{\zeta}} \\ \hat{\mathbf{u}} \end{bmatrix}\right) := \hat{\ell}_{\mathbf{J}}\left(s; \begin{bmatrix} \hat{\boldsymbol{\zeta}} \\ \hat{\mathbf{u}} \end{bmatrix}\right) + \hat{\ell}_{\mathbf{M}}\left(s; \begin{bmatrix} \hat{\boldsymbol{\zeta}} \\ \hat{\mathbf{u}} \end{bmatrix}\right).$$

Field energy for the deformed s-configuration can be written in terms of the linear form as

$$\mathcal{E}_F(s) = \frac{1}{2\mu_0} \hat{\ell}\left(s; \begin{bmatrix} -\hat{\boldsymbol{\psi}}_s \\ \hat{\mathbf{g}}_s \end{bmatrix}\right)$$

$$+ \mu_0 \int\limits_{\Gamma^0} \int\limits_{\Omega^0} G(\mathbf{T}_s^{\boldsymbol{\nu}}(\hat{\mathbf{x}}), \mathbf{T}_s^{\boldsymbol{\nu}}(\hat{\mathbf{y}})) \left(D\mathbf{T}_s^{\boldsymbol{\nu}}(\hat{\mathbf{y}}) \, \mathbf{curl M}(\hat{\mathbf{y}}) \right) \cdot \left(D\mathbf{T}_s^{\boldsymbol{\nu}}(\hat{\mathbf{x}}) \left\{ \mathbf{M}(\hat{\mathbf{x}}) \times \hat{\mathbf{n}}(\hat{\mathbf{x}}) \right\} \right) \, d\hat{\mathbf{y}} \, dS_{\hat{\mathbf{x}}}$$

$$+ \frac{\mu_0}{2} \int\limits_{\Gamma^0} \int\limits_{\Gamma^0} G(\mathbf{T}_s^{\boldsymbol{\nu}}(\hat{\mathbf{x}}), \mathbf{T}_s^{\boldsymbol{\nu}}(\hat{\mathbf{y}})) \left(D\mathbf{T}_s^{\boldsymbol{\nu}}(\hat{\mathbf{y}}) \left\{ \mathbf{M}(\hat{\mathbf{y}}) \times \hat{\mathbf{n}}(\hat{\mathbf{y}}) \right\} \right) \cdot \left(D\mathbf{T}_s^{\boldsymbol{\nu}}(\hat{\mathbf{x}}) \left\{ \mathbf{M}(\hat{\mathbf{x}}) \times \hat{\mathbf{n}}(\hat{\mathbf{x}}) \right\} \right) dS_{\hat{\mathbf{y}}} \, dS_{\hat{\mathbf{x}}}$$

$$+ \frac{\mu_0}{2} \int\limits_{\Omega^0} \int\limits_{\Omega^0} G(\mathbf{T}_s^{\boldsymbol{\nu}}(\hat{\mathbf{x}}), \mathbf{T}_s^{\boldsymbol{\nu}}(\hat{\mathbf{y}})) \left(D\mathbf{T}_s^{\boldsymbol{\nu}}(\hat{\mathbf{y}}) \, \mathbf{curl M}(\hat{\mathbf{y}}) \right) \cdot \left(D\mathbf{T}_s^{\boldsymbol{\nu}}(\hat{\mathbf{x}}) \, \mathbf{curl M}(\hat{\mathbf{x}}) \right) \, d\hat{\mathbf{y}} \, d\hat{\mathbf{x}}$$

$$+ \frac{\mu_0}{2} \int\limits_{\Omega_{\mathrm{src}}} \mathrm{N}(\mathbf{J}) \cdot \mathbf{J} \, d\mathbf{x}.$$

5.4.2.8 BIE-Constrained Shape Derivaive

To compute the shape derivative using the adjoint method, we start by defining the Lagrangian $\mathcal{L} : \mathbb{R} \times \boldsymbol{\mathcal{X}}_0 \times \boldsymbol{\mathcal{X}}_0 \to \mathbb{R}$,

$$
\mathcal{L}(s; \begin{bmatrix} \hat{\boldsymbol{\psi}} \\ \hat{\mathbf{g}} \end{bmatrix}, \begin{bmatrix} \hat{\boldsymbol{\zeta}} \\ \hat{\mathbf{u}} \end{bmatrix}) := \hat{\mathsf{b}}(s; \begin{bmatrix} \hat{\boldsymbol{\psi}} \\ \hat{\mathbf{g}} \end{bmatrix}, \begin{bmatrix} \hat{\boldsymbol{\zeta}} \\ \hat{\mathbf{u}} \end{bmatrix}) - \hat{\ell}(s; \begin{bmatrix} \hat{\boldsymbol{\zeta}} \\ \hat{\mathbf{u}} \end{bmatrix}) + \frac{1}{2\mu_0} \hat{\ell}(s; \begin{bmatrix} -\hat{\boldsymbol{\psi}} \\ \hat{\mathbf{g}} \end{bmatrix})
$$

$$
+ \mu_0 \int_{\Gamma^0} \int_{\Omega^0} G(\mathbf{T}_s^{\boldsymbol{\nu}}(\hat{\mathbf{x}}), \mathbf{T}_s^{\boldsymbol{\nu}}(\hat{\mathbf{y}})) \left(\mathsf{D}\mathbf{T}_s^{\boldsymbol{\nu}}(\hat{\mathbf{y}}) \, \mathbf{curl}\mathbf{M}(\hat{\mathbf{y}}) \right) \cdot \left(\mathsf{D}\mathbf{T}_s^{\boldsymbol{\nu}}(\hat{\mathbf{x}}) \big\{ \mathbf{M}(\hat{\mathbf{x}}) \times \hat{\mathbf{n}}(\hat{\mathbf{x}}) \big\} \right) d\hat{\mathbf{y}} \, dS_{\hat{\mathbf{x}}}
$$

$$
+ \frac{\mu_0}{2} \int_{\Gamma^0} \int_{\Gamma^0} G(\mathbf{T}_s^{\boldsymbol{\nu}}(\hat{\mathbf{x}}), \mathbf{T}_s^{\boldsymbol{\nu}}(\hat{\mathbf{y}})) \left(\mathsf{D}\mathbf{T}_s^{\boldsymbol{\nu}}(\hat{\mathbf{y}}) \big\{ \mathbf{M}(\hat{\mathbf{y}}) \times \hat{\mathbf{n}}(\hat{\mathbf{y}}) \big\} \right) \cdot
$$

$$
\left(\mathsf{D}\mathbf{T}_s^{\boldsymbol{\nu}}(\hat{\mathbf{x}}) \big\{ \mathbf{M}(\hat{\mathbf{x}}) \times \hat{\mathbf{n}}(\hat{\mathbf{x}}) \big\} \right) dS_{\hat{\mathbf{y}}} \, dS_{\hat{\mathbf{x}}}
$$

$$
+ \frac{\mu_0}{2} \int_{\Omega^0} \int_{\Omega^0} G(\mathbf{T}_s^{\boldsymbol{\nu}}(\hat{\mathbf{x}}), \mathbf{T}_s^{\boldsymbol{\nu}}(\hat{\mathbf{y}})) \left(\mathsf{D}\mathbf{T}_s^{\boldsymbol{\nu}}(\hat{\mathbf{y}}) \, \mathbf{curl}\mathbf{M}(\hat{\mathbf{y}}) \right) \cdot \left(\mathsf{D}\mathbf{T}_s^{\boldsymbol{\nu}}(\hat{\mathbf{x}}) \, \mathbf{curl}\mathbf{M}(\hat{\mathbf{x}}) \right) d\hat{\mathbf{y}} \, d\hat{\mathbf{x}}
$$

$$
+ \frac{\mu_0}{2} \int_{\Omega_{\mathrm{src}}} \mathrm{N}(\mathbf{J}) \cdot \mathbf{J} \, d\mathbf{x}.
$$

Pluggin in the pulled back state solution gives the field energy

$$
\mathcal{L}(s; \begin{bmatrix} \hat{\boldsymbol{\psi}}_s \\ \hat{\mathbf{g}}_s \end{bmatrix}, \begin{bmatrix} \hat{\boldsymbol{\zeta}} \\ \hat{\mathbf{u}} \end{bmatrix}) = \mathcal{E}_F(s) \quad \forall \begin{bmatrix} \hat{\boldsymbol{\zeta}} \\ \hat{\mathbf{u}} \end{bmatrix} \in \boldsymbol{\mathcal{X}}_0.
$$

The energy shape derivative can be computed as

$$
\frac{d\mathcal{E}_F}{ds}(0) = \frac{\partial \mathcal{L}}{\partial s}(0; \begin{bmatrix} \hat{\boldsymbol{\psi}}_0 \\ \hat{\mathbf{g}}_0 \end{bmatrix}, \begin{bmatrix} \hat{\boldsymbol{\lambda}} \\ \hat{\mathbf{p}} \end{bmatrix}),
$$

where $\begin{bmatrix} \hat{\boldsymbol{\lambda}} \\ \hat{\mathbf{p}} \end{bmatrix} \in \boldsymbol{\mathcal{X}}_0$ solves the adjoint equation

$$
\left\langle \frac{\partial \mathcal{L}}{\partial \begin{bmatrix} \hat{\boldsymbol{\psi}} \\ \hat{\mathbf{g}} \end{bmatrix}}(0; \begin{bmatrix} \hat{\boldsymbol{\psi}}_0 \\ \hat{\mathbf{g}}_0 \end{bmatrix}, \begin{bmatrix} \hat{\boldsymbol{\lambda}} \\ \hat{\mathbf{p}} \end{bmatrix}); \begin{bmatrix} \hat{\boldsymbol{\zeta}} \\ \hat{\mathbf{u}} \end{bmatrix} \right\rangle = 0 \quad \forall \begin{bmatrix} \hat{\boldsymbol{\zeta}} \\ \hat{\mathbf{u}} \end{bmatrix} \in V(\Gamma^0).
$$

Simplifying the above expression gives the adjoint equation in an explicit form

$$
\hat{\mathsf{b}}(0; \begin{bmatrix} \hat{\boldsymbol{\zeta}} \\ \hat{\mathbf{u}} \end{bmatrix}, \begin{bmatrix} \hat{\boldsymbol{\lambda}} \\ \hat{\mathbf{p}} \end{bmatrix}) = \frac{1}{2\mu_0} \hat{\ell}(0; \begin{bmatrix} \hat{\boldsymbol{\zeta}} \\ -\hat{\mathbf{u}} \end{bmatrix}) \quad \forall \begin{bmatrix} \hat{\boldsymbol{\zeta}} \\ \hat{\mathbf{u}} \end{bmatrix} \in \boldsymbol{\mathcal{X}}_0.
$$

Changing the sign of the test function $\hat{\mathbf{u}}$ gives

$$
\hat{\mathsf{b}}(0; \begin{bmatrix} \hat{\boldsymbol{\zeta}} \\ -\hat{\mathbf{u}} \end{bmatrix}, \begin{bmatrix} \hat{\boldsymbol{\lambda}} \\ \hat{\mathbf{p}} \end{bmatrix}) = \frac{1}{2\mu_0} \hat{\ell}(0; \begin{bmatrix} \hat{\boldsymbol{\zeta}} \\ \hat{\mathbf{u}} \end{bmatrix}) \quad \forall \begin{bmatrix} \hat{\boldsymbol{\zeta}} \\ \hat{\mathbf{u}} \end{bmatrix} \in \boldsymbol{\mathcal{X}}_0.
$$

We use the property

$$\hat{b}(s; \begin{bmatrix} \hat{\boldsymbol{\psi}} \\ \hat{\mathbf{g}} \end{bmatrix}, \begin{bmatrix} -\hat{\boldsymbol{\zeta}} \\ \hat{\mathbf{u}} \end{bmatrix}) = \hat{b}(s; \begin{bmatrix} \hat{\boldsymbol{\zeta}} \\ \hat{\mathbf{u}} \end{bmatrix}, \begin{bmatrix} -\hat{\boldsymbol{\psi}} \\ \hat{\mathbf{g}} \end{bmatrix}),$$

to get

$$\hat{b}(0; \begin{bmatrix} \hat{\boldsymbol{\lambda}} \\ -\hat{\mathbf{p}} \end{bmatrix}, \begin{bmatrix} \hat{\boldsymbol{\zeta}} \\ \hat{\mathbf{u}} \end{bmatrix}) = \frac{1}{2\mu_0}\hat{\ell}(0; \begin{bmatrix} \hat{\boldsymbol{\zeta}} \\ \hat{\mathbf{u}} \end{bmatrix}) \quad \forall \begin{bmatrix} \hat{\boldsymbol{\zeta}} \\ \hat{\mathbf{u}} \end{bmatrix} \in \boldsymbol{\mathcal{X}}_0,$$

which finally yields the adjoint solution as

$$\begin{bmatrix} \hat{\boldsymbol{\lambda}} \\ \hat{\mathbf{p}} \end{bmatrix} = \frac{1}{2\mu_0} \begin{bmatrix} \hat{\boldsymbol{\psi}}_0 \\ -\hat{\mathbf{g}}_0 \end{bmatrix}.$$

The shape derivative can then be computed as

$$\frac{d\mathcal{E}_F}{ds}(0) = \frac{\partial \mathcal{L}}{\partial s}(0; \begin{bmatrix} \hat{\boldsymbol{\psi}}_0 \\ \hat{\mathbf{g}}_0 \end{bmatrix}, \frac{1}{2\mu_0} \begin{bmatrix} \hat{\boldsymbol{\psi}}_0 \\ -\hat{\mathbf{g}}_0 \end{bmatrix}),$$

which simplifies to

$$\begin{aligned}
\frac{d\mathcal{E}_F}{ds}(0) ={}& \frac{1}{2\mu_0}\frac{\partial \hat{b}}{\partial s}(0; \begin{bmatrix} \hat{\boldsymbol{\psi}}_0 \\ \hat{\mathbf{g}}_0 \end{bmatrix}, \begin{bmatrix} \hat{\boldsymbol{\psi}}_0 \\ -\hat{\mathbf{g}}_0 \end{bmatrix}) + \frac{1}{\mu_0}\frac{\partial \hat{\ell}}{\partial s}(0; \begin{bmatrix} -\hat{\boldsymbol{\psi}}_0 \\ \hat{\mathbf{g}}_0 \end{bmatrix}) \\
&+ \mu_0 \int_{\Gamma^0}\int_{\Omega^0} \Big(\nabla_\mathbf{x}G(\hat{\mathbf{x}},\hat{\mathbf{y}})\cdot\boldsymbol{\mathcal{V}}(\hat{\mathbf{x}}) + \nabla_\mathbf{y}G(\hat{\mathbf{x}},\hat{\mathbf{y}})\cdot\boldsymbol{\mathcal{V}}(\hat{\mathbf{y}})\Big)\,\mathbf{curlM}(\hat{\mathbf{y}})\cdot\Big(\mathbf{M}(\hat{\mathbf{x}})\times\hat{\mathbf{n}}(\hat{\mathbf{x}})\Big)\,d\hat{\mathbf{y}}\,dS_{\hat{\mathbf{x}}} \\
&+ \mu_0 \int_{\Gamma^0}\int_{\Omega^0} G(\hat{\mathbf{x}},\hat{\mathbf{y}})\Big(\mathsf{D}\boldsymbol{\mathcal{V}}(\hat{\mathbf{y}})\,\mathbf{curlM}(\hat{\mathbf{y}})\Big)\cdot\Big(\mathbf{M}(\hat{\mathbf{x}})\times\hat{\mathbf{n}}(\hat{\mathbf{x}})\Big)\,d\hat{\mathbf{y}}\,dS_{\hat{\mathbf{x}}} \\
&+ \mu_0 \int_{\Gamma^0}\int_{\Omega^0} G(\hat{\mathbf{x}},\hat{\mathbf{y}})\,\mathbf{curlM}(\hat{\mathbf{y}})\cdot\Big(\mathsf{D}\boldsymbol{\mathcal{V}}(\hat{\mathbf{x}})\big\{\mathbf{M}(\hat{\mathbf{x}})\times\hat{\mathbf{n}}(\hat{\mathbf{x}})\big\}\Big)\,d\hat{\mathbf{y}}\,dS_{\hat{\mathbf{x}}} \\
&+ \frac{\mu_0}{2} \int_{\Gamma^0}\int_{\Gamma^0} \Big(\nabla_\mathbf{x}G(\hat{\mathbf{x}},\hat{\mathbf{y}})\cdot\boldsymbol{\mathcal{V}}(\hat{\mathbf{x}}) + \nabla_\mathbf{y}G(\hat{\mathbf{x}},\hat{\mathbf{y}})\cdot\boldsymbol{\mathcal{V}}(\hat{\mathbf{y}})\Big)\Big(\mathbf{M}(\hat{\mathbf{y}})\times\hat{\mathbf{n}}(\hat{\mathbf{y}})\Big)\cdot\Big(\mathbf{M}(\hat{\mathbf{x}})\times\hat{\mathbf{n}}(\hat{\mathbf{x}})\Big)dS_{\hat{\mathbf{y}}}\,dS_{\hat{\mathbf{x}}} \\
&+ \frac{\mu_0}{2} \int_{\Gamma^0}\int_{\Gamma^0} G(\hat{\mathbf{x}},\hat{\mathbf{y}})\Big(\mathsf{D}\boldsymbol{\mathcal{V}}(\hat{\mathbf{y}})\big\{\mathbf{M}(\hat{\mathbf{y}})\times\hat{\mathbf{n}}(\hat{\mathbf{y}})\big\}\Big)\cdot\Big(\mathbf{M}(\hat{\mathbf{x}})\times\hat{\mathbf{n}}(\hat{\mathbf{x}})\Big)dS_{\hat{\mathbf{y}}}\,dS_{\hat{\mathbf{x}}} \\
&+ \frac{\mu_0}{2} \int_{\Gamma^0}\int_{\Gamma^0} G(\hat{\mathbf{x}},\hat{\mathbf{y}})\Big(\mathbf{M}(\hat{\mathbf{y}})\times\hat{\mathbf{n}}(\hat{\mathbf{y}})\Big)\cdot\Big(\mathsf{D}\boldsymbol{\mathcal{V}}(\hat{\mathbf{x}})\big\{\mathbf{M}(\hat{\mathbf{x}})\times\hat{\mathbf{n}}(\hat{\mathbf{x}})\big\}\Big)dS_{\hat{\mathbf{y}}}\,dS_{\hat{\mathbf{x}}} \\
&+ \frac{\mu_0}{2} \int_{\Omega^0}\int_{\Omega^0} \Big(\nabla_\mathbf{x}G(\hat{\mathbf{x}},\hat{\mathbf{y}})\cdot\boldsymbol{\mathcal{V}}(\hat{\mathbf{x}}) + \nabla_\mathbf{y}G(\hat{\mathbf{x}},\hat{\mathbf{y}})\cdot\boldsymbol{\mathcal{V}}(\hat{\mathbf{y}})\Big)\,\mathbf{curlM}(\hat{\mathbf{y}})\cdot\mathbf{curlM}(\hat{\mathbf{x}})\,d\hat{\mathbf{y}}\,d\hat{\mathbf{x}} \\
&+ \frac{\mu_0}{2} \int_{\Omega^0}\int_{\Omega^0} G(\hat{\mathbf{x}},\hat{\mathbf{y}})\Big(\mathsf{D}\boldsymbol{\mathcal{V}}(\hat{\mathbf{y}})\,\mathbf{curlM}(\hat{\mathbf{y}})\Big)\cdot\mathbf{curlM}(\hat{\mathbf{x}})\,d\hat{\mathbf{y}}\,d\hat{\mathbf{x}}
\end{aligned}$$

$$+ \frac{\mu_0}{2} \int\limits_{\Omega^0} \int\limits_{\Omega^0} G(\hat{\mathbf{x}}, \hat{\mathbf{y}}) \, \mathbf{curlM}(\hat{\mathbf{y}}) \cdot \left(\mathsf{D}\boldsymbol{\mathcal{V}}(\hat{\mathbf{x}}) \, \mathbf{curlM}(\hat{\mathbf{x}}) \right) \, d\hat{\mathbf{y}} \, d\hat{\mathbf{x}}. \tag{5.4.28}$$

The partial derivative for the bilinear form can be computed based on the computations in 5.1.2.4. The partial derivative of the linear form can be computed using the partial derivatives of the two linear forms $\hat{\ell}_{\mathbf{J}}$ and $\hat{\ell}_{\mathbf{M}}$ which are given as

$$\frac{\partial \hat{\ell}_{\mathbf{J}}}{\partial s}\left(0; \begin{bmatrix} \hat{\boldsymbol{\zeta}} \\ \hat{\mathbf{u}} \end{bmatrix}\right) = \mu_0 \int\limits_{\Gamma^0} \int\limits_{\Omega_{\mathrm{src}}} \nabla_{\mathbf{x}} G(\mathbf{x}, \mathbf{y}) \cdot \boldsymbol{\mathcal{V}}(\mathbf{x}) \, \mathbf{J}(\mathbf{y}) \cdot \hat{\boldsymbol{\zeta}}(\mathbf{x}) \, d\mathbf{y} \, dS_{\mathbf{x}}$$

$$+ \mu_0 \int\limits_{\Gamma^0} \int\limits_{\Omega_{\mathrm{src}}} G(\mathbf{x}, \mathbf{y}) \, \mathbf{J}(\mathbf{y}) \cdot \left(\mathsf{D}\boldsymbol{\mathcal{V}}(\mathbf{x}) \, \hat{\boldsymbol{\zeta}}(\mathbf{x}) \right) \, d\mathbf{y} \, dS_{\mathbf{x}}$$

$$+ \mu_0 \int\limits_{\Gamma^0} \int\limits_{\Omega_{\mathrm{src}}} \left(\frac{d\nabla_{\mathbf{x}} G(\mathbf{T}_s^{\boldsymbol{\nu}}(\mathbf{x}), \mathbf{y})}{ds}\Big|_{s=0} \times \mathbf{J}(\mathbf{y}) \right) \cdot \left(\hat{\mathbf{n}} \times \hat{\mathbf{u}} \right)(\mathbf{x}) \, d\mathbf{y} \, dS_{\mathbf{x}}$$

$$+ \mu_0 \int\limits_{\Gamma^0} \int\limits_{\Omega_{\mathrm{src}}} \left(\nabla_{\mathbf{x}} G(\mathbf{x}, \mathbf{y}) \times \mathbf{J}(\mathbf{y}) \right) \cdot \left(\mathsf{D}\boldsymbol{\mathcal{V}}\{\hat{\mathbf{n}} \times \hat{\mathbf{u}}\} \right)(\mathbf{x}) \, d\mathbf{y} \, dS_{\mathbf{x}},$$

and

$$\frac{\partial \hat{\ell}_{\mathbf{M}}}{\partial s}\left(0; \begin{bmatrix} \hat{\boldsymbol{\zeta}} \\ \hat{\mathbf{u}} \end{bmatrix}\right) =$$

$$- \mu_0 \int\limits_{\Gamma^0} \int\limits_{\Omega^0} \left(\nabla_{\mathbf{x}} G(\mathbf{x}, \mathbf{y}) \cdot \boldsymbol{\mathcal{V}}(\mathbf{x}) + \nabla_{\mathbf{y}} G(\mathbf{x}, \mathbf{y}) \cdot \boldsymbol{\mathcal{V}}(\mathbf{y}) \right) \mathbf{curlM}(\mathbf{y}) \cdot \hat{\boldsymbol{\zeta}}(\mathbf{x}) \, d\mathbf{y} \, dS_{\mathbf{x}}$$

$$- \mu_0 \int\limits_{\Gamma^0} \int\limits_{\Omega^0} G(\mathbf{x}, \mathbf{y}) \left(\mathsf{D}\boldsymbol{\mathcal{V}}(\mathbf{y}) \, \mathbf{curlM}(\mathbf{y}) \right) \cdot \hat{\boldsymbol{\zeta}}(\mathbf{x}) \, d\mathbf{y} \, dS_{\mathbf{x}}$$

$$- \mu_0 \int\limits_{\Gamma^0} \int\limits_{\Omega^0} G(\mathbf{x}, \mathbf{y}) \, \mathbf{curlM}(\mathbf{y}) \cdot \left(\mathsf{D}\boldsymbol{\mathcal{V}}(\mathbf{x}) \, \hat{\boldsymbol{\zeta}}(\mathbf{x}) \right) \, d\mathbf{y} \, dS_{\mathbf{x}}$$

$$- \mu_0 \int\limits_{\Gamma^0} \int\limits_{\Omega^0} \left(\frac{d\nabla_{\mathbf{x}} G(\mathbf{T}_s^{\boldsymbol{\nu}}(\mathbf{x}), \mathbf{T}_s^{\boldsymbol{\nu}}(\mathbf{y}))}{ds}\Big|_{s=0} \times \mathbf{curlM}(\mathbf{y}) \right) \cdot \left(\hat{\mathbf{n}} \times \hat{\mathbf{u}} \right)(\mathbf{x}) \, d\mathbf{y} \, dS_{\mathbf{x}}$$

$$- \mu_0 \int\limits_{\Gamma^0} \int\limits_{\Omega^0} \left(\nabla_{\mathbf{x}} G(\mathbf{x}, \mathbf{y}) \times \left\{ \mathsf{D}\boldsymbol{\mathcal{V}}(\mathbf{y}) \, \mathbf{curlM}(\mathbf{y}) \right\} \right) \cdot \left(\hat{\mathbf{n}} \times \hat{\mathbf{u}} \right)(\mathbf{x}) \, d\mathbf{y} \, dS_{\mathbf{x}}$$

$$- \mu_0 \int\limits_{\Gamma^0} \int\limits_{\Omega^0} \left(\nabla_{\mathbf{x}} G(\mathbf{x}, \mathbf{y}) \times \mathbf{curlM}(\mathbf{y}) \right) \cdot \left(\mathsf{D}\boldsymbol{\mathcal{V}} \left\{ \hat{\mathbf{n}} \times \hat{\mathbf{u}} \right\} \right)(\mathbf{x}) \, d\mathbf{y} \, dS_{\mathbf{x}}$$

$$- \mu_0 \int\limits_{\Gamma^0} \int\limits_{\Gamma^0} \left(\nabla_{\mathbf{x}} G(\mathbf{x}, \mathbf{y}) \cdot \boldsymbol{\mathcal{V}}(\mathbf{x}) + \nabla_{\mathbf{y}} G(\mathbf{x}, \mathbf{y}) \cdot \boldsymbol{\mathcal{V}}(\mathbf{y}) \right) \left(\mathbf{M} \times \hat{\mathbf{n}} \right)(\mathbf{y}) \cdot \hat{\boldsymbol{\zeta}}(\mathbf{x}) \, dS_{\mathbf{y}} \, dS_{\mathbf{x}}$$

$$- \mu_0 \int\limits_{\Gamma^0} \int\limits_{\Gamma^0} G(\mathbf{x}, \mathbf{y}) \left(\mathsf{D}\boldsymbol{\mathcal{V}} \left\{ \mathbf{M} \times \hat{\mathbf{n}} \right\} \right)(\mathbf{y}) \cdot \hat{\boldsymbol{\zeta}}(\mathbf{x}) \, dS_{\mathbf{y}} \, dS_{\mathbf{x}}$$

$$- \mu_0 \int\limits_{\Gamma^0} \int\limits_{\Gamma^0} G(\mathbf{x}, \mathbf{y}) \left(\mathbf{M} \times \hat{\mathbf{n}} \right)(\mathbf{y}) \cdot \left(\mathsf{D} \boldsymbol{\mathcal{V}} \, \hat{\boldsymbol{\zeta}} \right)(\mathbf{x}) \, dS_\mathbf{y} \, dS_\mathbf{x}$$

$$- \mu_0 \int\limits_{\Gamma^0} \int\limits_{\Gamma^0} \left(\frac{d\nabla_\mathbf{x} G(\mathbf{T}_s^{\boldsymbol{\nu}}(\mathbf{x}), \mathbf{T}_s^{\boldsymbol{\nu}}(\mathbf{y}))}{ds} \Big|_{s=0} \times \left\{ \hat{\mathbf{n}}(\mathbf{y}) \times \hat{\mathbf{u}}(\mathbf{y}) \right\} \right) \cdot \left(\mathbf{M} \times \hat{\mathbf{n}} \right)(\mathbf{x}) \, dS_\mathbf{y} \, dS_\mathbf{x}$$

$$- \mu_0 \int\limits_{\Gamma^0} \int\limits_{\Gamma^0} \left(\nabla_\mathbf{x} G(\mathbf{x}, \mathbf{y}) \times \left\{ \mathsf{D} \boldsymbol{\mathcal{V}}(\mathbf{y}) \left(\hat{\mathbf{n}}(\mathbf{y}) \times \hat{\mathbf{u}}(\mathbf{y}) \right) \right\} \right) \cdot \left(\mathbf{M} \times \hat{\mathbf{n}} \right)(\mathbf{x}) \, dS_\mathbf{y} \, dS_\mathbf{x}$$

$$- \mu_0 \int\limits_{\Gamma^0} \int\limits_{\Gamma^0} \left(\nabla_\mathbf{x} G(\mathbf{x}, \mathbf{y}) \times \left\{ \hat{\mathbf{n}}(\mathbf{y}) \times \hat{\mathbf{u}}(\mathbf{y}) \right\} \right) \cdot \left(\mathsf{D} \boldsymbol{\mathcal{V}} \left\{ \mathbf{M} \times \hat{\mathbf{n}} \right\} \right)(\mathbf{x}) \, dS_\mathbf{y} \, dS_\mathbf{x}.$$

The partial derivative for $\nabla_x G(\mathbf{T}_s^{\boldsymbol{\nu}}(\hat{\mathbf{x}}), \mathbf{T}_s^{\boldsymbol{\nu}}(\hat{\mathbf{y}}))$ with respect to s is given as (5.1.38). We can also compute

$$\frac{d\nabla_\mathbf{x} G(\mathbf{T}_s^{\boldsymbol{\nu}}(\mathbf{x}), \mathbf{y})}{ds} \Big|_{s=0} = \mathsf{D}_x \nabla_x G(\mathbf{x}, \mathbf{y}) \, \boldsymbol{\mathcal{V}}(\mathbf{x}) = \nabla_x \nabla_x G(\mathbf{x}, \mathbf{y}) \, \boldsymbol{\mathcal{V}}(\mathbf{x}), \tag{5.4.29}$$

where $\nabla_x \nabla_x G(\mathbf{x}, \mathbf{y})$ is explicitly computed in (4.1.19).

5.4.2.9 Numerical Experiments

In this section we evaluate the shape derivatives numerically and investigate their performance. The shape derivative formulas we compare are (5.4.28) (called "BEM" in the plots) and the equivalent current model (5.4.12) (called "MST" in the plots). To keep things simple in terms to implementation, we choose the magnetization $\mathbf{M}$ such that $\mathbf{curl M} = 0$ inside Ω. This can be achieved by either using a constant magnetization, or a gradient free magnetization. This allows us to have purely boundary based expressions which can be evaluated by directly using the BEM solution obtained from a discretization of (5.4.26). The discrete spaces used are already introcuced in Section 5.1.2.8 as we have the same bilinear form on the left hand side in (5.1.31). The evaluation of discrete solution and the shape derivatives is thus carried out in an identical fashion. For convergence studies we evaluate the Galerkin solution and plug it into the shape derivative formulas for a decreasing meshwidth h. Forces and torques are computed using the recipe mentioned in Section 3.0.2 and dualnorm error is computed based on the procedure laid out in Section 4.4.7.1.

Experiment 35. Choosing $\mu_0 = 1$ and $\mathbf{M} \equiv (1, 0, 0)$ we consider a cube shaped permanent magnet in the presence of a source current. The geometrical situation is described in Figure 5.2 where the torus carries a unit tangential surface current density. The reference force and torque values are computed using the BEM based shape derivative at a refinement level of $h = 0.07$. Torque is computed about the point (4,0,0). The corresponding errors are plotted in Figure 5.65 and the convergence rates are tabulated in Table 5.25. It is clear that the BEM based shape derivative has an edge over the equivalent current model for the cube shaped geometry.
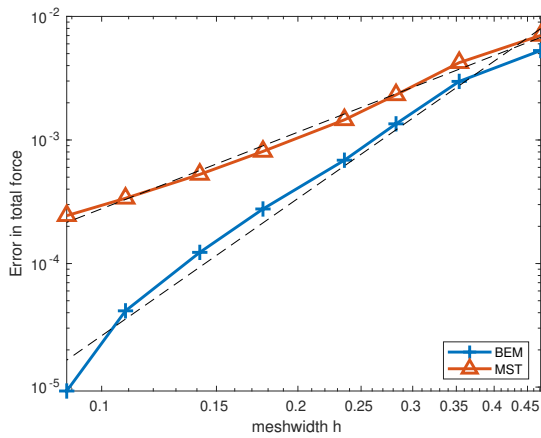
(a) Error in total force
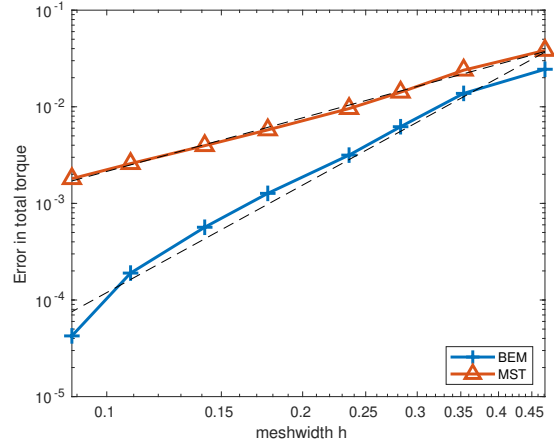
(b) Error in total torque

Figure 5.65: Error in force and torque computation for cube torus (Experiment 35)

Table 5.25: Asymptotic rate of algebraic convergence for Experiment 35

Method	Force	Torque
Pullback approach	3.691	3.696
Stress tensor	2.006	1.843

The performance of the two shape derivatives can also be compared via dual norm error computation which is presented in Figure 5.66. The reference values are computed using the BEM based shape derivative at the refinement level $h = 0.088$. This error computation cements the superiority of the BEM based shape derivative formula.

Figure 5.66: Dual norm error for Experiment 35

Experiment 36. Keeping $\mu_0 = 1$, we consider a spherical permanent magnet with $\mathbf{M} \equiv (1, 0, 0)$ as shown in Figure 5.5. The reference values for force and torque are computed using

216

the BEM based shape derivative at a refinement level $h = 0.039$, resulting in the error plot Figure 5.67 and convergence rates given in Table 5.26. Torque is computed about the point (4,0,0). We see similar convergence rates as expected for the smooth domain.

(a) Error in total force

(b) Error in total torque
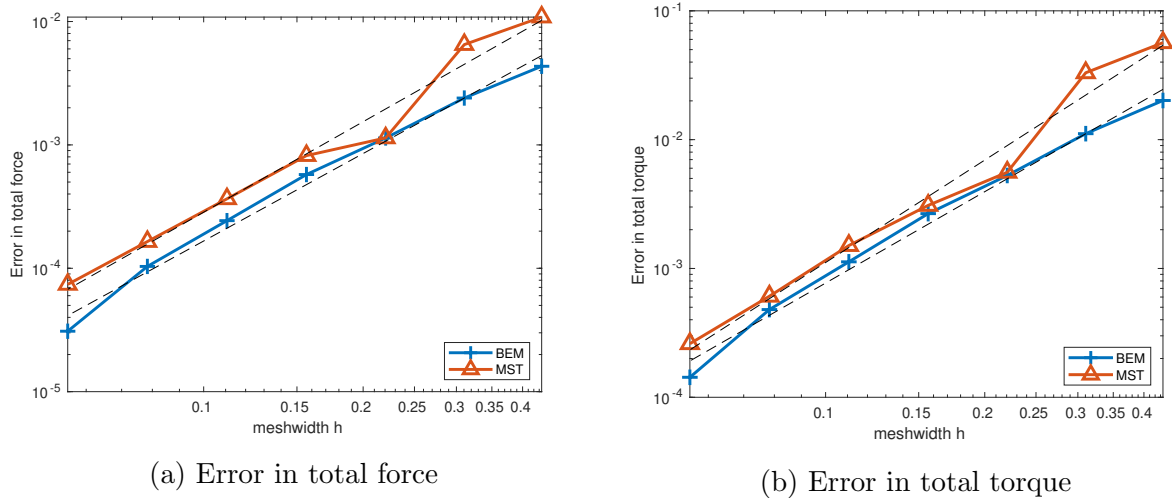
Figure 5.67: Error in force and torque computation for sphere and torus (Experiment 36)

Table 5.26: Asymptotic rate of algebraic convergence for Experiment 36

Method	Force	Torque
Pullback approach	2.355	2.357
Stress tensor	2.436	2.642

The dual norm errors are also compared where the reference values were computed using the BEM based shape derivative at a refinement level of $h = 0.039$. The results are shown in Figure 5.68. We see a sligtly superior performance from the BEM based shape derivative.
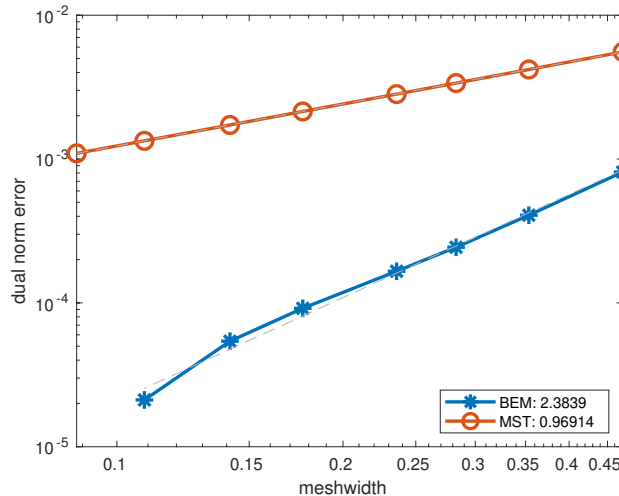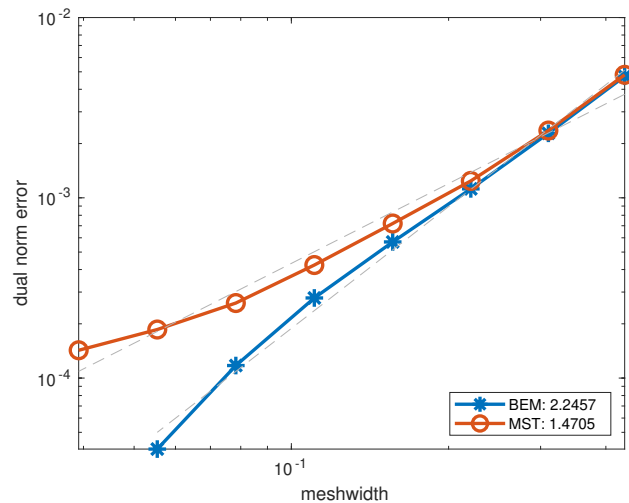

Figure 5.68: Dual norm error for Experiment 36

Experiment 37. Keeping $\mu_0 = 1$, we consider a brick shaped permanent magnet with $\mathbf{M} \equiv (1, 0, 0)$ as shown in Experiment 13. The reference values for force and torque are computed using the BEM based shape derivative at a refinement level $h = 0.05$, resulting in the error plot Figure 5.69 and convergence rates given in Table 5.27. Torque is computed about the point (4,0,0). We see a superior performance from the BEM based shape derivative for this non smooth case.

(a) Error in total force   (b) Error in total torque

Figure 5.69: Error in force and torque computation for cuboid and torus (Experiment 37)

Table 5.27: Asymptotic rate of algebraic convergence for Experiment 37

Method	Force	Torque
Pullback approach	3.61	3.73
Stress tensor	1.65	1.62

The dual norm errors are also compared where the reference values were computed using the BEM based shape derivative at a refinement level of $h = 0.064$. The results are shown in Figure 5.70 which confirms the superiority of the BEM based shape derivative.

Figure 5.70: Dual norm error for Experiment 37

Experiment 38. Keeping $\mu_0 = 1$, we consider a tetrahedral shaped permanent magnet with $\mathbf{M} \equiv (1, 0, 0)$ as shown in Experiment 14. The reference values for force and torque are computed using the BEM based shape derivative at a refinement level $h = 0.041$, resulting in the error plot Figure 5.71 and convergence rates given in Table 5.28. Torque is computed about the point (4,0,0). We see a superior performance from the BEM based shape derivative.

(a) Error in total force
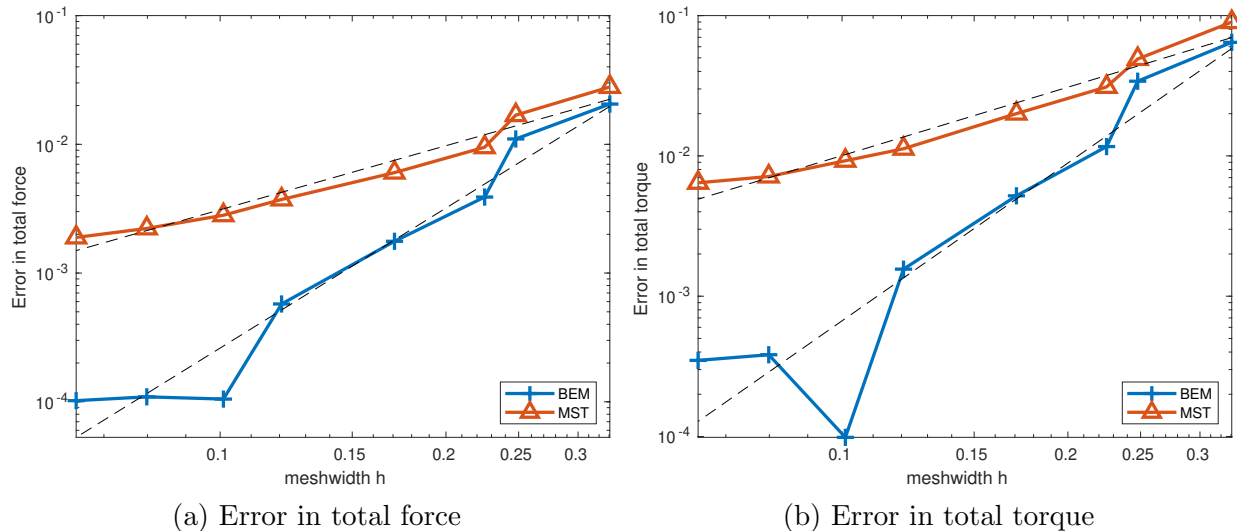
(b) Error in total torque
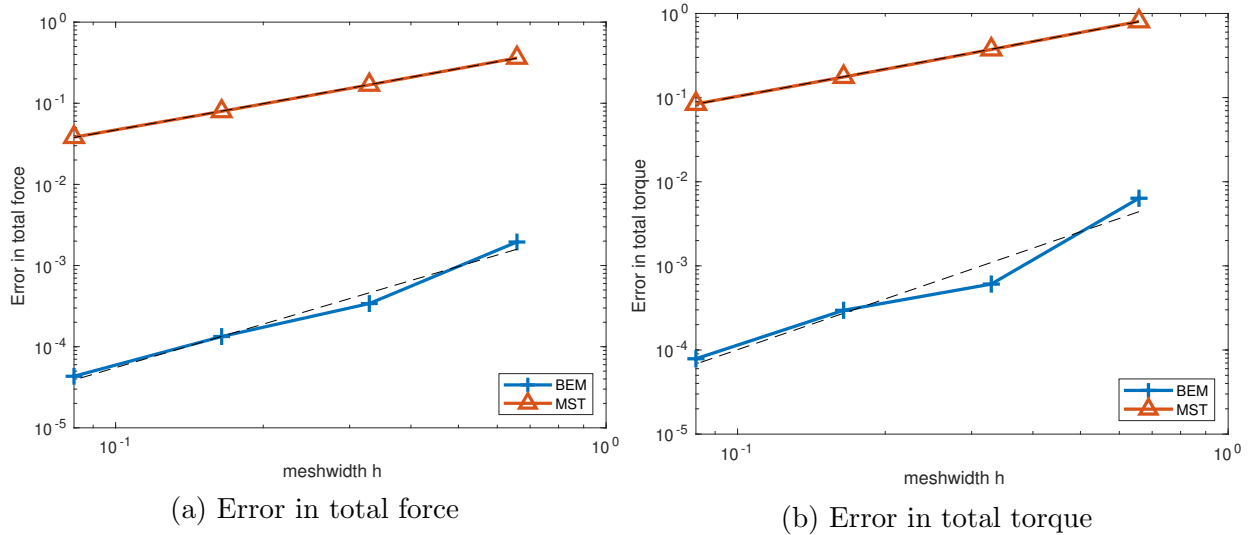
Figure 5.71: Error in force and torque computation for tetrahedron and torus (Experiment 38)

Table 5.28: Asymptotic rate of algebraic convergence for Experiment 38

Method	Force	Torque
Pullback approach	1.78	2.00
Stress tensor	1.08	1.09

The dual norm errors are also compared where the reference values were computed using the BEM based shape derivative at a refinement level of $h = 0.041$. The results are shown in Figure 5.72, which confirm the superiority of the BEM based shape derivative.
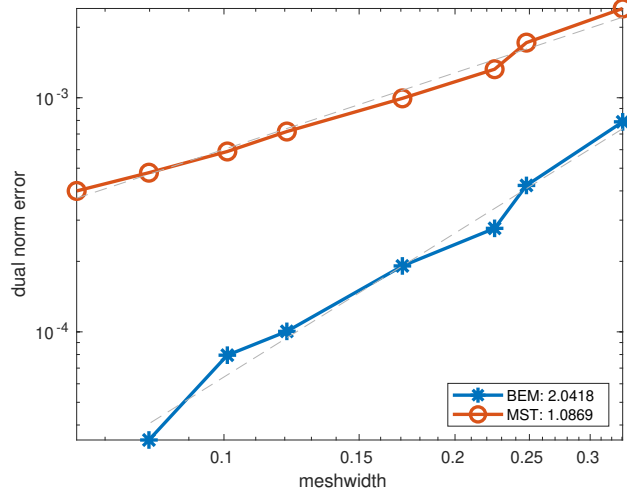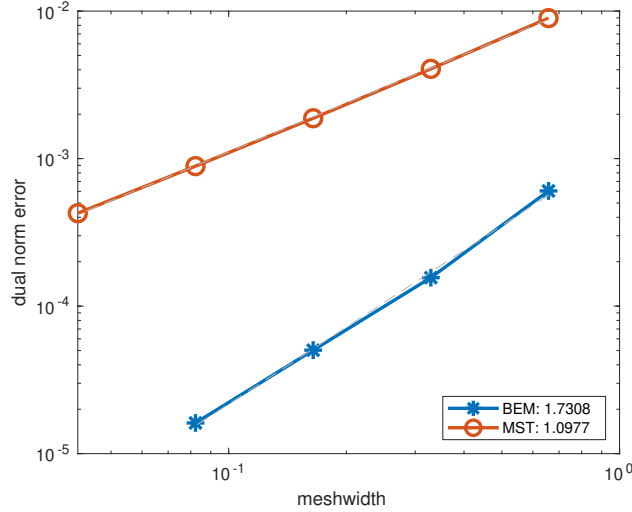

Figure 5.72: Dual norm error for Experiment 38

5.4.3   Scalar Potential Formulation

To get to the scalar potential formulation, we start with the magnetostatic equations

$$\operatorname{div} \mathbf{B} = 0 \quad \text{in } \mathbb{R}^3$$
$$\mathbf{curl}\mathbf{H} = \mathbf{J} \quad \text{in } \mathbb{R}^3.$$

We mention again that $\operatorname{supp}(\mathbf{J}) = \Omega_{\mathrm{src}} \Subset \mathbb{R}^3$, such that $\overline{\Omega}_{\mathrm{src}} \cap \overline{\Omega} = \phi$. Defining $\tilde{\mathbf{H}} := \mathbf{H} - \mathbf{H_J}$, where $\mathbf{H} := \int\limits_{\Omega_{\mathrm{src}}} G(\mathbf{x}, \mathbf{y}) \, \mathbf{J}(\mathbf{y}) \, d\mathbf{y}$, the equation for the field $\mathbf{H}$ can be written as

$$\mathbf{curl}\tilde{\mathbf{H}} = \mathbf{curl}(\mathbf{H} - \mathbf{H_J}) = 0 \quad \text{in } \mathbb{R}^3,$$

where $\mathbf{H_J}$ was already defined in (5.1.6). We can introduce a scalar potential u such that $\tilde{\mathbf{H}} = \nabla u$. Using the material law we have the relations

$$\mathbf{H} = \mu_0^{-1}\mathbf{B} - \mathbf{M} \quad \text{in } \Omega,$$
$$\mathbf{H} = \mu_0^{-1}\mathbf{B} \qquad \text{in } \Omega_c.$$

Combining them with $\Delta u = \operatorname{div} \tilde{\mathbf{H}} = \operatorname{div} \mathbf{H}$ $(\operatorname{div} \mathbf{H_J} = 0)$, we get

$$\Delta u = -\operatorname{div} \mathbf{M} \quad \text{in } \Omega,$$
$$\Delta u = 0 \qquad \text{in } \Omega_c.$$

Transmission condition for $\gamma_N u$ can be obtained as

$$0 = [\![\mathbf{B}]\!]_\Gamma \cdot \mathbf{n} = \mu_0 \, \mathbf{H}^+ \cdot \mathbf{n} - \mu_0 \, \mathbf{H}^- \cdot \mathbf{n} - \mu_0 \, \mathbf{M} \cdot \mathbf{n}$$

$$= \mu_0 \left(\nabla u^+ + \mathbf{H_J} \right) \cdot \mathbf{n} - \mu_0 \left(\nabla u^- + \mathbf{H_J} \right) \cdot \mathbf{n} - \mu_0 \, \mathbf{M} \cdot \mathbf{n}$$
$$= \mu_0 \, [\![\nabla u]\!]_\Gamma \cdot \mathbf{n} - \mu_0 \, \mathbf{M} \cdot \mathbf{n},$$

which gives

$$[\![\nabla u]\!]_\Gamma \cdot \mathbf{n} = \mathbf{M} \cdot \mathbf{n}.$$

To get the transmission condition for the Dirichlet trace, we consider

$$\mathbf{curl}_\Gamma \, [\![\gamma_D u]\!]_\Gamma = [\![\nabla u]\!]_\Gamma \times \mathbf{n} = \left[\!\!\left[\tilde{\mathbf{H}} \right]\!\!\right]_\Gamma \times \mathbf{n} = [\![\mathbf{H} - \mathbf{H_J}]\!]_\Gamma \times \mathbf{n} = [\![\mathbf{H}]\!]_\Gamma \times \mathbf{n} = 0.$$

Thus we can set $[\![\gamma_D u]\!]_\Gamma = 0$. We have the transmission problem

$$
\begin{aligned}
-\Delta u = \operatorname{div} \mathbf{M} = \rho & \quad \text{in } \Omega, \\
\Delta u = 0 & \quad \text{in } \Omega_c, \\
[\![\gamma_D u]\!]_\Gamma = 0 & \quad \text{on } \Gamma, \\
[\![\gamma_N u]\!]_\Gamma = \mathbf{M} \cdot \mathbf{n} = \lambda & \quad \text{on } \Gamma, \\
|u(\mathbf{x})| = O(\|\mathbf{x}\|^{-1}) & \quad \text{for } \|\mathbf{x}\| \to \infty.
\end{aligned}
\tag{5.4.30}
$$

5.4.3.1 Shape Derivative From Volume Based Variational Formulation

Assuming $\mathbf{M} \in H(\operatorname{div}; \Omega)$, the transmission problem (5.4.30) admits a weak solution $u \in H^1(\Delta; \mathbb{R}^3) := \{ u : \mathbb{R}^3 \to \mathbb{R} : \int_{\mathbb{R}^3} \|\nabla u\|^2 + \frac{u^2}{1+\|\mathbf{x}\|^2} \, d\mathbf{x} < \infty \}$ which solves the variational equation

$$\int_{\mathbb{R}^3} \nabla u(\mathbf{x}) \cdot \nabla v(\mathbf{x}) \, d\mathbf{x} = -\int_\Gamma v \, \mathbf{M} \cdot \mathbf{n} \, d\mathrm{S} + \int_\Omega \operatorname{div} \mathbf{M} \, v \, d\mathbf{x} \quad \forall v \in H^1(\Delta; \mathbb{R}^3). \tag{5.4.31}$$

The co-energy $\mathcal{J}_F$ can be written in terms of the bilinear form as

$$
\begin{aligned}
\mathcal{J}_F &= \frac{\mu_0}{2} \int_{\mathbb{R}^3} \|\mathbf{H}\|^2 \, d\mathbf{x} + \mu_0 \int_\Omega \mathbf{M} \cdot \mathbf{H} \, d\mathbf{x} \\
&= \frac{\mu_0}{2} \int_\Omega \|\nabla u\|^2 \, d\mathbf{x} + \frac{\mu_0}{2} \int_{\Omega_c} \|\nabla u\|^2 \, d\mathbf{x} + \frac{\mu_0}{2} \int_{\mathbb{R}^3} \|\mathbf{H_J}\|^2 \, d\mathbf{x} \\
&\quad + \mu_0 \int_\Omega \nabla u \cdot \mathbf{H_J} \, d\mathbf{x} + \mu_0 \int_{\Omega_c} \nabla u \cdot \mathbf{H_J} \, d\mathbf{x} + \mu_0 \int_\Omega \mathbf{M} \cdot \nabla u \, d\mathbf{x} + \mu_0 \int_\Omega \mathbf{M} \cdot \mathbf{H_J} \, d\mathbf{x} \\
&= -\frac{\mu_0}{2} \int_\Gamma g \, \mathbf{M} \cdot \mathbf{n} \, d\mathrm{S} + \frac{\mu_0}{2} \int_\Omega u \, \operatorname{div} \mathbf{M} \, d\mathbf{x} + \frac{\mu_0}{2} \int_{\mathbb{R}^3} \|\mathbf{H_J}\|^2 \, d\mathbf{x} \\
&\quad + 0 + \mu_0 \int_\Gamma g \, \mathbf{M} \cdot \mathbf{n} \, d\mathrm{S} - \mu_0 \int_\Omega u \, \operatorname{div} \mathbf{M} \, d\mathbf{x} + \mu_0 \int_\Omega \mathbf{M} \cdot \mathbf{H_J} \, d\mathbf{x} \\
&= -\frac{\mu_0}{2} \int_{\mathbb{R}^3} \|\nabla u\|^2 \, d\mathbf{x} + \frac{\mu_0}{2} \int_{\mathbb{R}^3} \|\mathbf{H_J}\|^2 \, d\mathbf{x} + \mu_0 \int_\Omega \mathbf{M} \cdot \mathbf{H_J} \, d\mathbf{x}.
\end{aligned}
$$

In the above manipulations we used Green's first identity, the transmission conditions and the fact that $\operatorname{div} \mathbf{H_J} = 0$.

5.4.3.2 Variational Formulation for Deformed Domain

We deform only the magnet and transform its magnetization as a 2-form to $\mathbf{M}_s \in H(\mathrm{div}; \Omega^s)$ such that $\mathbf{M}_s(\mathbf{T}_s^{\boldsymbol{\nu}}(\hat{\mathbf{x}})) = \frac{\mathrm{D}\mathbf{T}_s^{\boldsymbol{\nu}}(\hat{\mathbf{x}})}{\det \mathrm{D}\mathbf{T}_s^{\boldsymbol{\nu}}(\hat{\mathbf{x}})}\mathbf{M}(\hat{\mathbf{x}})$. Variational formulation for the deformed s-configuration has a similar structure to (5.4.31): seek $u_s \in H^1(\Delta; \mathbb{R}^3)$ such that

$$\int_{\mathbb{R}^3} \nabla u_s(\mathbf{x}) \cdot \nabla v(\mathbf{x}) \, d\mathbf{x} = -\int_{\Gamma^s} v \, \mathbf{M}_s \cdot \mathbf{n} \, dS + \int_{\Omega^s} \mathrm{div}\, \mathbf{M}_s \, v \, d\mathbf{x} \quad \forall v \in H^1(\Delta; \mathbb{R}^3).$$

To simplify the notation a bit, we will write

$$\mathrm{div}\, \mathbf{M}_s = \rho_s \in L^2(\Omega^s) \quad \text{in } \Omega^s, \quad \mathbf{M}_s \cdot \mathbf{n} = \lambda_s \in H^{-\frac{1}{2}}(\Gamma^s) \quad \text{on } \Gamma^s.$$

5.4.3.3 Transformation + Pullback

Using the perturbation map, the integrals can be written on reference domains. This gives us

$$\int_{\mathbb{R}^3} \nabla u_s(\mathbf{x}) \cdot \nabla v(\mathbf{x}) \, d\mathbf{x} = \int_{\mathbb{R}^3} \nabla u_s(\mathbf{T}_s^{\boldsymbol{\nu}}(\hat{\mathbf{x}})) \cdot \nabla v(\mathbf{T}_s^{\boldsymbol{\nu}}(\hat{\mathbf{x}})) \, \det \mathrm{D}\mathbf{T}_s^{\boldsymbol{\nu}}(\hat{\mathbf{x}}) \, d\hat{\mathbf{x}},$$

$$\int_{\Gamma^s} v \, \mathbf{H}_{\mathbf{J}} \cdot \mathbf{n} \, dS = \int_{\Gamma^0} v(\mathbf{T}_s^{\boldsymbol{\nu}}(\hat{\mathbf{x}})) \, \mathbf{H}_{\mathbf{J}}(\mathbf{T}_s^{\boldsymbol{\nu}}(\hat{\mathbf{x}})) \cdot \mathbf{n}(\mathbf{T}_s^{\boldsymbol{\nu}}(\hat{\mathbf{x}})) \, \omega_s(\hat{\mathbf{x}}) \, dS_{\hat{\mathbf{x}}},$$

$$\int_{\Gamma^s} v \, \lambda_s \, dS = \int_{\Gamma^0} v(\mathbf{T}_s^{\boldsymbol{\nu}}(\hat{\mathbf{x}})) \, \lambda_s(\mathbf{T}_s^{\boldsymbol{\nu}}(\hat{\mathbf{x}})) \, \omega_s(\hat{\mathbf{x}}) \, dS_{\hat{\mathbf{x}}},$$

$$\int_{\Omega^s} \rho_s \, v \, d\mathbf{x} = \int_{\Omega^0} \rho_s(\mathbf{T}_s^{\boldsymbol{\nu}}(\hat{\mathbf{x}})) \, v(\mathbf{T}_s^{\boldsymbol{\nu}}(\hat{\mathbf{x}})) \, \det \mathrm{D}\mathbf{T}_s^{\boldsymbol{\nu}}(\hat{\mathbf{x}}) \, d\hat{\mathbf{x}}.$$

Based on the pullbacks

$$\lambda(\hat{\mathbf{x}}) = \lambda_s(\mathbf{T}_s^{\boldsymbol{\nu}}(\hat{\mathbf{x}})) \, \omega_s(\hat{\mathbf{x}}), \quad \rho(\hat{\mathbf{x}}) = \rho_s(\mathbf{T}_s^{\boldsymbol{\nu}}(\hat{\mathbf{x}})) \, \det \mathrm{D}\mathbf{T}_s^{\boldsymbol{\nu}}(\hat{\mathbf{x}}), \quad \hat{u}(\hat{\mathbf{x}}) = u_s(\mathbf{T}_s^{\boldsymbol{\nu}}(\hat{\mathbf{x}})),$$

we define the pulled back hat (bi)linear forms

$$\hat{\mathsf{b}}(s; \hat{u}, \hat{v}) := \int_{\mathbb{R}^3} \left(\mathrm{D}\mathbf{T}_s^{\boldsymbol{\nu}}(\hat{\mathbf{x}})^{-T} \nabla \hat{u}(\hat{\mathbf{x}}) \right) \cdot \left(\mathrm{D}\mathbf{T}_s^{\boldsymbol{\nu}}(\hat{\mathbf{x}})^{-T} \nabla \hat{v}(\hat{\mathbf{x}}) \right) \, \det \mathrm{D}\mathbf{T}_s^{\boldsymbol{\nu}}(\hat{\mathbf{x}}) \, d\hat{\mathbf{x}},$$

$$\hat{\ell}(s; \hat{v}) := -\int_{\Gamma^0} \hat{v} \, \lambda \, dS + \int_{\Omega^0} \hat{v} \, \rho \, d\mathbf{x}.$$

The pulled back formulation reads: seek $\hat{u}_s \in V_0 := H^1(\Delta; \mathbb{R}^3)$ such that

$$\hat{\mathsf{b}}(s; \hat{u}_s, \hat{v}) = \hat{\ell}(s; \hat{v}) \quad \forall \hat{v} \in V_0.$$

Co-energy $\mathcal{J}_F$ for the deformed configuration can be expressed in terms of the pulled back bilinear form as

$$\mathcal{J}_F(s) = -\frac{\mu_0}{2} \hat{\mathsf{b}}(s; \hat{u}_s, \hat{u}_s) + \frac{\mu_0}{2} \int_{\mathbb{R}^3} \|\mathbf{H}_{\mathbf{J}}(\mathbf{T}_s^{\boldsymbol{\nu}}(\hat{\mathbf{x}}))\|^2 \, \det \mathrm{D}\mathbf{T}_s^{\boldsymbol{\nu}}(\hat{\mathbf{x}}) \, d\hat{\mathbf{x}}$$

$$+ \mu_0 \int_{\Omega^0} \left(\mathsf{D}\mathbf{T}_s^{\boldsymbol{\nu}}(\hat{\mathbf{x}}) \, \hat{\mathbf{M}}(\hat{\mathbf{x}}) \right) \cdot \mathbf{H_J}(\mathbf{T}_s^{\boldsymbol{\nu}}(\hat{\mathbf{x}})) \, d\hat{\mathbf{x}}.$$

In the above expression, it is assumed that $\mathbf{H_J}$ is not subject to the transformation.

5.4.3.4 Adjoint Method

To compute the shape derivative using the adjoint method, we start with the Lagrangian $\mathcal{L} : \mathbb{R} \times V_0 \times V_0 \to \mathbb{R}$,

$$\mathcal{L}(s; \hat{u}, \hat{v}) := \hat{\mathsf{b}}(s; \hat{u}, \hat{v}) - \hat{\ell}(s; \hat{v}) - \frac{\mu_0}{2} \hat{\mathsf{b}}(s; \hat{u}, \hat{u}) + \frac{\mu_0}{2} \int_{\mathbb{R}^3} \|\mathbf{H_J}(\mathbf{T}_s^{\boldsymbol{\nu}}(\hat{\mathbf{x}}))\|^2 \, \det \mathsf{D}\mathbf{T}_s^{\boldsymbol{\nu}}(\hat{\mathbf{x}}) \, d\hat{\mathbf{x}}$$

$$+ \mu_0 \int_{\Omega^0} \left(\mathsf{D}\mathbf{T}_s^{\boldsymbol{\nu}}(\hat{\mathbf{x}}) \, \hat{\mathbf{M}}(\hat{\mathbf{x}}) \right) \cdot \mathbf{H_J}(\mathbf{T}_s^{\boldsymbol{\nu}}(\hat{\mathbf{x}})) \, d\hat{\mathbf{x}}.$$

we get the co-energy after plugging in the state solution

$$\mathcal{J}_F(s) = \mathcal{L}(s; \hat{u}_s, \hat{v}) \quad \forall \hat{v} \in V_0.$$

The energy shape derivative can be computed as

$$\frac{d\mathcal{J}_F}{ds}(0) = \frac{\partial \mathcal{L}}{\partial s}(0; \hat{u}_0, \hat{p}),$$

where $\hat{p} \in V_0$ solves the adjoint equation

$$\left\langle \frac{\partial \mathcal{L}}{\partial \hat{u}}(0; \hat{u}_0, \hat{p}); \hat{v} \right\rangle = 0 \quad \forall \hat{v} \in V_0.$$

The adjoint equation simplifies to

$$\hat{\mathsf{b}}(0; \hat{v}, \hat{p}) = \mu_0 \, \hat{\mathsf{b}}(0; \hat{v}, \hat{u}_0) \quad \forall \hat{v} \in V_0,$$

which yields the adjoint solution in an explicit form as

$$\hat{p} = \mu_0 \, \hat{u}_0.$$

The shape derivative can be computed using formulas (3.0.12), (3.0.11) and $\frac{d}{ds} \mathbf{H_J}(\mathbf{T}_s^{\boldsymbol{\nu}}(\hat{\mathbf{x}}))|_{s=0} = \mathsf{D}\mathbf{H_J}(\hat{\mathbf{x}}) \, \boldsymbol{\mathcal{V}}(\hat{\mathbf{x}})$ and is given as

$$\frac{d\mathcal{J}_F}{ds}(0) = \frac{\partial \mathcal{L}}{\partial s}(0; \hat{u}_0, \mu_0 \, \hat{u}_0) = \frac{\mu_0}{2} \frac{\partial \hat{\mathsf{b}}}{\partial s}(0; \hat{u}_0, \hat{u}_0) - \frac{\partial \hat{\ell}}{\partial s}(0; \mu_0 \, \hat{u}_0)$$

$$+ \mu_0 \int_{\Omega^0} \left(\mathsf{D}\boldsymbol{\mathcal{V}} \, \mathbf{M} \right) \cdot \mathbf{H_J} + \left(\mathsf{D}\mathbf{H_J} \, \boldsymbol{\mathcal{V}} \right) \cdot \mathbf{M} \, d\mathbf{x}$$

$$= \frac{\mu_0}{2} \int_{\mathbb{R}^3} \left(- \nabla \hat{u}_0^T (\mathsf{D}\boldsymbol{\mathcal{V}}^T + \mathsf{D}\boldsymbol{\mathcal{V}}) \, \nabla \hat{u}_0 + \|\nabla \hat{u}_0\|^2 \, \nabla \cdot \boldsymbol{\mathcal{V}} \right) d\mathbf{x}$$

$$+ \mu_0 \int\limits_{\Omega^0} \left(\mathsf{D} \boldsymbol{\mathcal{V}} \, \mathbf{M} \right) \cdot \mathbf{H_J} + \left(\mathsf{D} \mathbf{H_J} \, \boldsymbol{\mathcal{V}} \right) \cdot \mathbf{M} \ d\mathbf{x}. \qquad (5.4.32)$$

Note that the partial derivative of $\hat{\ell}$ is zero. The integrand in the latter term is simplified as

$$\mathbf{H_J}^T \, \mathsf{D} \boldsymbol{\mathcal{V}} \, \mathbf{M} + \mathbf{M}^T \, \mathsf{D} \mathbf{H_J} \, \boldsymbol{\mathcal{V}} = \mathbf{H_J}^T \, \mathsf{D} \boldsymbol{\mathcal{V}} \, \mathbf{M} + \mathbf{M}^T \, \nabla \mathbf{H_J} \, \boldsymbol{\mathcal{V}} + \mathbf{M}^T \, \mathsf{D} \mathbf{H_J} \, \boldsymbol{\mathcal{V}} - \mathbf{M}^T \, \nabla \mathbf{H_J} \, \boldsymbol{\mathcal{V}}$$

$$= \mathbf{M}^T \left(\nabla \boldsymbol{\mathcal{V}} \, \mathbf{H_J} + \nabla \mathbf{H_J} \, \boldsymbol{\mathcal{V}} \right) + \mathbf{M}^T \left(\mathbf{curl} \mathbf{H_J} \times \boldsymbol{\mathcal{V}} \right)$$

$$= \mathbf{M} \cdot \nabla \left(\boldsymbol{\mathcal{V}} \cdot \mathbf{H_J} \right),$$

since $\mathbf{curl} \mathbf{H_J} = 0$ inside Ω^0. The latter integral then becomes

$$\int\limits_{\Omega^0} \mathbf{M} \cdot \nabla \left(\boldsymbol{\mathcal{V}} \cdot \mathbf{H_J} \right) \ d\mathbf{x} = \int\limits_{\Gamma^0} \boldsymbol{\mathcal{V}} \cdot \mathbf{H_J} \, \mathbf{M} \cdot \mathbf{n} \ dS - \int\limits_{\Omega^0} \boldsymbol{\mathcal{V}} \cdot \mathbf{H_J} \, \text{div} \, \mathbf{M} \ d\mathbf{x}.$$

The first term in (5.4.32) can be simplified in a similar fashion to Section 4.4.5 which leads to:

$$\frac{\mu_0}{2} \int\limits_{\mathbb{R}^3} \left(- \nabla \hat{u}_0^T (\mathsf{D} \boldsymbol{\mathcal{V}}^T + \mathsf{D} \boldsymbol{\mathcal{V}}) \, \nabla \hat{u}_0 + \| \nabla \hat{u}_0 \|^2 \, \nabla \cdot \boldsymbol{\mathcal{V}} \right) d\mathbf{x} = \mu_0 \int\limits_{\Omega} \nabla \cdot \left\{ \frac{\| \nabla \hat{u}_0 \|^2}{2} \mathsf{Id} - \nabla \hat{u}_0 \, \nabla \hat{u}_0^T \right\} d\mathbf{x}$$

$$+ \mu_0 \int\limits_{\Omega_c} \nabla \cdot \left\{ \frac{\| \nabla \hat{u}_0 \|^2}{2} \mathsf{Id} - \nabla \hat{u}_0 \, \nabla \hat{u}_0^T \right\} d\mathbf{x}$$

$$- \mu_0 \int\limits_{\Omega} \boldsymbol{\mathcal{V}} \cdot \nabla \hat{u}_0 \ \text{div} \, \mathbf{M} \ d\mathbf{x}.$$

Using the divergence theorem, we transform the integrals to the boundary and get the jump of the Maxwell Stress Tensor. Calling u_i the solution inside and u_o the solution outside, we see:

$$\left(\nabla u_o \, \nabla u_o \cdot \mathbf{n} - \frac{\| \nabla u_o \|^2}{2} \, \mathbf{n} \right) - \left(\nabla u_i \, \nabla u_i \cdot \mathbf{n} - \frac{\| \nabla u_i \|^2}{2} \, \mathbf{n} \right)$$

$$= (\nabla u_o \cdot \mathbf{n})^2 \, \mathbf{n} + (\nabla u_o \cdot \mathbf{n}) \, \mathbf{grad}_\Gamma \, u_o - \frac{(\nabla u_o \cdot \mathbf{n})^2}{2} \, \mathbf{n} - \frac{\| \mathbf{grad}_\Gamma \, u_o \|^2}{2} \, \mathbf{n}$$

$$- (\nabla u_i \cdot \mathbf{n})^2 \, \mathbf{n} - (\nabla u_i \cdot \mathbf{n}) \, \mathbf{grad}_\Gamma \, u_i + \frac{(\nabla u_i \cdot \mathbf{n})^2}{2} \, \mathbf{n} + \frac{\| \mathbf{grad}_\Gamma \, u_i \|^2}{2} \, \mathbf{n}$$

$$= \left((\nabla u_o \cdot \mathbf{n})^2 - (\nabla u_i \cdot \mathbf{n})^2 \right) \frac{\mathbf{n}}{2} + \left((\nabla u_o \cdot \mathbf{n}) - (\nabla u_i \cdot \mathbf{n}) \right) \mathbf{grad}_\Gamma \, g$$

$$= \left((\nabla u_o \cdot \mathbf{n}) - (\nabla u_i \cdot \mathbf{n}) \right) \left\{ \left((\nabla u_o \cdot \mathbf{n}) + (\nabla u_i \cdot \mathbf{n}) \right) \frac{\mathbf{n}}{2} + \mathbf{grad}_\Gamma \, g \right\}$$

$$= (\mathbf{M} \cdot \mathbf{n}) \left\{ \left((\nabla u_o \cdot \mathbf{n}) + (\nabla u_i \cdot \mathbf{n}) \right) \frac{\mathbf{n}}{2} + \mathbf{grad}_\Gamma \, g \right\}$$

$$= (\mathbf{M} \cdot \mathbf{n}) \, \{ \tilde{\mathbf{H}} \}.$$

So the shape derivative reduces to

$$\frac{d\mathcal{J}_F}{ds}(0) = \mu_0 \int_{\Gamma^0} \boldsymbol{\mathcal{V}} \cdot \mathbf{H_J} \, (\mathbf{M} \cdot \mathbf{n}) \, dS - \mu_0 \int_{\Omega^0} \boldsymbol{\mathcal{V}} \cdot \mathbf{H_J} \, \operatorname{div} \mathbf{M} \, d\mathbf{x}$$

$$+ \mu_0 \int_{\Gamma^0} \boldsymbol{\mathcal{V}} \cdot \{\tilde{\mathbf{H}}\} \, (\mathbf{M} \cdot \mathbf{n}) \, dS - \mu_0 \int_{\Omega^0} \boldsymbol{\mathcal{V}} \cdot \tilde{\mathbf{H}} \, \operatorname{div} \mathbf{M} \, d\mathbf{x}$$

$$= \mu_0 \int_{\Gamma^0} \boldsymbol{\mathcal{V}} \cdot \{\mathbf{H}\} \, (\mathbf{M} \cdot \mathbf{n}) \, dS - \mu_0 \int_{\Omega^0} \boldsymbol{\mathcal{V}} \cdot \mathbf{H} \, \operatorname{div} \mathbf{M} \, d\mathbf{x}. \qquad (5.4.33)$$

We identify the above expression with the equivalent charge model which is well known in literature [39, Section 2.A], [45, Section 2.A], [55, Equation 4], [56, Equation 5], [60, Section 2.2]. For computing the total force $\mathbf{F}$ on the magnet, we plug in constant velocity fields into (5.4.33). They can be taken out of the integral and we get a simple expression for the total force $\mathbf{F}$:

$$\mathbf{F} = \mu_0 \int_{\Gamma^0} \{\mathbf{H}\} \, (\mathbf{M} \cdot \mathbf{n}) \, dS - \mu_0 \int_{\Omega^0} \mathbf{H} \, \operatorname{div} \mathbf{M} \, d\mathbf{x}. \qquad (5.4.34)$$

Defining

$$\overleftrightarrow{\mathbf{T}} := \mathbf{H} \, \mathbf{H}^T - \frac{\|\mathbf{H}\|^2}{2} \mathsf{Id}, \qquad (5.4.35)$$

and using (5.1.23), (5.1.44), we see that

$$\nabla \cdot \overleftrightarrow{\mathbf{T}} = \mathrm{D}\mathbf{H} \, \mathbf{H} - \nabla \mathbf{H} \, \mathbf{H} + \nabla \cdot \mathbf{H} \, \mathbf{H} \qquad (5.4.36)$$

$$= \mathbf{curl}\mathbf{H} \times \mathbf{H} + \nabla \cdot \mathbf{H} \, \mathbf{H}. \qquad (5.4.37)$$

In free space, we see that $\mathbf{curl}\mathbf{H} = 0$ (no source currents) and $\operatorname{div} \mathbf{H} = \mu_0 \operatorname{div} \mathbf{B} = 0$, so $\nabla \cdot \overleftrightarrow{\mathbf{T}} = 0$. In the region occupied by the permanent magnet, we have $\mathbf{curl}\mathbf{H} = 0$ and using the material law $\mathbf{B} = \mu_0(\mathbf{H} + \mathbf{M})$, we have $\nabla \cdot \overleftrightarrow{\mathbf{T}} = \nabla \cdot \mathbf{H} \, \mathbf{H} = -\operatorname{div} \mathbf{M} \, \mathbf{H}$. Now we imagine $\Omega_m \Subset \mathbb{R}^3$ such that $\Omega \Subset \Omega_m$ and $\Omega_m \cap \Omega_{\mathrm{src}} = \phi$. Denoting the stress tensor in the exterior domain Ω_c by $\overleftrightarrow{\mathbf{T}}^+$, and using the divergence theorem over $\Omega_m \setminus \overline{\Omega}$ we get

$$\int_{\partial\Omega_m} \overleftrightarrow{\mathbf{T}}^+ \mathbf{n} \, dS = \int_{\Gamma} \overleftrightarrow{\mathbf{T}}^+ \mathbf{n} \, dS. \qquad (5.4.38)$$

Using the transmission conditions for $\mathbf{H}$ at the interface Γ, we can easily verify that

$$\left[\!\left[\overleftrightarrow{\mathbf{T}} \right]\!\right]_{\Gamma} \mathbf{n} = (\mathbf{M} \cdot \mathbf{n}) \, \{\mathbf{H}\}. \qquad (5.4.39)$$

Integrating over the interface Γ we get

$$\int_{\Gamma} \left[\!\left[\overleftrightarrow{\mathbf{T}} \right]\!\right]_{\Gamma} \mathbf{n} \, dS = \int_{\Gamma} (\mathbf{M} \cdot \mathbf{n}) \, \{\mathbf{H}\} \, dS. \qquad (5.4.40)$$

225

The expression on the LHS can be written as

$$\int_{\Gamma} \left[\!\!\left[\overleftrightarrow{\mathbf{T}} \right]\!\!\right]_{\Gamma} \mathbf{n} \, dS = \int_{\Gamma} \overleftrightarrow{\mathbf{T}}^{+} \mathbf{n} \, dS - \int_{\Gamma} \overleftrightarrow{\mathbf{T}}^{-} \mathbf{n} \, dS = \int_{\Gamma} \overleftrightarrow{\mathbf{T}}^{+} \mathbf{n} \, dS - \int_{\Omega} \nabla \cdot \overleftrightarrow{\mathbf{T}} \, d\mathbf{x} \qquad (5.4.41)$$

$$= \int_{\Gamma} \overleftrightarrow{\mathbf{T}}^{+} \mathbf{n} \, dS + \int_{\Omega} \operatorname{div} \mathbf{M} \, \mathbf{H} \, d\mathbf{x}. \qquad (5.4.42)$$

So we have

$$\int_{\Gamma} (\mathbf{M} \cdot \mathbf{n}) \, \{\mathbf{H}\} \, dS = \int_{\Gamma} \overleftrightarrow{\mathbf{T}}^{+} \mathbf{n} \, dS + \int_{\Omega} \operatorname{div} \mathbf{M} \, \mathbf{H} \, d\mathbf{x}. \qquad (5.4.43)$$

Using (5.4.38) we get

$$\int_{\partial\Omega_m} \overleftrightarrow{\mathbf{T}}^{+} \mathbf{n} \, dS = \int_{\Gamma} (\mathbf{M} \cdot \mathbf{n}) \, \{\mathbf{H}\} \, dS - \int_{\Omega} \operatorname{div} \mathbf{M} \, \mathbf{H} \, d\mathbf{x}. \qquad (5.4.44)$$

Thus

$$\mathbf{F} = \mu_0 \int_{\Gamma} (\mathbf{M} \cdot \mathbf{n}) \, \{\mathbf{H}\} \, dS - \mu_0 \int_{\Omega} \operatorname{div} \mathbf{M} \, \mathbf{H} \, d\mathbf{x} = \mu_0 \int_{\partial\Omega_m} \overleftrightarrow{\mathbf{T}}^{+} \mathbf{n} \, dS. \qquad (5.4.45)$$

Remark 12. Comparing (5.4.19) and (5.4.45) we can show the equivalence of the two models for computing total forces because in air we have $\mathbf{B} = \mu_0 \mathbf{H}$ and thus

$$\mu_0^{-1} \left(\mathbf{B} \, \mathbf{B}^T - \frac{\|\mathbf{B}\|^2}{2} \mathsf{Id} \right) = \mu_0 \left(\mathbf{H} \, \mathbf{H}^T - \frac{\|\mathbf{H}\|^2}{2} \mathsf{Id} \right). \qquad (5.4.46)$$

With (5.4.45) we have verified that the total force on the permanent magnet can also be computed by integrating the Maxwell Stress Tensor on an arbitrary interface enclosing the magnet, which doesn't intersect the magnet or the source current.

The alternative co-energy expression $\mathcal{J}_F'$

$$\mathcal{J}_F' = \frac{\mu_0}{2} \int_{\mathbb{R}^3} \|\mathbf{H}\|^2 \, d\mathbf{x},$$

can be written in terms of the scalar potential as

$$\mathcal{J}_F' = \frac{\mu_0}{2} \int_{\mathbb{R}^3} \|\nabla u\|^2 \, d\mathbf{x} + \frac{\mu_0}{2} \int_{\mathbb{R}^3} \|\mathbf{H_J}\|^2 \, d\mathbf{x}.$$

To compute its shape derivative, we use the adjoint approach again. We start with the Lagrangian $\mathcal{L}' : \mathbb{R} \times V_0 \times V_0 \to \mathbb{R}$,

$$\mathcal{L}'(s; \hat{u}, \hat{v}) := \hat{\mathsf{b}}(s; \hat{u}, \hat{v}) - \hat{\ell}(s; \hat{v}) + \frac{\mu_0}{2} \hat{\mathsf{b}}(s; \hat{u}, \hat{u}) + \frac{\mu_0}{2} \int_{\mathbb{R}^3} \|\mathbf{H_J}\|^2 \, d\mathbf{x}.$$

Plugging in the pulled back state solution we get

$$\mathcal{J}_F'(s) = \mathcal{L}'(s; \hat{u}_0, \hat{v}) \quad \forall \hat{v} \in V_0.$$

We can compute the shape derivative as

$$\frac{d\mathcal{J}_F'}{ds}(0) = \frac{\partial \mathcal{L}'}{\partial s}(0; \hat{u}_0, \hat{p}),$$

where $\hat{p} \in V_0$ solves

$$\frac{\partial \mathcal{L}'}{\partial \hat{u}}(0; \hat{u}_0, \hat{p})(\hat{v}) = 0 \quad \forall \hat{v} \in V_0.$$

Simplifying the adjoint equation gives

$$\hat{\mathsf{b}}(0; \hat{v}, \hat{p}) + \mu_0 \hat{\mathsf{b}}(0; \hat{u}_0, \hat{v}) = 0 \quad \forall \hat{v} \in V_0,$$

giving us $\hat{p} = -\mu_0 \hat{u}_0$. Thus the shape derivative is given as

$$
\begin{aligned}
\frac{d\mathcal{J}_F'}{ds}(0) = \frac{\partial \mathcal{L}'}{\partial s}(0; \hat{u}_0, -\mu_0 \hat{u}_0) &= -\frac{\mu_0}{2}\frac{\partial \hat{\mathsf{b}}}{\partial s}(0; \hat{u}_0, \hat{u}_0) \\
&= -\frac{\mu_0}{2}\int_{\mathbb{R}^3}\left(-\nabla \hat{u}_0^T(\mathsf{D}\boldsymbol{\mathcal{V}}^T + \mathsf{D}\boldsymbol{\mathcal{V}})\nabla \hat{u}_0 + \|\nabla \hat{u}_0\|^2 \ \nabla \cdot \boldsymbol{\mathcal{V}}\right) d\mathbf{x} \\
&= -\mu_0\int_{\Gamma^0}\boldsymbol{\mathcal{V}} \cdot \{\tilde{\mathbf{H}}\}\,(\mathbf{M} \cdot \mathbf{n})\,dS + \mu_0\int_{\Omega^0}\boldsymbol{\mathcal{V}} \cdot \nabla \hat{u}_0 \ \operatorname{div}\mathbf{M}\,d\mathbf{x}.
\end{aligned}
$$

$$(5.4.47)$$

Shape derivatives for $\mathcal{E}_F$ and $\mathcal{E}_F'$ can also be computed using relations in (5.4.6). We need the shape derivative of

$$\frac{\mu_0}{2}\int_{\Omega^s}\|\mathbf{M}_s\|^2 \ d\mathbf{x},$$

where $\mathbf{M}$ is transformed like a two form. In that case we have the shape derivative

$$\frac{\mu_0}{2}\int_{\Omega^0}\left\{\mathbf{M}^T\left(\mathsf{D}\boldsymbol{\mathcal{V}}(\hat{\mathbf{x}}) + \mathsf{D}\boldsymbol{\mathcal{V}}(\hat{\mathbf{x}})^T)\right)\mathbf{M} - \|\mathbf{M}\|^2 \ \nabla \cdot \boldsymbol{\mathcal{V}}(\hat{\mathbf{x}})\right\} d\hat{\mathbf{x}}.$$

The shape derivatives for different energy and co-energy functionals using vector potential formulation are summarized in Table 5.29.

(Co)Energy	Shape Derivative	
$\mathcal{E}_F$ (5.4.12)	$\displaystyle\int_\Omega \boldsymbol{\mathcal{V}} \cdot \Big(\mathbf{curl M} \times \mathbf{B}\Big)\, dx + \int_\Gamma \Big((\mathbf{M} \times \mathbf{n}) \times \{\mathbf{B}\}\Big) \cdot \boldsymbol{\mathcal{V}}\, dS$	Physical
$\mathcal{E}_F'$ (5.4.20)	$\displaystyle-\int_\Omega \boldsymbol{\mathcal{V}} \cdot \Big(\mathbf{curl M} \times \mathbf{B_M}\Big)\, dx - \int_\Gamma \Big((\mathbf{M} \times \mathbf{n}) \times \{\mathbf{B_M}\}\Big) \cdot \boldsymbol{\mathcal{V}}\, dS$	Non-physical
$\mathcal{J}_F'$	$\displaystyle-\int_\Omega \boldsymbol{\mathcal{V}} \cdot \Big(\mathbf{curl M} \times \mathbf{B_M}\Big)\, dx - \int_\Gamma \Big((\mathbf{M} \times \mathbf{n}) \times \{\mathbf{B_M}\}\Big) \cdot \boldsymbol{\mathcal{V}}\, dS$ $\displaystyle+\frac{\mu_0}{2}\int_{\Omega^0} \Big\{ -\mathbf{M}^T\big(\mathsf{D}\boldsymbol{\mathcal{V}} + \mathsf{D}\boldsymbol{\mathcal{V}}^T)\big)\mathbf{M} + \|\mathbf{M}\|^2\ \nabla \cdot \boldsymbol{\mathcal{V}} \Big\}\, d\hat{\mathbf{x}}$	Non-physical
$\mathcal{J}_F$	$\displaystyle\int_\Omega \boldsymbol{\mathcal{V}} \cdot \Big(\mathbf{curl M} \times \mathbf{B}\Big)\, dx + \int_\Gamma \Big((\mathbf{M} \times \mathbf{n}) \times \{\mathbf{B}\}\Big) \cdot \boldsymbol{\mathcal{V}}\, dS$ $\displaystyle-\frac{\mu_0}{2}\int_{\Omega^0} \Big\{ -\mathbf{M}^T\big(\mathsf{D}\boldsymbol{\mathcal{V}} + \mathsf{D}\boldsymbol{\mathcal{V}}^T)\big)\mathbf{M} + \|\mathbf{M}\|^2\ \nabla \cdot \boldsymbol{\mathcal{V}} \Big\}\, d\hat{\mathbf{x}}$	Physical

Table 5.29: Shape derivatives from vector potential formulation

We also summarize the results for the scalar potential formulation in Table 5.30.

(Co)Energy	Shape Derivative	
$\mathcal{E}_F$	$\displaystyle\mu_0\int_{\Gamma^0} \boldsymbol{\mathcal{V}} \cdot \{\mathbf{H}\}\,(\mathbf{M} \cdot \mathbf{n})\, dS - \mu_0 \int_{\Omega^0} \boldsymbol{\mathcal{V}} \cdot \mathbf{H}\ \mathrm{div}\,\mathbf{M}\, dx$ $\displaystyle+\frac{\mu_0}{2}\int_{\Omega^0} \Big\{ \mathbf{M}^T\big(\mathsf{D}\boldsymbol{\mathcal{V}} + \mathsf{D}\boldsymbol{\mathcal{V}}^T)\big)\mathbf{M} - \|\mathbf{M}\|^2\ \nabla \cdot \boldsymbol{\mathcal{V}} \Big\}\, d\hat{\mathbf{x}}$	Physical
$\mathcal{E}_F'$	$\displaystyle-\mu_0\int_{\Gamma^0} \boldsymbol{\mathcal{V}} \cdot \{\tilde{\mathbf{H}}\}\,(\mathbf{M} \cdot \mathbf{n})\, dS + \mu_0 \int_{\Omega} \boldsymbol{\mathcal{V}} \cdot \tilde{\mathbf{H}}\ \mathrm{div}\,\mathbf{M}\, dx$ $\displaystyle-\frac{\mu_0}{2}\int_{\Omega^0} \Big\{ \mathbf{M}^T\big(\mathsf{D}\boldsymbol{\mathcal{V}} + \mathsf{D}\boldsymbol{\mathcal{V}}^T)\big)\mathbf{M} - \|\mathbf{M}\|^2\ \nabla \cdot \boldsymbol{\mathcal{V}} \Big\}\, d\hat{\mathbf{x}}$	Non-physical
$\mathcal{J}_F'$ (5.4.47)	$\displaystyle-\mu_0\int_{\Gamma^0} \boldsymbol{\mathcal{V}} \cdot \{\tilde{\mathbf{H}}\}\,(\mathbf{M} \cdot \mathbf{n})\, dS + \mu_0 \int_{\Omega} \boldsymbol{\mathcal{V}} \cdot \tilde{\mathbf{H}}\ \mathrm{div}\,\mathbf{M}\, dx$	Non-physical
$\mathcal{J}_F$ (5.4.33)	$\displaystyle\mu_0\int_{\Gamma^0} \boldsymbol{\mathcal{V}} \cdot \{\mathbf{H}\}\,(\mathbf{M} \cdot \mathbf{n})\, dS - \mu_0 \int_{\Omega^0} \boldsymbol{\mathcal{V}} \cdot \mathbf{H}\ \mathrm{div}\,\mathbf{M}\, dx$	Physical

Table 5.30: Shape derivatives from scalar potential formulation

We see that with the vector potential formulation we get some sort of equivalent current model and only $\mathcal{E}_F$ gives us the equivalent current model known in literature. On the other hand, the scalar potential formulation always gives a variant of the equivalent charge model and we get the well known model in literature only with the shape derivative of $\mathcal{J}_F$.

5.4.3.5 Equivalence of Equivalent Charge and Equivalent Current Models

The relation in Equation (5.4.6) We can see from the tables above that the force field expressions for the equivalent magnetic current model and equivalent magnetic charge model are very different from one another. It has also been confirmed numerically in the work [39, 45, 55]. However, when computing total forces and torques, these methods turn out to be equivalent [39, 55, 60]. Using the shape derivative computation, it can also be proven. Notice the relation in Equation (5.4.6)

$$\mathcal{J}_F = \mathcal{E}_F - \frac{\mu_0}{2} \int_\Omega \|\mathbf{M}\|^2 \ d\mathbf{x}.$$

Considering deformations using a constant velocity field $\mathcal{V}$ we see that the transformations of the magnetization as a 1 form and 2 form coincide ($\mathsf{DT}_s^{\boldsymbol{\nu}} \equiv \mathsf{Id}, \omega_s \equiv 1$) which implies that the deformed configurations in the scalar potential and a vector potential formulation coincide, leading to the following relation between energy and co-energy of the deformed s-configuration

$$\mathcal{J}_F(s) = \mathcal{E}_F(s) - \frac{\mu_0}{2} \int_{\Omega^s} \|\mathbf{M}_s\|^2 \ d\mathbf{x}.$$

The integral of $\|\mathbf{M}_s\|^2$ turns out to be constant since the magnet is just translated by the constant velocity field. We immediately conclude that

$$\frac{d\mathcal{J}_F}{ds}(0) = \frac{d\mathcal{E}_F}{ds}(0).$$

Thus we have the equivalence of the two models for computing total forces. A similar argument can be made for the case of purely rotational fields of the form $\mathcal{V}(\mathbf{x}) := \boldsymbol{a} \times (\mathbf{x} - \mathbf{x}_0)$, $\boldsymbol{a} := (a_1, a_2, a_3)^T \in \mathbb{R}^3$. We can explicitly compute the Jacobian

$$\mathsf{D}\mathcal{V} = \begin{bmatrix} 0 & -a_3 & a_2 \\ a_3 & 0 & -a_1 \\ -a_2 & a_1 & 0. \end{bmatrix}$$

Thus we have $\mathsf{DT}_s^{\boldsymbol{\nu}} = \mathsf{Id} + s\mathsf{D}\mathcal{V}$, giving us $\det(\mathsf{DT}_s^{\boldsymbol{\nu}}) = 1 + s^2 \|\boldsymbol{a}\|^2$. Upon explicitly computing the $(\mathsf{DT}_s^{\boldsymbol{\nu}})^{-T}$ we get

$$(\mathsf{DT}_s^{\boldsymbol{\nu}})^{-T} = \frac{\mathbf{C}(\mathsf{DT}_s^{\boldsymbol{\nu}})}{\det(\mathsf{DT}_s^{\boldsymbol{\nu}})} = \frac{1}{\det \mathsf{DT}_s^{\boldsymbol{\nu}}} \left(\mathsf{Id} + s\mathsf{D}\mathcal{V} + O(s^2) \right) = \frac{\mathsf{DT}_s^{\boldsymbol{\nu}}}{\det(\mathsf{DT}_s^{\boldsymbol{\nu}})} + O(s^2).$$

We notice that the transformations as a 1-form and a 2-form are same up to order s. Thus the deformed model problems for the scalar and vector potential formulations coincide up to order s which is important since the shape derivative is a first order derivative in s. Since a rotational transformation would not change the integral of $\|\mathbf{M}\|_s^2$ over Ω^s, we again get the relation

$$\frac{d\mathcal{J}_F}{ds}(0) = \frac{d\mathcal{E}_F}{ds}(0).$$

Note that the equivalence would hold true for the boundary integral formulation as well.

5.4.3.6 Variational BIEs

The transmission problem (5.4.30) can be approached using boundary integral equations. We reuse the BIEs derived in (2.1.21) and (2.1.22). Since $\Delta u = -\rho$, we flip the sign in (2.1.21) to get a positive RHS. Thus we have

$$
\begin{bmatrix} -\mathrm{V} & \frac{\mathsf{Id}}{2} + \mathrm{K} \\ \frac{\mathsf{Id}}{2} - \mathrm{K}' & -\mathrm{W} \end{bmatrix} \begin{bmatrix} \gamma_N^- u \\ \gamma_D^- u \end{bmatrix} = \begin{bmatrix} \gamma_D^- \mathrm{N}(\rho) \\ \gamma_N^- \mathrm{N}(\rho) \end{bmatrix},
$$

$$
\begin{bmatrix} -\mathrm{V} & -\frac{\mathsf{Id}}{2} + \mathrm{K} \\ -\frac{\mathsf{Id}}{2} - \mathrm{K}' & -\mathrm{W} \end{bmatrix} \begin{bmatrix} \gamma_N^+ u \\ \gamma_D^+ u \end{bmatrix} = \begin{bmatrix} 0 \\ 0 \end{bmatrix}.
$$

Denoting the exterior traces as

$$
g = \gamma_D^+ u, \quad \gamma_N^+ u = \psi,
$$

the interior traces can be written using the transmission conditions as

$$
\gamma_D^- u = g, \quad \gamma_N^- u = \psi - \lambda.
$$

Using the notation above, the BIEs become

$$
\begin{bmatrix} -\mathrm{V} & \frac{\mathsf{Id}}{2} + \mathrm{K} \\ \frac{\mathsf{Id}}{2} - \mathrm{K}' & -\mathrm{W} \end{bmatrix} \begin{bmatrix} \psi - \lambda \\ g \end{bmatrix} = \begin{bmatrix} \gamma_D^- \mathrm{N}(\rho) \\ \gamma_N^- \mathrm{N}(\rho) \end{bmatrix},
$$

$$
\begin{bmatrix} -\mathrm{V} & -\frac{\mathsf{Id}}{2} + \mathrm{K} \\ -\frac{\mathsf{Id}}{2} - \mathrm{K}' & -\mathrm{W} \end{bmatrix} \begin{bmatrix} \psi \\ g \end{bmatrix} = \begin{bmatrix} 0 \\ 0 \end{bmatrix},
$$

and can be added to get

$$
\begin{bmatrix} -2\,\mathrm{V} & 2\,\mathrm{K} \\ -2\,\mathrm{K}' & -2\,\mathrm{W} \end{bmatrix} \begin{bmatrix} \psi \\ g \end{bmatrix} = \begin{bmatrix} \gamma_D^- \mathrm{N}(\rho) - \mathrm{V}(\lambda) \\ \gamma_N^- \mathrm{N}(\rho) + \frac{\lambda}{2} - \mathrm{K}'(\lambda) \end{bmatrix}.
$$

Testing the first equation with $\phi \in H^{-\frac{1}{2}}(\Gamma)$, second equation with $u \in H^{\frac{1}{2}}(\Gamma)$ and adding them up gives us the variational formulation: seek $\psi \in H^{-\frac{1}{2}}(\Gamma), g \in H^{\frac{1}{2}}(\Gamma)$

$$
-2\mathsf{b}_{\mathrm{V}}(\psi, \phi) + 2\mathsf{b}_{\mathrm{K}}(g, \phi) - 2\mathsf{b}_{\mathrm{K}'}(\psi, u) - 2\mathsf{b}_{\mathrm{W}}(g, u) =
$$

$$
\left\langle \gamma_D^- \mathrm{N}(\rho), \phi \right\rangle - \mathsf{b}_{\mathrm{V}}(\lambda, \phi) + \left\langle \gamma_N^- \mathrm{N}(\rho), u \right\rangle + \frac{1}{2}\left\langle \lambda, u \right\rangle - \mathsf{b}_{\mathrm{K}'}(\lambda, u) \quad \forall \phi \in H^{-\frac{1}{2}}(\Gamma),\ u \in H^{\frac{1}{2}}(\Gamma).
$$
$$
(5.4.48)
$$

We know that traces of the potential u satisfying (5.4.30) satisfy (5.4.48). Unique solvability can be shown using Theorem 2.

In the above equation, $\langle \cdot, \cdot \rangle$ denotes the duality pairing between $H^{-\frac{1}{2}}(\Gamma)$ and $H^{\frac{1}{2}}(\Gamma)$. We focus on the shape derivative of $\mathcal{J}_F$ as that gave us a meaningful physical shape derivative in (5.4.33). Using Green's formula, the co-enery expression $\mathcal{J}_F$ in (5.4.5) can be written as

$$
\mathcal{J}_F = \frac{\mu_0}{2} \int_{\mathbb{R}^3} \|\nabla u + \mathbf{H_J}\|^2 \, d\mathbf{x} + \mu_0 \int_{\Omega} \mathbf{M} \cdot (\nabla u + \mathbf{H_J}) \, d\mathbf{x}
$$

$$= \frac{\mu_0}{2} \int_{\mathbb{R}^3} \|\nabla u\|^2 \, d\mathbf{x} + \frac{\mu_0}{2} \int_{\mathbb{R}^3} \|\mathbf{H_J}\|^2 \, d\mathbf{x} + \mu_0 \int_{\mathbb{R}^3} \nabla u \cdot \mathbf{H_J} \, d\mathbf{x} + \mu_0 \int_\Omega \mathbf{M} \cdot (\nabla u + \mathbf{H_J}) \, d\mathbf{x}$$

$$= \frac{\mu_0}{2} \int_{\mathbb{R}^3} \|\nabla u\|^2 \, d\mathbf{x} + \mu_0 \int_\Omega \mathbf{M} \cdot \nabla u \, d\mathbf{x} + \frac{\mu_0}{2} \int_{\mathbb{R}^3} \|\mathbf{H_J}\|^2 \, d\mathbf{x} + \mu_0 \int_\Omega \mathbf{M} \cdot \mathbf{H_J} \, d\mathbf{x}$$

$$= -\frac{\mu_0}{2} \int_{\mathbb{R}^3} \|\nabla u\|^2 \, d\mathbf{x} + \frac{\mu_0}{2} \int_{\mathbb{R}^3} \|\mathbf{H_J}\|^2 \, d\mathbf{x} + \mu_0 \int_\Omega \mathbf{M} \cdot \mathbf{H_J} \, d\mathbf{x}$$

$$= -\frac{\mu_0}{2} \int_\Omega u \,\, \mathrm{div}\, \mathbf{M} \, d\mathbf{x} + \frac{\mu_0}{2} \int_\Gamma g \, \mathbf{M} \cdot \mathbf{n} \, dS + \frac{\mu_0}{2} \int_{\mathbb{R}^3} \|\mathbf{H_J}\|^2 \, d\mathbf{x} + \mu_0 \int_\Omega \mathbf{M} \cdot \mathbf{H_J} \, d\mathbf{x}.$$

Plugging in the representation formula for u in Ω (2.1.20) we get

$$\mathcal{J}_F = -\frac{\mu_0}{2} \int_\Omega \Big(\mathrm{N}(\rho)(\mathbf{x}) + \psi_{\mathrm{SL}} \left(\gamma_N^- u \right)(\mathbf{x}) - \psi_{\mathrm{DL}} \left(g \right)(\mathbf{x}) \Big) \,\, \mathrm{div}\, \mathbf{M}(\mathbf{x}) \, d\mathbf{x}$$

$$+ \frac{\mu_0}{2} \int_\Gamma g \, \mathbf{M} \cdot \mathbf{n} \, dS + \frac{\mu_0}{2} \int_{\mathbb{R}^3} \|\mathbf{H_J}\|^2 \, d\mathbf{x} + \mu_0 \int_\Omega \mathbf{M} \cdot \mathbf{H_J} \, d\mathbf{x}$$

$$= -\frac{\mu_0}{2} \int_\Omega \int_\Omega G(\mathbf{x}, \mathbf{y}) \, \rho(\mathbf{y}) \, \rho(\mathbf{x}) \, d\mathbf{y} \, d\mathbf{x}$$

$$- \frac{\mu_0}{2} \left\langle \gamma_D^- \mathrm{N}(\rho), \psi \right\rangle + \frac{\mu_0}{2} \left\langle \gamma_D^- \mathrm{N}(\rho), \lambda \right\rangle$$

$$+ \frac{\mu_0}{2} \left\langle \gamma_N^- \mathrm{N}(\rho), g \right\rangle + \frac{\mu_0}{2} \left\langle \lambda, g \right\rangle$$

$$+ \frac{\mu_0}{2} \int_{\mathbb{R}^3} \|\mathbf{H_J}\|^2 \, d\mathbf{x} + \mu_0 \int_\Omega \mathbf{M} \cdot \mathbf{H_J} \, d\mathbf{x}.$$

To find the adjoint solution explicitly later on, it is useful to express the co-energy in terms of the linear form. Denoting the RHS of (5.4.48) as $\ell\left(\begin{bmatrix} \phi \\ u \end{bmatrix} \right)$, we observe that

$$\ell\left(\begin{bmatrix} -\psi \\ g \end{bmatrix} \right) = - \left\langle \gamma_D^- \mathrm{N}(\rho), \psi \right\rangle + \mathsf{b}_V(\lambda, \psi) + \left\langle \gamma_N^- \mathrm{N}(\rho), g \right\rangle + \frac{1}{2} \left\langle \lambda, g \right\rangle - \mathsf{b}_{K'}(\lambda, g),$$

which gives us

$$- \left\langle \gamma_D^- \mathrm{N}(\rho), \psi \right\rangle + \left\langle \gamma_N^- \mathrm{N}(\rho), g \right\rangle = \ell\left(\begin{bmatrix} -\psi \\ g \end{bmatrix} \right) - \mathsf{b}_V(\lambda, \psi) - \frac{1}{2} \left\langle \lambda, g \right\rangle + \mathsf{b}_{K'}(\lambda, g).$$

Plugging this in the co-energy expression we get

$$\mathcal{E}_F = -\frac{\mu_0}{2} \int_\Omega \int_\Omega G(\mathbf{x}, \mathbf{y}) \, \rho(\mathbf{y}) \, \rho(\mathbf{x}) \, d\mathbf{y} \, d\mathbf{x}$$

$$+ \frac{\mu_0}{2} \ell\left(\begin{bmatrix} -\psi \\ g \end{bmatrix} \right) - \frac{\mu_0}{2} \mathsf{b}_V(\lambda, \psi) - \frac{\mu_0}{4} \left\langle \lambda, g \right\rangle + \frac{\mu_0}{2} \mathsf{b}_{K'}(\lambda, g)$$

$$+ \frac{\mu_0}{2} \left\langle \gamma_D^- \mathrm{N}(\rho), \lambda \right\rangle + \frac{\mu_0}{2} \left\langle \lambda, g \right\rangle$$

$$+ \frac{\mu_0}{2} \int_{\mathbb{R}^3} \|\mathbf{H_J}\|^2 \ d\mathbf{x} + \mu_0 \int_{\Omega} \mathbf{M} \cdot \mathbf{H_J} \ d\mathbf{x}.$$

Testing the first BIE for the interior traces with λ and scaling, we get

$$-\frac{\mu_0}{2}\mathsf{b}_{\mathrm{V}}(\psi, \lambda) + \frac{\mu_0}{4} \left\langle g, \lambda \right\rangle + \frac{\mu_0}{2}\mathsf{b}_{\mathrm{K}}(g, \lambda) = \frac{\mu_0}{2} \left\langle \gamma_D^- \mathrm{N}(\rho), \lambda \right\rangle - \frac{\mu_0}{2}\mathsf{b}_{\mathrm{V}}(\lambda, \lambda).$$

This finally leads to the desired relation

$$\mathcal{E}_F = \frac{\mu_0}{2}\ell(\begin{bmatrix} -\psi \\ g \end{bmatrix}) - \frac{\mu_0}{2} \int_{\Omega} \int_{\Omega} G(\mathbf{x}, \mathbf{y}) \ \rho(\mathbf{y}) \ \rho(\mathbf{x}) \ d\mathbf{y} \ d\mathbf{x}$$

$$+ \mu_0 \left\langle \gamma_D^- \mathrm{N}(\rho), \lambda \right\rangle - \frac{\mu_0}{2}\mathsf{b}_{\mathrm{V}}(\lambda, \lambda)$$

$$+ \frac{\mu_0}{2} \int_{\mathbb{R}^3} \|\mathbf{H_J}\|^2 \ d\mathbf{x} + \mu_0 \int_{\Omega} \mathbf{M} \cdot \mathbf{H_J} \ d\mathbf{x}.$$

5.4.3.7 Variational BIEs on Deformed Domain

We consider deformations of only the permanent magnet as in the vector potential case. The magnetization $\mathbf{M}$ is moved as a 2-form now, which is natural considering that its divergence and normal traces show up in the formulation. Variational problem for the deformed s-configuration has a similar structure to (5.4.48): seek $\psi_s \in H^{-\frac{1}{2}}(\Gamma^s), u_s \in H^{\frac{1}{2}}(\Gamma^s)$ such that

$$\mathsf{b}(s)(\begin{bmatrix} \psi_s \\ g_s \end{bmatrix}, \begin{bmatrix} \phi \\ u \end{bmatrix}) = \ell(s)(\begin{bmatrix} \phi \\ u \end{bmatrix}) \quad \forall \phi \in H^{-\frac{1}{2}}(\Gamma^s), \ \forall u \in H^{\frac{1}{2}}(\Gamma^s),$$

where

$$\mathsf{b}(s)(\begin{bmatrix} \psi \\ g \end{bmatrix}, \begin{bmatrix} \phi \\ u \end{bmatrix}) := -2\mathsf{b}_{\mathrm{V}}(s)(\psi, \phi) + 2\mathsf{b}_{\mathrm{K}}(s)(g, \phi) - 2\mathsf{b}_{\mathrm{K}'}(s)(\psi, u) - 2\mathsf{b}_{\mathrm{W}}(s)(g, u).$$

The bilinear forms $\mathsf{b}_*(s)$ contain integrals over Γ^s. The linear form is defined as

$$\ell(s)(\begin{bmatrix} \phi \\ u \end{bmatrix}) := \left\langle \gamma_D^- \mathrm{N}(\rho_s), \phi \right\rangle_{\Gamma^s} - \mathsf{b}_{\mathrm{V}}(s)(\lambda_s, \phi) + \left\langle \gamma_N^- \mathrm{N}(\rho_s), u \right\rangle_{\Gamma^s} + \frac{1}{2} \left\langle \lambda_s, u \right\rangle_{\Gamma^s} - \mathsf{b}_{\mathrm{K}'}(s)(\lambda_s, u),$$

where $\left\langle \cdot, \cdot \right\rangle_{\Gamma^s}$ denotes the the duality pairing between $H^{-\frac{1}{2}}(\Gamma^s)$ and $H^{\frac{1}{2}}(\Gamma^s)$.

5.4.3.8 Equivalent BIEs on Reference Domain

Using the perturbation map, we transform the integrals in the (bi)linear forms back to the reference domains. These computations have already been done for the bilinear forms in Section 4.4.3 so we only mention the transformation for the linear form

$$\ell(s)(\begin{bmatrix} \phi \\ u \end{bmatrix}) =$$

$$\int_{\Gamma^0}\int_{\Omega^0} G(\mathbf{T}_s^{\boldsymbol{\nu}}(\hat{\mathbf{x}}), \mathbf{T}_s^{\boldsymbol{\nu}}(\hat{\mathbf{y}}))\, \rho_s(\mathbf{T}_s^{\boldsymbol{\nu}}(\hat{\mathbf{y}}))\, \phi(\mathbf{T}_s^{\boldsymbol{\nu}}(\hat{\mathbf{x}}))\, \det \mathsf{D}\mathbf{T}_s^{\boldsymbol{\nu}}(\hat{\mathbf{y}})\, \omega_s(\hat{\mathbf{x}})\, d\hat{\mathbf{y}}\, dS_{\hat{\mathbf{x}}}$$

$$+\int_{\Gamma^0}\int_{\Omega^0} \nabla_{\mathbf{x}} G(\mathbf{T}_s^{\boldsymbol{\nu}}(\hat{\mathbf{x}}), \mathbf{T}_s^{\boldsymbol{\nu}}(\hat{\mathbf{y}}))\cdot \mathbf{n}(\mathbf{T}_s^{\boldsymbol{\nu}}(\hat{\mathbf{x}}))\, \rho_s(\mathbf{T}_s^{\boldsymbol{\nu}}(\hat{\mathbf{y}}))\, u(\mathbf{T}_s^{\boldsymbol{\nu}}(\hat{\mathbf{x}}))\, \det \mathsf{D}\mathbf{T}_s^{\boldsymbol{\nu}}(\hat{\mathbf{y}})\, \omega_s(\hat{\mathbf{x}})\, d\hat{\mathbf{y}}\, dS_{\hat{\mathbf{x}}}$$

$$-\int_{\Gamma^0}\int_{\Gamma^0} G(\mathbf{T}_s^{\boldsymbol{\nu}}(\hat{\mathbf{x}}), \mathbf{T}_s^{\boldsymbol{\nu}}(\hat{\mathbf{y}}))\, \lambda_s(\mathbf{T}_s^{\boldsymbol{\nu}}(\hat{\mathbf{y}}))\, \phi(\mathbf{T}_s^{\boldsymbol{\nu}}(\hat{\mathbf{x}}))\, \omega_s(\hat{\mathbf{x}})\, \omega_s(\hat{\mathbf{y}})\, dS_{\hat{\mathbf{y}}}\, dS_{\hat{\mathbf{x}}}$$

$$-\int_{\Gamma^0}\int_{\Gamma^0} \nabla_y G(\mathbf{T}_s^{\boldsymbol{\nu}}(\hat{\mathbf{x}}), \mathbf{T}_s^{\boldsymbol{\nu}}(\hat{\mathbf{y}}))\cdot \left(\frac{\mathbf{C}(\mathsf{D}\mathbf{T}_s^{\boldsymbol{\nu}}(\hat{\mathbf{y}})\, \hat{\mathbf{n}}(\hat{\mathbf{y}}))}{\omega_s(\hat{\mathbf{y}})}\right) u(\mathbf{T}_s^{\boldsymbol{\nu}}(\hat{\mathbf{y}}))\, \lambda_s(\mathbf{T}_s^{\boldsymbol{\nu}}(\hat{\mathbf{x}}))\, \omega_s(\hat{\mathbf{x}})\, \omega_s(\hat{\mathbf{y}})\, dS_{\hat{\mathbf{y}}}\, dS_{\hat{\mathbf{x}}}$$

$$+\frac{1}{2}\int_{\Gamma^0} \lambda_s(\mathbf{T}_s^{\boldsymbol{\nu}}(\hat{\mathbf{x}}))\, u(\mathbf{T}_s^{\boldsymbol{\nu}}(\hat{\mathbf{x}}))\, \omega_s(\hat{\mathbf{x}})\, dS_{\hat{\mathbf{x}}}.$$

We use the following pullbacks

$$u(\mathbf{T}_s^{\boldsymbol{\nu}}(\hat{\mathbf{x}})) = \hat{u}(\hat{\mathbf{x}}),$$

$$\psi(\mathbf{T}_s^{\boldsymbol{\nu}}(\hat{\mathbf{x}})) = \frac{\hat{\psi}(\hat{\mathbf{x}})}{\omega_s(\hat{\mathbf{x}})},$$

$$\mathbf{curl}_\Gamma\, u(\mathbf{T}_s^{\boldsymbol{\nu}}(\hat{\mathbf{x}})) = \frac{\mathsf{D}\mathbf{T}_s^{\boldsymbol{\nu}}(\hat{\mathbf{x}})}{\omega_s(\hat{\mathbf{x}})}\, \mathbf{curl}_\Gamma\, \hat{u}(\hat{\mathbf{x}}).$$

We use the following pullbacks for λ_s and ρ_s

$$\lambda_s(\mathbf{T}_s^{\boldsymbol{\nu}}(\hat{\mathbf{x}})) = \frac{\lambda(\hat{\mathbf{x}})}{\omega_s(\hat{\mathbf{x}})}, \quad \rho_s(\mathbf{T}_s^{\boldsymbol{\nu}}(\hat{\mathbf{x}})) = \frac{\rho(\hat{\mathbf{x}})}{\det \mathsf{D}\mathbf{T}_s^{\boldsymbol{\nu}}(\hat{\mathbf{x}})}.$$

The pulled back bilinear forms are defined in Section 4.4.3, and the pulled back linear form is defined as

$$\hat{\ell}\left(s; \begin{bmatrix}\hat{\phi}\\\hat{u}\end{bmatrix}\right) := \int_{\Gamma^0}\int_{\Omega^0} G(\mathbf{T}_s^{\boldsymbol{\nu}}(\hat{\mathbf{x}}), \mathbf{T}_s^{\boldsymbol{\nu}}(\hat{\mathbf{y}}))\, \rho(\hat{\mathbf{y}})\, \hat{\phi}(\hat{\mathbf{x}})\, d\hat{\mathbf{y}}\, dS_{\hat{\mathbf{x}}}$$

$$+\int_{\Gamma^0}\int_{\Omega^0} \nabla_{\mathbf{x}} G(\mathbf{T}_s^{\boldsymbol{\nu}}(\hat{\mathbf{x}}), \mathbf{T}_s^{\boldsymbol{\nu}}(\hat{\mathbf{y}}))\cdot \left(\mathbf{C}(\mathsf{D}\mathbf{T}_s^{\boldsymbol{\nu}}(\hat{\mathbf{x}}))\, \hat{\mathbf{n}}(\hat{\mathbf{x}})\right) \rho(\hat{\mathbf{y}})\, \hat{u}(\hat{\mathbf{x}})\, d\hat{\mathbf{y}}\, dS_{\hat{\mathbf{x}}}$$

$$-\hat{\mathsf{b}}_{\mathrm{V}}(s; \lambda, \hat{\phi}) - \hat{\mathsf{b}}_{\mathrm{K}'}(s; \lambda, \hat{u}) + \frac{1}{2}\int_{\Gamma^0} \lambda\, \hat{u}\, dS.$$

Co-energy for the deformed s-configuration can be written in terms of the pulled back linear form as

$$\mathcal{J}_F(s) = \frac{\mu_0}{2}\hat{\ell}\left(s; \begin{bmatrix}-\hat{\psi}_s\\\hat{g}_s\end{bmatrix}\right) - \frac{\mu_0}{2}\int_{\Omega^0}\int_{\Omega^0} G(\mathbf{T}_s^{\boldsymbol{\nu}}(\hat{\mathbf{x}}), \mathbf{T}_s^{\boldsymbol{\nu}}(\hat{\mathbf{y}}))\, \rho(\hat{\mathbf{y}})\, \rho(\hat{\mathbf{x}})\, d\hat{\mathbf{y}}\, d\hat{\mathbf{x}}$$

$$+\mu_0\int_{\Gamma^0}\int_{\Omega^0} G(\mathbf{T}_s^{\boldsymbol{\nu}}(\hat{\mathbf{x}}), \mathbf{T}_s^{\boldsymbol{\nu}}(\hat{\mathbf{y}}))\, \rho(\hat{\mathbf{y}})\, \lambda(\hat{\mathbf{x}})\, d\hat{\mathbf{y}}\, dS_{\hat{\mathbf{x}}} - \frac{\mu_0}{2}\hat{\mathsf{b}}_{\mathrm{V}}(s; \lambda, \lambda) + \frac{\mu_0}{2}\int_{\mathbb{R}^3} \|\mathbf{H}_{\mathbf{J}}\|^2\, d\mathbf{x}$$

$$+ \mu_0 \int_{\Omega^0} \left(\mathsf{D}\mathbf{T}_s^{\boldsymbol{\nu}}(\hat{\mathbf{x}}) \, \mathbf{M}(\hat{\mathbf{x}}) \right) \cdot \mathbf{H_J}(\mathbf{T}_s^{\boldsymbol{\nu}}(\hat{\mathbf{x}})) \, d\hat{\mathbf{x}}.$$

The pulled back variational problem is given as: seek $\hat{\psi}_s, \hat{g}_s \in V_0 := H^{-\frac{1}{2}}(\Gamma^0) \times H^{\frac{1}{2}}(\Gamma^0)$ such that

$$\hat{\mathsf{b}}(s; \begin{bmatrix} \hat{\psi}_s \\ \hat{g}_s \end{bmatrix}, \begin{bmatrix} \hat{\phi} \\ \hat{u} \end{bmatrix}) = \hat{\ell}(s; \begin{bmatrix} \hat{\phi} \\ \hat{u} \end{bmatrix}) \quad \forall \begin{bmatrix} \hat{\phi} \\ \hat{u} \end{bmatrix} \in V_0,$$

where

$$\hat{\mathsf{b}}(s; \begin{bmatrix} \hat{\psi} \\ \hat{g} \end{bmatrix}, \begin{bmatrix} \hat{\phi} \\ \hat{u} \end{bmatrix}) := -2\mathsf{b}_{\mathrm{V}}(s; \hat{\psi}, \hat{\phi}) + 2\mathsf{b}_{\mathrm{K}}(s; \hat{g}, \hat{\phi}) - 2\mathsf{b}_{\mathrm{K}'}(s; \hat{\psi}, \hat{u}) - 2\mathsf{b}_{\mathrm{W}}(s; \hat{g}, \hat{u}).$$

5.4.3.9 BIE-Constrained Shape Derivaive

We start by defining the Lagrangian $\mathcal{L} : \mathbb{R} \times V_0 \times V_0 \to \mathbb{R}$,

$$\mathcal{L}(s; \begin{bmatrix} \hat{\psi} \\ \hat{g} \end{bmatrix}, \begin{bmatrix} \hat{\phi} \\ \hat{u} \end{bmatrix}) := \hat{\mathsf{b}}(s; \begin{bmatrix} \hat{\psi} \\ \hat{g} \end{bmatrix}, \begin{bmatrix} \hat{\phi} \\ \hat{u} \end{bmatrix}) - \hat{\ell}(s; \begin{bmatrix} \hat{\phi} \\ \hat{u} \end{bmatrix}) + \frac{\mu_0}{2} \hat{\ell}(s; \begin{bmatrix} -\hat{\psi} \\ \hat{g} \end{bmatrix})$$

$$- \frac{\mu_0}{2} \int_{\Omega^0} \int_{\Omega^0} G(\mathbf{T}_s^{\boldsymbol{\nu}}(\hat{\mathbf{x}}), \mathbf{T}_s^{\boldsymbol{\nu}}(\hat{\mathbf{y}})) \, \rho(\hat{\mathbf{y}}) \, \rho(\hat{\mathbf{x}}) \, d\hat{\mathbf{y}} \, d\hat{\mathbf{x}}$$

$$+ \mu_0 \int_{\Gamma^0} \int_{\Omega^0} G(\mathbf{T}_s^{\boldsymbol{\nu}}(\hat{\mathbf{x}}), \mathbf{T}_s^{\boldsymbol{\nu}}(\hat{\mathbf{y}})) \, \rho(\hat{\mathbf{y}}) \, \lambda(\hat{\mathbf{x}}) \, d\hat{\mathbf{y}} \, dS_{\hat{\mathbf{x}}}$$

$$- \frac{\mu_0}{2} \hat{\mathsf{b}}_{\mathrm{V}}(s; \lambda, \lambda) + \frac{\mu_0}{2} \int_{\mathbb{R}^3} \|\mathbf{H_J}\|^2 \, d\mathbf{x}$$

$$+ \mu_0 \int_{\Omega^0} \left(\mathsf{D}\mathbf{T}_s^{\boldsymbol{\nu}}(\hat{\mathbf{x}}) \, \mathbf{M}(\hat{\mathbf{x}}) \right) \cdot \mathbf{H_J}(\mathbf{T}_s^{\boldsymbol{\nu}}(\hat{\mathbf{x}})) \, d\hat{\mathbf{x}}.$$

Plugging in the state solution, we see that

$$\mathcal{J}_F(s) = \mathcal{L}(s; \begin{bmatrix} \hat{\psi}_s \\ \hat{g}_s \end{bmatrix}, \begin{bmatrix} \hat{\phi} \\ \hat{u} \end{bmatrix}) \quad \forall \begin{bmatrix} \hat{\phi} \\ \hat{u} \end{bmatrix} \in V_0.$$

We can compute the shape derivative as

$$\frac{d\mathcal{E}_F}{ds}(0) = \frac{\partial \mathcal{L}}{ds}(0; \begin{bmatrix} \hat{\psi}_0 \\ \hat{g}_0 \end{bmatrix}, \begin{bmatrix} \hat{\eta} \\ \hat{p} \end{bmatrix}),$$

where $\begin{bmatrix} \hat{\eta} \\ \hat{p} \end{bmatrix} \in V_0$ solves the adjoint equation

$$\left\langle \frac{\partial \mathcal{L}}{\partial \begin{bmatrix} \hat{\psi} \\ \hat{g} \end{bmatrix}}(0; \begin{bmatrix} \hat{\psi}_0 \\ \hat{g}_0 \end{bmatrix}, \begin{bmatrix} \hat{\eta} \\ \hat{p} \end{bmatrix}); \begin{bmatrix} \hat{\phi} \\ \hat{u} \end{bmatrix} \right\rangle = 0 \quad \forall \begin{bmatrix} \hat{\phi} \\ \hat{u} \end{bmatrix} \in V_0,$$

which simplifies to

$$\hat{\mathsf{b}}(0; \begin{bmatrix} \hat{\phi} \\ \hat{u} \end{bmatrix}, \begin{bmatrix} \hat{\eta} \\ \hat{p} \end{bmatrix}) + \frac{\mu_0}{2}\hat{\ell}(0; \begin{bmatrix} -\hat{\phi} \\ \hat{u} \end{bmatrix}) = 0 \quad \forall \begin{bmatrix} \hat{\phi} \\ \hat{u} \end{bmatrix} \in V_0.$$

Changing the sign of the test function $\hat{\phi}$ in the adjoint equation we get

$$\hat{\mathsf{b}}(0; \begin{bmatrix} -\hat{\phi} \\ \hat{u} \end{bmatrix}, \begin{bmatrix} \hat{\eta} \\ \hat{p} \end{bmatrix}) + \frac{\mu_0}{2}\hat{\ell}(0; \begin{bmatrix} \hat{\phi} \\ \hat{u} \end{bmatrix}) = 0 \quad \forall \begin{bmatrix} \hat{\phi} \\ \hat{u} \end{bmatrix} \in V_0.$$

Finally, using the property

$$\hat{\mathsf{b}}(0; \begin{bmatrix} -\hat{\phi} \\ \hat{u} \end{bmatrix}, \begin{bmatrix} \hat{\eta} \\ \hat{p} \end{bmatrix}) = \hat{\mathsf{b}}(0; \begin{bmatrix} -\hat{\eta} \\ \hat{p} \end{bmatrix}, \begin{bmatrix} \hat{\phi} \\ \hat{u} \end{bmatrix}),$$

the adjoint equation becomes

$$\hat{\mathsf{b}}(0; \begin{bmatrix} -\hat{\eta} \\ \hat{p} \end{bmatrix}, \begin{bmatrix} \hat{\phi} \\ \hat{u} \end{bmatrix}) = -\frac{\mu_0}{2}\hat{\ell}(0; \begin{bmatrix} \hat{\phi} \\ \hat{u} \end{bmatrix}) \quad \forall \begin{bmatrix} \hat{\phi} \\ \hat{u} \end{bmatrix} \in V_0,$$

which yields the adjoint solution

$$\begin{bmatrix} \hat{\eta} \\ \hat{p} \end{bmatrix} = \frac{\mu_0}{2}\begin{bmatrix} \hat{\psi}_0 \\ -\hat{g}_0 \end{bmatrix}.$$

The shape derivative is then given as

$$\frac{d\mathcal{J}_F}{ds}(0) = \frac{\partial\mathcal{L}}{ds}(0; \begin{bmatrix} \hat{\psi}_0 \\ \hat{g}_0 \end{bmatrix}, \begin{bmatrix} \hat{\eta} \\ \hat{p} \end{bmatrix}) = \frac{\partial\mathcal{L}}{ds}(0; \begin{bmatrix} \hat{\psi}_0 \\ \hat{g}_0 \end{bmatrix}, \frac{\mu_0}{2}\begin{bmatrix} \hat{\psi}_0 \\ -\hat{g}_0 \end{bmatrix})$$

$$= \frac{\mu_0}{2}\frac{\partial\hat{\mathsf{b}}}{\partial s}(0; \begin{bmatrix} \hat{\psi}_0 \\ \hat{g}_0 \end{bmatrix}, \begin{bmatrix} \hat{\psi}_0 \\ -\hat{g}_0 \end{bmatrix}) + \mu_0\frac{\partial\hat{\ell}}{\partial s}(0; \begin{bmatrix} -\hat{\psi}_0 \\ \hat{g}_0 \end{bmatrix})$$

$$- \frac{\mu_0}{2}\int_{\Omega^0}\int_{\Omega^0}\Big(\nabla_{\mathbf{x}}G(\mathbf{x},\mathbf{y})\cdot\mathcal{V}(\mathbf{x}) + \nabla_{\mathbf{y}}G(\mathbf{x},\mathbf{y})\cdot\mathcal{V}(\mathbf{y})\Big)\,\rho(\mathbf{y})\,\rho(\mathbf{x})\,d\mathbf{y}\,d\mathbf{x}$$

$$+ \mu_0\int_{\Gamma^0}\int_{\Omega^0}\Big(\nabla_{\mathbf{x}}G(\mathbf{x},\mathbf{y})\cdot\mathcal{V}(\mathbf{x}) + \nabla_{\mathbf{y}}G(\mathbf{x},\mathbf{y})\cdot\mathcal{V}(\mathbf{y})\Big)\,\rho(\mathbf{y})\,\lambda(\mathbf{x})\,d\mathbf{y}\,d\mathrm{S}_{\mathbf{x}}$$

$$- \frac{\mu_0}{2}\int_{\Gamma^0}\int_{\Gamma^0}\Big(\nabla_{\mathbf{x}}G(\mathbf{x},\mathbf{y})\cdot\mathcal{V}(\mathbf{x}) + \nabla_{\mathbf{y}}G(\mathbf{x},\mathbf{y})\cdot\mathcal{V}(\mathbf{y})\Big)\,\lambda(\mathbf{y})\,\lambda(\mathbf{x})\,d\mathrm{S}_{\mathbf{y}}\,d\mathrm{S}_{\mathbf{x}}$$

$$+ \mu_0\int_{\Omega^0}\Big(\mathsf{D}\mathcal{V}\,\mathbf{M}\Big)\cdot\mathbf{H_J} + \Big(\mathsf{D}\mathbf{H_J}\,\mathcal{V}\Big)\cdot\mathbf{M}\,d\mathbf{x}. \tag{5.4.49}$$

The partial derivatives for the bilinear forms have been computed already in (5.1.20). The partial derivative for the linear form is given as

$$\frac{\partial\hat{\ell}}{\partial s}(0; \begin{bmatrix} \hat{\phi} \\ \hat{u} \end{bmatrix}) = \int_{\Gamma^0}\int_{\Omega^0}\Big(\nabla_{\mathbf{x}}G(\mathbf{x},\mathbf{y})\cdot\mathcal{V}(\mathbf{x}) + \nabla_{\mathbf{y}}G(\mathbf{x},\mathbf{y})\cdot\mathcal{V}(\mathbf{y})\Big)\,\rho(\hat{\mathbf{y}})\,\hat{\phi}(\hat{\mathbf{x}})\,d\hat{\mathbf{y}}\,d\mathrm{S}_{\hat{\mathbf{x}}}$$

$$
+ \int\limits_{\Gamma^0} \int\limits_{\Omega^0} \frac{d\left(\nabla_{\mathbf{x}} G(\mathbf{T}_s^{\boldsymbol{\nu}}(\hat{\mathbf{x}}), \mathbf{T}_s^{\boldsymbol{\nu}}(\hat{\mathbf{y}}))\right)}{ds}\Big|_{s=0} \cdot \hat{\mathbf{n}}(\hat{\mathbf{x}}) \, \rho(\hat{\mathbf{y}}) \, \hat{u}(\hat{\mathbf{x}}) \, d\hat{\mathbf{y}} \, dS_{\hat{\mathbf{x}}}
$$

$$
+ \int\limits_{\Gamma^0} \int\limits_{\Omega^0} \nabla_{\mathbf{x}} G(\hat{\mathbf{x}}, \hat{\mathbf{y}}) \cdot \left(\nabla \cdot \boldsymbol{\mathcal{V}}(\hat{\mathbf{x}}) \, \hat{\mathbf{n}}(\hat{\mathbf{x}}) - \mathsf{D}\boldsymbol{\mathcal{V}}^T(\hat{\mathbf{x}}) \, \hat{\mathbf{n}}(\hat{\mathbf{x}})\right) \rho(\hat{\mathbf{y}}) \, \hat{u}(\hat{\mathbf{x}}) \, d\hat{\mathbf{y}} \, dS_{\hat{\mathbf{x}}}
$$

$$
- \int\limits_{\Gamma^0} \int\limits_{\Gamma^0} \left(\nabla_{\mathbf{x}} G(\mathbf{x}, \mathbf{y}) \cdot \boldsymbol{\mathcal{V}}(\mathbf{x}) + \nabla_{\mathbf{y}} G(\mathbf{x}, \mathbf{y}) \cdot \boldsymbol{\mathcal{V}}(\mathbf{y})\right) \lambda(\mathbf{y}) \, \hat{\phi}(\mathbf{x}) \, dS_{\mathbf{y}} \, dS_{\mathbf{x}}
$$

$$
- \frac{\partial \hat{\mathsf{b}}_{\mathrm{K}}}{\partial s}(0; \hat{u}, \lambda).
$$

The partial derivative for $\nabla_{\mathbf{x}} G(\mathbf{T}_s^{\boldsymbol{\nu}}(\hat{\mathbf{x}}), \mathbf{T}_s^{\boldsymbol{\nu}}(\hat{\mathbf{y}}))$ with respect to s is computed in (5.1.38).

Remark 13. For a constant velocity field $\boldsymbol{\mathcal{V}}$, we see a massive simplification of (5.4.49) and the shape derivative formula reduces to

$$
\frac{d\mathcal{J}_F}{ds}(0) = \mu_0 \int\limits_{\Omega^0} \left(\mathsf{D}\boldsymbol{\mathcal{V}} \, \mathbf{M}\right) \cdot \mathbf{H_J} + \left(\mathsf{D}\mathbf{H_J} \, \boldsymbol{\mathcal{V}}\right) \cdot \mathbf{M} \, d\mathbf{x}, \tag{5.4.50}
$$

which is precisely the last term in (5.4.32) which was obtained via a volume based variational formulation.

5.4.3.10 Numerical Experiments

In this section we compute the shape derivatives (5.4.49) (called "BEM" in the plots) and (5.4.33) (Called "MST" in the plots) numerically. To keep computations entirely boundary based, we restrict ourselves to magnetizations $\mathbf{M}$ which are either constant or are obtained from a curl. Then we can compute boundary data using a BEM formulation based on (5.4.48) and use it directly to evaluate the shape derivatives. We don't mention the discrete spaces again as the setting is very similar to the one in Section 5.1.1.9 since we have the same structure as the variational problem in (5.1.15). The total force and torque is computed from the shape derivative as mentioned in Section 3.0.2 for a sequence of meshes with decreasing meshwidth h. For computing the dualnorm error, we use the procedure laid out in Section 4.4.7.1.

Experiment 39. We have the same setting as in Experiment 35 (cube shaped magnet) with the same constant magnetization $\mathbf{M} = (1, 0, 0)$, now approached with a scalar potential formulation. The reference values for force and torque are computed usig the BEM based shape derivative at a refinement level $h = 0.07$. Torque is computed about the point $(4,0,0)$. The resulting error in force and torque is plotted in Figure 5.73 and the asymptotic convergence rates are tabulated in Table 5.31. For total force, we see the exact same performance, whereas for total torque, we see a superior performance from the BEM based shape derivative.

(a) Error in total force
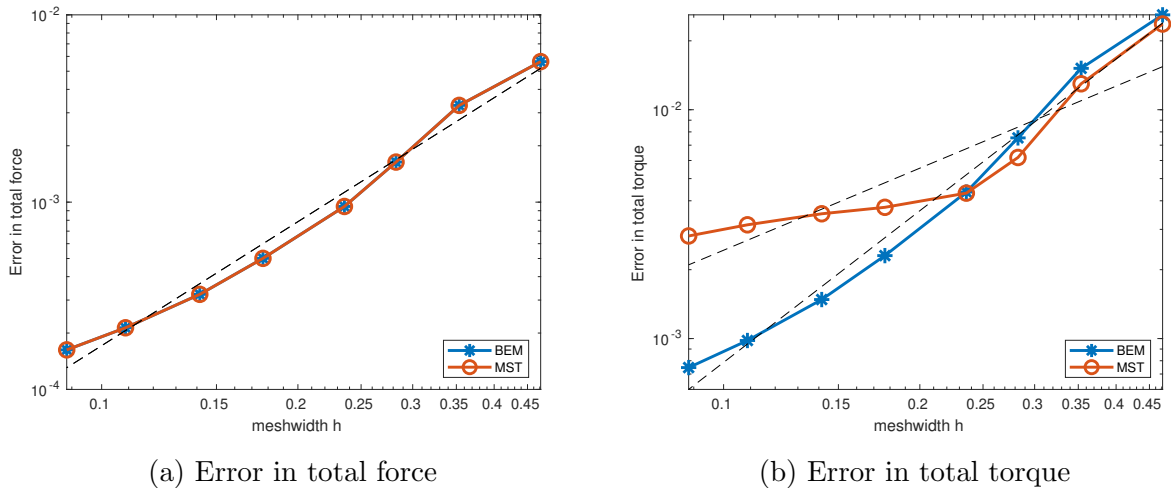
(b) Error in total torque

Figure 5.73: Error in force and torque computation for cube torus (Experiment 39)

Table 5.31: Asymptotic rate of algebraic convergence (Experiment 39)

Method	Force	Torque
Pullback approach	2.199	2.202
Stress tensor	2.199	1.1912

The shape derivatives can also be compared using the dual norm error. The reference value is again computed using the BEM based shape derivative at a refinement level $h = 0.088$. The resulting errors are plotted in Figure 5.74 which show the superiority of the BEM based shape derivative.
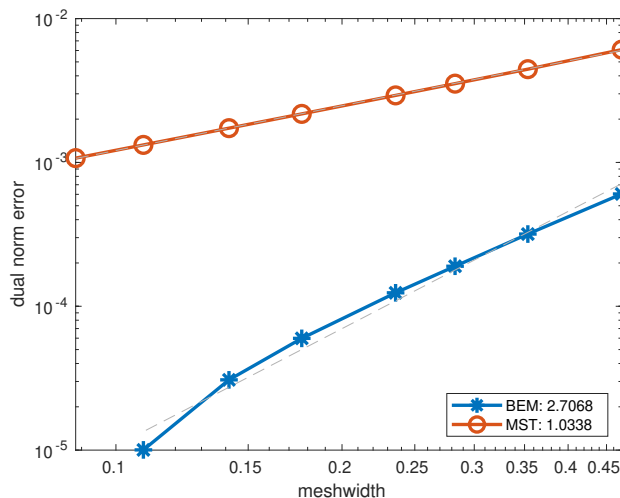
Figure 5.74: Dual norm error for Experiment 39

Experiment 40. We have the same setting as in Experiment 36 (spherical magnet) with the constant magnetization $\mathbf{M} = (1, 0, 0)$, now approached using a scalar potential formulation.

The reference values of force and torque are computed using the BEM based shape derivative at a refinement level $h = 0.039$, leading to the error plot Figure 5.75. Torque is computed about the point (4,0,0). The asymptotic convergence rates are tabulated in Table 5.32. We see a similar performance for the two methods which is expected for the case of a smooth domain.
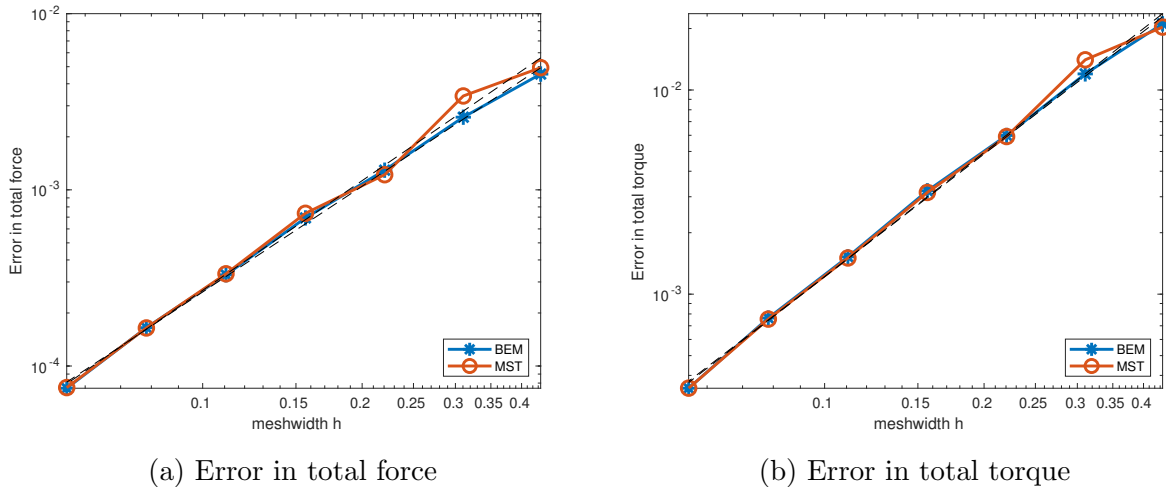

(a) Error in total force   (b) Error in total torque

Figure 5.75: Error in force and torque computation for sphere and torus (Experiment 40)

Table 5.32: Asymptotic rate of algebraic convergence (Experiment 40)

Method	Force	Torque
Pullback approach	1.994	1.995
Stress tensor	2.068	2.019

The dualnorm errors for the shape derivatives are given in Figure 5.76, computed using reference values computed using BEM based shape derivative at a refinement level $h = 0.055$. We again see a similar performance for the two shape derivatives.
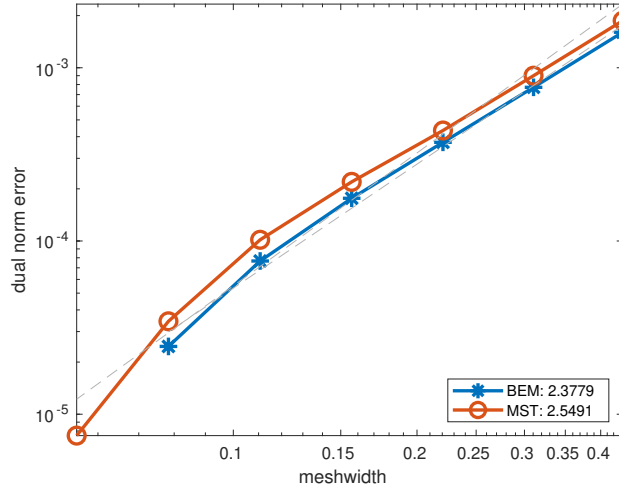
Figure 5.76: Dual norm error for Experiment 40

Experiment 41. We have the same setting as in Experiment 37 (brick shaped magnet) with the constant magnetization $\mathbf{M} = (1, 0, 0)$, now approached using a scalar potential formulation. The reference values of force and torque are computed using the BEM based shape derivative at a refinement level $h = 0.05$, leading to the error plot Figure 5.77. Torque is computed about the point $(4,0,0)$. The asymptotic convergence rates are tabulated in Table 5.33. We see the exact same performance for total force computation and only a slightly superior performance for total torque computation.
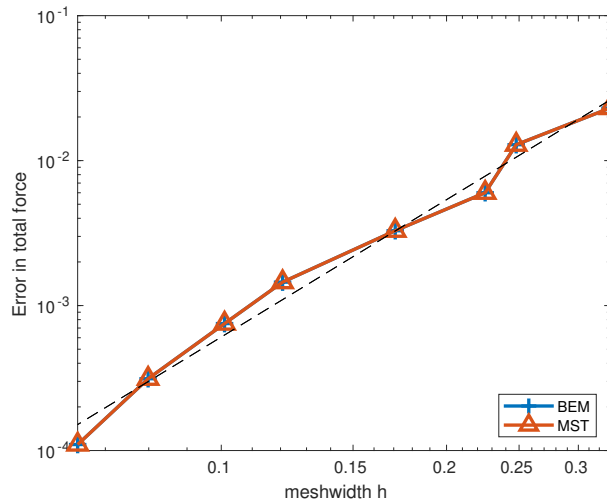
(a) Error in total force
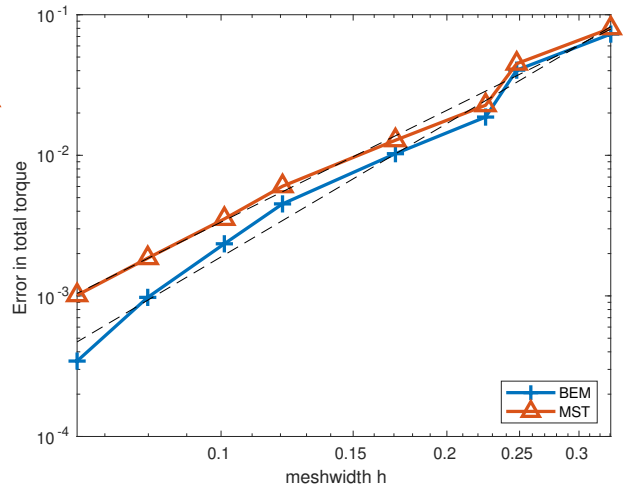
(b) Error in total torque

Figure 5.77: Error in force and torque computation for cuboid and torus (Experiment 41)

Table 5.33: Asymptotic rate of algebraic convergence (Experiment 41)

Method	Force	Torque
Pullback approach	3.15	3.15
Stress tensor	3.15	2.64

The dualnorm errors for the shape derivatives are given in Figure 5.78, computed using reference values computed using BEM based shape derivative at a refinement level $h = 0.064$. For general velocity fields $\mathcal{V}$, we see a superior performance from the BEM based shape derivative.
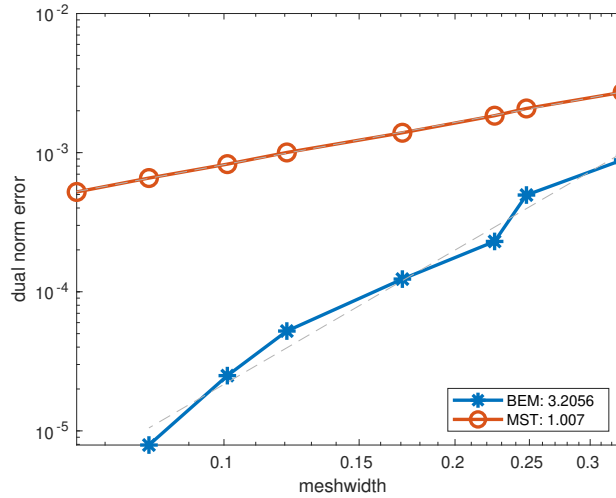

Figure 5.78: Dual norm error for Experiment 41

Experiment 42. We have the same setting as in Experiment 38 (tetrahedral magnet) with the constant magnetization $\mathbf{M} = (1, 0, 0)$, now approached using a scalar potential formulation. The reference values of force and torque are computed using the BEM based shape derivative at a refinement level $h = 0.041$, leading to the error plot Figure 5.79. Torque is computed about the point (4,0,0). The asymptotic convergence rates are tabulated in Table 5.34. We see similar convergence rates for the two shape derivatives but a lower absolute error for the BEM based shape derivative.

(a) Error in total force
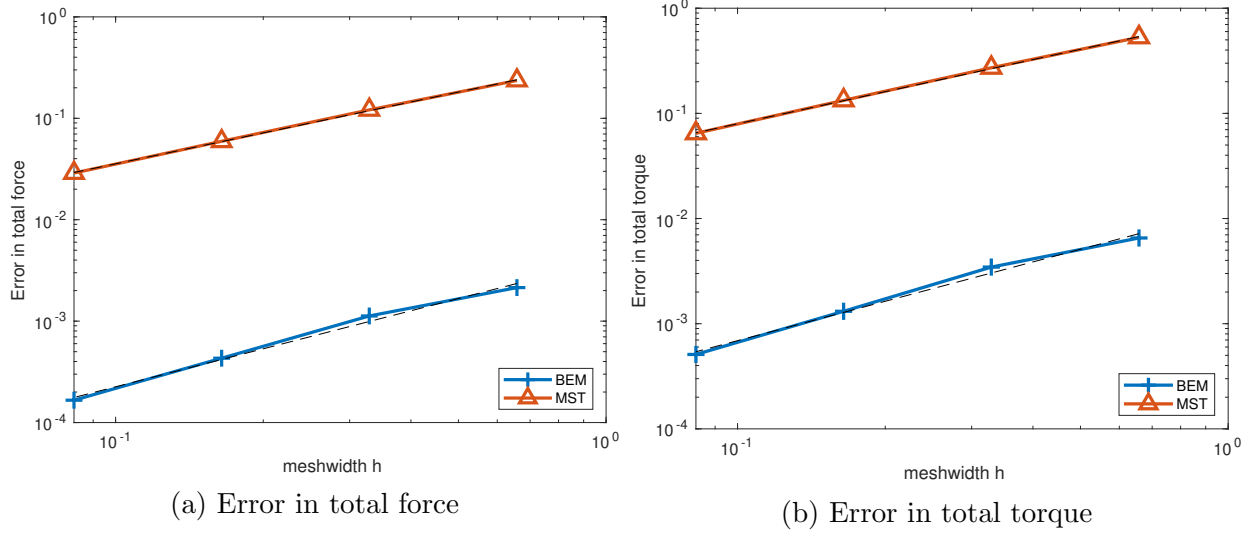

(b) Error in total torque

Figure 5.79: Error in force and torque computation for tetrahedron and torus (Experiment 42)

Table 5.34: Asymptotic rate of algebraic convergence (Experiment 42)

Method	Force	Torque
Pullback approach	1.24	1.24
Stress tensor	1.01	1.01

The dualnorm errors for the shape derivatives are given in Figure 5.80, computed using reference values computed using BEM based shape derivative at a refinement level $h = 0.041$. We see a slightly superior performance of the BEM based shape derivative.
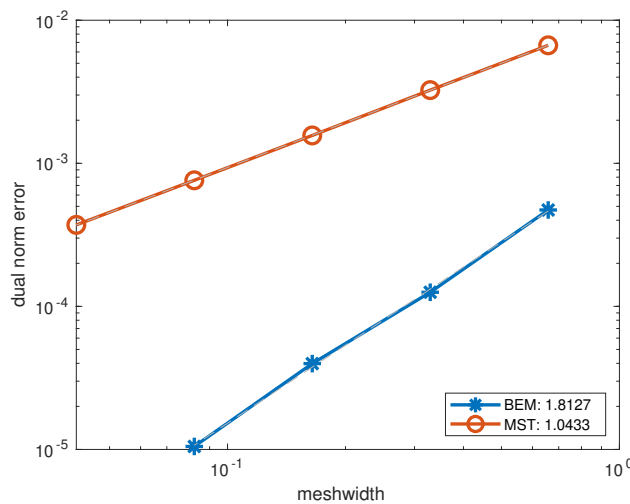

Figure 5.80: Dual norm error for Experiment 42

Chapter 6

Implementation

In this chapter, we go over the numerical implementation of BEM based shape derivatives derived in the previous chapters. All the 3D implementation codes can be found in the git repository [1], which is a fork of the open-source Gypsilab repository [2]. The 2D implementation for the Dirichlet BVP from Section 4.1 can be found in the FCSC repository [3], whereas the implementation for 2D dielectric case from Section 4.3 can be found in the FCSCD repository [4], both of which are based on the 2DParametricBEM library [5]. For evaluating the BEM solutions for various model problems presented, we rely on the available implementation for assembling the BIOs in these libraries.

Having the BEM solution, the critical part of the implementation of shape derivatives involves evaluating singular integrals of the (general) form

$$I = \int_\Gamma \int_\Gamma \mathsf{K}(\mathbf{x}, \mathbf{y}) \, \psi(\mathbf{y}) \, g(\mathbf{x}) \, dS_\mathbf{y} \, dS_\mathbf{x}, \tag{6.0.1}$$

where $\mathsf{K}(\mathbf{x}, \mathbf{y})$ is a singular kernel for $\mathbf{x} = \mathbf{y}$. The dependence on $\boldsymbol{\mathcal{V}}$ could appear anywhere in the integral, either the kernel K or the functions ψ and g.

Remark 14. Note that we may have a vector-valued kernel with vector-valued trial and test functions which are coupled through cross products and dot products. The evaluation strategy is similar to the scalar case.

In 2D the BEM based shape derivatives can be evaluated by switching to polar coordinates as elaborated in [47, Section 3.2] for each of the terms appearing in (4.1.16). In 3D the evaluation is done using the Sauter and Schwab quadrature rule [54, Chapter 5].

Assuming that we have a triangular mesh $\mathcal{M}_h$ of the boundary Γ, the integral I is decomposed as

$$I = \sum_{\tau \in \mathcal{M}_h} \sum_{t \in \mathcal{M}_h} \int_\tau \int_t \mathsf{K}(\mathbf{x}, \mathbf{y}) \, \psi(\mathbf{y}) \, g(\mathbf{x}) \, dS_\mathbf{y} \, dS_\mathbf{x}. \tag{6.0.2}$$

---

[1]https://github.com/piyushplcr7/gypsilab_forces
[2]https://github.com/matthieuaussal/gypsilab
[3]https://gitlab.ethz.ch/ppanchal/fcsc
[4]https://github.com/gninr/FCSCD
[5]https://gitlab.ethz.ch/ppanchal/2dparametricbem

The evaluation then involves treatment of the singular cases where the triangular elements τ and t have an intersection: common vertex, common edge or identical elements. The quadrature rules for these cases have been summarized in [54, Section 5.2.4]. If there is no intersection, the singularity is not hit and the integral can be simply evaluated by numerical quadrature.

During the actual evaluation, we have the BEM solution in terms of basis functions of a BEM space, for example $\psi(\mathbf{x}) = \sum_{i=1}^{N} b_i \; \beta_i(\mathbf{x})$ and $g(\mathbf{x}) = \sum_{i=1}^{M} a_i \; \alpha_i(\mathbf{x})$, where $\{\beta_i(\mathbf{x})\}_{i=1}^{N}$ and $\{\alpha_i(\mathbf{x})\}_{i=1}^{M}$ are the basis functions. The integral I can then be written as

$$I = \boldsymbol{a}^T \, \mathbf{M} \, \boldsymbol{b}, \qquad \boldsymbol{a} := [a_1, a_2, ..., a_M]^T, \; \boldsymbol{b} := [b_1, b_2, ..., b_N]^T, \tag{6.0.3}$$

and

$$\mathbf{M}_{i,j} := \int_\Gamma \int_\Gamma \mathsf{K}(\mathbf{x}, \mathbf{y}) \, \beta_j(\mathbf{y}) \, \alpha_i(\mathbf{x}) \, d\mathrm{S}_\mathbf{y} \, d\mathrm{S}_\mathbf{x}, \quad i \in \{1, ..., M\}, \; j \in \{1, ..., N\}. \tag{6.0.4}$$

So the integral (6.0.4) is evaluated for all pairs of trial and test basis functions, all of which have compact support in a few triangular elements in the mesh. The basis functions for general triangular elements are obtained via appropriate transformations of the reference shape functions which are defined on the reference triangle $\hat{K}$ with vertices (0,0), (1,0) and (1,1). For assembling the matrix in (6.0.4), we compute for each possible pair $\tau, t \in \mathcal{M}_h \times \mathcal{M}_h$ the local matrices

$$\mathbf{L}_{p,q}^{\tau,t} := \int_{\hat{K}} \int_{\hat{K}} \mathsf{K}(\chi_\tau(\hat{\mathbf{x}}), \chi_t(\hat{\mathbf{y}})) \; \hat{\beta}_q(\hat{\mathbf{y}}) \; \hat{\alpha}_p(\hat{\mathbf{x}}) \, \omega_\tau(\hat{\mathbf{x}}) \, \omega_t(\hat{\mathbf{y}}) \, d\mathrm{S}_{\hat{\mathbf{y}}} \, d\mathrm{S}_{\hat{\mathbf{x}}}, \quad p \in \{1, ..., m\}, \; q \in \{1, ..., n\},$$

$$\tag{6.0.5}$$

where ω_τ, ω_t are the Jacobians of the transformations $\chi_\tau : \hat{K} \to \tau$, $\chi_t : \hat{K} \to t$, and $\hat{\alpha}_p$, $\hat{\beta}_q$ are the reference shape functions of the corresponding BEM spaces. For each pair of a reference shape function and a mesh element, there is a unique global basis function index. Using this local to global mapping, the final global matrix (6.0.4) is assembled from all local matrices (6.0.5). A similar panel-oriented assembly is used for the 2D computations where the local matrices are evaluated for all element pairs and mapped to the global location.

The Sauter and Schwab quadrature rule for evaluating the integrals (6.0.5) is based on integration on a unit four dimensional cube $[0,1]^4$. We use a tensor product Gauss Legendre quadrature rule of order 5 to generate the points and weights which are then transformed according to the expressions presented in [54, Section 5.2.4] to get the final quadrature points and weights, which are simply plugged into the integrands in (6.0.5). We use the same evaluation technique for the case of the strongly singular kernel present in (5.1.36) as the Sauter and Schwab quadrature technique can be applied to such integrals [54, Section 5.1.2].

6.0.1   2D Implementation (2DParametricBEM)

2D BEM implementations are based on the 2DParametricBEM library which consists of parametric meshes, handled by the object 'ParametrizedMesh'. The mesh contains the

sequence of mesh elements which are just parametrized curves, allowing the possibility of pointwise evaluation of the curve and its derivative. The library implements parametrizations like fourier sum, line segment and polynomial parametrization. The functionality to assemble BIOs is already there in the library using the method GalerkinMatrix in the namespaces 'single_layer', 'double_layer' and 'hypersingular'. Below is an example of solving the direct first kind BIE $V\psi = (\frac{1}{2}\mathsf{Id} + K)g$ for given Dirichlet data g. Note that 2DParametricBEM uses the C++ based Eigen library to handle matrices and linear algebra operations.

```
Eigen::VectorXd solve(const ParametrizedMesh &mesh,
std::function<double(double, double)> g, unsigned order) {
        // Lowest order space of piece-wise constants (P0)
        DiscontinuousSpace<0> trial_space;
        DiscontinuousSpace<0> test_space;
        // Space used for interpolation of Dirichlet data (P1)
        ContinuousSpace<1> g_interpol_space;
        // Computing V matrix
        Eigen::MatrixXd V = single_layer::GalerkinMatrix(mesh,
            trial_space, order);
        // Computing K matrix
        Eigen::MatrixXd K =
        double_layer::GalerkinMatrix(mesh, g_interpol_space, test_space
            , order);
        // Computing mass matrix
        Eigen::MatrixXd M = MassMatrix(mesh, test_space,
            g_interpol_space, order);
        // Interpolating Dirichlet data
        Eigen::VectorXd g_N = g_interpol_space.Interpolate(g, mesh);
        // Build rhs for solving
        Eigen::VectorXd rhs = (0.5 * M + K) * g_N;
        // Solving for coefficients
        //Eigen::FullPivLU<Eigen::MatrixXd> dec(V);
        Eigen::HouseholderQR<Eigen::MatrixXd> dec(V);
        Eigen::VectorXd sol = dec.solve(rhs);
        return sol;
}
```

Evaluation of the terms in the shape derivative is done in a similar fashion to the evaluation of boundary integral operators.

6.0.2   3D Implementation (Gypsilab)

All 3D implementations are done using Gypsilab. Triangular meshes in Gypsilab are handled by the "msh" class which provides methods for accessing the mesh elements, vertices, normals etc. There are some built-in methods for generating spherical meshes ("mshSphere"), cuboidal meshes ("mshCube") and toroidal meshes ("mshTorus"). These can be found in the sub-directory Gypsi_files/openMsh.

Given a msh object, we can construct a "dom" object which contains information about

quadrature weights and points associated with the mesh. This can be constructed using a mesh by the command dom(mesh,order) where order is the quadrature order per mesh element. There are only a certain number of quadrature orders available in the library.

With the msh object, we can also construct a "fem" object which represents a discrete space associated with the mesh elements. Is is constructed using the command fem(mesh,type) where type specifies the type of the space. There are several options like 'P0' (piece-wise constants), 'P1' (piece-wise linear function), 'NED' (Nedelec edge elements) and 'RWG' (Rao-Wilton-Glisson) for constructing the fem object. It is also possible to apply some operators to these spaces using the fem object as shown in the code snippet below

```
% Spherical boundary mesh with radius 1
mesh = mshSphere(50,1);
% Dom object for quadrature of order 3 per triangle
Gamma = dom(mesh,3);

% Piece-wise linear functions on the mesh
P1 = fem(mesh,'P1');
% Piece-wise constant functions on the mesh
P0 = fem(mesh,'P0');
% Nedelec edge elements on the mesh
NED = fem(mesh,'NED');
% RWG basis functions on the mesh
RWG = fem(mesh,'RWG');

% Applying nxgrad operator to P1
nxgradP1 = P1.nxgrad;
% Applying surface divergence to RWG
divRWG = RWG.div;
```

With the mesh, quadrature and discrete spaces at our disposal, we can assemble BIOs required for our case. For this task, we utilize the "integral" functionality in the library which allows us to evaluate various integrals. In the library, the quadrature is directly applied using the singular kernel and whenever it is close to 0, it is assigned the value 0. To get the correct integrals, the library offers a "regularize" method which needs to be used after applying the "integral" method for singular kernels. These computations have been wrapped in the functions like "single_layer", "double_layer_laplace", "double_layer_magnetostatics" etc. for a high level access. The implementation for "single_layer" is shown here for reference

```
function MV = single_layer(Gamma,test,trial)
        % Kernel for single layer
        Gxy = @(X,Y)femGreenKernel(X,Y,'[1/r]',0);
        % Evaluating the integral
        MV = integral(Gamma,Gamma,test,Gxy,trial)/(4*pi);
        % Regularizing the integral to get the final Galerkin matrix
        MV = MV + 1/(4*pi)*regularize(Gamma,Gamma,test,'[1/r]',trial);
end
```

In the code snippet above, 'test' and 'trial' represent the test and trial spaces respectively.

The BIOs can then be easily combined together into a block structure if needed as they are full matrices. Solving for the unknowns is straightforward for which we use the backslash operator in Matlab. Below is a simple example of solving the direct first kind BIE $V\psi = (\frac{1}{2}\mathsf{Id} + K)g$ with a given Dirichlet data $g(\mathbf{x}) \equiv \boldsymbol{a}\cdot\mathbf{x}$ for some constant $\boldsymbol{a} \in \mathbb{R}^3$

```matlab
% Spherical boundary mesh with radius 1
mesh = mshSphere(50,1);
% Dom object for quadrature of order 3 per triangle
Gamma = dom(mesh,3);

% Piece-wise linear functions on the mesh
P1 = fem(mesh,'P1');
% Piece-wise constant functions on the mesh
P0 = fem(mesh,'P0');

% BIOs
V = single_layer(Gamma,P0,P0);
K = double_layer_laplace(Gamma,P0,P1);
M = mass_matrix(Gamma,P0,P1);

% Constant vector a
a = [1 2 3];
% Dirichlet data as a function (assumes input of size N X 3)
g = @(X) X * a';

% Quadrature points
[X,~] = Gamma.qud;
% Evaluating Dirichlet data at all quadrature points
g_values = g(X);
% Projecting the data to the space P1 and getting the coefficients
g_coeffs = proj(g_values,Gamma,P1);

% Solving the linear system to get psi
psi = V\((0.5 * M + K) * g_coeffs);
```

6.0.2.1 CUDA Acceleration

For evaluating the BEM based shape derivatives, we use a CUDA based implementation, especially for the evaluation of the dual norm as mentioned in Section 4.4.7.1 where the shape derivative needs to be evaluated for multiple velocity fields. The CUDA codes are compiled to .ptx format using the NVCC compiler and the CUDA kernel is launched directly from Gypsilab. The .cu and .ptx files are available in the repository [6] in the sub-directory "Piyush's codes/CUDA".

Since the computation of the local matrices (6.0.5) are independent from each other, they can be done in parallel if there are enough computing resources available and GPUs provide

---

[6]https://github.com/piyushplcr7/gypsilab_forces

the perfect hardware to do that. They contain thousands of cores (up to 16000 for RTX 4090) which can take up a small chunk of all the possible triangle pairs τ, t. Assuming that the total number of triangle pairs is N_{el}^2 where N_{el} is the number of triangular elements in the mesh $\mathcal{M}_h$, and total number of available CUDA threads is $N_{threads}$, each thread computes ceil($N_{el}^2/N_{threads}$) interactions (except for the last one) for all reference shape functions.

For the computations, we pass the required BEM coefficients $\boldsymbol{a}, \boldsymbol{b}$ to the GPU along with information about the mesh like vertices, elements, areas and normals. We also pass the quadrature rules for the different interaction cases (common edge, common vertex, identical panel and far away panel) to the GPU. A skeleton of the CUDA kernel is shown below

```
/*
This function computes the shape derivative Tnu' * M * Tdu using CUDA
    parallelism.

Parameters:
NInteractions (int): The total number of interaction pairs.
NThreads (int): The number of CUDA threads to be used for parallel
    computation.
I (const int*): Array of length NInteractions containing the indices of
    the first elements of the interaction pairs.
J (const int*): Array of length NInteractions containing the indices of
    the second elements of the interaction pairs.
relation (const int*): Array of length NInteractions containing the
    type of relation for each interaction pair (ranging from 0 to 3,
    representing the number of vertices intersecting between two
    triangular elements).
WK (const double*): Array of length NqK containing the weights for the
    first set of quadrature points of interaction type K = {0,1,2,3}.
XK (const double*): Array of length NqK containing the coordinates for
    the first set of quadrature points of interaction type K =
    {0,1,2,3}.
NqK (int): The number of quadrature points for the interaction type K =
    {0,1,2,3}.
Tdu (const double*): Coefficients for trial function
Tnu (const double*): Coefficients for test function.
Elements (const int*): Array containing the elements of the mesh.
Vertices (const double*): Array containing the vertices of the mesh.
Normals (const double*): Array containing the normals of the mesh
    elements.
Areas (const double*): Array containing the areas of the mesh elements.
Elt2DofTest (const int*): Array containing the element to dof mapping
    for the test space.
Elt2DofTrial (const int*): Array containing the element to dof mapping
    for the trial space.
*/
__global__ void computeShapeDerivative( int NInteractions,
int NThreads, const int *I, const int *J, const int *relation,
```

```
const double *W0, const double *X0, int Nq0,
const double *W1, const double *X1, int Nq1,
const double *W2, const double *X2, int Nq2,
const double *W3, const double *X3, int Nq3,
double *shapeDerivative,
const double *Tdu, const double *Tnu,
const int *Elements, const double *Vertices, const double *Normals,
const double *Areas,
const int *Elt2DofTest, const int *Elt2DofTrial) {
        // Get thread ID (Assuming 1D block and grid)
        int ThreadID = blockIdx.x * blockDim.x + threadIdx.x;

        // No. of interactions assigned per thread
        int InteractionsPerThread = ceil(double(NInteractions) / double
            (NThreads));
        for (int idx = 0; idx < InteractionsPerThread; ++idx) {
                // The interaction number
                int InteractionIdx = ThreadID * InteractionsPerThread +
                    idx;

                // Make sure that the last thread stays in limit
                if (InteractionIdx >= NInteractions)
                        break;

                // The pair of interacting elements
                int i = I[InteractionIdx], j = J[InteractionIdx];

                // Processing the interaction i,j
        }


}
```

For evaluating the shape derivative, we don't need to assemble the matrix (6.0.4). Instead, we accumulate to the shape derivative value from all the local interactions as soon as they are computed. This is very efficient in terms of memory usage, which can be limited on a GPU. Writing to a global shape derivative repeatedly by each thread needs atomic compare and swap operations which can be time consuming. Instead, the threads accumulate the shape derivatives to the shared memory based on all the interactions assigned to them and write to a global location only at their end, reducing the amount of atomic operations. For dual norm computations, each thread also loops over all the velocity fields and accumulates the associated shape derivatives at different positions in shared memory which are eventually written at different positions in the global memory.

There are some things to keep in mind for CUDA implementation. Since there is no branch prediction on GPUs, it is not a good idea to use conditional statements. The threads are executed in groups of a certain size called warps under the SIMD (single instruction multiple data) paradigm. This means that the threads visit both the branches of a condi-

tional statement which is wasted computing effort. To get rid of if conditions in our CUDA implementation, we do some pre-processing on the CPU. There are a few places where these conditions could be used: selection of the quadrature rule based on the type of interaction between a pair of triangles, evaluation of the type of intersection between a given pair and ordering of the vertices while performing integration. In our implementation, we pre-compute the interaction type for all pairs on the CPU, along with the required permutation the vertices need to be in while computing the integrals. This information is passed to the CUDA kernel and used directly, allowing us to get rid of conditional statements.

With GPU computations, it is very important to make use of the registers, shared memory and constant memory for the fastest memory accesses. The information transferred to GPU is stored in global memory and access to it is much more time consuming and often the cause of performance problems. With that in mind, our implementation is sub-optimal as we don't use the faster memory accesses for the quadrature points, which is by far the largest chunk of data to be read. This is because the quadrature rule takes up much more space than available in the shared memory or constant memory, which is up to 96 Kb in modern GPU architectures. This problem is remedied a bit by using the __ldg functionality in CUDA which loads the data from cache if available, reducing the number of global memory accesses, as the quadrature points and weights are stored as a contiguous array. But this is not the optimal solution. The alternative of dividing the quadrature points across all threads might not be the best solution either because then the threads have to compute all the interactions. The optimal solution would be dividing both quadrature points and interactions across CUDA threads by using large block sizes and larger number of blocks. The end goal is to limit the amount of memory usage per block which would allow all the necessary information to be stored in the shared memory or constant memory, allowing for a faster read time and ultimately faster computations. Keeping the memory usage light for a given block, the hardware allows for more performance optimization: A streaming multiprocessor, the computing unit which executes the warps in a lockstep with each other, can handle different warps or different blocks simultaneously. If it requires some additional clock cycles for a given warp, to fetch some data for example, if can execute another one meanwhile if it is ready for execution. This could be exploited if multiple blocks or warps need to work on the same chunk of the quadrature data, which has already been loaded into the shared memory.

Since the GPU computations are independent of the CPU computations, we can also compute things in parallel on the CPU. This is also used in our implementation where the shape derivative computations are divided into a Sauter and Schwab based part and the rest. The prior is sent to the GPU for computation while the latter is processed on the CPU at the same time. It is obviously possible to use parllelization on the CPU side as well to speed up the computations but in our case, the Sauter and Schwab based computations take up more time.

Chapter 7

Conclusion and Outlook

In this work, we explored energy shape derivatives for various electrostatic and magnetostatic model problems, both with a volume-based variational formulation and a boundary integral formulation constraint. We mainly worked with linear, isotropic and homogeneous materials and for the case of permanent magnets, chose an affine material law. We observed that the volume-based variational constraint yields shape derivatives that recover the Maxwell Stress Tensor-based formulas, whereas the BIE constraint yields novel expressions for the energy shape derivatives, containing double integrals resembling boundary integral operators. In the case of electrostatics, we theoretically argued that these BIE-constrained shape derivatives are continuous on energy trace spaces, compared to the MST-based expressions on the boundary which lack continuity. The continuity of the shape derivative was crucial in showing supercovergence during numerical evaluation as seen in Proposition 1. This was also evident in all the numerical experiments, both in 2D and 3D, where we observed the superior performance of the BIE-based shape derivatives, especially in cases with non-smooth domains where the solutions exhibit corner singularities. We observed a performance that was superior even to volume-based (egg-shell) computations in Section 4.1. We confirmed the superior convergence rate of the BEM based shape derivatives with a more general evaluation via the dual norm. It would be interesting to extend the technique presented in this work to analytical non-linear material laws, for example a magnetic material where the $\mathbf{B} - \mathbf{H}$ curve passes through the origin.

In the case of permanent magnets, the affine material law led to inevitable volume-based terms depending on either $\mathbf{curl M}$ or $\mathrm{div}\,\mathbf{M}$, even with BEM based shape derivatives. In this work, we restricted ourselves to the simple case where the volume terms go to zero by assuming that $\mathbf{curl}M = 0$ or $\mathrm{div}\,\mathbf{M} = 0$. Evaluation with a more general magnetization $\mathbf{M}$ is a possible extension of the numerical experiments for the permanent magnet case. However it requires treatment of singular integration for tetrahedron interactions (double integrals over Ω) and tetrahedron-triangle interactions (double integral involving Ω and $\partial\Omega$). For constant velocity fields $\boldsymbol{\mathcal{V}}$ we saw that the BEM based shape derivative for a scalar potential formulation of a permanent magnet reduced to an MST-like expression (see Remark 13). This also explained why in some experiments in Section 5.4.3.10 we saw an exact overlap of the BEM based and MST-based approaches. However, the BEM based shape derivative still retained its superior convergence during more general dual-norm computations.

For the case of permanent magnets, we explored shape derivatives for two energies and two

co-energies in a brute force approach to a-posteriori find out meaningful shape derivatives. We saw that our approach gave a physically plausible result only for specific choices of the energy and co-energy as seen in tables Table 5.30 and Table 5.29, whereas the others gave a force density which ignored the existence of the current source and reported just the interaction of the magnet with itself. We used these "right" (co)energies for the BEM based shape derivative evaluation. It is still unclear what is the right (co)energy to use and what is the true force density inside a permanent magnets. It has been a topic of interest and confusion for a long time because as we saw, the two different models of the magnet we used give the same total force and torque. This also implies that the BEM based shape derivative could be used to compute these quantities reliably at a faster convergence rate. The question of the true force density for permanent magnets still remains open.

We currently lack a theoretical argument to show the superiority of the BIE-constrained shape derivatives obtained via a vector potential formulation or even to demonstrate that the partial derivatives obtained via the vectorial double-layer potential are defined as weakly singular integrals. Nevertheless, implementing them using Sauter and Schwab quadrature works just fine and yields these amazing results, hinting at the possibility of demonstrating their existence as weakly singular integrals and nice mapping properties.

We also discovered how the idea of holding the fluxes constant, as described by Henrotte and Hameyer, emerges as a natural consequence of our method: that forces can be obtained via shape differentiation by transforming the reference fields and potentials as the appropriate differential forms. With this approach, we also proved the equivalence of the equivalent current and equivalent charge model of a permanent magnet for computing the total force and total torque.

The work here was restricted to a static setting. It would be interesting to extend this approach to an electrodynamic setting or exploring other types of elliptic problems where force is a derived quantity and of interest. For the sake of curiosity, such derivations could also be attempted at a more abstract level where we don't work with integral representations of the BIOs.

A missing result in this work is showing the equivalence of the BEM based and MST shape derivatives after they have been computed. Showing this would allow us to express the BIE-constrained shape derivatives in Hadamard form.

Finally, there is potential for improvement in the numerical implementation, especially the CUDA acceleration which can lead to drastic performance improvements. This would be an interesting direction for not just computing BEM based shape derivatives but for BEM solvers in general.

Bibliography

[1] Dominic Amann, Andreas Blaszczyk, Günther Of, and Olaf Steinbach. Simulation of floating potentials in industrial applications by boundary element methods. *Journal of Mathematics in Industry*, 4(1):13, Oct 2014.

[2] Martin Berggren. A unified discrete–continuous sensitivity analysis method for shape optimization. In W. Fitzgibbon, Y.A. Kuznetsov, Pekka Neittaanmäki, Jacques Périaux, and Olivier Pironneau, editors, *Applied and Numerical Partial Differential Equations*, volume 15 of *Computational Methods in Applied Sciences*, pages 25–39. Springer Netherlands, 2010.

[3] Timo Betcke, Alexander Haberl, and Dirk Praetorius. Adaptive boundary element methods for the computation of the electrostatic capacity on complex polyhedra. *J. Comput. Phys.*, 397:108837, 19, 2019.

[4] A. Bossavit. Forces in magnetostatics and their computation. *Journal of Applied Physics*, 67(9):5812–5814, 1990.

[5] A. Bossavit. Applied differential geometry: A compendium. Unpublished Lecture Notes, 2002.

[6] A. Bossavit. Bulk forces and interface forces in assemblies of magnetized pieces of matter. *IEEE Transactions on Magnetics*, 52(3):1–4, March 2016.

[7] Alain Bossavit. Magnetic forces in and on a magnet. *Discrete Contin. Dyn. Syst. Ser. S*, 12(6):1589–1600, 2019.

[8] A. Buffa and P. Ciarlet. On traces for functional spaces related to Maxwell's equations. Part I: An integration by parts formula in Lipschitz polyhedra. Technical Report 1147, Instituto di Analisi Numerica, CNR, Pavia, Italy, 1999.

[9] A. Buffa and P. Ciarlet. On traces for functional spaces related to Maxwell's equations. Part II: Hodge decompositions on the boundary of Lipschitz polyhedra and applications. *Math. Meth. Appl. Sci.*, 24(1):31–48, 2001.

[10] A. Buffa, M. Costabel, and D. Sheen. On traces for $\mathbf{H}(\mathbf{curl}, \Omega)$ in Lipschitz domains. *J. Math. Anal. Appl.*, 276(2):845–867, 2002.

[11] Anthony Carpentier, Nicolas Galopin, Olivier Chadebec, Gérard Meunier, and Christophe Guérin. Application of the virtual work principle to compute magnetic forces with a volume integral method. *International Journal of Numerical Modelling: Electronic Networks, Devices and Fields*, 27(3):418–432, 2014.

[12] Philippe G. Ciarlet. *Linear and nonlinear functional analysis with applications.* Society for Industrial and Applied Mathematics, Philadelphia, PA, 2013.

[13] Xavier Claeys and Ralf Hiptmair. First-kind Galerkin boundary element methods for the Hodge-Laplacian in three dimensions. *Math. Methods Appl. Sci.*, 43(8):4974–4994, 2020.

[14] D. Colton and R. Kress. *Integral equation methods in scattering theory.* Pure and Applied Mathematics. John Wiley & Sons, 1983.

[15] J.L. Coulomb. A methodology for the determination of global electromechanical quantities from a finite element analysis and its application to the evaluation of magnetic forces, torques and stiffness. *IEEE Trans. Magnetics*, 19(6):2514–2519, 1983.

[16] Monique Dauge. *Elliptic boundary value problems on corner domains*, volume 1341 of *Lecture Notes in Mathematics.* Springer-Verlag, Berlin, 1988. Smoothness and asymptotics of solutions.

[17] Georges de Rham. *Differentiable manifolds*, volume 266 of *Grundlehren der Mathematischen Wissenschaften [Fundamental Principles of Mathematical Sciences].* Springer-Verlag, Berlin, 1984. Forms, currents, harmonic forms, Translated from the French by F. R. Smith, With an introduction by S. S. Chern.

[18] M. C. Delfour and J.-P. Zolésio. *Shapes and geometries*, volume 22 of *Advances in Design and Control.* Society for Industrial and Applied Mathematics (SIAM), Philadelphia, PA, second edition, 2011. Metrics, analysis, differential calculus, and optimization.

[19] M.C. Delfour and J.-P. Zolésio. *Shapes and Geometries*, volume 22 of *Advances in Design and Control.* SIAM, Philadelphia, 2nd edition, 2010.

[20] Geoffrey Deliége François Henrotte, Hans Vande Sande and Kay Hameyer. Electromagnetic force density in a ferromagnetic material. *IEEE Transactions On Magnetics, Vol. 40, No. 2*, 2004.

[21] Heiko Gimperlein, Fabian Meyer, Ceyhun Özdemir, David Stark, and Ernst P. Stephan. Boundary elements with mesh refinements for the wave equation. *Numer. Math.*, 139(4):867–912, 2018.

[22] Wei Gong and Shengfeng Zhu. On Discrete Shape Gradients of Boundary Type for PDE-constrained Shape Optimization. *SIAM J. Numer. Anal.*, 59(3):1510–1541, 2021.

[23] David J Griffiths. *Introduction to electrodynamics.* Pearson, 2013.

[24] P. Grisvard. *Elliptic Problems in Nonsmooth Domains.* Pitman, Boston, 1985.

[25] Joachim Gwinner and Ernst Peter Stephan. *Advanced boundary element methods*, volume 52 of *Springer Series in Computational Mathematics*. Springer, Cham, 2018. Treatment of boundary value, transmission and contact problems.

[26] W. Hackbusch. *Integral equations. Theory and numerical treatment.*, volume 120 of *International Series of Numerical Mathematics*. Birkhäuser, Basel, 1995.

[27] F. Henrotte, G. Deliege, and K. Hameyer. The eggshell approach for the computation of electromagnetic forces in 2D and 3D. *COMPEL*, 23(4):996–1005, 2004.

[28] F. Henrotte and K. Hameyer. A theory for electromagnetic force formulas in continuous media. *IEEE Transactions on Magnetics*, 43(4):1445–1448, April 2007.

[29] François Henrotte and Kay Hameyer. Computation of electromagnetic force densities: Maxwell stress tensor vs. virtual work principle. *J. Comput. Appl. Math.*, 168(1-2):235–243, 2004.

[30] N. Heuer and E.P. Stephan. The *hp*-version of the boundary element method on polygons. *J. Integral Equations Appl.*, 8:173–212, 1996.

[31] M. Hinze, R. Pinnau, M. Ulbrich, and S. Ulbrich. *Optimization with PDE constraints*, volume 23 of *Mathematical Modelling: Theory and Applications*. Springer, New York, 2009.

[32] R. Hiptmair. Finite elements in computational electromagnetism. *Acta Numer.*, 11:237–339, 2002.

[33] R. Hiptmair. Symmetric coupling for eddy current problems. *SIAM J. Numer. Anal.*, 40(1):41–65, 2002.

[34] R. Hiptmair, A. Paganini, and S. Sargheini. Comparison of approximate shape gradients. *BIT Numerical Mathematics*, 55:459–485, 2014.

[35] Ralf Hiptmair. Maxwell's equations: Continuous and discrete. *Lecture Notes in Mathematics*, 2148, 01 2015.

[36] Ralf Hiptmair and Jingzhi Li. Shape derivatives in differential forms I: an intrinsic perspective. *Ann. Mat. Pura Appl. (4)*, 192(6):1077–1098, 2013.

[37] Se Hee Lee Hong Soon Choi and Il Han Park. General formulation of equivalent magnetic chargemethod for force density distribution on interfaceof different materials. *IEEE Transactions On Magnetics, Vol. 41, No. 5*, 2005.

[38] J.D. Jackson. *Classical electrodynamics*. John Wiley, 3rd edition, 1998.

[39] G. Meunier L.H. de Medeiros, G. Reyne. About the distribution of forces in permanent magnets. *IEEE Transactions on Magnetics*, 1999.

[40] Gilbert Reyne Luiz H. de Medeiros and Gérard Meunier. A unique distribution of forces in permanent magnets using scalar and vector potential formulations. *IEEE TRANSACTIONS ON MAGNETICS, VOL. 36, NO. 5*, 2000.

[41] M. Maischak and E. P. Stephan. The *hp*-version of the boundary element method in $\mathbf{R}^3$: the basic approximation results. *Math. Methods Appl. Sci.*, 20(5):461–476, 1997.

[42] S. McFee, J.P. Webb, and D.A. Lowther. A tunable volume integration formulation for force calculation in finite-element based computational magnetostatics. *IEEE Trans. Magnetics*, 24(1):439–442, 1988.

[43] W. McLean. *Strongly Elliptic Systems and Boundary Integral Equations*. Cambridge University Press, Cambridge, UK, 2000.

[44] J.-C. Nédélec. *Acoustic and Electromagnetic Equations: Integral Representations for Harmonic Problems*, volume 44 of *Applied Mathematical Sciences*. Springer-Verlag, Berlin, 2001.

[45] Pascal Brochet Olivier Barré and Michel Hecquet. Experimental validation of magnetic and electric local force formulations associated to energy principle. *IEEE Transactions On Magnetics, Vol. 42, No. 4*, 2006.

[46] A. Paganini. *Numerical shape optimization with finite elements*. Eth dissertation 23212, ETH Zurich, 2016.

[47] Piyush Panchal. Electrostatic force computation using shape calculus. Master's thesis, ETH Zurich, 2019.

[48] Piyush Panchal and Ralf Hiptmair. Electrostatic Force Computation with Boundary Element Methods. *The SMAI journal of computational mathematics*, 8:49–74, 2022.

[49] Piyush Panchal and Ralf Hiptmair. Electrostatic forces on conductors with boundary element methods in 3d. In Martijn van Beurden, Neil V. Budko, Gabriela Ciuprina, Wil Schilders, Harshit Bansal, and Ruxandra Barbulescu, editors, *Scientific Computing in Electrical Engineering*, pages 102–110, Cham, 2024. Springer Nature Switzerland.

[50] Piyush Panchal, Ning Ren, and Ralf Hiptmair. Force computation for dielectrics using shape calculus. *Computational Methods in Applied Mathematics*, 23(2):425–444, 2023.

[51] R. Vives-Fos R. Sanchez-Grandia, a and V. Aucejo-Galindo. Magnetostatic maxwell's tensors in magnetic media applying virtual works method from either energy or co-energy. *Eur. Phys. J. Appl. Phys. 35, 61–68*, 2006.

[52] A. Usieto Galve R. Vives Fos R. Sánchez Grandía, V. Aucejo Galindo. General formulation for magnetic forces in linear materials and permanent magnets. *IEEE TRANSACTIONS ON MAGNETICS*, 2008.

[53] F.H. Read. Improved extrapolation technique in the boundary element method to find the capacitances of the unit square and cube. *Journal of Computational Physics*, 133(1):1–5, 1997.

[54] S. Sauter and C. Schwab. *Boundary Element Methods*, volume 39 of *Springer Series in Computational Mathematics*. Springer, Heidelberg, 2010.

[55] Do-Kyung Kim Shihab Elborai Hong-Soon Choi Il-Han Park Se-Hee Lee, Xiaowei He and Markus Zahn. Evaluation of the mechanical deformation in incompressible linear and nonlinear magnetic materials using various electromagnetic force density methods. *Journal of Applied Physics*, 2005.

[56] Il-han Park Se-hee Lee and Ki sik Lee. Comparison of mechanical deformations due to different force distributions of two equivalent magnetization models. *IEEE Transactions on Magnetics, Vol. 34, No. 4*, 2000.

[57] J. Sokolowski and J.-P. Zolesio. *Introduction to shape optimization*, volume 16 of *Springer Series in Computational Mathematics*. Springer, Berlin, 1992.

[58] Olaf Steinbach. *Numerical approximation methods for elliptic boundary value problems.* Springer, New York, 2008.

[59] Ernst P. Stephan. The *hp*-version of BEM-fast convergence, adaptivity and efficient preconditioning. *J. Comput. Math.*, 27(2-3):348–359, 2009.

[60] Hao Zhang-Xukun Su Shuailing Sun Xiaoyu Chen Yuyang Zhang, Yonggang Leng and Junjie Xu. Comparative study on equivalent models calculating magnetic force between permanent magnets. *Journal of Intelligent Manufacturing and Special Equipment Vol. 1, No. 1*, 2020.